12
3-14-95 JS(1)

PNL-10359, Vol. 2
UC-[redacted]
2020

Property/Composition Relationships for Hanford High-Level Waste Glasses Melting at 1150°C

Volume 2: Chapters 12 – 16 and Appendices A – K

P. R. Hrma
G. F. Piepel
M. J. Schweiger
D. E. Smith
D.-S. Kim
P. E. Redgate
J. D. Vienna
C. A. LoPresti
D. B. Simpson
D. K. Peeler
M. H. Langowski

December 1994

Prepared for the U.S. Department of Energy
under Contract DE-AC06-76RLO 1830

Pacific Northwest Laboratory
Operated for the U.S. Department of Energy
by Battelle Memorial Institute

Battelle

PNL-10359, Vol. 2

DISTRIBUTION OF THIS DOCUMENT IS UNLIMITED

DISCLAIMER

This report was prepared as an account of work sponsored by an agency of the United States Government. Neither the United States Government nor any agency thereof, nor Battelle Memorial Institute, nor any of their employees, makes **any warranty, expressed or implied, or assumes any legal liability or responsibility for the accuracy, completeness, or usefulness of any information, apparatus, product, or process disclosed, or represents that its use would not infringe privately owned rights.** Reference herein to any specific commercial product, process, or service by trade name, trademark, manufacturer, or otherwise does not necessarily constitute or imply its endorsement, recommendation, or favoring by the United States Government or any agency thereof, or Battelle Memorial Institute. The views and opinions of authors expressed herein do not necessarily state or reflect those of the United States Government or any agency thereof.

PACIFIC NORTHWEST LABORATORY
operated by
BATTELLE MEMORIAL INSTITUTE
for the
UNITED STATES DEPARTMENT OF ENERGY
under Contract DE-AC06-76RLO 1830

Printed in the United States of America

Available to DOE and DOE contractors from the Office of Scientific and Technical Information, P.O. Box 62, Oak Ridge, TN 37831; prices available from (615) 576-8401. FTS 626-8401.

Available to the public from the National Technical Information Service, U.S. Department of Commerce, 5285 Port Royal Rd., Springfield, VA 22161.

The contents of this report were printed on recycled paper

DISCLAIMER

Portions of this document may be illegible in electronic image products. Images are produced from the best available original document.

PNL-10359, VOL. 2
UC-[redacted]
2020

PROPERTY/COMPOSITION RELATIONSHIPS FOR HANFORD HIGH-LEVEL WASTE GLASSES MELTING AT 1150°C

Volume 2: Chapters 12 - 16 and Appendices A - K

Principal Investigators and Authors
P. R. Hrma
G. F. Piepel

Other Significant Contributors and Authors
M. J. Schweiger
D. E. Smith
D.-S. Kim
P. E. Redgate
J. D. Vienna
C. A. LoPresti
D. B. Simpson
D. K. Peeler
M. H. Langowski

December 1994

Prepared for
the U.S. Department of Energy
under Contract DE-AC06-76RLO 1830

MASTER

DISTRIBUTION OF THIS DOCUMENT IS UNLIMITED

Pacific Northwest Laboratory
Richland, Washington 99352

ABSTRACT

A Composition Variation Study (CVS) is being performed within the Pacific Northwest Laboratory[a] Vitrification Technology Development (PVTD) project in support of a future high-level nuclear waste vitrification plant at the Hanford site in Washington. From 1989 to 1994, over 120 nonradioactive glasses were melted and properties measured in five statistically-designed experimental phases. Glass composition is represented by the 10 components SiO_2, B_2O_3, Al_2O_3, Fe_2O_3, ZrO_2, Na_2O, Li_2O, CaO, MgO, and Others (all remaining components). The properties measured include viscosity (η), electrical conductivity (ϵ), glass transition temperature (T_g), thermal expansion of solid glass (α_s) and molten glass (α_m), crystallinity (quenched and canister centerline cooled glasses), liquidus temperature (T_L), durability based on normalized elemental releases from the Materials Characterization Center-1 28-day dissolution test (MCC-1, r_{Mi}) and the 7-day Product Consistency Test (PCT, r_{Pi}), and solution pHs from MCC-1 and PCT. Amorphous phase separation was also evaluated.

Empirical first- and second-order mixture models were fit using the CVS data to relate the various properties to glass composition. Equations for calculating the uncertainty associated with property values predicted by the models were also developed. The models were validated using both internal and external data. Other modeling approaches (e.g., non-bridging oxygen, free energy of hydration, phase-equilibria T_L) were investigated for specific properties. A preliminary Qualified Composition Region was developed to identify glass compositions with high confidence of being processable in a melter and meeting waste form acceptance criteria.

Models expressed in mass and mole fractions of the 10 components have similar goodness of fit (R^2) values. First- and second-order models fit the CVS data for: η and ϵ from 950 to 1250°C with R^2 from 0.93 to 0.98; T_g with R^2 from 0.88 to 0.97; α_s with R^2 from 0.87 to 0.93; α_m with R^2 from 0.43 to 0.75; r_{Pi} with R^2 from 0.73 to 0.92; r_{Mi} with R^2 from 0.60 to 0.83; T_L with

---

(a) Pacific Northwest Laboratory is operated by Battelle Memorial Institute for the U.S. Department of Energy under Contract DE-AC06-76RLO 1830.

R^2 = 0.90 for clinopyroxene, R^2 = 0.64 for spinel, and R^2 = 0.79 for Zr-containing crystals. The other modeling approaches investigated did not fit the CVS data as well as the CVS first- and second-order models.

Within the composition range studied: Li_2O and Na_2O decrease η, T_g, T_L, and durability (MCC-1 and PCT), and increase ϵ. SiO_2 increases durability, η, and T_g and decreases ϵ. In addition, Al_2O_3 increases η and durability; ZrO_2 increases η, T_g, durability, and T_L for clinopyroxene and Zr-containing phases; MgO increases T_L and decreases durability; Fe_2O_3 increases T_L for Fe-containing phases; B_2O_3 decreases durability and T_L for spinel and clinopyroxene.

The crystalline phases observed in canister centerline cooled samples of CVS glasses were spinel, clinopyroxene, and Zr-containing phases (zircon, ZrO_2, and Na-Zr silicate), orthopyroxene, nepheline, olivine, $CaSiO_3$, and SiO_2 (cristobalite and quartz). Hematite, Li_2SiO_3, and $LiAlSi_2O_6$ crystallized less frequently. Durability appeared to be decreased by crystallization of nepheline, $LiAlSi_2O_6$, and cristobalite. A method for predicting amorphous phase separation in multicomponent glasses was applied to 123 CVS glasses. Nine glasses were predicted as prone to amorphous phase separation.

The results (both data and models) from the CVS so far constitute an important contribution to vitrification knowledge and technology. However, research and its interpretation will be required as new problems and needs arise.

CONTENTS--VOLUME 2

ABSTRACT iii

12.0 GLASS DURABILITY RESULTS AND DISCUSSION 12.1

12.1 FIRST-ORDER MODELS AND COMPONENT EFFECTS FOR MCC-1 RELEASES 12.1

12.2 INVESTIGATION OF POTENTIAL BIASES IN MCC-1 RELEASE DATA DUE TO CVS PHASES 12.13

12.3 SECOND-ORDER MODELS FOR MCC-1 RELEASES 12.20

12.4 VALIDATION OF FIRST- AND SECOND-ORDER MODELS FOR MCC-1 RELEASES 12.20

12.5 FIRST-ORDER MODELS AND COMPONENT EFFECTS FOR PCT RELEASES 12.30

12.6 INVESTIGATION OF POTENTIAL BIASES IN PCT RELEASE DATA DUE TO CVS PHASES 12.43

12.7 SECOND-ORDER MODELS FOR PCT RELEASES 12.44

12.8 VALIDATION OF FIRST- AND SECOND-ORDER MODELS FOR PCT RELEASES 12.48

12.9 OTHER MODEL FORMS INVESTIGATED FOR PCT RELEASES 12.54

12.10 FIRST-ORDER MODELS AND COMPONENT EFFECTS FOR PCT AND MCC-1 SOLUTION pH 12.55

12.11 GLASS DURABILITY DISCUSSION 12.69

12.11.1 Component Effects on MCC-1 and PCT Durability . . 12.69

12.11.2 Single Component Change Study 12.72

12.11.3 Glasses with Extreme Normalized Boron Releases . . 12.84

12.11.4 Amorphous Phase Separation and Anomalous Glasses 12.90

12.11.5 Normalized Releases of Si, Li, Na, Mo, and Cs . . 12.108

12.12 EFFECT OF CRYSTALLINITY ON DURABILITY OF SELECTED CVS GLASSES 12.112

13.0 MISCELLANEOUS GLASS PROPERTY DATA INVESTIGATIONS 13.1

13.1 CORRELATIONS AMONG GLASS PROPERTIES 13.1

13.2 EFFECTS OF VARYING OTHERS COMPOSITION 13.4

13.3 OVERCHECK RESULTS 13.8

13.3.1 Viscosity and Electrical Conductivity Overchecks. . 13.8

13.3.2 Durability Overchecks 13.12

13.3.3 Glass Composition Overchecks 13.22

14.0 APPLYING CVS RESULTS 14.1

14.1 USING THE CVS MODELS AND UNCERTAINTIES 14.1

14.1.1 Predicting Property Values With CVS Models 14.1

14.1.2 Statistical Statements About Model Predictions . . 14.2

14.2 QUALIFIED COMPOSITION REGION 14.4

14.4.1 Predicted Acceptable Composition Region 14.5

14.2.2 Accounting for Model Uncertainty in the QCR 14.6

14.2.3 Mathematical Constraints Defining the QCR 14.9

14.2.4 QCR Discussion 14.15

14.2.5 QCR Applications 14.25

15.0 CONCLUSIONS AND FUTURE RESEARCH 15.1

15.1 CONCLUSIONS 15.1

15.2 SUGGESTIONS FOR FUTURE RESEARCH 15.11

16.0 REFERENCES 16.1

APPENDIX A -- CVS GLASS COMPOSITIONS AND UNCERTAINTIES A.1

APPENDIX B -- VISCOSITY AT TEMPERATURE DATA AND RESULTS FROM FITTING THE FULCHER EQUATION B.1

APPENDIX C -- ELECTRICAL CONDUCTIVITY AT TEMPERATURE DATA AND RESULTS FROM FITTING THE ARRHENIUS EQUATION C.1

APPENDIX D -- NORMALIZED ELEMENTAL RELEASES AND STANDARD DEVIATIONS FROM DUPLICATE MCC-1 AND PCT DISSOLUTION TESTS D.1

APPENDIX E -- THERMAL PROPERTY AND LIQUIDUS TEMPERATURE DATA E.1

APPENDIX F -- PROPERTY VALUE UNCERTAINTIES F.1

APPENDIX G -- DATA FOR VALIDATING FITTED PROPERTY MODELS G.1

APPENDIX H -- MODELING NORMALIZED BORON RELEASE AS A FUNCTION OF COMPUTED FREE ENERGY OF HYDRATION H.1

APPENDIX I -- UNCERTAINTIES AND STATISTICAL INTERVALS FOR GLASS PROPERTY MODEL PREDICTIONS I.1

APPENDIX J -- QUALITY ASSURANCE J.1

APPENDIX K -- ACRONYMS, TERMS, SYMBOLS, AND ABBREVIATIONS K.1

FIGURES--VOLUME 2

12.1a Predicted Versus Measured MCC-1 B Release for the First-Order Mixture Model Using Mass Fractions Fitted to the Full Data Set (from Table 12.2a) 12.14

12.1b Predicted Versus Measured MCC-1 B Release for the First-Order Mixture Model Using Mole Fractions Fitted to the Full Data Set (from Table 12.2b) 12.15

12.2a Predicted Versus Measured MCC-1 B Release for the First-Order Mixture Model Using Mass Fractions Fitted to the Reduced Data Set (from Table 12.3a) 12.16

12.2b Predicted Versus Measured MCC-1 B Release for the First-Order Mixture Model Using Mole Fractions Fitted to the Reduced Data Set (from Table 12.3b) 12.17

12.3 Predicted Component Effects on MCC-1 B Release Relative to the HW-39-4 Composition, Based on the First-Order Mixture Model Using Mass Fractions Fitted to the Reduced Data Set (in Column 3 of Table 12.3a) 12.18

12.4 Predicted Versus Measured MCC-1 B Release for the Second-Order Mixture Model #2 Fitted to the Reduced Data Set (from Table 12.4) 12.23

12.5 Predicted MCC-1 Boron Release from the First-Order Mixture Model After CVS-II Phase 2 (from Table 12.8) Versus Measured MCC-1 Boron Releases (from Table 12.1) for the CVS-II Phase 3 Data 12.26

12.6a Predicted MCC-1 Boron Release from the Second-Order Mixture Model #1 After CVS-II Phase 2 (from Table 12.8) Versus Measured MCC-1 Boron Releases (from Table 12.1) for the CVS-II Phase 3 Data 12.27

12.6b Predicted MCC-1 Boron Release from the Second-Order Mixture Model #2 After CVS-II Phase 2 (from Table 12.8) Versus Measured MCC-1 Boron Releases (from Table 12.1) for the CVS-II Phase 3 Data 12.28

12.6c Predicted MCC-1 Boron Release from the Second-Order Mixture Model #3 After CVS-II Phase 2 (from Table 12.8) Versus Measured MCC-1 Boron Releases (from Table 12.1) for the CVS-II Phase 3 Data 12.29

12.7a Predicted Versus Measured PCT B Release for the First-Order Mixture Model Using Mass Fractions (from Table 12.10a) 12.40

FIGURES--VOLUME 2 (continued)

12.7b Predicted Versus Measured PCT B Release for the First-Order Mixture Model Using Mole Fractions (from Table 12.10b) 12.41

12.8 Predicted Component Effects on PCT B Release Relative to the HW-39-4 Composition, Based on First-Order Mixture Model Using Mass Fractions (in Column 3 of Table 12.10a) 12.42

12.9 Predicted Versus Measured PCT B Release for the Second-Order Mixture Model #2 (from Table 12.11) 12.47

12.10 Predicted Normalized PCT Boron Release from the First-Order Mixture Model After CVS-II Phase 2 (from Table 12.15) Versus Measured PCT Boron Releases (from Table 12.9) for the CVS-II Phase 3 Data 12.50

12.11a Predicted Normalized PCT Boron Release from the Second-Order Mixture Model #1 After CVS-II Phase 2 (from Table 12.15) Versus Measured PCT Boron Releases (from Table 12.9) for the CVS-II Phase 3 Data 12.51

12.11b Predicted Normalized PCT Boron Release from the Second-Order Mixture Model #2 After CVS-II Phase 2 (from Table 12.15) Versus Measured PCT Boron Releases (from Table 12.9) for the CVS-II Phase 3 Data 12.52

12.11c Predicted Normalized PCT Boron Release from the Second-Order Mixture Model #3 After CVS-II Phase 2 (from Table 12.15) Versus Measured PCT Boron Releases (from Table 12.9) for the CVS-II Phase 3 Data 12.53

12.12a Predicted Versus Measured PCT B Release for the Alfred University "Ratio to SiO_2" Model Using Mass Fractions 12.57

12.12b Predicted Versus Measured PCT B Release for the Alfred University "Ratio to SiO_2" Model Using Mole Fractions 12.58

12.13a Predicted Versus Measured MCC-1 pH for the First-Order Mixture Model Using Mass Fractions (from Table 12.18) 12.61

12.13b Predicted Versus Measured MCC-1 pH for the First-Order Mixture Model Using Mole Fractions (from Table 12.18) 12.62

12.14a Predicted Versus Measured PCT pH for the First-Order Mixture Model Using Mass Fractions (from Table 12.18) 12.63

12.14b Predicted Versus Measured PCT pH for the First-Order Mixture Model Using Mole Fractions (from Table 12.18) 12.64

FIGURES--VOLUME 2 (continued)

12.15 Predicted Component Effects on MCC-1 pH Relative to the HW-39-4 Composition, Based on the Fitted First-Order Mixture Model Using Mass Fractions 12.66

12.16 Predicted Component Effects on PCT pH Relative to the HW-39-4 Composition, Based on the Fitted First-Order Mixture Model Using Mass Fractions 12.67

12.17 Coefficients of First-Order Mixture Models Using Mass Fractions for pH of MCC-1 Dissolution Test Solutions Versus for pH of PCT Dissolution Test Solutions 12.68

12.18 Plot of MCC-1 Versus PCT Normalized Boron Release First-Order Mixture Model Coefficients 12.70

12.19 Ternary Plot of the Normalized Compositions of CVS2-102 Through CVS2-123 Glasses 12.73

12.20 Effect of Varying the SiO_2 Mass Fraction of HW-39-4 Glass on Normalized Boron Release by: • MCC-1, ○ PCT of quenched glass, □ PCT of CCC glass, and X CVS measurements of HW-39-4 glass 12.76

12.21 Effect of Varying the B_2O_3 Mass Fraction of HW-39-4 Glass on Normalized Boron Release by: • MCC-1, ○ PCT of quenched glass, □ PCT of CCC glass, and X CVS measurements of HW-39-4 glass 12.77

12.22 Effect of Varying the Na_2O Mass Fraction of HW-39-4 Glass on Normalized Boron Release by: • MCC-1, ○ PCT of quenched glass, □ PCT of CCC glass, and X CVS measurements of HW-39-4 glass 12.78

12.23 Effect of Varying the Li_2O Mass Fraction of HW-39-4 Glass on Normalized Boron Release by: • MCC-1, ○ PCT of quenched glass, □ PCT of CCC glass, and X CVS measurements of HW-39-4 glass 12.79

12.24 Effect of Varying the CaO Mass Fraction of HW-39-4 Glass on Normalized Boron Release by: • MCC-1, ○ PCT of quenched glass, □ PCT of CCC glass, and X CVS measurements of HW-39-4 glass 12.81

12.25 Effect of Varying the MgO Mass Fraction of HW-39-4 Glass on Normalized Boron Release by: • MCC-1, ○ PCT of quenched glass, □ PCT of CCC glass, and X CVS measurements of HW-39-4 glass 12.82

FIGURES--VOLUME 2 (continued)

12.26 Effect of Varying the Al_2O_3 Mass Fraction of HW-39-4 Glass on Normalized Boron Release by: • MCC-1, ○ PCT of quenched glass, □ PCT of CCC glass, and X CVS measurements of HW-39-4 glass 12.83

12.27 Plot of MCC-1 and PCT Normalized Boron Releases With Lines Representing Different PCT/MCC-1 Release Ratios Superimposed 12.87

12.28 Ratio of Silicon-to-Boron Releases (r_{Si}/r_B) After Dissolution in H_2O at 90°C Versus $(S/V)t^{1/2}$ for CVS2-23 and CVS2-39 Glasses 12.89

12.29 Various Normalized Alkali Borosilicate Submixtures Categorizing the 123 CVS-I and CVS-II Phase 1, 2, and 3 Glasses in Terms of High and Low MCC-1 Durability of Quenched Samples 12.96

12.30 Compositional Positions of the 24 CVS Glasses Selected for Analysis Within the (a) NBS and (b) NLBS Normalized Submixtures 12.102

12.31 Compositional Positions of the High-Release Glasses Within the (a) NBS and (b) NLBS Normalized Submixtures 12.107

12.32 Component-Wise Differences Between Coefficients of First-Order Mixture Models for Si, Na, and Li Normalized Elemental Releases With That of B for PCT 12.111

12.33 Component-Wise Differences Between Coefficients of First-Order Mixture Models for Si, Na, and Li Normalized Elemental Releases With That of B for MCC-1 . . . . . 12.111

12.34 7-Day PCT Normalized Boron Releases from Quenched and Heat-Treated Glasses 12.115

13.1 CVS and CELS Viscosity Data on the CVS Internal Standard and HW-39-4 Glasses 13.10

13.2 CVS and CELS Electrical Conductivity Data on the CVS Internal Standard and HW-39-4 Glasses 13.11

13.3 Comparison of MCC-1 B and Li Releases (ppm) Obtained by PNL, SRTC, and ANL for the CVS Internal Standard Glass and HW-39-4 . . . . . 13.20

FIGURES--VOLUME 2 (continued)

13.4 Comparison of PCT B and Li Releases (ppm) Obtained by PNL, SRTC, and ANL for the CVS Internal Standard Glass and HW-39-4 . . . . . 13.20

14.1 Histograms of Predicted Property Values for Shrunken Versions of the Vertices and Centroid of Each Property Constraint That Lie on the Boundary of the Qualified Composition Region Defined by 95% Confidence Intervals 14.19

14.2 Histograms of Predicted Property Values for Shrunken Versions of the Vertices and Centroid of Each Property Constraint That Lie on the Boundary of the Qualified Composition Region Defined by 95% Confidence Bands 14.22

H.1 Natural Log of 28-Day MCC-1 Boron Release Versus Free Energy of Hydration for CVS Glasses H.8

H.2 Natural Log of 28-Day MCC-1 Boron Release Versus pH-Corrected Free Energy of Hydration for CVS Glasses H.9

H.3 Natural Log of 7-Day PCT Boron Release Versus Free Energy of Hydration for CVS Glasses H.10

H.4 Natural Log of 7-Day PCT Boron Release Versus pH-Corrected Free Energy of Hydration for CVS Glasses H.11

TABLES--VOLUME 2

12.1 Si, B, Li, Na, Mo, and Cs Normalized Releases and Solution pHs Averaged Over Duplicate 28-day MCC-1 Dissolution Tests of CVS-I and CVS-II Glasses 12.2

12.2a Coefficients and Goodness-of-Fit Statistics for First-Order Mixture Models (Using Component Mass Fractions) Fitted to Natural Logarithms of Averaged 28-Day MCC-1 Normalized Elemental Releases (g/m^2) for CVS-I and CVS-II Phase 1, 2, and 3 Glasses 12.9

12.2b Coefficients and Goodness-of-Fit Statistics for First-Order Mixture Models (Using Component Mole Fractions) Fitted to Natural Logarithms of Averaged 28-Day MCC-1 Normalized Elemental Releases (g/m^2) for CVS-I and CVS-II Phase 1, 2, and 3 Glasses 12.10

12.3a Coefficients and Goodness-of-Fit Statistics for First-Order Mixture Models (Using Component Mass Fractions) Fitted to Natural Logarithms of Averaged 28-Day MCC-1 Normalized Elemental Releases (g/m^2) for CVS-I and CVS-II Phase 1, 2, and 3 Glasses After Deleting the High Release Data Corresponding to Glasses CVS1-4,6,9,13,15,21 and CVS2-82 . . . 12.11

12.3b Coefficients and Goodness-of-Fit Statistics for First-Order Mixture Models (Using Component Mole Fractions) Fitted to Natural Logarithms of Averaged 28-Day MCC-1 Normalized Elemental Releases (g/m^2) for CVS-I and CVS-II Phase 1, 2, and 3 Glasses After Deleting the High Release Data Corresponding to Glasses CVS1-4,6,9,13,15,21 and CVS2-82 . . . 12.12

12.4 Candidate Scheffé Second-Order Models Using Mass Fractions for MCC-1 ln(Boron) Release Fitted to the Reduced Data Set 12.21

12.5 Candidate Scheffé Second-Order Models Using Mass Fractions for MCC-1 ln(Silica) Release Fitted to the Reduced Data Set 12.21

12.6 Candidate Scheffé Second-Order Models Using Mass Fractions for MCC-1 ln(Lithium) Release Fitted to the Reduced Data Set 12.22

12.7 Candidate Scheffé Second-Order Models Using Mass Fractions for MCC-1 ln(Sodium) Release Fitted to the Reduced Data Set 12.22

TABLES--VOLUME 2 (continued)

12.8 First-Order Model and Three Candidate Second-Order Models for MCC-1 ln(Boron) Release Fitted to CVS-I and CVS-II Phase 1 and 2 Data Without High Release Data Points 12.24

12.9 Si, B, Li, Na, Mo, and Cs Normalized Releases and Solution pHs Averaged Over Duplicate 7-day PCT Dissolution Tests of CVS-I and CVS-II Glasses 12.31

12.10a Coefficients and Goodness-of-Fit Statistics for First-Order Mixture Models (Using Component Mass Fractions) Fitted to Natural Logarithms of Averaged 7-Day PCT Normalized Elemental Releases (g/m^2) for CVS-I and CVS-II Phase 1, 2, and 3 Glasses 12.38

12.10b Coefficients and Goodness-of-Fit Statistics for First-Order Mixture Models (Using Component Mole Fractions) Fitted to Natural Logarithms of Averaged 7-Day PCT Normalized Elemental Releases (g/m^2) for CVS-I and CVS-II Phase 1, 2, and 3 Glasses 12.39

12.11 Candidate Scheffé Second-Order Models Using Mass Fractions for PCT ln(Boron) Release 12.45

12.12 Candidate Scheffé Second-Order Models Using Mass Fractions for PCT ln(Silica) Release 12.45

12.13 Candidate Scheffé Second-Order Models Using Mass Fractions for PCT ln(Lithium) Release 12.46

12.14 Candidate Scheffé Second-Order Models Using Mass Fractions for PCT ln(Sodium) Release 12.46

12.15 First-Order Model and Three Candidate Second-Order Models Using Mass Fractions for PCT ln(Boron) Release Fitted to CVS-I and CVS-II Phase 1 and 2 Data 12.49

12.16 Coefficients for Mass and Mole Fraction Versions of Alfred University "Ratio to SiO_2" Model for Normalized PCT B Release 12.56

12.17 R^2 Values for the Alfred University "Ratio to SiO_2" Model and the CVS First-Order Mixture Model for Normalized PCT Boron Release Using Mass and Mole Fractions 12.56

12.18 Coefficients and Goodness of Fit Statistics for First-Order Mixture Models (Using Mass and Mole Fractions) Fitted to pH Data from MCC-1 and PCT Tests 12.60

12.19 Classification of Individual CVS Glass Components Regarding Their Effects On Glass Durability 12.71

12.20 Slopes of ln(Boron Release) Versus Single-Component Additions to the HW-39-4 Glass Composition 12.74

12.21 Microstructural Analysis of 24 Canister-Centerline-Cooled CVS Glasses by SEM 12.103

12.22 Crystalline Phases and Estimated Volume % in CVS Glasses After CCC Heat Treatment 12.113

12.23 PCT Normalized Releases of Quenched and Canister-Centerline-Cooled Heat-Treated CVS Glasses 12.115

13.1 Pairwise Correlations Among Untransformed Glass Properties 13.2

13.2 Pairwise Correlations Among Transformed Glass Properties 13.3

13.3 Property Values for Sets of Glasses with the Same 10-Component Compositions but Different Others Mixes 13.5

13.4 CELS Viscosity and Electrical Conductivity Measurements for the CVS Internal Standard Glass 13.9

13.5 B and Li Concentrations (ppm) from PCT Overcheck Tests 13.14

13.6 B and Li Concentrations (ppm) from MCC-1 Overcheck Tests . . . 13.15

13.7 Percent Relative Differences (%RD) in Elemental Releases Between Two Labs Detectable With 95% Confidence and 5% False-Alarm Rate 13.18

13.8 As-Batched and Analyzed Compositions (wt%) of the CVS Internal Standard and HW-39-4 Glasses 13.21

14.1 Region of Validity for CVS Property Models 14.3

14.2 CVS Glass Property Transformations and Inverse Transformations 14.3

14.3 Overall Centroid and Eight-Dimensional Face Centroid Glass Compositions (mass fractions) for the Preliminary PACR 14.7

14.4 Constraints Defining the Qualified Composition Region (QCR) 14.10

TABLES--VOLUME 2 (continued)

14.5 Model Coefficients ($\hat{\beta}$), $(X'X)^{-1}$, Experimental Error Standard Deviations (σ), and Multipliers for Preliminary QCR 14.14

14.6 Number of Vertices of Predicted Acceptable Composition Region Violating the Stand-In Crystallinity Constraints 14.15

14.7 Summary of Shrinkage Factors for Each Property Model-Constraint Boundary of the Qualified Composition Region for Both 95% Confidence Intervals and 95% Confidence Bands 14.18

15.1 First-Order Mass Fraction Mixture Model Coefficients for Various Properties 15.3

A.1 As-Batched (B) and Analyzed (A) Compositions (in mass fractions) for CVS-I Glasses A.13

A.2 As-Batched (B) and Analyzed (A) Compositions (in mass fractions) for CVS-II Phase 1 and Phase 2 Glasses A.18

A.3 As-Batched (B) and Analyzed (A) Compositions (in mass fractions) for Selected CVS-II Phase 3 Glasses A.30

A.4 Results of Statistical Tests on Differences Between Analyzed and As-Batched Values of Oxide Components for CVS-I Glasses A.33

A.5 Results of Statistical Tests on Differences Between Analyzed and As-Batched Values of Oxide Components for CVS-II Phase 1 Glasses A.34

A.6 Results of Statistical Tests on Differences Between Analyzed and As-Batched Values of Oxide Components for CVS-II Phase 2 Glasses CVS2-20 to CVS2-51 . . . . . A.35

A.7 Results of Statistical Tests on Differences Between Analyzed and As-Batched Values of Oxide Components for Selected CVS-II Phase 3 Glasses A.36

A.8 Summary of Analyzed - Batched Differences by Oxide Component for CVS-I, CVS-II Phase 1, CVS-II Phase 2, and CVS-II Phase 3 Glasses A.37

A.9 As-Batched and Analyzed Compositions (in mass fractions) for Six Replicate Analyses of Glass CVS1-19 Conducted Over Three Months A.38

TABLES--VOLUME 2 (continued)

A.10 Summary Statistics for Six Replicate Analyses of CVS-I Glass CVS1-19 Conducted Over Three Months A.39

A.11 As-Batched and Analyzed Compositions (in mass fractions) for Replicate Analyses of the CVS Internal Standard Glass . . . A.40

A.12 Redox Ratios of Selected Test Glasses A.41

B.1 Viscosity at Temperature Data for CVS-I and CVS-II Phase 1, 2, and 3 Glasses B.2

B.2 Results of Fitting the Fulcher Equation to the Viscosity at Temperature Data for Each CVS-I and CVS-II Phase 1, 2, and 3 Glass B.17

C.1 Electrical Conductivity at Temperature Data for CVS-I and CVS-II Phase 1 and 2 Glasses C.2

C.2 Electrical Conductivity at Temperature Data for CVS-II Phase 3 Glasses C.7

C.3 Results of Fitting the Arrhenius Equation to the Electrical Conductivity at Temperature Data for Each CVS-I and CVS-II Phase 1, 2, and 3 Glass C.12

D.1 Normalized Elemental Release and pH Data from Duplicate 28-Day MCC-1 Tests (90°C, DIW, $10m^{-1}$) Performed on CVS-I and CVS-II Glasses D.2

D.2 Normalized Elemental Release and pH Data from Duplicate 7-day PCTs (90°C, DIW, $2000m^{-1}$) Performed on CVS-I and CVS-II Glasses D.13

D.3 Standard Deviations (SD) and Percent Relative Standard Deviations (%RSD) Before and After Natural Logarithmic Transformations of Normalized Si, B, Li, and Na Release Data from Duplicate 28-Day MCC-1 Dissolution Tests D.24

D.4 Standard Deviations (SD) and Percent Relative Standard Deviations (%RSD) Before and After Natural Logarithmic Transformations of Normalized Si, B, Li, and Na Release Data from Duplicate 7-Day PCT Dissolution Tests D.26

D.5 Normalized Elemental Release and pH Data from Duplicate 7-day PCTs (90°C, DIW, $2000m^{-1}$) Performed on CVS-II Phase 4 Glasses D.28

TABLES--VOLUME 2 (continued)

E.1 Glass Transition Temperature (T_g), Thermal Expansion Coefficients for Solid Glass (α_s) and Molten Glass (α_m), and Older Liquidus Temperature Results for CVS-I and CVS-II Phase 1, 2, and 3 Glasses E.2

F.1 Viscosity, Electrical Conductivity, and Thermal Property Values for Glasses Replicated During CVS. F.2

F.2 PCT Elemental Releases for Glasses Replicated During CVS . . . F.3

F.3 MCC-1 Elemental Releases for Glasses Replicated During CVS . . F.4

F.4 Standard Deviations of Untransformed and Transformed Glass and Melt Property Data from Replicate Glasses F.5

F.5 Standard Deviations of Natural Log Transformed PCT Si, B, Li, and Na Release (g/m²) Data from Replicate Glasses F.6

F.6 Standard Deviations of Natural Log Transformed MCC-1 Si, B, Li, and Na Release (g/m²) Data from Replicate Glasses F.8

F.7 Standard Deviations of PCT pH and MCC-1 pH Data from Replicate Glasses F.10

F.8 Liquidus Temperature Data and Their Means, Standard Deviations, and % Relative Standard Deviations for Glasses Replicated During CVS F.11

G.1 Summary of Model Validation Database Contents G.3

G.2 Oxide Composition Regions in Mass Fractions Delimited by Nominal CVS Oxide Component Bounds and Relaxed CVS Bounds G.3

G.3 Data for 160 Glasses from Historical Database Used to Validate Models for Viscosity at 1150°C G.6

G.4 Data for 209 Glasses from Historical Database Used to Validate Models for Electrical Conductivity at 1150°C . . . G.12

G.5 Data for 143 Glasses from Historical Database Used to Validate Models for Glass Transition Temperature G.19

H.1 Computed Free Energy of Hydration Values With and Without PCT and MCC-1 pH Corrections Versus PCT and MCC-1 Normalized Boron Releases H.2

TABLES--VOLUME 2 (continued)

I.1 $(X'X)^{-1}$ for the First-Order Mixture Model Using Mass Fractions for ln(Viscosity at 1150°C) (from Table 7.3) I.4

I.2 $(X'X)^{-1}$ for the First-Order Mixture Model Using Mass Fractions for ln(Electrical Conductivity at 1150°C) (from Table 8.2) I.4

I.3 $(X'X)^{-1}$ for the First-Order Mixture Models Using Mass Fractions for ln(PCT Elemental Releases) (from Table 12.10a) and for PCT pH (from Table 12.18) I.5

I.4 $(X'X)^{-1}$ for the First-Order Mixture Models Using Mass Fractions for ln(MCC-1 Elemental Releases) Fitted to the "Reduced Data" (from Table 12.3a) I.5

I.5 $(X'X)^{-1}$ for the First-Order Mixture Models Using Mass Fractions for ln(MCC-1 Elemental Releases) Fitted to the "Full Data" (from Table 12.2a) and for T_g (from Table 9.2) I.6

I.6 $(X'X)^{-1}$ for the First-Order Mixture Model Using Mass Fractions for MCC-1 pH (from Table 12.18) I.6

I.7 $(X'X)^{-1}$ for the First-Order Mixture Model Using Mass Fractions for Thermal Expansion of Molten Glass (from Table 10.2) I.7

I.8 $(X'X)^{-1}$ for the First-Order Mixture Model Using Mass Fractions for Thermal Expansion of Solid Glass (from Table 10.2) I.7

I.9 $(X'X)^{-1}$ for the First-Order Mixture Model Using Mass Fractions for Liquidus Temperature of Clinopyroxene (from Table 11.7) I.8

I.10 $(X'X)^{-1}$ for the First-Order Mixture Model Using Mass Fractions for Liquidus Temperature of Spinel (from Table 11.7) I.8

I.11 $(X'X)^{-1}$ for the First-Order Mixture Model Using Mass Fractions for Liquidus Temperature of Zr-Containing Phases (from Table 11.7) I.9

I.12 $\hat{\sigma}^2$ Values Corresponding to First-Order Mass Fraction Property Models I.10

TABLES--VOLUME 2 (continued)

J.1 Design and Analysis Results That Require QA SCP Verification J.4

J.2 Design and Analysis Results That Do Not Require QA SCP Verification, Organized by Reason Why J.5

12.0 GLASS DURABILITY RESULTS AND DISCUSSION

In this chapter, MCC-1 and PCT data and models relating the data to glass composition are presented and discussed. The MCC-1 test and the PCT provide different information about glass dissolution. The amount of glass dissolved per unit surface area is large in the MCC-1 test compared to the PCT. The solution at the end of the PCT is much closer to saturation than in the MCC-1 test. In this chapter, the results are discussed in the order of degree of saturation at the end of the test (i.e., MCC-1 first, then PCT). The PCT is currently the basis for determining acceptability of HLW glass.

The Si, B, Li, Na, Mo, and Cs elemental releases and estimates of short-term uncertainties from duplicate 28-day MCC-1 and 7-day PCT dissolution tests of CVS glasses are contained in Appendix D. Long-term uncertainty estimates based on replicate glass results are presented in Appendix F. Overcheck MCC-1 and PCT testing of several glasses was performed at the Savannah River Technology Center (SRTC), Rensselaer Polytechnic Institute (RPI), and Argonne National Laboratory (ANL) and the results are discussed in Section 13.3.2.

The extent of glass dissolution is calculated using the concentrations of glass components in solution. As explained in Section 5.8, the extent of glass dissolution is represented by normalized elemental releases. The normalized release of B provides the best representation of glass dissolution extent for the following reasons: 1) all B dissolved from glass enters into solution and does not precipitate in the gel layer, 2) B is released only by dissolution of the glass network, not by a diffusion process, 3) B_2O_3 is present in CVS glasses in a sufficiently high concentration, and 4) B concentration in solution is determined by ICP with satisfactory precision.

12.1 FIRST-ORDER MODELS AND COMPONENT EFFECTS FOR MCC-1 RELEASES

The Si, B, Li, Na, Mo, and Cs release values averaged over duplicate 28-day MCC-1 results (see Table D.1) for all CVS-I and CVS-II (Phase 1, 2, 3, and 4) glasses are contained in Table 12.1. The MCC-1 averaged normalized B releases ranged from roughly 2.7 to 690 g/m^2. Eight CVS-I glasses and ten CVS-II glasses have MCC-1 normalized boron releases above 50 g/m^2.

TABLE 12.1. Si, B, Li, Na, Mo, and Cs Normalized Releases and Solution pHs Averaged Over Duplicate 28-day MCC-1 Dissolution Tests of CVS-I and CVS-II Glasses

Glass [b]	ID[c] #	PS[d]	Averaged 28-day MCC-1 Normalized Elemental Releases (g/m²)[a] Si	B	Li	Mo	Na	Cs	pH
CVS1-1 (1)	1	M	8.99	12.47	11.95	12.24	12.36	9.68	9.95
CVS1-2	2	1	6.82	7.46	7.19	8.24	7.41	8.48	10.04
CVS1-3	3	1	10.84	15.57	15.56	15.50	15.62	10.25	9.58
CVS1-4 (2)	4	1	64.85	189.71	161.94	177.29	180.44	102.50	9.65
CVS1-5	5	1	10.42	11.48	10.46	11.59	10.83	14.00	10.07
CVS1-6	6	1	45.38	121.30	108.60	118.38	92.99	9.86	9.91
CVS1-7	7	1	7.50	11.00	10.50	11.31	10.75	10.25	9.85
CVS1-8 (3)	8	1	11.73	17.88	16.73	18.29	17.31	15.57	9.72
CVS1-9	9	1	45.79	158.72	148.82	124.10	150.30	69.38	9.24
CVS1-10	10	1	2.70	2.74	3.33	2.37	2.80	2.38	8.51
CVS1-11	11	1	6.77	8.25	8.17	7.83	8.32	5.92	9.17
CVS1-12	12	1	49.35	118.48	122.58	118.66	122.68	106.44	10.86
CVS1-13	13	1	187.62	690.51	652.69	665.87	637.30	102.50	10.59
CVS1-14	14	1	23.94	73.63	68.06	45.93	57.69	10.05	10.09
CVS1-15	15	1	73.40	210.29	172.04	199.20	172.50	57.36	12.37
CVS1-16	16	1	11.38	16.85	15.38	18.01	16.01	16.36	10.48
CVS1-17	17	1	20.24	39.10	40.86	38.11	40.85	37.06	10.96
CVS1-18	18	1	5.91	24.05	23.66	20.56	23.24	13.15	11.03
CVS1-19 (1)	19	M	8.95	13.02	13.18	12.29	13.05	10.17	9.88
CVS1-20 (1)	20	M	8.84	12.50	12.50	11.91	12.49	9.20	9.88
CVS1-21 (2)	21	1	61.10	205.79	177.74	194.04	192.42	102.50	9.65
CVS1-22 (3)	22	1	11.61	17.36	17.10	17.45	16.99	15.77	9.77
CVS1-23 (e)	23	M	12.02	15.37	15.71	14.64	15.63	14.00	9.96
CVS2-1	24	2	9.37	12.24	12.61	11.99	11.84	12.96	9.46
CVS2-2	25	2	7.29	8.44	9.54	9.23	9.16	7.78	9.61
CVS2-3	26	2	7.36	8.87	9.56	9.23	9.12	10.18	9.29

(a) Release rates normalized using as-batched compositions in Table 4.15.

(b) The numbers in parentheses represent replicate sets of glasses.

(c) ID# is a consecutive integer numbering of all CVS glasses.

(d) PS is the plotting symbol used in plots associated with this data: 1 = CVS-I boundary, 2 = CVS-II Phase 1 interior, 3 = CVS-II Phase 2a boundary, 4 = CVS-II Phase 2b interior, 5 = CVS-II Phase 3 boundary, 6 = CVS-II Phase 4 one-component-at-a-time, M = middle compositions, O = other than NCAW waste glasses, A = EA glass.

(e) The result from one of two duplicate tests--the other was obviously erroneous.

TABLE 12.1. Si, B, Li, Na, Mo, and Cs Normalized Releases and Solution pHs Averaged Over Duplicate 28-day MCC-1 Dissolution Tests of CVS-I and CVS-II Glasses (continued)

Glass [b]	ID[c] #	PS[d]	Averaged 28-day MCC-1 Normalized Elemental Releases (g/m²)[a] Si	B	Li	Mo	Na	Cs	pH
CVS2-4	27	2	9.55	9.73	10.87	10.79	10.38	13.26	9.52
CVS2-5	28	2	9.22	10.40	11.82	10.49	10.98	8.93	9.04
CVS2-6	29	2	13.56	17.48	18.74	18.50	18.82	15.05	9.66
CVS2-7	30	2	9.48	5.02	4.78	13.87	24.24	11.36	9.76
CVS2-8	31	2	15.03	18.50	19.92	19.19	19.17	14.08	9.81
CVS2-9	32	2	11.42	13.20	14.40	13.84	13.16	11.13	9.51
CVS2-10	33	2	10.99	12.28	12.79	11.99	11.02	7.50	8.92
CVS2-11	34	2	11.66	19.85	21.70	20.28	17.92	15.61	9.94
CVS2-12	35	2	8.44	9.86	10.28	10.56	9.67	9.54	9.25
CVS2-13	36	2	10.63	13.36	14.00	12.85	16.60	14.21	9.73
CVS2-14	37	2	8.24	15.10	15.52	16.28	14.96	8.05	9.48
CVS2-15	38	2	11.10	25.10	33.04	9.75	5.38	8.52	9.03
CVS2-16 (4)	39	M	14.41	18.08	18.22	17.37	18.22	14.74	9.46
CVS2-17 (1)	40	M	9.23	12.32	14.02	12.85	13.48	10.60	9.31
CVS2-18 (4)	41	M	15.74	19.72	20.32	19.28	23.37	14.84	9.38
CVS2-19 (5)	42	M	11.18	13.69	13.76	14.61	13.07	9.66	9.34
CVS2-20	43	3	7.22	8.43	7.28	(f)	7.69	6.31	9.55
CVS2-21	44	3	9.39	11.81	10.31	(f)	11.25	9.27	9.37
CVS2-22	45	3	11.44	15.60	13.50	(f)	14.56	10.65	9.74
CVS2-23	46	3	10.27	11.21	10.49	(f)	11.63	10.06	9.86
CVS2-24	47	3	10.10	19.86	17.37	(f)	15.92	0.95	9.38
CVS2-25	48	3	21.27	34.50	31.49	(f)	33.65	32.58*	10.27
CVS2-26	49	3	17.80	39.15	35.02	(f)	37.25	9.07	9.75
CVS2-27	50	3	8.78	11.22	9.90	(f)	10.98	11.44	9.64
CVS2-28	51	3	8.86	9.84	8.87	(f)	9.98	8.08	9.51

(a) Release rates normalized using as-batched compositions in Table 4.15.

(b) The numbers in parentheses represent replicate sets of glasses.

(c) ID# is a consecutive integer numbering of all CVS glasses.

(d) PS is the plotting symbol used in plots associated with this data: 1 = CVS-I boundary, 2 = CVS-II Phase 1 interior, 3 = CVS-II Phase 2a boundary, 4 = CVS-II Phase 2b interior, 5 = CVS-II Phase 3 boundary, 6 = CVS-II Phase 4 one-component-at-a-time, M = middle compositions, O = other than NCAW waste glasses, A = EA glass.

(f) Mo release was not measured during CVS-II.

* Based on re-analysis of samples.

TABLE 12.1. Si, B, Li, Na, Mo, and Cs Normalized Releases and Solution pHs Averaged Over Duplicate 28-day MCC-1 Dissolution Tests of CVS-I and CVS-II Glasses (continued)

Glass [b]	ID[c] #	PS[d]	Averaged 28-day MCC-1 Normalized Elemental Releases (g/m²)[a] Si	B	Li	Mo	Na	Cs	pH
CVS2-29	52	3	20.76	42.29	37.74	(f)	40.63	25.63	9.14
CVS2-30	53	3	8.11	24.44	21.08	(f)	18.31	1.97	8.76
CVS2-31	54	3	22.40	47.02	42.69	(f)	44.20	15.97	9.41
CVS2-32	55	3	13.62	16.62	14.12	(f)	16.04	8.28	10.07
CVS2-33	56	3	9.23	14.51	12.71	(f)	13.95	9.86	10.26
CVS2-34 (6)	57	3	12.80	29.24	26.17	(f)	22.81	3.55	9.98
CVS2-35	58	3	9.65	11.61	10.83	(f)	12.03	13.01	10.22
CVS2-36	59	3	15.49	21.09	19.01	(f)	20.35	18.53	10.13
CVS2-37	60	3	9.30	9.64	8.40	(f)	9.05	7.49	9.33
CVS2-38	61	3	16.94	23.65	20.36	(f)	22.33	15.18	9.27
CVS2-39	62	3	10.49	16.30	14.21	(f)	15.34	10.25	10.17
CVS2-40	63	4	9.45	12.21	10.65	(f)	11.68	9.26	9.79
CVS2-41	64	4	7.93	9.43	8.10	(f)	8.93	7.23	9.60
CVS2-42	65	4	10.99	14.31	12.20	(f)	13.41	14.85	9.86
CVS2-43	66	4	8.62	11.33	9.92	(f)	10.87	7.56	9.23
CVS2-44	67	4	8.79	10.28	8.85	(f)	9.88	7.23	9.56
CVS2-45	68	4	8.79	11.60	9.85	(f)	10.91	8.73	9.43
CVS2-46	69	4	9.07	10.99	9.59	(f)	10.36	8.44	9.32
CVS2-47	70	4	8.76	11.56	10.01	(f)	10.93	10.70	9.83
CVS2-48	71	4	8.41	10.63	9.21	(f)	10.11	5.63	9.42
CVS2-49	72	4	9.48	11.35	9.79	(f)	10.71	7.03	9.01
CVS2-50 (1)	73	M	8.37	11.43	9.84	(f)	10.81	9.93	9.45
CVS2-51 (5)	74	M	10.23	12.35	10.32	(f)	12.18	7.61	9.48
CVS2-52	75	5	8.99	10.08	8.71	(f)	9.55	7.85	9.47
CVS2-53	76	5	(g)	(g)	(g)	(g)	(g)	(g)	(g)
CVS2-54	77	M	(g)	(g)	(g)	(g)	(g)	(g)	(g)

(a) Release rates normalized using as-batched compositions in Table 4.15.

(b) The numbers in parentheses represent replicate sets of glasses.

(c) ID# is a consecutive integer numbering of all CVS glasses.

(d) PS is the plotting symbol used in plots associated with this data: 1 = CVS-I boundary, 2 = CVS-II Phase 1 interior, 3 = CVS-II Phase 2a boundary, 4 = CVS-II Phase 2b interior, 5 = CVS-II Phase 3 boundary, 6 = CVS-II Phase 4 one-component-at-a-time, M = middle compositions, O = other than NCAW waste glasses, A = EA glass.

(f) Mo release was not measured during CVS-II.

(g) MCC-1 testing not performed on radioactive glasses CVS2-53 and CVS2-54.

TABLE 12.1. Si, B, Li, Na, Mo, and Cs Normalized Releases and Solution pHs Averaged Over Duplicate 28-day MCC-1 Dissolution Tests of CVS-I and CVS-II Glasses (continued)

Glass [b]	ID[c] #	PS[d]	Averaged 28-day MCC-1 Normalized Elemental Releases (g/m²)[a] Si	B	Li	Mo	Na	Cs	pH
CVS2-55	78	0	13.11	15.91	13.73	(f)	14.92	0.33	9.52
CVS2-56	79	0	14.36	17.23	14.99	(f)	16.30	0.33	9.57
CVS2-57	80	0	12.13	15.28	13.32	(f)	14.39	0.33	9.55
CVS2-58	81	4	8.66	13.15	11.45	(f)	12.72	4.34	9.36
CVS2-59	82	5	9.76	11.98	10.20	(f)	11.69	8.52	9.85
CVS2-60	83	5	10.72	16.52	14.62	(f)	16.41	1.66	10.44
CVS2-61	84	5	10.32	10.90	9.58	(f)	10.72	7.74	9.75
CVS2-62	85	5	9.96	12.39	11.58	(f)	12.58	8.08	9.32
CVS2-63	86	5	7.93	9.64	10.54	(f)	9.58	8.48	9.61
CVS2-64	87	0	10.69	12.32	10.72	(f)	12.31	10.25	9.85
CVS2-65	88	0	7.80	9.40	8.33	(f)	9.02	(h)	9.59
CVS2-66	89	0	10.32	11.74	10.48	(f)	11.68	(h)	9.61
CVS2-67	90	0	10.92	11.14	9.96	(f)	11.23	(h)	9.11
CVS2-68	91	0	10.18	10.56	9.42	(f)	10.56	(h)	9.21
CVS2-69	92	0	9.44	9.88	8.75	(f)	9.84	(h)	9.45
CVS2-70	93	0	11.01	11.56	10.42	(f)	11.78	(h)	9.22
CVS2-71	94	5	10.13	12.00	10.55	(f)	11.80	9.52	9.78
CVS2-72	95	5	10.32	11.74	10.48	(f)	12.24	8.88	9.71
CVS2-73	96	5	6.15	6.64	5.87	(f)	6.34	5.60	9.10
CVS2-74	97	5	8.68	9.88	8.75	(f)	9.84	8.18	9.49
CVS2-75	98	5	7.92	8.62	7.78	(f)	8.63	5.82	9.12
CVS2-76	99	5	20.22	26.53	23.65	(f)	27.32	19.71	10.70
CVS2-77	100	5	26.54	49.58	43.01	(f)	45.30	13.14	11.17
CVS2-78	101	5	20.41	32.15	27.94	(f)	31.00	10.15	9.15

(a) Release rates normalized using as-batched compositions in Table 4.15.

(b) The numbers in parentheses represent replicate sets of glasses.

(c) ID# is a consecutive integer numbering of all CVS glasses.

(d) PS is the plotting symbol used in plots associated with this data: 1 = CVS-I boundary, 2 = CVS-II Phase 1 interior, 3 = CVS-II Phase 2a boundary, 4 = CVS-II Phase 2b interior, 5 = CVS-II Phase 3 boundary, 6 = CVS-II Phase 4 one-component-at-a-time, M = middle compositions, 0 = other than NCAW waste glasses, A = EA glass.

(f) Mo release was not measured during CVS-II.

(h) Cs release was not measured for some CVS-II Phase 3 glasses.

TABLE 12.1. Si, B, Li, Na, Mo, and Cs Normalized Releases and Solution pHs Averaged Over Duplicate 28-day MCC-1 Dissolution Tests of CVS-I and CVS-II Glasses (continued)

Glass [b]	ID[c] #	PS[d]	Averaged 28-day MCC-1 Normalized Elemental Releases (g/m²)[a] Si	B	Li	Mo	Na	Cs	pH
CVS2-79	102	5	23.40	32.15	29.32	(f)	31.00	12.26	8.84
CVS2-80	103	5	26.10	45.22	39.10	(f)	43.12	15.08	9.10
CVS2-81	104	5	48.56	107.18	89.09	(f)	97.16	39.62	11.60
CVS2-82	105	5	362.48	643.09	506.91	(f)	591.49	87.72	11.79
CVS2-83	106	5	29.00	37.19	33.84	(f)	37.81	28.47	10.72
CVS2-84	107	5	22.78	30.01	26.11	(f)	29.95	18.53	10.76
CVS2-85	108	5	15.30	18.49	15.98	(f)	19.10	17.08	10.45
CVS2-86	109	5	7.18	8.30	7.90	(f)	8.61	7.22	9.53
CVS2-87	110	5	7.72	9.44	8.66	(f)	9.73	7.88	9.58
CVS2-88	111	5	6.97	9.11	8.29	(f)	9.51	7.49	10.06
CVS2-89	112	5	21.12	38.44	34.41	(f)	37.82	19.81	10.04
CVS2-90	113	5	26.14	29.14	25.96	(f)	29.84	14.09	9.56
CVS2-91	114	5	26.33	44.21	38.71	(f)	43.64	12.70	9.12
CVS2-92	115	5	20.64	86.42	70.66	(f)	72.78	5.48	10.56
CVS2-93	116	5	97.13	216.45	176.66	(f)	194.94	48.18	10.89
CVS2-94 (i)	117	5	44.68	87.42	77.68	(f)	84.23	15.28	10.74
CVS2-95 (7)	118	A	34.48	49.16	40.95	(f)	46.78	0.00	10.26
CVS2-96 (1)	119	M	8.90	12.53	11.16	(f)	12.63	8.90	9.57
CVS2-97 (5)	120	M	10.43	12.89	10.95	(f)	13.13	10.58	9.49
CVS2-98 (6)	121	5	13.23	30.44	27.68	(f)	25.94	1.78	10.08
CVS2-99	122	5	10.06	13.94	11.78	(f)	12.44	(h)	9.48
CVS2-100	123	5	10.03	14.12	11.91	(f)	12.49	(h)	9.62
CVS2-101(7)	124	A	48.20	90.76	76.62	(f)	79.44	(h)	10.64

(a) Release rates normalized using as-batched compositions in Table 4.15.

(b) The numbers in parentheses represent replicate sets of glasses.

(c) ID# is a consecutive integer numbering of all CVS glasses.

(d) PS is the plotting symbol used in plots associated with this data: 1 = CVS-I boundary, 2 = CVS-II Phase 1 interior, 3 = CVS-II Phase 2a boundary, 4 = CVS-II Phase 2b interior, 5 = CVS-II Phase 3 boundary, 6 = CVS-II Phase 4 one-component-at-a-time, M = middle compositions, O = other than NCAW waste glasses, A = EA glass.

(f) Mo release was not measured during CVS-II.

(h) Cs release was not measured for some CVS-II Phase 3 glasses.

(i) The duplicate results used to obtain the average releases were quite different (see Table D.1 in Appendix D).

TABLE 12.1. Si, B, Li, Na, Mo, and Cs Normalized Releases and Solution pHs Averaged Over Duplicate 28-day MCC-1 Dissolution Tests of CVS-I and CVS-II Glasses (continued)

Glass [b]	ID[c] #	PS[d]	Averaged 28-day MCC-1 Normalized Elemental Releases (g/m²)[a] Si	B	Li	Mo	Na	Cs	pH
CVS2-102(4)	125	M	15.37	19.24	17.49	(f)	17.37	(j)	9.54
CVS2-103	126	6	25.80	52.91	49.70	(f)	45.77	(j)	10.22
CVS2-104	127	6	20.18	30.97	28.34	(f)	27.83	(j)	9.87
CVS2-105	128	6	17.01	22.67	20.88	(f)	20.73	(j)	9.68
CVS2-106	129	6	11.06	13.38	12.71	(f)	12.43	(j)	9.37
CVS2-107	130	6	10.15	12.54	11.89	(f)	11.28	(j)	9.56
CVS2-108	131	6	23.74	22.73	28.03	(f)	28.05	(j)	9.47
CVS2-109	132	6	46.88	90.95	83.45	(f)	76.36	(j)	9.40
CVS2-110	133	6	8.58	10.13	9.39	(f)	9.30	(j)	9.08
CVS2-111	134	6	20.21	25.97	24.26	(f)	23.81	(j)	9.87
CVS2-112	135	6	53.14	98.26	89.08	(f)	80.86	(j)	10.76
CVS2-113	136	6	10.48	12.77	11.08	(f)	11.54	(j)	9.18
CVS2-114	137	6	21.05	20.33	20.07	(f)	19.75	(j)	9.86
CVS2-115	138	6	22.31	29.40	26.27	(f)	26.04	(j)	10.05
CVS2-116	139	6	14.75	19.77	17.68	(f)	17.58	(j)	9.57
CVS2-117	140	6	16.23	19.99	18.21	(f)	18.41	(j)	9.56
CVS2-118	141	6	15.55	20.39	18.21	(f)	18.79	(j)	9.59
CVS2-119	142	6	38.60	56.67	50.12	(f)	49.14	(j)	9.76
CVS2-120	143	6	11.08	13.51	12.37	(f)	12.26	(j)	9.45
CVS2-121	144	6	8.45	10.11	9.01	(f)	9.18	(j)	9.24
CVS2-122	145	6	7.80	9.31	8.58	(f)	8.19	(j)	8.93
CVS2-123(5)	146	M	12.43	15.65	13.55	(f)	14.92	(j)	9.50

(a) Release rates normalized using as-batched compositions in Table 4.15.

(b) The numbers in parentheses represent replicate sets of glasses.

(c) ID# is a consecutive integer numbering of all CVS glasses.

(d) PS is the plotting symbol used in plots associated with this data: 1 = CVS-I boundary, 2 = CVS-II Phase 1 interior, 3 = CVS-II Phase 2a boundary, 4 = CVS-II Phase 2b interior, 5 = CVS-II Phase 3 boundary, 6 = CVS-II Phase 4 one-component-at-a-time, M = middle compositions, 0 = other than NCAW waste glasses, A = EA glass.

(f) Mo release was not measured during CVS-II.

(j) Cs release was not measured for CVS-II Phase 4 glasses.

First-order mixture models of the form (6.1) using mass and mole fractions were fitted to the natural logs of the averaged Si, B, Li, and Na, elemental MCC-1 releases from Table 12.1 using the as-batched compositions from Table 4.15. The data for CVS-I and CVS-II Phases 1, 2, and 3 glasses (ID#s 1 through 124) were used. The first-order mixture models were also refitted after deleting the data points corresponding to glasses CVS1-4, CVS1-6, CVS1-9, CVS1-13, CVS1-15, CVS1-21, and CVS2-82 (which have the seven highest B releases). These seven data points were considered anomalous and are discussed in Section 12.11.4.5. These seven data points had strong influences on fitted first-order models, causing them to overpredict lower releases for which good predictive ability is desired. Glass CVS1-12 had moderately high B release similar to that of CVS1-6, but it agreed well with fitted models, so it was not deleted. The CVS-I test matrix consisted mainly of glasses at the vertices of the composition experimental region defined in Table 4.2. The fact that vertices have many components simultaneously at extreme values of their ranges is probably why several of the CVS-I glasses exhibited high elemental releases. High releases are likely due to nonlinear or interactive effects of components, which first-order models can't address. Constraints to avoid glasses with very high releases were added in subsequent phases of the CVS. Additional discussions of high-release glasses are given in Section 12.11.3 and Section 12.11.4.5.

The coefficients and R^2 statistics for the first-order models fitted to the full and reduced sets of data for both mass and mole fractions are given in Tables 12.2a and 12.2b (for the full data set) and 12.3a and 12.3b (for the reduced data set). Focusing on the models for MCC-1 B release, the R^2 statistics for the full data set model using mass fractions are $R^2 = 0.6683$, $R^2(ADJ) = 0.6414$, and $R^2(PRESS) = 0.5853$, while for the full data set model using mole fractions they are $R^2 = 0.6633$, $R^2(ADJ) = 0.6359$, and $R^2(PRESS) = 0.5828$. The R^2 statistics for the reduced data set model using mass fractions are $R^2 = 0.6520$, $R^2(ADJ) = 0.6219$, and $R^2(PRESS) = 0.5701$, while for the reduced data set model using mole fractions they are $R^2 = 0.6591$, $R^2(ADJ) = 0.6296$, and $R^2(PRESS) = 0.5800$. Note there is little difference between the R^2 values for the mass and mole fraction models for either the full or reduced data sets. Because the total sum of squares for the full and reduced data

TABLE 12.2a. Coefficients and Goodness-of-Fit Statistics for First-Order Mixture Models (Using Component Mass Fractions) Fitted to Natural Logarithms of Averaged 28-Day MCC-1 Normalized Elemental Releases (g/m^2) for CVS-I and CVS-II Phase 1, 2, and 3 Glasses

Component	MCC-1 Si	MCC-1 B	MCC-1 Li	MCC-1 Na
SiO_2	1.5252	0.7520	0.6351	0.8122
B_2O_3	8.3034	11.7667	11.5572	11.6800
Na_2O	8.6025	11.2400	10.9281	10.6536
Li_2O	10.9643	12.7971	11.4779	13.0459
CaO	1.1008	2.5548	3.5185	2.4552
MgO	3.8410	7.9369	7.7192	7.7582
Fe_2O_3	1.2457	1.3389	1.6427	1.4738
Al_2O_3	-8.9277	-11.8976	-11.3414	-11.5527
ZrO_2	-5.6850	-5.2635	-4.9116	-5.4273
Others	0.1499	1.3988	1.7904	1.0045
# points[a]	121	121	121	121
R^2[b]	0.6254	0.6683	0.6586	0.6701
R^2(ADJ)[b]	0.5950	0.6414	0.6309	0.6434
R^2(PRESS)[b]	0.5275	0.5853	0.5733	0.5864
LOF?[c]	Yes (>99%)	Yes (>99%)	Yes (>99%)	Yes (>99%)

(a) Data for only 121 of the 124 CVS-I and CVS-II Phase 1, 2, and 3 glasses in Table 12.1 were used in fitting the MCC-1 normalized elemental release models because MCC-1 tests were not performed on the radioactive glasses CVS2-53 and CVS2-54 and because the data for CVS2-101 was not available at the time these models were fitted.

(b) R^2, R^2(ADJ), and R^2(PRESS) statistics take values between 0.0 and 1.0, and provide different measures of the proportion of variation in the property data accounted for by a fitted model. See Section 6.1.5 for the definitions of these statistics.

(c) A statistical F-test for lack-of-fit (LOF) was performed using the estimates of experimental variation obtained from four replicate tests. "Yes" and "No" entries indicate whether the LOF was statistically significant at a 90% confidence level. The actual confidence level at which a LOF can be declared significant is given in parentheses following the "Yes" or "No" for each model.

TABLE 12.2b. Coefficients and Goodness-of-Fit Statistics for First-Order Mixture Models (Using Component Mole Fractions) Fitted to Natural Logarithms of Averaged 28-Day MCC-1 Normalized Elemental Releases (g/m^2) for CVS-I and CVS-II Phase 1, 2, and 3 Glasses

Component	MCC-1 Si	MCC-1 B	MCC-1 Li	MCC-1 Na
SiO_2	1.5954	0.9013	0.7965	0.9632
B_2O_3	8.7819	12.5175	12.2892	12.4212
Na_2O	8.3887	10.9915	10.6869	10.3939
Li_2O	6.4309	7.4954	6.8492	7.6055
CaO	1.3782	2.6799	3.4971	2.5918
MgO	3.4988	6.2731	6.0933	6.1539
Fe_2O_3	-0.8377	-1.2628	-0.4263	-0.8911
Al_2O_3	-15.7455	-20.7918	-19.8778	-20.2107
ZrO_2	-13.2679	-12.9492	-12.2151	-13.2367
Others	-3.4440	-0.9782	-0.0682	-2.0502
# points[a]	121	121	121	121
R^2[b]	0.6147	0.6633	0.6535	0.6646
R^2(ADJ)[b]	0.5835	0.6359	0.6254	0.6374
R^2(PRESS)[b]	0.5186	0.5828	0.5708	0.5831
LOF?[c]	Yes (>99%)	Yes (>99%)	Yes (>99%)	Yes (>99%)

(a) Data for only 121 of the 124 CVS-I and CVS-II Phase 1, 2, and 3 glasses in Table 12.1 were used in fitting the MCC-1 normalized elemental release models because MCC-1 tests were not performed on the radioactive glasses CVS2-53 and CVS2-54 and because the data for CVS2-101 was not available at the time these models were fitted.

(b) R^2, R^2(ADJ), and R^2(PRESS) statistics take values between 0.0 and 1.0, and provide different measures of the proportion of variation in the property data accounted for by a fitted model. See Section 6.1.5 for the definitions of these statistics.

(c) A statistical F-test for lack-of-fit (LOF) was performed using the estimates of experimental variation obtained from four replicate tests. "Yes" and "No" entries indicate whether the LOF was statistically significant at a 90% confidence level. The actual confidence level at which a LOF can be declared significant is given in parentheses following the "Yes" or "No" for each model.

TABLE 12.3a. Coefficients and Goodness-of-Fit Statistics for First-Order Mixture Models (Using Component Mass Fractions) Fitted to Natural Logarithms of Averaged 28-Day MCC-1 Normalized Elemental Releases (g/m²) for CVS-I and CVS-II Phase 1, 2, and 3 Glasses After Deleting the High Release Data Corresponding to Glasses CVS1-4,6,9,13,15,21 and CVS2-82

Component	MCC-1 Si	MCC-1 B	MCC-1 Li	MCC-1 Na
SiO_2	0.9025	-0.0993	-0.2319	-0.0587
B_2O_3	6.8360	9.6800	9.4346	9.6671
Na_2O	7.1851	9.5454	9.1998	8.9623
Li_2O	9.6783	11.8108	10.5425	12.2173
CaO	2.0185	3.7572	4.7685	3.6144
MgO	1.8500	5.1079	4.9844	5.0078
Fe_2O_3	4.6516	5.7008	6.0434	5.7557
Al_2O_3	-4.6186	-6.2911	-5.6794	-6.0434
ZrO_2	-2.1819	-0.6283	-0.2328	-0.7562
Others	1.9548	3.6529	4.1125	3.4126
# points[a]	114	114	114	114
R^2[b]	0.5996	0.6520	0.6525	0.6532
R^2(ADJ)[b]	0.5650	0.6219	0.6224	0.6232
R^2(PRESS)[b]	0.4960	0.5701	0.5727	0.5702
LOF?[c]	Yes (>99%)	Yes (>99%)	Yes (>99%)	Yes (>99%)

(a) Data for only 114 of the 124 CVS-I and CVS-II Phase 1, 2, and 3 glasses listed in Table 12.1 were used in fitting the MCC-1 normalized elemental release models because: (i) the seven highest-release glasses CVS1-4, 6,9,13,15,21 and CVS2-82 were omitted, (ii) MCC-1 tests were not performed on the radioactive glasses CVS2-53 and CVS2-54, and (iii) CVS2-101 was not part of the data set at the time these models were fitted.

(b) R^2, R^2(ADJ), and R^2(PRESS) statistics take values between 0.0 and 1.0, and provide different measures of the proportion of variation in the property data accounted for by a fitted model. See Section 6.1.5 for the definitions of these statistics.

(c) A statistical F-test for lack-of-fit (LOF) was performed using the estimates of experimental variation obtained from four replicate tests. "Yes" and "No" entries indicate whether the LOF was statistically significant at a 90% confidence level. The actual confidence level at which a LOF can be declared significant is given in parentheses following the "Yes" or "No" for each model.

TABLE 12.3b. Coefficients and Goodness-of-Fit Statistics for First-Order Mixture Models (Using Component Mole Fractions) Fitted to Natural Logarithms of Averaged 28-Day MCC-1 Normalized Elemental Releases (g/m²) for CVS-I and CVS-II Phase 1, 2, and 3 Glasses After Deleting the High Release Data Corresponding to Glasses CVS1-4,6,9,13,15,21 and CVS2-82

Component	MCC-1 Si	MCC-1 B	MCC-1 Li	MCC-1 Na
SiO_2	0.9838	0.0695	-0.0410	0.1138
B_2O_3	7.2136	10.3037	10.0370	10.2930
Na_2O	7.0527	9.3841	9.0584	8.7928
Li_2O	5.8360	7.0087	6.3874	7.1971
CaO	2.1229	3.6507	4.5082	3.5286
MgO	2.1698	4.3944	4.2783	4.3325
Fe_2O_3	7.8481	9.9125	10.7650	10.0591
Al_2O_3	-8.8615	-11.8231	-10.8682	-11.4100
ZrO_2	-6.3643	-3.8095	-3.0536	-4.0341
Others	1.2613	4.9512	5.9449	4.2410
# points[a]	114	114	114	114
R^2[b]	0.6033	0.6591	0.6576	0.6593
R^2(ADJ)[b]	0.5690	0.6296	0.6280	0.6298
R^2(PRESS)[b]	0.4997	0.5800	0.5799	0.5785
LOF?[c]	Yes (>99%)	Yes (>99%)	Yes (>99%)	Yes (>99%)

(a) Data for only 114 of the 124 CVS-I and CVS-II Phase 1, 2, and 3 glasses listed in Table 12.1 were used in fitting the MCC-1 normalized elemental release models because: (i) the seven highest-release glasses CVS1-4, 6,9,13,15,21 and CVS2-82 were omitted, (ii) MCC-1 tests were not performed on the radioactive glasses CVS2-53 and CVS2-54, and (iii) CVS2-101 was not part of the data set at the time these models were fitted.

(b) R^2, R^2(ADJ), and R^2(PRESS) statistics take values between 0.0 and 1.0, and provide different measures of the proportion of variation in the property data accounted for by a fitted model. See Section 6.1.5 for the definitions of these statistics.

(c) A statistical F-test for lack-of-fit (LOF) was performed using the estimates of experimental variation obtained from four replicate tests. "Yes" and "No" entries indicate whether the LOF was statistically significant at a 90% confidence level. The actual confidence level at which a LOF can be declared significant is given in parentheses following the "Yes" or "No" for each model.

sets are quite different, it is not appropriate to compare the R^2 statistics for models fit to the two data sets.

The general indication from the R^2 statistics in Tables 12.2 and 12.3 is that the first-order mixture models provide some predictive ability, but leave considerable room for improvement. The plots of predicted versus measured MCC-1 B release values in Figures 12.1a (mass fraction model) and 12.1b (mole fraction model) for the full data set and in Figures 12.2a (mass fraction model) and 12.2b (mole fraction model) for the reduced data set confirm that there is room for improvement on the first-order models. These figures show that the first-order models have a tendency to underpredict larger MCC-1 B releases and overpredict smaller MCC-1 B releases. A statistical test for model lack-of-fit (LOF) (see Section 6.1.5) indicated that first-order mixture models (using mass and mole fractions) fitted to both the full and reduced data sets have statistically significant LOFs at greater than 99% confidence.

The component effects plot for the first-order mixture model using mass fractions fitted to MCC-1 normalized B releases for the reduced set of data is shown in Figure 12.3. Only the single-component constraints and not the stand-in crystallinity constraints in Tables 4.2 and 4.6 were used to limit the effects plot (both were used in previous effects plots). As a result, effects are evaluated over wider ranges than in the past for several components involved in the stand-in constraints (most notably Al_2O_3 and SiO_2). MCC-1 B release of HW-39-4 glass is predicted to be increased the most by Li_2O, B_2O_3, and Na_2O. Al_2O_3 and SiO_2 are predicted to decrease B release of HW-39-4 glass the most, while ZrO_2 is predicted to decrease it to a lesser degree. Fe_2O_3 may mildly increase B release of HW-39-4 glass, although this effect is questionable due to the uncertainty in the fitted first-order model.

12.2 INVESTIGATION OF POTENTIAL BIASES IN MCC-1 RELEASE DATA DUE TO CVS PHASES

As discussed in Section 6.1.1, a model of the form (6.3) was fitted to the Si, B, Li, and Na normalized MCC-1 release data for CVS-I and CVS-II Phases 1, 2, and 3 to ascertain whether any biases (block effects) are present in the data because of performing the CVS in phases.

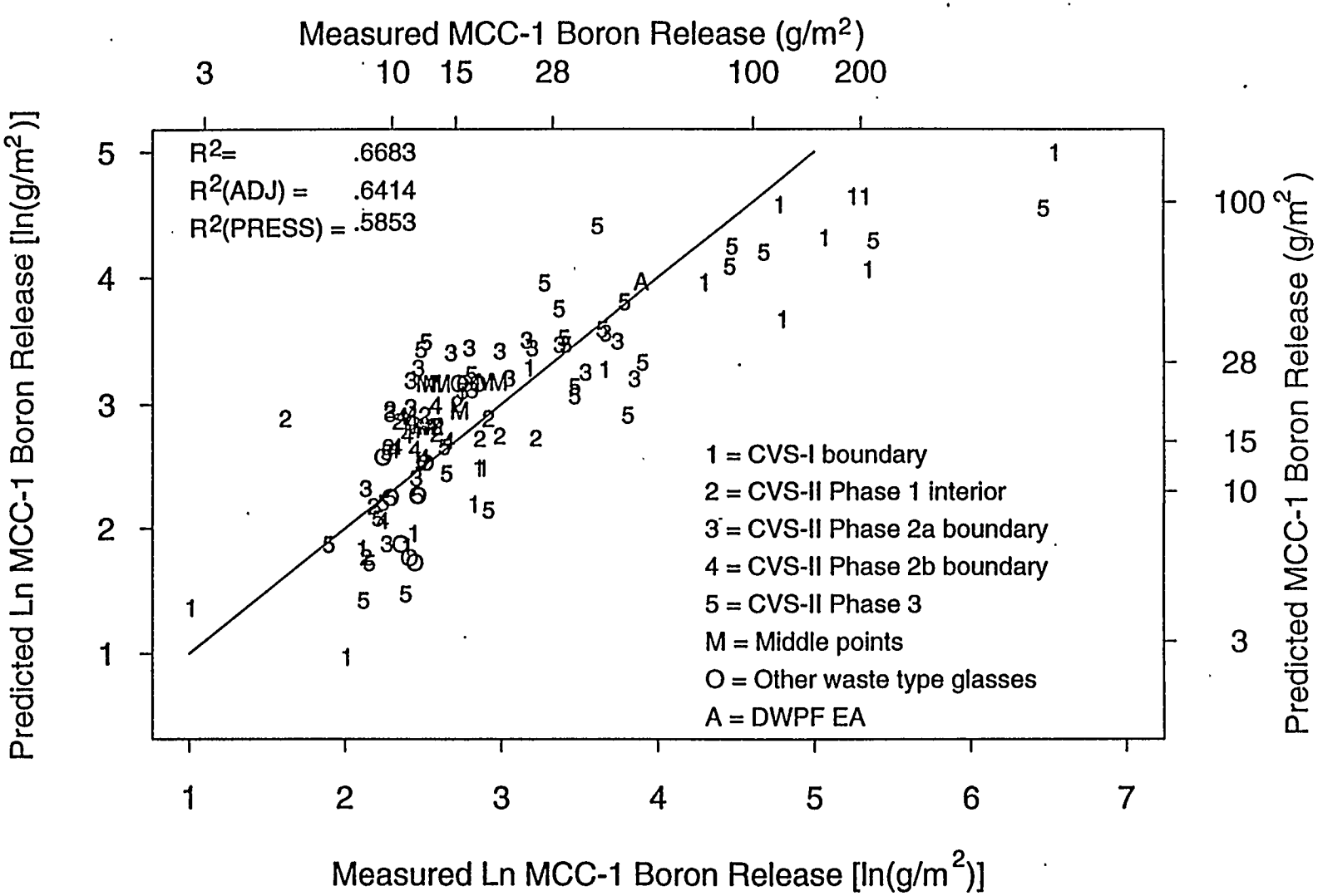

FIGURE 12.1a. Predicted Versus Measured MCC-1 B Release for the First-Order Mixture Model Using Mass Fractions Fitted to the Full Data Set (from Table 12.2a)

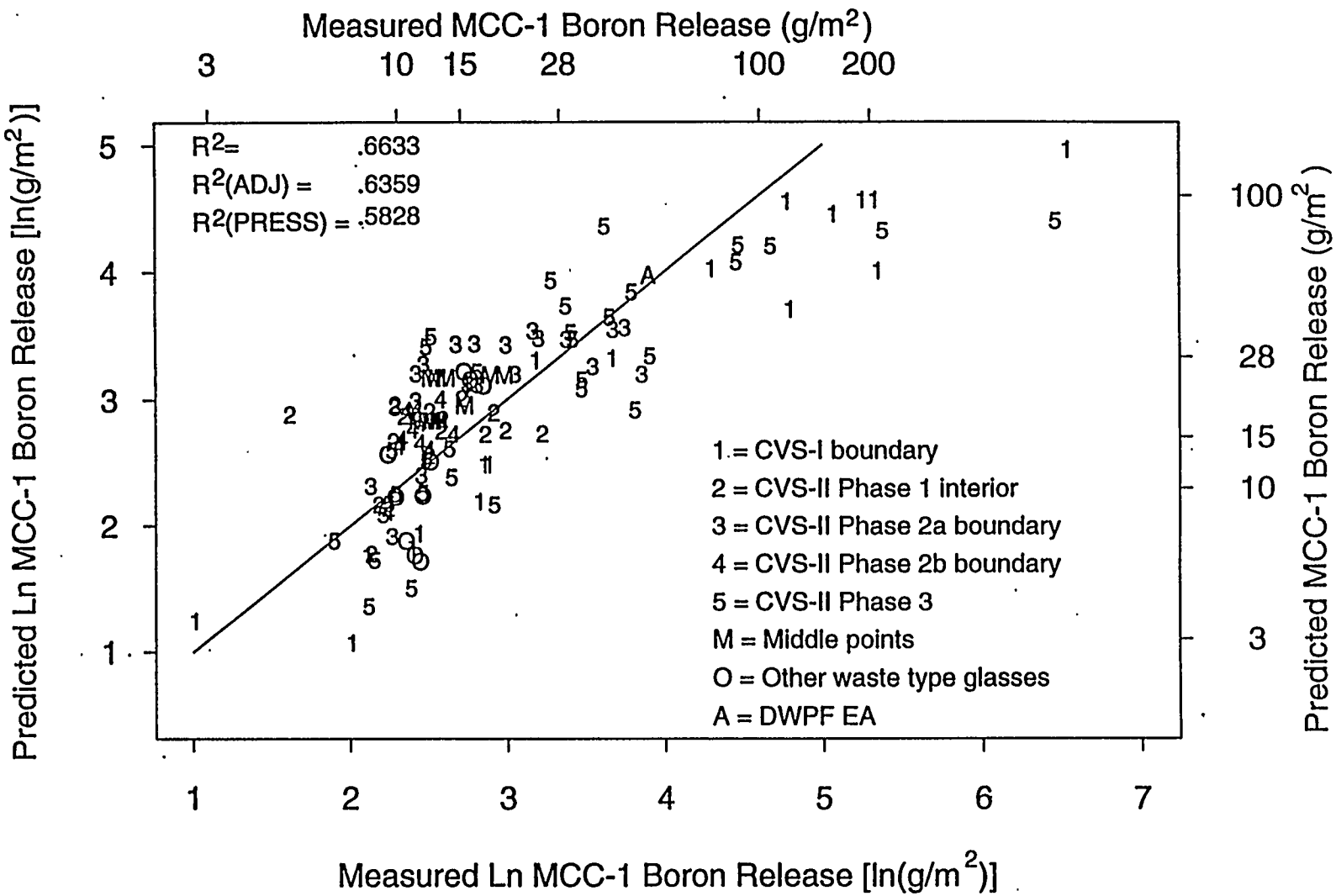

FIGURE 12.1b. Predicted Versus Measured MCC-1 B Release for the First-Order Mixture Model Using Mole Fractions Fitted to the Full Data Set (from Table 12.2b)

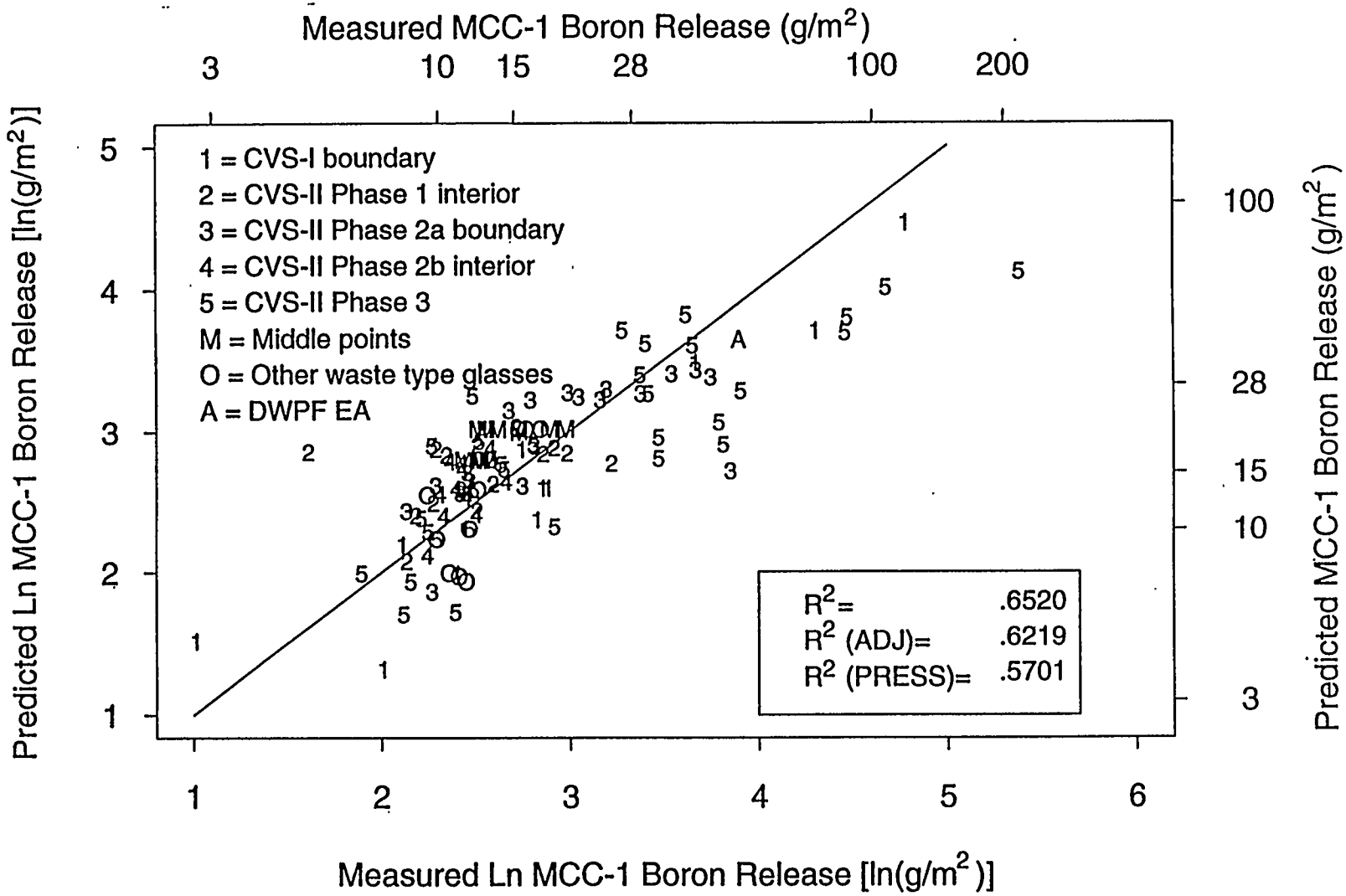

FIGURE 12.2a. Predicted Versus Measured MCC-1 B Release for the First-Order Mixture Model Using Mass Fractions Fitted to the Reduced Data Set (from Table 12.3a)

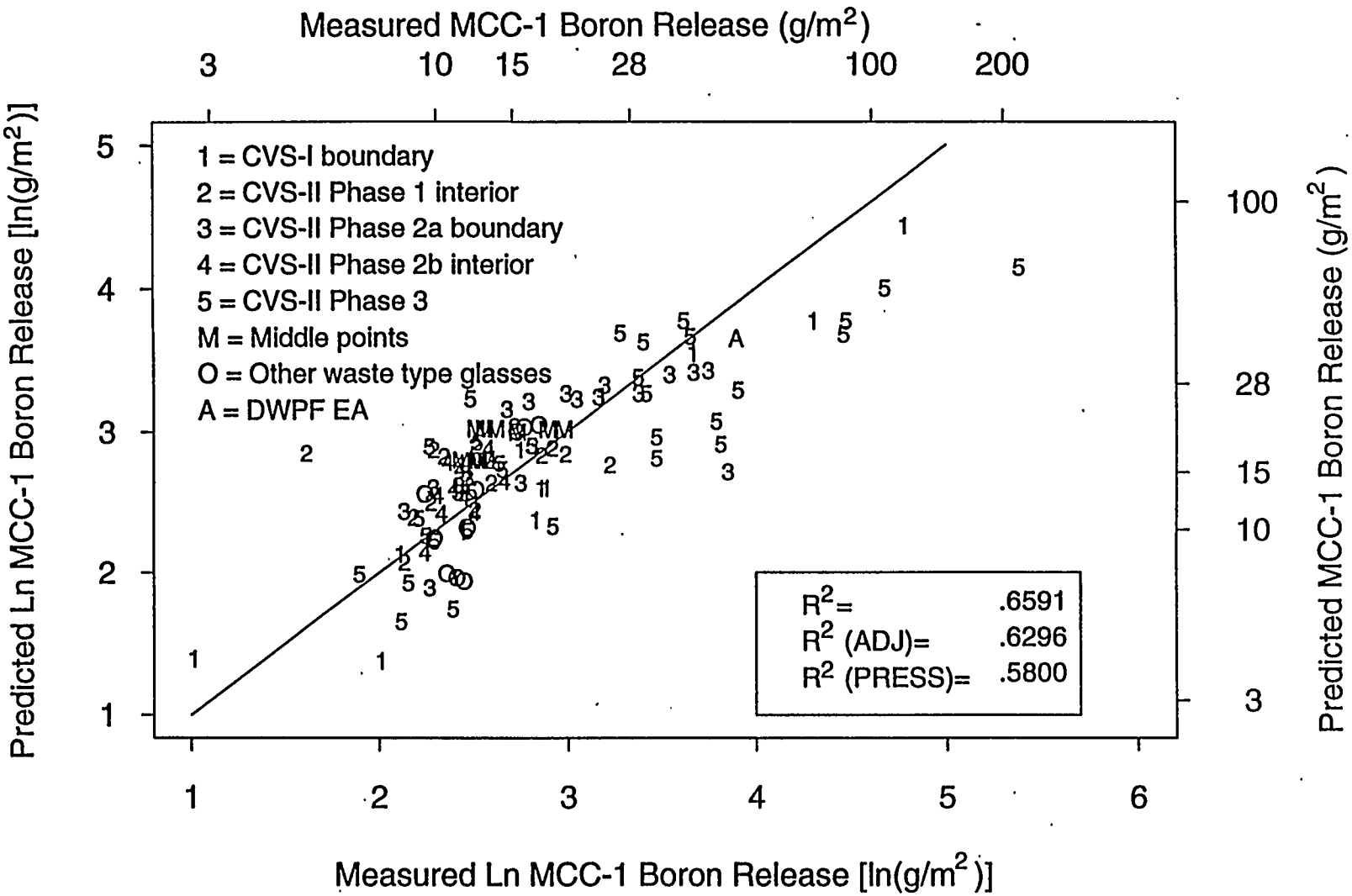

FIGURE 12.2b. Predicted Versus Measured MCC-1 B Release for the First-Order Mixture Model Using Mole Fractions Fitted to the Reduced Data Set (from Table 12.3b)

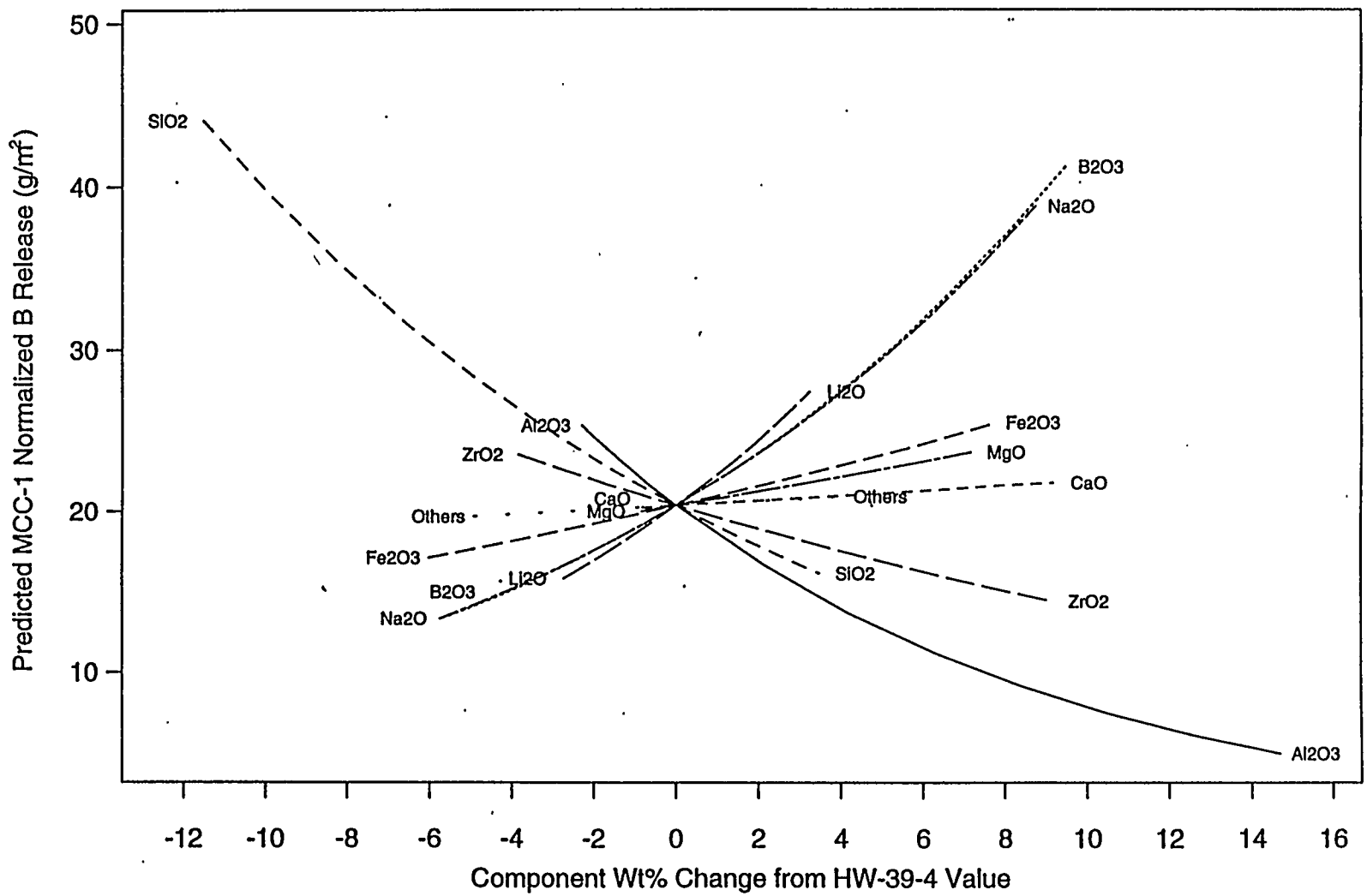

FIGURE 12.3. Predicted Component Effects on MCC-1 B Release Relative to the HW-39-4 Composition, Based on the First-Order Mixture Model Using Mass Fractions Fitted to the Reduced Data Set (in Column 3 of Table 12.3a)

The mass fraction versions of (6.3) fitted to the full data set yielded $R^2 = 0.7015$ for Si, $R^2 = 0.7473$ for B, $R^2 = 0.7465$ for Li, and $R^2 = 0.7561$ for Na. These values can be compared to the corresponding values (from Table 12.2a) for the first-order mass fraction models (6.1) without the block effect terms, which were $R^2 = 0.6254$ for Si, $R^2 = 0.6683$ for B, $R^2 = 0.6586$ for Li, and $R^2 = 0.6701$ for Na. Thus, the block effect terms improved the R^2 values by about 0.08, a substantial although not monumental improvement. The mole fraction version of (6.3) fitted to the full data set and the mass fraction version of (6.3) fitted to the reduced data set yielded similar R^2 values.

Several statistically significant block effects were detected for both mass and mole fraction versions of the model (6.3) for Si, B, Li, and Na normalized MCC-1 releases. CVS-I was found to have a positive block effect (increased releases) for all four elements. This could be due to all CVS-I normalized releases being biased high, or to the large-release data points in CVS-I. CVS-II Phase 1 was found to have a negative block effect (decreased releases) for B and Na, while CVS-II Phase 2 was found to have a negative block effect (decreased releases) for all four elements. The same results were obtained for the mass fraction model fitted to the reduced data set. These results could be because the normalized release values were biased low for all or a substantial portion of the glasses in the respective CVS phases. Alternatively, the results could be because a reduced subregion of the full CVS composition region was explored for CVS-II Phase 1, and that compositions with restricted ranges of releases were investigated in CVS-II Phases 1 and 2 (see Table 4.6). Finally, CVS-II Phase 3 was found to have a positive block effect (increased releases) for Si release (B and Na also had indications of block effects, although they were only significant at about the 85-88% confidence level). When the mass fraction model was fitted to the reduced data set, CVS-II Phase 3 was found to have a positive block effect (increased releases) for all elements. These results could be because the normalized release values were biased high for all or a substantial portion of the glasses in CVS-II Phase 3. Alternatively, they could be because new, more extreme portions of composition space with larger release values were explored for CVS-II Phase 3 (see Section 4.5). Data for replicate glasses in Table F.3 in Appendix F do not provide strong support for the "biased data" hypotheses.

Because of the uncertainty as to whether the statistically significant block (CVS phase) effects detected for MCC-1 normalized release data are due to biased data or merely differences in how each phase was designed, it was decided not to try to adjust the data and refit models.

12.3 SECOND-ORDER MODELS FOR MCC-1 RELEASES

Three candidate Scheffé second-order mixture models (using mass fractions of the component oxides) for each of B, Si, Li, and Na normalized MCC-1 releases fitted to the reduced set of data (the CVS-I and CVS-II Phase 1, 2, and 3 data points in Table 12.1 minus the data for CVS1-4,6,9,13,15,21 and CVS2-82 and CVS2-101) are given in Tables 12.4 to 12.7. These models consist of the first-order mixture model terms and several second-order terms selected using statistical variable selection techniques (see Section 6.1.4). It was not necessary to apply the pseudocomponent transformation (see Section 6.1.3), so the usual glass oxide component mass fractions were used in fitting the models. The candidate sets of second-order mixture models in Tables 12.4 to 12.7 provide better fits than the corresponding "reduced data set" first-order mixture models, based on comparing the R^2 statistics in Tables 12.4 to 12.7 to those in Table 12.3a. Figure 12.4 displays the predicted versus measured MCC-1 B release values for the second-order mixture model #2 from Table 12.4. This figure still shows a tendency for the second-order model to underpredict larger B releases and overpredict smaller releases. Considerable scatter also is found in the middle of the range of B releases studied. Thus, considerable room for improvement in modeling MCC-1 normalized releases still appears to exist. LOF test results for the second-order models in Tables 12.4 through 12.7 confirm this.

12.4 VALIDATION OF FIRST- AND SECOND-ORDER MODELS FOR MCC-1 RELEASES

The CVS-II Phase 3 data were used to validate the first- and second-order Scheffé mixture models (based on mass fractions) for normalized MCC-1 B release developed using data up through CVS-II Phase 2. These models were reported in an earlier version of this report, but for convenience they are listed in Table 12.8. (Recall that validation involves using data not used to

TABLE 12.4. Candidate Scheffé Second-Order Models Using Mass Fractions for MCC-1 ln(Boron) Release Fitted to the Reduced Data Set

Model #1		Model #2		Model #3	
Terms	Coefficients	Terms	Coefficients	Terms	Coefficients
SiO2	-1.0431	SiO2	-1.5667	SiO2	-0.4642
B2O3	15.3309	B2O3	15.8843	B2O3	13.6642
Na2O	10.2358	Na2O	11.4422	Na2O	10.3786
Li2O	12.8952	Li2O	13.3587	Li2O	12.8656
CaO	-23.8810	CaO	-39.7866	CaO	4.1984
MgO	7.0291	MgO	13.6312	MgO	21.8462
Fe2O3	6.1197	Fe2O3	6.3236	Fe2O3	6.5020
Al2O3	-12.3180	Al2O3	-8.8417	Al2O3	-26.2208
ZrO2	-1.5048	ZrO2	-1.2666	ZrO2	-1.0044
Others	4.8330	Others	5.4600	Others	-12.7585
Al2O3 x Al2O3	81.9049	Al2O3 x Al2O3	69.0532	SiO2 x Al2O3	25.0721
B2O3 x Al2O3	-69.5330	B2O3 x Al2O3	-80.0411	B2O3 x Al2O3	-45.6289
SiO2 x CaO	56.8185	SiO2 x CaO	70.1922	MgO x MgO	-204.0895
		Na0 x MgO	-58.4244	Al2O3 x Al2O3	81.0670
		CaO x CaO	111.8019	Others x Others	164.9226
R^2	= .7878	R^2	= .8080	R^2	= .7913
R^2(ADJ)	= .7626	R^2(ADJ)	= .7808	R^2(ADJ)	= .7618
R^2(PRESS)	= .7281	R^2(PRESS)	= .7409	R^2(PRESS)	= .7104
LOF?[a]	Yes (>99%)		Yes (>99%)		Yes (>99%)

(a) A statistical F-test for lack-of-fit (LOF) was performed using the estimates of experimental variation obtained from four replicate tests. "Yes" and "No" entries indicate whether the LOF was statistically significant at a 90% confidence level. The actual confidence level at which a LOF can be declared significant is given in parentheses following the "Yes" or "No" for each model.

TABLE 12.5. Candidate Scheffé Second-Order Models Using Mass Fractions for MCC-1 ln(Silica) Release Fitted to the Reduced Data Set

Model #1		Model #2		Model #3	
Terms	Coefficients	Terms	Coefficients	Terms	Coefficients
SiO2	0.8109	SiO2	0.8096	SiO2	0.5715
B2O3	9.9358	B2O3	10.5784	B2O3	9.8100
Na2O	7.2742	Na2O	7.4819	Na2O	21.8997
Li2O	12.4018	Li2O	13.4812	Li2O	11.8732
CaO	1.6129	CaO	1.9270	CaO	-29.3913
MgO	2.8732	MgO	0.2600	MgO	27.0021
Fe2O3	3.5621	Fe2O3	0.2762	Fe2O3	-1.7298
Al2O3	-10.5311	Al2O3	-9.7530	Al2O3	-5.0812
ZrO2	-0.2189	ZrO2	-0.8051	ZrO2	-4.4873
Others	1.9029	Others	-0.2012	Others	-0.5063
Al2O x Al2O3	60.8662	Al2O3 x Al2O3	57.6366	Al2O3 x Al2O3	66.5894
B2O3 x Al2O3	-48.6020	B2O3 x Al2O3	-53.9386	B2O3 x Al2O3	-72.5241
Li2O x ZrO2	-75.0298	Li2O x ZrO2	-68.8168	SiO2 x Na2O	-23.4248
		MgO x Fe2O3	62.2353	SiO2 x CaO	60.1717
		Fe2O3 x Others	55.0261	B2O3 x CaO	44.4026
				Na2O x MgO	-109.6402
				Na2O x Al2O3	-36.7088
				Li2O x Cao	-88.0401
				Li2O x MgO	-250.5230
				Li2O x Fe2O3	58.4976
				Fe2O3 x Others	64.0741
R^2	= .7458	R^2	= .7747	R^2	= .8393
R^2(ADJ)	= .7156	R^2(ADJ)	= .7428	R^2(ADJ)	= .8047
R^2(PRESS)	= .6589	R^2(PRESS)	= .6833	R^2(PRESS)	= .7522

TABLE 12.6. Candidate Scheffé Second-Order Models Using Mass Fractions for MCC-1 ln(Lithium) Release Fitted to the Reduced Data Set

Model #1		Model #2		Model #3	
Terms	Coefficients	Terms	Coefficients	Terms	Coefficients
SiO2	-1.1528	SiO2	-1.6883	SiO2	-1.1150
B2O3	14.7349	B2O3	15.2981	B2O3	12.3492
Na2O	9.8519	Na2O	11.0969	Na2O	26.4194
Li2O	11.5657	Li2O	12.0219	Li2O	12.8982
CaO	-21.6299	CaO	-37.6365	CaO	-55.2341
MgO	6.7635	MgO	13.6295	MgO	32.3014
Fe2O3	6.4941	Fe2O3	6.7044	Fe2O3	4.3775
Al2O3	-10.9846	Al2O3	-7.4666	Al2O3	-26.4947
ZrO2	-0.9867	ZrO2	-0.7522	ZrO2	-1.1580
Others	5.2492	Others	5.8900	Others	3.9643
Al2O3 x Al2O3	74.9705	Al2O3 x Al2O3	62.1538	SiO2 x Na2O	-29.4838
SiO2 x CaO	54.2838	SiO2 x CaO	67.8571	SiO2 x CaO	86.5234
B2O3 x Al2O3	-65.0841	B2O3 x Al2O3	-75.9724	SiO2 x Al2O3	32.8964
		CaO x CaO	111.8127	B2O3 x Cao	49.9035
		Na2O x MgO	-60.8414	B2O3 x Al2O3	-51.7399
				Na2O x MgO	-107.9588
				Li2O x MgO	-126.7497
				Fe2O3 x Others	42.9904
				CaO x CaO	152.7413
				MgO x MgO	-99.0069
				Al2O3 x Al2O	63.1657
R^2	= .7747	R^2	= .7965	R^2	= .8352
R^2(ADJ)	= .7479	R^2(ADJ)	= .7677	R^2(ADJ)	= .7997
R^2(PRESS)	= .7137	R^2(PRESS)	= .7274	R^2(PRESS)	= .7424

TABLE 12.7. Candidate Scheffé Second-Order Models Using Mass Fractions for MCC-1 ln(Sodium) Release Fitted to the Reduced Data Set

Model #1		Model #2		Model #3	
Terms	Coefficients	Terms	Coefficients	Terms	Coefficients
SiO2	-0.9477	SiO2	-1.1037	SiO2	0.0250
B2O3	15.1851	B2O3	15.0355	B2O3	14.4120
Na2O	9.6350	Na2O	10.0800	Na2O	10.1378
Li2O	13.2710	Li2O	13.8558	Li2O	7.6326
CaO	-23.0024	CaO	-38.2146	CaO	-7.5924
MgO	6.9085	MgO	17.6842	MgO	21.2753
Fe2O3	6.1125	Fe2O3	6.0535	Fe2O3	4.8714
Al2O3	-12.2784	Al2O3	-11.1392	Al2O3	-11.5820
ZrO2	-1.6759	ZrO2	-1.5430	ZrO2	-1.2609
Others	4.5414	Others	4.4476	Others	-23.1645
Al2O3 x Al2O3	81.8311	SiO2 x CaO	62.6082	Al2O3 x Al2O3	81.3509
B2O3 x Al2O3	-67.9671	B2O3 x Al2O3	-63.3972	B2O3 x Al2O3	-62.2355
SiO2 x CaO	54.7095	CaO x Cao	135.5845	SiO2 x CaO	32.6569
		Mgo x Mgo	-142.7077	MgO x MgO	-206.5971
		Al2O3 x Al2O3	72.1920	Li2O x Others	130.6189
				Others x Others	189.2346
				Fe2O3 x Others	57.2294
				Na2O x CaO	-44.0500
R^2	= .7933	R^2	= .8124	R^2	= .8372
R^2(ADJ)	= .7687	R^2(ADJ)	= .7859	R^2(ADJ)	= .8083
R^2(PRESS)	= .73505	R^2(PRESS)	= .7527	R^2(PRESS)	= .7623

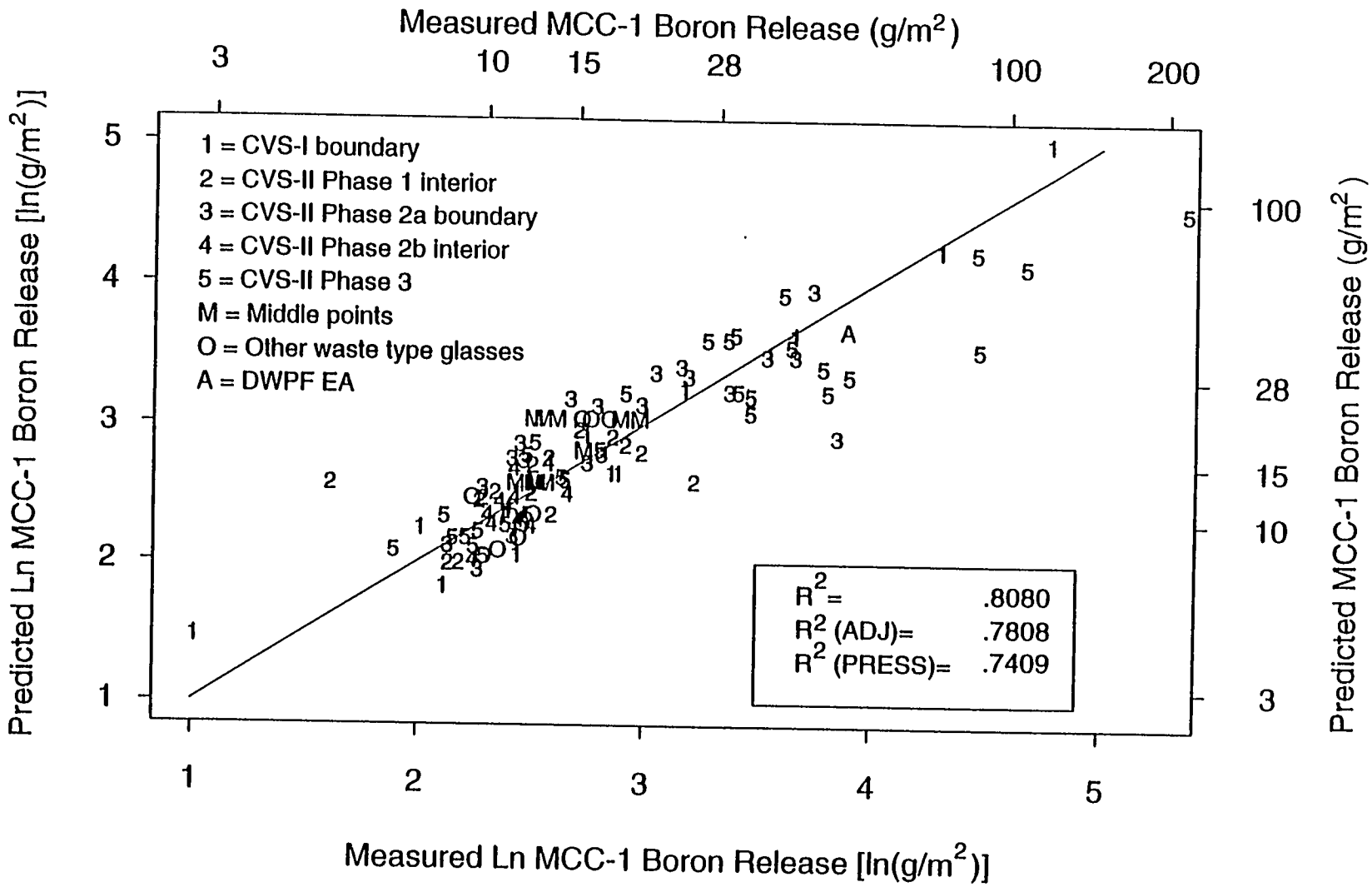

FIGURE 12.4. Predicted Versus Measured MCC-1 B Release for the Second-Order Mixture Model #2 Fitted to the Reduced Data Set (from Table 12.4)

TABLE 12.8. First-Order Model and Three Candidate Second-Order Models Using Mass Fractions for MCC-1 ln(Boron) Release Fitted to CVS-I and CVS-II Phase 1 and 2 Data Without High Release Data Points[a]

First-Order Model		Three Candidate Second-Order Models					
		Model #1		Model #2		Model #3	
Terms	Coefficients	Terms	Coefficients	Terms	Coefficients	Terms	Coefficients
SiO2	0.3406	SiO2	2.6055	SiO2	-1.5069	SiO2	3.4256
B2O3	8.9920	B2O3	-0.7681	B2O3	12.4247	B2O3	-5.5002
Na2O	9.0513	Na2O	27.8667	Na2O	11.9782	Na2O	26.0694
Li2O	9.1772	Li2O	7.3163	Li2O	-21.2031	Li2O	6.4803
CaO	7.3108	CaO	5.6589	CaO	8.9903	CaO	5.4435
MgO	6.2883	MgO	5.9660	MgO	9.8573	MgO	4.5177
Fe2O3	5.0714	Fe2O3	3.2967	Fe2O3	6.3714	Fe2O3	3.0065
Al2O3	-7.0336	Al2O3	-33.9815	Al2O3	-33.5161	Al2O3	-8.8350
ZrO2	-0.5414	ZrO2	-2.5321	ZrO2	0.1851	ZrO2	-2.3333
Others	0.4687	Others	0.0591	Others	2.5320	Others	-0.5088
		B2O3 x B2O3	41.9163	SiO2 x Al2O3	34.3108	B2O3 x B2O3	55.6853
		SiO2 x Na2O	-39.7479	SiO2 x Li2O	64.4461	SiO2 x Na2O	-38.8016
		SiO2 x Al2O3	35.3721	Al2O3 x Al2O3	77.3193		
		Al2O3 x Al2O3	57.5762				
R^2	= .7082	R^2	= .8197	R^2	= .7861	R^2	= .7799
R^2(ADJ)	= .6665	R^2(ADJ)	= .7800	R^2(ADJ)	= .7433	R^2(ADJ)	= .7402
R^2(PRESS)	= .5720	R^2(PRESS)	= .7081	R^2(PRESS)	= .6644	R^2(PRESS)	= .6614
LOF?[b]	Yes (>99%)		Yes (>99%)		Yes (>99%)		Yes (>99%)

(a) Glasses CVS1-4,6,9,13,15,21 had high MCC-1 releases and were deleted prior to fitting these models. MCC-1 testing was not performed on the radioactive glasses CVS2-53 and CVS2-54, so those glasses were also not used to fit the models.

(b) A statistical F-test for lack-of-fit (LOF) was performed using the estimates of experimental variation obtained from four replicate tests. "Yes" and "No" entries indicate whether the LOF was statistically significant at a 90% confidence level. The actual confidence level at which a LOF can be declared significant is given in parentheses following the "Yes" or "No" for each model.

fit the models to assess their predictive performance--see Section 6.1.6.) For other properties (viscosity, electrical conductivity, and transition temperature), historical data were also used to validate models. However, not enough time was available to do this using the historical MCC-1 data. The results of the validation investigation using CVS-II Phase 3 data follow.[a]

Figures 12.5, 12.6a, 12.6b, and 12.6c contain the validation results using the CVS-II Phase 3 data for the first-order and three candidate second-order mixture models (using mass fractions) for normalized PCT B release. These figures contain plots of the predicted versus measured MCC-1 B release values along with a superimposed 45° line that represents perfect prediction. The error bars on the plotted points represent 95% two-sided prediction intervals for the MCC-1 B release values. If the error bars for a given point overlap the 45° line, the model is validated for that point, in the sense that no statistically significant difference exists between the predicted and measured values after accounting for model and measurement uncertainties. Various plotting symbols are used in Figures 12.5, 12.6a, 12.6b, and 12.6c to identify the specific nature of some of the CVS-II Phase 3 points. Points that are not otherwise specifically identified are plotted with a "5" as the plotting symbol.

Figure 12.5 shows that the first-order MCC-1 B release model from Table 12.8 is not validated very well for the CVS-II Phase 3 data points, in spite of the wide error bars. The first-order model appears to underpredict larger values of MCC-1 B release (> 28 g/m^2) for the CVS-II Phase 3 data. The plot for the first-order MCC-1 B release model fitted to the full data set after CVS-II Phase 2 (not shown) was very similar. The poor predictive performance for the larger release values contributes to the rather poor R^2(VAL) = 0.3932 in Figure 12.5.

(a) It would also be possible to use CVS-II Phase 4 data to validate MCC-1 models developed from data up through CVS-II Phase 3. However, the CVS-II Phase 4 data were not available in time to include such validation work in the report.

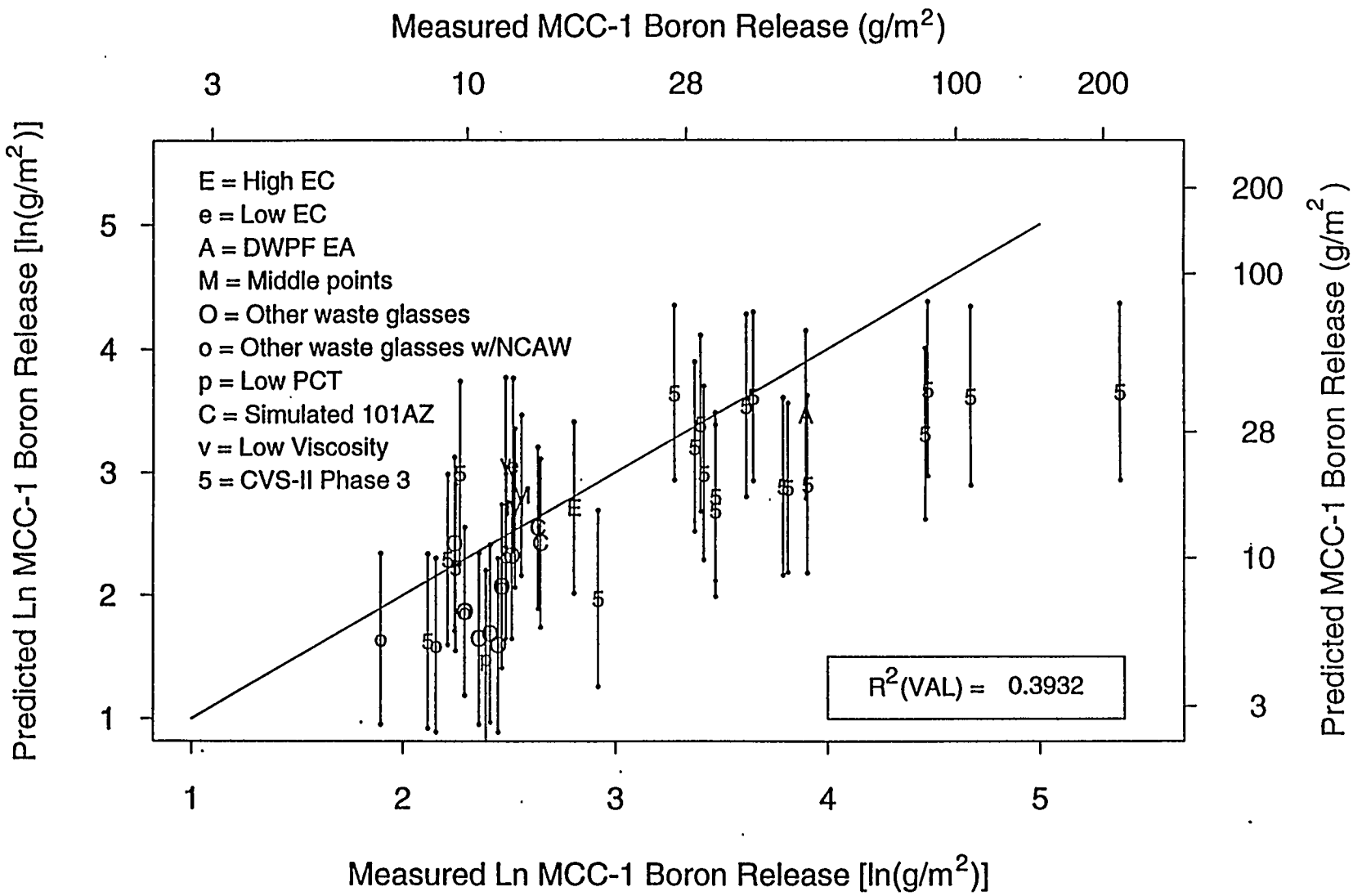

FIGURE 12.5. Predicted MCC-1 Boron Releases from the First-Order Mixture Model After CVS-II Phase 2 (from Table 12.8) Versus Measured MCC-1 Boron Releases (from Table 12.1) for the CVS-II Phase 3 Data

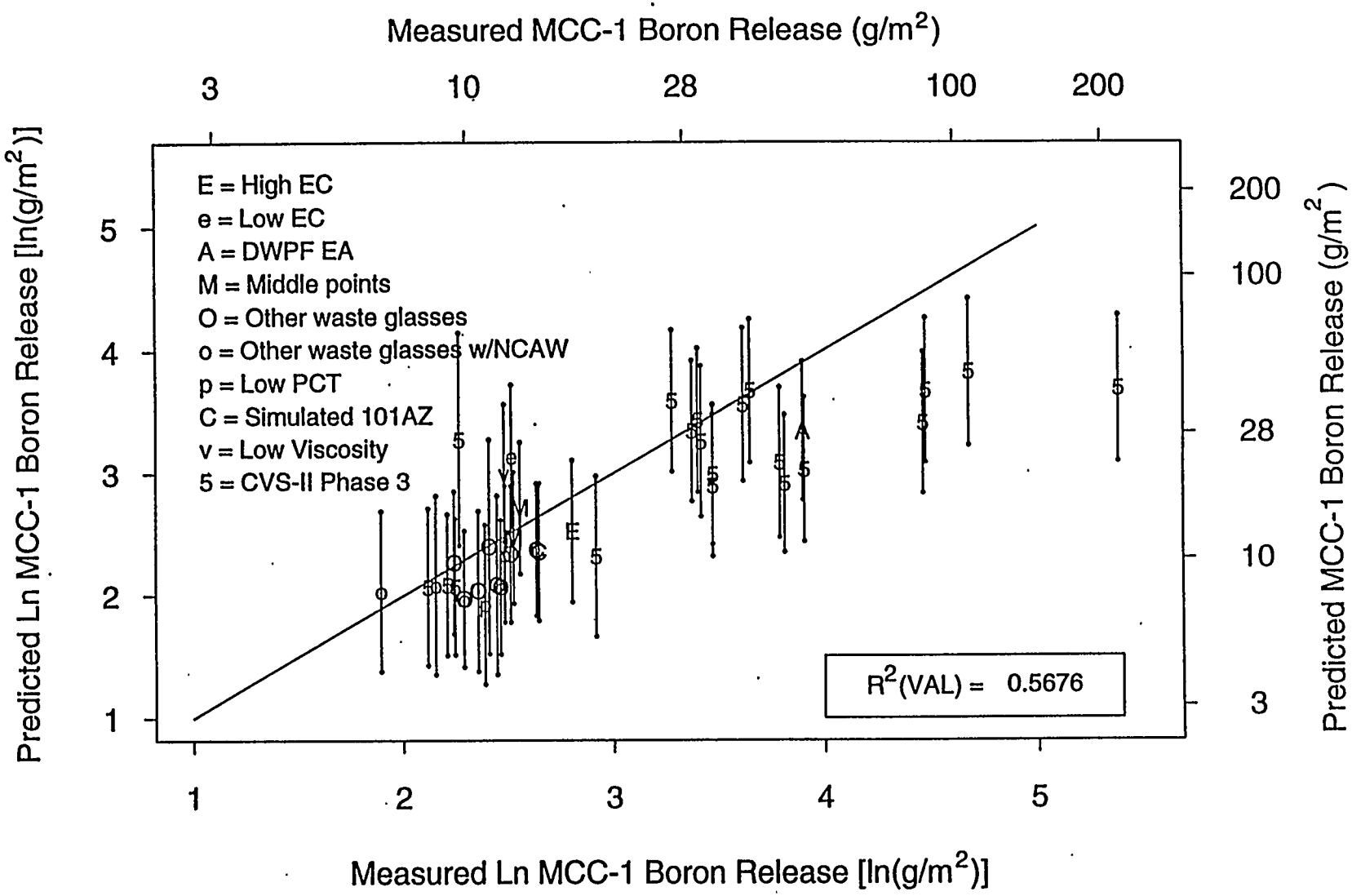

FIGURE 12.6a. Predicted MCC-1 Boron Releases from the Second-Order Mixture Model #1 After CVS-II Phase 2 (from Table 12.8) Versus Measured MCC-1 Boron Releases (from Table 12.1) for the CVS-II Phase 3 Data

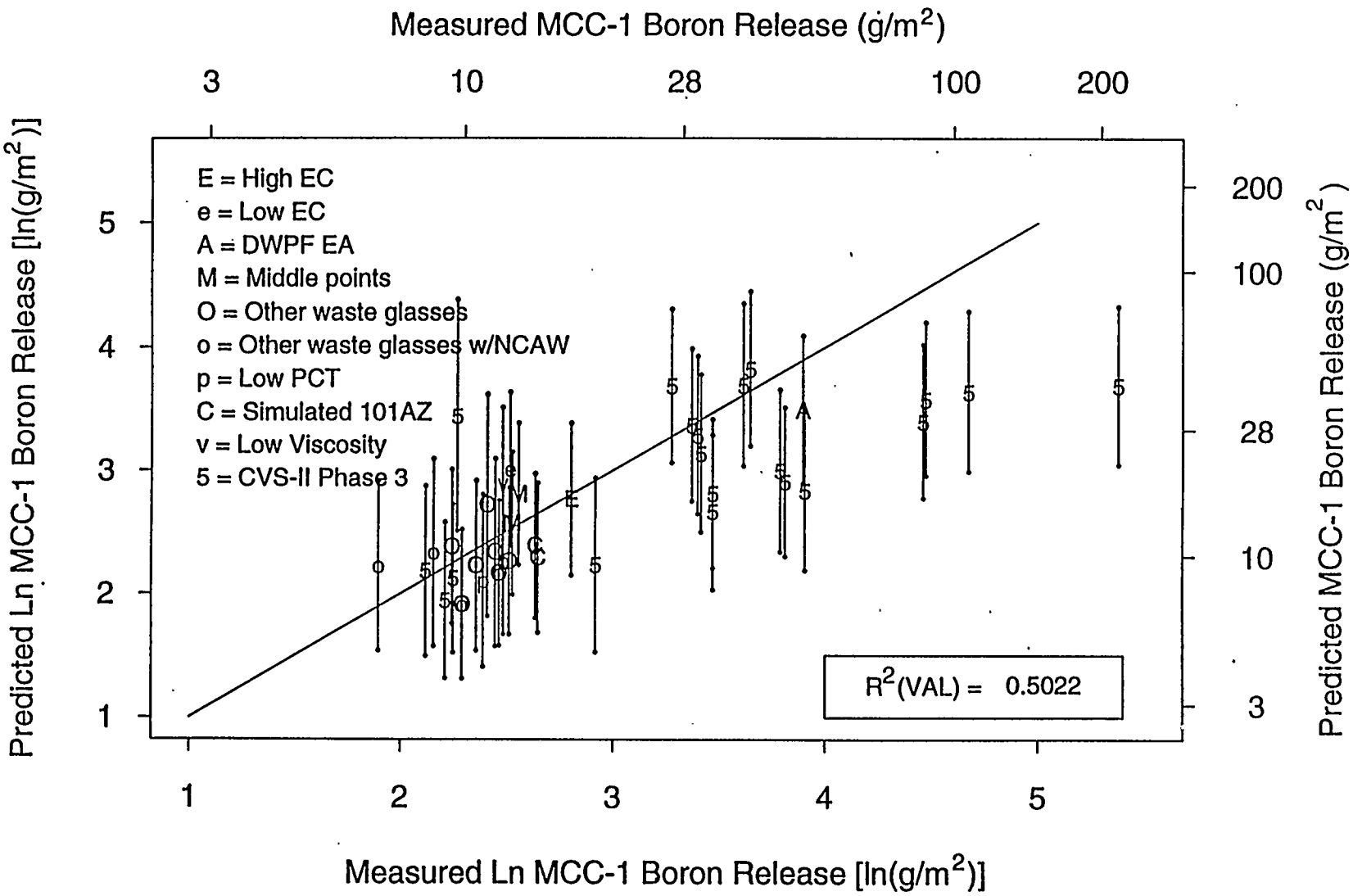

FIGURE 12.6b. Predicted MCC-1 Boron Releases from the Second-Order Mixture Model #2 After CVS-II Phase 2 (from Table 12.8) Versus Measured MCC-1 Boron Releases (from Table 12.1) for the CVS-II Phase 3 Data

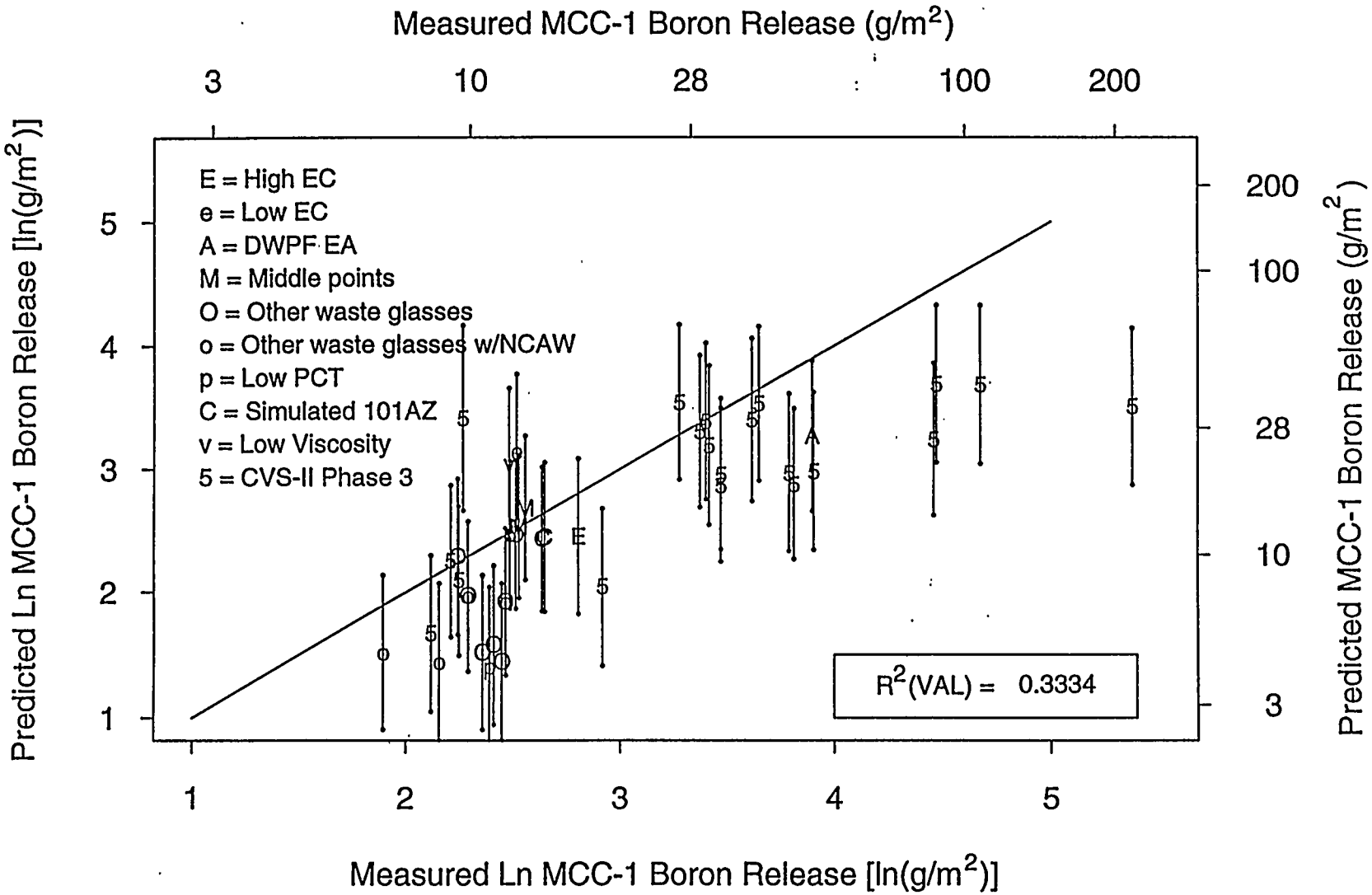

FIGURE 12.6c. Predicted MCC-1 Boron Releases from the Second-Order Mixture Model #3 After CVS-II Phase 2 (from Table 12.8) Versus Measured MCC-1 Boron Releases (from Table 12.1) for the CVS-II Phase 3 Data

Figure 12.6c shows that second-order model #3 for MCC-1 B release has slightly worse predictive ability for the CVS-II Phase 3 data compared to the first-order model. Figures 12.6b and 12.6a show that second-order models #2 and #1 have better predictive abilities for the CVS-II Phase 3 data than the first-order model and second-order model #3 (models #2 and #1 contain more second-order terms than model #3). The extra second-order terms in models #2 and #1 (compared to the first-order model and second-order model #3) appear to mainly improve predictions for glasses with lower MCC-1 B releases. The poor predictions for larger MCC-1 B releases cause the R^2(VAL) values (see Section 6.1.6) to still be rather low for second-order models #2 [R^2(VAL) = 0.5022] and #1 [R^2(VAL) = 0.5676]. This may be because the high-release data were not used in fitting the models (in Table 12.8) being validated. Second-order models were not fitted to the full data set because of concerns that second-order terms would be selected to fit the few available high-release data points and not provide good predictive ability for other compositions.

It should be recalled that the CVS-II Phase 3 data are not ideal validation data, because they are not uniformly spread over the full CVS composition region. Part of the goal of CVS-II Phase 3 was to collect data for more extreme compositions and property values than had been obtained previously. This, together with validating models fitted without higher release data, explains why none of the models validated well across the board. Still, it appears that second-order model #1 performed reasonably well in predicting MCC-1 B releases below about 28 g/m^2.

12.5 FIRST-ORDER MODELS AND COMPONENT EFFECTS FOR PCT RELEASES

The Si, B, Li, Na, Mo, and Cs release values averaged over duplicate 7-day PCT results (see Table D.2) for all CVS-I and CVS-II (Phase 1, 2, 3, and 4) glasses are contained in Table 12.9. The PCT averaged normalized B releases ranged from roughly 0.07 to 44 g/m^2. Six CVS-I glasses and nine CVS-II glasses have PCT normalized boron releases above 10 g/m^2. An additional two CVS-I glasses and 15 CVS-II glasses have PCT normalized boron releases above 5 g/m^2.

TABLE 12.9. Si, B, Li, Na, Mo, and Cs Normalized Releases and Solution pHs Averaged Over Duplicate 7-day PCT Dissolution Tests of CVS-I and CVS-II Glasses

Glass [b]	ID[c] #	PS[d]	Averaged 7-day PCT Normalized Elemental Releases (g/m²)[a] Si	B	Li	Mo	Na	Cs	pH
CVS1-1 (1)	1	M	0.167	0.521	0.529	0.439	0.403	0.056	10.92
CVS1-2 (e)	2	1	0.054	0.066	0.154	0.061	0.064	0.057	11.42
CVS1-3	3	1	0.172	0.864	0.791	0.468	0.580	0.042	9.85
CVS1-4 (2)	4	1	0.540	20.639	16.935	23.033	17.034	1.735	9.67
CVS1-5	5	1	0.318	0.355	0.462	0.327	0.191	0.148	11.22
CVS1-6	6	1	0.312	6.113	4.892	4.188	3.046	0.124	10.07
CVS1-7	7	1	0.114	0.287	0.331	0.304	0.339	0.143	10.91
CVS1-8 (3)	8	1	0.265	1.238	0.744	1.160	0.805	0.074	10.42
CVS1-9	9	1	0.345	10.993	8.602	7.399	7.897	0.922	8.69
CVS1-10	10	1	0.104	0.127	0.386	0.094	0.095	0.029	9.76
CVS1-11	11	1	0.041	0.099	0.187	0.066	0.099	0.057	9.99
CVS1-12	12	1	0.825	4.662	4.171	4.739	4.395	1.606	11.12
CVS1-13	13	1	0.786	14.072	12.903	13.122	12.413	1.104	10.37
CVS1-14	14	1	0.149	9.847	8.011	1.312	5.790	0.311	9.63
CVS1-15	15	1	0.967	18.778	11.198	19.125	13.995	2.799	13.03
CVS1-16	16	1	0.241	0.523	0.266	0.468	0.540	0.152	12.01
CVS1-17	17	1	0.663	2.235	2.075	2.234	2.304	0.940	11.57
CVS1-18	18	1	1.531	11.238	8.065	10.732	8.040	1.569	12.25
CVS1-19 (1)	19	M	0.166	0.523	0.533	0.448	0.433	0.065	10.29
CVS1-20 (1)	20	M	0.156	0.455	0.468	0.396	0.396	0.051	10.16
CVS1-21 (2)	21	1	0.459	18.850	15.591	19.543	15.536	1.744	9.68
CVS1-22 (3)	22	1	0.259	1.119	0.704	1.122	0.760	0.067	9.81
CVS1-23	23	M	0.229	0.525	0.535	0.487	0.487	0.063	10.29
CVS2-1	24	2	0.170	0.312	0.369	0.300	0.208	0.048	10.21
CVS2-2	25	2	0.075	0.128	0.276	0.118	0.188	0.068	10.92
CVS2-3	26	2	0.064	0.137	0.222	0.060	0.125	0.063	10.08
CVS2-4	27	2	0.101	0.158	0.300	0.150	0.182	0.100	10.40

(a) Release rates normalized using as-batched compositions in Table 4.15.

(b) The numbers in parentheses represent replicate sets of glasses.

(c) ID# is a consecutive integer numbering of all CVS glasses.

(d) PS is the plotting symbol used in plots associated with this data: 1 = CVS-I boundary, 2 = CVS-II Phase 1 interior, 3 = CVS-II Phase 2a boundary, 4 = CVS-II Phase 2b interior, 5 = CVS-II Phase 3 boundary, M = middle compositions, O = other than NCAW waste glasses, A = EA glass.

(e) Elemental release values are from one of two duplicate dissolution tests.

TABLE 12.9. Si, B, Li, Na, Mo, and Cs Normalized Releases and Solution pHs Averaged Over Duplicate 7-day PCT Dissolution Tests of CVS-I and CVS-II Glasses (continued)

Glass [b]	ID[c] #	PS[d]	Averaged 7-day PCT Normalized Elemental Releases (g/m²)[a] Si	B	Li	Mo	Na	Cs	pH
CVS2-5	28	2	0.106	0.284	0.382	0.165	0.284	0.030	9.58
CVS2-6	29	2	0.421	1.185	1.303	1.254	1.284	0.238	10.48
CVS2-7	30	2	0.164	0.740	0.812	0.204	0.343	0.004	9.89
CVS2-8	31	2	0.263	0.484	0.523	0.483	0.445	0.044	10.75
CVS2-9	32	2	0.241	0.560	0.620	0.568	0.374	0.014	10.34
CVS2-10	33	2	0.115	1.332	1.322	0.128	0.828	0.006	9.46
CVS2-11	34	2	0.510	1.587	1.564	1.676	1.370	0.076	11.46
CVS2-12	35	2	0.075	0.194	0.262	0.133	0.184	0.061	9.90
CVS2-13	36	2	0.182	0.360	0.362	0.308	0.478	0.080	11.14
CVS2-14	37	2	0.261	1.656	1.468	1.781	1.268	0.354	10.46
CVS2-15	38	2	0.180	0.331	0.451	0.281	0.608	0.158	11.30
CVS2-16 (4)	39	M	0.558	2.937	2.349	2.760	2.182	0.017	10.36
CVS2-17 (1)	40	M	0.167	0.495	0.572	0.464	0.474	0.023	10.27
CVS2-18 (4)	41	M	0.546	2.578	2.094	2.475	1.886	0.016	10.34
CVS2-19 (5)	42	M	0.450	1.990	1.654	2.070	1.481	0.128	10.35
CVS2-20	43	3	0.187	0.347	0.386	(f)	0.279	0.048*	10.89
CVS2-21	44	3	0.506	3.854	2.534	(f)	2.089	0.054	10.26
CVS2-22	45	3	2.249	9.646	5.453	(f)	6.097	0.434	11.72
CVS2-23	46	3	0.144	0.173	0.604	(f)	0.809	0.077*	11.81
CVS2-24	47	3	0.179	4.522	3.226	(f)	2.060	0.042	9.80
CVS2-25	48	3	1.214	4.662	2.765	(f)	3.526	0.400	11.91
CVS2-26	49	3	0.275	1.628	1.436	(f)	1.349	0.123	10.11
CVS2-27	50	3	0.890	3.270	1.835	(f)	2.342	0.266	11.87
CVS2-28	51	3	1.654	5.144	3.682	(f)	3.538	0.326	11.54
CVS2-29	52	3	0.192	1.286	1.355	(f)	1.273	0.316	9.11

(a) Release rates normalized using as-batched compositions in Table 4.15.

(b) The numbers in parentheses represent replicate sets of glasses.

(c) ID# is a consecutive integer numbering of all CVS glasses.

(d) PS is the plotting symbol used in plots associated with this data: 1 = CVS-I boundary, 2 = CVS-II Phase 1 interior, 3 = CVS-II Phase 2a boundary, 4 = CVS-II Phase 2b interior, 5 = CVS-II Phase 3 boundary, M = middle compositions, O = other than NCAW waste glasses, A = EA glass.

(f) Mo release was not measured during CVS-II.

* Based on re-analysis of samples.

TABLE 12.9. Si, B, Li, Na, Mo, and Cs Normalized Releases and Solution pHs Averaged Over Duplicate 7-day PCT Dissolution Tests of CVS-I and CVS-II Glasses (continued)

Glass [b]	ID[c] #	PS[d]	Averaged 7-day PCT Normalized Elemental Releases (g/m²)[a] Si	B	Li	Mo	Na	Cs	pH
CVS2-30	53	3	0.174	6.512	4.194	(f)	2.552	0.015	8.74
CVS2-31	54	3	0.121	0.411	0.460	(f)	0.318	0.170	9.54
CVS2-32	55	3	2.747	9.646	5.527	(f)	5.896	0.464	12.31
CVS2-33	56	3	0.516	1.723	1.438	(f)	1.608	0.374	11.94
CVS2-34 (6)	57	3	0.265	4.340	3.468	(f)	2.700	0.054	11.55
CVS2-35	58	3	0.204	0.320	0.580	(f)	0.910	0.262	11.90
CVS2-36	59	3	0.276	0.480	0.630	(f)	0.654	0.246	11.34
CVS2-37	60	3	0.206	0.246	0.300	(f)	0.177	0.036	10.45
CVS2-38	61	3	0.280	1.119	0.726	(f)	0.807	0.065	9.56
CVS2-39	62	4	1.612	12.701	6.528	(f)	7.668	0.758	12.50
CVS2-40	63	4	0.172	0.337	0.328	(f)	0.399	0.210	11.13
CVS2-41	64	4	0.104	0.177	0.260	(f)	0.188	0.088	10.89
CVS2-42	65	4	0.574	1.694	1.220	(f)	1.337	0.118	11.19
CVS2-43	66	4	0.196	0.767	0.697	(f)	0.451	0.012	9.97
CVS2-44	67	4	0.128	0.255	0.294	(f)	0.194	0.060	10.31
CVS2-45	68	4	0.186	0.500	0.478	(f)	0.374	0.032	10.05
CVS2-46	69	4	0.148	0.317	0.346	(f)	0.188	0.027	10.19
CVS2-47	70	4	0.434	1.159	1.124	(f)	1.055	0.188	11.39
CVS2-48	71	4	0.102	0.307	0.318	(f)	0.284	0.048	10.09
CVS2-49	72	4	0.136	0.303	0.334	(f)	0.217	0.016	9.97
CVS2-50 (1)	73	M	0.150	0.442	0.426	(f)	0.368	0.030	10.23
CVS2-51 (5)	74	M	0.411	1.764	1.496	(f)	1.283	0.056	10.30
CVS2-52	75	4	0.294	0.557	0.554	(f)	0.260	0.022	10.16
CVS2-53	76	4	0.176	0.304	0.305	(f)	0.202	0.060	10.02
CVS2-54	77	M	0.571	2.761	1.715	(f)	1.612	0.112	10.23

(a) Release rates normalized using as-batched compositions in Table 4.15.

(b) The numbers in parentheses represent replicate sets of glasses.

(c) ID# is a consecutive integer numbering of all CVS glasses.

(d) PS is the plotting symbol used in plots associated with this data: 1 = CVS-I boundary, 2 = CVS-II Phase 1 interior, 3 = CVS-II Phase 2a boundary, 4 = CVS-II Phase 2b interior, 5 = CVS-II Phase 3 boundary, M = middle compositions, O = other than NCAW waste glasses, A = EA glass.

(f) Mo release was not measured during CVS-II.

TABLE 12.9. Si, B, Li, Na, Mo, and Cs Normalized Releases and Solution pHs Averaged Over Duplicate 7-day PCT Dissolution Tests of CVS-I and CVS-II Glasses (continued)

Glass [b]	ID[c] #	PS[d]	Averaged 7-day PCT Normalized Elemental Releases (g/m²)[a] Si	B	Li	Mo	Na	Cs	pH
CVS2-55	78	0	0.352	1.342	1.127	(f)	0.880	0.002	10.19
CVS2-56	79	0	0.368	1.419	1.218	(f)	0.946	0.002	10.20
CVS2-57	80	0	0.346	1.164	1.081	(f)	0.842	0.002	10.26
CVS2-58	81	4	0.138	0.778	0.636	(f)	0.620	0.034	9.87
CVS2-59	82	5	0.268	1.591	1.287	(f)	1.222	0.019	11.47
CVS2-60	83	5	0.415	1.624	1.158	(f)	1.523	0.035	11.96
CVS2-61	84	5	0.195	0.222	0.280	(f)	0.230	0.064	10.89
CVS2-62	85	5	0.268	1.002	0.862	(f)	0.928	0.026	9.56
CVS2-63	86	5	0.079	0.332	0.222	(f)	0.390	0.186	10.59
CVS2-64	87	0	0.234	0.379	0.376	(f)	0.342	0.054	10.62
CVS2-65	88	0	0.148	0.335	0.355	(f)	0.200	(g)	10.62
CVS2-66	89	0	0.164	0.210	0.247	(f)	0.223	(g)	10.54
CVS2-67	90	0	0.230	0.512	0.480	(f)	0.214	(g)	9.73
CVS2-68	91	0	0.254	0.308	0.340	(f)	0.127	(g)	9.84
CVS2-69	92	0	0.186	0.226	0.302	(f)	0.112	(g)	10.18
CVS2-70	93	0	0.286	0.312	0.381	(f)	0.128	(g)	9.89
CVS2-71	94	5	0.244	0.411	0.427	(f)	0.350	0.031	10.78
CVS2-72	95	5	0.153	0.210	0.226	(f)	0.228	0.038	10.48
CVS2-73	96	5	0.179	0.244	0.301	(f)	0.074	0.010	9.96
CVS2-74	97	5	0.163	0.226	0.279	(f)	0.147	0.048	10.41
CVS2-75	98	5	0.220	0.278	0.334	(f)	0.100	0.032	9.88
CVS2-76	99	5	4.045	14.871	7.571	(f)	12.541	3.203	12.46
CVS2-77	100	5	2.290	9.512	6.221	(f)	6.552	1.434	12.26
CVS2-78	101	5	0.191	0.934	0.698	(f)	0.593	0.012	9.21
CVS2-79	102	5	0.190	0.744	0.684	(f)	0.660	0.035	8.96
CVS2-80	103	5	0.195	0.764	0.672	(f)	0.600	0.005	9.15

(a) Release rates normalized using as-batched compositions in Table 4.I5.

(b) The numbers in parentheses represent replicate sets of glasses.

(c) ID# is a consecutive integer numbering of all CVS glasses.

(d) PS is the plotting symbol used in plots associated with this data: 1 = CVS-I boundary, 2 = CVS-II Phase 1 interior, 3 = CVS-II Phase 2a boundary, 4 = CVS-II Phase 2b interior, 5 = CVS-II Phase 3 boundary, M = middle compositions, O = other than NCAW waste glasses, A = EA glass.

(f) Mo release was not measured during CVS-II.

(g) Cs release was not measured for some CVS-II Phase 3 glasses.

TABLE 12.9. Si, B, Li, Na, Mo, and Cs Normalized Releases and Solution pHs Averaged Over Duplicate 7-day PCT Dissolution Tests of CVS-I and CVS-II Glasses (continued)

Glass [b]	ID[c] #	PS[d]	Averaged 7-day PCT Normalized Elemental Releases (g/m²)[a] Si	B	Li	Mo	Na	Cs	pH
CVS2-81	104	5	3.036	16.613	8.064	(f)	12.824	0.338	12.51
CVS2-82	105	5	16.884	44.000	19.969	(f)	35.377	8.574	12.18
CVS2-83	106	5	11.447	34.656	19.228	(f)	27.890	0.832	12.33
CVS2-84	107	5	0.493	12.460	6.682	(f)	8.236	0.922	12.42
CVS2-85	108	5	0.291	0.456	0.422	(f)	0.749	0.146	11.68
CVS2-86	109	5	0.082	0.115	0.091	(f)	0.254	0.074	10.98
CVS2-87	110	5	0.114	0.178	0.131	(f)	0.286	0.054	10.90
CVS2-88	111	5	0.162	0.308	0.376	(f)	0.473	0.094	11.52
CVS2-89	112	5	0.364	1.716	1.236	(f)	1.348	0.044	11.04
CVS2-90	113	5	0.716	5.577	3.764	(f)	3.481	0.036	9.98
CVS2-91	114	5	0.468	8.642	6.774	(f)	6.738	0.246	9.38
CVS2-92	115	5	1.214	18.590	12.442	(f)	11.792	0.865	11.12
CVS2-93	116	5	1.967	13.227	7.757	(f)	10.010	1.566	11.76
CVS2-94	117	5	0.935	4.070	3.066	(f)	3.350	0.123	11.84
CVS2-95 (7)	118	A	2.008	9.976	4.271	(f)	7.259	(g)	11.81
CVS2-96 (1)	119	M	0.159	0.493	0.429	(f)	0.410	0.032	10.24
CVS2-97 (5)	120	M	0.391	1.434	1.052	(f)	1.134	0.066	10.25
CVS2-98 (6)	121	5	0.267	4.520	3.497	(f)	2.796	0.065	11.58
CVS2-99	122	5	0.131	0.232	0.246	(f)	0.199	(g)	10.10
CVS2-100	123	5	0.170	0.326	0.343	(f)	0.226	(g)	10.34
CVS2-101(7)	124	A	1.819	8.644	3.831	(f)	6.586	(g)	11.92

(a) Release rates normalized using as-batched compositions in Table 4.15.

(b) The numbers in parentheses represent replicate sets of glasses.

(c) ID# is a consecutive integer numbering of all CVS glasses.

(d) PS is the plotting symbol used in plots associated with this data: 1 = CVS-I boundary, 2 = CVS-II Phase 1 interior, 3 = CVS-II Phase 2a boundary, 4 = CVS-II Phase 2b interior, 5 = CVS-II Phase 3 boundary, M = middle compositions, O = other than NCAW waste glasses, A = EA glass.

(f) Mo release was not measured during CVS-II.

(g) Cs release was not measured for some CVS-II Phase 3 glasses.

TABLE 12.9. Si, B, Li, Na, Mo, and Cs Normalized Releases and Solution pHs Averaged Over Duplicate 7-day PCT Dissolution Tests of CVS-I and CVS-II Glasses (continued)

Glass [b]	ID[c] #	PS[d]	Averaged 7-day PCT Normalized Elemental Releases (g/m²)[a] Si	B	Li	Mo	Na	Cs	pH
CVS2-102(4)	125	M	0.559	2.672	1.921	(f)	1.677	(h)	10.28
CVS2-103	126	6	0.691	6.073	4.066	(f)	4.082	(h)	11.61
CVS2-104	127	6	0.712	5.548	3.633	(f)	3.668	(h)	11.29
CVS2-105	128	6	0.687	4.590	3.132	(f)	2.974	(h)	10.82
CVS2-106	129	6	0.447	1.651	1.348	(f)	1.165	(h)	10.18
CVS2-107	130	6	0.348	0.788	0.662	(f)	0.620	(h)	10.68
CVS2-108	131	6	0.357	2.144	1.646	(f)	1.387	(h)	9.79
CVS2-109	132	6	0.313	5.707	4.494	(f)	3.584	(h)	9.54
CVS2-110	133	6	0.160	0.314	0.402	(f)	0.118	(h)	9.61
CVS2-111	134	6	1.199	6.135	3.894	(f)	4.043	(h)	11.35
CVS2-112	135	6	0.454	14.400	7.794	(f)	9.603	(h)	12.04
CVS2-113	136	6	0.216	0.612	0.630	(f)	0.510	(h)	9.63
CVS2-114	137	6	1.838	7.116	4.928	(f)	4.599	(h)	11.41
CVS2-115	138	6	1.942	9.406	5.837	(f)	5.765	(h)	11.55
CVS2-116	139	6	0.606	3.012	2.203	(f)	2.030	(h)	10.43
CVS2-117	140	6	0.445	1.590	1.337	(f)	1.099	(h)	10.19
CVS2-118	141	6	0.606	3.630	2.609	(f)	2.394	(h)	10.40
CVS2-119	142	6	0.829	3.803	2.688	(f)	2.574	(h)	10.32
CVS2-120	143	6	0.154	0.291	0.324	(f)	0.231	(h)	10.09
CVS2-121	144	6	0.129	0.199	0.311	(f)	0.137	(h)	10.06
CVS2-122	145	6	0.128	0.193	0.363	(f)	0.089	(h)	9.91
CVS2-123(5)	146	M	0.391	1.473	1.125	(f)	1.075	(h)	10.22

(a) Release rates normalized using as-batched compositions in Table 4.15.

(b) The numbers in parentheses represent replicate sets of glasses.

(c) ID# is a consecutive integer numbering of all CVS glasses.

(d) PS is the plotting symbol used in plots associated with this data: 1 = CVS-I boundary, 2 = CVS-II Phase 1 interior, 3 = CVS-II Phase 2a boundary, 4 = CVS-II Phase 2b interior, 5 = CVS-II Phase 3 boundary, 6 = CVS-II Phase 4 one-component-at-a-time, M = middle compositions, O = other than NCAW waste glasses, A = EA glass.

(f) Mo release was not measured during CVS-II.

(h) Cs release was not measured for CVS-II Phase 4 glasses.

First-order mixture models of the form (6.1) using mass and mole fractions were fitted to the natural logs of the averaged Si, B, Li, and Na elemental PCT releases from Table 12.9 using the as-batched compositions from Table 4.15. The data for CVS-I and CVS-II Phases 1, 2, and 3 glasses (ID#s 1 through 124) were used. The model coefficients are given in Tables 12.10a and 12.10b for models using mass and mole fractions, respectively. First-order mixture models were also fitted to a reduced set of data obtained by deleting the data points corresponding to glasses CVS1-4, 9, 13, 15, 18, and 21 (which had the six largest PCT B release values). However, these data points agreed fairly well with the models fit to all of the data, and it was decided that "reduced data set" models were not required for the PCT results. See Sections 12.11.3 and 12.11.4.5 for additional discussion of high-release glasses.

Focusing on PCT B release, the R^2 statistics for the first-order model using mass fractions are $R^2 = 0.8114$, $R^2(ADJ) = 0.7964$, and $R^2(PRESS) = 0.7715$, while for the first-order model using mole fractions they are $R^2 = 0.8057$, $R^2(ADJ) = 0.7903$, and $R^2(PRESS) = 0.7644$. These R^2 values are somewhat higher than were the corresponding values for the first-order models fit to the full and reduced MCC-1 data sets. The general indication from the R^2 statistics in Tables 12.10a and 12.10b is that the PCT first-order mixture models provide reasonable predictive ability, but leave considerable room for improvement. The plots of predicted versus measured PCT B release values in Figures 12.7a (mass fractions) and 12.7b (mole fractions) confirm that there is room for improvement on the first-order model. The model tends to under-predict both lower and higher B releases, and shows a considerable scatter for middle values. A statistical test for model lack-of-fit (LOF) (see Section 6.1.5) indicated that first-order mixture models (using mass and mole fractions) have statistically significant LOFs at greater than 99% confidence.

The component effects plot produced using the PCT normalized B release first-order mixture model fitted to all the CVS data set (from Table 12.11) is given in Figure 12.8. Only the single-component constraints and not the stand-in crystallinity constraints in Tables 4.2 and 4.6 were used to limit the effects plot (both were used in previous effects plots). As a result, effects are evaluated over wider ranges than in the past for several

TABLE 12.10a. Coefficients and Goodness-of-Fit Statistics for First-Order Mixture Models (Using Component Mass Fractions) Fitted to Natural Logarithms of Averaged 7-Day PCT Normalized Elemental Releases (g/m^2) for CVS-I and CVS-II Phase 1, 2, and 3 Glasses

Component	PCT Si	PCT B	PCT Li	PCT Na
SiO_2	-2.9671	-4.3173	-3.2278	-4.4118
B_2O_3	-0.6148	11.9791	10.1496	9.4049
Na_2O	10.7384	17.6068	14.0017	19.4013
Li_2O	19.7370	22.5791	18.4159	19.0635
CaO	-6.0415	-8.7114	-5.3528	-1.9567
MgO	2.9296	10.9210	7.1181	11.8228
Fe_2O_3	-4.2315	-3.2009	-4.5113	-4.0953
Al_2O_3	-17.3377	-25.4071	-22.3095	-25.4294
ZrO_2	-10.8139	-10.5613	-10.0618	-11.4209
Others	-0.7297	0.1587	0.6181	-0.6647
# points[a]	123	123	123	123
R^2[b]	0.7377	0.8114	0.7905	0.8457
R^2(ADJ)[b]	0.7168	0.7964	0.7738	0.8334
R^2(PRESS)[b]	0.6791	0.7715	0.7465	0.8151
LOF?[c]	Yes (>99%)	Yes (>99%)	Yes (>99%)	Yes (>99%)

(a) All CVS-I and CVS-II Phase 1, 2, and 3 data in Table 12.9 except CVS2-101 (which was originally not part of the CVS data set) were used in fitting the PCT normalized elemental release models.

(b) R^2, R^2(ADJ), and R^2(PRESS) statistics take values between 0.0 and 1.0, and provide different measures of the proportion of variation in the property data accounted for by a fitted model. See Section 6.1.5 for the definitions of these statistics.

(c) A statistical F-test for lack-of-fit (LOF) was performed using the estimates of experimental variation obtained from four replicate tests. "Yes" and "No" entries indicate whether the LOF was statistically significant at a 90% confidence level. The actual confidence level at which a LOF can be declared significant is given in parentheses following the "Yes" or "No" for each model.

TABLE 12.10b. Coefficients and Goodness-of-Fit Statistics for First-Order Mixture Models (Using Component Mole Fractions) Fitted to Natural Logarithms of Averaged 7-Day PCT Normalized Elemental Releases (g/m^2) for CVS-I and CVS-II Phase 1, 2, and 3 Glasses

Component	PCT Si	PCT B	PCT Li	PCT Na
SiO_2	-2.7729	-3.9171	-2.9040	-3.9940
B_2O_3	-0.6037	13.0094	11.0442	10.2374
Na_2O	10.4147	17.2575	13.7189	18.9374
Li_2O	8.3858	10.4311	8.4870	8.6882
CaO	-5.2639	-7.4729	-4.6291	-1.7696
MgO	1.5497	7.0436	4.5915	7.4833
Fe_2O_3	-9.1948	-9.0271	-12.0510	-10.9748
Al_2O_3	-27.1596	-41.0770	-36.0781	-41.0700
ZrO_2	-20.0818	-21.2458	-20.1523	-22.7515
Others	-0.1302	-1.0674	0.2465	-2.8252
# points[a]	123	123	123	123
R^2[b]	0.7268	0.8057	0.7854	0.8403
R^2(ADJ)[b]	0.7050	0.7903	0.7684	0.8276
R^2(PRESS)[b]	0.6674	0.7644	0.7400	0.8085
LOF?[c]	Yes (>99%)	Yes (>99%)	Yes (>99%)	Yes (>99%)

(a) All CVS-I and CVS-II Phase 1, 2, and 3 data in Table 12.9 except CVS2-101 (which was originally not part of the CVS data set) were used in fitting the PCT normalized elemental release models.

(b) R^2, R^2(ADJ), and R^2(PRESS) statistics take values between 0.0 and 1.0, and provide different measures of the proportion of variation in the property data accounted for by a fitted model. See Section 6.1.5 for the definitions of these statistics.

(c) A statistical F-test for lack-of-fit (LOF) was performed using the estimates of experimental variation obtained from four replicate tests. "Yes" and "No" entries indicate whether the LOF was statistically significant at a 90% confidence level. The actual confidence level at which a LOF can be declared significant is given in parentheses following the "Yes" or "No" for each model.

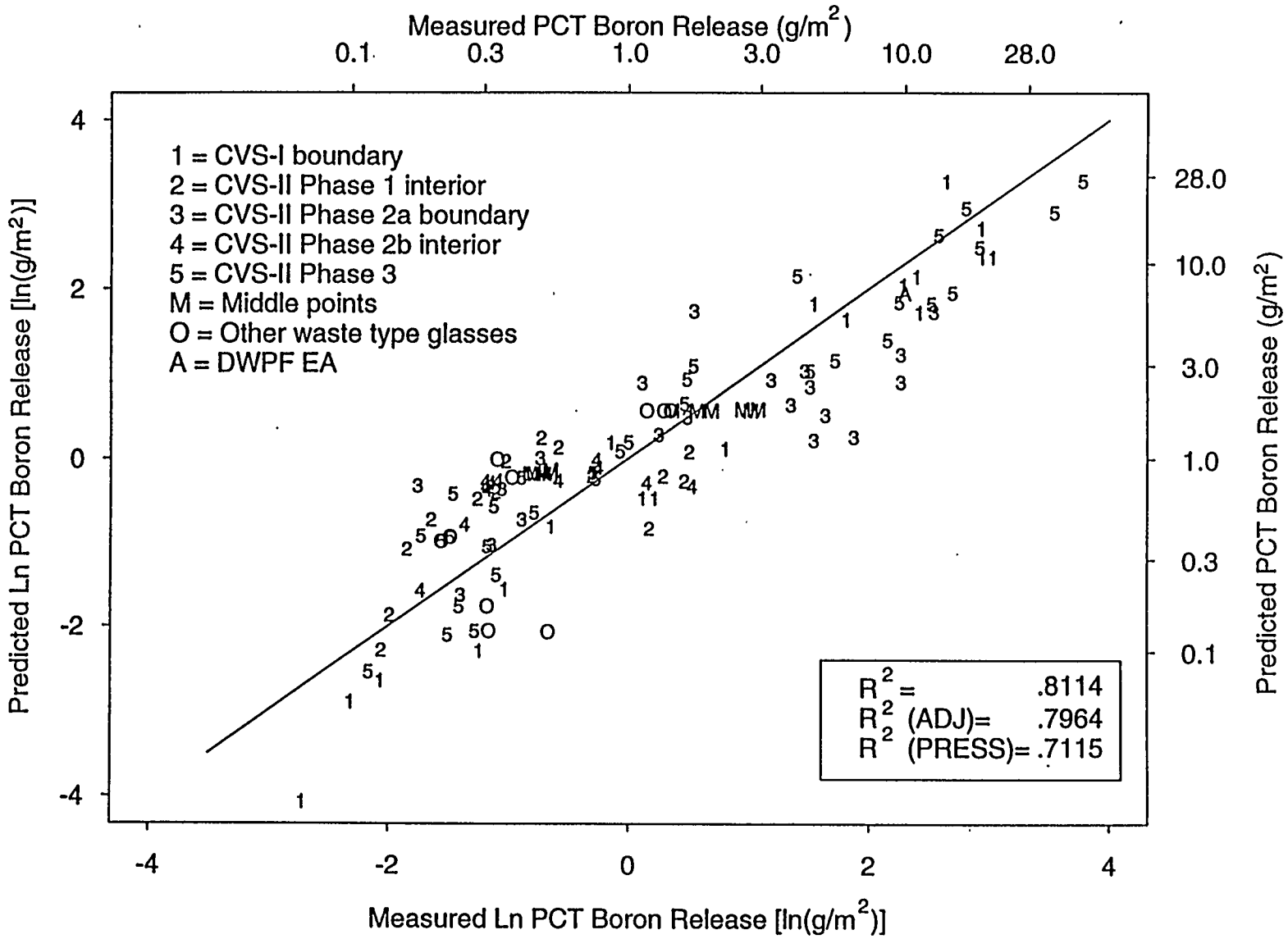

FIGURE 12.7a. Predicted Versus Measured PCT B Release for the First-Order Mixture Model Using Mass Fractions (from Table 12.10a)

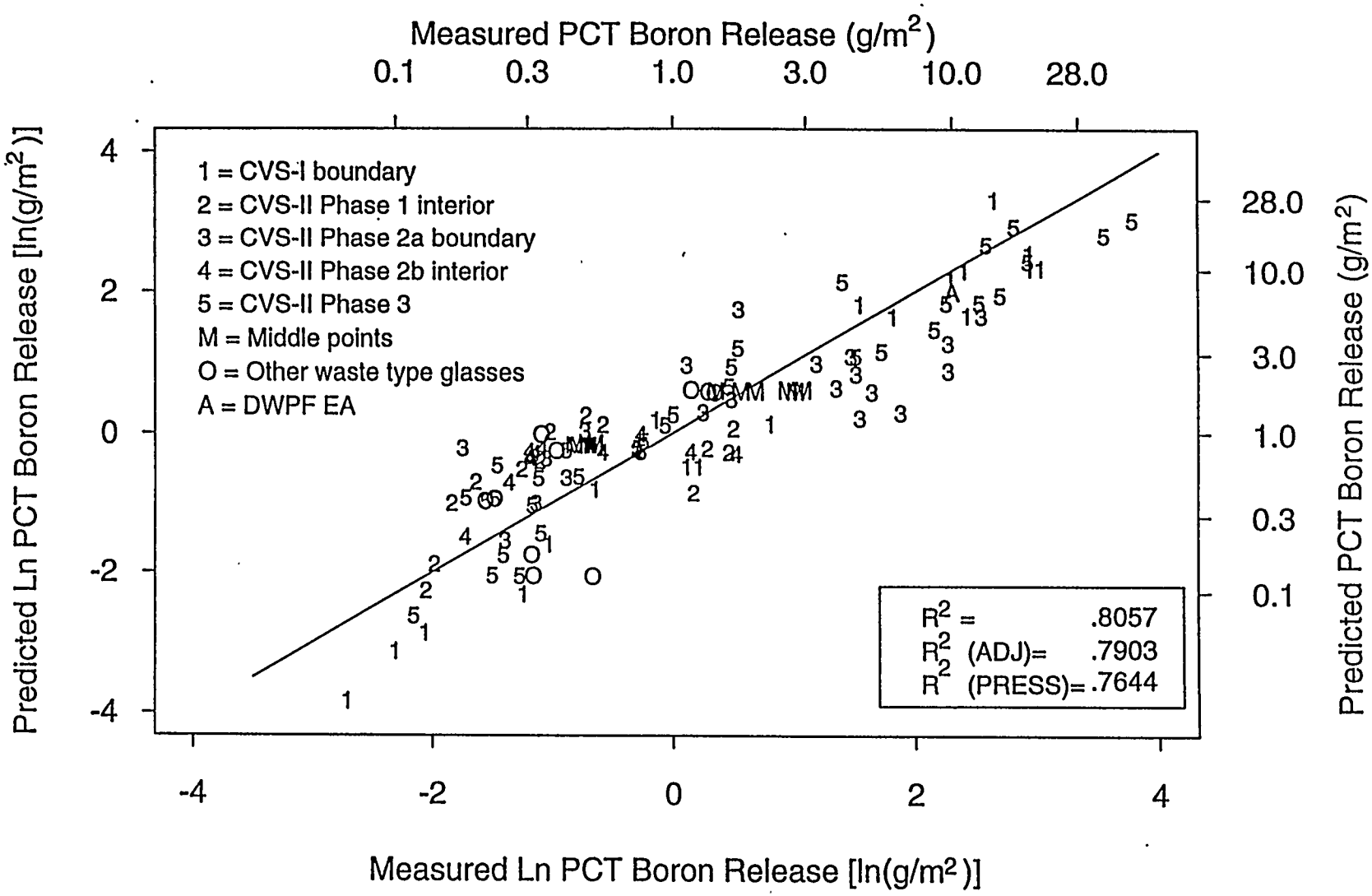

FIGURE 12.7b. Predicted Versus Measured PCT B Release for the First-Order Mixture Model Using Mole Fractions (from Table 12.10b)

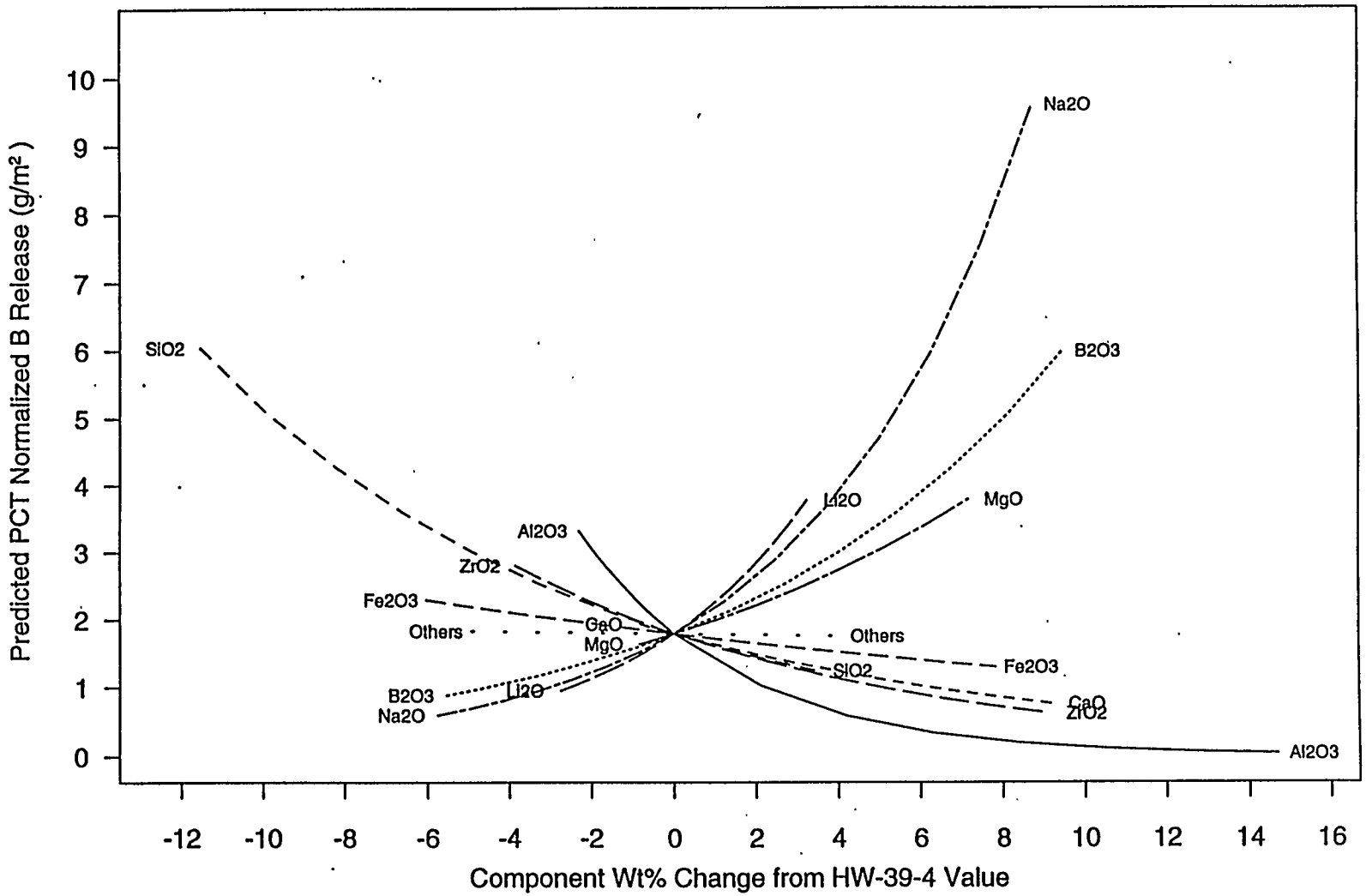

FIGURE 12.8. Predicted Component Effects on PCT B Release Relative to the HW-39-4 Composition, Based on First-Order Mixture Model Using Mass Fractions (in Column 3 of Table 12.10a)

components involved in the stand-in constraints (most notably Al_2O_3 and SiO_2). The components Li_2O, Na_2O, B_2O_3, and MgO (in that order) are predicted to increase PCT B release of HW-39-4 glass, while Al_2O_3 and SiO_2 are predicted to decrease PCT B release of HW-39-4. ZrO_2 and CaO also appear to decrease PCT B release of HW-39-4 glass, but this is not clear due to uncertainty in the fitted model. The Others and Fe_2O_3 components appear to have negligible effects on PCT B release of HW-39-4.

12.6 INVESTIGATION OF POTENTIAL BIASES IN PCT RELEASE DATA DUE TO CVS PHASES

As discussed in Section 6.1.1, a model of the form (6.3) was fitted to the Si, B, Li, and Na normalized PCT release data for CVS-I and CVS-II Phases 1, 2, and 3 to ascertain whether any biases (block effects) were present in the data because of performing the CVS in phases. The mass fraction versions of (6.3) yielded $R^2 = 0.7485$ for Si, $R^2 = 0.8200$ for B, $R^2 = 0.8110$ for Li, and $R^2 = 0.8517$ for Na. These values can be compared to the corresponding values (from Table 12.10a) for the first-order mass fraction models (6.1) without the block effect terms, which were $R^2 = 0.7377$ for Si, $R^2 = 0.8114$ for B, $R^2 = 0.7905$ for Li, and $R^2 = 0.8457$ for Na. Thus, the block effect terms improved the R^2 values only marginally. The results for mole fraction model R^2 values were similar.

Statistically significant block effects were detected for only two of the four CVS phases, with the same effects being significant for both mass and mole fraction versions of the model (6.3). CVS-I was found to have a positive block effect (increased releases) for B, Li, and Na. This could be due to all CVS-I normalized releases being biased high, or to the large release data points in CVS-I. CVS-II Phase 3 was found to have a negative block effect (decreased releases) for Li, and a positive block effect (increased releases) for Si. This result is somewhat perplexing, because Si and Li releases are generally positively correlated (see Tables 13.1 and 13.2). One possible explanation is that chemical analyses of PCT solutions could have been biased for particular elements during CVS-II Phase 3. The results could be due to the fact that CVS-II Phase 3 explored more extreme portions of composition space with larger PCT release values (see Section 4.5), although this would

have tended to yield higher releases for all properties. Data for replicate glasses in Table F.2 in Appendix F does not provide strong support for the "biased data" hypotheses.

Because of the uncertainty as to whether the statistically significant block (CVS phases) effects detected for PCT normalized release data are due to biased data or merely differences in how each phase was designed, it was decided not to try to adjust the data and refit models.

12.7 SECOND-ORDER MODELS FOR PCT RELEASES

Three candidate Scheffé second-order mixture models (using mass fractions of the component oxides) for each of B, Si, Li, and Na normalized PCT releases are given in Tables 12.11 to 12.14. These models consist of the first-order mixture model terms and several second-order terms selected using statistical variable selection techniques (see Section 6.1.4). It was not necessary to apply the pseudocomponent transformation (see Section 6.1.3), so the usual glass oxide component mass fractions were used in fitting the models. All CVS-I and CVS-II Phase 1, 2, and 3 glasses were used to develop the candidate second-order models (with the exceptions of the radioactive glasses CVS2-53 and CVS2-54, and the EA glass CVS2-101).

The candidate sets of second-order mixture models in Tables 12.11 to 12.14 provide better fits than the corresponding first-order mixture models, based on comparing the R^2 statistics in Tables 12.11 to 12.14 to those in Table 12.10a. Figure 12.9 displays the predicted versus measured PCT B release values for the second-order mixture model #2 from Table 12.11. This plot confirms that the second-order model fits the data better than the first-order model. However, there still appears to be room for improvement in modeling PCT normalized releases. The lack-of-fit of the first-order PCT B release model was tested (see Section 6.1.5) and found to be statistically significant (see Table 12.11).

Second-order mixture models for PCT releases using mole fractions were also investigated. The second-order terms selected by the statistical procedures and the R^2 statistics obtained were almost the same as for mass fractions. Hence, it was decided not to present the mole fraction models.

TABLE 12.11. Candidate Scheffé Second-Order Models Using Mass Fractions for PCT ln(Boron) Release

Model #1		Model #2		Model #3	
Terms	Coefficients	Terms	Coefficients	Terms	Coefficients
SiO2	-3.3000	SiO2	-4.3800	SiO2	-4.1267
B2O3	11.6288	B2O3	-3.0800	B2O3	-2.7803
Na2O	17.7140	Na2O	21.4405	Na2O	19.7648
Li2O	22.7698	Li2O	24.1740	Li2O	25.1279
CaO	-98.2559	CaO	14.0697	CaO	7.8944
MgO	11.3756	MgO	-49.7288	MgO	-51.2479
Fe2O3	-3.6844	Fe2O3	-1.3114	Fe2O3	-0.7342
Al2O3	-46.9147	Al2O3	-39.5782	Al2O3	-39.6897
ZrO2	-11.9546	ZrO2	-11.4163	ZrO2	-21.8129
Others	0.9622	Others	4.2083	Others	4.3558
Al2O3 x Al2O3	129.7378	Al2O3 x Al2O3	104.2185	Al2O3 x Al2O3	105.2815
		B2O3 x B2O3	76.6582	SiO2 x MgO	119.5209
		SiO2 x MgO	117.1719	Na2O x ZrO2	70.4225
		Na2O x CaO	-120.8841	CaO x ZrO2	101.8736
		B2O3 x CaO	-91.1406	B2O3 x CaO	-80.9291
		MgO x ZrO2	122.0852	Na2O x CaO	-90.8996
				MgO x ZrO2	146.7060
				B2O3 x B2O3	76.5449
R^2	= .8638	R^2	= .9012	R^2	= .9106
R^2(ADJ)	= .8517	R^2(ADJ)	= .8873	R^2(ADJ)	= .8961
R^2(PRESS)	= .8294	R^2(PRESS)	= .8572	R^2(PRESS)	= .8671
LOF?[a]	Yes (>99%)		Yes (>99%)		Yes (>99%)

(a) A statistical F-test for lack-of-fit (LOF) was performed using the estimates of experimental variation obtained from four replicate tests. "Yes" and "No" entries indicate whether the LOF was statistically significant at a 90% confidence level. The actual confidence level at which a LOF can be declared significant is given in parentheses following the "Yes" or "No" for each model.

TABLE 12.12. Candidate Scheffé Second-Order Models Using Mass Fractions for PCT ln(Silica) Release

Model #1		Model #2		Model #3	
Terms	Coefficients	Terms	Coefficients	Terms	Coefficients
SiO2	-2.6378	SiO2	-1.2553	SiO2	-2.3415
B2O3	-1.5180	B2O3	-5.2433	B2O3	2.2959
Na2O	13.7318	Na2O	10.6964	Na2O	17.8263
Li2O	18.5257	Li2O	-1.6936	Li2O	18.0258
CaO	-5.7286	CaO	-8.8074	CaO	11.2689
MgO	3.2630	MgO	3.5842	MgO	-1.7491
Fe2O3	-4.3537	Fe2O3	-3.7775	Fe2O3	-5.6296
Al2O3	-28.6325	Al2O3	-28.5725	Al2O3	-28.9796
ZrO2	-11.9002	ZrO2	-11.5979	ZrO2	-17.2431
Others	-0.2859	Others	0.2360	Others	-2.5487
Al2O3 x Al2O3	101.2231	B2O3 x Li2O	94.3587	Al2O3 x Al2O3	96.5647
Na2O x Al2O3	-47.6957	B2O3 x CaO	37.3563	Na2O x Al2O3	-53.2773
		Na2O x Li2O	91.9995	CaO x ZrO2	95.2066
		Na2O x Al2O3	-47.4447	MgO x ZrO2	109.7168
		Al2O3 x Al2O3	104.8281	B2O3 x Na2O	-40.6487
				SiO2 x CaO	-43.2976
R^2	= .8181	R^2	= .8376	R^2	= .8471
R^2(ADJ)	= .8001	R^2(ADJ)	= .8165	R^2(ADJ)	= .8257
R^2(PRESS)	= .7610	R^2(PRESS)	= .7749	R^2(PRESS)	= .7800

TABLE 12.13. Candidate Scheffé Second-Order Models Using Mass Fractions for PCT ln(Lithium) Release

Model #1		Model #2		Model #3	
Terms	Coefficients	Terms	Coefficients	Terms	Coefficients
SiO2	-2.2167	SiO2	-2.9517	SiO2	-3.3159
B2O3	-7.4085	B2O3	-5.8288	B2O3	12.4446
Na2O	14.4113	Na2O	18.7421	Na2O	16.3850
Li2O	20.2462	Li2O	18.9041	Li2O	16.9458
CaO	4.0630	CaO	14.0667	CaO	20.5631
MgO	13.0413	MgO	14.4795	MgO	12.1879
Fe2O3	-3.8672	Fe2O3	-5.6310	Fe2O3	-5.5866
Al2O3	-30.2543	Al2O3	-31.3808	Al2O3	-37.6244
ZrO2	-9.6787	ZrO2	-10.2112	ZrO2	-10.3597
Others	2.2841	Others	2.6523	Others	-19.0889
Al2O3 x Al2O3	65.9792	Al2O3 x Al2O3	94.0252	B2O3 x CaO	-119.8254
B2O3 x B2O3	84.1979	B2O3 x B2O3	76.9459	Na2O x CaO	-120.7020
MgO x Al2O3	-107.5930	MgO x Al2O3	-134.7076	Li2O x MgO	165.6870
B2O3 x CaO	-83.6549	B2O3 x CaO	-94.6921	MgO x Al2O3	-153.5615
		Na2O x CaO	-81.9280	MgO x Others	-104.2277
		Na2O x Al2O3	-43.3511	Fe2O3 x Al2O3	82.5595
		Fe2O3 x Al2O3	75.9884	Al2O3 x Al2O3	99.7873
				Others x Others	224.4631
R^2	= .8801	R^2	= .9001	R^2	= .9058
R^2(ADJ)	= .8658	R^2(ADJ)	= .8850	R^2(ADJ)	= .8906
R^2(PRESS)	= .8421	R^2(PRESS)	= .8621	R^2(PRESS)	= .8649

TABLE 12.14. Candidate Scheffé Second-Order Models Using Mass Fractions for PCT ln(Sodium) Release

Model #1		Model #2		Model #3	
Terms	Coefficients	Terms	Coefficients	Terms	Coefficients
SiO2	-2.5180	SiO2	-2.5768	SiO2	-1.7652
B2O3	-9.8368	B2O3	-10.5462	B2O3	-10.4721
Na2O	19.8630	Na2O	15.2841	Na2O	12.5007
Li2O	20.0227	Li2O	4.5529	Li2O	7.5967
CaO	-1.6743	CaO	7.5329	CaO	8.5246
MgO	11.6129	MgO	-30.2283	MgO	-17.0361
Fe2O3	-3.4063	Fe2O3	-1.3070	Fe2O3	-2.8512
Al2O3	-39.3089	Al2O3	-34.6467	Al2O3	-32.6424
ZrO2	-11.5920	ZrO2	-9.2165	ZrO2	16.1412
Others	1.3827	Others	2.4961	Others	0.7069
Al2O3 x Al2O3	92.9406	SiO2 x MgO	75.0612	Al2O3 x Al2O3	89.9973
B2O3 x B2O3	82.4463	B2O3 x CaO	-77.1027	B2O3 x B2O3	94.9874
		Na2O x Li2O	126.1367	Na2O x Li2O	152.3524
		B2O3 x B2O3	98.2860	B2O3 x CaO	-96.6209
		Li2O x MgO	133.3324	SiO2 x MgO	57.6768
		Al2O3 x Al2O3	81.6175	SiO2 x ZrO2	-53.2743
				Li2O x Al2O3	-86.3851
R^2	= .8980	R^2	= .9197	R^2	= .9238
R^2(ADJ)	= .8879	R^2(ADJ)	= .9084	R^2(ADJ)	= .9123
R^2(PRESS)	= .8708	R^2(PRESS)	= .8888	R^2(PRESS)	= .8924

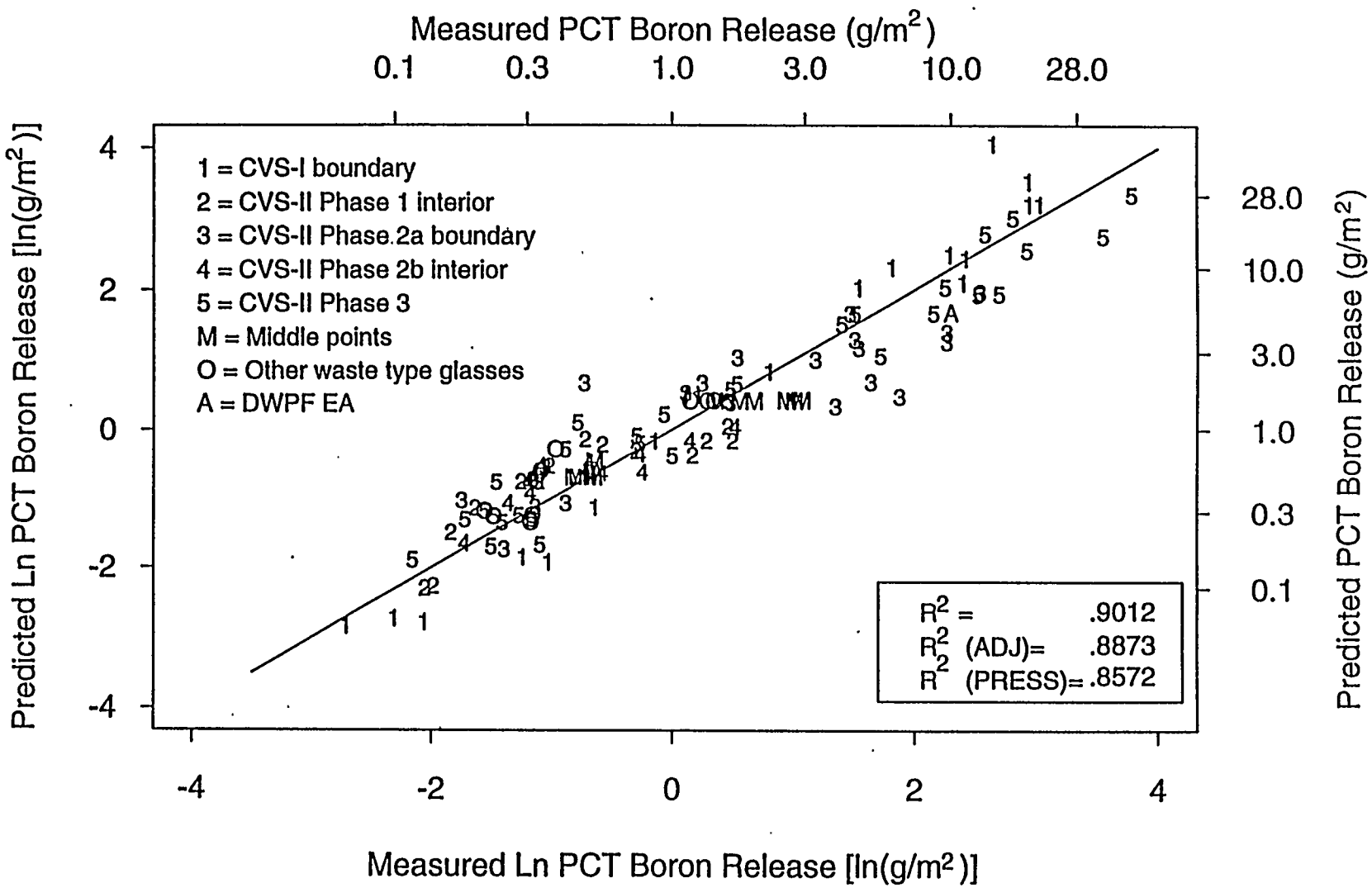

FIGURE 12.9. Predicted Versus Measured PCT B Release for the Second-Order Mixture Model #2 (from Table 12.11)

12.8 VALIDATION OF FIRST- AND SECOND-ORDER MODELS FOR PCT RELEASES

The CVS-II Phase 3 data were used to validate the first- and second-order Scheffé mixture models (based on mass fractions) for normalized PCT B release developed using data through the end of CVS-II Phase 2. These models were reported in an earlier version of this report, but for convenience they are listed in Table 12.15. (Recall that validation involves using data that was not used to fit the models to assess their predictive performance--see Section 6.1.6.) For other properties (viscosity, electrical conductivity, and transition temperature), historical data were also used to validate models. However, the PCT is a relatively new test and the historical data base used did not contain PCT data. PCT data that could be used for validating CVS models were obtained from SRTC, but time was insufficient to complete the validation and include the results in this report. The results of the validation investigation using CVS-II Phase 3 data are discussed in the following paragraphs.[a]

Figures 12.10, 12.11a, 12.11b, and 12.11c contain the validation results using the CVS-II Phase 3 data for the first-order and three candidate second-order models (using mass fractions) for normalized PCT B release. These figures contain plots of the predicted versus measured PCT B release values together with a superimposed 45° line that represents perfect prediction. The error bars on the plotted points represent 95% two-sided prediction intervals for the predicted PCT B values. If the error bars for a given point overlap the 45° line, the model is validated for that point, in the sense that no statistically significant difference exists between the predicted and measured values after accounting for the uncertainties in the predicted and measured values. Various plotting symbols are used in Figures 12.10, 12.11a, 12.11b, and 12.11c to identify the specific nature of some of the CVS-II Phase 3 points. Points that are not otherwise specifically identified are plotted with a "5" as the plotting symbol.

(a) It would also be possible to use CVS-II Phase 4 data to validate PCT models developed from data up through CVS-II Phase 3. However, the CVS-II Phase 4 data were not available in time to include such validation work in the report.

TABLE 12.15. First-Order Model and Three Candidate Second-Order Models Using Mass Fractions for PCT ln(Boron) Release Fitted to CVS-I and CVS-II Phase 1 and 2 Data[a]

First-Order Model		Three Candidate Second-Order Models: Model #1		Model #2		Model #3	
Terms	Coefficients	Terms	Coefficients	Terms	Coefficients	Terms	Coefficients
SiO2	-3.4520	SiO2	-2.5087	SiO2	-2.2717	SiO2	-2.1186
B2O3	10.5302	B2O3	-16.5500	B2O3	-17.3413	B2O3	-28.1878
Na2O	15.2856	Na2O	13.1692	Na2O	15.8287	Na2O	15.6606
Li2O	18.6680	Li2O	19.1440	Li2O	20.5960	Li2O	20.2263
CaO	-8.9534	CaO	-9.3952	CaO	-9.5700	CaO	-8.4922
MgO	10.9238	MgO	-48.2284	MgO	-41.8317	MgO	-36.0019
Fe2O3	-2.2142	Fe2O3	2.2885	Fe2O3	1.1134	Fe2O3	2.0287
Al2O3	-26.1028	Al2O3	-33.3525	Al2O3	-35.1342	Al2O3	-19.0994
ZrO2	-8.6732	ZrO2	-11.1879	ZrO2	-5.3533	ZrO2	-4.1143
Others	1.6666	Others	16.1779	Others	6.6125	Others	6.7180
		B2O3 x B2O3	128.3213	B2O3 x B2O3	120.4075	B2O3 x B2O3	166.5814
		SiO2 x MgO	115.4480	SiO2 x MgO	103.6567	SiO2 x MgO	93.5007
		Al2O3 x Al2O3	113.0015	Al2O3 x Al2O3	113.1687		
		B2O3 x Others	-75.6968				
		Na2O x ZrO2	69.1946				
R^2	= .7776	R^2	= .8838	R^2	= .8640	R^2	= .8472
R^2(ADJ)	= .7485	R^2(ADJ)	= .8584	R^2(ADJ)	= .8393	R^2(ADJ)	= .8221
R^2(PRESS)	= .6994	R^2(PRESS)	= .8073	R^2(PRESS)	= .7939	R^2(PRESS)	= .7790
LOF?[b]	Yes (>99%)		Yes (>99%)		Yes (>99%)		Yes (>99%)

(a) Although PCT testing was performed the radioactive glasses CVS2-53 and CVS2-54, the data were not used in fitting the models.

(b) A statistical F-test for lack-of-fit (LOF) was performed using the estimates of experimental variation obtained from four replicate tests. "Yes" and "No" entries indicate whether the LOF was statistically significant at a 90% confidence level. The actual confidence level at which a LOF can be declared significant is given in parentheses following the "Yes" or "No" for each model.

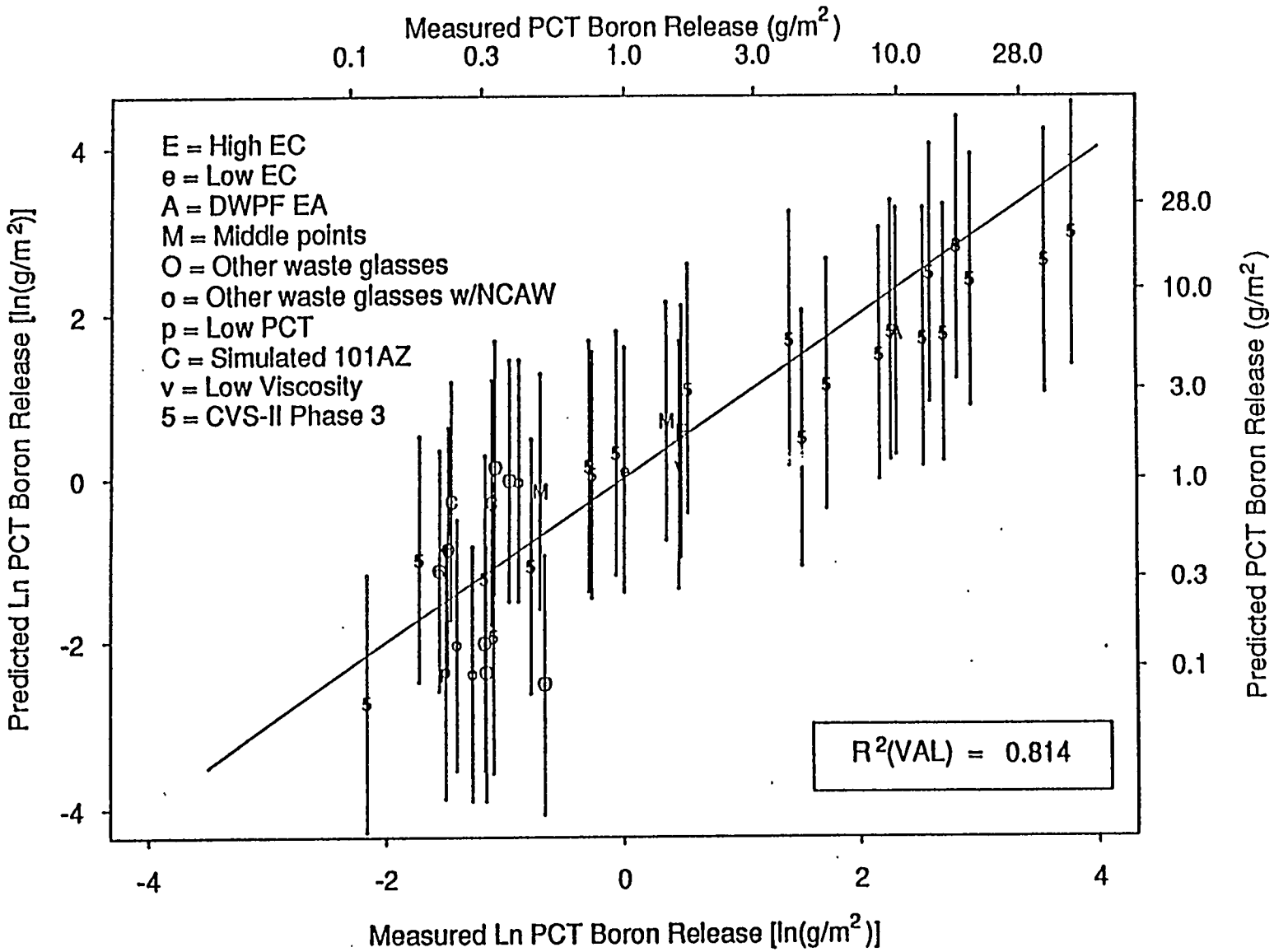

FIGURE 12.10. Predicted Normalized PCT Boron Release from the First-Order Mixture Model After CVS-II Phase 2 (from Table 12.15) Versus Measured PCT Boron Releases (from Table 12.9) for the CVS-II Phase 3 Data

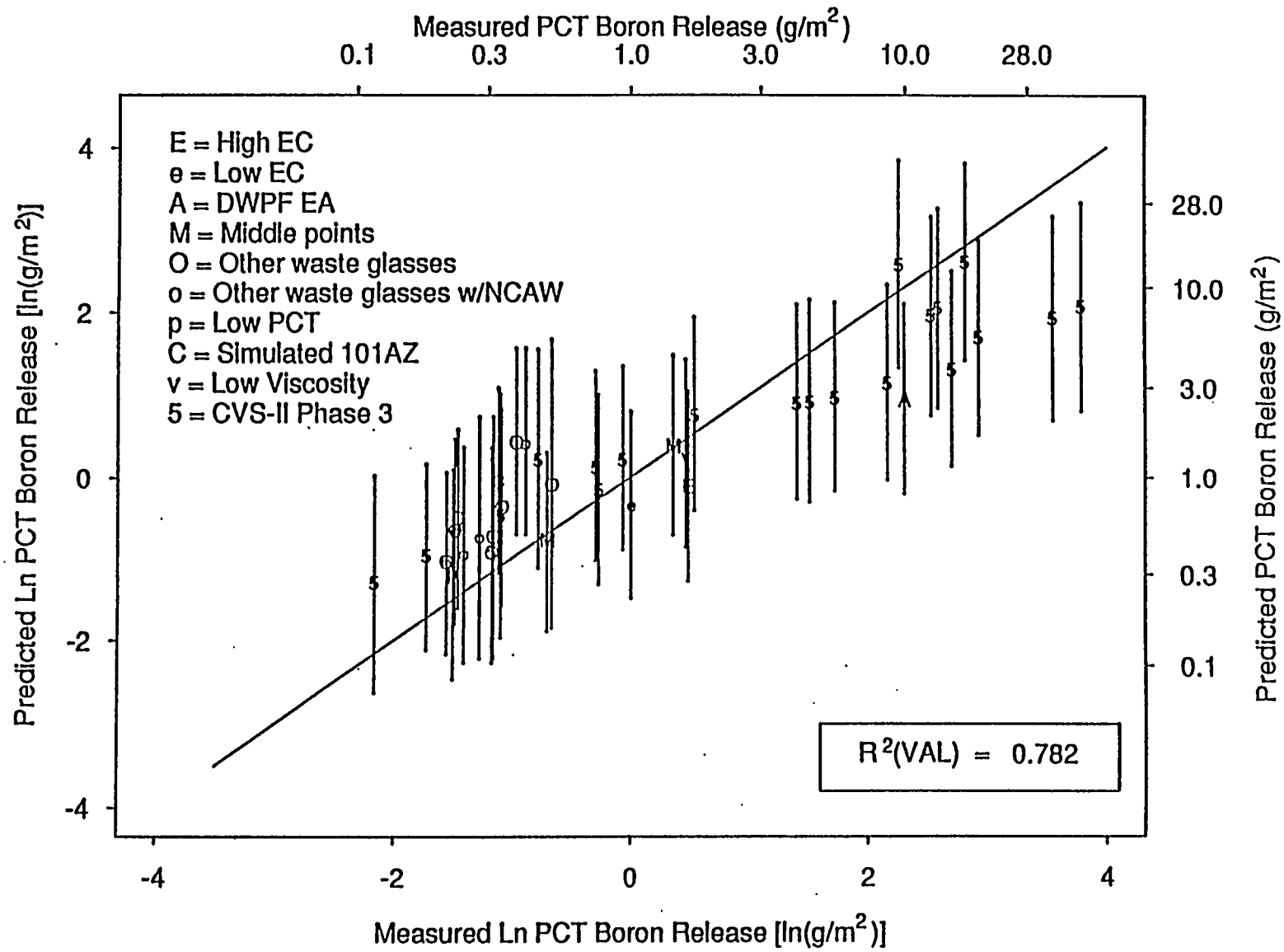

FIGURE 12.11a. Predicted Normalized PCT Boron Release from the Second-Order Mixture Model #1 After CVS-II Phase 2 (from Table 12.15) Versus Measured PCT Boron Releases (from Table 12.9) for the CVS-II Phase 3 Data

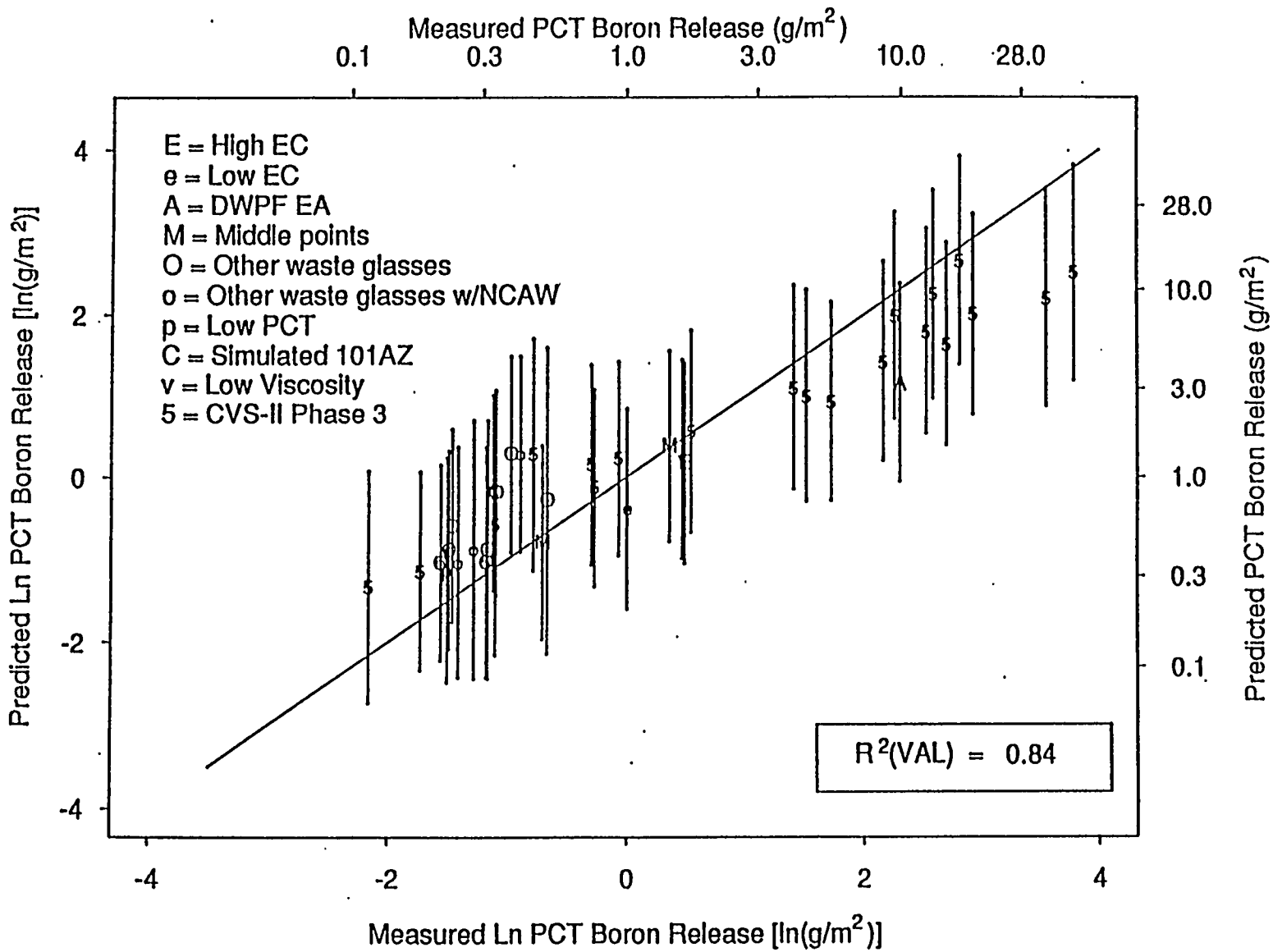

FIGURE 12.11b. Predicted Normalized PCT Boron Release from the Second-Order Mixture Model #2 After CVS-II Phase 2 (from Table 12.15) Versus Measured PCT Boron Releases (from Table 12.9) for the CVS-II Phase 3 Data

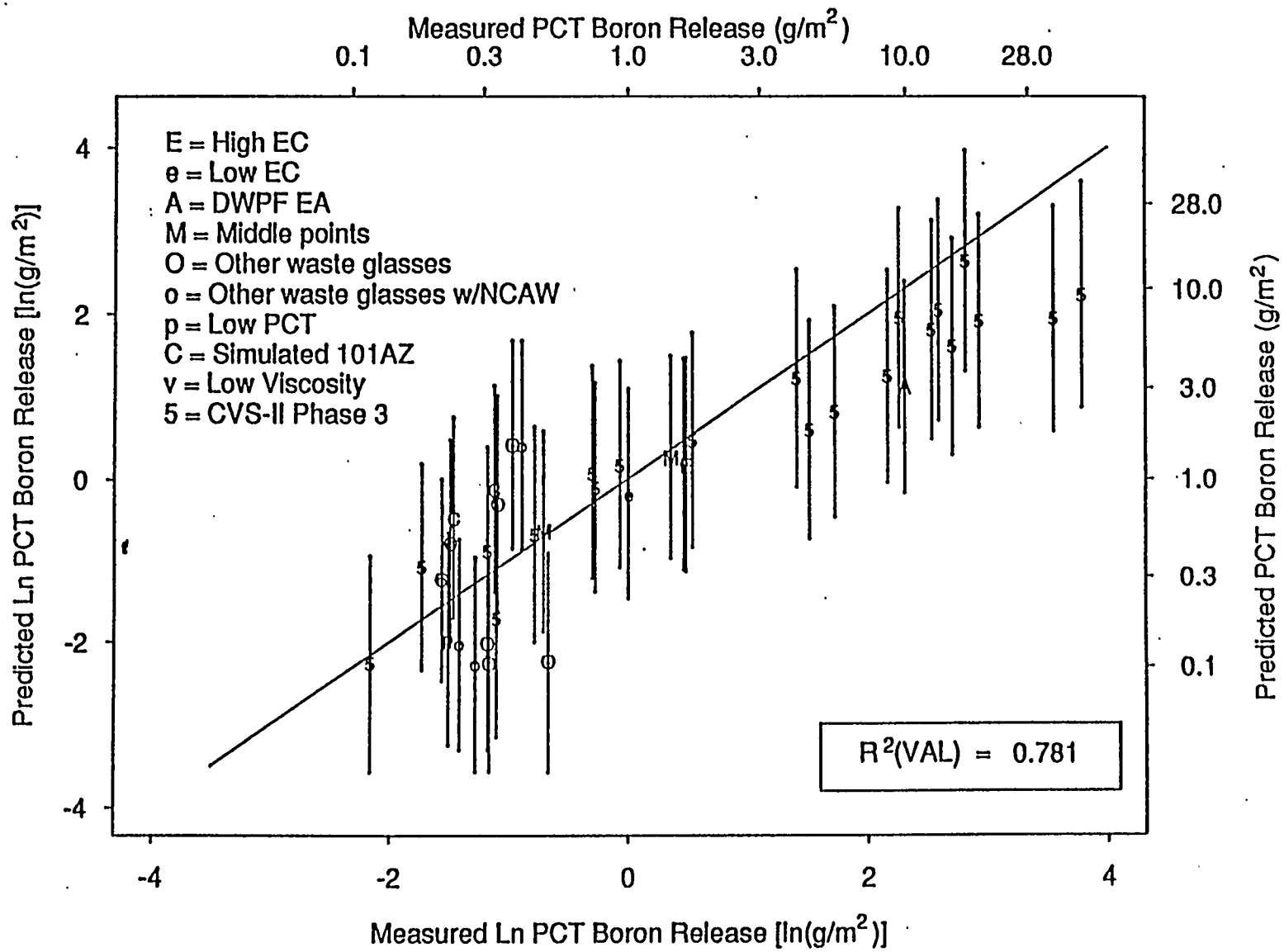

FIGURE 12.11c. Predicted Normalized PCT Boron Release from the Second-Order Mixture Model #3 After CVS-II Phase 2 (from Table 12.15) Versus Measured PCT Boron Releases (from Table 12.9) for the CVS-II Phase 3 Data

Figure 12.10 shows that the first-order PCT B release model is validated for nearly all of the CVS-II Phase 3 data points, although the wide error bars contribute to this. The first-order model appears to slightly underpredict larger values of PCT B release (> 3.0 g/m^2) for the CVS-II Phase 3 data.

Figures 12.11a, 12.11b, and 12.11c show that the three candidate second-order models are also validated reasonably well for the CVS-II Phase 3 data, in spite of smaller prediction uncertainties than those of the first-order model. Overlaying Figures 12.11a, 12.11b, and 12.11c on Figure 12.10 shows that some predictions from the second-order models are better than from the first-order model, some are worse, and many are only minimally changed. The extra second-order terms in models #2 and #1 (compared to the first-order model and second-order model #3) appear to reduce the scatter of predictions for glasses with PCT B release below 0.5 - 1.0 g/m^2. The R^2(VAL) values (see Section 6.1.6) for the three second-order PCT B release models range from slightly smaller to slightly larger than the R^2(VAL) for the first-order PCT B release model. These results suggest that possibly only second-order model #2 provides better predictive performance than the first-order model, at least for the CVS-II Phase 3 data. It should be recalled that the CVS-II Phase 3 data is not an ideal validation data set, because it is not uniformly spread over the full CVS composition region. Part of the goal of CVS-II Phase 3 was to collect data for more extreme compositions and property values than had been obtained previously. This is a potential reason why the second-order models did not (as a group) predict any better than the first-order model for these data. However, the fact that the first-order model yielded R^2(VAL) = 0.814 in spite of these aspects of the CVS-II Phase 3 data indicates that it is a fairly good model.

12.9 OTHER MODEL FORMS INVESTIGATED FOR PCT RELEASES

Another approach for modeling PCT elemental release was considered based on a similar approach for viscosity that was included in a November 1992 draft report, "Statistical Analysis of Viscosity Composition Data", submitted to the Savannah River Technical Center, by Dolun Oksoy of Alfred University (see

Section 7.6.2). Based on this approach, a model for PCT B release of the form

$$\ln(PCT\ B) = \sum_{i=1}^{9} b_i (x_i / SiO_2) + b_{10}(B_2O_3 / SiO_2)^2 \qquad (12.1)$$

was investigated, where x_i is either the mass or mole fraction of the i-th oxide component (excluding SiO_2), b_i is the coefficient corresponding to the first-order term involving x_i/SiO_2, and b_{10} is the coefficient corresponding to the quadratic term $(B_2O_3/SiO_2)^2$. This model could be applied to any PCT (or even MCC-1) elemental release, but attention was focused on PCT B release to see if additional attention was warranted for this model form.

Mass and mole fraction versions of model (12.1) were fitted to normalized PCT B release values for 123 CVS-I and CVS-II Phases 1, 2, and 3 glasses (the result for CVS2-101 was not available at the time of this work). The model coefficients are given in Table 12.16. The predicted versus measured plots of normalized PCT B release for the mass and mole fraction versions of (12.1) are given in Figures 12.12a and 12.12b.

The R^2, R^2(ADJ), and R^2(PRESS) values for the mass and mole fraction versions of (12.1) are given in Table 12.17 along with the values for the mass and mole fraction versions of the first-order mixture model discussed in Section 12.5. The predicted versus measured plots for the mass and mole fraction versions of (12.1) in Figures 12.12a and 12.12b may be compared to the corresponding first-order mixture model plots in Figures 12.7a and 12.7b. Comparison of these plots and the various R^2 values indicates that the model form (12.1) does not fit the CVS data any better than the first-order mixture model.

12.10 FIRST-ORDER MODELS AND COMPONENT EFFECTS FOR PCT AND MCC-1 SOLUTION pH

Solution pH is a fundamental factor that affects glass dissolution rate. In static tests (e.g., MCC-1 and PCT), pH is an indicator of durability, and is affected by the glass surface area to volume ratio of the durability test. Models for MCC-1 and PCT pH data from CVS glasses will help reveal the effects of composition and test method (MCC-1 or PCT) on solution pH, and hence, on

TABLE 12.16. Coefficients for Mass and Mole Fraction Versions of Alfred University "Ratio to SiO_2" Model for Normalized PCT B Release

Variable	Mass Fractions	Mole Fractions
Intercept	-1.035265	-1.005813
B_2O_3/SiO_2	-0.787584	-0.936271
Na_2O_3/SiO_2	8.440505	8.703721
Li_2O/SiO_2	9.911421	4.942952
CaO/SiO_2	-4.716429	-4.422127
MgO/SiO_2	4.608401	3.076100
Fe_2O_3/SiO_2	-2.311685	-6.184310
Al_2O_3/SiO_2	-12.780182	-21.748324
ZrO_2/SiO_2	-6.003842	-12.362880
$Others/SiO_2$	-0.384759	-1.731038
$(B_2O_3/SiO_2)^2$	12.723930	17.131328

TABLE 12.17. R^2 Values for the Alfred University "Ratio to SiO_2" Model and the CVS First-Order Mixture Model for Normalized PCT Boron Release Using Mass and Mole Fractions

PCT Model	Mass or Mole Fractions	R^2	R^2(ADJ)	R^2(PRESS)
Alfred Univ. "Ratio to SiO_2"	Mass	.8075	.7903	.7630
	Mole	.8078	.7906	.7632
First-Order Mixture	Mass	.8114	.7964	.7715
	Mole	.8057	.7903	.7644

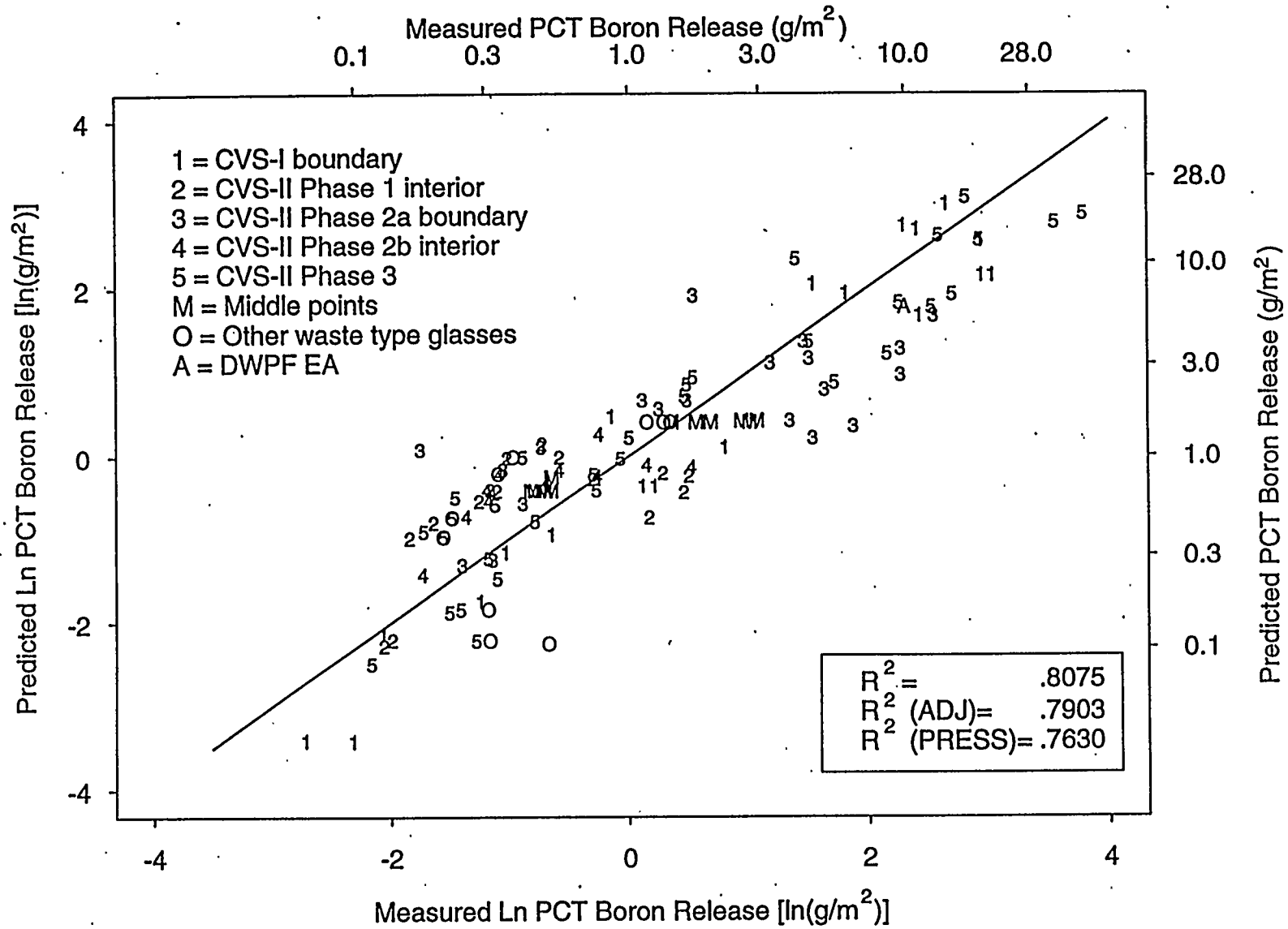

FIGURE 12.12a. Predicted Versus Measured PCT B Release for the Alfred University "Ratio to SiO_2" Model Using Mass Fractions

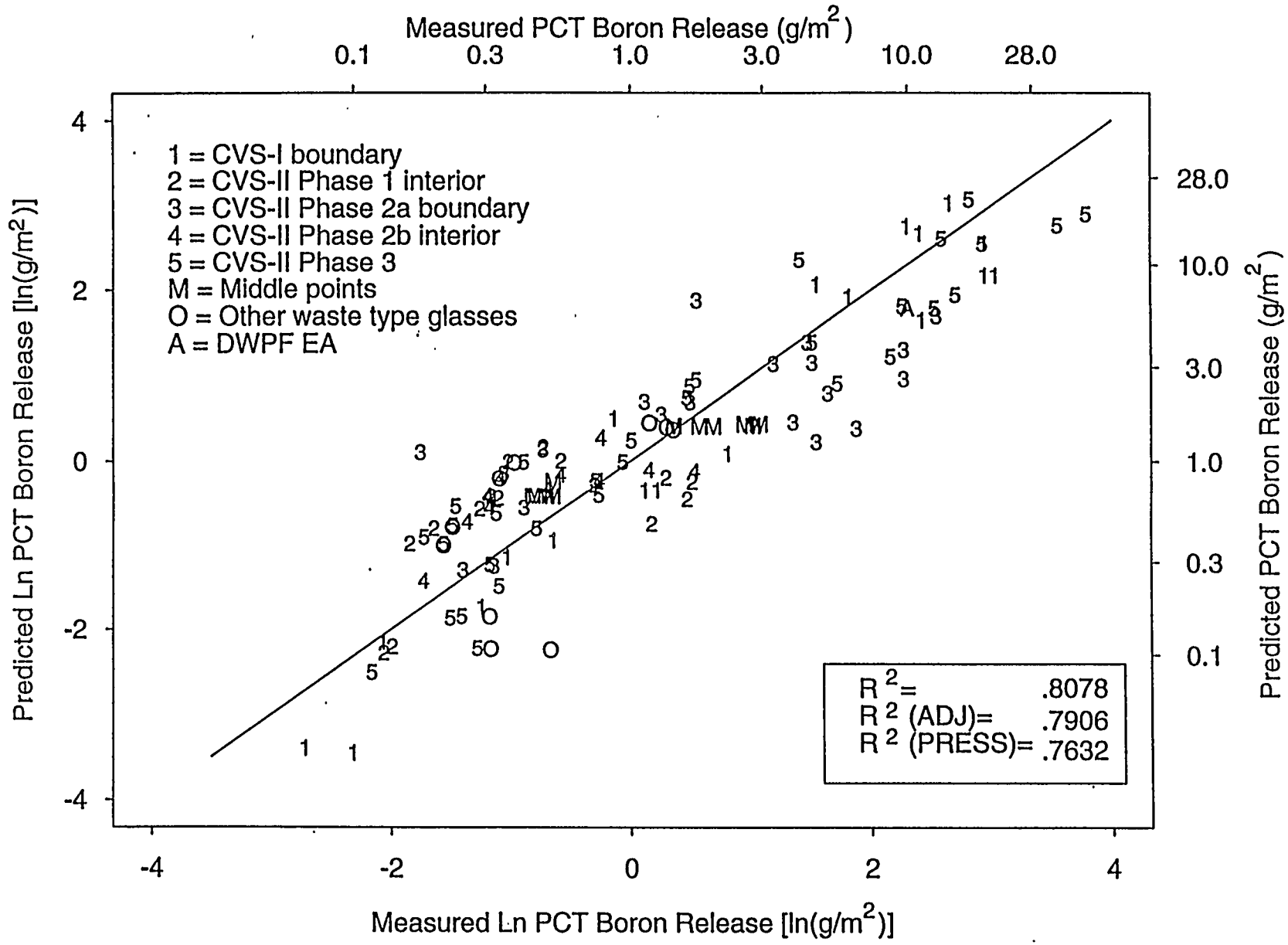

FIGURE 12.12b. Predicted Versus Measured PCT B Release for the Alfred University "Ratio to SiO_2" Model Using Mole Fractions

glass dissolution rate. Also, durability models based on a priori assumptions about glass dissolution mechanisms based on composition (e.g., hydration energy model) use pH corrections (see Appendix H). For these reasons, the collection, study, and modeling of MCC-1 and PCT pH data is of interest and important.

First-order mixture models of the form (6.1) using both mass and mole fractions were fitted to the averaged MCC-1 and PCT solution pH values listed in Table 12.1 (MCC-1) and in Table 12.9 (PCT). Data for all CVS-I and CVS-II Phase 1, 2, and 3 glasses except CVS2-101 were used in developing the PCT pH first-order mixture models. Data for all CVS-I and CVS-II Phase 1, 2, and 3 glasses (except the two radioactive glasses CVS2-53 and CVS2-54, CVS1-15, and CVS2-101) were used in developing the MCC-1 pH first-order models. The MCC-1 test was not performed on the radioactive glasses. The CVS1-15 MCC-1 pH value was the largest observed in the data set, and stood out as a significant outlier when it was included in fitting the first-order model. Hence, the MCC-1 pH models were fitted without that data point. The MCC-1 and PCT pH data for CVS2-101 were not available at the time the models were fit, and so were not used. The coefficients and goodness-of-fit statistics for the MCC-1 and PCT pH first-order models are given in Table 12.18.

The R^2 statistics for the MCC-1 and PCT pH first-order models shown in Table 12.18 indicate that the mole fraction versions of the models fit the data about the same as the mass fraction versions. The R^2 statistics also indicate that the PCT pH models (mass and mole fraction versions) fit fairly well (over 90% of the variability in the PCT pH data is accounted for), but that the MCC-1 pH models do not fit as well (only about 75% of the variability in the MCC-1 pH data is accounted for). The plots of predicted versus measured pH values are given in Figure 12.13a (MCC-1 mass fractions), Figure 12.13b (MCC-1 mole fractions), Figure 12.14a (PCT mass fractions), and Figure 12.14b (PCT mole fractions). These predicted versus measured plots confirm that there is room for improvement on the MCC-1 and PCT pH first-order models. No evidence of biased predictions is found in Figures 12.13a, 12.13b, 12.14a or 12.14b, except possibly in underpredicting the very largest values. There is some scatter in Figures 12.14a and 12.14b (PCT pH), with considerably more

TABLE 12.18. Coefficients and Goodness of Fit Statistics for First-Order Mixture Models (Using Mass and Mole Fractions) Fitted to pH Data from MCC-1 and PCT Tests[a]

Component	MCC-1 pH		PCT pH	
	Mass Fractions	Mole Fractions	Mass Fractions	Mole Fractions
SiO_2	7.3414	7.4906	8.1926	8.3851
B_2O_3	9.1180	9.0435	3.3332	2.7418
Na_2O	17.8061	17.5280	23.6171	23.1901
Li_2O	24.4490	16.5150	31.2448	20.1349
CaO	13.3174	12.8219	17.2056	16.1830
MgO	13.1459	11.8995	15.3354	13.5105
Fe_2O_3	10.1817	11.0900	8.5939	5.7790
Al_2O_3	4.0454	0.7704	5.3578	2.1983
ZrO_2	7.5917	5.7380	7.6111	4.7502
Others	8.6750	7.4352	9.2689	7.2951
# points[a]	120	120	123	123
R^2[b]	0.7487	0.7455	0.9092	0.9042
R^2(ADJ)[b]	0.7281	0.7246	0.9020	0.8965
R^2(PRESS)[b]	0.6810	0.6788	0.8863	0.8801
LOF?[c]	Yes (99%)	Yes (99%)	Yes (93.2%)	Yes (94.6%)

(a) First-order mixture models were fitted to average pH values calculated from the duplicate dissolution tests of each type (MCC-1 and PCT). All CVS-I and CVS-II Phase 1, 2, and 3 data for MCC-1 (from Table 12.1) and PCT (Table 12.9) were used with the following exceptions. The CVS2-101 data were not available at the time the models were fit for MCC-1 or PCT. For MCC-1, tests were not performed on the radioactive glasses CVS2-53 and CVS2-54, and glass CVS1-15 had an outlying pH value. Hence, these glasses were not used to fit the MCC-1 pH models.

(b) R^2, R^2(ADJ), and R^2(PRESS) statistics take values between 0.0 and 1.0, and provide different measures of the proportion of variation in the property data accounted for by a fitted model. See Section 6.1.5 for the definitions of these statistics.

(c) A statistical F-test for lack-of-fit (LOF) was performed using the estimates of experimental variation obtained from four replicate tests. "Yes" and "No" entries indicate whether the LOF was statistically significant at a 90% confidence level. The actual confidence level at which a LOF can be declared significant is given in parentheses following the "Yes" or "No" for each model.

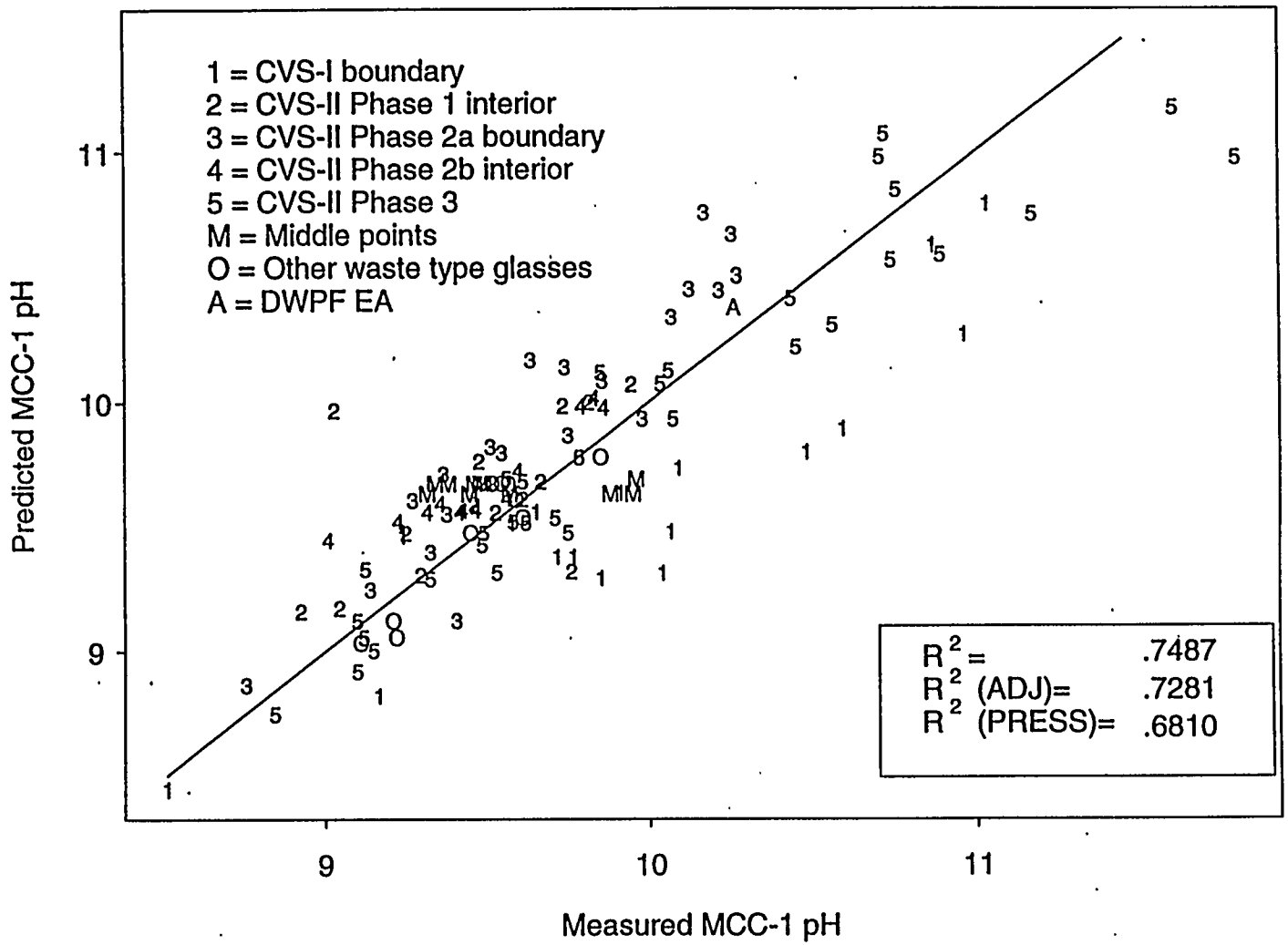

FIGURE 12.13a. Predicted Versus Measured MCC-1 pH for the First-Order Mixture Model Using Mass Fractions (from Table 12.18)

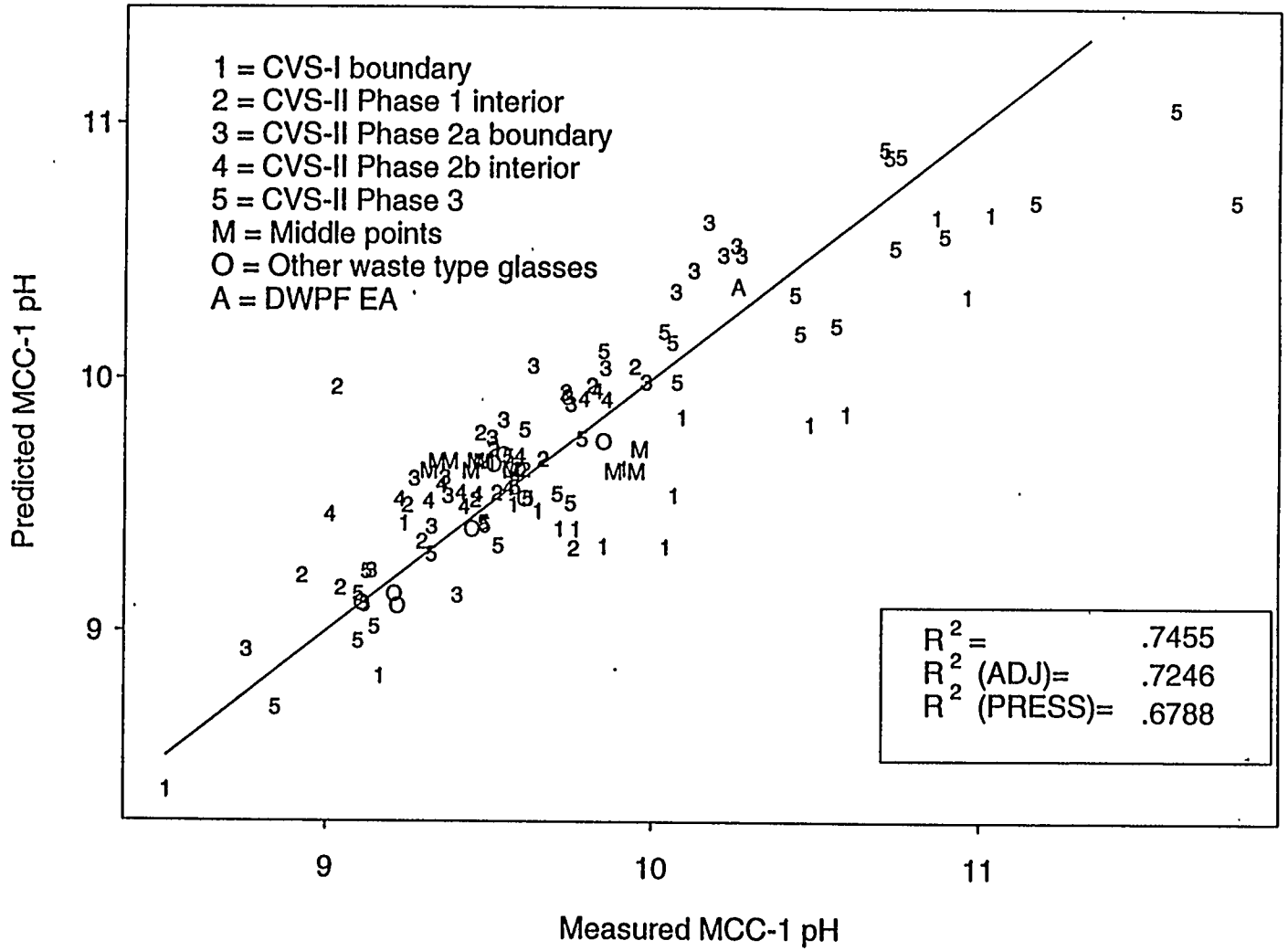

FIGURE 12.13b. Predicted Versus Measured MCC-1 pH for the First-Order Mixture Model Using Mole Fractions (from Table 12.18)

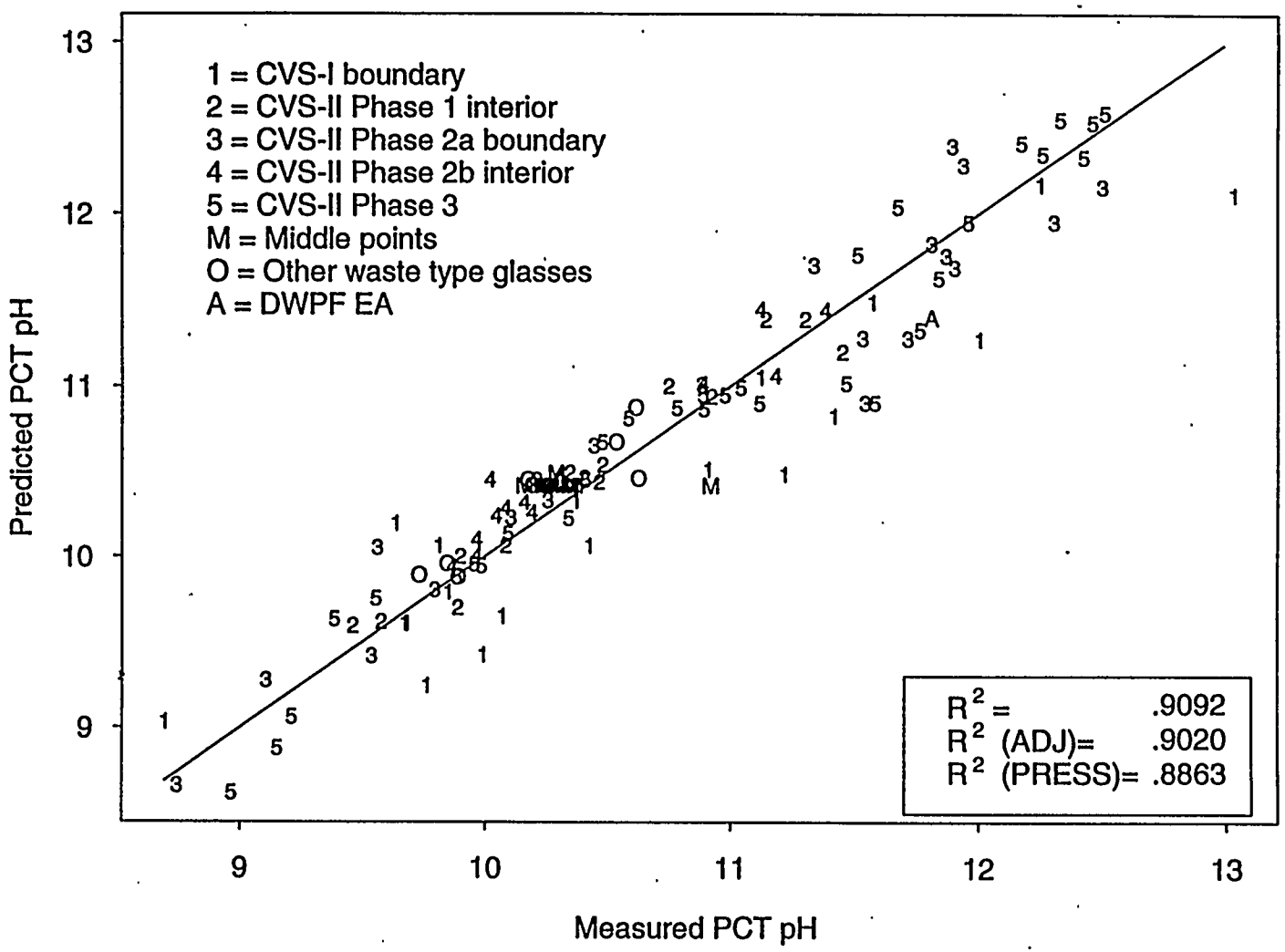

FIGURE 12.14a. Predicted Versus Measured PCT pH for the First-Order Mixture Model Using Mass Fractions (from Table 12.18)

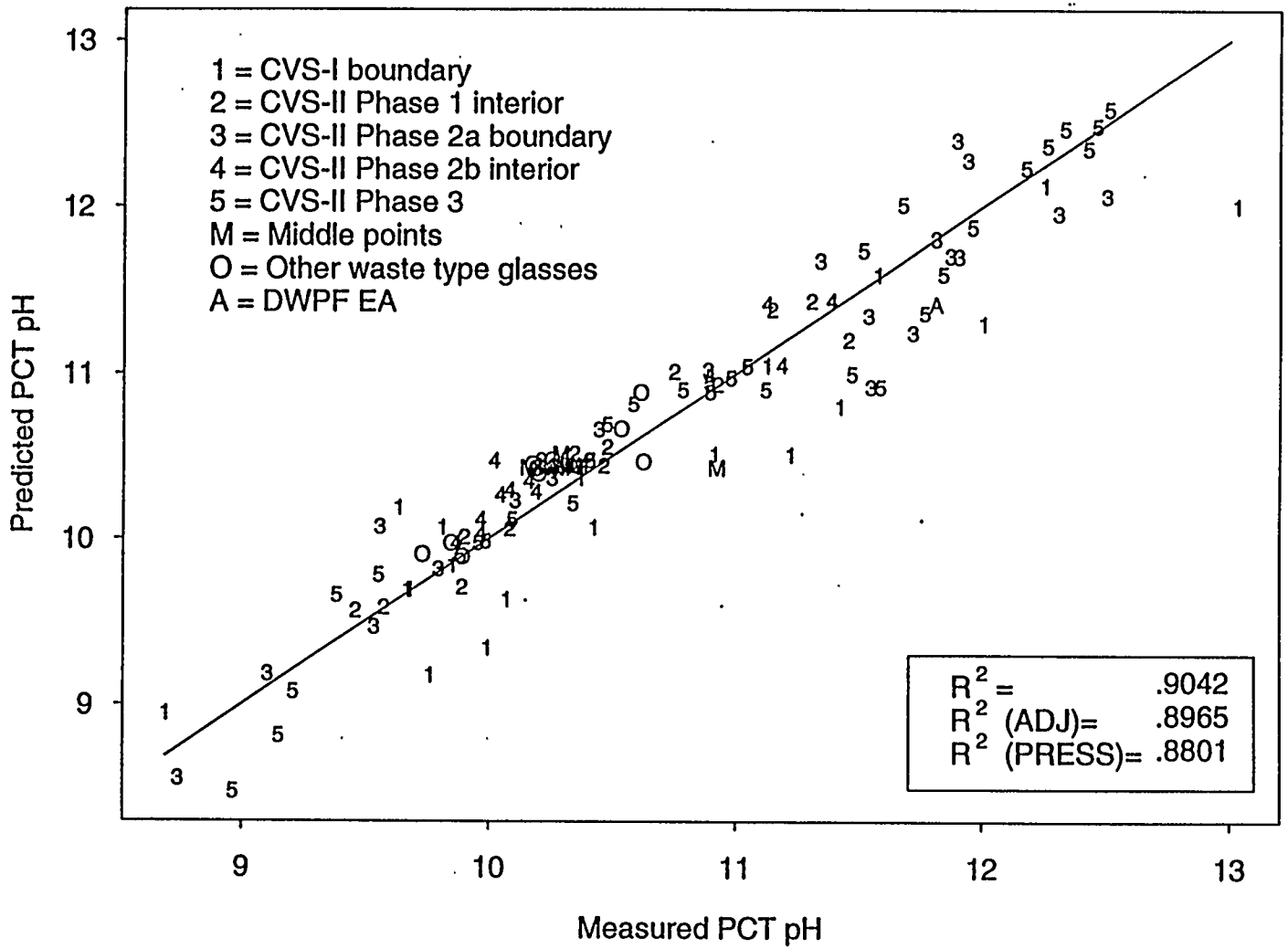

FIGURE 12.14b. Predicted Versus Measured PCT pH for the First-Order Mixture Model Using Mole Fractions (from Table 12.18)

scatter in Figures 12.13a and 12.13b (MCC-1 pH). Statistical tests for model lack-of-fit (LOF) (see Section 6.1.5) indicate that the MCC-1 and PCT pH first-order mixture models have statistically significant LOFs (at greater than 99% confidence for MCC-1 pH, and greater than 93% confidence for PCT pH). Model validation has not been performed on these models, so their predictive ability for data not used to fit them is unknown.

The component effects plots for the MCC-1 and PCT pH first-order mixture models using mass fractions are given in Figures 12.15 and 12.16. Only the single-component constraints and not the stand-in crystallinity constraints in Tables 4.2 and 4.6 were used to limit the effects plot (both were used in previous effects plots). As a result, effects are evaluated over wider ranges than in the past for several components involved in the stand-in constraints (most notably Al_2O_3 and SiO_2). Figure 12.15 indicates that MCC-1 solution pH is predicted to be: (1) increased the most by Li_2O and Na_2O, with CaO and MgO having lesser but still significant effects, (2) decreased the most by Al_2O_3, SiO_2, and ZrO_2, and (3) little affected by B_2O_3, Others, and Fe_2O_3. Figure 12.16 indicates that PCT pH is predicted to be: (1) increased the most by Li_2O and Na_2O, with MgO and CaO having lesser but still significant effects, (2) decreased the most by B_2O_3, Al_2O_3, and SiO_2, and (3) slightly to negligibly decreased by ZrO_2, Fe_2O_3, and Others.

The final level of solution pH depends on glass composition and, to even a greater extent, on the glass surface to solution volume ratio (this ratio determines the extent of the initial alkali ion exchange). Therefore, PCT solutions exhibited generally higher levels of pH than MCC-1 solutions. Figure 12.17 plots the first-order model coefficients from MCC-1 pH versus PCT pH. The figure indicates that the higher PCT pHs were mainly due to Na_2O and Li_2O, since the first-order coefficients of those two alkalis are significantly higher for PCT than for MCC-1. As was shown by Feng and Pegg (1994), the initial ion exchange of Na^+ and Li^+, and thus the solution pH, increases as the glass surface area to solution volume ratio increases. Boron oxide, which is also preferentially leached during the initial stage of dissolution, also effects pH in PCT differently than MCC-1. These differences are attributed to a difference in glass surface area to volume of leachant.

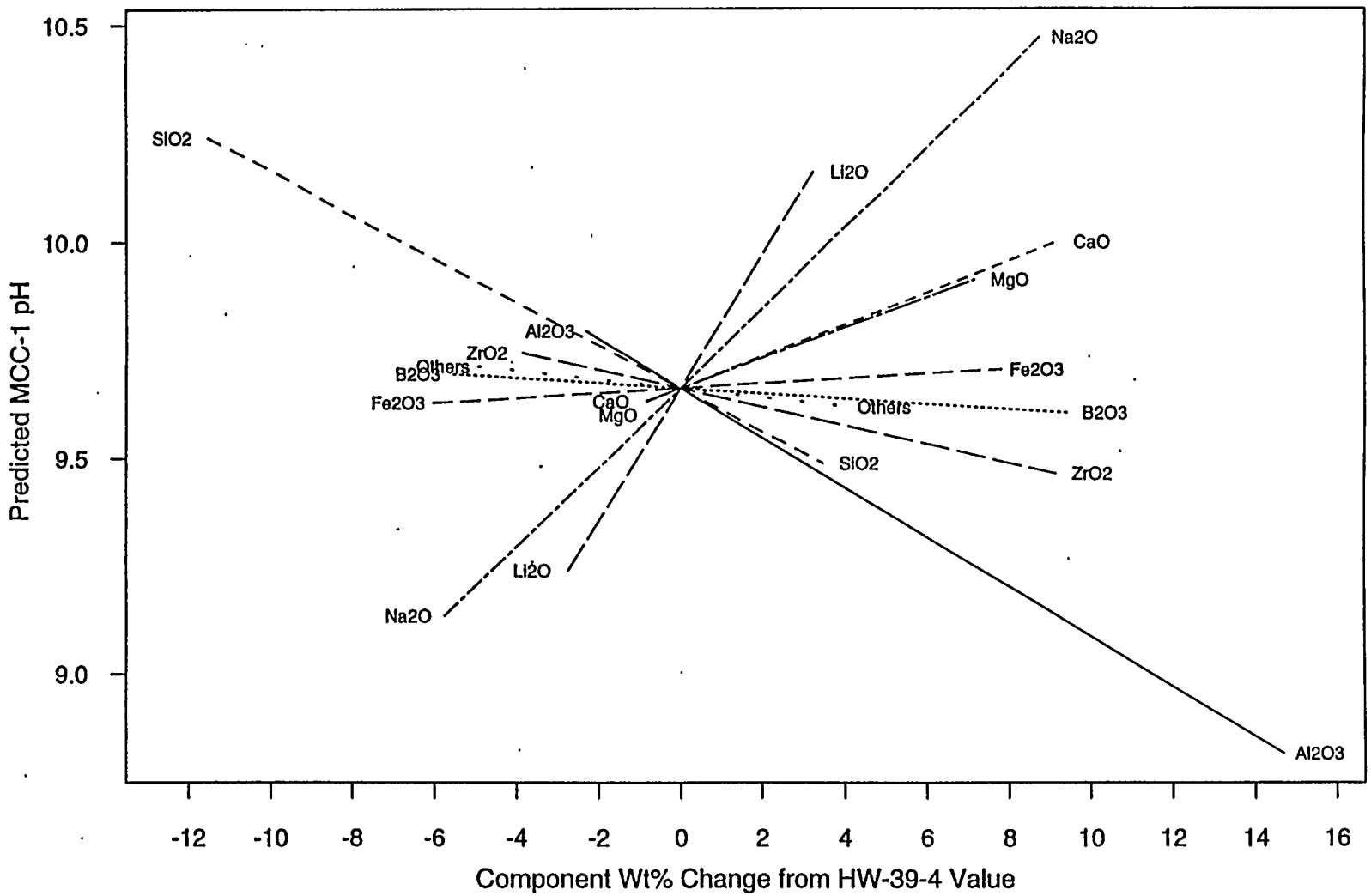

FIGURE 12.15. Predicted Component Effects on MCC-1 pH Relative to the HW-39-4 Composition, Based on the Fitted First-Order Mixture Model Using Mass Fractions

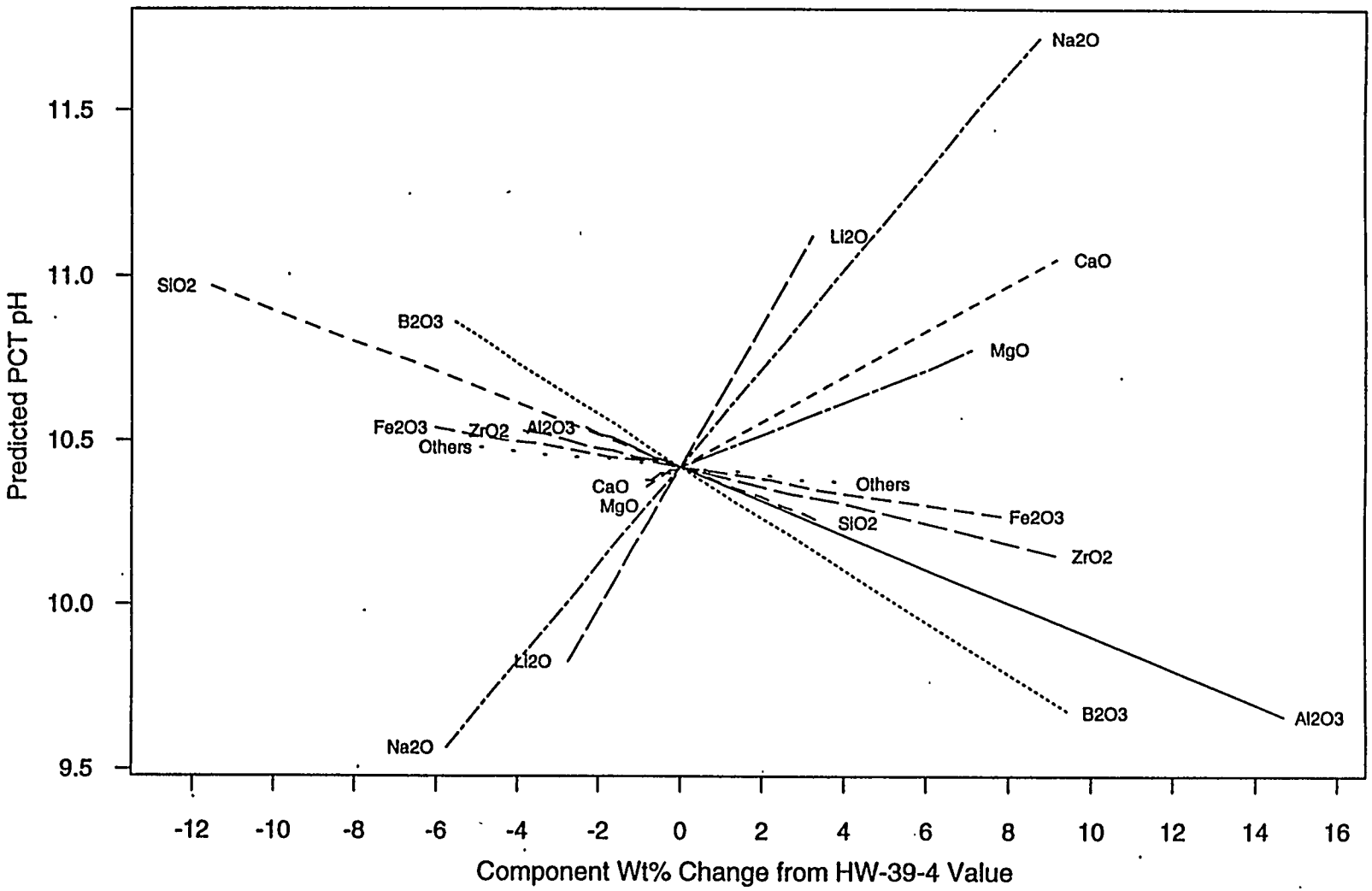

FIGURE 12.16. Predicted Component Effects on PCT pH Relative to the HW-39-4 Composition, Based on the Fitted First-Order Mixture Model Using Mass Fractions

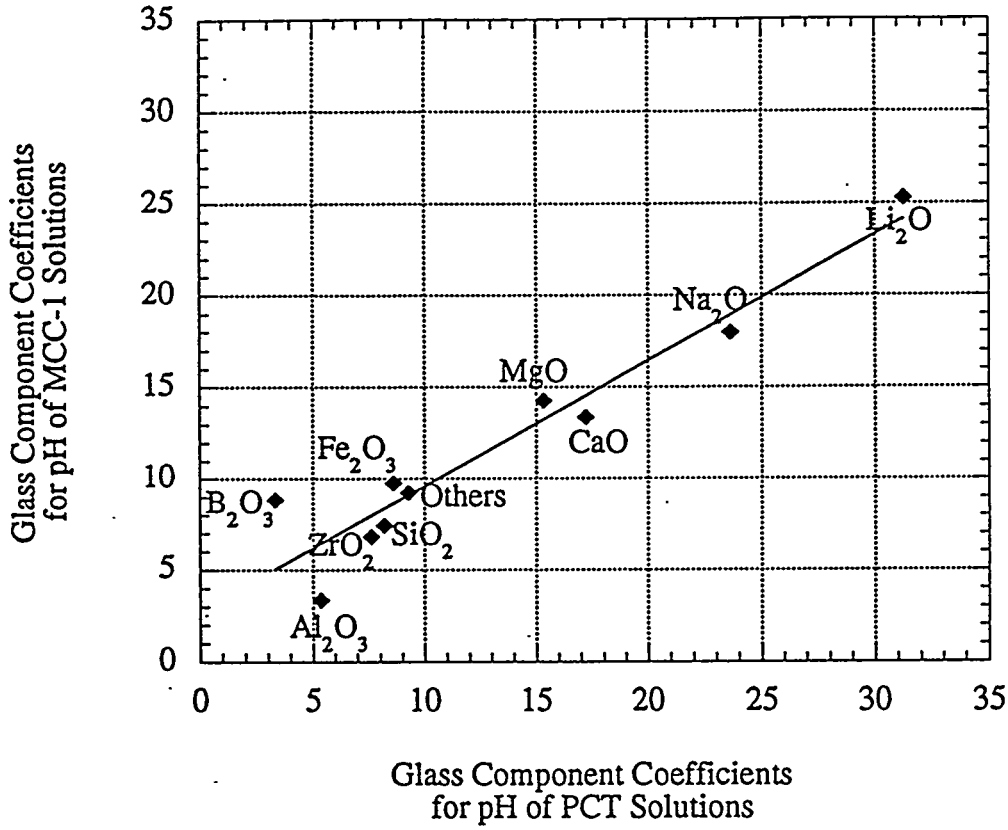

FIGURE 12.17. Coefficients of First-Order Mixture Models Using Mass Fractions for pH of MCC-1 Dissolution Test Solutions Versus for pH of PCT Dissolution Test Solutions

Alkali earth oxides also increase solution pH, but to a lesser extent than Na_2O and Li_2O. Na^+, Li^+, and Ca^{2+} display the common trend of preferential dissolution.

12.11 GLASS DURABILITY DISCUSSION

The following subsections are devoted to the discussion of how individual components affect glass durability, as reflected by normalized elemental releases. Section 12.11.1 discusses these effects as expressed by the first-order coefficients for normalized boron release. (Section 6.3 contains a general discussion of component effects on glass properties.) Section 12.11.2 discusses the CVS-II Phase 4 study in which components were changed one-at-a-time. Section 12.11.3 discusses some individual glass compositions and groups of compositions that exhibit extreme (high or low) durability. Section 12.11.4 discusses anomalous glasses that cannot be fitted by first-order models. Section 12.11.5 deals with normalized releases of elements other than boron.

12.11.1 Component Effects on MCC-1 and PCT Durability

Figure 12.18 plots the first-order mixture model coefficients for MCC-1 normalized boron release versus the coefficients for PCT normalized boron release. Based on Figure 12.18 and the component effects plots in Figures 12.3 and 12.8, the 10 major CVS glass components[(a)] were roughly divided into three groups: components that increase durability (durability risers), components that decrease durability (durability reducers), and components that have little effect (indifferent components). This division is relative, because some of the indifferent components can be viewed as durability risers if more potent risers are absent from (or present in lower mass fractions for) a particular glass. Roughly, durability risers/reducers have component coefficients for normalized boron release significantly lower/higher than that

---

(a) Iron oxide was treated as a single component, namely Fe_2O_3. The Fe(II)/Fe ratio was not specifically addressed as a variable affecting glass durability in CVS. As was shown by S.O. Bates in an 1989 unpublished project report, the Fe(II)/Fe ratio did not exhibit a measurable effect on dissolution of studied glasses over the range from 0 to 0.53. The actual Fe(II)/Fe value for the CVS glasses is within the range 0 to 0.04 (see Section A.4) because iron is added as Fe_2O_3 and no reducing agents are introduced in the batches. However, the Fe(II)/Fe ratio can significantly effect durability of low durability glasses (see Feng et al. 1991) or glasses with high transition metal content.

of SiO_2. Components classified as indifferent have normalized boron release coefficients close to that of SiO_2. The exception to this is that SiO_2 is clearly a durability riser according to Figures 12.3 and 12.8.

The classification of components according to their effects on durability is shown in Table 12.19. Within each classification, components are listed left to right in order of the strength of their effects. Component effects can be dependent on the dissolution test method, as is seen for CaO in Figure 12.18.

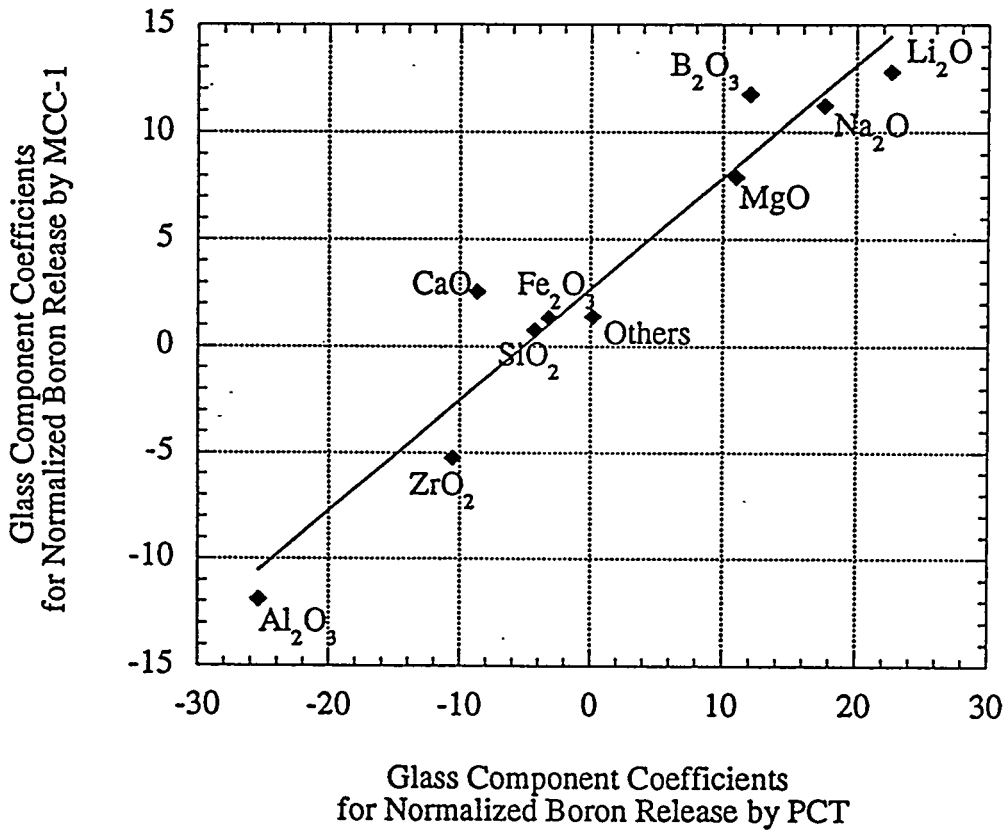

FIGURE 12.18. Plot of MCC-1 Versus PCT Normalized Boron Release First-Order Mixture Model Coefficients

TABLE 12.19. Classification of Individual CVS Glass Components Regarding Their Effects on Glass Durability

Effect	Component
Risers	Al_2O_3, SiO_2, ZrO_2
Indifferent	CaO, Fe_2O_3, Others
Reducers	Li_2O, Na_2O, B_2O_3, MgO

According to the component coefficient values and Figures 12.3 and 12.8, the most powerful durability riser is Al_2O_3. The only additional durability riser according to component coefficient values is ZrO_2, although its effect on the durability of glasses in this composition range is significantly smaller than that of Al_2O_3. This difference holds true on both mass and molar bases, because the molecular masses of ZrO_2 and Al_2O_3 differ by only 20%. Figures 12.3 and 12.8 clearly show that SiO_2 is a durability riser also, so it is included in Table 12.19 as such. Components that display an indifferent effect on durability are CaO, Fe_2O_3, and Others.

The most potent durability reducer on a mass basis is Li_2O. It is very closely followed by Na_2O, B_2O_3, and MgO. Because the molecular mass of Li_2O is less than half of that of Na_2O and B_2O_3, the latter two oxides are more effective durability reducers on a molar basis than Li_2O. PCT durability is reduced by Na_2O less than by Li_2O, and by B_2O_3 less than by Na_2O, but these differences may be within the limits of uncertainty of the models. The alkali and boron oxides are commonly used to control viscosity. Although Li_2O has the strongest effect on durability, it has a stronger effect on viscosity. Hence, Li_2O is the most effective additive for lowering viscosity while maintaining high durability. MgO decreases durability in both durability test methods and is not used to lower glass viscosity. MgO also increased the liquidus temperature for zircon, clinopyroxene, and spinel; therefore, its use as a frit component is undesirable.

12.11.2 Single Component Change Study

Glass dissolution is a complex process that is affected by many factors including glass composition, temperature, aqueous medium, surface area, and time. In general, the dissolution of glass in water follows these stages (Bourcier et al. 1993):

- Ion exchange: The alkali ions in glass (R^+) are replaced by protons (H^+) or hydronium ions (H_3O^+) from the water.
- Selective hydrolysis at NBOs: Non-bridging oxygen (NBO) atoms are attacked by water molecules to form hydrolyzed silica.
- Network hydrolysis: Network bonds are hydrolyzed. The glass forms high surface area gel.
- Precipitation of insoluble components: As the dissolution process continues, the saturation limit of soluble species (such as silicic acid) may be reached. These components then precipitate on the glass or container surface through nucleation and growth.

Ion exchange occurs as the dissolution begins. As the concentration of alkalis in solution and the diffusion distances increase, ion exchange slows and eventually reaches the glass dissolution rate. Hydrolysis occurs at easily attacked NBOs at the onset of ion exchange. This process is slower than ion exchange at the beginning of the dissolution process and eventually equals the glass dissolution rate. Due to the difference in reaction rates at the onset of glass dissolution, an alteration layer is formed. It is a hydrolysed silica layer that is often the site of mineral deposition. The alteration layer in some glasses impedes further dissolution (protective); while in other glasses, the layer has little effect (non-protective) (Maurer et al. 1985).

To measure the effects of several CVS glass components (SiO_2, B_2O_3, Na_2O, Li_2O, CaO, MgO, and Al_2O_3) on PCT and MCC-1 durability, a central composition (HW-39-4) was altered one-component-at-a-time while keeping the remaining components in the same relative proportions. This study is denoted CVS-II Phase 4, and is discussed in detail in Section 4.6. The specific compositions

tested are listed in Table 4.14. For most components, the concentration range in this study was large enough to span the CVS composition range of the component. The exceptions are CaO and MgO. These components have been used in frit to improve glass durability, although empirical models show that they decrease durability over the larger ranges investigated in prior phases of the CVS study. It has been reported that at low concentrations their effects may be positive (Paul 1990). Hence, the effects of CaO and MgO at small concentrations (0 to 2 wt%) were measured. The normalized composition of 21 glasses tested in this study are plotted on a Li_2O+Na_2O - B_2O_3 - $SiO_2+Al_2O_3$ ternary diagram in Figure 12.19. The normalized Si, B, Li, and Na releases for the 21 glasses studied are given in Table 12.1 (MCC-1) and Table 12.9 (PCT).

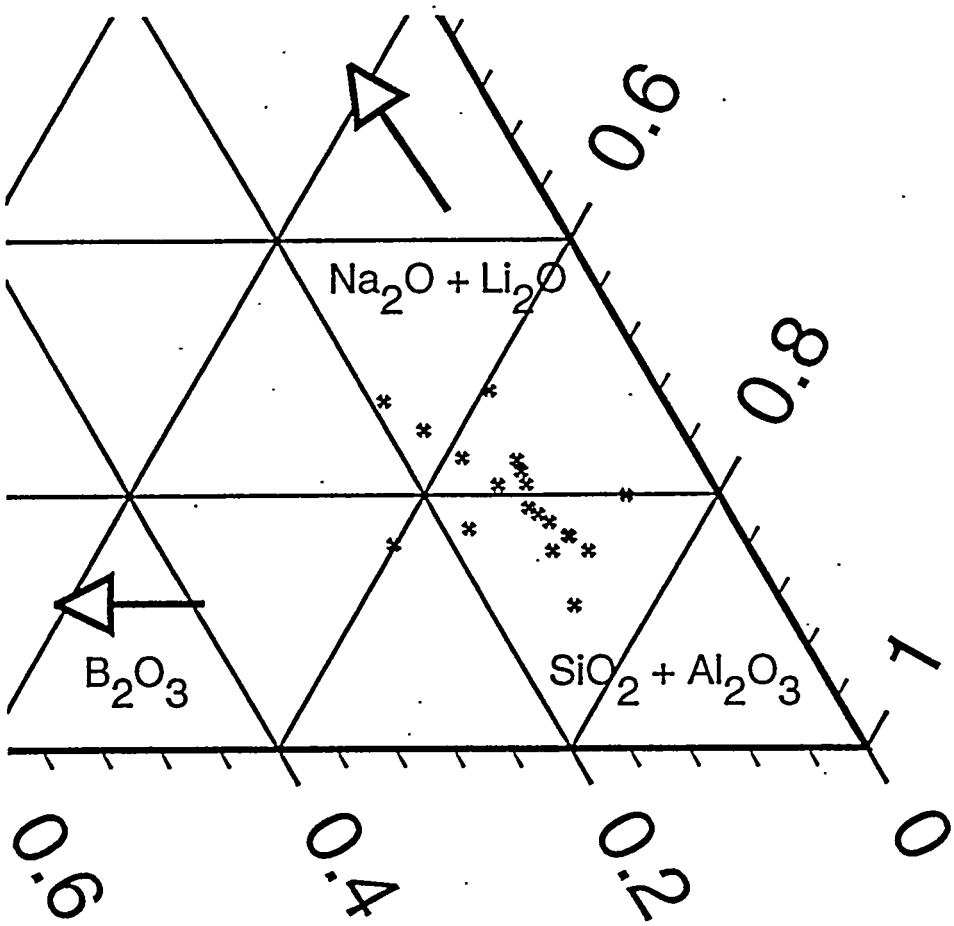

FIGURE 12.19. Ternary Plot of the Normalized Compositions of CVS2-102 Through CVS2-123 Glasses

Figures 12.20 to 12.26 show the effects of varying the composition of HW-39-4 one-component-at-a-time on normalized PCT and MCC-1 boron releases (averaged over two duplicate tests). In each figure, the natural log of normalized boron release [$\ln(r_B)$] is plotted versus the component mass fraction on the upper horizontal axis, and versus the change in the component concentration from the HW-39-4 value on the lower horizontal axis. In the plots: squares indicate glasses which have been heat treated according to the canister centerline cooling (CCC) schedule (Table 5.1); circles represent quenched glasses (empty for PCT and solid for MCC-1); Xs show the CVS results of the HW-39-4 glass; and lines represent first-order mass fraction model predictions of $\ln(r_B)$.

The model predictions of $\ln(r_B)$ in Figures 12.20 to 12.26 are based on the models in Table 12.2a for MCC-1 and Table 12.10a for PCT. The slopes of these predicted lines, $\partial\ln(r_B)/\partial x_i$, also referred to as component effects, were calculated using Equation (6.14) and are tabulated in Table 12.20. Also tabulated in Table 12.20 are the slopes of best fit lines with the measured single-component data for quenched MCC-1, quenched PCT, and CCC PCT. These slopes (component effects) can be used to compare the CVS model-predicted effect of a glass component with the measured effect from this study (CVS-II Phase 4). This comparison shows a good match between measured and predicted

TABLE 12.20. Slopes of ln(Boron Release) Versus Single-Component Additions to the HW-39-4 Glass Composition

Method	SiO_2	B_2O_3	Na_2O	Li_2O	CaO	MgO	Al_2O_3
PCT							
CVS First-Order Model	-10.5	12.7	19.2	22.9	-9.4	10.4	-25.6
Single-Component Study	-8.2	11.7	25.6	45.3	10.2	40.4	-20.9
CCC Single-Component Study	-9.5	11.2	11.6	47.0	3.7	27.0	-20.4
MCC-1							
CVS First-Order Model	-5.2	9.6	9.1	10.0	2.3	4.8	-15.4
Single-Component Study	-7.9	12.3	14.5	13.9	-0.6	1.2	-9.4

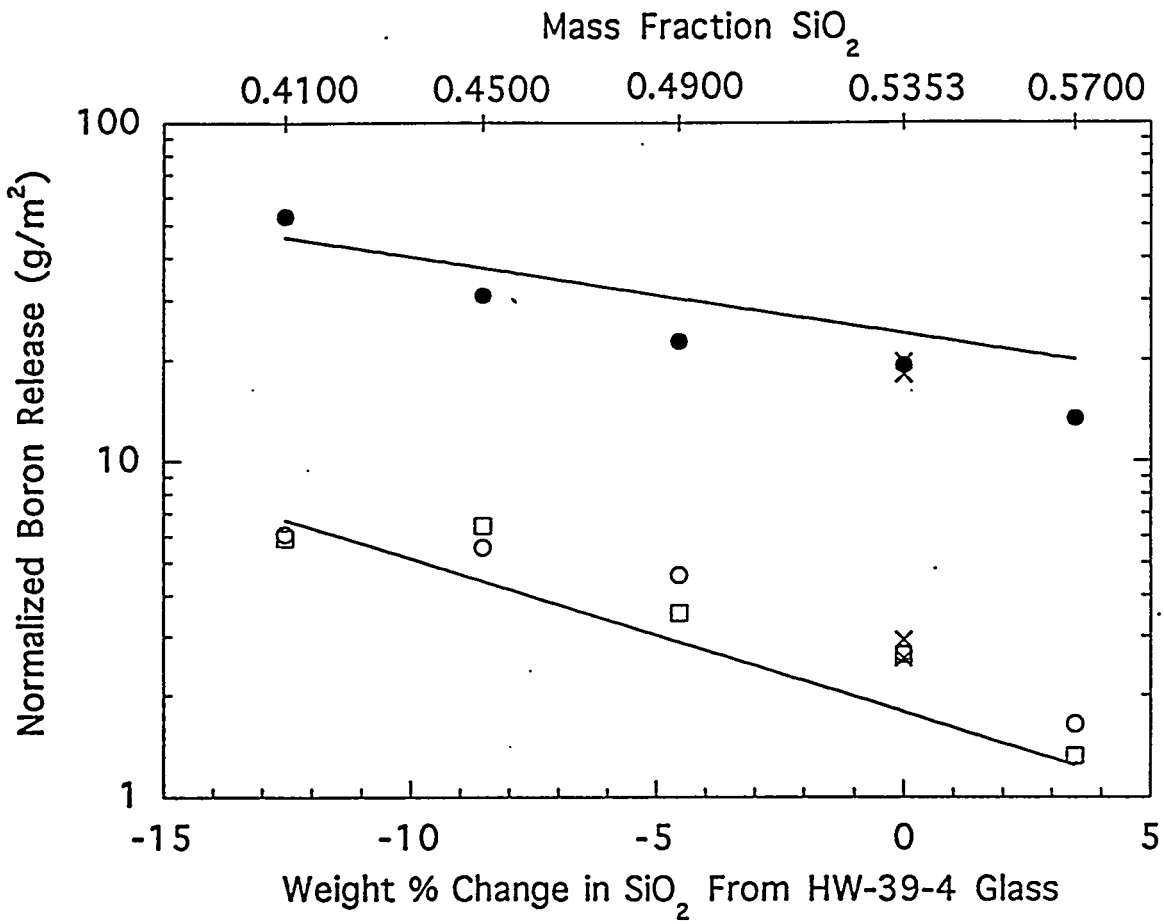

FIGURE 12.20. Effect of Varying the SiO_2 Mass Fraction of HW-39-4 Glass on Normalized Boron Release by: • MCC-1, ○ PCT of quenched glass, □ PCT of CCC glass, and X CVS measurements of HW-39-4 glass. Lines represent the first-order mass fraction model predictions of boron release.

B_2O_3

Boron is also a network forming element in both three-fold and four-fold coordinations. A conversion from three- to four-fold boron occurs as alkali concentration increases, which is known as the boron anomaly (LaCourse and Stevens 1977). When in silicate glass, however, only four-fold boron increases durability. When in three-fold coordination, boron decreases silicate glass durability by forming NBOs. B_2O_3 is predicted to have a negative effect on durability by CVS empirical models. This effect was shown to be nonlinear by second-order models (see Sections 12.3 and 12.7) over a

effects of SiO_2, B_2O_3, and Al_2O_3 for PCT, and between measured and predicted effects of SiO_2, B_2O_3, Li_2O, and Al_2O_3 for MCC-1. The effects of CaO and MgO cannot be fairly compared using the limited data measured here. The largest slope difference is seen for PCT with Li_2O, where the measured slope is more than twice that of the one predicted by the first-order mixture model.

Results for each of the seven components based on Figures 12.20 to 12.26 are discussed in turn.

SiO_2

Quatra-valent network forming elements such as Si and Zr increase glass durability. They increase the connectivity of the glass and are strongly (covalently) bonded to oxygen atoms. Thus, as expected, Figure 12.20 shows that increasing SiO_2 concentration has a positive effect on glass durability over the entire composition range. No discontinuity in boron release (such as shown by Feng (1988) in West Valley glass WV205) is seen in the composition range tested. However, nonlinear behavior appears to be starting with the 41 wt% SiO_2 glass for MCC-1 and is expected for PCT below 41 wt% SiO_2. The small degree of nonlinearity suggests that first- or second-order mixture models can describe, with sufficient accuracy, the effect of SiO_2 in the measured composition region.

Figure 12.20 shows that r_B is underpredicted by the PCT first-order model and overpredicted by the MCC-1 first-order model for SiO_2 above 45 wt%. However, the differences are within the uncertainties of the model and the measured values. The r_B of the 41 wt% SiO_2 glass falls slightly below the first-order PCT model prediction and slightly above the MCC-1 prediction. Both differences are within model and measurement uncertainties.

Over most of the region, the effect of SiO_2 on measured PCT and MCC-1 boron release ($\partial \ln(r_B)/\partial x_i$) is similar. The effect of SiO_2 concentration on measured $\ln(r_B)$ is -8.2 and -7.9 for PCT and MCC-1, respectively (Table 12.20). At lower silica concentrations, the SiO_2 change versus release curve is concave [$\partial^2 \ln(r_B)/\partial g_i^2 < 0$] for PCT and slightly convex [$\partial^2 \ln(r_B)/\partial g_i^2 > 0$] for MCC-1. If SiO_2 concentration decreases to low enough levels, the effect must also become convex for PCT due to a breakdown of the glass structure.

wide range of B_2O_3 concentration (5 to 20 wt %). However, as Figure 12.21 shows, the effect on PCT of modifying the B_2O_3 mass fraction of HW-39-4 is surprisingly linear. As expected, it is more curved at high B_2O_3 mass fractions with MCC-1. Figure 12.21 also shows the effect of B_2O_3 is predicted with good relative accuracy by the first-order models for both PCT and MCC-1. The r_B values for both MCC-1 and PCT are also predicted with good accuracy.

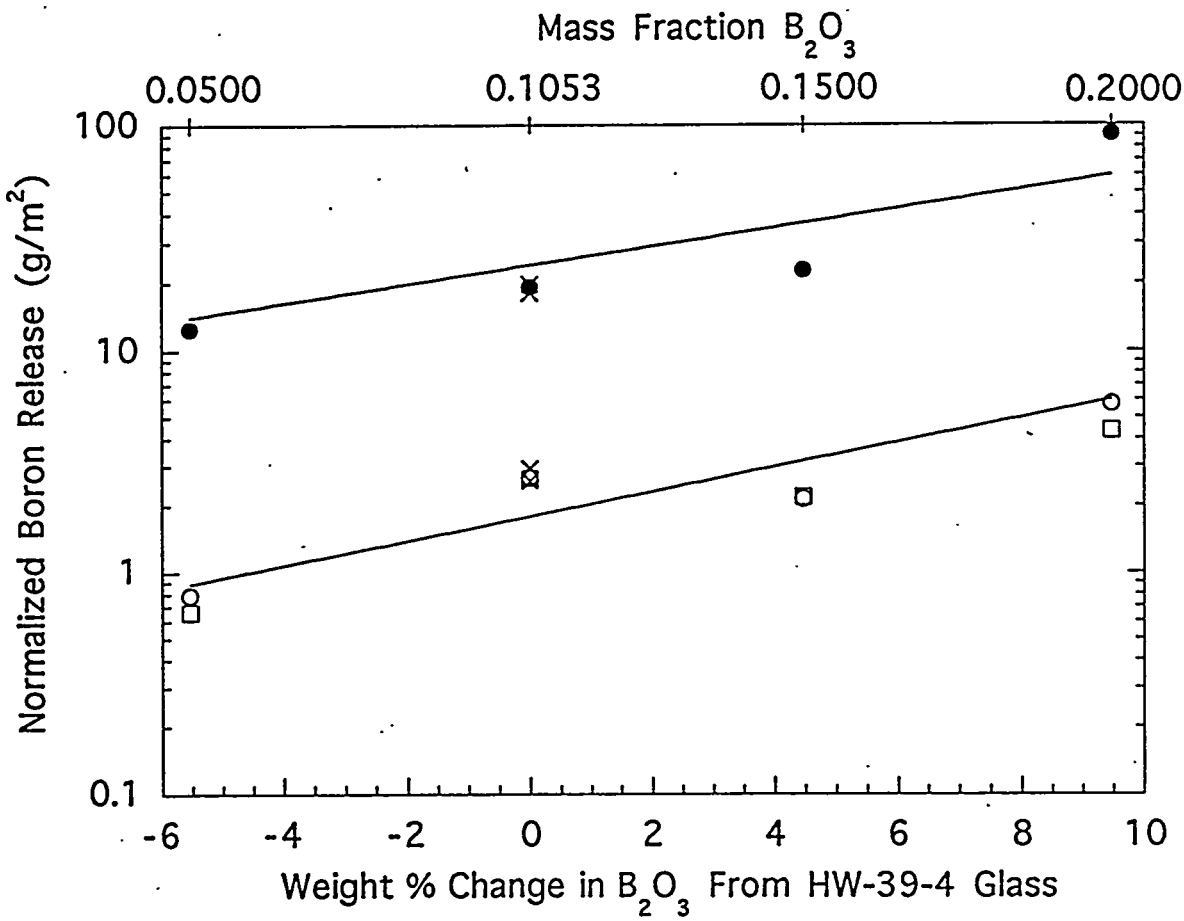

FIGURE 12.21. Effect of Varying the B_2O_3 Mass Fraction of HW-39-4 Glass on Normalized Boron Release by: • MCC-1, ○ PCT of quenched glass, □ PCT of CCC glass, and X CVS measurements of HW-39-4 glass. Lines represent the first-order mass fraction model predictions of boron release.

Na_2O

Alkali ions create NBOs which "loosen" the glass network thus creating less durable glass. The effect of a single alkali (i.e., Na or Li) is expected to be linear. The mixed alkali effect (LaCourse and Stevens 1977, Day 1976) is also important in durability. If more than one alkali is used, the effect of alkali ions is less pronounced and nonlinear at low concentrations. Low alkali glasses are also prone to phase separation in alkali-boro-silicate glass systems (see Figure 12.30), which is likely to alter the glass dissolution rate.

Figure 12.22 shows that both PCT and MCC-1 first-order models underpredict r_B of quenched glasses at the largest Na_2O addition to HW-39-4 glass and overpredict at the largest Na_2O removal from HW-39-4. However, the

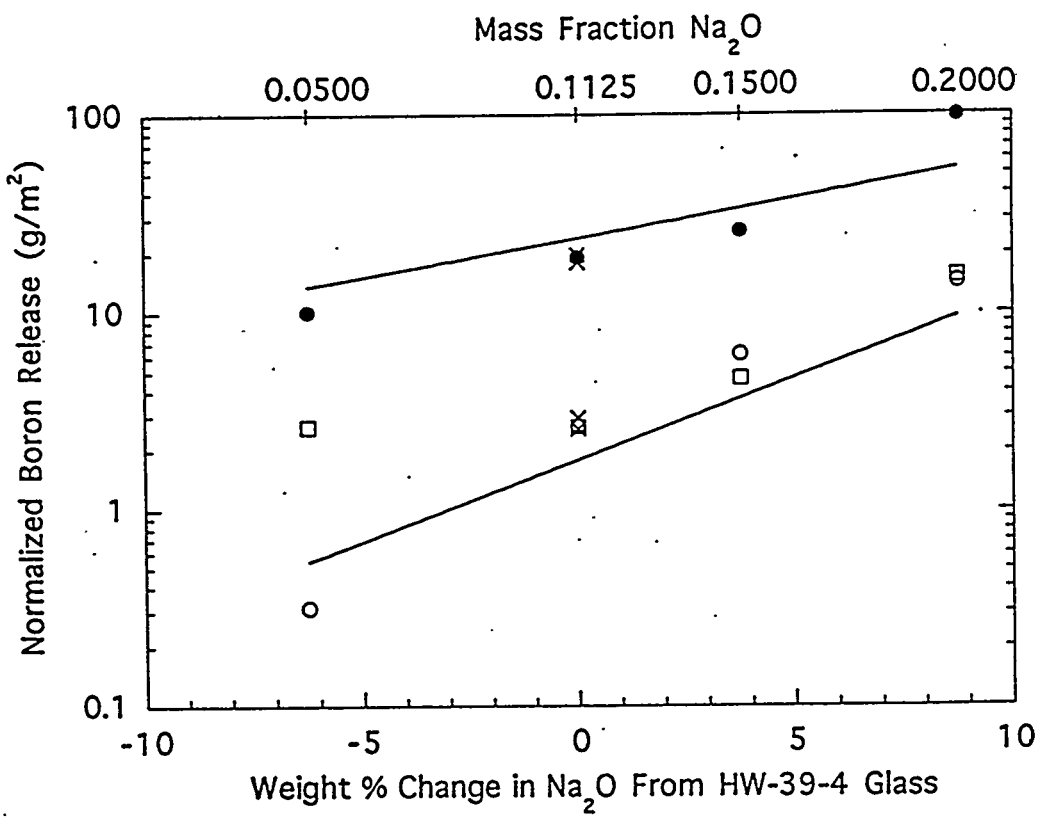

FIGURE 12.22. Effect of Varying the Na_2O Mass Fraction of HW-39-4 Glass on Normalized Boron Release by: • MCC-1, o PCT of quenched glass, □ PCT of CCC glass, and X CVS measurements of HW-39-4 glass. Lines represent the first-order mass fraction model predictions of boron release.

differences are within the uncertainties of the model and measured values. Still, the tendency to overpredict at one Na_2O extreme and underpredict at the other is an indication that curvature or interactive effects of Na_2O may exist that cannot be accounted for by the first-order model. The slope of the Na_2O change versus normalized release curve is underpredicted by first-order PCT and MCC-1 models (see Table 12.20).

Li_2O

Figure 12.23 shows that the PCT first-order model underpredicts r_B at the two largest Li_2O additions to HW-39-4 glass and overpredicts at the largest Li_2O removal from HW-39-4. However, these differences are within the uncertainties of the model and measured values. Still, the tendency to

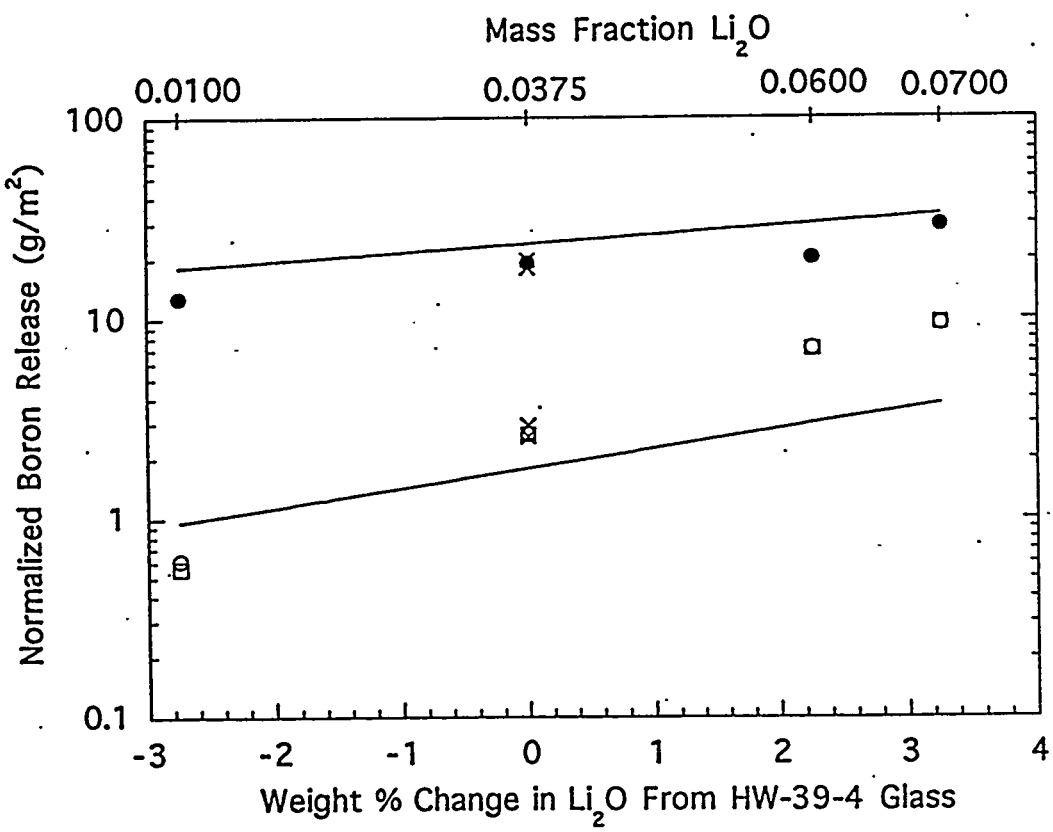

FIGURE 12.23. Effect of Varying the Li_2O Mass Fraction of HW-39-4 Glass on Normalized Boron Release by: • MCC-1, o PCT of quenched glass, □ PCT of CCC glass, and X CVS measurements of HW-39-4 glass. Lines represent the first-order mass fraction model predictions of boron release.

overpredict at one Li_2O extreme and underpredict at the other is an indication that curvature or interactive effects of Li_2O may exist that cannot be accounted for by the first-order model. Figure 12.23 shows that the first-order MCC-1 predicts the effect of Li_2O on r_B more accurately.

Table 12.20 indicates that the slope of the Li_2O change versus normalized release curve is underpredicted by both first-order PCT and MCC-1 models, although the underprediction is slight for MCC-1 and is probably within the model and data uncertainties.

CaO

Alkaline earth elements often lower the durability of glass by creation of two NBOs per atom. However, if the alteration layer contains divalent (alkaline earth) ions, diffusion of alkali ions is slowed and the layer is protective (Maurer et al. 1985). Hence, at low concentrations divalent ions are capable of increasing glass durability. The effects of Mg and Ca on durability are important because these components have traditionally been added to soda-lime glass in order to increase durability. Empirical CVS models predict MgO to decrease glass durability and CaO to have little effect (in the range of 0 to 10 % for CaO and 0 to 8 % for MgO).

Figure 12.24 indicates that adding approximately 1.2 wt% CaO to the HW-39-4 glass has a slight negative effect on PCT durability and essentially no effect on MCC-1 durability. The difference in PCT results for the two glasses represented in Figure 12.24 is within the uncertainty of the data. Hence, no reason is apparent for the addition of CaO to glasses in this composition range.

Figure 12.24 shows that the mass fraction first-order model underpredicts normalized boron PCT releases and overpredicts MCC-1 releases. Table 12.20 also shows that the first-order models predict component effects with opposite signs than the measured data. However, these differences are within the uncertainties of the models and measured values.

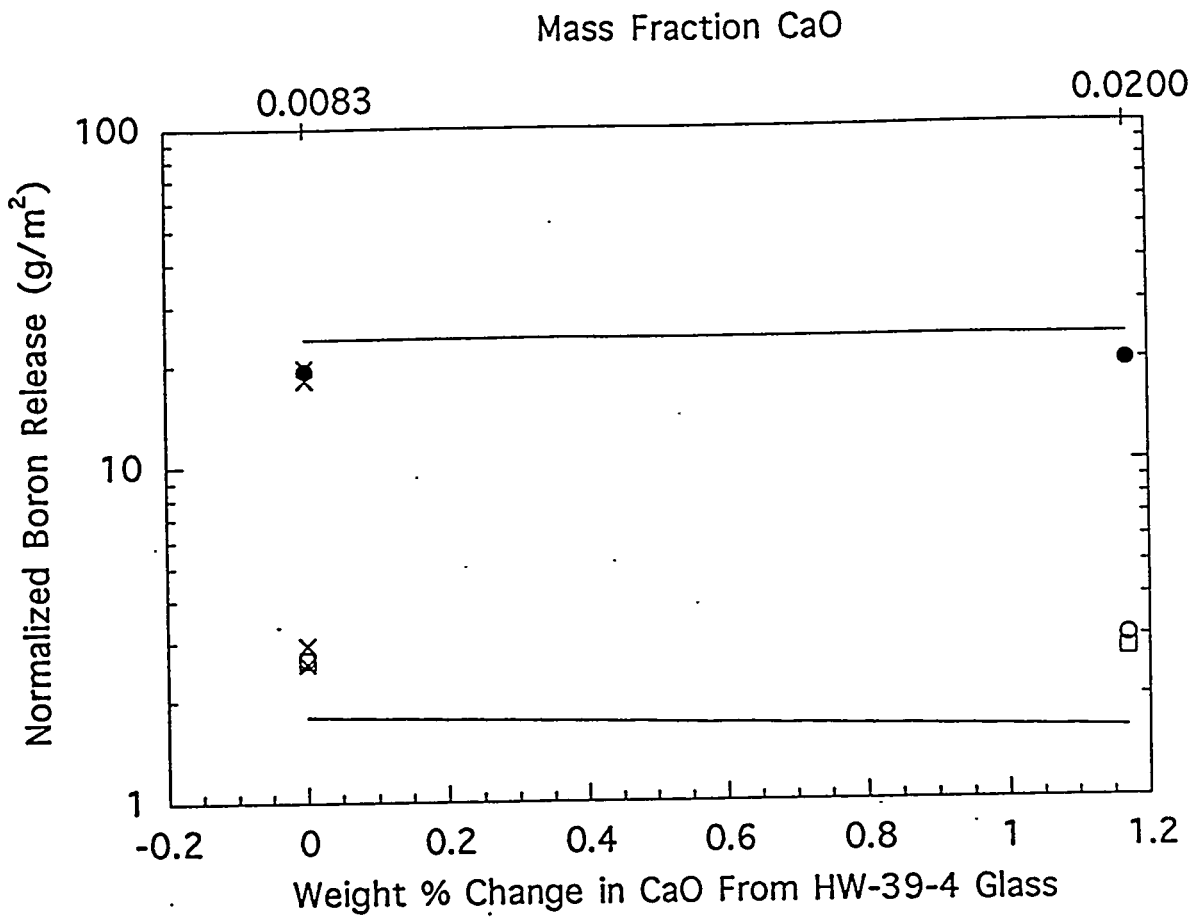

FIGURE 12.24. Effect of Varying the CaO Mass Fraction of HW-39-4 Glass on Normalized Boron Release by: • MCC-1, ○ PCT of quenched glass, □ PCT of CCC glass, and X CVS measurements of HW-39-4 glass. Lines represent the first-order mass fraction model predictions of boron release.

MgO

MgO is detrimental to glass durability even at low concentrations (as discussed in the preceding CaO section) and it also tends to promote crystallinity. Therefore, MgO should be avoided in waste glasses in this composition region if possible. As seen in Figure 12.25 and Table 12.20, the PCT first-order model underpredicts this detrimental effect. The MCC-1 model predicts a slightly increasing effect of MgO, where the measured effect of changing MgO showed little effect. The differences in predicted and measured r_B values and predicted and measured component effects are within the uncertainties of the model and measured data, however.

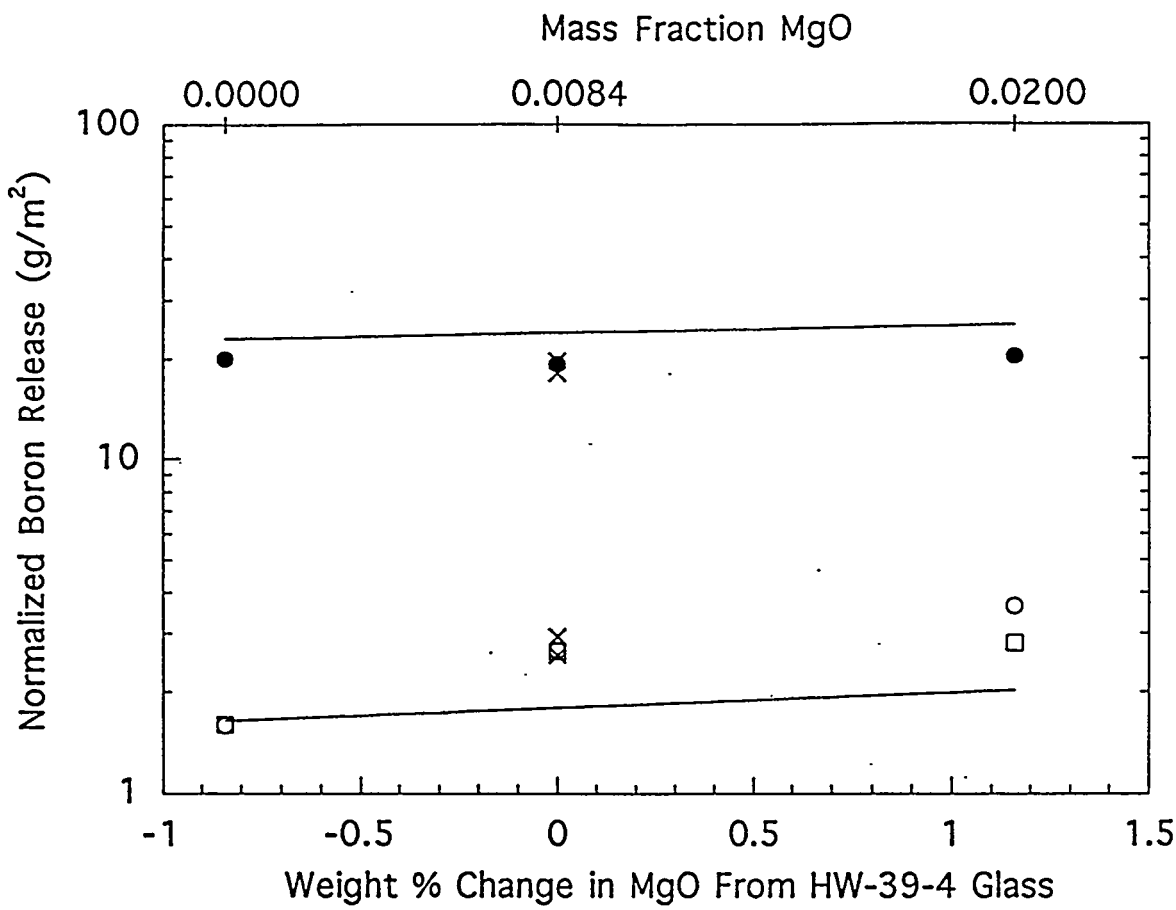

FIGURE 12.25. Effect of Varying the MgO Mass Fraction of HW-39-4 Glass on Normalized Boron Release by: • MCC-1, o PCT of quenched glass, □ PCT of CCC glass, and X CVS measurements of HW-39-4 glass. Lines represent the first-order mass fraction model predictions of boron release.

Al_2O_3

Figure 12.26 indicates that the effect of adding Al_2O_3 to HW-39-4 is nonlinear and is characterized by an abrupt drop in r_B. The drop appears to be more pronounced in the PCT data than in the MCC-1 data, but is present in both. Similar behavior was demonstrated by Feng (1988) for a West Valley reference glass (WV205). This type of nonlinearity suggests that first-order (and possibly second-order) models are not capable of accurately modelling the effect of Al_2O_3 mass fraction on r_B over the composition range from 0 to 15 wt% Al_2O_3. Still, the differences between measured and predicted values are within model and measurement uncertainties (although this may be because model uncertainties are relatively large).

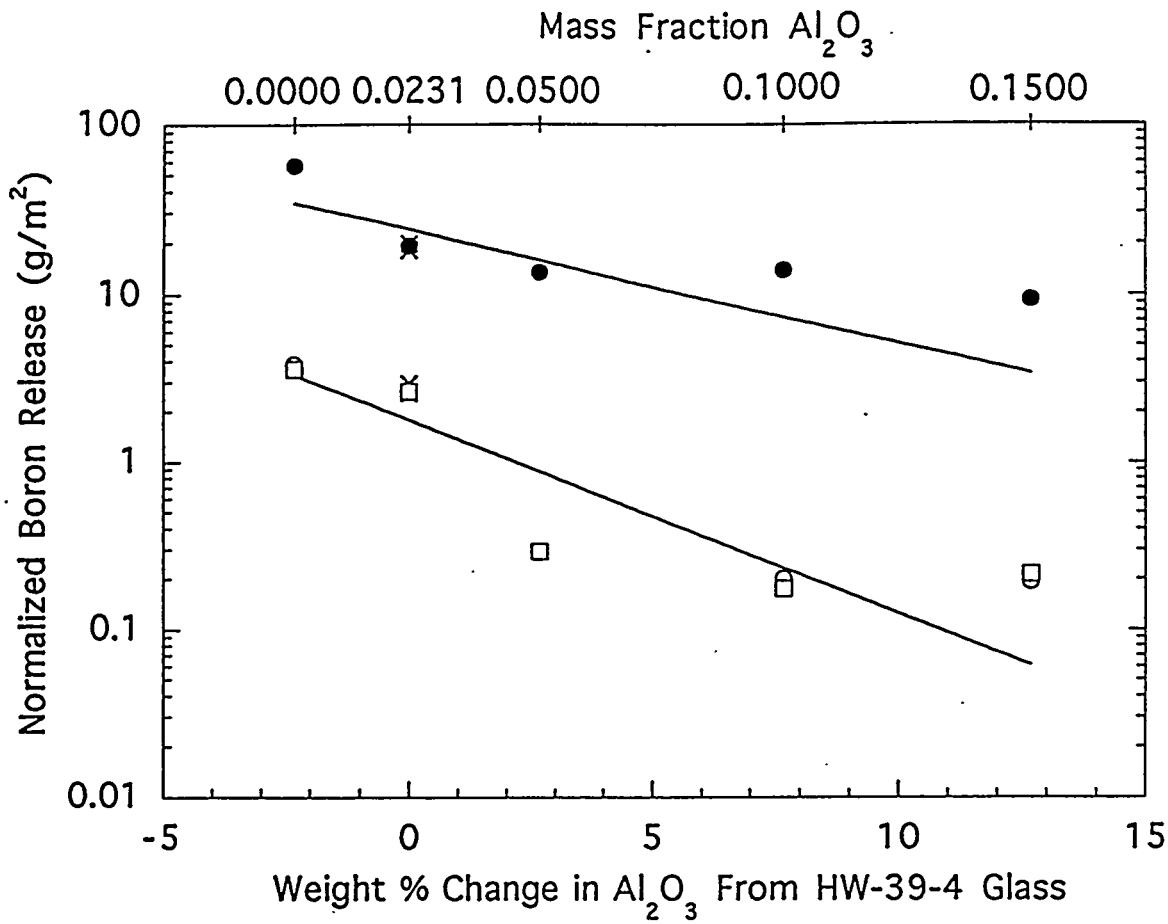

FIGURE 12.26. Effect of Varying the Al_2O_3 Mass Fraction of HW-39-4 Glass on Normalized Boron Release by: • MCC-1, o PCT of quenched glass, □ PCT of CCC glass, and X CVS measurements of HW-39-4 glass. Lines represent the first-order mass fraction model predictions of boron release.

Effect of CCC Heat Treatment

The normalized Si, B, Li, and Na release data for PCT of CCC samples of CVS-II Phase 4 glasses are given in Table D.5 of Appendix D. The effect of CCC on PCT r_B can be seen in Figures 12.20 to 12.26. Generally, CCC affects glass properties by favoring crystallization (see Chapter 11) or amorphous phase separation (see Section 12.11.4). There is very little difference seen between quenched and CCC PCT r_B for most CVS-II Phase 4 glasses. One marked difference is seen for the lowest Na_2O glass in Figure 12.22. The increased r_B after CCC is attributed to the location of the glass composition within the

immiscibility dome (see Section 12.11.4.3). A second possibility is high crystallinity, which is promoted by decreasing Na_2O.

12.11.3 Glasses with Extreme Normalized Boron Releases

The averaged normalized boron releases ranged roughly from 3 to 700 g/m² for 28-day MCC-1 and from 0.07 to 44 g/m² for 7-day PCT. These wide ranges, together with the differences in component effects on PCT and MCC-1 tests, reflect a rich variety of durability behavior. To develop an intuitive grasp of this variety, it is useful to look at glasses that exhibit unusual or extreme behavior with respect to durability. Four groups of such glasses (from CVS-I and CVS-II Phases 1, 2, and 3) are discussed:

Group A: Glasses with extreme normalized boron releases for both PCT and MCC-1

Group B: Glasses with extreme normalized boron releases for PCT or MCC-1 individually (i.e., regardless of the release level measured by the other method)

Group C: Glasses with extreme PCT/MCC-1 ratios of normalized boron releases

Group D: Anomalous glasses (glasses not predicted accurately by first-order property models).

Extreme release is arbitrarily set as normalized boron release outside the range $0.2 \leq r_B \leq 10.0$ g/m^2 for PCT and $9.0 \leq r_B \leq 100.0$ g/m^2 for MCC-1. The first three groups of glasses exhibit extreme (high or low) values of normalized boron releases and are discussed in this subsection. Subsection 12.11.4 is reserved for anomalous glasses.

Group A

Six CVS glasses showed extreme low releases by PCT and MCC-1: CVS1-2, CVS1-10, CVS1-11, CVS2-2, CVS2-3, and CVS2-86. With the exception of CVS2-2 and CVS2-3, these glasses have higher than acceptable viscosity at 1150°C. The remaining four glasses have high levels of durability increasers SiO_2, Al_2O_3, and ZrO_2 and are accurately predicted by first-order durability models.

These observations suggest a correlation between durability and viscosity because the components which are most potent viscosity reducers

(alkali oxides) or viscosity risers (alumina) are also the most potent durability reducers or risers, respectively. The statistical correlations presented in Chapter 13 (Tables 13.1 and 13.2) do not indicate a strong correlation between durability and viscosity, but that is because they are based on variations of all components as determined by the test matrix. If a frit is designed for vitrification of particular waste (such as NCAW), only glass-forming and -modifying components (SiO_2, Al_2O_3, B_2O_3, Li_2O, and Na_2O) can vary. If the fractions of B_2O_3, Li_2O, and Na_2O decrease, both viscosity and durability increase. Hence, production of glasses with high viscosity would allow an increase in durability. This situation would be possible if the melting temperature could be increased above 1150°C. Viscosity at 1150°C should not exceed 10 Pa.s, but if it is maintained as close to this level as practically possible, glasses with higher durability can be produced. As is explained in Sections 7.0 and 8.0, it is better for glass durability if viscosity is adjusted using Li_2O rather than Na_2O or B_2O_3. Such glasses (using Li_2O to adjust viscosity) will have relatively high electrical conductivity.

Eight CVS glasses showed extremely high release by both PCT and MCC-1: CVS1-4, CVS1-9, CVS1-13, CVS1-15, CVS1-21, CVS2-81, CVS2-82, and CVS2-93. Three of these glasses (CVS2-81, CVS2-82, and CVS2-93) have lower than acceptable viscosity at 1150°C due to high alkali concentration (>19 wt%). Glasses CVS1-4, CVS1-9, CVS1-15, and CVS1-21 have no Al_2O_3 or ZrO_2 (the only two durability raisers besides SiO_2) and glass CVS1-13 has a mass fraction Al_2O_3 of only 0.0038 and no ZrO_2. Glasses CVS1-4, CVS1-9, CVS1-13, and CVS1-21 have high B_2O_3 (a durability reducer).

Many of the high release glasses are considered anomalous due to over- or underprediction of boron release. CVS1-4, CVS1-9, and CVS1-13 are more than 40% underpredicted by the first-order PCT model in Table 12.10a. CVS1-2 and CVS2-86 are underpredicted by the first-order MCC-1 model in Table 12.2a by 50% or more, and CVS1-10 is overpredicted by more than 40%. Some of these anomalous glasses are further discussed in terms of MCC-1 release in Section 12.11.4.

Group B

Glasses exhibiting the highest values of durability (lowest values of normalized B release) by PCT or MCC-1 tests, and possessing acceptable viscosity, are CVS2-2, CVS2-3, CVS2-4, CVS2-12, CVS2-23, CVS2-41, CVS2-73, and CVS2-75. These glasses are relatively high in SiO_2 (minimum 46.5 wt%) and Al_2O_3 (minimum 6 wt%), and have moderate contents of B_2O_3 (7 to 17 wt%), ZrO_2 (maximum 4 wt%), and Fe_2O_3 (maximum 4.5 wt%). Most have low alkali content (maximum 21 wt% Na_2O + Li_2O) and are low in MgO (maximum 2 wt%). Their range of CaO and Others is wide. Some of the components are restricted, mainly due to the constraints imposed by viscosity, electrical conductivity, and stand-in constraints. At the time of test matrix design, it was thought that high concentrations of Al_2O_3+ZrO_2 and other combinations would lead to excessive crystallization, so stand-in constraints were formulated (see Tables 4.2 and 4.6). These stand-in constraints where later found to be inadequate (see Section 11.6). However, data are not currently available in the composition regions eliminated by the stand-in constraints.

Glasses with lowest durability (highest normalized B release) by PCT or MCC-1 tests, and possessing acceptable viscosity, are CVS1-13, CVS1-15, CVS1-4 (with its replicate CVS1-21), CVS1-9, CVS1-14, CVS1-17, CVS2-25, CVS2-30, CVS2-24, and CVS2-16 (with its replicate CVS2-18). These glasses are arranged approximately in the order of increasing durability as far as the differences between MCC-1 and PCT allowed such ordering. These glasses occupy the full range of composition with respect to SiO_2, B_2O_3, Li_2O, CaO, MgO, Fe_2O_3, and Others, and almost the full range of Na_2O (5 to 19 wt%). With two exceptions, they are low in Al_2O_3 and ZrO_2. These two exceptions are CVS1-14 with 13 wt% ZrO_2 and CVS2-24 with 9.6 wt% Al_2O_3. Both are low in SiO_2 and high in B_2O_3 and alkali oxides.

Group C

Figure 12.27 shows nine glasses have high PCT normalized B releases relative to the corresponding MCC-1 normalized B releases (PCT/MCC-1 ratio > 0.3). These glasses are (in order of decreasing PCT/MCC-1 boron release ratio): CVS2-83, CVS2-39, CVS2-22, CVS2-32, CVS2-76, CVS2-28, CVS1-18, CVS2-84, and CVS2-21. Most of these glasses have zero CaO content. Six of them

are low in B_2O_3 (≤ 6 wt%), while CVS2-83 has 9 wt% B_2O_3 and CVS2-21 has 13 wt% B_2O_3.

The eight glasses with the lowest PCT/MCC-1 boron release ratios (≤ 0.015) are, in increasing order, CVS2-31, CVS1-2, CVS1-11, CVS2-15, CVS2-86, CVS2-2, CVS2-23, and CVS2-3. These glasses are represented by the data points to the left of the line PCT = 0.015 MCC-1 (indicated as P=0.015M) in Figure 12.27. All of these glasses have high CaO concentration (6 to 10 wt%), except for CVS2-86 with 4 wt% CaO.

These results illustrate and confirm the dissimilar effect of CaO on different durability test methods (shown in Figures 12.3, 12.8, and 12.18). Note that some glasses with both zero and high levels of CaO can have medium

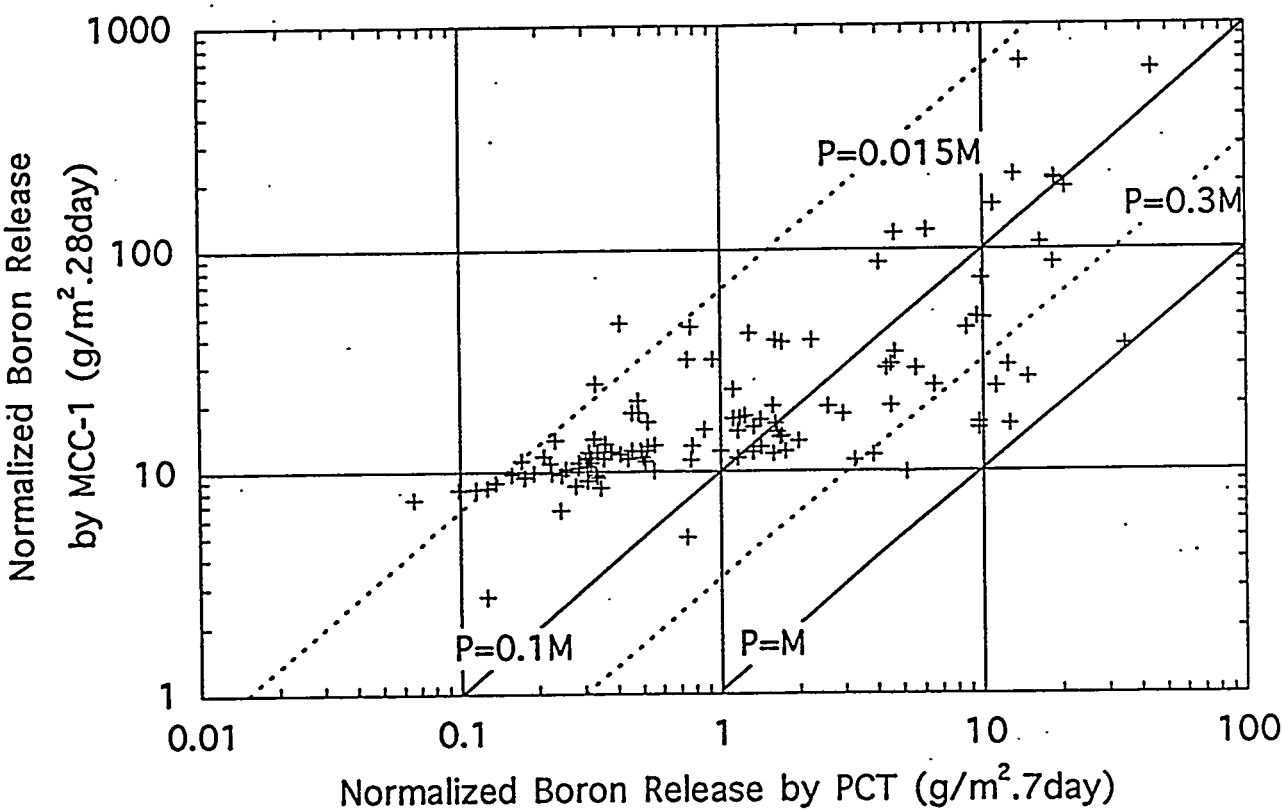

FIGURE 12.27. Plot of MCC-1 and PCT Normalized Boron Releases With Lines Representing Different PCT/MCC-1 Release Ratios Superimposed. P and M stand for the normalized boron release from PCT and MCC-1, respectively.

values of PCT/MCC-1 boron release ratios because of the compensating effects of components other than CaO.

The effect of CaO on PCT/MCC-1 ratio is difficult to rationalize. Two simple explanations can be suggested. First, extremely high PCT/MCC-1 values can be caused by a dramatic increase in the pH of the solution with advancing reaction progress. This hypothesis is not supported by the data (see Figure 12.17, in which no differences in CaO coefficients for pH are seen for PCT and MCC-1). The pH values in solutions are predominately affected by the alkali ion exchange due to diffusion at early stages of dissolution, in which CaO does not participate. Second, extremely high PCT/MCC-1 values of r_B can be caused by precipitation of silicate minerals. Such a reaction probably does not take place when CaO is present until a higher degree of reaction progress is reached than is achieved in PCT. In addition, components (such as MgO) that react with silicic acid are not present in high CaO glasses because of the multiple-component stand-in constraints. If precipitation does not occur, high concentrations of silicic acid develop at advanced stages of reaction progress and the ratio r_{Si}/r_B (normalized Si release divided by normalized B release) is low. This ratio is below 0.33 for the nine glasses previously listed as having high values of PCT/MCC-1 normalized boron release ratios. The ratio is above 0.41 for the eight glasses previously listed as having low values of PCT/MCC-1 normalized boron release ratios. Thus, the second hypothesis is supported by the data.

Direct evidence of this effect has been obtained through additional study of two glasses, CVS2-23 and CVS2-39. CVS2-23 is high in CaO, has no MgO, and has a PCT/MCC-1 ratio of 0.015. CVS2-39 is high in MgO, has no CaO, and has a PCT/MCC-1 of 0.779. The overall composition of these glasses is otherwise similar (see Table 4.15). Powdered glass (+200, -100 mesh) was added to DI water in glass surface area to solution volume ratios (S/V) of 20, 200, 2000, and 20000 m^{-1} in Teflon vessels. The glass was then dissolved at 90°C for 1, 10, 100, and 1000 hours and normalized boron release measured.

Figure 12.28 shows the ratio r_{Si}/r_B as a function of the scaling factor $(S/V)t^{1/2}$ for the two glasses. The figure shows the r_{Si}/r_B ratio is low and increases in both glasses at low $(S/V)t^{1/2}$ values. This change occurs due to

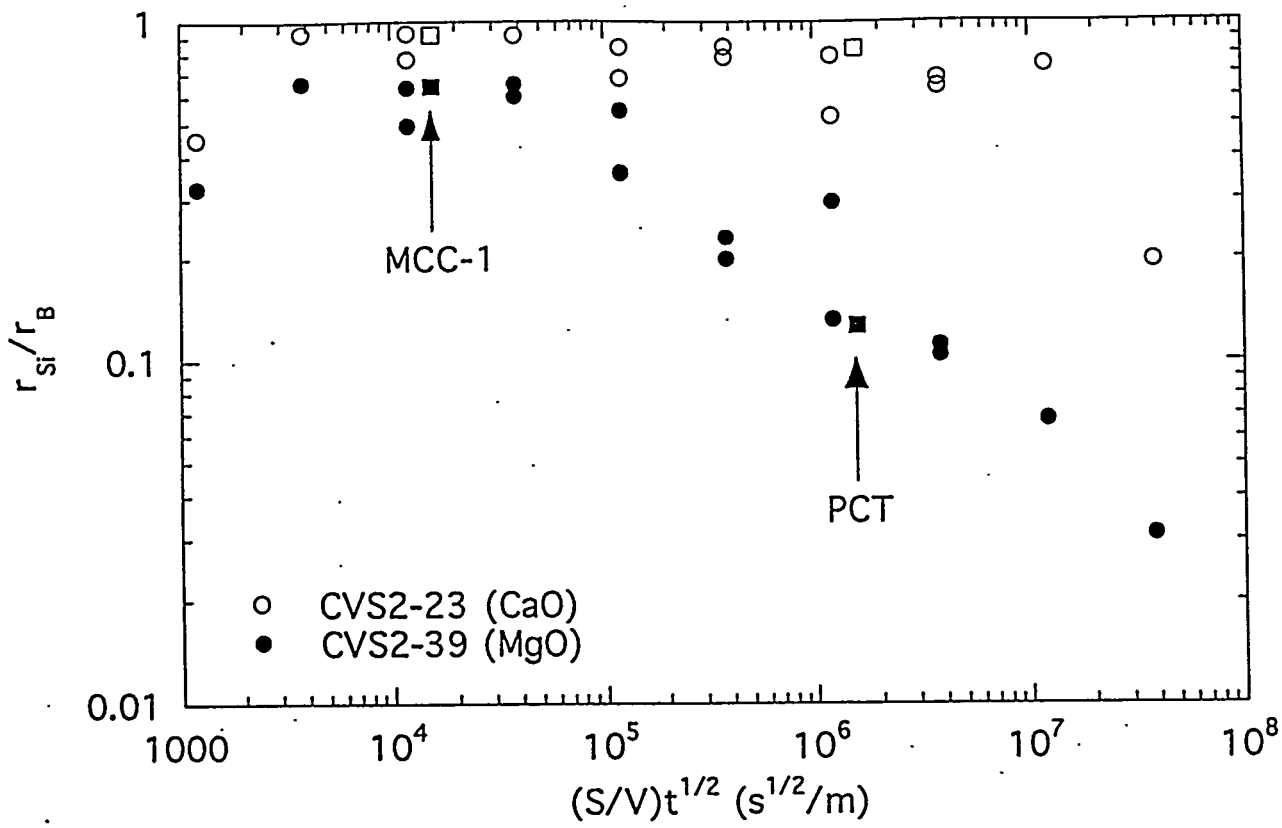

FIGURE 12.28. Ratio of Silicon-to-Boron Releases (r_{Si}/r_B) After Dissolution in H_2O at 90°C Versus $(S/V)t^{1/2}$ for CVS2-23 and CVS2-39 Glasses

preferential dissolution of B at the start of the dissolution process. As dissolution continues, the rate of Si dissolution matches that of B dissolution. At higher $(S/V)t^{1/2}$ values, the high MgO glass (CVS2-39) shows a marked decrease in r_{Si}/r_B. This situation is due to precipitation of silicon-containing phases. The high CaO glass (CVS2-23) continues to dissolve without increased r_{Si}/r_B until reaching a very high level of reaction progress. It can be concluded that precipitation occurs earlier in the high MgO glass, which suggests that MgO aids in the precipitation of silicon-containing phases. Calcium is likely to precipitate as $CaCO_3$ (Grambow and Strachan 1988) and evidence indicates Si precipitates as $Mg_2Si_3O_7(OH)_4$ and other magnesium silicates (Chick and Turcotte 1983).

CaO is commonly used as a frit component because it improves the durability of soda-lime glasses (Paul 1990, Chick et al. 1984). For nuclear waste glasses, however, the role of CaO as a frit component is ambiguous,

depending on which test is used to measure durability. If MCC-1 is used, CaO should be avoided as a frit component. If PCT is relevant, CaO addition may be mildly beneficial[a]. However this beneficial effect was not seen with a small CaO increase in HW-39-4 glass in the single-component study (see Section 12.11.2). Also, CaO may be detrimental if added to a glass with P_2O_5 present (Bunnell 1988).

12.11.4 Amorphous Phase Separation and Anomalous Glasses

An overview of amorphous phase separation in silicate and borosilicate glasses is given in Section 12.11.4.1. Methods to predict the development of amorphous phase separation are discussed in Section 12.11.4.2. The effect of amorphous phase separation on durability is discussed in Section 12.11.4.3. Section 12.11.4.4 evaluates Taylor's immiscibility model for CVS-I and CVS-II Phase 1, 2, and 3 glasses. Anomalous and high-release glasses are discussed in Section 12.11.4.5.

12.11.4.1 Overview of Amorphous Phase Separation

Amorphous phase separation is defined as the separation, upon cooling, of a homogeneous melt into two or more liquids. Borosilicate glasses are prone to glass-in-glass phase separation. Depending on the developing microstructure, phase separation can profoundly affect glass properties, in particular, durability towards aqueous dissolution. Two domains, differing in composition, typically develop when an alkali borosilicate glass undergoes glass-in-glass phase separation. The microstructure is usually composed of one domain which is silica-rich while the other is an alkali-boron enriched phase. Multicomponent borosilicate glasses tend to partition in a similar manner (Ehrt et al. 1977, Taylor 1990).

Tomozawa (1979) recognizes three microstructural types depending upon whether the separation kinetics are governed by nucleation/growth or spinodal

---

(a) The main difference between MCC-1 and PCT is in the final level of solution saturation (or the degree of reaction progress)--this level is considerably higher in PCT than in MCC-1.

decomposition mechanisms. The three different microstructures are:

Type A: Both phases are highly interconnected and continuous structures. (Spinodal decomposition)

Type B: The more durable phase is dispersed as discrete droplets in a continuous matrix of the less durable phase. (Nucleation/Growth)

Type C: The less durable phase exists as discrete droplets in a continuous matrix of the more durable phase. (Nucleation/Growth)

The durability of a glass in an aqueous environment usually deteriorates upon the development of a Type A or Type B microstructure because the less durable phase is continuous in both cases. The development of a Type C microstructure usually has little effect on durability, but in some cases has been shown to improve the durability (Danilova et al. 1971, Taylor et al. 1987). If two immiscible phases exist, a sharp change in durability can occur within a narrow compositional range due to decomposition mechanism differences. The rate controlling factor in the dissolution process is primarily defined in terms of the durability of the continuous matrix phase when amorphous phase separation is of concern.

Although phase separation may be advantageous with respect to aqueous dissolution, the concern for nuclear waste disposal purposes is a deterioration in durability. This concern is heightened by the fact that most metal oxides and fission products tend to partition into the more soluble alkali-boron enriched phase (Taylor 1990).

Several alkali (R_2O) and alkaline earth (MO) binary silicate systems show limited compositional regions of immiscibility (Kawamoto and Tomozawa 1981). The $MO-SiO_2$ systems generally have more extensive miscibility gaps than the R_2O-SiO_2 systems. The extent of immiscibility is typically discussed in terms of the polarization power (or field strength) of the modifier cation (Dietzel 1942, Warren and Pincus 1940). In general, the higher the polarization power, the greater the extent of immiscibility in terms of both temperature and composition.

As in binary silicate systems, the extent of immiscibility in alkali-borosilicate systems increases with increasing polarization power of the

alkali cation ($Li^+ > Na^+ > K^+ > Rb^+ > Cs^+$). The same holds for alkaline earth borosilicate systems ($Zn^{2+} \sim Mg^{2+} > Ca^{2+} > Sr^{2+} > Ba^{2+} \sim Pb^{2+}$). The relationship between the extent of immiscibility and polarization power breaks down with the most polarizing cation (Al^{3+}), which usually enters the structure as a network-former rather than a modifying cation. Suppression of amorphous phase separation typically results when sufficient Al_2O_3 is incorporated into the glass composition. To a lesser extent, additions of ZrO_2 will also suppress the development of amorphous phase separation.

The development of amorphous phase separation is not only a function of composition but also is highly dependent upon kinetic factors, of which thermal history is of primary importance. Sufficient heat treatment may be necessary for kinetic development of amorphous separation even if glass composition is favorable for its development. Thermal history not only determines the formation probability of amorphous phase separation, but also has a strong influence on the scale to which the microstructure develops.

Because phase separation is sensitive to the heat treatment, the durability of phase-separated glasses is also expected to be sensitive to heat treatment. The effect of heat treatment on waste glass durability was observed by Bickford and Jantzen (1984) and Jantzen and Bickford (1985). They found that crystallization produces only a minor effect on the dissolution of alumina-containing glasses with up to 30 vol% of crystalline phase (spinel and acmite). The authors concluded that devitrification affects durability less than changes in chemical composition. Phase separation was unlikely to occur in most of their glasses because of the Al_2O_3 content of 5.6 and 11.1 wt% (Bickford and Jantzen 1986). However, they ran an MCC-1 test on a glass with a lower Al_2O_3 content (SRL-165 High Fe, which contained 2.2 wt% Al_2O_3 and 6.5 wt% B_2O_3) and found more than 10 times higher B release after heat treatment (Jantzen and Bickford 1985). They attributed this finding to cracking caused by the thermal expansion mismatch of the glass and crystals. The possibility that the low durability could be caused by phase separation was not considered. No explanation was given of how cracking could cause a substantial decrease in durability. Only a few percent of the increase in B release can be attributed

to an increase in the surface area. The rest is attributable to internal stresses and other factors discussed in Section 12.12.

12.11.4.2 Predictability of Immiscibility Within Multicomponent Systems

Equally important to the effect of amorphous phase separation on the glass durability is the predictability of immiscibility within multicomponent systems. In binary silicate glasses, as well as several alkali and alkaline earth borosilicate systems, determination of miscibility boundaries has been well-documented. But as the systems become progressively more complex (i.e., binary to ternary to multicomponent systems), detailed mapping of immiscibility domes requires an extensive study involving the preparation and evaluation of numerous glasses. Therefore, it would be advantageous to model the immiscibility domes of multicomponent systems based on the knowledge of simpler systems and single-component effects of modifying cations in ternary systems.

Several attempts have been made to empirically or theoretically predict immiscibility behavior within multicomponent systems. Kawamoto and Tomozawa (1981) have proposed a "simple and reliable" method to estimate the miscibility boundaries in ternary silicate systems. This method is based on the similarity in shape of observed boundaries of binary silicate systems and a pseudo-binary regular mixing equation. They suggest that if boundaries of two binary silicate systems are defined, immiscibility within the common ternary system can be determined. Although this method has been successful in predicting immiscibility in several ternary silicate systems, it has not been applied to the multicomponent systems typical of nuclear waste vitrification.

Charles (1967), based on cryoscopic data, thermodynamically estimated the immiscibility boundary of the $BaO-Li_2O-SiO_2$ system. This technique can only be applied to systems where thermodynamic data exists. Levin and Block (1957) applied the principles of crystal chemistry to interpret and calculate the immiscibility behavior of 19 binary and a limited number of ternary systems. Strand and Strand (1978) calculated the miscibility boundaries of various ternary systems based on thermodynamic relations obtained by equating the chemical potentials of the equilibrium component phases. Burnett and

Douglas (1970) use a number of simple empirical relations to approximate the immiscibility dome of a single ternary silicate system. All predictive techniques mentioned thus far have been limited to binary and a few select ternary systems, but have not been applied to multicomponent systems.

Limited work has been performed on quaternary systems in terms of mapping the immiscibility domes. Most work has involved the X_2O-MO-B_2O_3-SiO_2 systems, where X = Na or K, and M = Mg, Ba, Ca, Mn (Taylor et al. 1981, 1983, 1984). Chick et al. (1981), as well as Tomozawa (1979), have observed glass-in-glass phase separation in various nuclear waste glasses. These studies respectively involved the observation of phase separation by Scanning Electron Miscroscopy (SEM) and the evaluation of additives to suppress its formation, yet no attempt was made to predict immiscibility.

Taylor (1990) has evaluated immiscibility in multicomponent systems through work performed within the Canadian Nuclear Fuel Waste Management program. His review not only emphasizes the immiscibility limits within binary, ternary, and several quaternary systems, but also models the prediction of immiscibility within multicomponent systems. Taylor's model to predict immiscibility limits in multicomponent systems is based on simpler systems and single component effects in ternary systems. Taylor draws several conclusions from the influence of various additive oxides on the phase separation behavior in borate, silicate, and borosilicate systems. A summary of those conclusions are:

1. The oxides of cations more weakly polarizing than Na (K, Rb, Cs) show very limited regions of immiscibility in their respective borosilicate systems. These oxides tend to suppress amorphous phase separation when <u>substituted</u> for Na_2O in a Na_2O-B_2O_3-SiO_2 (NBS) system.

2. A large number of cations, more polarizing than Na (Li, Ca, Ba, etc.), show more extensive regions of immiscibility in borosilicate glasses. These cations tend to promote phase separation when <u>added</u> to a glass composition lying within the sodium borosilicate immiscibility dome.

3. The higher polarizing cations do not tend to induce phase separation when added to a sodium borosilicate composition lying outside the immiscibility dome.

4. When substituted for Na, the higher polarizing cations may induce phase separation, if the Na content is reduced sufficiently for the composition to enter the immiscibility dome.

Taylor's rules are based on the position of a NBS submixture from the multicomponent system with respect to the immiscibility dome. The submixture proportions (mass fractions) are obtained by totaling the proportions of Na_2O, B_2O_3, and SiO_2 in the glass and then dividing by the total. If the NBS submixture lies outside the immiscibility dome, Taylor predicts that additions of various oxides will not promote phase separation in multicomponent systems. If the NBS submixture lies within the dome, additions of oxides with highly polarizing cations will induce phase separation. These rules are based on the assumption that problematic components (such as sulfates, phosphates, and molydates) are minimized.

12.11.4.3 Relationship Between Durability, Composition, and Phase Separation in CVS Glasses

Figure 12.29(a) shows all CVS glasses within a normalized NBS submixture. The immiscibility boundary shown is that defined by Haller et. al (1970). The solid points and open circles indicate high and low durability for quenched glasses. The distinction between high durability and low durability is based on whether glasses have MCC-1 (MCC 1983) normalized B release below or above 28 g/m^2, respectively. Because B is not involved in aqueous reactions, its normalized elemental release accurately measures the glass dissolution process.

PCT normalized B releases were not used to determine high and low durability in Figure 12.29 because a similar compositional dependency was not observed using the EA glass limit ($B \leq 8.2$ g/m^2, see Table 3.1) as the delineator. However, if the durability limit is set to a B release value of 2-3 g/m^2, the relationship is similar but not identical. The differences may

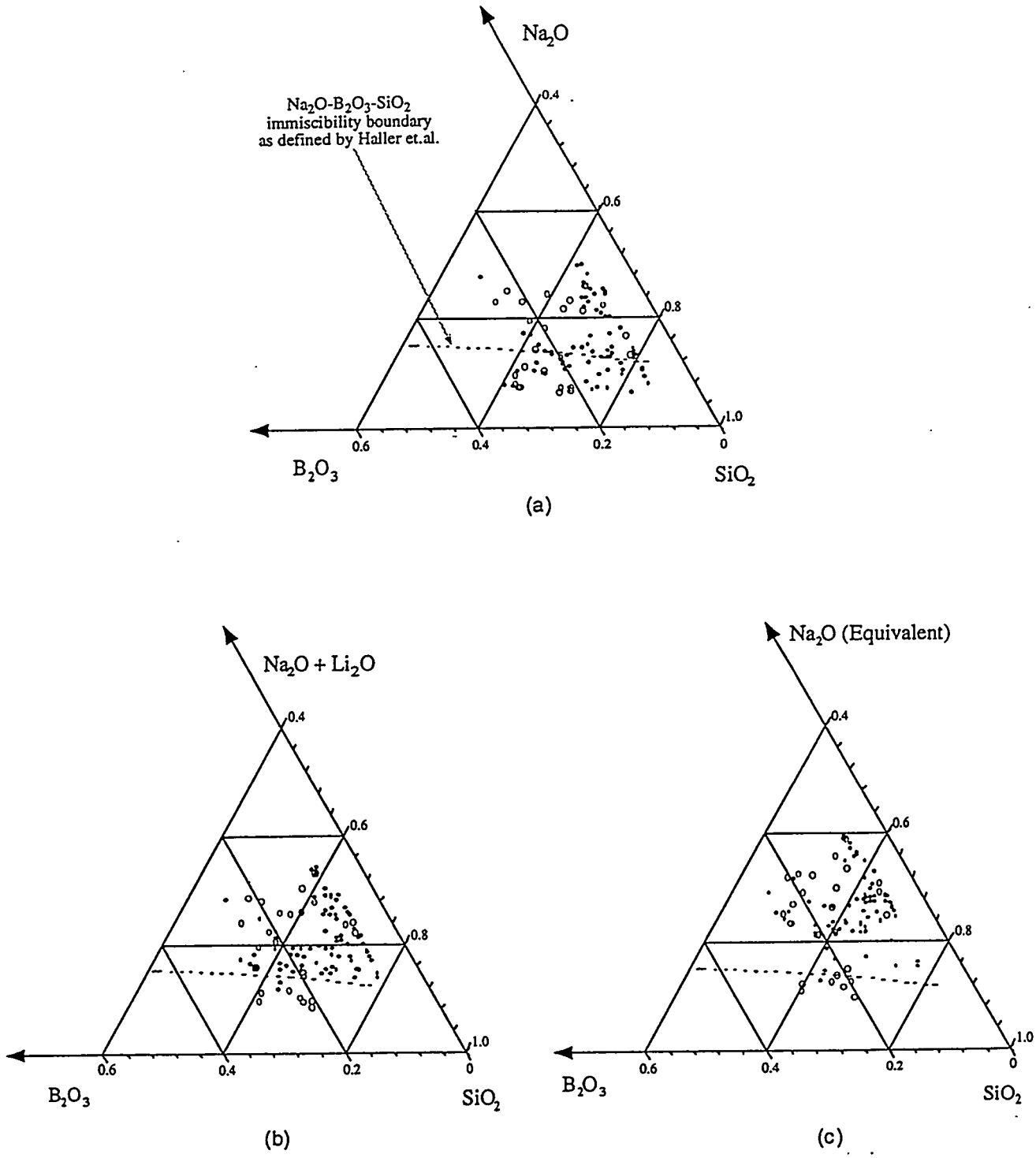

FIGURE 12.29. Various Normalized Alkali Borosilicate Submixtures Categorizing the 123 CVS-I and CVS-II Phase 1, 2, and 3 Glasses in Terms of High (•) and Low (○) MCC-1 Durability of Quenched Samples. Submixtures are (a) NBS, (b) NLBS, and (c) NBS-equivalent. The dashed line is the immiscibility boundary.

be explained by the complex compositional effects on PCT and MCC-1 test results (see Sections 12.10 and 12.11.1). Ion exchange occurs rapidly during the initial stage of the PCT test. This behavior is due to the high surface area to volume ratio between the powdered sample and the solution. The results are the rapid formation of a saturated solution and a dramatic increase in pH. Solubility limits of certain elements may be reached as dissolution proceeds, resulting in selective precipitation of various minerals. High pH solutions also tend to attack the silica network more readily. During the MCC-1 test, ion exchange occurs over a longer period of time, causing a gradual increase in pH as the solution becomes progressively more concentrated. Mechanisms of dissolution in the two tests may also differ. The effect of selective precipitation due to solution saturation and/or the prominence of ion exchange accounts for the high degree of complexity of the compositional/durability relationship in the PCT data.

Figure 12.29(a) suggests a relationship between MCC-1 durability and the position within the normalized submixture. The majority of the low durability glasses lie either within the immiscibility dome or toward the SiO_2-deficient regions of the ternary. Development of a Type A or Type B microstructure (discussed in Section 12.11.4.1) or the lack of structural integrity may be the result of the low durability CVS glasses lying within the dome. No clear distinction exists between the low and high durability glasses in the SiO_2-deficient region. A semi-defined pocket of high durability glasses exists toward the higher SiO_2 contents. As expected, the high SiO_2 glasses should provide a continuous 3-D network, resulting in a high durability system.

Another important oxide is Li_2O. As previously discussed, additions of highly polarizing cations generally expand the immiscibility dome in terms of both temperature and composition. The effect of adding Li_2O to the NBS submixture (denoted the NLBS submixture) is shown in Figure 12.29(b). Upon the addition of Li_2O to the alkali corner (on a mass fraction basis) the relationship between chemical durability and composition becomes more clearly defined. Specifically, the pocket of high durability glasses becomes more distinct and moves entirely outside the dome (with the exceptions of CVS1-11

and CVS2-30). The majority of the low durability glasses remain on the outskirts of this pocket in the SiO_2-deficient or phase separation regions.

The NLBS submixture in Figure 12.29(b) appears to contain three distinct regions. The first region is defined by submixture compositions with low durability positioned within the immiscibility dome. The developing microstructure and/or lack of structural integrity determines the durability of these glasses. Although these glasses are prone to amorphous phase separation, the quenching process limits and virtually prevents (except CVS1-9) the development of phase separation (as detected by SEM). Following the CCC heat treatment, three of these glasses (CVS2-29, CVS2-31, CVS1-4) were characterized by amorphous phase separation. When comparing MCC-1 durability results of quenched (non-phase separated) and CCC (phase separated) samples of CVS2-29 and CVS2-31, very little difference in B release values were observed. This suggests that the development of amorphous phase separation has little effect on the overall MCC-1 durability in these glasses. Compositionally, CVS2-29 and CVS2-31 have low content of Al_2O_3 and ZrO_2, i.e., the components which may enter the structure as network formers and provide structural integrity. CVS2-29 contains 0 wt% Al_2O_3 and 8.3 wt% ZrO_2; CVS2-31 contains 5.3 wt% Al_2O_3 and 0 wt% ZrO_2. The low durability of these glasses is caused by the lack of structural integrity rather than the development of amorphous phase separation. The second region consists of SiO_2-deficient submixtures having low durability. These glasses generally lack sufficient network formers to develop a continuous three-dimensional network. The third region is defined by a pocket of high durability glasses located toward the high-SiO_2 corner of the ternary and a ridge of high durability glasses along the low B_2O_3 edge. The glasses along this ridge contain approximately 5 wt% B_2O_3 (unnormalized). As the B_2O_3 content is reduced, the composition moves toward low durability Na_2O-SiO_2-based systems.

Although the composition/durability relationship becomes more distinct in the NLBS submixture, a few low durability glasses exist within the high durability pocket, as well as select high durability glasses scattered within the normalized SiO_2-deficient region (< 60 wt% SiO_2). Eight high durability glasses are intermixed with the low durability glasses in the SiO_2-deficient

region, with normalized B_2O_3 contents of at least 20 wt%. These glasses include CVS1-3, CVS2-10, CVS2-24, CVS2-58, CVS2-59, CVS2-60, CVS2-63, and CVS2-67. Glasses in this region are assumed to lack a continuous three-dimensional network that provides the structural integrity characterized by high durability systems. Not only will the SiO_2 content play a significant role in forming this continuous network, Al_2O_3 and ZrO_2 (other potential network formers) contents may also be important. All eight high durability glasses in the SiO_2-deficient region possess high Al_2O_3 contents (from 10 wt% to 20 wt%), but have extremely low ZrO_2 contents (from 0 wt% to a maximum of 1 wt%). Although these glasses lie in the SiO_2-deficient region and contain less than 1 wt% ZrO_2, their high Al_2O_3 contents seem to supplement and provide adequate network forming oxides, which results in the high durability outcomes.

A total of 10 low durability glasses that contain an average of 2.0 wt% Al_2O_3 lie in the SiO_2-deficient region. Although three of these low durability glasses (CVS1-6, CVS1-14, and CVS2-26) contain relatively high ZrO_2 contents (12, 13, and 10 wt%, respectively), the continuous network is not developed due to the low SiO_2 and Al_2O_3 contents. This result suggests that adequate SiO_2 and Al_2O_3 contents are required for the structural development of the continuous 3D network with less emphasis on the ZrO_2 content. Modifying the submixture to include Al_2O_3 and ZrO_2 is discussed in Section 12.11.4.4.

Six low durability glasses (CVS1-15, CVS1-17, CVS2-25, CVS2-82, CVS2-90, and CVS2-91) lie within the high durability pocket but outside the immiscibility dome of the NLBS submixture. Three of these glasses (CVS1-15, CVS1-17, and CVS2-25) are positioned toward the low B_2O_3 edge of the submixture with approximately 70 normalized wt% SiO_2 (the unnormalized SiO_2 values for these three glasses are approximately 56, 45, and 51 wt%, respectively). CVS1-15 and CVS1-17 contain (unnormalized) 0 wt% Al_2O_3 and 0 wt% ZrO_2, while CVS2-25 contains 0.3 wt% Al_2O_3 and 0 wt% ZrO_2. Both CVS2-90 and CVS2-91 (positioned just outside the immiscibility dome) and CVS2-82 (positioned toward higher alkali contents) also contain low Al_2O_3 and ZrO_2 contents, 2 wt% and 0.5 wt%, respectively. The inability of these six low

durability glasses to develop a 3-D continuous network may be the result of insufficient content of oxides that act as network formers.

Figure 12.29(c) categorizes the CVS glasses based on a normalized NLBS submixture, but instead of adding Li_2O on a mass fraction basis and normalizing, the Li_2O is added as an equivalent Na_2O content on a molar basis. The equivalent Na_2O content is defined as:

$$Na_2O \text{ (equivalent)} = \kappa * Li_2O \text{ (Mass \%)} + Na_2O \text{ (Mass \%)} \tag{12.2}$$

where $\kappa = 61.98/29.88$, the ratio of the molecular masses of Na_2O and Li_2O, respectively. This submixture is identified as NBS (equivalent) throughout the remainder of this section.

The most noticeable effect is a shift of the majority of glasses toward the alkali corner of the ternary leaving a select number of glasses below the constant normalized 20% Na_2O (+Li_2O) line. The low durability glasses remain relatively stable with respect to their position within this particular submixture.

The different normalized submixtures provide only limited insight into the relationship between MCC-1 durability of quenched glass and compositional effects (i.e., phase separation and/or network formation). For the NBS submixture, both low and high durability glasses exist within the immiscibility dome. With the addition of Li_2O to the alkali corner of the ternary, the distinction between the majority of low durability and high durability glasses becomes more well-defined. Of particular interest are the low durability glasses that remain within the dome. Not only may the formation of amorphous phase separation or the lack of a continuous 3-D network result in a low durability system, but other interrelated effects, such as crystallization, need to be considered.

12.11.4.4 Evaluation of Taylor's Immiscibility Model

Besides providing limited insight into the durability/composition relationship, the data in Figure 12.29(a) also provide a template from which various CVS glasses can be selected to evaluate the effectiveness of using

various submixtures to predict immiscibility. A series of 24 normalized NBS submixture compositions were chosen [Figure 12.30(a)] that would allow a direct evaluation of Taylor's immiscibility prediction model. Although both high- and low-durability glasses were selected from within the immiscibility boundary, of primary interest was to isolate a particular submixture that could predict the development of amorphous phase separation in canistered glasses. The reference to durability in this section is only intended for identification/tracking purposes. The position of the submixture composition with respect to the immiscibility boundary and the microstructural development after CCC is of primary interest.

All glasses evaluated have a thermal history corresponding to the predicted CCC schedule in Table 5.1. For the detection of amorphous phase separation, a freshly fractured glass surface was etched with a 5% HF solution at room temperature and analyzed by SEM. Enhanced etching will occur in low durability areas (SiO_2-deficient), providing surface relief if amorphous phase separation exists. If the sample is homogeneous with respect to amorphous phase separation, no selective etching results.

Table 12.21 shows the SEM results for the 24 selected CVS glasses in terms of amorphous phase separation for the three normalized submixtures. The descriptive microstructural characteristics are based on the SEM analyses and are divided into three categories defined as homogeneous or non-phase separated (•), phase separated (o), and highly crystalline (*). The position of each glass with respect to the immiscibility dome is also given for each submixture. "Yes" corresponds to a glass composition lying within the immiscibility dome, while "-" relates to a composition outside the dome.

As predicted by Taylor's rules, glasses lying outside the immiscibility dome in the NBS normalized submixture show no sign of amorphous phase separation. Contrary to Taylor's predictions none of the "high-durability" glasses lying within the immiscibility boundary show signs of amorphous phase separation by SEM analysis after CCC. Amorphous phase separation or a high degree of crystallinity was detected by SEM in six of the eight "low-durability" CCC glasses lying inside the dome. The high crystallinity of CVS1-9 is the result of the centerline canister cooling schedule. Within the

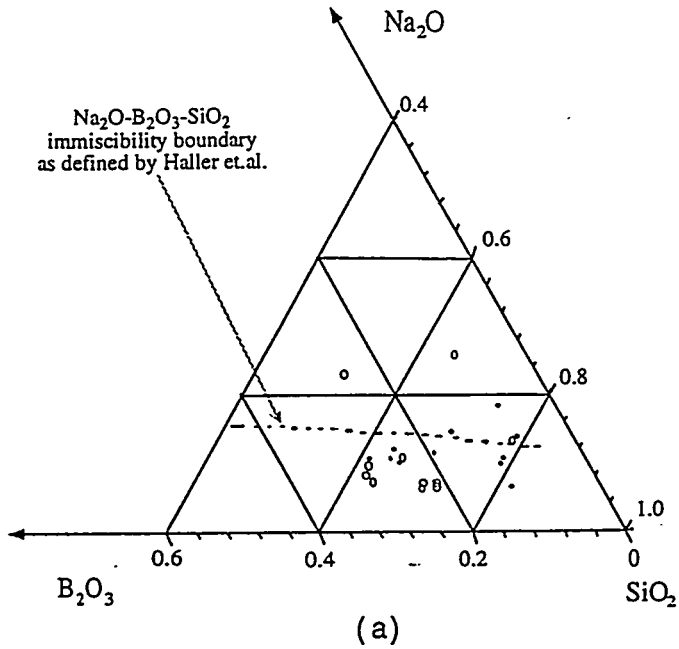

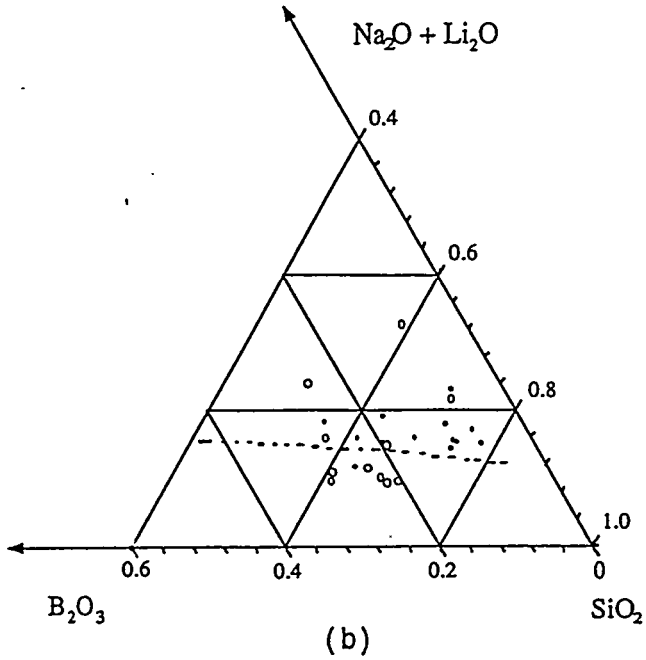

FIGURE 12.30. Compositional Positions of the 24 CVS Glasses Selected for Analysis Within the (a) NBS and (b) NLBS Normalized Submixtures

TABLE 12.21. Microstructural Analysis of 24 Canister-Centerline-Cooled CVS Glasses by SEM[a]

	CVS Glass	SEM	NBS	NLBS	NBS-Equiv
High Durability	CVS2-30	•	YES	YES	YES
	CVS1-11	•	YES	YES	-
	CVS2-52	•	YES	-	-
	CVS2-6	•	YES	-	-
	CVS2-43	•	YES	-	-
	CVS2-74	•	YES	-	-
	CVS2-24	•	YES	-	-
	CVS1-10	•	YES	-	-
	CVS2-12	•	YES	-	-
	CVS2-73	•	YES	-	-
	CVS1-7	•	-	-	-
	CVS2-47	•	-	-	-
	CVS2-38	•	-	-	-
Low Durability	CVS2-29	o	YES	YES	YES
	CVS1-9	*	YES	YES	YES
	CVS1-4	o	YES	YES	YES
	CVS2-31	o	YES	YES	YES
	CVS2-80	*	YES	YES	YES
	CVS2-78	*	YES	YES	YES
	CVS2-90	•	YES	-	-
	CVS2-26	•	YES	-	-
	CVS1-14	•	-	-	-
	CVS2-25	•	-	-	-
	CVS2-81	•	-	-	-

(a) Microstructural characteristics as defined by the SEM are categorized into three classes. Symbols representing each class are (•) non-phase separated or homogeneous, (o) phase separated, and (*) highly crystalline. To define each compositional position with respect to the immiscibility boundary for each submixture, "Yes" indicates a composition lying within the dome while "-" defines a composition lying outside the dome.

susceptible region of crystallization, the average cooling rate is approximately 20°C per hour. This slower cooling rate (relative to quenching) kinetically favors crystallization, if crystallization is thermodynamically favorable. It has also been shown that amorphous phase separation may be a precursor to crystallization (Burnett and Douglas 1971). Therefore, the high

degree of crystallinity may have been aided by prior amorphous phase separation. In fact, amorphous phase separation and less extensive crystallization was detected in a quenched sample of CVS1-9, showing the effect of thermal history on the developing microstructure. Of the 24 glasses studied, one-half conflict with Taylor's rules for immiscibility prediction within multicomponent systems.

Figure 12.30(b) shows the 24 glasses within the NLBS submixture. As was shown in Figure 12.29(b), the addition of Li_2O causes several glasses to shift relative to the immiscibility dome. This effect can also be seen in Table 12.21 as the majority of the non-phase separated glasses shift outside the immiscibility dome for the NLBS submixture that initially were within the dome for the NBS submixture. Note CVS2-90 and CVS2-26 show no sign of amorphous phase separation. They also shift outside the dome in the NLBS submixture, thereby increasing the efficiency in predicting immiscibility.

Glasses which are characterized by either amorphous phase separation or a high degree of crystallinity remain within the immiscibility boundary of the NLBS submixture. Only two glasses (CVS2-30 and CVS1-11) do not follow the modified rules for predicting immiscibility in multicomponent systems. Amorphous phase separation was not detected in either glass, but both lie within the immiscibility dome. Of particular interest is CVS1-11 which contains 14 wt% Al_2O_3, known to suppress amorphous phase separation. No CVS glasses lying outside the dome in the NLBS submixture show signs of amorphous phase separation.

Very little difference is found between the NLBS and NBS (equivalent) submixtures in terms of predictability effectiveness (Table 12.21). Although, of the two anomalous glasses in the previous submixture (CVS1-11 and CVS2-30), only CVS2-30 cannot be accounted for by the NLBS submixture. As expected, no compositions outside the dome show signs of amorphous phase separation.

With the addition of Li_2O to the NBS submixture, either as an equivalent Na_2O content or strictly normalized on a mass basis, the experimental results indicate that amorphous phase separation may be more accurately predicted. This increased prediction accuracy is illustrated by the submixture's ability to effectively sort those glasses that were experimentally determined to be

phase separated from the "homogeneous" glasses. Although both the NLBS and NBS (equivalent) submixtures seem to adequately predict amorphous phase separation (see Table 12.21), neither submixture is 100% accurate based on the SEM analysis. This situation is not surprising due to the compositional complexity of the glasses involved. The addition of Li_2O, in either system, also served to more clearly define the relationship between durability and normalized composition.

A limited number of glasses have been evaluated by Transmission Electron Microscopy (TEM) to detect amorphous phase separation on a scale undetectable by SEM. Although there were no disagreements in terms of the predicted development of phase separation and the limited TEM results, further study would be beneficial (for predictability of phase separation and also for isolating the effect of amorphous phase separation on durability).

Due to the limited number of glasses evaluated, it is difficult to conclude which of the two NLBS submixtures [NLBS and NBS(equivalent)] should be used to predict immiscibility behavior. The NLBS and NBS (equivalent) submixtures yield the same results except for two glasses. The predictability difference between the two NLBS submixtures may be a function of the specific submixture or an effect of composition.

Other submixtures need to be evaluated for their ability to predict immiscibility within these complex glasses. For example, a normalized Na_2O+Li_2O - B_2O_3 - $SiO_2+Al_2O_3+ZrO_2$ submixture may enhance the prediction accuracy since Al_2O_3 and ZrO_2 usually suppresses phase separation and may aid in the development of the 3-D network.

Statistical methods for predicting categorical data (phase separation) from quantitative data (composition), such as discriminant analysis and tree-based regression methods, could also be investigated. Such methods are able to produce more complicated functions of components (than the renormalized sums of components considered previously) to predict phase separation. However, to work well, these methods require a significant proportion of the data to be on phase separated glasses.

12.11.4.5 Anomalous and High Release Glasses

Among the 12 CVS glasses [CVS1-4, CVS1-6, CVS1-9, CVS1-12, CVS1-13, CVS1-15, CVS1-21 (a replicate of CVS1-4), CVS2-81, CVS2-82, CVS2-92, CVS2-93, and CVS2-94] with the largest observed MCC-1 normalized boron releases (ranging from 86 g/m^2 to 690 g/m^2), eight (CVS1-4, CVS1-6, CVS1-9, CVS1-13, CVS1-15, CVS1-21, CVS2-82 and CVS2-93) have vastly different measured B release values than that predicted by the first-order mixture model from Table 12.2a. Hence, they fall into the category of anomalous glasses with the difference between measured and predicted release values exceeding 80 g/m^2.

The first-order release-composition model predicts MCC-1 release values that are relatively consistent with measured values for the remaining four glasses (CVS1-12, CVS2-81, CVS2-92, and CVS2-94). The high release values may also be due to structural deficiency and/or amorphous phase separation.

Figure 12.31(a) and (b) show the position of the 12 high release glasses relative to the immiscibility dome within the normalized NBS and NLBS submixtures, respectively. Three of these glasses (CVS1-4, CVS-21 (replicate) and CVS1-9) are within the NLBS immiscibility dome. Two (CVS1-4 and CVS1-9) have been experimentally evaluated by SEM and are characterized by phase separation and/or high crystallinity. Compositionally, these two glasses, as well as CVS1-12 and CVS1-21, contain no Al_2O_3 or ZrO_2, which are known to suppress phase separation.

Microstructural analysis of CVS1-12 and CVS1-6 by SEM/TEM techniques would provide insight into the inter-related or independent effects of submixture effectiveness for predictability (because both move outside the dome in the NLBS system). Such analysis would also provide insight as to what extent, if any, Al_2O_3 and ZrO_2 affect the formation of phase separation in multicomponent systems.

The low durabilities of the glasses lying outside the immiscibility dome are probably the result of structural deficiency or the lack of a developed 3-D network. With one exception (CVS1-15), all of these glasses lie in the low SiO_2 regions of the NBS ternary. Upon addition of Li_2O, these glasses

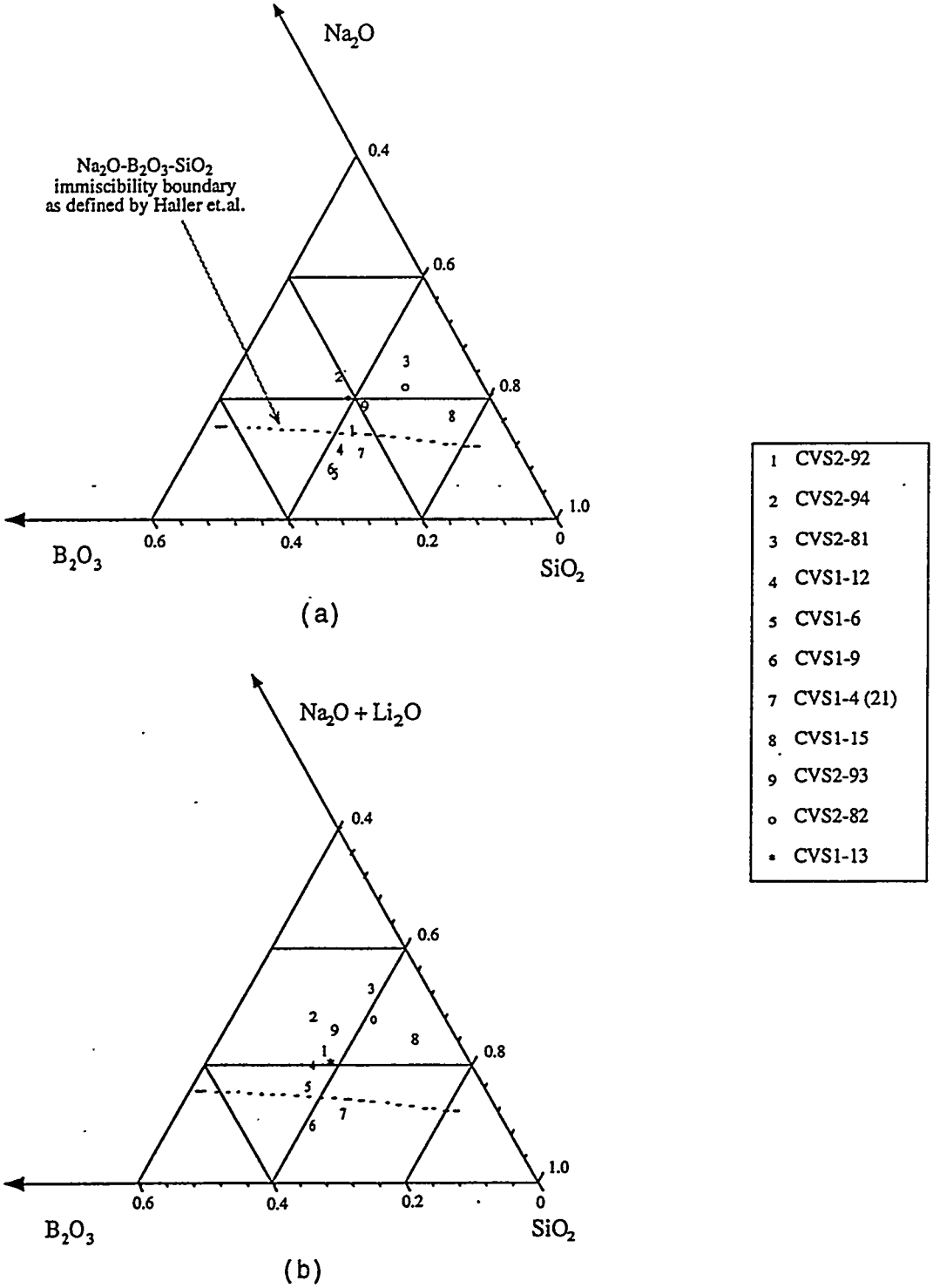

FIGURE 12.31. Compositional Positions of the High Release Glasses Within the (a) NBS and (b) NLBS Normalized Submixtures

remain in the low SiO_2 regions outside the dome. As discussed in Section 12.11.4.3, the formation of the 3-D continuous network is dependent upon adequate content of network formers (SiO_2, Al_2O_3, and ZrO_2). CVS1-15 contains no Al_2O_3 or ZrO_2 which decreases the formation probability of the continuous network. The low durability must be associated with this structural deficiency rather than devitrification effects (CVS1-15 contains 0% crystallization) or amorphous phase separation (lying outside the immiscibility dome for all submixtures).

SEM analyses of CVS2-81 and CVS2-94 show no sign of amorphous phase separation. This result is in agreement with the modified predictability model. Because CVS2-81 contains less than 3.0 wt% Al_2O_3 and ZrO_2, the low durability is expected, although the composition is located in close proximity to the 5% B_2O_3 high durability ridge.

Durability of these multicomponent glasses seems to be a function of several interrelated characteristics that define the microstructure. These characteristics include not only the formation of amorphous phase separation, the microstructural type, and possibly the scale of separation, but also the development of a continuous 3-D network and the type and extent of crystallization. These factors are primarily influenced by the overall composition and the thermal history of each system.

12.11.5 Normalized Releases of Si, Li, Na, Mo, and Cs

According to a personal communication with D.M. Strachan in 1990, alkali ion (Li^+, Na^+, Cs^+) extraction occurs simultaneously with glass dissolution and releases additional alkali ions at the beginning of the process (Pederson et al. 1986). If, for example, $r_{Li} - r_B = 1$ g/m², the equivalent lithium-depleted depth is $\delta = (r_{Li} - r_B)/\rho = 400$ nm, where ρ is glass density (2.6×10^6 g/m^3). Apart from being extracted, alkali ions may also be partly absorbed in the alteration (gel) layer (Strachan et al. 1982). In addition, Na^+ and Cs^+ may form solid compounds with silica and other oxides in an aqueous environment. Hence, normalized releases of alkali oxides can be lower or higher than the normalized releases of boron, according to whether alkali extraction or precipitation/gel layer absorption dominates.

Alkali ion extraction (also referred to as alkali ion exchange) is caused by diffusion of water (or hydronium, H_3O^+) into the glass and diffusion of Na^+ and OH^- out of the glass back to the solution at the beginning of the glass-water interactive process. The integrity of the silicate network is presumed. This initial ion exchange is the cause of the early increase of the solution pH. This pH increase gets larger as the glass surface to water volume ratio increases (Feng et al. 1991). Thus, PCT solutions have generally higher pH values than MCC-1 solutions (see Section 12.10).

Normalized Mo and Cs releases for MCC-1 and PCT were obtained and modeled in CVS-I (see Piepel, Hrma, et al. 1993), but were dropped from further study in CVS-II for several reasons (e.g., the focus on B, Li, and Na releases in WAPS revisions, less precision in Cs and Mo normalized releases due to low Cs_2O and MoO_3 mass fractions in glass, different analytical procedure required for Cs, and the similarity of Mo and B releases).

During the initial stage of dissolution, preferential extraction of B occurs, after which the normalized Si release is progressively lower than that of B because the solution approaches the saturation level of Si during dissolution. This phenomena is illustrated in Figure 12.28 for two CVS glasses. Additional hydrolyzed Si is retained in an alteration (or gel) layer on the glass surface or in the form of colloids.

The normalized B release is, by the first-order model,

$$\ln r_B = \sum_{i=1}^{10} (a_B)_i x_i, \tag{12.3}$$

where $(a_B)_i$ is the i-th component first-order coefficient for normalized B release. Similar equations can be written for other elements. For example, the normalized Si release is

$$\ln r_{Si} = \sum_{i=1}^{10} (a_{Si})_i x_i, \tag{12.4}$$

where $(a_{Si})_i$ is the i-th component first-order coefficient for normalized Si release. Subtracting equations (12.2 and 12.3) results in

$$\ln \frac{r_{Si}}{r_B} = \sum_{i=1}^{10} [(a_{Si})_i - (a_B)_i] x_i . \qquad (12.5)$$

As was stated in the introduction to Chapter 12, r_B best represents dissolution of the glass network. On the other hand, r_{Si} represents only that part of the silicate network that remained in solution (and did not precipitate as a mineral or remain in the form of a hydrated silica gel). The ratio r_{Si}/r_B is the fraction of dissolved silicon that remains in solution. The difference $(a_{Si})_i$ - $(a_B)_i$ reflects the effects of glass components (i = 1, 2, ..., 10) on the fraction of Si in solution. Elements that tend to increase this fraction will reduce the driving force for glass dissolution and thus increase durability. Hence, the driving force for dissolution is related to the concentration of Si in solution. Elements that tend to decrease r_{Si}/r_B will decrease durability. These elements decrease the solubility of silicon in solution or aid in the precipitation of silicon containing phases, increasing the driving force (chemical affinity) of network dissolution.

The differences between the oxide component coefficients for the normalized releases of Si and B are plotted in Figure 12.32 for PCT and Figure 12.33 for MCC-1. If this difference is positive for the i-th oxide, this oxide will tend to increase the concentration of Si in solution or decrease the concentration of B. The difference is positive for Al_2O_3 (for MCC-1 and PCT), and hence Al_2O_3 decreases r_B and slows the dissolution rate by strengthening glass structure. The difference is also positive for CaO, which supports results from Figure 12.28. Components that reduce glass durability (B_2O_3, Na_2O, Li_2O, and MgO) cause the Si minus B component coefficient difference to be negative. B_2O_3 additions increase glass dissolution which in turn increases the absolute concentration of Si in solution above the solubility limit and hence decreases r_{Si}/r_B. Alkaline components (Na_2O and Li_2O) increase solution pH. As pH increases, the solubility of Si increases, however, glass dissolution rate also increases. The increase in dissolution increases Si concentration above the increase in Si solubility, hence alkalis decrease r_{Si}/r_B. MgO decreases r_{Si}/r_B due to formation of magnesium silicates, which reduces the amount of silica in solution. Components other than

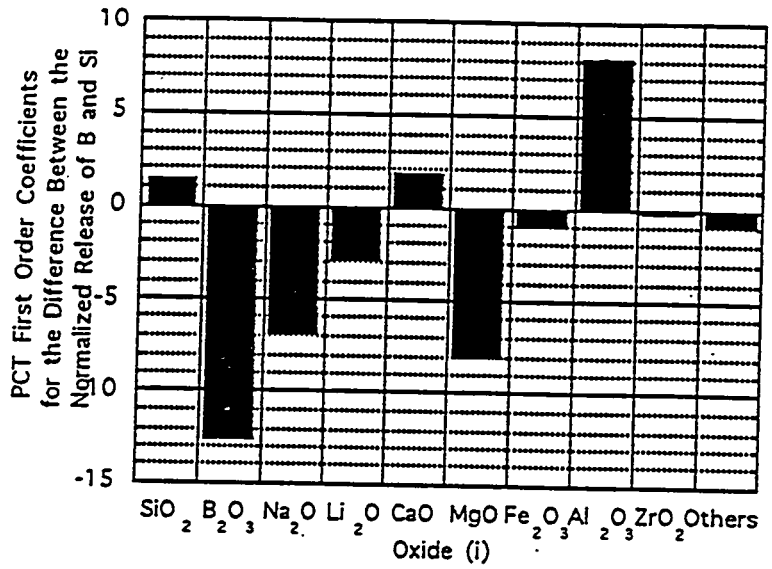

FIGURE 12.32. Component-Wise Differences Between Coefficients of First-Order Mixture Models for Si, Na, and Li Normalized Elemental Releases With That of B for PCT

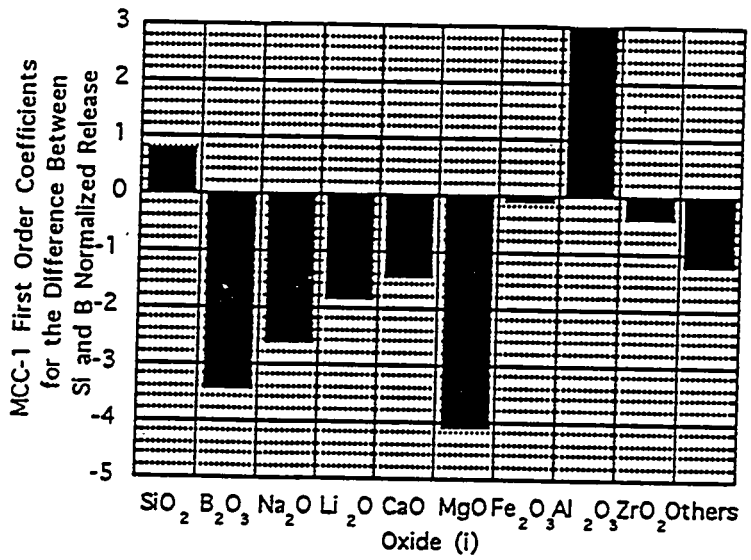

FIGURE 12.33. Component-Wise Differences Between Coefficients of First-Order Mixture Models for Si, Na, and Li Normalized Elemental Releases With That of B for MCC-1

alkalis, alkali earths, Al_2O_3, and B_2O_3 (i.e., SiO_2, Fe_2O_3, ZrO_2, and Others) have negligible effects on r_{Si}/r_B.

12.12 EFFECT OF CRYSTALLINITY ON DURABILITY OF SELECTED CVS GLASSES

Some canistered nuclear waste glasses will contain crystalline phases that will precipitate during cooling. Crystallization can affect glass durability by mechanical effects (internal stresses, cracks, and pores) and by changing the composition of the glass matrix. Glass durability as a function of crystallization was studied at the Savannah River Laboratory for Savannah River defense waste glasses (Jantzen and Bickford 1985). The crystalline phases precipitated from Savannah River glasses after simulated canister centerline cooling were spinel (nominally $NiFe_2O_4$), acmite ($NaFeSi_2O_6$, one of the clinopyroxenes), and nepheline ($NaAlSiO_4$). Crystallization of spinel and acmite totaling 5 to 20 vol% caused a one- to three-times increase of boron release compared to the non-crystallized glass of the same composition. Crystallization of nepheline caused additional loss of durability.

The effect of crystallization on glass durability was studied on selected CVS glasses (see Table 12.22) that were subjected to canister centerline cooling (CCC) heat treatment (see Table 5.1 in Section 5.5). (Tables 11.1 and 11.2 contain crystallinity results for CCC samples of all CVS glasses, and the analysis of durability data on CCC samples for all CVS compositions will be available at the end of FY 1994.) The internal standard glass (CVS2-51) was also isothermally heat treated for 48 hours at 600°C, 700°C, and 800°C. These samples contained crystals after the heat treatment as seen by optical microscopy. X-ray diffraction analysis showed that the amount of crystalline material (clinopyroxene) was below the detection limit of approximately 1 vol% in the 600°C and 800°C samples. The 700°C sample had 7-8 vol% clinopyroxene. This sample was selected for further testing.

Crystalline phases detected by X-ray diffraction in the CCC heat treated glasses are listed in Table 12.22. The heat treated glasses were also examined by optical and scanning electron microscopy. The CVS1-6 sample had isolated crystals completely surrounded by glass. The CVS1-16, CVS2-22,

TABLE 12.22. Crystalline Phases and Estimated Volume % in CVS Glasses After CCC Heat Treatment

Glass	Crystalline Phases	Vol%
CVS1-6	Zircon ($ZrSiO_4$)	8-10
CVS1-16	Nepheline ($NaAlSiO_4$)	15-18
CVS2-22	Lithium Silicate (Li_2SiO_3)	7
	Orthopyroxene [$(Mg,Fe)SiO_3$]	7
CVS2-29	Phase separation (b)	--
CVS2-30	Hematite (Fe_2O_3)	9
	Cristobalite (SiO_2)	2
CVS2-42	Clinopyroxene (c)	20
	Lithium Silicate (Li_2SiO_3)	10-15
CVS2-51	None	--
CVS2-51 (a)	Clinopyroxene (c)	7-8

(a) Heat treated at 700°C for 48 h.

(b) Detected by SEM.

(c) Typical composition: $(Na,Ca)(Fe^{2+},Fe^{3+},Mg)(SiO_3)_2$.

CVS2-30, and CVS2-42 samples exhibited a network of crystals, making it difficult to examine the samples with transmitted light. The CVS2-30 glass was permeated with thin plates of hematite. In the CVS1-16, CVS2-22 and CVS2-42 glasses, crystals were close to each other and connected with each other in some areas. Heavily crystallized areas were porous, probably because of the density mismatch between crystalline and amorphous phases. Only a few pores were observed in CVS1-16, where the density of nepheline (~2.6 g/cm^3) is similar to that of the glass. A large number of pores were found in CVS2-22 and CVS2-42, where the densities of orthopyroxene (~3.6 g/cm^3) and clinopyroxene (~3.5 g/cm^3) are greater than the density of the glass. The absence of pores in CVS2-30 with high-density hematite (~5.2 g/cm^3) can probably be attributed to the high temperature at which hematite precipitates (>1100°C) and where the viscous glass matrix can easily accommodate changes in volume.

The CVS2-29 glass was quite different than the other CCC heat-treated glasses. A layer of clear glass existed near the crucible walls. In the center of the crucible, an opaque material displayed a variety of colors dispersed in a swirling pattern, which indicates amorphous phase separation. Amorphous phase separation in the CCC sample of CVS2-29 was verified through SEM analysis.

The CCC heat-treated samples (listed in Table 12.22) and the internal standard glass sample isothermally treated at 700°C were tested in duplicate for PCT durability and the solutions were analyzed by ICP. The averaged (across duplicate results) Si, B, Na, and Li normalized releases (g/m^2) for both CCC heat-treated glasses and quenched glasses are given in Table 12.23. The normalized boron releases for quenched and CCC heat-treated glasses are compared graphically in Figure 12.34.

The PCT results indicate that the CCC heat-treated internal standard glass (CVS2-51) is slightly more durable than the quenched glass, but the difference is negligible. The 48-hour heat treatment of the same glass at 700°C led to an increase of PCT boron release by 41% compared to the quenched glass.

The CVS1-6, CVS2-22 and CVS2-29 glasses experienced no significant changes in PCT durability for crystallized samples compared to quenched samples of the same composition. The CVS2-29 glass had no crystallinity after CCC heat treatment, but was amorphous phase separated. No change in PCT durability was observed between CCC heat-treated and quenched samples of CVS2-29. The effect of amorphous phase separation on CVS glass durability is discussed in more detail in Section 12.11.4.3.

The sharpest increase in PCT boron release after CCC heat treatment was observed in CVS1-16, from 0.51 to 21.2 g/m^2. This strong effect is probably a result of removing aluminum oxide and silica from the glass matrix. The PCT boron release from CVS2-30 and CVS2-42 increased 3.4 and 5.4 times, respectively, after CCC heat treatment. These increased releases were probably caused by mechanical stress due to crystallization in CVS2-30 (cristobalite and hematite) and CVS2-42 (clinopyroxene and lithium silicate) and by a mechanically damaged matrix in CVS2-42. Stresses will only be partly

TABLE 12.23. PCT Normalized Releases of Quenched and Canister-Centerline-Cooled Heat-Treated CVS Glasses

	Normalized Elemental Release (g/m^2)[a]							
	Silica		Boron		Sodium		Lithium	
Glass	Q	CCC	Q	CCC	Q	CCC	Q	CCC
CVS1-6	0.331	0.322	6.368	6.238	2.836	2.196	5.560	4.800
CVS1-16	0.246	1.579	0.513	21.162	0.581	7.745	0.312	10.487
CVS2-22	2.249	2.062	9.646	9.003	6.097	5.593	5.453	4.378
CVS2-29	0.193	0.186	1.286	1.206	1.273	1.048	1.355	1.129
CVS2-30	0.174	0.237	6.511	22.106	2.551	9.314	4.194	16.667
CVS2-42	0.574	1.883	1.695	9.325	1.337	4.528	1.220	4.762
CVS2-51	0.411	0.381	1.764	1.529	1.283	1.134	1.496	1.091
CVS2-51		0.461[b]		2.608[b]		1.522[b]		1.903[b]

(a) All numbers are averages of two test results.

(b) Sample heat treated at 700°C for 48 hours.

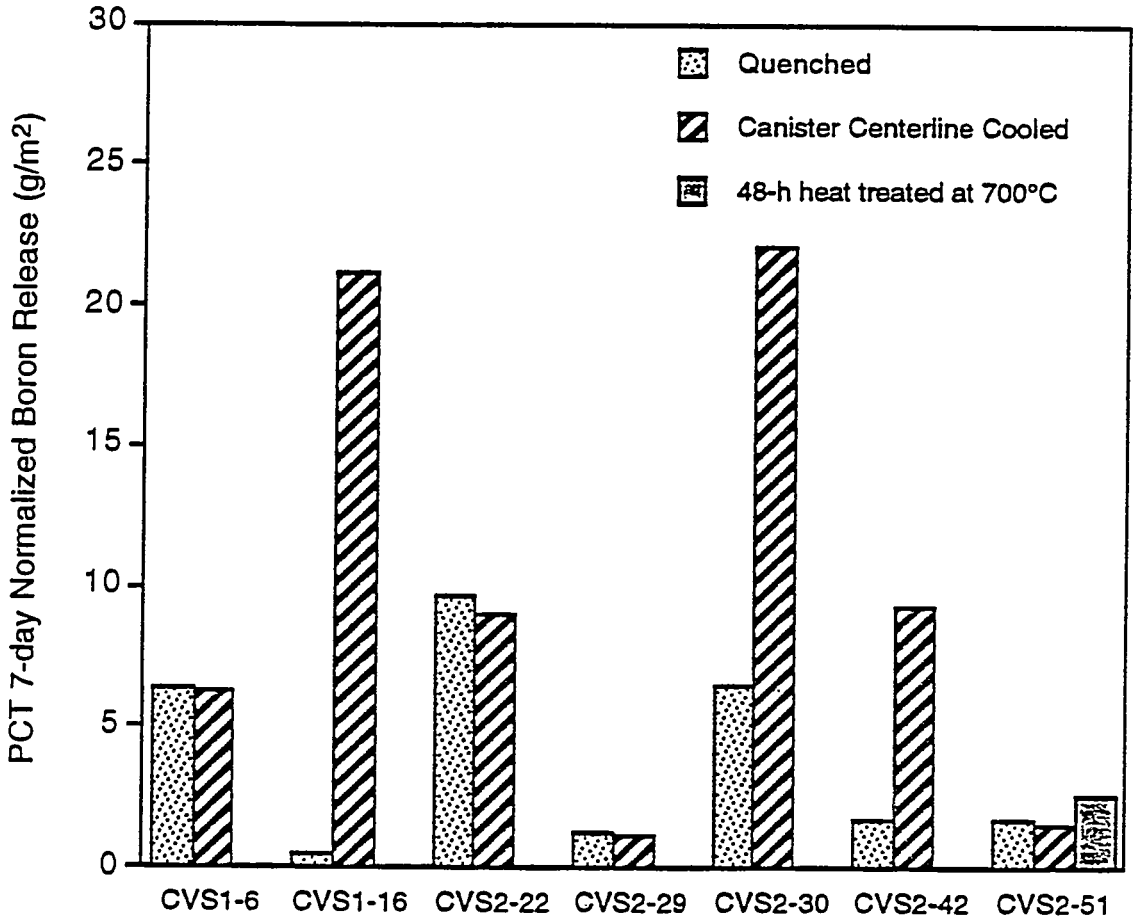

FIGURE 12.34. 7-Day PCT Normalized Boron Releases from Quenched and Heat-Treated Glasses

relieved by crushing the glass, dependent on the size of the crystals (which are generally smaller than the glass particles).

Although glass durability can be increased, decreased, or unaffected by crystallization, only decreases or "no effects" were observed in the samples tested. The decrease in durability seems to be produced by chemical alteration of the glassy matrix and by mechanical causes, such as stress, cracks and porosity. The extent of mechanical damage depends on the volume fraction of the crystalline phase, the density mismatch between the crystals and glassy matrix (which produces permanent stresses during cooling), and the glass viscosity at the time of crystallization (which allows stress relaxation by flow). A general conclusion about the effect of crystallinity on durability of CVS glass can be made only after the analysis of the CCC glass durability data for all CVS glasses are completed.

13.0 MISCELLANEOUS GLASS PROPERTY DATA INVESTIGATIONS

Relationships among glass property values are investigated in Section 13.1. The effects of varying the composition of the Others component in several CVS glasses is discussed in Section 13.2. Results and discussion of overcheck tests and analyses performed at various offsite labs are contained in Section 13.3.

13.1 CORRELATIONS AMONG GLASS PROPERTIES

Pairwise Pearson correlation coefficients for the untransformed and transformed (see Table 6.1) glass and melt properties are given in Tables 13.1 and 13.2, respectively. Pairwise property correlations are investigated to gain an understanding of the relationships between glass properties over a range of compositions. A Pearson correlation coefficient of +1.0 (or -1.0) for a pair of properties would indicate the pair is perfectly linearly related with a positive (or negative) slope. A value of 0.0 would indicate absolutely no linear relationship exists between the properties. Thus, the closer a correlation value is to +1.0 or -1.0, the stronger the linear relationship between the pair of properties.

In Table 13.1, the strongest pairwise correlations (above 0.99) among untransformed property values occur among the normalized 28-day MCC-1 releases of B, Li, and Na, indicating that the results for these elements are strongly linearly related. MCC-1 Si releases are also highly correlated with MCC-1 B, Li, and Na releases (correlation coefficients above 0.95). Normalized 7-day PCT releases for B, Li, and Na are also highly correlated (correlation coefficients above 0.97). Smaller correlations between PCT Si releases and PCT B, Li, and Na releases are probably due to the tendency of Si to saturate the solution prior to completion of the tests. Pairwise correlations among PCT B, Li, and Na releases and MCC-1 Si, B, Li, and Na releases range from roughly 0.7 - 0.8. PCT Si releases do not correlate well with MCC-1 Si, B, Li, and Na releases (correlation coefficients in the range 0.28 to 0.38), again possibly due to Si saturation in PCT tests.

TABLE 13.1. Pairwise Correlations[a] Among Untransformed Glass Properties

	η_{1150}	ϵ_{1150}	T_g	α_s	α_m	28-Day MCC-1 Release				7-Day PCT Release		
						Si	B	Li	Na	Si	B	Li
ϵ_{1150}	-.427											
T_g	.451	-.792										
α_s	-.449	.677	-.665									
α_m	-.368	.002	-.035	.035								
MCC-1 Si	-.130	.171	-.095	.041	.205							
MCC-1 B	-.130	.103	-.029	-.027	.168	.959						
MCC-1 Li	-.134	.096	-.013	-.036	.183	.951	.996					
MCC-1 Na	-.129	.092	-.018	-.025	.176	.959	.994	.992				
PCT Si	-.199	.484	-.450	.504	.069	.380	.298	.284	.302			
PCT B	-.201	.302	-.252	.193	.066	.704	.752	.736	.745	.668		
PCT Li	-.189	.221	-.147	.089	.078	.715	.798	.788	.795	.540	.973	
PCT Na	-.201	.284	-.242	.205	.075	.740	.783	.768	.782	.667	.987	.970

(a) Pearson correlation coefficients take values between -1 and +1, which represent perfect negative and positive correlation, respectively.

(b) Data for glasses CVS1-13, CVS2-75, CVS2-82, and CVS2-83 were identified as outliers (for at least one property for each glass) and were not used in computing the correlation coefficients shown in this table.

TABLE 13.2. Pairwise Correlations[a] Among Transformed[b] Glass Properties

	η_{1150}	ϵ_{1150}	T_g	α_s	α_m	28-Day MCC-1 Release Si	B	Li	Na	7-Day PCT Release Si	B	Li
ϵ_{1150}	-.638											
T_g	.582	-.805										
α_s	-.585	.714	-.675									
α_m	-.378	.048	.005	.015								
MCC-1 Si	-.413	.085	-.106	.144	.255							
MCC-1 B	-.439	.042	-.064	.096	.260	.956						
MCC-1 Li	-.437	.028	-.041	.089	.267	.947	.995					
MCC-1 Na	-.440	.037	-.064	.127	.262	.960	.973	.966				
PCT Si	-.493	.451	-.481	.510	.156	.613	.577	.554	.582			
PCT B	-.516	.231	-.260	.285	.209	.702	.754	.737	.751	.835		
PCT Li	-.518	.220	-.243	.264	.220	.707	.764	.753	.762	.806	.983	
PCT Na	-.542	.247	-.275	.356	.198	.723	.775	.764	.767	.827	.970	.963

(a) Pearson correlation coefficients take values between -1 and +1, which represent perfect negative and positive correlation, respectively.

(b) The property transformations are identified in Table 6.1, and consist of natural log transformations on all properties except T_g, α_s, and α_m, which are not transformed.

(c) Data for at least one property of CVS2-75 were identified as outliers and were not used in computing the correlation coefficients shown in this table.

Relatively large correlations (greater than 0.6 in absolute value) exist between T_g and ϵ_{1150} (-0.792), α_s and ϵ_{1150} (0.677), and α_s and T_g (-0.665) in Table 13.1. Moderate negative correlation between η_{1150} and ϵ_{1150} (-0.427) indicates some tendency for these properties to vary inversely, but it is not a strong tendency due to different transport mechanisms of electric charge and mechanical momentum within the glass melt network. Whereas electric charge is transported predominantly by alkali ions moving inside the borosilicate network, viscous flow requires breaking the network bonds.

In Table 13.2, the property transformations increase the correlation between η_{1150} and ϵ_{1150} (-0.638), but it is still not extremely strong. Correlations among and between normalized MCC-1 and PCT Si, B, Na, and Li releases are similar to untransformed values. Also similar are the relatively large correlations between T_g and ϵ_{1150} (-0.805), α_s and ϵ_{1150} (0.714), and α_s and T_g (-0.675).

13.2 EFFECTS OF VARYING OTHERS COMPOSITION

Most of the glasses studied in the CVS have had the same Others mix of minor components (corresponding to the NCAW waste type, see Table 4.1). However, the Others composition will vary within and between the various wastes to be vitrified in the Hanford HLW vitrification plant, and so several glasses with different Others mixes have been tested to determine the impact, if any, on glass properties.

Table 13.3 contains the property values for several sets of glasses. Each set contains a base glass and one or more other glasses with the same composition as the base glass except for different Others mixes. The standard deviations in Tables F.4, F.5, F.6, and F.8 that estimate random and experimental error variability (based on all replicate glasses) are useful in comparing property values within a data set. Descriptions of each set and the effects of different Others mixes on property values are given in the following paragraphs.

The first set of glasses (CVS2-1 versus CVS2-53) provides only for assessing the impact of substituting UO_2 for Nd_2O_3 on PCT durability, because that was the only property measured for the radioactive glass CVS2-53. These

Table 13.3. Property Values for Sets of Glasses with the Same 10-Component Compositions but Different Others Mixes

Set	Glass #	Others (a) Description	Viscosity at 1150°C (Pa·s)	EC at 1150°C (S/m)	MCC-1 B Release (g/m^2)	PCT B Release (g/m^2)	T_g (°C)	α_s (10^{-6}/K)	α_m (10^{-6}/K)	Non-Spinel T_L (°C)	Spinel T_L (°C)
1	CVS2-1	NCAW	7.74	32.55	12.24	0.312	474.5	8.8	114.2	929	~1048
	CVS2-53	UO_2 replaced Nd_2O_3	-.--(b)	--.-	-.--	0.304	---.-	-.--	--.-	----	----
2	CVS2-19	Internal Standard	6.76	27.55	13.69	1.990	493.0	9.8	99.3	862	>883
	CVS2-51	Internal Standard	7.07	28.30	12.35	1.764	478.0	9.39	94.2	856	~899
	CVS2-97	Internal Standard	7.25	24.56	12.89	1.434	489.3	10.1	104.1	858	~887
	CVS2-123	Internal standard	-.--(b)	--.-	15.65	1.473	---.-	-.--	--.-	----	----
	CVS2-54	UO_2 replaced Nd_2O_3	-.--(b)	--.-	--.--	2.761	---.-	-.--	--.-	----	----
	CVS2-55	Simplified CC	6.26	27.02	15.91	1.342	502.2	8.73	85.8	944	>1118
	CVS2-56	Simplified PFP	6.12	27.83	17.23	1.419	496.6	9.05	98.9	910	~1117
	CVS2-57	Simplified NCRW	6.74	28.13	15.28	1.164	512.1	8.95	87.6	1036	~953
3	CVS2-71	NCAW	8.50	38.46	12.00	0.411	470.9	8.7	97.1	890	~1004
	CVS2-64	Revised NCAW	8.89	39.53	12.32	0.379	471.8	10.0	80.9	895	~983
4	CVS2-72	NCAW	7.81	36.88	11.74	0.210	462.7	8.4	76.3	794	>868
	CVS2-66	CC	8.24	37.74	11.74	0.210	470.1	8.8	79.3	799	>1114
5	CVS2-73	NCAW	8.67	36.85	6.64	0.244	476.4	8.3	71.7	840	none
	CVS2-68	CC	17.05	35.28	10.56	0.308	465.7	7.7	74.0	>1114	none
6	CVS2-74	NCAW	9.55	35.40	9.88	0.226	470.3	8.8	83.3	850	~1066
	CVS2-69	PFP	22.15	36.01	9.88	0.226	488.2	8.9	62.5	>1114	>1114
7	CVS2-75	NCAW	8.66	36.40	8.62	0.278	469.1	-.-	77.1	826	none
	CVS2-70	PFP	10.80	36.97	11.56	0.312	484.2	8.4	94.0	>1114	none

EC = Electrical Conductivity
T_g = Transition Temperature
T_L = Liquidus Temperature

α_s = Thermal Expansion of Solid Glass
α_m = Thermal Expansion of Molten Glass

(a) See Tables 4.1, 4.8, 4.10, and 4.13 for the Others compositions of the various CVS glasses.

(b) Only PCT testing was performed on the radioactive glasses, CVS2-53 and CVS2-54.

two glasses had similar normalized releases for B, Li, Na, and Si. For example, the PCT normalized B release was 0.312 g/m^2 for CVS2-1 and 0.304 g/m^2 for CVS2-53. The PCT uranium release for CVS2-53 was below detection limits. Therefore, substituting UO_2 for Nd_2O_3 had negligible effects on the PCT of this glass.

The second set of glasses (CVS2-19, CVS2-51, CVS2-97, and CVS2-123 versus CVS2-54, CVS2-55, CVS2-56, and CVS2-57) provide the basis for a number of comparisons. The availability of results from four replicates of the CVS internal standard base glass (CVS2-19, CVS2-51, CVS2-97, and CVS2-123) aids in the comparisons, because they give an idea of the random experimental and measurement error for this particular glass composition. Observations that can be made for this set of glasses include:

- CVS2-54, a UO_2-doped glass, has moderately higher PCT normalized B release (2.76 g/m^2) than the base glasses (1.99, 1.76, and 1.43 g/m^2). This fact is interesting in light of the negligible difference for the first set of glasses (which were more durable to begin with). This suggests that further testing of U effects is needed.

- CVS2-55, -56, and -57 (the simplified CC, PFP, and NCRW Others glasses) have moderately larger MCC-1 normalized B releases and slightly smaller PCT normalized B releases than the base glasses with the NCAW-based Others mix. Liquidus temperatures for both spinel and non-spinel crystals were significantly higher for CVS2-55, -56, and -57 compared to the base glasses. The differences for viscosity at 1150°C, electrical conductivity at 1150°C, transition temperature, and both thermal expansion coefficients were slight to negligible.

In the third set of glasses, CVS2-71 is the base glass with NCAW Others, while CVS2-64 has a revised NCAW Others mix (see Table 4.13). There does not appear to be any significant differences between the glasses for any of the properties.

In the fourth set of glasses, CVS2-72 is the base glass with NCAW Others, while CVS2-66 has a CC Others mix (see Table 4.13). No significant differences between the glasses are apparent for any of the properties.

In the fifth set of glasses, CVS2-73 is the base glass with NCAW Others, while CVS2-68 has a CC Others mix (see Table 4.13). CVS2-68 has a significantly larger viscosity at 1150°C value than CVS2-72, which may be due

to its high (3%) Cr_2O_3 content and the possibility of undissolved Cr affecting viscosity. CVS2-68 also had a significantly larger non-spinel liquidus temperature value than CVS2-72. CVS2-68 has slightly larger PCT and MCC-1 normalized boron release values compared to CVS2-72. The differences for other properties appear to be slight to negligible.

In the sixth set of glasses, CVS2-74 is the base glass with NCAW Others, while CVS2-69 has a PFP Others mix (see Table 4.13). CVS2-69 has a significantly larger viscosity at 1150°C than CVS2-74. CVS2-69 had 2.4% Cr_2O_3 and contained both spinel and Cr_2O_3 crystals. CVS2-74 contained much less Cr_2O_3 (< 0.21 wt%) and contained only spinel crystals (no Cr_2O_3 crystals). The combination of Cr_2O_3 and spinel crystals may have increased viscosity in CVS2-69 if their size and/or shape favored agglomeration. CVS2-69 also had 3.3% P_2O_5, a significant amount compared to the 0.16% present in CVS2-74. Scoping tests results indicated that P_2O_5 may also increase viscosity slightly. In addition, CVS2-69 had a much larger non-spinel liquidus temperature value (>1114°C) than CVS2-74 (850°C). The spinel liquidus temperature for CVS2-69 (>1114°C) was also larger than for CVS2-74 (~1066°C). Other properties were in good agreement.

In the seventh set of glasses, CVS2-75 is the base glass with NCAW Others, while CVS2-70 has a PFP TRUEX Others mix (see Table 4.13). CVS2-70 had a slightly larger viscosity at 1150°C and a significantly larger non-spinel liquidus temperature value than CVS2-75 (see Table 13.3). The amount of Cr_2O_3 in CVS2-70 (1.17 wt% Cr_2O_3) was larger than in CVS2-75 (0.07 wt%). Cr_2O_3 crystals were not detected in CVS2-75, but were detected in CVS2-70. Spinel was not detected in either glass. Thus, the reason the viscosity increase from CVS2-75 to CVS2-70 was not nearly as large as from CVS2-74 to CVS2-69 may be due to the lack of spinel and Cr_2O_3 crystals in combination. CVS2-70 had larger PCT and MCC-1 normalized boron releases values when compared to CVS2-75. Other properties were in good agreement.

Based on these limited investigations, it appears that variations in Others compositions can affect some glass properties [viscosity at 1150°C, MCC-1 and PCT normalized B releases, and liquidus temperature (spinel and non-spinel)] depending on the composition of the glass and the composition of

Others. Other properties such as electrical conductivity at 1150°C, transition temperature, and thermal expansion appear to be only slightly affected, if at all, by varying Others compositions.

13.3 OVERCHECK RESULTS

Results of overcheck testing and analyses of selected CVS glasses (as discussed in Section 5.9) are presented and discussed in this section.

13.3.1 Viscosity and Electrical Conductivity Overchecks

Samples of the CVS internal standard glass were sent to Corning Engineering Laboratory Services (CELS) for viscosity and electrical conductivity overcheck testing. CELS measured the glasses within the temperature interval from 650°C to 1000°C, whereas CVS data were obtained in the interval from 950°C to 1250°C.[a] The CELS viscosity and electrical conductivity results for the CVS internal standard glass are listed in Table 13.4. CVS viscosity and electrical conductivity results for replicate measurements of the internal standard glass (CVS2-19, CVS2-51, and CVS2-97) and replicate fabrications and measurements of the compositionally similar[b] HW-39-4 glass (CVS2-16, CVS2-16A, and CVS2-18)[c] are listed in Table B.1 (viscosity) and Tables C.1 and C.2[d] (electrical conductivity).

Figures 13.1 and 13.2 display the CELS and CVS viscosity and electrical conductivity results in two panels. Panel (a) of each figure shows the data over the combined CELS and CVS temperature interval (roughly 650 to 1250°C).

(a) It would have been desirable for the Corning data to overlap the CVS temperature interval more, but they could only measure viscosity and electrical conductivity over the lower temperature interval.

(b) The CVS internal standard glass was designed to approximate the HW-39-4 composition with the exception of several minor components.

(c) Viscosity of CVS2-16 was measured twice during CVS, and the second measurement is denoted CVS2-16A. The viscosity and electrical conductivity results for CVS2-16 and CVS2-18 are from separate fabrications and measurements of the HW-39-4 glass composition.

(d) The 1k frequency values were used in CVS.

TABLE 13.4. CELS Viscosity and Electrical Conductivity Measurements for the CVS Internal Standard Glass

Temperature (°C)	Viscosity (Pa·s)	Electrical Conductivity (S/m)
989	37.23	11.250
979	43.19	9.160
949	67.1	7.870
916	112.1	7.030
882	200.6	5.880
851	368.9	4.690
814	821.2	3.390
777	2133	2.400
743	6062	1.650
720	12450	1.240
707	20000	1.030
672	81570	0.598
659	152700	0.492

Panel (b) of each figure shows the subset of the data in the temperature interval from 850 to 1150°C, which includes the overlap between the CELS and CVS data. In Figures 13.1 and 13.2, the CVS viscosity and electrical conductivity data show good agreement between the internal standard and HW-39-4 glasses, and also within the replicates of these glasses. In Figure 13.1(b), the agreement between CELS and CVS viscosity results is also good. In Figure 13.2 [both panels (a) and (b)], the CELS and CVS data appear to yield slightly different relationships as a function of composition. However, the wavy pattern of the CELS data is nonstandard, and suggests problems may exist in the data.

A least squares line ($\ln \eta = A + B/T$, which is the Arrhenius equation with T the Kelvin temperature) was fitted to the viscosity data in the 950°C to 1250°C interval, and is displayed in panels (a) and (b) of Figure 13.1. A slight nonlinearity of the data can be detected in the lower temperature portion of the 950°C to 1250°C interval, and the nonlinearity increases for temperatures below 950°C (°C scale shown at top of panels). Consequently, the applicability of the Arrhenius relationship is restricted to a narrow temperature interval. The slight departure from Arrhenius behavior

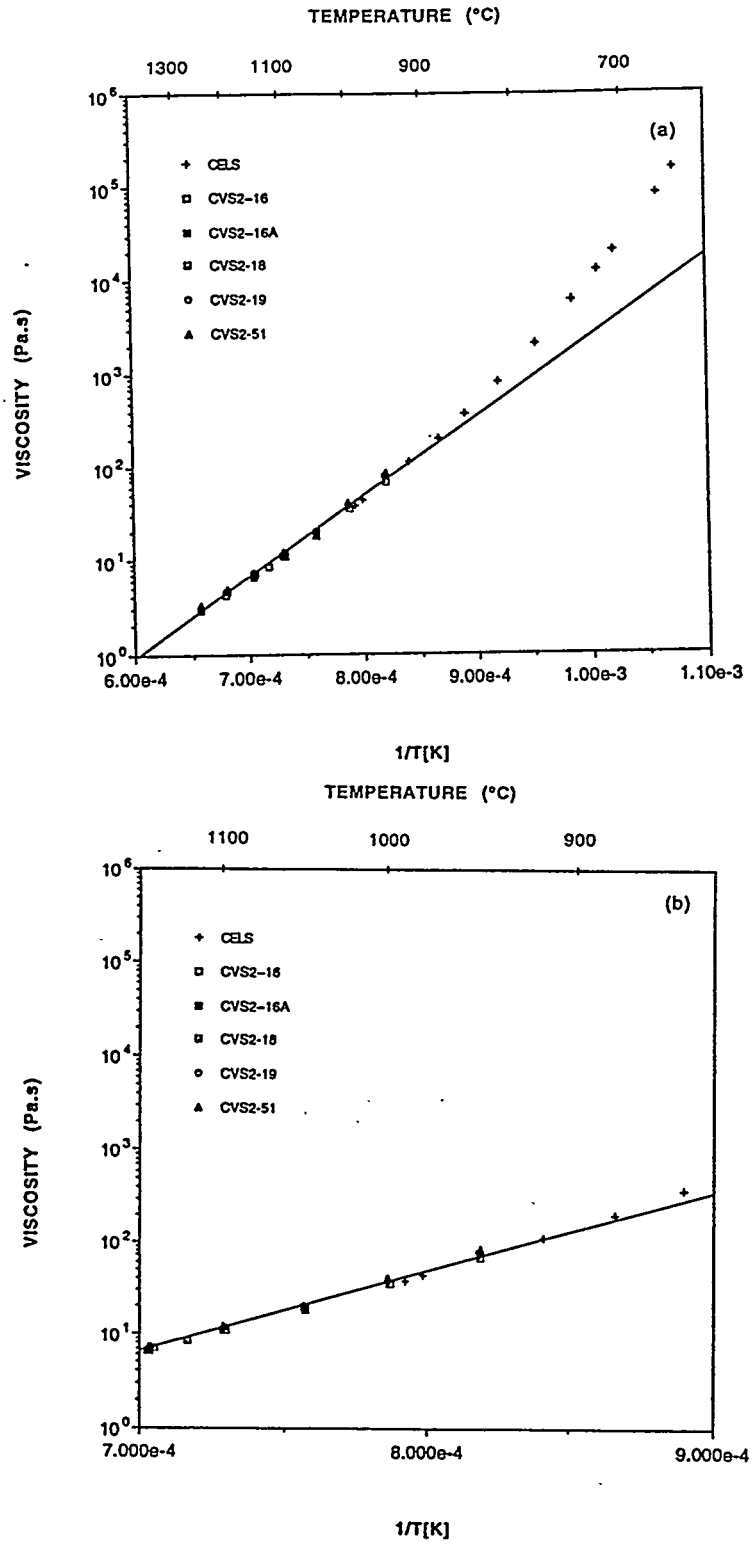

FIGURE 13.1. CVS and CELS Viscosity Data on the CVS Internal Standard and HW-39-4 Glasses: (a) 650 to 1250°C, (b) 850 to 1150°C

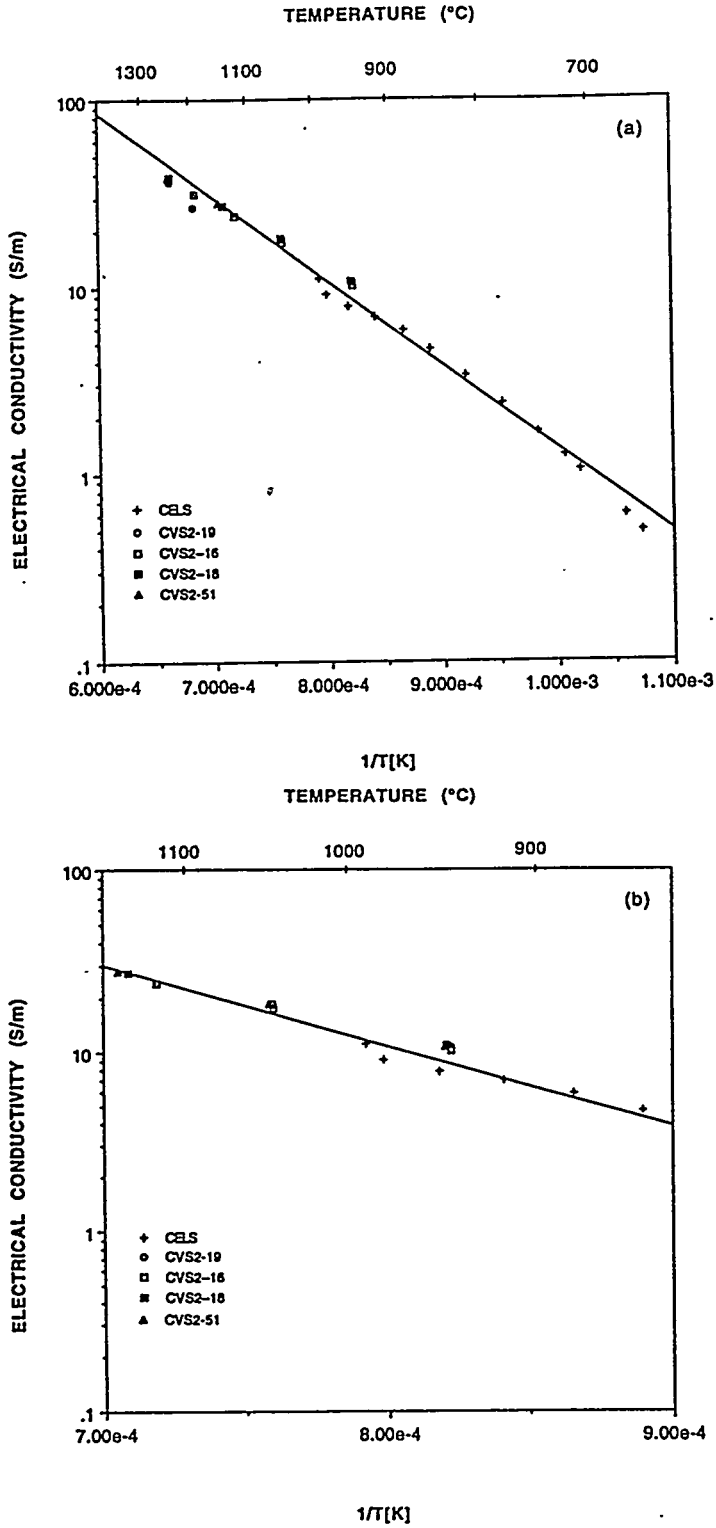

FIGURE 13.2. CVS and CELS Electrical Conductivity Data on the CVS Internal Standard and HW-39-4 Glasses: (a) 650 to 1250°C, (b) 850 to 1150°C

in the interval from 950°C to 1250°C (and larger departures from Arrhenius behavior for other CVS glasses, see Appendix B) justifies fitting the Fulcher equation to the CVS data. However, the temperature interval from 950°C to 1250°C is too narrow to allow reliable extrapolation with the Fulcher equation (see related discussion in Section 7.1).

A least-squares line ($\ln \epsilon = A + B/T$, which is the Arrhenius equation with T the Kelvin temperature) was fitted to the electrical conductivity data over the full 650°C to 1250°C interval, and is displayed in panels (a) and (b) of Figure 13.2. Although a small departure from linearity is noticeable in panel (a), the plot supports the hypothesis that the Arrhenius equation is applicable to electrical conductivity over a wider temperature interval than for viscosity.

13.3.2 Durability Overchecks

Samples of CVS-II glasses were sent to Savannah River Technology Center (SRTC), Rensselaer Polytechnic Institute (RPI), and Argonne National Laboratory (ANL) for durability testing using the MCC-1 and PCT dissolution tests. Five samples were sent to SRTC: two samples of the internal standard glass, two samples of vertex glasses (CVS2-5 and CVS2-7), and a sample of the CVS-I center point replicate (CVS2-17). Three samples were sent to RPI [CVS2-18 (HW-39-4 glass), CVS2-52, and CVS2-74]. Three samples were sent to ANL (CVS2-37, CVS2-39, and CVS2-51). Glass samples sent to SRTC and ANL were taken from remaining portions of glass fabricated and tested in CVS. The glasses sent to RPI were remade because there were insufficient quantities of the glasses remaining.

The CVS internal standard glass was prepared in 1990 and has been tested during each phase of CVS-II (as CVS2-19 during 1990 in CVS-II Phase 1, as CVS2-51 during 1991 in CVS-II Phase 2, as CVS2-97 during 1992-93 in CVS-II Phase 3, and as CVS2-123 during 1993 in CVS-II Phase 4). Its composition is close to that of HW-39-4 (given in Table 13.8 later), although the internal standard contains 0.49 wt% ZnO, whereas HW-39-4 does not contain ZnO. Also, the internal standard does not contain Sm_2O_3, SrO, PdO, Rb_2O, Rh_2O_3, and Y_2O_3.

PCT and MCC-1 tests were performed in duplicate at PNL (CVS) and ANL. At SRTC, PCT was performed in triplicate, while MCC-1 was performed in duplicate. At RPI, MCC-1 was performed in triplicate, while PCT was only performed once. The B and Li concentrations (ppm) in the PCT and MCC-1 test solutions from PNL, SRTC, RPI, and ANL are listed in Table 13.5 (PCT) and Table 13.6 (MCC-1). Also listed are percent relative differences (% RD) and natural logarithm differences between the PNL results and the results of the other laboratories. Both the % RD values and "ln difference" values (see footnotes of Tables 13.5 and 13.6) in Tables 13.5 and 13.6 were computed using the ppm release data, but the values would be the same if normalized release data in g/m^2 units had been used[(a)].

13.3.2.1 Assessment of Differences Between PNL/CVS and Other Labs

To judge whether any of the %RD values in Tables 13.5 and 13.6 are large enough to be of concern, it is necessary to know how large differences can be and still be due to random variation between laboratories performing the same dissolution test (PCT or MCC-1) on the same glass. The following formula computes the %RD detectable with specified confidence and false alarm rate:

$$\%RDD = \left[2\left(t_{f;1-\alpha/2} + t_{f;1-\beta}\right)^2 \left(RSDL^2 + \frac{RSDP^2}{n} + \frac{RSDA^2}{nm} \right) \right]^{0.5} \quad (13.1)$$

where %RDD = the percent relative difference in elemental releases (ppm) between two labs detectable at specified α and β error rates, where the lab values are averages over n dissolution tests and m chemical analyses per glass,

α = the probability of incorrectly deciding a difference exists (i.e., a false alarm), so that $100(1-\alpha)\%$ is the confidence,

(a) This is assuming the same CVS as-batched glass compositions used to normalize the PNL ppm release data were used to normalize the data from the other laboratories, and that as-batched compositions and A/V values used to normalize data are treated as being without error.

TABLE 13.5. B and Li Concentrations (ppm) from PCT Overcheck Tests

Glass	PNL/CVS[a] B	PNL/CVS[a] Li	SRTC[b] B	SRTC[b] Li	% RD[d] B	% RD[d] Li	ln Difference[e] B	ln Difference[e] Li
CVS2-19	125	52.9	70.6	31.3[f]	-43.5	-40.8	-0.571	-0.525
			99.4	42.3[f]	-20.5	-20.0	-0.229	-0.224
CVS2-51	115	51.9	70.6	31.3[f]	-38.6	-39.7	-0.488	-0.506
			99.4	42.3[f]	-13.6	-18.5	-0.146	-0.205
CVS2-97	93.5	36.5	70.6	31.3[f]	-24.5	-14.2	-0.281	-0.154
			99.4	42.3[f]	6.3	15.9	0.061	0.147
CVS2-123	96	39	70.6	31.3[f]	-26.5	-19.7	-0.307	-0.220
			99.4	42.3[f]	3.5	8.5	0.035	0.081
CVS2-5	27.2	6.1	30.4	6.3	11.8	3.3	0.111	0.032
CVS2-7	72.2	37.4	73.1	35.3	1.2	-5.6	0.012	-0.058
CVS2-17	35.0	17.6	27.9	13.8	-20.3	-21.6	-0.227	-0.243

Glass	PNL/CVS[a] B	PNL/CVS[a] Li	RPI[c] B	RPI[c] Li	% RD[d] B	% RD[d] Li	ln Difference[e] B	ln Difference[e] Li
CVS2-16	190.0	78.7	199.8	125.1[g]	5.2	59.0	0.050	0.463
CVS2-18	170.0	71.1	199.8	125.1[g]	17.5	75.9	0.162	0.565
CVS2-102	175.0	67.0	199.8	125.1[g]	14.2	86.7	0.133	0.624
CVS2-52	28.3	40.6	38.7	67.2	36.7	65.5	0.313	0.504
CVS2-74	11.0	18.5	10.1	24.1	-8.2	30.3	-0.085	0.264

Glass	PNL/CVS[a] B	PNL/CVS[a] Li	ANL[a] B	ANL[a] Li	% RD[d] B	% RD[d] Li	ln Difference[e] B	ln Difference[e] Li
CVS2-37	12.9	19.5	13.5	21.4	4.7	9.7	0.045	0.093
CVS2-39	395	425	446.0	520.0	12.9	22.4	0.121	0.202
CVS2-51	115	51.9	106.5	43.1	-7.4	-17.0	-0.077	-0.186

(a) Averages of duplicate tests.

(b) Averages of triplicate tests.

(c) Results from a single test.

(d) % RD = percent relative difference = 100(LAB - PNL)/PNL, where LAB is SRTC, RPI, or ANL. Note that the %RD values would be the same if calculated using normalized releases (g/m^2) instead of unnormalized releases (ppm).

(e) ln Difference = ln(LAB) - ln(PNL), where LAB is SRTC, RPI, or ANL. Note that the ln Difference values would be the same if calculated using normalized releases (g/m^2) instead of unnormalized releases (ppm).

(f) SRTC tested the CVS internal standard glass twice, but there is no natural pairing with the CVS results labeled CVS2-19, CVS2-51, CVS2-97, and CVS2-123. The two SRTC results are listed with each of the four CVS results and %RD values are shown for each pairing.

(g) RPI only tested the HW-39-4 glass once, but the RPI results were used to compute %RD values relative to the CVS results from replicates tests of HW-39-4 (CVS2-16, CVS2-18, and CVS2-102).

TABLE 13.6. B and Li Concentrations (ppm) from MCC-1 Overcheck Tests

Glass	PNL/CVS[a] B	PNL/CVS[a] Li	SRTC[a] B	SRTC[a] Li	% RD[c] B	% RD[c] Li	ln Difference[d] B	ln Difference[d] Li
CVS2-19	4.3	2.2	5.46	2.66[e]	27.0	20.9	0.239	0.190
			5.05	2.46[e]	17.4	11.8	0.161	0.112
CVS2-51	4.03	1.79	5.46	2.66[e]	35.5	48.6	0.304	0.396
			5.05	2.46[e]	25.3	37.4	0.226	0.318
CVS2-97	4.2	1.9	5.46	2.66[e]	30.0	40.0	0.262	0.336
			5.05	2.46[e]	20.2	29.5	0.184	0.258
CVS2-123	5.1	2.35	5.46	2.66[e]	7.1	13.2	0.068	0.124
			5.05	2.46[e]	-1.0	4.7	-0.010	0.046
CVS2-5	5.0	0.935	5.02	0.93	0.4	-0.5	0.004	-0.005
CVS2-7	2.45	1.1	2.58	1.14	5.3	3.6	0.052	0.036
CVS2-17	4.35	2.15	4.80	2.25	10.3	4.7	0.098	0.045

Glass	PNL/CVS[a] B	PNL/CVS[a] Li	RPI[b] B	RPI[b] Li	% RD[c] B	% RD[c] Li	ln Difference[d] B	ln Difference[d] Li
CVS2-16	5.85	3.05	4.3	2.6[f]	-26.5	-14.8	-0.308	-0.160
CVS2-18	6.5	3.45	4.3	2.6[f]	-33.8	-24.6	-0.413	-0.283
CVS2-102	6.3	3.05	4.3	2.6[f]	-31.7	-14.8	-0.382	-0.160
CVS2-52	2.6	3.2	1.6	2.7	-38.5	-15.6	-0.486	-0.170
CVS2-74	2.4	2.9	1.3	2.7	-45.8	-6.9	-0.613	-0.071

Glass	PNL/CVS[a] B	PNL/CVS[a] Li	ANL[a] B	ANL[a] Li	% RD[c] B	% RD[c] Li	ln Difference[d] B	ln Difference[d] Li
CVS2-37	2.52	2.74	2.18	2.51	-13.5	-8.4	-0.145	-0.088
CVS2-39	2.54	4.63	2.53	5.08	-0.4	9.7	-0.004	0.093
CVS2-51	4.03	1.79	4.23	2.00	5.0	11.7	0.048	0.111

(a) Averages of duplicate tests.

(b) Averages from triplicate tests, except that the results for CVS2-74 are from a single test.

(c) % RD = percent relative difference = 100(LAB - PNL)/PNL, where LAB is SRTC, RPI, or ANL. Note that the %RD values would be the same if calculated using normalized releases (g/m^2) instead of unnormalized releases (ppm).

(d) ln Difference = ln(LAB) - ln(PNL), where LAB is SRTC, RPI, or ANL. Note that the ln Difference values would be the same if calculated using normalized releases (g/m^2) instead of unnormalized releases (ppm).

(e) SRTC tested the CVS internal standard glass twice, but there is no natural pairing with the CVS results labeled CVS2-19, CVS2-51, CVS2-97, and CVS2-123. The two SRTC results are listed with each of the four CVS results and %RD values are shown for each pairing.

(f) RPI only tested the HW-39-4 glass once, but the RPI results were used to compute %RD values relative to the CVS results from replicates tests of HW-39-4 (CVS2-16, CVS2-18, and CVS2-102).

$1-\beta$ = the probability of detecting a percent relative difference of magnitude %RDD (i.e., the power to detect %RDD with $100(1-\alpha)\%$ confidence),

$t_{f;1-\alpha/2}$, $t_{f;1-\beta}$ = upper $1-\alpha/2$ and $1-\beta$ percentiles of the Student's t distribution with f degrees of freedom,

f = the effective degrees of freedom associated with the estimated variance $RSDL^2 + RSDP^2/n + RSDA^2/nm$,

RSDL = the lab-to-lab %RSD associated with performing the dissolution test and chemically analyzing the solution,

RSDP = the long-term within-lab %RSD associated with performing the dissolution test,

RSDA = the long-term within-lab %RSD associated with chemically analyzing the solution,

n = the number of times the dissolution test is performed on a given glass,

m = the number of times the solution from a dissolution test is chemically analyzed.

This formula assumes that each lab has the same RSDL (by default), RSDP, RSDA, n, and m. The overcheck program and data were not designed to estimate RSDL, RSDP and RSDA, so values based on CVS data and the literature are discussed and used below. All of the values in Tables 13.5 and 13.6 are based on m = 1, but n = 1, 2, or 3 depending on the lab and dissolution test. The fact that n is not the same for all labs is considered in the following discussion.

Results in Tables F.5 and F.6 in Appendix F indicate that for PNL/CVS data, the long-term within-lab standard deviation for natural logarithm normalized B and Li releases is about 0.10 to 0.14 for both PCT and MCC-1 tests.[a] These values roughly correspond to 10 to 14 %RSD values for

---

(a) Most of the data used to produce the standard deviations in Tables F.5 and F.6 include variations from replicate fabrication of glasses as well as replicate dissolution testing and chemical analyses. This should tend to inflate the uncertainty estimates for dissolution testing and analyses. However, data without replicate glass fabrication variation had comparable or larger uncertainty as data with fabrication variation, so use of results in Tables F.5 and F.6 is deemed reasonable.

normalized releases without the natural logarithm transformation. As noted previously, these values would be the same for %RSDs of unnormalized ppm releases. In CVS, no effort was made to separately estimate RSDP and RSDA. Hence, based on Tables F.5 and F.6, $(RSDP^2 + RSDA^2)^{0.5}$ is estimated to be in the 10 to 14% range for the PNL/CVS data. The same range is assumed for SRTC, RPI, and ANL.

Piepel, Jones, Eggett, and Mellinger (1989, Table C.2) report results from a PCT round robin study on four different glasses. They reported combined within-lab and lab-to-lab %RSDs for B and Li PCT releases (ppm) of 5 to 12%, depending on glass composition. This range of values is lower than the range of long-term within-lab %RSDs experienced in the CVS, as described in the previous paragraph. However, the time-frame of within-lab variations is much different for the two studies. The PCT round robin included variations in a three-week time frame, whereas CVS includes variations over months and years. Piepel et al. (1989, Table C.2) also reported separate estimates of lab-to-lab %RSD values, which were in the 1 to 8% range for B and Li PCT releases.

Johnston, Mendel, and Daniel (1981, pp. 90-91) and Johnston and Daniel (1982) reported the results of an MCC-1 round robin study. They reported "optimistic characterizations" of MCC-1 precisions as 6 to 11 %RSD within-lab and 25 to 40 %RSD lab-to-lab, and "pessimistic characterizations" as 11 to 25 %RSD within-lab and 40 to 75 %RSD lab-to-lab.

Table 13.7 contains computed values of %RDD from the formula in (13.1) using m = 1, n = 1, 2, or 3, and the above literature references as guidelines for values of RSDL and $(RSDP^2 + RSDA^2)^{0.5}$ [(a)]. Values of $\alpha = 0.05$ and $\beta = 0.05$ were used, so that the %RDDs in Table 13.7 are those detectable with 95% confidence and 5% false-alarm rate. The effective degrees of freedom for the Student's t values were assumed to be infinite (i.e., $f = \infty$) to provide a conservative basis for comparing detectable %RDs to the values in Tables 13.5 and 13.6. Specifically, using $f = \infty$ yields the smallest possible Student's t

(a) Note that RSDP and RSDA can be treated together because all of the labs involved in the overcheck testing performed just one chemical analysis per dissolution test solution (i.e., m = 1).

TABLE 13.7. Percent Relative Differences (%RD) in Elemental Releases Between Two Labs Detectable With 95% Confidence and 5% False-Alarm Rate

RSDL	$(RSDP^2 + RSDA^2)^{0.5}$	%RD Values[a] n = 1	n = 2	n = 3[b]
10	5	57.0	54.1	53.1
10	10	72.1	62.4	58.9
10	15	91.9	74.3	67.4
10	20	114.0	88.3	77.9
20	5	105.1	103.5	103.0
20	10	114.0	108.2	106.1
20	15	127.5	115.4	111.1
20	20	144.2	124.9	117.7
30	5	155.1	154.0	153.7
30	10	161.2	157.1	155.8
30	15	171.0	162.2	159.2
30	20	183.8	169.1	163.9
50	5	256.2	255.5	255.3
50	10	260.0	257.4	256.6
50	15	266.1	260.6	258.7
50	20	274.5	264.9	261.6
75	5	383.2	382.8	382.7
75	10	385.8	384.1	383.5
75	15	389.9	386.2	384.9
75	20	395.7	389.1	386.9

(a) %RDs calculated from Equation (13.1) with $m = 1$, $\alpha = 0.05$, $\beta = 0.05$, $f = \infty$, $t_{\infty,0.975} = 1.96$, and $t_{\infty,0.95} = 1.645$. Using $f = \infty$ implies that RSDL and the combination of RSDP and RSDA are known without error. This is obviously not the case, but it is conservative for computing detectable %RDs for comparison with values in Tables 13.5 and 13.6.

(b) n = the number of times a lab performs a dissolution test on a given glass, where the n results are then averaged.

values for the chosen α and β, and thus the smallest possible detectable %RDDs for the chosen α and β and given values of RSDL and $(RSDP^2 + RSDA^2)^{0.5}$. This makes it easier to say the values in Tables 13.5 and 13.6 are statistically significant.

All of the %RDs in Table 13.6 and all except 4 of the %RDs in Table 13.5 are smaller (in absolute value) than 50%. Relative differences of that

magnitude or smaller are not statistically significant according to Table 13.7. The four %RDs in Table 13.5 larger than 50% are all for PCT Li differences between PNL/CVS and RPI. Three of the four %RDs (59.0, 75.9, and 86.7%) are between RPI's single PCT Li result (i.e., n = 1) for the HW-39-4 glass and the PNL/CVS PCT results (averages of two PCTs) for three replicates of HW-39-4 (CVS2-16, CVS2-18, and CVS2-102). The fourth %RD (65.5%) is between RPI's single PCT Li result and the PNL/CVS result (average of two PCTs) for CVS2-52. Table 13.7 indicates that none of these four %RDs is statistically significant if the lab-to-lab %RSD (i.e., RSDL) is at least 20%.

In summary, the differences between PNL/CVS durability results and results from SRTC, ANL, and RPI are within what is possible given magnitudes of within-lab and lab-to-lab random variations.

13.3.2.2 Comparison of Internal Standard and HW-39-4 Results

Figures 13.3 and 13.4 compare the B and Li MCC-1 and PCT releases (ppm) for the HW-39-4 glass tested in CVS (CVS2-16, CVS2-18, and CVS2-102), the sample of HW-39-4 tested by RPI (CVS2-18), the four replicates of the CVS internal standard glass tested in CVS (CVS2-19, CVS2-51, CVS2-97, and CVS2-123), the two samples of internal standard glass tested by SRTC, and the sample of the internal standard glass tested by ANL. It is of interest to compare the release results for the internal standard glass and HW-39-4, which have approximately the same compositions. Table 13.8 contains the as-batched and analyzed compositions of the internal standard and HW-39-4 glasses. Figures 13.3 and 13.4 show that the internal standard glass is noticeably more durable (has lower PCT and MCC-1 releases) than the HW-39-4 glass. The difference could be caused by the presence in the internal standard glass of ZnO,[a] which is known to increase glass durability (Lutze 1988).

(a) The internal standard glass was produced from a large quantity of black frit available at PNL that had been procured by another project to match the major components of the HW-39-4 composition. The black frit contained ZnO, which is not a component of CVS glasses.

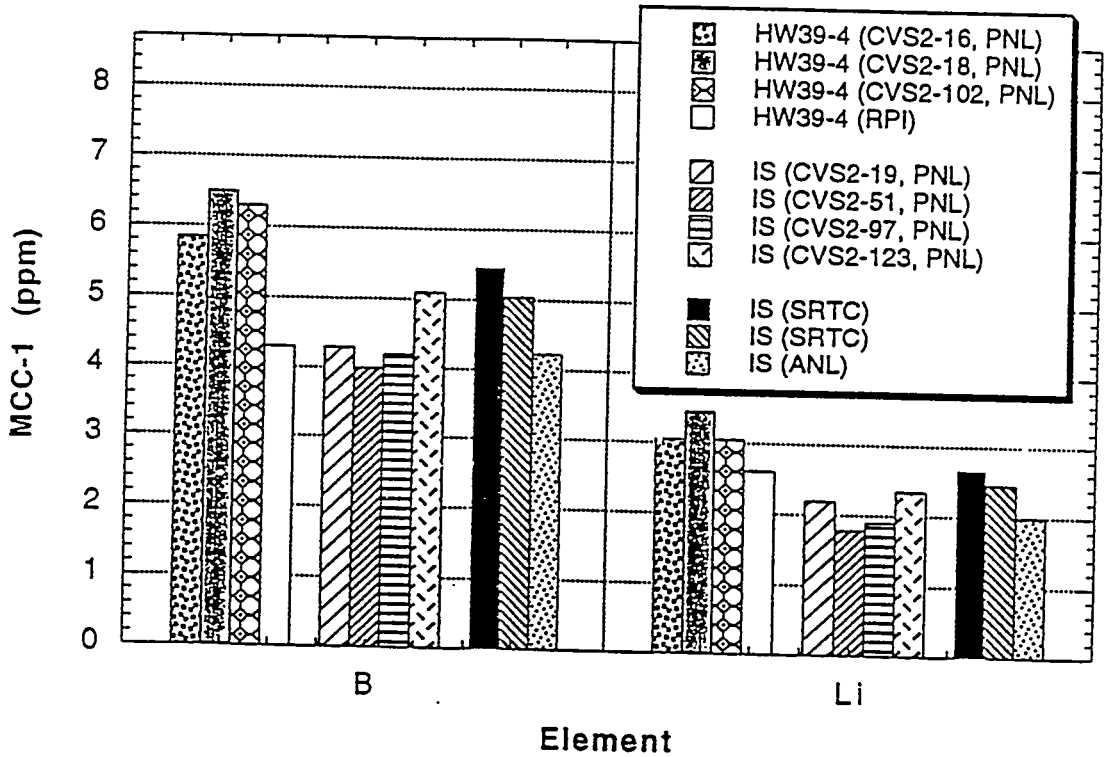

FIGURE 13.3. Comparison of MCC-1 B and Li Releases (ppm) Obtained by PNL, SRTC, and ANL for the CVS Internal Standard Glass and HW-39-4

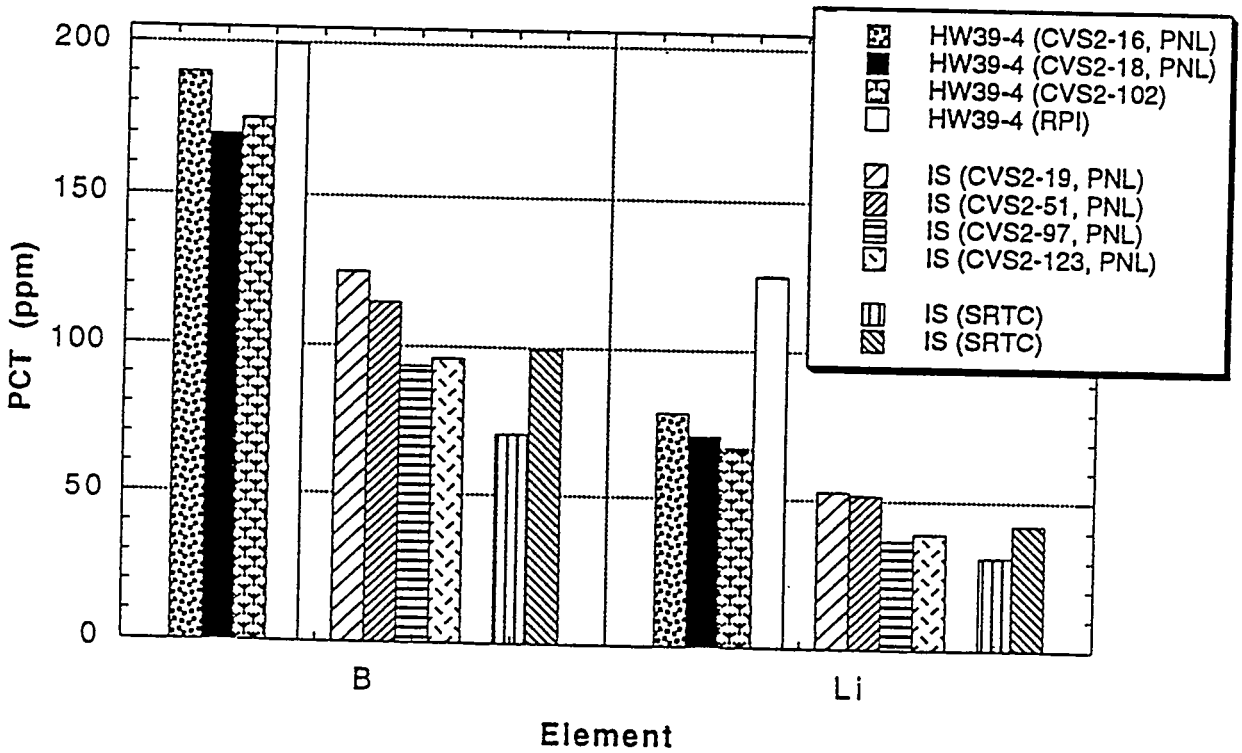

FIGURE 13.4. Comparison of PCT B and Li Releases (ppm) Obtained by PNL, SRTC, and ANL for the CVS Internal Standard Glass and HW-39-4

TABLE 13.8. As-Batched and Analyzed Compositions (wt%) of the CVS Internal Standard and HW-39-4 Glasses

Oxide	As-Batched Internal Standard	PNL Analyses of Internal Standard			SRTC Analyses of Internal Standard[a]				As-Batched HW-39-4	PNL Analyses of HW-39-4	
		CVS2-19	CVS2-51	CVS2-97	1A	1B	2A	2B		CVS2-16	CVS2-18
Al_2O_3	2.35	3.00	2.85	2.87	2.73	3.14	2.97	2.75	2.31	2.30	2.35
B_2O_3	10.48	10.10	9.75	9.94	10.73	12.23	9.96	10.10	10.53	10.40	10.60
BaO	0.099	0.230	0.215	0.233	0.11	0.24	0.23	0.23	0.106	0.10	0.10
CaO	0.82	1.08	0.99	0.975	1.09	1.07	1.08	1.06	0.83	0.92	0.93
CdO	0.65	0.641	0.59	0.601	0.62	0.62	0.62	0.62	0.795	0.79	0.80
CeO_2	0.017	0.098	0.21	0.017	0.16	0.16	0.16	0.16	0.159	0.23	0.22
Co_2O_3	--	--	0.036	0.043	--	--	--	--	--	--	--
Cr_2O_3	0.129	0.104	0.096	0.105	0.18	0.18	0.20	0.20	0.133	0.16	0.17
Cs_2O	0.15	0.018	0.158	0.15	0.16	0.16	0.16	0.16	0.159	0.146	0.15
CuO	0.158	0.214	0.185	0.199	0.20	0.21	0.20	0.20	0.159	0.16	0.16
F	0.19	0.19*	0.19*	0.19*	--	--	--	--	0.318	0.318*	0.318*
FeO	--	--	--	--	0.59	0.77	0.83	0.78	--	--	--
Fe_2O_3	7.33	6.10	5.70	5.90	5.84	5.62	5.51	5.51	7.19	7.00	7.05
K_2O	--	--	--	--	0.29	0.21	0.27	0.28	--	3.10	2.80
La_2O_3	1.54	2.12	2.05	1.96	0.95	3.48	1.80	1.82	0.662	0.605	0.615
Li_2O	3.73	3.44	3.20	3.28	3.40	3.40	3.38	3.36	3.75	3.60	3.65
MgO	0.84	0.809	0.72	0.775	0.84	0.84	0.83	0.82	0.84	0.855	0.855
MnO_2	0.158	0.241	0.21	0.230	0.21#	0.20#	0.21#	0.21#	0.159	0.24	0.27
MoO_3	0.31	0.277	0.28	0.29	0.29	0.27	0.29	0.28	0.318	0.315	0.315
Na_2O	11.29	11.60	12.00	11.40	11.11	10.96	10.76	10.76	11.25	10.50	10.90
Nd_2O_3	0.57	0.70	0.645	0.655	1.31	1.31	1.31	1.31	1.308	1.10	1.90
NiO	0.60	0.629	0.59	0.60	0.67	0.67	0.68	0.67	0.610	0.65	0.66
P_2O_5	0.099	0.099*	0.15	0.15	0.17	0.17	0.21	0.17	0.106	0.106*	0.106*
PdO	--	--	--	--	--	--	--	--	0.053	0.053*	0.053*
Pr_6O_{11}	0.188	0.188*	0.188*	0.188*	--	--	--	--	0.106	0.106*	0.106*
Rb_2O	--	--	--	--	--	--	--	--	0.053	0.053*	0.053*
Rh_2O_3	--	--	--	--	--	--	--	--	0.053	0.053*	0.053*
RuO_2	0.151	0.151*	0.13	0.10	--	--	--	--	0.159	0.19	0.18
SiO_2	53.28	51.10	46.00	48.50	48.74	53.32	50.86	52.17	53.53	54.00	53.20
Sm_2O_3	--	--	--	--	--	--	--	--	0.053	0.053*	0.053*
SO_3	0.44	0.44*	0.44*	0.44*	--	--	--	--	0.292	0.292*	0.292*
SrO	--	--	0.008	--	0.01	0.01	0.01	0.01	0.106	0.10	0.10
TiO_2	--	0.103	0.106	0.115	--	--	--	--	--	0.02	0.025
Y_2O_3	--	--	0.007	--	0.05	0.05	0.05	0.05	0.053	0.05	0.055
ZnO	0.49	0.482	0.43	0.48	0.59	0.59	0.59	0.58	--	--	--
ZrO_2	3.92	3.97	3.40	3.67	3.93	3.97	3.94	3.93	3.85	3.80	4.00
Sum	99.797	98.124	91.524	94.056	94.97	103.85	97.11	98.19	100.00	102.365	103.089

(a) Two independent analyses from sample 1 are denoted as 1A and 1B, and from sample 2 as 2A and 2B.

* Was not analyzed or analytical value was below detection limits, so the as-batched value was assumed.

\# MnO.

13.3.3 Glass Composition Overchecks

Although not contracted to do so, SRTC also analyzed the composition of the CVS internal standard glass four times (two analyses each of the two samples provided to them). The SRTC results, as well as the CVS as-batched and analyzed results, are listed in Table 13.8.

14.0 APPLYING CVS RESULTS

The fitted glass property models and the corresponding model uncertainty equations developed in CVS are basic "building blocks" that can be applied in many ways to meet the needs of an eventual Hanford HLW vitrification plant. Section 14.1 discusses the use of CVS property models and corresponding uncertainties, while Section 14.2 discusses application of these "building blocks" to the development of a Qualified Composition Region. It is beyond the scope of this document to discuss other potential uses of the CVS property models and uncertainty equations, but some possible uses are mentioned in Section 14.2.5.

14.1 USING THE CVS MODELS AND UNCERTAINTIES

Section 14.1.1 discusses using the fitted models to predict property values, while Section 14.1.2 discusses uncertainties related to the property models and the types of statistical statements that can be made.

14.1.1 Predicting Property Values With CVS Models

Predicting property values with the fitted empirical models intuitively involves substituting a 10-component glass composition into a model and performing the arithmetic to yield the predicted value. However, the following several points should be kept in mind.

1. Because various models in this report are provided in both mass and mole fraction forms, care must be taken to substitute the proper composition form into a particular model. In general, no advantage was found to using mole fraction models instead of mass fraction models. Thus, for simplicity, the use of mass fraction models is recommended.

2. The glass composition must be in terms of mass or mole fractions (not mass or mole percents) of the 10 components SiO_2, B_2O_3, Na_2O, Li_2O, CaO, MgO, Fe_2O_3, Al_2O_3, ZrO_2, and Others. The sum of these 10 components should be 1.0 to at least two or three decimal places to avoid making biased predictions with the property models. Analyzed compositions typically will not sum to 1.0, and bias correction and normalization

procedures (see Section A.6 of Appendix A) will be required to yield compositions that do sum to 1.0 to at least two or three decimal places.

3. The 10-component composition must be within the region of validity for the CVS property models, as summarized in Table 14.1.

4. If a second-order model is being used that is based on the L-pseudo-component transformations of the 10 components, then glass compositions for which predictions are desired should be transformed to L-pseudo-components, as defined in Section 6.1.3. (Currently, none of the property models listed in Sections 7 through 12 utilize the L-pseudo-component transformation. However, this discussion is retained in case such transformations become necessary in the future).

5. To make a property prediction, substitute the glass component composition or pseudocomponent composition (as appropriate) into the model being used and perform the arithmetic.

6. If appropriate, apply the inverse property transformation to obtain the predicted property value in original property units. Be aware that international units are used in CVS, and these may differ from units sometimes used for a property. Table 14.2 lists the transformations, inverse transformations, and units for each property.

Using statistical statements to account for the uncertainty in predictions made with fitted property models is discussed in the next subsection.

14.1.2 Statistical Statements About Model Predictions

Equations for quantifying uncertainties in property model predictions due to model and composition uncertainties were briefly discussed in Section 6.2 and are presented and illustrated in Section I.3 of Appendix I. In this section, several types of statistical statements that can be developed using the fitted property models and their corresponding uncertainty equations are discussed.

Three basic types of statistical statements can be made about glass property model predictions: confidence intervals, prediction intervals, and

TABLE 14.1. Region of Validity for CVS Property Models[a]

Individual Component Mass Fraction Constraints

Oxide	Lower Bound	Upper Bound
SiO_2	.42	.57
B_2O_3	.05	.20
Na_2O	.05	.20
Li_2O	.01	.07
CaO	0	.10
MgO	0	.08
Fe_2O_3	0	.15
Al_2O_3	0	.17
ZrO_2	0	.13
Others	.01	.10

Stand-In Crystallinity Constraints[b]

Oxide Ratio or Sum	Lower Bound	Upper Bound
SiO_2/Al_2O_3	3.0	---
MgO+CaO	---	.10
$Fe_2O_3+Al_2O_3+ZrO_2$+Others	---	.24
$Al_2O_3+ZrO_2$	---	.16
$MgO+CaO+ZrO_2$	---	.18

(a) This table is preliminary at this point and is based on the range of glasses studied in CVS-I through CVS-II Phase 3.

(b) Eventually these stand-in crystallinity constraints will be dropped from the definition of the region of validity as liquidus temperature models (and thus constraints) improve and additional data are collected.

TABLE 14.2. CVS Glass Property Transformations and Inverse Transformations

Property	Units	Transformation	Inverse Transformation
Viscosity	Pa·s	ln(·)	exp(·)
Electrical Conductivity	S/m	ln(·)	exp(·)
Liquidus Temperature	°C	none	none
PCT and MCC-1 Durability	g/m^2	ln(·)	exp(·)
Transition Temperature	°C	none	none
Coefficients of Thermal Expansion (solid & molten)	$10^{-6}/K$	none	none

tolerance intervals. A confidence interval is a statement about the mean property value for a given point (composition), a prediction interval is a statement about a single property value for a given point (composition), while a tolerance interval is a statement about a specified proportion of the distribution of property values for a given point (composition). Confidence, prediction, and tolerance intervals can be one-sided lower, one-sided upper, or two-sided.

Each of the three basic types of statements can be made about one point (composition) at a time, or about all possible points (compositions) simultaneously. In the simultaneous cases, the statements are referred to as simultaneous confidence intervals (sometimes referred to as confidence bands), simultaneous prediction intervals (sometimes referred to as prediction bands), and simultaneous tolerance intervals (sometimes referred to as tolerance bands).

The formulas for one-sided and two-sided versions of the various types of statistical intervals discussed above are given in Section I.4 of Appendix I.

14.2 QUALIFIED COMPOSITION REGION

Roughly, the Qualified Composition Region (QCR) is intended to be a subregion of the composition region studied in CVS that satisfies, with high confidence, the viscosity, electrical conductivity, liquidus temperature, and PCT durability constraints in Table 3.1. The QCR must be a subregion of the region of glass compositions studied in the CVS because the fitted empirical property models will be used in constructing the QCR, and extrapolation with fitted empirical models is generally to be avoided. Hence, the QCR will not contain all glasses with acceptable property values, but only glasses within the CVS composition study region for which high confidence of acceptable property values exists.

The mention of "high confidence" in the preceding paragraph is because fitted property models are subject to uncertainty, and the uncertainty must be accounted for in defining the QCR. However, it will be useful to define the Predicted Acceptable Composition Region (PACR) concept as a precursor to the

QCR, where the PACR does not account for the uncertainty in fitted property models. The PACR concept is further defined and discussed in Section 14.2.1. Accounting for property model uncertainty so as to convert the PACR into the QCR is discussed in Section 14.2.2. The mathematical constraints specifying the QCR are presented and discussed in Section 14.2.3. Issues regarding the use of the QCR are discussed in Section 14.2.4. Section 14.2.5 briefly mentions possible areas of application for the QCR.

14.2.1 Predicted Acceptable Composition Region

Intuitively, the PACR is the subregion of glass compositions in the CVS experimental region that remains after eliminating compositions predicted by empirical glass property models to violate the lower and/or upper limits on glass properties given in Table 3.1. Mathematically, it can be defined by the CVS experimental region composition constraints, and equations obtained by equating empirical glass property models to lower and/or upper property limits. Tables 14.3 and 14.4 (discussed in Section 14.2.3) contain this information, except that glass property model uncertainty is also addressed in those tables. Versions of those tables with the model uncertainty portions deleted could have been included here, but were not because of the duplication that would have ensued. Although discussed in more detail in Section 14.2.3, it is noted here that the stand-in crystallinity constraints (from Table 14.1) were not used in defining the PACR or the QCR.

The preliminary PACR is a nine-dimensional composition region that can be described in terms of the 10 CVS oxide components (mass fractions thereof, since we have chosen to work with mass fraction property models). Some boundaries of the PACR are due to equating single components to their lower or upper limits (as shown in the top portion of the first page of Table 14.4). Other boundaries are due to equating first-order property models (given in Table 14.5) to lower or upper property limits (or natural log transformations thereof, as applicable). Both kinds of boundaries are multidimensional

planes[a], so that the preliminary PACR is a multidimensional polyhedron. A routine in the MIXSOFT (Piepel 1992) software package was used to generate the center point, 3868 vertices, and 30 eight-dimensional face centroids (the center points of the 30 boundary faces) of the polyhedral preliminary PACR. These points help describe the PACR, and were used in investigations discussed in Section 14.2.4. The overall centroid and the 30 eight-dimensional face centroids are listed in Table 14.3. There are too many vertices to include them in the table.

14.2.2 Accounting for Model Uncertainty in the QCR

Fitted property models and statistical statements accounting for the uncertainty in the model fits will be used in constructing the QCR. The statistical statements discussed in Section 14.1.2 are intended to address model imprecision only--it is assumed that the fitted models predict properties accurately without significant bias. Model adequacy needs to be assessed from both statistical and practical perspectives. That is, models must be assessed to determine if they have a statistically significant lack-of-fit, and if so, whether it is practically significant.

Estimated compositions to be supplied to the fitted models during HLW vitrification plant production will also be subject to uncertainty (batch-to-batch, within-batch sampling/inhomogeneity, and analytical), but such uncertainty will not be factored into the construction of the QCR. The main reason for this is that composition uncertainty will depend on: (1) the magnitudes of batch-to-batch, sampling/inhomogeneity, and analytical uncertainties (as characterized by covariance matrices for these various sources of uncertainty), (2) the number of batches sampled, (3) the number of

---

(a) The decision to use all first-order property models was made to simplify initial efforts in defining the preliminary PACR and QCR. At the time the PACR and QCR work was started, comparisons of first- and second-order models were still in progress. This work indicated that second-order models may be better than first-order models for some properties. However, the investigations discussed in Section 14.2.4 could not be done (using existing software) if second-order models were chosen, so it was decided to use only first-order models for the preliminary PACR and QCR work.

TABLE 14.3. Overall Centroid and Eight-Dimensional Face Centroid Glass Compositions (mass fractions) for the Preliminary PACR

Point Description	SiO_2	B_2O_3	Na_2O	Li_2O	CaO	MgO	Fe_2O_3	Al_2O_3	ZrO_2	Others
Overall centroid	.4829	.1152	.1177	.0356	.0388	.0373	.0482	.0370	.0373	.0500
Face Centroids Coresponding to Component Lower and Upper Bounds										
SiO_2 = .42	.4200	.1258	.1290	.0294	.0418	.0337	.0556	.0689	.0399	.0558
SiO_2 = .57	.5700	.0964	.1060	.0422	.0379	.0383	.0355	.0120	.0223	.0395
B_2O_3 = .05	.4934	.0500	.1422	.0444	.0413	.0377	.0508	.0412	.0455	.0535
B_2O_3 = .20	.4664	.2000	.0804	.0259	.0390	.0367	.0434	.0375	.0259	.0447
Na_2O = .05	.4959	.1412	.0500	.0491	.0478	.0380	.0440	.0403	.0350	.0588
Na_2O = .20	.4704	.0751	.2000	.0266	.0257	.0220	.0447	.0473	.0478	.0404
Li_2O = .01	.4674	.1293	.1423	.0100	.0471	.0370	.0569	.0303	.0283	.0515
Li_2O = .07	.5021	.0843	.0945	.0700	.0299	.0345	.0386	.0529	.0489	.0443
CaO = 0	.4850	.1137	.1300	.0410	.0000	.0362	.0608	.0420	.0408	.0505
CaO = .10	.4764	.1100	.0966	.0297	.1000	.0379	.0273	.0387	.0321	.0514
MgO = 0	.4803	.1179	.1249	.0369	.0409	.0000	.0645	.0424	.0425	.0496
MgO = .08	.4897	.1173	.1037	.0349	.0406	.0800	.0203	.0330	.0296	.0509
Fe_2O_3 = 0	.4889	.1158	.1194	.0382	.0478	.0423	.0000	.0514	.0442	.0520
Fe_2O_3 = .15	.4617	.1079	.1304	.0293	.0184	.0105	.1500	.0159	.0282	.0477
Al_2O_3 = 0	.5046	.1144	.1107	.0331	.0431	.0361	.0596	.0000	.0437	.0548
Al_2O_3 = .17	.4294	.0962	.1159	.0508	.0419	.0252	.0140	.1700	.0226	.0340
ZrO_2 = 0	.4951	.1206	.1183	.0333	.0405	.0364	.0539	.0507	.0000	.0512
ZrO_2 = .13	.4913	.0560	.1911	.0654	.0053	.0048	.0054	.0144	.1300	.0363
Others = .01	.4929	.1220	.1278	.0372	.0379	.0360	.0527	.0453	.0383	.0100
Others = .10	.4696	.1086	.1054	.0330	.0387	.0369	.0453	.0277	.0348	.1000
Face Centroids Corresponding to Glass Property Lower and Upper Limits										
η_{1150} = 2 Pa•s	.4621	.1123	.1286	.0449	.0431	.0349	.0545	.0275	.0427	.0495
η_{1150} = 10 Pa•s	.5078	.1124	.1009	.0282	.0345	.0367	.0387	.0566	.0338	.0503
ϵ_{1150} = 10 S/m	.5000	.1811	.0606	.0144	.0689	.0493	.0265	.0205	.0228	.0560
ϵ_{1150} = 100 S/m	.5212	.0515	.1987	.0694	.0040	.0031	.0080	.0039	.1236	.0164
PCT B = 8.2 g/m^2	.4597	.1277	.1427	.0343	.0047	.0457	.0898	.0206	.0362	.0386
PCT Li = 4.8 g/m^2	.4972	.1426	.1234	.0345	.0210	.0416	.0395	.0143	.0354	.0504
PCT Na = 6.6 g/m^2	.4847	.0958	.1655	.0278	.0316	.0457	.0502	.0167	.0382	.0439
T_L spinel = 1050°C	.4727	.1168	.0919	.0348	.0443	.0496	.0709	.0413	.0268	.0511
T_L clino = 1050°C	.4749	.0581	.0708	.0443	.0917	.0706	.0100	.0242	.0654	.0899
T_L Zr = 1050°C	.4633	.1152	.1097	.0370	.0382	.0411	.0432	.0281	.0747	.0495

samples per batch, and (4) the number of analyses per sample. Because this information is not known at this time, it cannot be factored into the construction of the QCR. Even if this information were known, additional flexibility is provided by dealing separately with model and composition uncertainties. Hence, only model uncertainty is factored into the construction of the QCR, while composition uncertainties are left to be accounted for (where appropriate) at the time the QCR is used.

It was stated earlier that the QCR should provide high confidence that the viscosity, electrical conductivity, liquidus temperature, and PCT durability constraints are met. It remains to define what is meant by high confidence (i.e., which of the statistical intervals discussed in Section 14.1.2 should be used), and whether high confidence is required for each property separately or for all properties simultaneously.

To illustrate the difference between separate and simultaneous confidence for multiple property constraints, consider an example of four constraints. Suppose that 95% confidence is desired that each property constraint separately is satisfied. If the four properties were statistically independent, the simultaneous confidence that all four property constraints are satisfied would only be 81.5%[a]. If a higher simultaneous confidence than this were required, it could be achieved by increasing the separate confidences. For example, the simultaneous confidence would be approximately 96% (assuming independence) if separate confidences of 99% were used for each property.

It was decided that statistical confidences should be specified separately for each property constraint rather than simultaneously across all property constraints. This approach provides the flexibility to: (1) use a different confidence level for each property constraint if desired, and (2) modify the QCR by working with only one constraint or any subset of the constraints. Also, the nature of the property constraints and the way a HLW

(a) Glass properties are neither totally statistically independent or dependent, in which case the simultaneous confidence would be somewhere between 81.5 and 95%. However, this discussion is mainly intended to illustrate the concept.

vitrification plant will be operated are such that only one or two property constraints at a time will have any chance of being violated. Thus, the simultaneous confidence question is not an issue for the most part.

The final aspect required to complete the QCR concept is the type of statistical statement to be used in accounting for the uncertainties in the fitted property models. Six types of statistical statements were introduced in Section 14.1.2, and their formulas and more detailed discussions are contained in Section I.4 of Appendix I. Of these six types, it appears that confidence intervals or confidence bands (simultaneous confidence intervals) are the most appropriate choices. From the standpoint of wanting to know whether a single composition in the QCR will have acceptable properties with a specified confidence (say 95%) for each property, constructing the QCR as a collection of individual confidence intervals is the appropriate thing to do. From the standpoint of wanting to know whether all of the compositions in the QCR will have acceptable properties with a specified confidence (say 95%) for each property, constructing the QCR as a collection of simultaneous confidence intervals (confidence bands) is the appropriate thing to do. Because the only difference between individual and simultaneous confidence interval formulas is the statistical multiplier used [see Equations (I.8) and (I.11) in Section I.4 of Appendix I], it is easy to construct the QCR both ways and investigate the difference between them.

14.2.3 Mathematical Constraints Defining the QCR

The mathematical constraints defining the QCR are given in three sets in Table 14.4, corresponding to three parts of the QCR definition. The first set of constraints is the single-component constraints that restrict attention to the ranges of the components studied during the CVS. The second set of constraints is the critical solubility constraints from Table 4.2 (or updated estimates thereof--see the discussion in Section 4.2.2). The third set of constraints is the "statistical statement" property constraints (individual or simultaneous confidence intervals, as discussed in Section 14.2.2) that implement the property limits from Table 3.1 via the fitted empirical models

TABLE 14.4. Constraints Defining the Qualified Composition Region (QCR)

Single-Component Constraints[a]				
.42	≤	SiO_2	≤	.57
.05	≤	B_2O_3	≤	.20
.05	≤	Na_2O	≤	.20
.01	≤	Li_2O	≤	.07
0	≤	CaO	≤	.10
0	≤	MgO	≤	.08
0	≤	Fe_2O_3	≤	.15
0	≤	Al_2O_3	≤	.17
0	≤	ZrO_2	≤	.13
.01	≤	Others	≤	.10

Critical Solubility Constraints[b]	
Cr_2O_3	≤ 0.005
F	≤ 0.017
P_2O_5	≤ 0.010
SO_3	≤ 0.005
Rh_2O_3, PdO, and Ru_2O_3	≤ 0.025

"Statistical Statement" Property Constraints

The "statistical statements" used to define the following constraints have the general form:

(Model prediction at x) +/- (Multiplier) * (Standard Deviation of model prediction at x)

which is written in vector and matrix notation (see Appendix I for definitions of the notation) as

$$(x'\hat{\beta}) \text{ +/- (Multiplier) } * ([x'(X'X)^{-1}x]^{0.5}\ \hat{\sigma})$$

The constraints based on these statistical statements take the form of 9-dimensional hyperbolic surfaces in the 10-component CVS composition space.

Viscosity at 1150°C, Pa·s

$$\ln(2) \le x'\hat{\beta}(\eta_{1150}) - \text{Multiplier} * [x'(X'X)^{-1}x]^{0.5}\ \hat{\sigma}(\eta_{1150}) \qquad (14.1)$$

$$x'\hat{\beta}(\eta_{1150}) + \text{Multiplier} * [x'(X'X)^{-1}x]^{0.5}\ \hat{\sigma}(\eta_{1150}) \le \ln(10) \qquad (14.2)$$

where $\hat{\beta}(\eta_{1150})$, $(X'X)^{-1}$, $\hat{\sigma}(\eta_{1150})$, and the choices for Multiplier are given in Table 14.5.

(a) An implicit constraint on the components is that their mass fractions must sum to 1.0.

(b) The critical solubility constraints are implicitly constraints on the upper limit of the Others component. Considering them in this way allows maintaining the 10-component approach used throughout CVS. Also, as discussed in Section 4.2.2, these critical solubility constraints should be considered preliminary and may be updated in the future.

TABLE 14.4. Constraints Defining the Qualified Composition Region (QCR) (continued)

"Statistical Statement" Property Constraints (continued)

Electrical Conductivity at 1150°C, S/m [d]

$$\ln(10) \le x'\hat{\beta}(\epsilon_{1150}) - \text{Multiplier} * [x'(X'X)^{-1}x]^{0.5}\,\hat{\sigma}(\epsilon_{1150}) \tag{14.3}$$

$$x'\hat{\beta}(\epsilon_{1150}) + \text{Multiplier} * [x'(X'X)^{-1}x]^{0.5}\,\hat{\sigma}(\epsilon_{1150}) \le \ln(100) \tag{14.4}$$

where $\hat{\beta}(\epsilon_{1150})$, $(X'X)^{-1}$, $\hat{\sigma}(\epsilon_{1150})$, and the choices for Multiplier are given in Table 14.5.

PCT Normalized B, Li, and Na Releases, g/m^2 [e]

$$x'\hat{\beta}(PCT_B) + \text{Multiplier} * [x'(X'X)^{-1}x]^{0.5}\,\hat{\sigma}(PCT_B) \le \ln(8.2) \tag{14.5}$$

where $\hat{\beta}(PCT_B)$, $(X'X)^{-1}$, $\hat{\sigma}(PCT_B)$, and the choices for Multiplier are given in Table 14.5.

$$x'\hat{\beta}(PCT_{Li}) + \text{Multiplier} * [x'(X'X)^{-1}x]^{0.5}\,\hat{\sigma}(PCT_{Li}) \le \ln(4.8) \tag{14.6}$$

where $\hat{\beta}(PCT_{Li})$, $(X'X)^{-1}$, $\hat{\sigma}(PCT_{Li})$, and the choices for Multiplier are given in Table 14.5.

$$x'\hat{\beta}(PCT_{Na}) + \text{Multiplier} * [x'(X'X)^{-1}x]^{0.5}\,\hat{\sigma}(PCT_{Na}) \le \ln(6.6) \tag{14.7}$$

where $\hat{\beta}(PCT_{Na})$, $(X'X)^{-1}$, $\hat{\sigma}(PCT_{Na})$, and the choices for Multiplier are given in Table 14.5.

(d) See Section 3.2 for the rationale of the 10 - 100 S/m acceptable range for electrical conductivity at 1150°C.

(e) The numerical limits given are based on PCT testing of the EA glass at the Savannah River Technology Center.

TABLE 14.4. Constraints Defining the Qualified Composition Region (QCR) (continued)

"Statistical Statement" Property Constraints (continued)

Liquidus Temperature, °C [f]

Clinopyroxene:

$$x'\hat{\beta}(T_L \text{ clino}) + \text{Multiplier} * [x'(X'X)^{-1}x]^{0.5}\,\hat{\sigma}(T_L \text{ clino}) \leq 1050 \qquad (14.8)$$

where $\hat{\beta}(T_L \text{ clino})$, $(X'X)^{-1}$, $\hat{\sigma}(T_L \text{ clino})$, and the choices for Multiplier are given in Table 14.5.

Spinel:

$$x'\hat{\beta}(T_L \text{ spinel}) + \text{Multiplier} * [x'(X'X)^{-1}x]^{0.5}\,\hat{\sigma}(T_L \text{ spinel}) \leq 1050 \qquad (14.9)$$

where $\hat{\beta}(T_L \text{ spinel})$, $(X'X)^{-1}$, $\hat{\sigma}(T_L \text{ spinel})$, and the choices for Multiplier are given in Table 14.5.

Zr-containing crystals:

$$x'\hat{\beta}(T_L \text{ Zr}) + \text{Multiplier} * [x'(X'X)^{-1}x]^{0.5}\,\hat{\sigma}(T_L \text{ Zr}) \leq 1050 \qquad (14.10)$$

where $\hat{\beta}(T_L \text{ Zr})$, $(X'X)^{-1}$, $\hat{\sigma}(T_L \text{ Zr})$, and the choices for Multiplier are given in Table 14.5.

(f) Only three primary phases had sufficient liquidus temperature data for fitting first-order models, and two of the three models do not fit the data very well. Hence, the liquidus temperature constraints are very preliminary at this time. To the extent the preliminary liquidus temperature constraints are active in defining boundaries of the QCR, the QCR will also be very preliminary.

It should also be kept in mind that applying the three liquidus temperature constraints may over-restrict the QCR, because currently there is no way to know or predict for a given composition the primary crystalline phase at the liquidus temperature. Applying all three constraints to every composition may be very over-restrictive, but that is the only solution until better models for predicting liquidus temperature and the corresponding primary crystalline phase become available.

and their corresponding uncertainties. Table 14.5 contains information concerning the fitted empirical models and their corresponding uncertainties used to define the preliminary QCR.

It was decided not to include the stand-in crystallinity constraints from Table 14.1 in the definition of the QCR. Although technically the stand-in constraints partially define the composition region studied to date in the CVS, the desire to drop them was strong because of their arbitrary nature. It was decided instead to use constraints based on liquidus temperature models. To investigate the consequence of dropping the stand-in crystallinity constraints from the definition of the QCR, the vertices of the predicted acceptable composition region (PACR, the region defined by ignoring the model uncertainty portion of the QCR) were constructed using a routine in MIXSOFT (Piepel 1992). The total number of vertices and the number violating each of the stand-in crystallinity constraints are given in Table 14.6. The results in Table 14.6 indicate that portions of the PACR are outside of the CVS composition region studied to date. Thus, model predictions for compositions in such subregions will be extrapolations.[a] Hence, model prediction uncertainties will be larger and the QCR will shrink further from the PACR in such subregions. The extent to which the QCR shrinks relative to the PACR is discussed in Section 14.2.4.

The QCR constraints in Table 14.4 define the boundary of a multi-faceted compositional region. If the uncertainty (multiplier times model prediction standard deviation) portions of the constraints were deleted, they would define planes in 9-dimensional composition space. With the uncertainty portions, the constraints define hyperbolic surfaces in 9-dimensional composition space. Glass compositions that satisfy all the constraints (including the uncertainty portions) are either on the boundary of or inside the QCR, while glass compositions that fail one or more of the constraints are

---

(a) Subregions of the PACR outside the CVS study region are of great interest for future experimental investigation. Expansion of the CVS study region into such subregions will allow extending CVS property models so that interpolative predictions with smaller prediction uncertainties can be made.

TABLE 14.5. Model Coefficients ($\hat{\beta}$), $(X'X)^{-1}$, Experimental Error Standard Deviations ($\hat{\sigma}$), and Multipliers for Preliminary QCR

	$\ln(\eta_{1150})$	$\ln(\epsilon_{1150})$	ln(PCT B)	ln(PCT Li)	ln(PCT Na)	T_L clino	T_L spinel	T_L Zr
SiO2	8.967982	0.8471	-4.3173	-3.2278	-4.4118	955.65	989.31	753.78
B2O3	-6.204318	2.2518	11.9791	10.1496	9.4049	314.72	666.42	1095.83
Na2O	-11.016616	11.0396	17.6068	14.0017	19.4013	38.83	3.77	74.31
Li2O	-34.239274	23.5355	22.5791	18.4159	19.0635	-207.05	-128.77	-956.39
CaO	-7.466158	1.4129	-8.7114	-5.3528	-1.9567	1372.44	1366.21	886.76
MgO	-2.776217	1.0565	10.9210	7.1181	11.8228	2387.62	2830.58	2458.47
Fe2O3	-0.036918	2.5863	-3.2009	-4.5113	-4.0953	1506.69	2256.00	1461.04
Al2O3	11.306471	1.3108	-25.4071	-22.3095	-25.4294	1319.78	1735.03	1138.06
ZrO2	7.433982	1.1224	-10.5613	-10.0618	-11.4209	1844.50	928.11	4541.99
Others	-0.155959	3.4531	0.1587	-0.6181	-0.6647	1357.40	1005.56	657.99
$(X'X)^{-1}$ (a)	Table I.1	Table I.2	Table I.3	Table I.3	Table I.3	Table I.9	Table I.10	Table I.11
$\hat{\sigma}$ (b)	0.253	0.158	0.686	0.604	0.593	17.670	50.648	51.650
Multiplier 95% CI (c)	1.658 (d)	1.659	1.658	1.658	1.658	1.734	1.729	1.782
Multiplier 95% CB (c)	4.068 (d)	4.071	4.069	4.069	4.069	4.446	4.422	4.677

(a) The table numbers given are from Appendix I, where these matrices are listed.

(b) The square root of the mean square error from fitting each property model.

(c) Values of multipliers for both 95% confidence intervals (CI) and 95% confidence bands (CB) are given. The multipliers for 95% CIs are upper 95th percentiles of a t-distribution $[t_{.95}(n-p)]$, while multipliers for 95% CBs are based on the upper 90th percentile of an F-distribution $[p\ F_{.90}(p,n-p)]^{0.5}$, where n is the number of data points used to fit the model and p is the number of fitted parameters (coefficients) in the model.

(d) Multiplier values are rounded to three decimal places, although more were used in actual calculations.

TABLE 14.6. Number of Vertices of Predicted Acceptable Composition Region Violating the Stand-In Crystallinity Constraints

Stand-In Crystallinity Constraint	Number of Vertices Violating Constraint
$SiO_2/Al_2O_3 \geq 3.0$	394
$MgO + CaO \leq 0.10$	935
$Fe_2O_3 + Al_2O_3 + ZrO_2 + \text{Others} \leq 0.24$	813
$Al_2O_3 + ZrO_2 \leq 0.16$	461
$MgO + CaO + ZrO_2 \leq 0.18$	562
Total Number of Vertices for Predicted Acceptable Composition Region	3868

outside the QCR. Because all constraints maintain their identity, it will be easy to determine the cause and potential remedies for glass compositions that are outside the QCR.

14.2.4 QCR Discussion

The QCR, being a 9-dimensional composition region defined by the matrix and vector notation given in Table 14.4, is not very understandable or easy to visualize. Using the TWEAT software (developed as part of the PVTD project) to visualize the QCR and the consequences of model uncertainty in a waste-frit-recycle ternary plot was considered, but TWEAT currently cannot display the QCR as defined in Table 14.4. Also considered was computing and comparing the volume of the QCR to that of the PACR. However, computing the volume of such regions is difficult and provides no basis for understanding the consequences of uncertainty for each property model separately.

In order to help understand the QCR and the consequences of property model uncertainty, selected points on the boundary of the QCR were determined for each property constraint, and two kinds of information about these points

were summarized. The points were selected by starting with the vertices and 8-dimensional face centroids[a] of the PACR and shrinking them toward the center of the PACR. If a line is drawn from a point on the boundary of the PACR (e.g., a vertex or an 8-dimensional face centroid) to the overall center of the PACR, the line will intersect the boundary of the QCR, yielding a shrunken version of the point. The shrunken versions of the PACR vertices and 8-dimensional face centroids lying on the QCR were the points for which two kinds of information were summarized.

The first kind of information summarized is referred to as the shrinkage factor, which is the ratio of: (a) the distance between the center of the PACR and a shrunken version of a PACR vertex or 8-dimensional face centroid on the surface of the QCR, to (b) the distance between the center of the PACR and the vertex or 8-dimensional face centroid on the surface of the PACR. The shrinkage factor can be thought of as the proportion of the distance between a point on the surface of the PACR and the overall center point that remains after accounting for model uncertainty.

If the PACR were shrunken to the QCR in an even manner, or all linear dimensions of the surface were decreased by the same proportion, the shrinkage factor would have the same value for every point on the surface of the QCR. This is not the case, however. Each of the constraints listed in Table 14.4 define an 8-dimensional face on the surface of the QCR. Because each of the property constraints has a different model uncertainty, the faces will not shrink by the same proportion. In addition, the model uncertainty on a particular face of the QCR will vary from point to point due to the form of the uncertainty equations. For these reasons the shrinkage factors due to model uncertainty are not uniform over the QCR. Obviously shrinkage factors cannot be computed for every point on the surface of the PACR because the number of points on any surface is infinite. Rather than arbitrarily pick

---

(a) Eight-dimensional face centroids are center points of the 8-dimensional composition faces that make up the boundary of the QCR. An 8-dimensional face exists for each oxide component or glass property constraint defining the QCR.

points on the surface, it was decided to use the vertices and 8-dimensional face centroids, so that each face would be equally represented in some sense.

The shrinkage factors are summarized in Table 14.7. This table shows the range of shrinkage factors obtained for each constraint that has model uncertainty. The constraints with no uncertainty did not shrink inward, so all of their shrinkage factors were 1.0. As discussed in Section 4.1.2, two ways of statistically accounting for model uncertainty can be considered appropriate at various times, namely confidence bands and confidence intervals. The shrinkage factor results for both types of statistical statement are given in Table 14.7. These results vary greatly, which shows the effect of the type of statistical statement used to account for uncertainty. The shrinkage factor values listed for the confidence bands are much smaller than those listed for the confidence intervals. This fact indicates that much more of the region is eliminated for confidence bands than is eliminated using confidence intervals. As an example of how to interpret the numbers, the range listed under confidence bands for the viscosity lower limit is 0.53 to 0.77. This range indicates that 47% [=100(1-0.53)] to 23% [=100(1-0.77)] of the distances between the center of the region and the points on the "low viscosity boundary" of the PACR were lost due to accounting for uncertainty in the viscosity at 1150°C model in defining the QCR. Keep in mind that the distance lost for points on the interior of the PACR may be considerably less.

The second kind of information summarized for the shrunken versions of PACR vertices and 8-dimensional face centroids is the predicted property values for the shrunken points. After the shrinkage factors were calculated, the shrunken versions of points (compositions) could be calculated, and then these compositions were substituted into the property models to obtain predicted values. Because this information might give the reader a more understandable interpretation of the consequences of model uncertainty than the shrinkage factors themselves, histograms of the predicted property values were made for each property model-constraint combination. Figure 14.1 contains the histograms for the QCR defined using 95% confidence intervals to account for model uncertainty. Figure 14.2 contains the histograms for the

TABLE 14.7. Summary of Shrinkage Factors for Each Property Model-Constraint Boundary of the Qualified Composition Region for Both 95% Confidence Intervals (C.I.) and 95% Confidence Bands (C.B.)

Property Constraint	Range of Shrinkage Factor Values[a] 95% C.I.	95% C.B.
Lower viscosity (η_{1150}= 2 Pa·s)	0.76 - 0.90	0.53 - 0.77
Upper viscosity (η_{1150}= 10 Pa·s)	0.80 - 0.93	0.61 - 0.84
Lower conductivity (ϵ_{1150}= 10 S/m)	0.88 - 0.93	0.74 - 0.83
Upper conductivity (ϵ_{1150}= 100 S/m)	0.93 - 0.95	0.85 - 0.88
Upper PCT B (8.2 g/m^2)	0.74 - 0.85	0.51 - 0.66
Upper PCT Li (4.8 g/m^2)	0.64 - 0.83	0.36 - 0.61
Upper PCT Na (6.6 g/m^2)	0.69 - 0.85	0.43 - 0.65
Upper T_L clinopyroxene (1050°C)	0.67 - 0.78	0.40 - 0.56
Upper T_L spinel (1050°C)	0.17 - 0.60	0.18 - 0.35 (b)
Upper T_L Zr-containing (1050°C)	0.26 - 0.70	0.15 - 0.37 (b)

(a) A shrinkage factor is a unitless quantity representing the ratio of the distance from the PACR center point to a point on the QCR (obtained by shrinking a PACR boundary point toward the PACR center point) to the distance from the PACR center point to the PACR boundary point.

(b) The uncertainties for these property models were so large for some compositions (when accounted for using 95% confidence bands) that shrinking PACR points toward the PACR center point either did not yield intersections with the QCR (in which case shrinkage factors could not be calculated) or yielded negative shrinkage factors (indicating the PACR center point is outside the QCR. The ranges shown are for the subset of points for which positive values were obtained.

QCR defined using 95% confidence bands to account for model uncertainty. The histograms display the distributions of predicted property values obtained for the shrunken versions of the vertices on each of the PACR 8-dimensional faces corresponding to a given property model-constraint combination. The vertical line in each histogram represents the predicted property value at the shrunken version of the centroid of each PACR 8-dimensional face. These shrunken versions of PACR points lie on the boundary of the QCR.

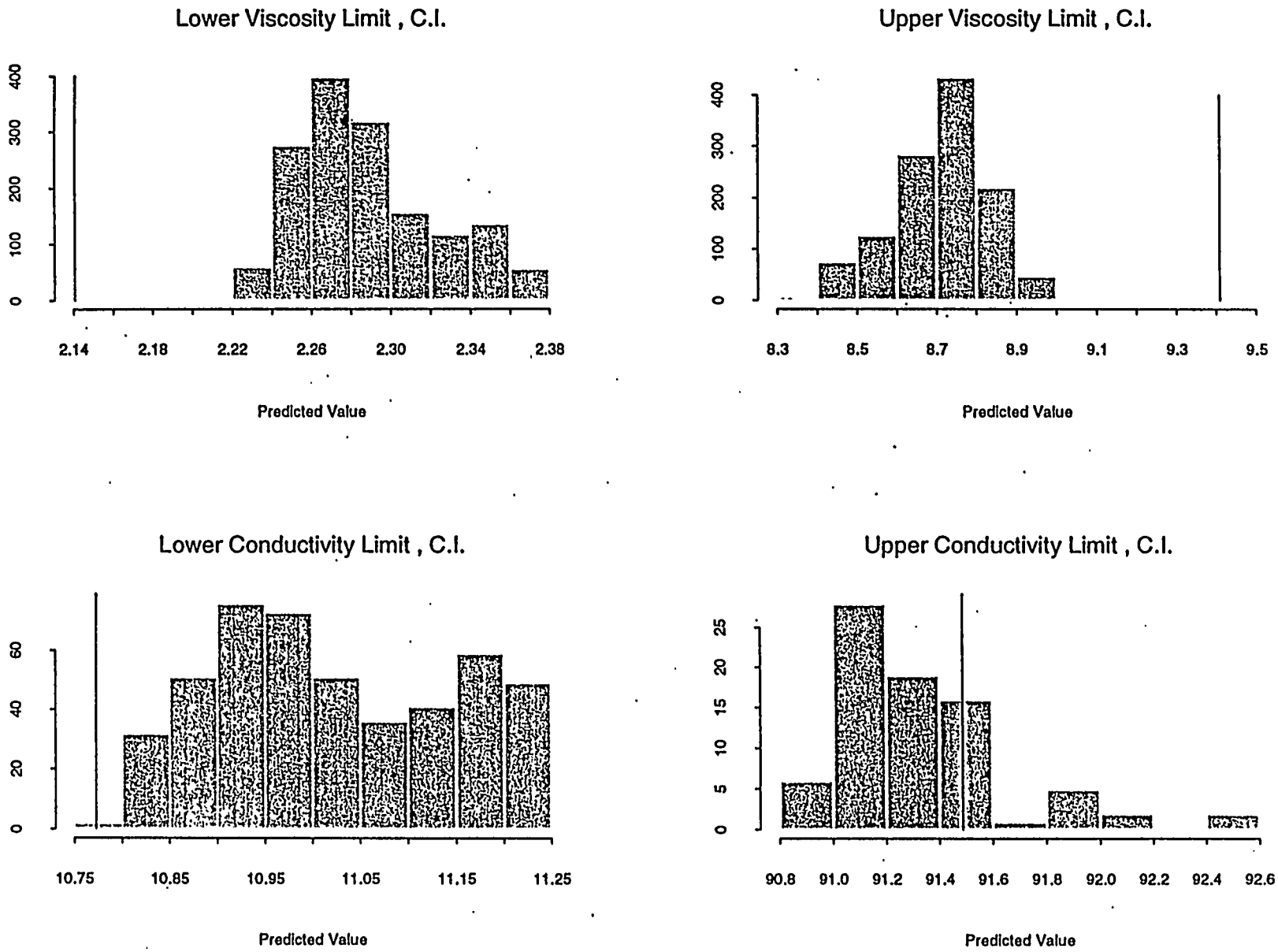

FIGURE 14.1. Histograms of Predicted Property Values for Shrunken Versions of the Vertices and Centroid of Each Property Constraint That Lie on the Boundary of the Qualified Composition Region Defined by 95% Confidence Intervals

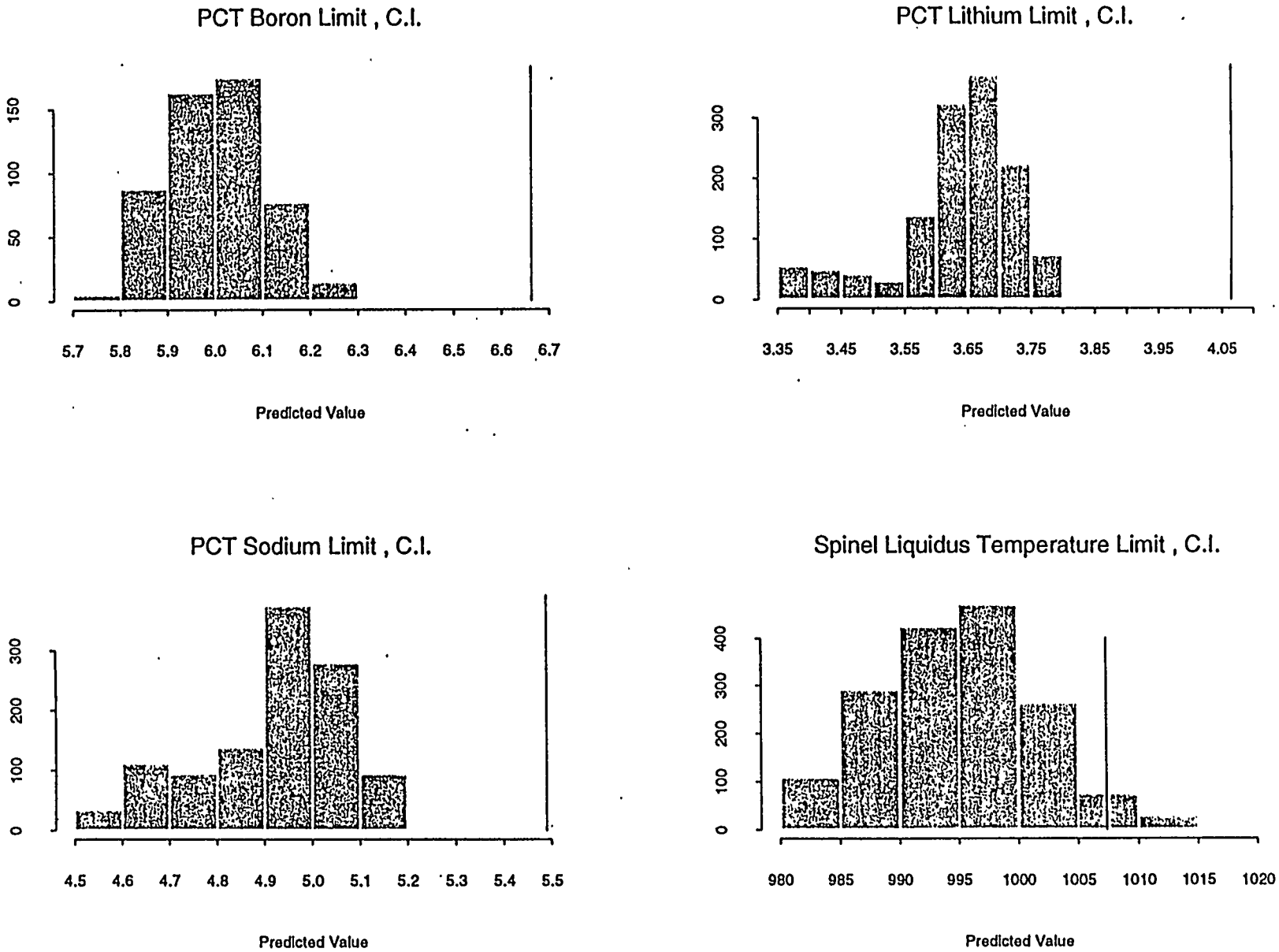

FIGURE 14.1. Histograms of Predicted Property Values for Shrunken Versions of the Vertices and Centroid of Each Property Constraint That Lie on the Boundary of the Qualified Composition Region Defined by 95% Confidence Intervals (continued)

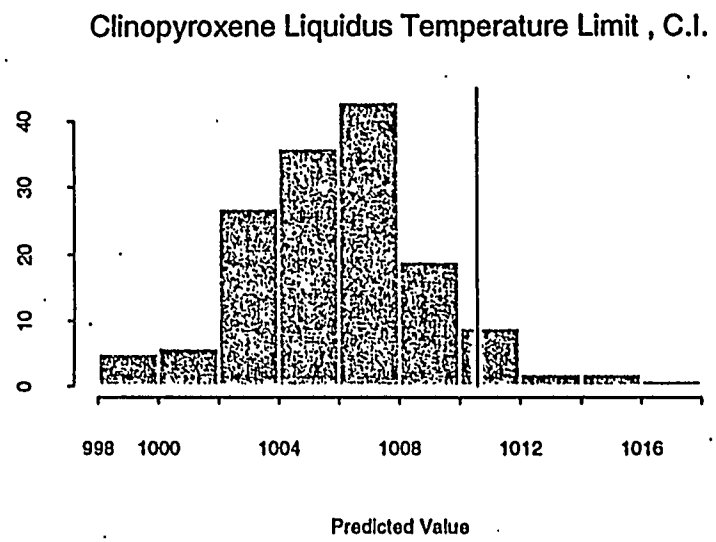

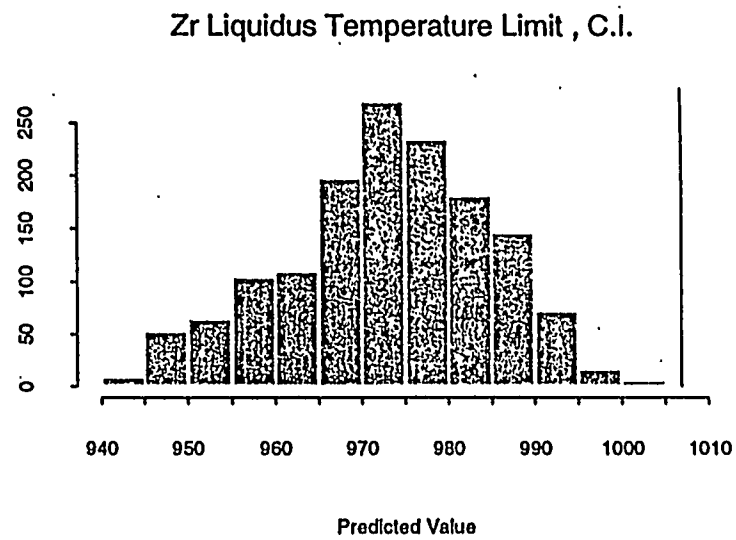

FIGURE 14.1. Histograms of Predicted Property Values for Shrunken Versions of the Vertices and Centroid of Each Property Constraint That Lie on the Boundary of the Qualified Composition Region Defined by 95% Confidence Intervals (continued)

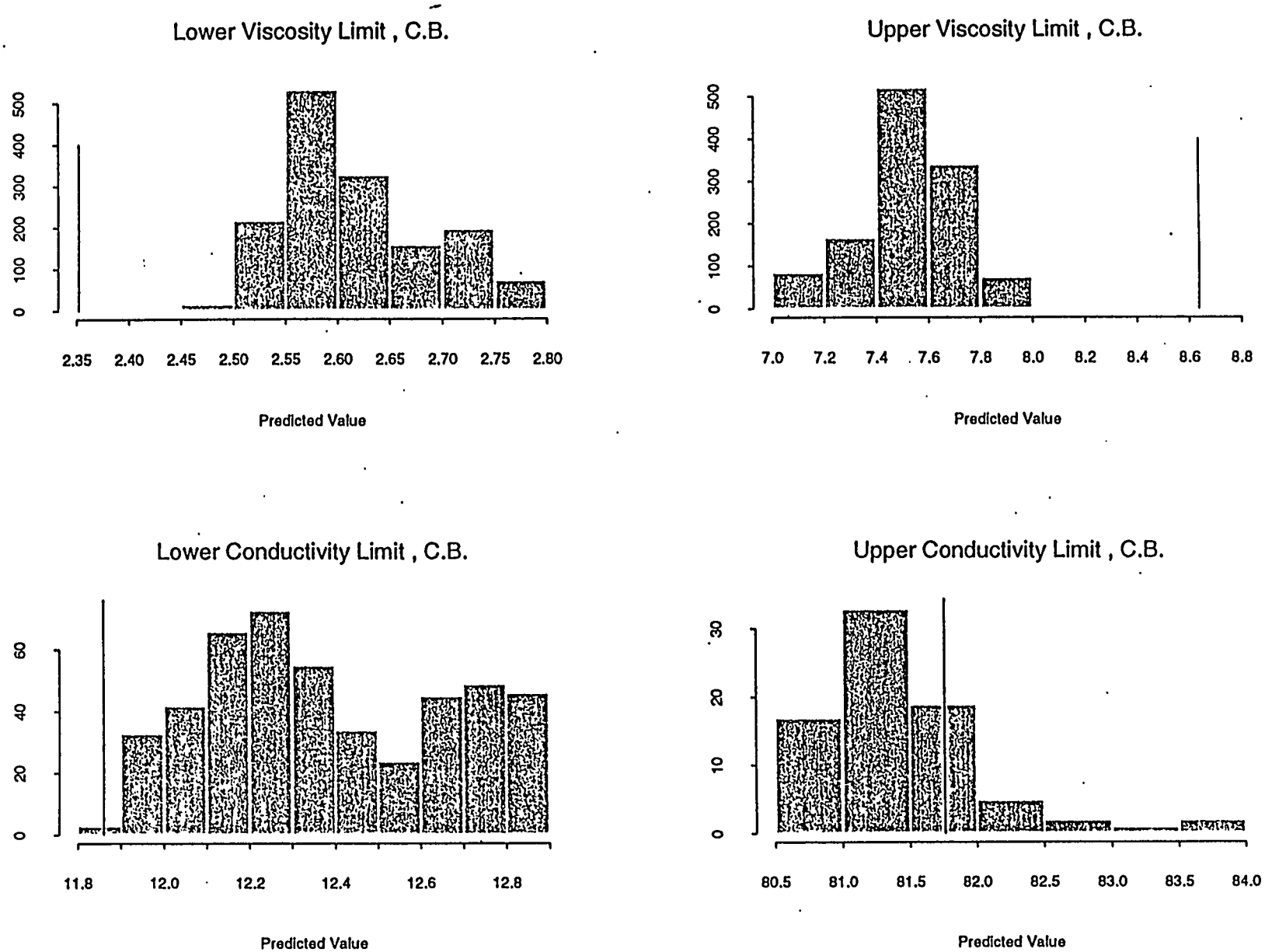

FIGURE 14.2. Histograms of Predicted Property Values for Shrunken Versions of the Vertices and Centroid of Each Property Constraint That Lie on the Boundary of the Qualified Composition Region Defined by 95% Confidence Bands

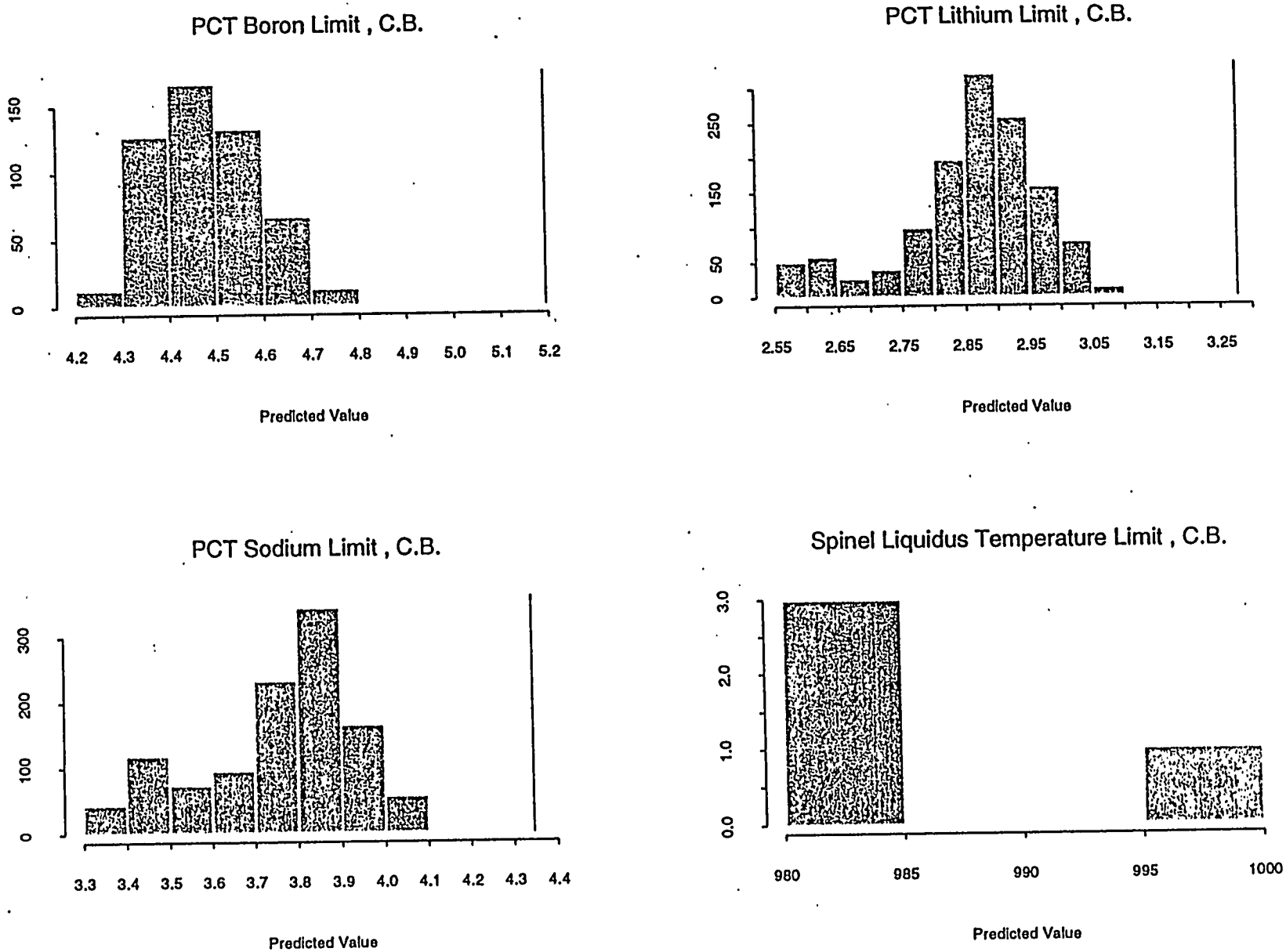

FIGURE 14.2. Histograms of Predicted Property Values for Shrunken Versions of the Vertices and Centroid of Each Property Constraint That Lie on the Boundary of the Qualified Composition Region Defined by 95% Confidence Bands (continued)

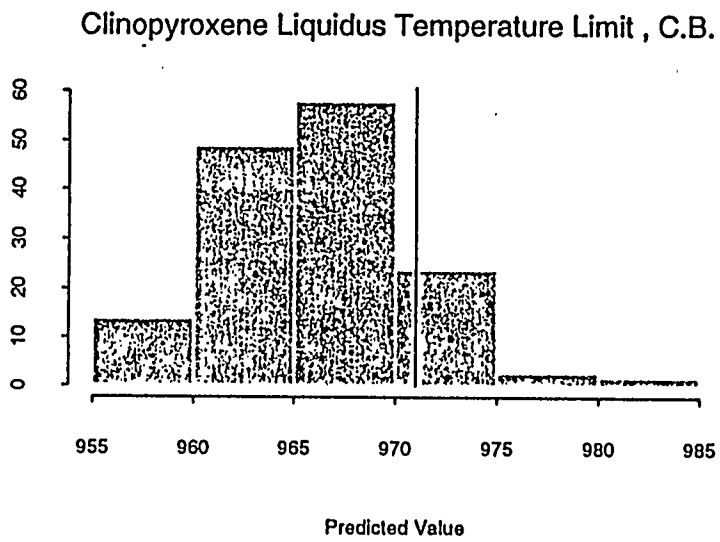

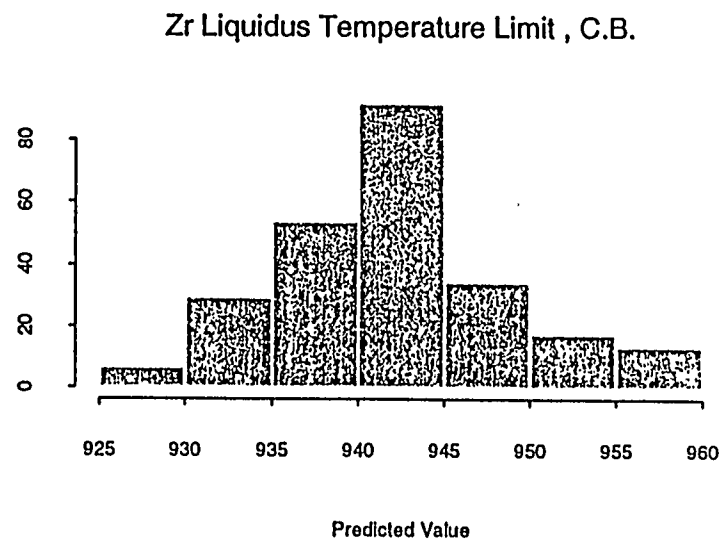

FIGURE 14.2. Histograms of Predicted Property Values for Shrunken Versions of the Vertices and Centroid of Each Property Constraint That Lie on the Boundary of the Qualified Composition Region Defined by 95% Confidence Bands (continued)

To illustrate the interpretation of the histogram results, in Figure 14.2 consider the histogram for the viscosity lower limit when a 95% confidence band is used to account for the uncertainty in the viscosity at 1150°C model. The values in the histogram range from 2.45 to 2.80 Pa·s for the shrunken versions of the vertices of the low viscosity PACR face, while the shrunken version of the centroid for that face has a predicted value of about 2.35 Pa·s. So, in order to satisfy the lower limit of 2 Pa·s for viscosity at 1150°C with 95% confidence, the worst glass on the low viscosity boundary of the QCR would have to have a predicted viscosity greater than 2.80 Pa·s. Of course, it is unlikely that a glass composition selected for use during production will be on the QCR boundary for a number of properties (e.g., viscosity and electrical conductivity), in which case uncertainties in various property models will need to be accounted for in the vicinity of the desired composition. This process would use the same tools as those used to help understand the consequences of applying model uncertainty to the PACR to obtain the QCR.

Note in Figure 14.2 that the histogram for spinel liquidus temperature only includes the results for four vertices. This is because the uncertainty in the first-order model for spinel liquidus temperature is so large that only four vertices on the spinel liquidus temperature constraint face of the PACR had positive shrinkage values. Practically, this means that large portions of the PACR are being "cut off" by uncertainty in the first-order spinel liquidus temperature models. This observation indicates that the QCR defined and described in Section 14.2 should be considered as very preliminary.

14.2.5 QCR Applications

The QCR (and/or the fitted glass property models and uncertainty equations used to construct it) will be useful[a] for several applications

---

(a) Although the QCR presented in this report is very preliminary at this time due to limitations in liquidus temperature models, other property models and their uncertainty equations can be used for glass formulation and other needs. It is envisioned that adequate models and uncertainty equations for all glass properties, and one or more QCRs, will be available by the time a Hanford HLW vitrification plant begins operation.

including: selecting optimal frit and glass compositions, selecting target compositions for process batches during operation of the Hanford HLW vitrification plant, judging acceptability of a SME batch for passing forward to the MFT, showing compliance with the WAPS 1.3 product consistency (PCT durability) specification, and other waste form qualification efforts. Recall, however, that the QCR accounts only for uncertainty in the fitted property models and not for composition uncertainty due to sampling or inhomogeneity within a process feed batch, chemical analysis, or batch-to-batch variations. Such composition uncertainties must be appropriately accounted for in the statistical algorithms and techniques designed to address the various applications mentioned at the beginning of this subsection. The development and application of these algorithms and techniques is within the work scope of the Process/Product Model Development activity of the PVTD project.

15.0 CONCLUSIONS AND FUTURE RESEARCH

Conclusions from the CVS experimental and data analysis work through CVS-II Phase 4 are presented in Section 15.1. Suggestions for future research are presented in Section 15.2.

15.1 CONCLUSIONS

Conclusions based on CVS data (from CVS-I and CVS-II Phases 1, 2, 3, and 4), property modeling, and other data analyses are given. The conclusions are organized according to several topic areas: (1) Data and Test Methods, (2) Glass Property Models, (3) Viscosity, (4) Electrical Conductivity, (5) Glass Transition Temperature, (6) Thermal Expansion, (7) PCT and MCC-1 Durability, (8) Liquidus Temperature and Crystallinity, (9) Amorphous Phase Separation, (10) Different Others Compositions, and (11) Model Uncertainty and the Qualified Composition Region.

Data and Test Methods

- The CVS was planned to study glasses with acceptable and somewhat unacceptable property values, so as to provide the basis for predicting when unacceptable behavior occurs. Generally, the CVS was successful in collecting data satisfying this goal.

- CVS viscosity and electrical conductivity data compared very well with overcheck results performed at Corning Engineering Laboratory Services. CVS PCT and MCC-1 durability results showed some differences compared to overcheck results performed at Savannah River Technology Center, Rensselaer Polytechnic Institute, and Argonne National Laboratory. However, the differences were within lab-to-lab random variations.

- Percent relative standard deviations (%RSD) for glass properties based on replicate glasses and measurements made at different times during the CVS are as follows: 3.5% for viscosity at 1150°C; 9.3% for electrical conductivity at 1150°C; 6.1%, 9.7%, 13.6%, and 10.5% for Si, B, Li, and Na normalized PCT releases; and 5.4%, 6.4%, 11.3%, and 9.5% for Si, B, Li, and Na normalized MCC-1 releases. For properties whose experimental and measurement uncertainty was constant on an absolute basis, standard deviations are: 6.5°C for glass transition temperature, 0.53×10^{-6}/K for thermal expansion of solid glass, 11.3×10^{-6}/K for thermal expansion of molten glass, and 3 to 13°C for liquidus temperature.

Glass Property Models

- There was no advantage for the CVS data of fitting first- and second-order mixture models using mole fractions of components instead of mass fractions. Because of this and because working in terms of mass fractions avoids the extra steps of transforming between mass and mole fractions, mass fraction models were used in CVS analyses requiring fitted models.

- The first-order (mass fraction) mixture model coefficients for various properties are summarized in Table 15.1.

- The first- and second-order glass property models were fitted to data from a constrained composition region. These models have predictive performances for other compositions in the constrained region comparable to those for the compositions used to fit the models. Models for viscosity at 1150°C showed some ability to be extrapolated (i.e., applied to compositions outside the constrained composition region). Models for electrical conductivity at 1150°C and glass transition temperature did not perform well when extrapolated, however. Thus, in general, the fitted CVS models should not be extrapolated.

- Many of the first- and second-order glass property models have statistically significant lack-of-fits (LOFs) at higher than 90% confidence, even though in some cases R^2 values are 0.90 and above. This means that the differences between predicted and measured property values are larger than can be explained by long-term within-lab experimental and measurement uncertainty. However, such LOFs may not be of practical significance if experimental and measurement uncertainty is rather small and somewhat larger prediction uncertainties can be tolerated (e.g., if glasses for the vitrification plant will have some properties targeted to the middle of their acceptable ranges).

Viscosity

- A model consisting of the Fulcher equation with its coefficients (A, B, and T_0) expanded in the forms of first-order mixture models fit CVS measured viscosity data in the 950 to 1250°C range quite well (R^2 = 0.984), but had inappropriate values for some coefficients. The measured data were augmented with a "data point" for each glass consisting of the approximate viscosity value of $10^{11.3}$ Pa·s at the glass transition temperature, and the Fulcher-mixture model was refitted. Compared to the model fitted without the augmented data, the resulting model has: slightly degraded predictive ability in the 950 to 1250°C range (R^2 = 0.937), appropriate coefficient estimates, and better expected predictive ability outside the 950 to 1250°C range.

- A model consisting of the Arrhenius equation with its coefficients (A and B) expanded in the forms of first-order mixture models fit CVS measured viscosity data in the 950 to 1250°C range quite well (R^2 = 0.970). Its predictive ability in the 950 to 1250°C range was not quite

TABLE 15.1. First-Order Mass Fraction Mixture Model Coefficients for Various Properties

	ln(PCT) Release				ln(MCC-1) Release				pH				
Oxide	Si	B	Li	Na	Si	B	Li	Na	PCT	MCC-1	T_g	α_s	α_m
SiO_2	-2.9671	-4.3173	-3.2278	-4.4118	1.5252	0.7520	0.6351	0.8122	8.1926	7.3414	622.973	1.634	56.866
B_2O_3	-0.6148	11.9791	10.1496	9.4049	8.3034	11.7667	11.5572	11.6800	3.3332	9.1180	584.939	0.747	186.560
Na_2O	10.7384	17.6068	14.0017	19.4013	8.6025	11.2400	10.9281	10.6536	23.6171	17.8061	128.504	38.479	81.991
Li_2O	19.7370	22.5791	18.4159	19.0635	10.9643	12.7971	11.4779	13.0459	31.2448	24.4490	-571.109	46.968	342.580
CaO	-6.0415	-8.7114	-5.3528	-1.9567	1.1008	2.5548	3.5185	2.4552	17.2056	13.3174	621.517	19.455	171.985
MgO	2.9296	10.9210	7.1181	11.8228	3.8410	7.9369	7.7192	7.7582	15.3354	13.1459	494.391	12.941	105.643
Fe_2O_3	-4.2315	-3.2009	-4.5113	-4.0953	1.2457	1.3389	1.6427	1.4738	8.5939	10.1817	427.129	10.170	194.435
Al_2O_3	-17.3377	-25.4071	-22.3095	-25.4294	-8.9277	-11.8976	-11.3414	-11.5527	5.3578	4.0454	544.451	3.990	-74.456
ZrO_2	-10.8139	-10.5613	-10.0618	-11.4209	-5.6850	-5.2635	-4.9116	-5.4273	7.6111	7.5917	730.071	3.751	-71.236
Others	-0.7297	0.1587	0.6181	-0.6647	0.1499	1.3988	1.7904	1.0045	9.2689	8.6750	363.637	10.174	48.886
R^2	0.7377	0.8114	0.7905	0.8457	0.6254	0.6683	0.6586	0.6701	0.9092	0.7487	0.8865	0.8709	0.4291

	ln(Viscosity)						ln(Electrical Conductivity)			Liquidus Temperature		
	Arrhenius		Fulcher				Arrhenius					
Oxide	A	B	A	B	To	1150°C	A	B	1150°C	Clinopyroxene	Spinel	Zr-Containing
SiO_2	-11.084	28539.00	-10.590	19236.326	76.113	8.968	8.12	-10283.00	0.8471	955.65	989.31	753.78
B_2O_3	-13.659	10868.00	-24.413	15922.841	263.485	-6.204	12.82	-15135.00	2.2518	314.72	666.42	1095.83
Na_2O	-9.604	-1217.06	2.020	-12965.418	425.716	-11.016	6.05	7089.48	11.0396	38.83	3.77	74.31
Li_2O	-4.514	-42288.00	5.456	-39177.204	474.430	-34.239	7.47	22484.00	23.5355	-207.05	-128.77	-956.39
CaO	-22.750	21522.00	3.954	-18671.453	1065.825	-7.466	14.41	-18769.00	1.4129	1372.44	1366.21	886.76
MgO	-21.105	25767.00	5.309	-11943.961	752.242	-2.776	10.39	-13414.00	1.0565	2387.62	2830.58	2458.47
Fe_2O_3	-6.404	8773.98	-13.633	14559.334	43.638	-0.036	9.94	-10608.00	2.5863	1506.69	2256.00	1461.04
Al_2O_3	-4.089	21186.00	1.500	9524.439	178.525	11.306	7.14	-8227.18	1.3108	1319.78	1735.03	1138.06
ZrO_2	-31.323	54574.00	-0.359	4618.146	540.509	7.434	7.93	-9723.86	1.1224	1844.50	928.11	4541.99
Others	-17.017	23027.00	-2.382	1710.206	270.741	-0.156	18.11	-20653.00	3.4531	1357.40	1005.56	657.99
R^2	------- 0.9704 -------		---------- 0.9958 ----------			0.9391	----- 0.9582 ------		0.9314	0.9054	0.6433	0.7902

as good as for the Fulcher-mixture model fit without the augmented data (R^2 = 0.984), but was better than the Fulcher-mixture model fit with the augmented data (R^2 = 0.937).

- The Fulcher-mixture and Arrhenius-mixture models discussed in the preceding two bulleted items showed a tendency towards slightly underpredicting viscosities below about 1 to 2 Pa·s.

- The Arrhenius "B" coefficient is the activation energy for viscous flow for a CVS glass in the temperature interval from 950 to 1250°C (assuming a linear relationship between ln(viscosity) and inverse temperature). High activation energies indicate that a glass will remain in a workable viscosity range for a short temperature interval (or a short glass). Components which increase "B" will shorten glass while components that decrease "B" will lengthen it. Based on first-order models fit to CVS data, Li_2O and Na_2O are predicted to have the largest lengthening effects on glass while ZrO_2 and SiO_2 are predicted to have the largest shortening effects.

- First- and second-order mixture models for viscosity at 1150°C fit the CVS data quite well (R^2 ranged from 0.94 to 0.98). These models show no evidence of biased predictions for CVS glasses with viscosity at 1150°C below ~15 Pa·s, but show a tendency to underpredict above this value. Second-order models appear to have a negligible to slight advantage over the first-order model for predicting viscosity at 1150°C. Both first- and second-order models have statistically significant LOFs, although the LOFs may not be of practical concern (as discussed previously).

- Based on a first-order mixture model fitted to CVS data, Li_2O and Na_2O are predicted to have the strongest effects decreasing viscosity, while SiO_2, Al_2O_3, and ZrO_2 are predicted to have the strongest effects increasing viscosity.

- A non-bridging oxygen (NBO) modeling approach (used by DWPF) was compared to CVS first- and second-order models for viscosity at 1150°C. The CVS models performed significantly better than the NBO model for the CVS data (R^2 ranged from 0.94 to 0.97 for CVS models, whereas R^2 ranged from 0.70 to 0.76 for the NBO models).

- An empirical modeling approach using oxide/SiO_2 ratios was investigated for viscosity at 1150°C. The first- and second-order CVS models were found to perform slightly better than the oxide/SiO_2 ratio models.

Electrical Conductivity

- A model consisting of the Arrhenius equation with its coefficients (A and B) expanded in the forms of first-order mixture models fit CVS measured electrical conductivity data in the 950 to 1250°C range quite well (R^2 = 0.958). The model showed a tendency to overpredict electrical conductivity values below about 3 S/m and above about 50 S/m.

- First- and second-order mixture models for electrical conductivity at 1150°C fit the CVS data quite well (R^2 ranged from 0.93 to 0.98). The first-order model shows a tendency to overpredict electrical conductivity at 1150°C values about 8 S/m and above about 60 S/m. Second-order models #2 and #3 (Table 8.3) corrected these shortcomings and appear to have an advantage over the first-order model for predicting electrical conductivity at 1150°C. The first-order model has a statistically significant LOF at greater than 90% confidence, but second-order models #2 and #3 do not. Second-order model #3 does not fit the data much better than #2, even though it contains several more terms. Hence, second-order model #2 is recommended.

- Based on a first-order mixture model fitted to CVS data, Li_2O and Na_2O are predicted to have the strongest effects increasing electrical conductivity, while SiO_2 is predicted to have the strongest effect decreasing electrical conductivity. The remaining components are predicted to have negligible effects.

Glass Transition Temperature

- First- and second-order mixture models for glass transition temperature fit the CVS data fairly well (R^2 ranged from 0.88 to 0.97). The first-order model shows some tendency to overpredict glass transition temperature values below about 425°C, and to underpredict values above about 550°C. Second-order models fitted the CVS data better than the first-order model and eliminated biased predictions. The first-order model and second-order model #1 have statistically significant LOFs for the CVS data, but second-order models #2 and #3 (Table 9.3) do not. For data not used to fit the models, however, second-order models did not predict any better than the first-order model. Hence, it is unclear at this time whether second-order models provide a worthwhile improvement over the first-order model.

- Based on a first-order mixture model fitted to CVS data, Li_2O and Na_2O are predicted to have the strongest effects decreasing glass transition temperature, while SiO_2 and ZrO_2 are predicted to have the strongest effects increasing glass transition temperature.

Thermal Expansion

- First- and second-order mixture models for thermal expansion of solid glass fit the CVS data fairly well (R^2 ranged from 0.87 to 0.93). The first-order model shows some tendency to overpredict thermal expansion of solid glass values below about 7×10^{-6}/K. Second-order models fitted the CVS data slightly better than the first-order model and eliminated biased predictions at lower values. The first- and second-order models do not have statistically significant LOFs for the CVS data, presumably due to larger experimental error (reflecting the difficulty in reproducibly measuring thermal expansion of solid glass).

- Based on a first-order mixture model fitted to CVS data, Li_2O and Na_2O are predicted to have the strongest effects increasing thermal expansion of solid glass, while SiO_2 and B_2O_3 are predicted to have the strongest effects decreasing thermal expansion of solid glass.

- The first-order mixture model for thermal expansion of molten glass fit the CVS data rather poorly (R^2 = 0.43), and showed tendencies towards biased predictions over the whole range of data. Second-order models fitted the CVS data noticeably better than the first-order model (R^2 = 0.72 to 0.75). The first-order model had a statistically significant LOF for the CVS data, but the second-order models did not. The non-significant LOF for second-order models in spite of relatively low R^2 values is presumably due to larger experimental error (reflecting the difficulty in reproducibly measuring thermal expansion of molten glass).

- Based on a first-order mixture model fitted to CVS data, Li_2O, $B_2O_3 \approx Fe_2O_3$ and CaO are predicted to have the strongest effects increasing thermal expansion of molten glass, while Al_2O_3, ZrO_2, and SiO_2 are predicted to have the strongest effects decreasing thermal expansion of molten glass.

PCT and MCC-1 Durability

- Most of the PCT and MCC-1 durability results in this report are for quenched glass. However, PCTs of canister centerline cooled samples of all CVS glasses were completed late in FY94, and will be addressed in a subsequent report. Unless stated otherwise, the following conclusions are for PCT and MCC-1 tests of quenched CVS glasses.

- Ranking the CVS glasses according to MCC-1 dissolution test results does not yield the same order as ranking according to PCT dissolution test results. Glasses acceptable by PCT can be poor performers by MCC-1 and vice versa. The differences in the ranking of glasses according to different dissolution tests is attributed to solution reactions. A durability study of two CVS glasses shows that precipitation of minerals occurs at higher surface area to volume ratios. Precipitation of silicates removes silicic acid from the solution and thus increases the driving force for dissolution and dissolution rate. Glass composition dictates solution composition and, hence, affects precipitation.

- First- and second-order mixture models for PCT normalized B, Li, and Na releases fit the CVS data reasonably well (R^2 ranged from 0.73 to 0.92). Both first- and second-order models show some tendency to underpredict releases above 3 g/m^2, although second-order models seem to lessen this tendency. Both first- and second-order models have LOFs that are statistically significant at greater than 99% confidence, and the LOFs may be practically significant.

- First- and second-order mixture models for MCC-1 normalized B, Li, and Na releases did not fit the CVS data as well as the PCT release models (R^2 ranged from 0.60 to 0.83). Both first- and second-order models show

- The current version of the phase-equilibria liquidus temperature model (which considers composition only in terms of the nine major CVS components and the Others component) does not predict the CVS data very well. However, the model is expected to improve after it is updated to account for solid solutions and minor components. Also, whether the CVS data may be affected by kinetic and other factors is being investigated.

- Approximately one-half of the CVS-I and CVS-II Phase 1, 2, and 3 glasses exhibited crystallinity after canister centerline cooling heat treatment. The crystalline phases occurring most frequently were spinel, Li_2SiO_3, and clinopyroxene, followed by olivine, SiO_2, hematite, zircon, orthopyroxene, and nepheline.

- Crystallization of nepheline and SiO_2 after canister centerline cooling had a strong negative effect on glass durability. Crystallization of clinopyroxenes and zircon only slightly affected glass durability. These conclusions are based on a study of selected CVS glasses, and are thus preliminary.

Amorphous Phase Separation

- Of the 123 CVS-I and CVS-II Phase 1, 2, and 3 glasses, only nine are prone to amorphous phase separation, as predicted by a modified Taylor model using Na_2O+Li_2O - B_2O_3 - SiO_2 (NLBS) and Na_2O equivalent - B_2O_3 - SiO_2 submixtures. Experimentally, amorphous phase separation has only been observed in three CCC glasses and one quenched glass by SEM/TEM analysis.

- The NLBS submixture also suggests a relationship between composition and durability for both quenched MCC-1 and PCT data. Based on MCC-1 data and SEM results, glasses within the immiscibility dome show low durability as a result of insufficient network forming oxides (compositional deficiency), not the development of amorphous phase separation. The developing microstructure was determined to possess a B-rich continuous phase with dispersed Si-rich particles. The effects of structural integrity on durability was also dependent on position within the submixture. Glasses located within the high durability pocket positioned near the SiO_2-rich corner of the NLBS submixture possess a continuous 3-D network (or structural integrity). Glasses positioned in the SiO_2-deficient region of the submixture generally produced low durability unless sufficient Al_2O_3 and ZrO_2 were present.

Different Others Compositions

- Based on limited testing, varying the composition of the Others component from that used in most of the CVS glasses (which corresponds to NCAW) seems to affect some properties and not others. Viscosity, MCC-1 and PCT normalized B releases, and liquidus temperature (spinel and non-spinel) can be affected depending on the composition of the glass and the composition of Others. Electrical conductivity, glass

some tendency to underpredict releases above about 40-50 g/m^2, but glasses with such higher releases are not of much interest. These models also overpredicted releases below 5 g/m^2 for two glasses. Both first- and second-order models have LOFs that are statistically significant at greater than 99% confidence. The LOFs are due to these tendencies towards biased predictions and considerable scatter in plots of predicted versus measured releases, and hence are of considerable practical concern.

- Based on first-order PCT and MCC-1 normalized B release models fitted to CVS data, Li_2O, Na_2O, and B_2O_3 are predicted to have the strongest effects increasing B release, while Al_2O_3, SiO_2, and ZrO_2 are predicted to have the strongest effects decreasing B release.

- Experimentally varying components one-at-a-time from their values in the HW-39-4 glass showed that the effects of most components on PCT and MCC-1 are roughly linear over the ranges studied. Nonlinearity was seen for SiO_2, Al_2O_3, and B_2O_3 (MCC-1 only).

- Plots of natural logarithms of PCT and MCC-1 normalized boron release versus free energy of hydration show essentially no relationship for CVS data (or any subset thereof). Correcting free energy of hydration for pH effects does not improve the relationships. Hence, the DWPF approach of modeling PCT and MCC-1 releases based on free energy of hydration does not appear applicable to the wide range of CVS glass compositions.

Liquidus Temperature and Crystallinity

- The prevailing primary crystalline phases within the CVS composition region are spinel, clinopyroxene, and Zr-containing phases (zircon, ZrO_2, and Na-Zr silicate), followed by orthopyroxene, nepheline, olivine, $CaSiO_3$, and SiO_2. Less frequent are Li_2SiO_3, $LiAlSi_2O_6$, and hematite. Liquidus temperatures (T_L) of two-thirds of the CVS glasses lie within the 800 to 1000°C range. The crystalline phases with T_L > 1050°C were mainly limited to spinels and Zr-containing phases.

- The first-order mixture model for T_L of clinopyroxene fits the CVS data fairly well, but the models for spinel and Zr-containing crystals need improvement. There were not sufficient glasses having each of these primary crystalline phases to reliably fit second-order models.

- Based on the first-order mixture models, alkali oxides (Na_2O and Li_2O) are predicted to decrease T_L of all three crystalline phases, with Li_2O always having the stronger effect. B_2O_3 is predicted to decrease T_L of glasses containing clinopyroxene and spinel, but slightly increase T_L for glasses with Zr-containing crystals. MgO and Fe_2O_3 are predicted to be most effective in increasing T_L of glasses containing clinopyroxene or spinel. The T_L of Zr-containing phases is predicted to be most strongly increased by ZrO_2 followed by MgO. The strong predicted effect of MgO in increasing T_L of all three crystalline phases suggests caution when using MgO as an additive component.

transition temperature, and thermal expansion appear to be only slightly affected, if at all, by varying Others composition.

- The presence of higher levels of Cr_2O_3 in some Others mixes seems to be a possible explanation for some of the significant changes in property values.

Model Uncertainty and the Qualified Composition Region (QCR)

- The QCR is intended to be a subregion of the composition region studied in CVS that satisfies, with high confidence, processability and Waste Acceptance Product Specification (WAPS) constraints. The preliminary QCR discussed in this report was based on the viscosity, electrical conductivity, liquidus temperature, and PCT durability constraints and single-component constraints in Table 14.3.

- First-order property models and the corresponding uncertainty expressions were used to construct the preliminary QCR presented in this report. For some properties second-order models were determined to be better, but there wasn't time to modify the QCR calculations to accommodate second-order models.

- Six types of statistical approaches were considered to account for property model uncertainty in constructing the QCR: confidence intervals, prediction intervals, tolerance intervals, confidence bands, prediction bands, and tolerance bands. Confidence intervals and confidence bands were determined to be the most appropriate.

  -- From the standpoint of wanting to know whether a single composition in the QCR will have acceptable properties with a specified confidence (say 95%) for each property, constructing the QCR as a collection of individual confidence intervals is the appropriate thing to do.

  -- From the standpoint of wanting to know whether all of the compositions in the QCR will have acceptable properties with a specified confidence (say 95%) for each property, constructing the QCR as a collection of simultaneous confidence intervals (confidence bands) is the appropriate thing to do.

- The preliminary QCR is a nine-dimensional composition region defined using matrix equations (having slightly different forms depending on whether confidence intervals or confidence bands are used), and is thus impossible to visualize directly. The QCR can be thought of as a shrunken version of the PACR, where the shrinkage occurs due to model uncertainty. The following two bullets summarize the results of two investigations to help understand how much smaller the QCR is than the PACR due to model uncertainty.

- The percentage of the distance from the center of the CVS composition region to each PACR property boundary remaining after accounting for

model uncertainty in the QCR ranged as follows (results are combined for properties with both lower and upper constraints):

-- Using 95% confidence intervals: 76-93% for viscosity at 1150°C, 88-95% for electrical conductivity at 1150°C, 65-85% for PCT B, Li, and Na releases, 67-78% for clinopyroxene liquidus temperature, 17-60% for spinel liquidus temperature, and 26-70% for Zr-containing crystals liquidus temperature

-- Using 95% confidence bands: 53-84% for viscosity at 1150°C, 74-88% for electrical conductivity at 1150°C, 36-66% for PCT B, Li, and Na releases, 40-56% for clinopyroxene liquidus temperature, 0-35% for spinel liquidus temperature, and 0-37% for Zr-containing crystals liquidus temperature.

These percentage numbers give an intuitive idea how much smaller the QCR is than the PACR due to model uncertainty. Smaller percentage numbers correspond to models with more uncertainty. Also, it is clear that a considerable price is paid for wanting to make statistical statements about all compositions in the QCR (with confidence bands) compared to wanting to make statistical statements about individual compositions in the QCR (with confidence intervals).

- For glass compositions on each boundary of the preliminary QCR corresponding to a property constraint[a], the predicted property value farthest from the constraint value (i.e., the property limit) indicates the size and consequence of model uncertainty. The farther the predicted property value from the property limit, the greater the size and consequence of model uncertainty. The worst values for each property constraint are as follows.

  -- Using 95% confidence intervals: 2.38 Pa·s compared to lower viscosity at 1150°C limit of 2 Pa·s, 8.40 Pa·s compared to upper viscosity at 1150°C limit of 10 Pa·s, 11.25 S/m compared to lower electrical conductivity at 1150°C limit of 10 S/m, 90.8 S/m compared to upper electrical conductivity at 1150°C limit of 100 S/m, 5.7 g/m^2 compared to upper PCT B release limit of 8.2 g/m^2, 3.35 g/m^2 compared to upper PCT Li release limit of 4.8 g/m^2, 4.5 g/m^2 compared to upper PCT Na release limit of 6.6 g/m^2. Values for clinopyroxene, spinel, and Zr-containing crystals liquidus temperature to compare to the upper limit of 1050°C could not be obtained due to the large model uncertainties.

  -- Using 95% confidence bands: 2.80 Pa·s compared to lower viscosity at 1150°C limit of 2 Pa·s, 7.0 Pa·s compared to upper viscosity at

---

(a) There is a boundary (or "face") of the QCR corresponding to each glass property constraint used in defining the QCR. The equations of the boundaries are given by Equations (14.1) to (14.10) in Table 14.4 of Chapter 14.

1150°C limit of 10 Pa·s, 12.9 S/m compared to lower electrical conductivity at 1150°C limit of 10 S/m, 80.5 S/m compared to upper electrical conductivity at 1150°C limit of 100 S/m, 4.2 g/m^2 compared to upper PCT B release limit of 8.2 g/m^2, 2.55 g/m^2 compared to upper PCT Li release limit of 4.8 g/m^2, and 3.3 g/m^2 compared to upper PCT Na release limit of 6.6 g/m^2. Values for clinopyroxene, spinel, and Zr-containing crystals liquidus temperature to compare to the upper limit of 1050°C could not be obtained due to the large model uncertainties.

- The preliminary QCR presented in this report should be considered a demonstration effort and not relied on, due to the very preliminary nature of the liquidus temperature models used. The PCT durability models also have more uncertainty than is desirable.

15.2 SUGGESTIONS FOR FUTURE RESEARCH

This report concludes a study of a composition region of glasses with melting temperature in the range 1100 to 1200°C. The composition region was originally built around NCAW and was later extended to encompass the NCRW, CC, and PFP DST wastes. The previously planned HWVP envisioned relatively low waste loadings (25-28 wt%), although the region studied did include some higher waste-loaded compositions. This philosophy changed at the end of FY 1993, when a wider melting temperature range (1050-1500°C) and unlimited waste loading began to be considered for both DST and SST high-level Hanford wastes. With adjustable melting temperature, viscosity is no longer a constraining property. Viscosity, along with electrical conductivity, can be used to determine the operation (and even the design) of the melter rather than adjusting these properties for a pre-selected melter. Further, with no a priori limitation imposed on waste loading, waste-loading maximization became a more important objective in waste glass formulation.

As the waste loading increases, four different thresholds can be recognized:

- Spinel threshold is the lowest waste loading at which spinel appears in the glass in the melter.
- Crystallization threshold is the lowest waste loading at which crystals other than spinel precipitate in the melter.
- Molten salt segregation threshold is the lowest waste loading at which segregated molten salts, such as sulfate, accumulate in the melter.

- Durability threshold is the highest waste loading at which glass durability is acceptable by the chosen standard.

The effect of the first three thresholds on the maximum acceptable waste loading depends on the melter type. Melters with long residence times are sensitive to accumulation of solids, especially if the solid particles are large or form large agglomerates. Spinels are evaluated separately because their crystals are usually small (<10 μm) and well dispersed, so only a tolerable amount of spinel sludge accumulates during the melter service time. Crystals other than spinels are larger and can put a continuous melter out of service within a short time. Molten salts can segregate and accumulate in the melter, on the top or at the bottom of melt, depending on the density. Segregated molten salts are tolerable only in special melters with mechanical stirring or molten salt drains.

The durability threshold is independent of the method of melting and depends solely on glass composition and the durability standard applied. When the fraction of modifying components in the glass increases and the fraction of network-forming components decreases to the point that the network breaks down, the elemental releases of waste components increase above the acceptable level.

The order in which different thresholds occur as waste loading increases depends on the waste type. The waste loading of high-alkaline wastes (Hanford low-level waste) is limited by durability. Wastes with high level(s) of S, P, Mo, etc., are likely to first reach the limit for the segregation of molten salts. Generally, Hanford high-level waste compositions are rich in refractory components (some major and some minor), such as Al_2O_3, Fe_2O_3, ZrO_2, Cr_2O_3, and RuO_2. With increasing waste loading, spinel will occur first if the fraction of Fe is large enough. Spinel precipitation will be followed by the formation of another crystalline phase, such as baddeleyite (ZrO_2) and zircon. RuO_2 is virtually insoluble in a borosilicate glass, but its concentration in Hanford wastes is considered tolerable. The durability threshold is likely to be reached in Hanford high-level wastes at high values of waste loading, after a high fraction of crystals has precipitated. Since 25 wt% Na_2O is typical for Hanford high-level wastes, the glass network will

break down at 70 to 80 wt% waste loading, when a high fraction of Na_2O brings about structural deterioration of the glass phase.

For common types of melters, the dominating factor that limits waste loading for Hanford high-level wastes is crystallinity. Unfortunately, no reliable models for crystallinity are available at present. Unlike other properties, liquidus temperature and composition of crystalline phases may be substantially affected by minor components. A semi-empirical liquidus temperature model based on thermodynamics has been developed for a system defined by the major CVS components. The current version of the model ignores minor components, redox, H_2O, and solid solutions, but is being updated to address these aspects.

Improvement of the liquidus temperature model may be hindered by the lack of reliable data. Liquidus temperatures determined from gradient furnace testing are possibly affected by the kinetics of nucleation and crystallization and by fluid flow induced in the melt due to the temperature gradient. Gradient furnace results do not provide data directly relevant to the melter because of the differences in the time scale and nucleation conditions. In the melter, glass may stay on slow streamlines for many days before it is removed, and melter walls provide nucleation sites for crystallization. In addition, the crystals that precipitate from nuclear waste glasses are often complex solid solutions for which no data exist in the literature. Improvement of the thermodynamic liquidus temperature model is being pursued, but empirical models for T_L and an approach based on an operational definition for T_L related to melter conditions may also be pursued.

To predict sludge formation in the melter, kinetic factors must also be considered. Liquidus temperature alone is insufficient for such a prediction. Sluggish kinetic or nucleation barriers may allow safe operation below the liquidus temperature and thus increase waste loading.

Prediction of molten salts segregation is even more difficult than prediction of crystallization because salts can probably segregate in the cold cap below their solubility limits in molten glass. The development of thermodynamic models for molten salt segregation have recently been initiated.

Experimental study of molten salt segregation in Hanford glasses has also started.

To summarize, the ability to predict maximum acceptable waste loadings for Hanford waste types can be enhanced by progress on: 1) developing thermodynamic models for crystallization and molten salts segregation, 2) developing the database for liquidus temperature and solubility limits, 3) crystallization and salt segregation kinetic studies, and 4) case studies targeted at specific Hanford waste types as the waste feeds become better defined.

Specific suggestions for future studies are given in the following bullets. The suggestions are organized according to several topic areas.

Glass Composition and Properties

- Viscosity of glasses should be measured over a wider temperature range than the 950 to 1250°C range used so far in CVS. Viscosity data over a wider temperature range will yield more accurate Fulcher viscosity models, which are needed to predict viscosities and melting temperatures for higher-temperature, higher-waste-loaded glasses.

- Develop parallel models expressing temperature as a function of viscosity and composition. This will provide for predicting melting temperature as a function of composition for specified viscosities.

- Increase the database for glasses in composition regions of more interest where sufficient data do not exist (e.g., glass composition regions having higher concentrations of waste components, high durability, and high melting temperature).

- Perform case studies to optimize glass composition for given waste types. This optimization will entail use of CVS models with experimental verification and will lead to a better understanding of the practical limitations of CVS models and point the way for future model development.

Glass Durability

- Develop PCT and MCC-1 elemental release models focusing on the glass composition region with higher durabilities (i.e., focus less attention on modeling for glasses with very high releases) to increase the predictability of elemental releases for higher durability glasses. Employ second- and higher-order terms and new model forms to account for nonlinearity and interactive effects of components on release.

- Collect recent glass composition and corresponding PCT and MCC-1 release data from Savannah River Technology Center and other sites. As appropriate, use this data to validate CVS models and to augment CVS data for additional model development/improvement work.

- Perform both PCT and MCC-1 dissolution tests for future CVS investigations. Both tests have been performed since the start of the CVS and provide different views of glass durability because of differences in reaction progress.

- Study the effects of dissolution test parameters on glass durability of selected glasses (e.g., flow-through testing).

Crystallinity, Liquidus Temperature, and Solubility Limits

- Improve the first-order models for the liquidus temperature of glasses with clinopyroxene, spinel, and Zr-containing phases by including points with high liquidus temperatures. Develop second-order models if sufficient data points are obtained for each phase.

- Investigate empirical models for predicting the primary crystalline phase at the liquidus temperature, and for predicting whether liquidus temperature is above or below a specified limit.

- Update the phase-equilibria liquidus temperature model by expanding the underlying database to include FeO, NiO, CrO, Cr_2O_3, MnO, and Bi_2O_3. Investigate the incorporation of F, S, P, and H_2O into the database to predict the solubility of minor components.

- Complete investigation of the effect of crystallinity after CCC on the durability of all CVS glasses. Identify those composition regions where CCC glass durability differs from that of quenched glass. Develop first- and second-order models for durability of CCC glasses.

- Study crystallization in glasses that precipitate phases such as nepheline and SiO_2. Investigate the durability of glasses containing durability-reducing crystalline phases as a function of crystallinity. Determine the component effects on the crystallization of durability-reducing phases.

- Perform case studies to determine waste-loading thresholds. Compare the results with predictions/estimates.

- Determine the solubility limits for Cr_2O_3, P_2O_5, and SO_3 as functions of glass composition and temperature history. Determine the impact of these oxides on vitrification of Hanford wastes.

- The effects of noble metals on melter performance are subjects of independent studies. Although the form of RuO_2 (undissolved RuO_2 or RuO_2 needles) is affected by glass composition to some degree, behavior of noble metals is probably not directly influenced by glass composition

within the range of CVS. Support the studies of metal behavior in the melter by determining: (i) the form of noble metals precipitated when simulants are used instead of chemicals, and (ii) the tendency of noble metals to agglomerate, settle, and form unremovable sludge.

- Fluorine and chlorine, which are also sensitive components, are not present in any estimated Hanford high-level waste in high concentration. If, however, high levels of fluorides and chlorides should be mixed with the feed, determine their solubilities, maximum acceptable concentrations, and effects on melter performance. Obtain the effect of fluorine on viscosity and durability.

Effects of Various Glass Components

- Investigate the effects of oxygen concentration (or redox) on glass properties. In particular, study the effect of batch chemistry on Fe-II/Fe and its effect on durability.

- The redox of CVS glasses may have been affected by ammonium phosphate used in the Others component mixes. Determine whether the effects of Others fraction and redox on properties are compounded.

- Study the effect of FeO on glass properties, including durability and crystallinity. Discuss the effect of FeO on glass processability and acceptability. There is expected to be some variability in the redox state of glasses processed by the high-level waste vitrification plant due to waste pretreatment effects and reduction due to heat treatment, and this may impact crystallization.

- To extend property models for possible application to vitrification of single shell tank wastes, determine the effect of high concentrations of Bi_2O_3, MnO, UO_2, P_2O_5 and other oxides (if necessary) on glass properties.

Glass Property Models

- Update or improve glass property models as additional CVS data or off-site data become available. This includes extending models to incorporate new components and expanded component ranges.

- Collect and utilize adequate data (glass compositions and property values) for validating the CVS empirical glass property models. Validating empirical models with data other than those used to develop them is an essential aspect of the empirical modeling process. Both nonradioactive and radioactive glass data are required for validation.

- Continue to assess uncertainty (bias and imprecision) in glass property models as they are updated or developed. Least squares model fitting theory provides formulas for calculating imprecision of model predictions. Validating a model with data not used to fit it provides for assessing whether the model yields biased predictions and whether imprecision is larger than calculated by least squares theory.

16.0 REFERENCES

Babcock, C.L. 1977. Silicate Glass Technology Methods, John Wiley & Sons, New York.

Bansal, N.P. and R.H. Doremus. 1986. Handbook of Glass Properties, Academic Press, New York, pp. 381-449.

Bashkirov, L.A. and M.G. Bashkirova. 1981. Figure from R.S. Roth, T. Negas, and L.P. Cooke, Phase Diagrams for Ceramists, Vol. 4, American Ceramic Society, Columbus, Ohio.

Begley, E.R. 1974. "Refractories" in The Handbook of Glass Manufacture, edited by F.V. Tooley, Books for Industry, Inc., New York.

Bourcier, W.L., W.L. Ebert, X. Feng. 1993. "Modeling Surface Area to Volume Effects on Borosilicate Glass Dissolution", Materials Research Society Symposium Proceedings, 294, 577-582.

Bickford, D.F. and C.M. Jantzen. 1984. "Devitrification Behavior of SRL Defense Waste Glass", Materials Research Society Symposium Proceedings, 26, 557-566.

Bickford, D.F. and C.M. Jantzen. 1986. "Devitrification of Defense Nuclear Waste Glasses", Journal of Non-Crystalline Solids, 84, 299-307.

Bickford, D.F., A. Applewhite-Ramsey, C.M. Jantzen, and K.G. Brown. 1990. "Control of Radioactive Waste Glass Melters--Part 1. Preliminary General Limits at Savannah River", Journal of the American Ceramic Society, 73, 10, 2896-2902.

Box, G.E.P. and N.R. Draper. 1987. Empirical Model Building and Response Surfaces, John Wiley and Sons, New York.

Bunnell, L.R. 1988. Laboratory Work in Support of West Valley Glass Development, PNL-6539, Pacific Northwest Laboratory, Richland, Washington.

Burnett, D.G. and R.W. Douglas. 1970. "Liquid-Liquid Phase Separation in the Soda-Lime-Silica System", Physics and Chemistry of Glasses, 11, 125-135.

Burnett, D.G. and R.W. Douglas. 1971. "Nucleation and Crystallization in the Soda-Baria-Silica System", Physics and Chemistry of Glasses, 12, 117-124.

Cahn, R.W. and P. Haasen. 1983. Physical Metallurgy, Third Edition. Elsevier Publishing, NY.

Charles, R.J. 1967. "Metastable Immiscibility in the $BaO-Li_2O-SiO_2$ System", Physics and Chemistry of Glasses, 8, 185-189.

Chick, L.A., G.F. Piepel, G.B. Mellinger, R.P. May, W.J. Gray, and C.O. Buckwalter. 1981. The Effects of Composition on Properties in an 11-Component Nuclear Waste Glass System, PNL-3188, Pacific Northwest Laboratory, Richland, Washington.

Chick, L.A. and G.F. Piepel. 1984. "Statistically Designed Optimization of a Glass Composition", Journal of the American Ceramic Society, 67, 763-768.

Chick, L.A. and R.P. Turcotte. 1983. Glass Leaching Performance, PNL-4576, Pacific Northwest Laboratory, Richland, Washington.

Chick, L.A., J.L. Swanson, and D.S. Goldman. 1984. "Nuclear Waste Glass Composition Limitations", Proceedings of Fuel Reprocessing and Waste Management, Vol. 1, pp. 371-385. American Nuclear Society, Inc., LaGrange Park, Illinois.

Cooper, M.F., M.L. Elliott, L.L. Eyler, C.J. Freeman, J.J. Higginson, L.A. Mahoney, and M.R. Powell. 1994. Research-Scale Melter Test Report, PNL-9428, Pacific Northwest Laboratory, Richland, Washington.

Cornell, J.A. 1990. Experiments with Mixtures: Design, Models, and the Analysis of Mixture Data, Second Edition, John Wiley and Sons, New York.

Cox, D.R. 1971. "A Note on Polynomial Response Functions for Mixtures", Biometrika, 58, 155-159.

Danilova, N.P., O.V. Mazurin, and T.S. Tschomskaya. 1971. "The Influence of the Structure of Phase Separated Glasses on Their Chemical Durability", Proceedings International Congress Glass (9th), Volume 9, Part 1, Institute dur Verre, Paris, pp. 825-841.

Day, D.E. 1976. "Mixed Alkali Glasses--Their Properties and Uses", Journal of Non-Crystalline Solids, 21, 343-372.

Deer, W.A., R.A. Howie, and J. Zussman. 1982. Rock-Forming Minerals, Vol. 1A: Orthosilicates, Second Edition, John Wiley and Sons, Inc., New York.

Deer, W.A., R.A. Howie, and J. Zussman. 1986. Rock-Forming Minerals, Vol. 1B: Disilicates and Ring Silicates, Second Edition, John Wiley and Sons, Inc., New York.

Deer, W.A., R.A. Howie, and J. Zussman. 1978. Rock-Forming Minerals, Vol. 2A: Single-Chain Silicates, Second Edition, John Wiley and Sons, Inc., New York.

Dietzel, A. 1942. "The Cation Field Strength and the Relation to Devitrifying Processes, to Compound Formation, and to the Melting Points of Silicates", Zeitschrift Electrochemic, 48, 9-23.

DOE. 1982. Environmental Assessment: Waste-Form Selection for SRP High-Level Waste, Report DOE/EA 0179, U.S. Department of Energy, Washington, D.C.

DOE. 1987. Waste Acceptance Preliminary Specifications for the West Valley Demonstration Project High Level Waste Form, DOE/RW-0136, U.S. Department of Energy, Washington, D.C.

DOE. 1988. Waste Acceptance Preliminary Specifications for the Defense Waste Processing Facility High Level Waste Form Rev. 1, ORG/B-8, Draft for Concurrence, April 1988, U.S. Department of Energy, Washington, D.C.

DOE. 1990. Quality Assurance Requirements Document, DOE/RW-0214, Office of Civilian Radioactive Waste Management, U.S. Department of Energy, Washington, D.C.

DOE. 1993. Waste Acceptance Product Specifications for Vitrified High-Level Waste Forms, February 1993, Office of Environmental Restoration and Waste Management, U.S. Department of Energy, Washington, D.C.

Draper, N.R. and H. Smith. 1981. Applied Regression Analysis, Second Edition, John Wiley and Sons, New York.

Edwards, R.E. 1987. SGM Run 8--Canister and Glass Temperature During Filling and Cooldown. DPST-87-801, Savannah River Laboratory.

Ehrt, D., H. Reiss, and W. Vogel. 1977. "Microstructural Study of CoO-containing Na_2O-B_2O_3-SiO_2 Glasses," Silikattechnik, 28, 359-364.

Feng, X. 1988. Composition Effects on Chemical Durability and Viscosity of Nuclear Waste Glasses--Systematic Studies and Structural Thermodynamics, Ph.D. thesis, Catholic University, Washington, D.C.

Feng, X., I.L. Pegg, Q. Yan, X. Mao, and P.B. Macedo. 1991. "Effects of pH on the Leaching Mechanism of Nuclear Waste Glass," Ceramic Transactions, 23, 95-104.

Feng, X. and I.L. Pegg. 1994. "A Glass Dissolution Model for the Effects of S/V on pH," Ceramic Transactions, Vol. 39, American Ceramic Society, Westerville, OH.

Fuller, W.A. 1987. Measurement Error Models, John Wiley and Sons, New York, NY.

GAO. 1993. NUCLEAR WASTE: Hanford Tank Waste Program Needs Cost, Schedule, and Management Changes, GAO/RCED-93-99, United States General Accounting Office, Washington, D.C.

Goles, R.W. and R.K. Nakaoka. 1990. Hanford Waste Vitrification Program Pilot-Scale Ceramic Melter Test Number 23 Summary Report, PNL-7142, Pacific Northwest Laboratory, Richland, Washington.

Grambow, B. and D.M. Strachan. 1988. "A Comparison of the Performance of Nuclear Waste Glasses by Modelling", Materials Research Society Symposium Proceedings, 112, 713-724.

Graybill, F.A. 1976. Theory and Application of the Linear Model, Duxbury Press, North Scituate, Massachusetts.

Hagy, H.E., W.H. Barney, J.S. McCartney, C.J. Parker, W.A. Plummer, and F.V. Tooley. 1974. "Physical Properties of Glass", Chapter 17 in The Handbook of Glass Manufacture, ed. F.V. Tooley, pp. 933-937, Books For Industry, Inc., New York.

Haller, W., D.H. Blackburn, F.E. Wagstaff, and R.J. Charles. 1970. "Metastable Immiscibility Surface in the System Na_2O-B_2O_3-SiO_2", Journal of the American Ceramic Society, 53, 34-39.

Hrma, P.R., G.F. Piepel, M.J. Schweiger, and D.E. Smith. 1992. "First-Order Model for Durability of Hanford Waste Glasses As a Function of Composition," High Level Radioactive Waste Management, American Nuclear Society, La Grange Park, Illinois, 1236-1243.

Li, H. and M. Tomozawa. 1994. Effect of Water on Properties of the Simulated Nuclear Waste Glasses, final report submitted to Pacific Northwest Laboratory, Rensselaer Polytechnic Institute, Troy, NY.

Jantzen, C.M. 1988. "Prediction of Glass Durability as a Function of Glass Composition and Test Conditions: Thermodynamics and Kinetics", Proceedings of the First International Conference on Advances in the Fusion of Glass, pp. 24.1-24.17, American Ceramic Society, Westerville, OH.

Jantzen, C.M., N.E. Bibler, D.C. Beam, W.G. Ramsay, and B.J. Waters. 1992. Nuclear Waste Glass Product Consistency, Version 5.0, Rev. 2, WSRC-TR-90-539-Rev 2. Westinghouse Savannah River Company, Aiken, South Carolina.

Jantzen, C.M. and D.F. Bickford. 1985. "Leaching of Devitrified Glass Containing Simulated SRP Nuclear Waste", Materials Research Society Symposium Proceedings, 44, 135-146.

Jantzen, C.M. and K.G. Brown. 1993. "Statistical Process Control of Glass Manufactured for the Disposal of Nuclear Waste", American Ceramic Society Bulletin, May 1993, pp. 55-59.

Jantzen, C.M. and M.J. Plodinec. 1984. "Thermodynamic Model of Natural, Medieval, and Nuclear Waste Glass Durability", Journal of Non-Crystalline Solids, 67, 207-223.

Jantzen, C.M., N.E. Bibler, D.C. Beam, C.L. Crawford, and M.A. Pickett. 1993. Characterization of the Defense Waste Processing Facility (DWPF) Environmental Assessment (EA) Glass Standard Reference Material, WSRC-TR-92-346, Rev. 1. Westinghouse Savannah River Company, Aiken, SC.

Johnston, J.W. and J.L. Daniel. 1982. Summary Report for the Interlaboratory Round Robin on the MCC-1 Static Leach Test Method, PNL-4249, Pacific Northwest Laboratory, Richland, Washington.

Johnston, J.W., J.E. Mendel, and J.L. Daniel. 1981. "Estimating Analytical and Procedural Components of Variance from a Round Robin on a Static Leach Test", Proceedings of the 1981 DOE Statistical Symposium, BNL 51535, pp. 85-93, Brookhaven National Laboratory, Upton, Long Island, New York.

Katsura, T. and A. Muan. 1985. Figure from E.M. Levin, C.R. Robbins, and H.F. McMurdie, Phase Diagrams for Ceramists, 1969 Supplement, American Ceramic Society, Columbus, Ohio.

Kawamoto, Y. and M. Tomozawa. 1981. "Prediction of Immiscibility Boundaries of Ternary Silicate Glasses", Physics and Chemistry of Glasses, 22, 11-16.

Kruger, O.L. 1990. Hanford Waste Vitrification Plant Applied Technology Plan, WHC-EP-0350, Westinghouse Hanford Company, Richland, Washington.

Kruger, O.L., R.A. Watrous and G.F. Piepel. 1990. Progress in the Development of Glass Compositions for Vitrification Hanford High Level Transuranic Wastes, WHC-SA-0841, Westinghouse Hanford Company, Richland, Washington.

LaCourse, W.C. and H.J. Stevens. 1977. "Properties of Silica Glasses Containing Small Amounts of B_2O_3", Materials Science Research, 12, 539-548.

Lee, L. 1989. Thermal Analysis of DWPF Canister During Pouring and Cooldown. DPST-89-269, Savannah River Laboratory, Aiken, SC.

Levin, E.M. and S. Block. 1957. "Structural Interpretation of Immiscibility in Oxide Systems: I, Analysis and Calculation of Immiscibility", Journal of the American Ceramic Society, 40, 95-106.

Lutze, W. 1988. "Silicate Glasses." In Radioactive Waste Forms for the Future, W. Lutze and R.C. Ewing, editors, North-Holland, Amsterdam, pp. 27-28.

Malow G., J.A.C. Marples, and C. Sombret. 1980. "Thermal and Radiation Effects on Properties of High Level Waste Products." In Radioactive Waste Management and Disposal, R. Simon and S. Orlowski, editors, Harwood Academic Publishers, Chur, Switzerland, pp. 341-359.

Maurer, C., D.E. Clark, L.L. Hench. 1985. "Solubility Effects on the Corrosion of Nuclear Defense Waste Glasses", Nuclear and Chemical Waste Management, 5, 193-201.

MCC-1 STATIC LEACH TEST METHOD. 1983. Materials Characterization Center, Pacific Northwest Laboratory, Richland, Washington.

Mendel, J.E. and J.L. McElroy. 1972. Waste Solidification Program Volume 10, Evaluation of Solidified Waste Products, BNWL-1666, Pacific Northwest Laboratory, Richland, Washington.

Mendel, J.E., W.A. Ross, F.P. Roberts, Y.B. Katayama, J.H. Westsik, Jr., R.P. Turcotte, J.W. Wald, and D.J. Bradley. 1977. Annual Report on the Characteristics of High-Level Waste Glasses. BNWL-2252, Pacific Northwest Laboratory, Richland, Washington.

Miller, A.J. 1990. Subset Selection in Regression, Chapman and Hall, New York, NY.

Miller, R.G. 1981. Simultaneous Statistical Inference, Second Edition, Springer-Verlag, New York.

Moynihan, C.T. 1993. "Correlation Between the Width of the Glass Transition Region and the Temperature Dependence of the Viscosity of High-T_g Glasses", Journal of the American Ceramic Society, 76, 1081-1087.

Nelson, J.L. 1988. Preliminary Hanford Waste Vitrification Plant Waste Form Qualification Plan - FY 1988 Update, WHC-EP-0045, Westinghouse Hanford Company, Richland, Washington.

Paul, A. 1990. Chemistry of Glasses, Second Edition, Chapman and Hall, London.

Pederson, L.R., D.R. Baer, G.L. McVay, and M.H. Engelhard. 1986. "Reaction of Soda Lime Silicate Glass in Isotopically Labelled Water", Journal of Non-Crystalline Solids, 86, 369-380.

Pelton, A.D. and G. Eriksson. 1988. "A Thermodynamic Database Computing System for Multicomponent Glasses", Advances in the Fusion of Glass, The American Ceramic Society, Westerville, Ohio, pp. 27.1-27.11.

Pelton, A.D., P. Wu, and G. Eriksson. 1992. Development of Models and Software for Liquidus Temperatures of Glasses of HWVP Products, Centre for Research in Computational Thermochemistry, Ecole Polytechnique, Montreal, Quebec, Canada.

Piepel, G.F. 1982. "Measuring Component Effects in Constrained Mixture Experiments", Technometrics, 24, 29-39.

Piepel, G.F. 1988. "Programs for Generating Extreme Vertices and Centroids of Linearly Constrained Experimental Regions", Journal of Quality Technology, 20, 125-139.

Piepel, G.F. 1989. MIXSOFT and MIXSOFT USER'S GUIDE, Version 1.0, MIXSOFT--Mixture Experiment Software, Richland, Washington.

Piepel, G.F. 1992. MIXSOFT and MIXSOFT USER'S GUIDE, Version 2.07, MIXSOFT--Mixture Experiment Software, Richland, Washington.

Piepel, G.F., P.R. Hrma, S.O. Bates, M.J. Schweiger, and D.E. Smith. 1993. First-Order Study of Property/Composition Relationships for Hanford Waste Vitrification Plant Glasses, PNL-8502, Pacific Northwest Laboratory, Richland, Washington.

Piepel, G.F., T.E. Jones, D.L. Eggett, and G.B. Mellinger. 1989. Product Consistency Test Round Robin Conducted by the Materials Characterization Center--Summary Report, PNL-6967, Pacific Northwest Laboratory, Richland, Washington.

Piepel, G.F., G.B. Mellinger, and M.A. Reimus. 1989. "A Statistical Approach for Characterizing Chemical Durability Within A Waste Glass Compositional Region", Waste Management, 9, 3-11.

PNL 1989. Procedures for Quality Assurance Program. PNL-7005, Pacific Northwest Laboratory, Richland, Washington.

PRODUCT CONSISTENCY TEST METHOD FOR DEFENSE WASTE PROCESSING FACILITY (DWPF) GLASS REV. 2.1. 1989. E.I. du Pont de Nemours & Company, Inc., Aiken, South Carolina.

Robertus, R.J., R. Lambert, and P. Hrma. 1993. "Ternary Waste Envelope Assessment Tool", Proceedings of the 1993 Symposium on Waste Management, pp. 1081-1084, Waste Management Symposia, Inc., Tuscon, Arizona.

Rumble, D. III. 1976. Reviews in Mineralogy, Vol. 3: Oxide Minerals, Mineralogical Society of America, Washington D.C.

SAS Institute Inc. 1985a. SAS User's Guide: Statistics, Version 5 Edition. SAS Institute Inc., Cary, NC.

SAS Institute Inc. 1985b. SAS/GRAPH User's Guide, Version 5 Edition. SAS Institute Inc., Cary, NC.

SAS Institute Inc. 1990. SAS/STAT User's Guide, Version 6, Fourth Edition. SAS Institute Inc., Cary, NC.

Sexton, R.A. 1988. Hanford Waste Vitrification Plant Technology Plan, WHC-EP-0139, Westinghouse Hanford Company, Richland, Washington.

Scheffé, H. 1958. "Experiments with Mixtures", Journal of the Royal Statistical Society, B, 20, 344-360.

StatSci. 1991. S-PLUS Reference Manual, Statistical Sciences, Inc., Seattle, Washington.

Strachan, D.M. 1983. "Effect of Gamma Irradiation on Simulated Waste Glass Leaching and on the Leach Vessel", Journal of the American Ceramic Society, 66, C158-C160.

Strachan, D.M., R.P. Turcotte, and B.O. Barnes. 1982. "MCC-1: A Standard Leach Test for Nuclear Waste Forms", Nuclear Technology, 56, 306-312.

Strand, Z. and P. Strand. 1978. "Calculation of Metastable Two-Liquid Tie Lines in Ternary Glass-Forming Systems", Journal of the American Ceramic Society, 61, 283-286.

Taylor, P. 1990. A Review of Phase Separation in Borosilicate Glasses, with Reference to Nuclear Fuel Waste Immobilization, AECL-10173, Whiteshell Nuclear Research Establishment, Pinawa, Manitoba, Canada.

Taylor, P. and D.G. Owen. 1981. "Liquid Immiscibility in the System Na_2O-ZnO-B_2O_3-SiO_2", Journal of the American Ceramic Society, 64, 360-367.

Taylor, P., A.B. Campbell, and D.G. Owen. 1983. "Liquid Immiscibility in the Systems X_2O-MO-B_2O_3-SiO_2 (X = Na, K; M = Mg, Ca, Ba) and Na_2O-MgO-BaO-B_2O_3-SiO_2", Journal of the American Ceramic Society, 66, 347-351.

Taylor, P., S.D. Ashmore, and A.B. Campbell. 1984. "Liquid Immiscibility in the Systems Na_2O-Yb_2O_3-B_2O_3-SiO_2 and K_2O-Yb_2O_3-B_2O_3-SiO_2", Journal of the American Ceramic Society, 67, C-186.

Taylor, P., S.D. Ashmore, and D.G. Owen. 1987. "Chemical Durability of Some Sodium Borosilicate Glasses Improved by Phase Separation", Journal of the American Ceramic Society, 70, 333-338.

Tomozawa, M. 1979. "Phase Separation in Glass", Treatise on Materials Science and Technology, Vol. 17; Glass II, M. Tomozawa and R.H. Doremus, editors, Academic Press, New York.

Tomozawa, M., G.M. Singer, Y. Oka, and J.T. Warden. 1979. "Phase Separation in Nuclear Waste Glasses", Ceramics in Nuclear Waste Management, Proceedings of Symposium in Cincinnati, OH, April/May. Edited by T.D. Chikalla and J.E. Mendel, U.S. Department of Energy, Technical Information Center, pp. 193-197.

Tooley, F.V. 1974. The Handbook of Glass Manufacture, Vol. 1, Books for Industry, New York, NY.

Truesdell, C. 1969. Rational Thermodynamics. McGraw-Hill, New York.

Vogel, W. 1971. Structure and Crystallization of Glasses, Pergammon Press, Oxford.

Warren, B.E. and A.G Pincus. 1940. "Atomic Considerations of Immiscibility in Glass Systems", Journal of the American Ceramic Society, 23, 301-304.

Welch, W.J. 1987. ACED, Algorithms for the Construction of Experimental Designs, User's Guide Version 1.6.1, University of Waterloo, Waterloo, Ontario, Canada.

WSRC 1993. Defense Waste Processing Facility Waste Form Qualification Report, Volume 5: Technical Bases for the DWPF Glass Product Control Program, WSRC-IM-91-116-5, Westinghouse Savannah River Company, Aiken, SC.

APPENDIX A

CVS GLASS COMPOSITIONS AND UNCERTAINTIES

APPENDIX A

CVS GLASS COMPOSITIONS AND UNCERTAINTIES

During CVS-I and CVS-II Phases 1 and 2, samples of all glasses were submitted for chemical analysis by ICP to serve as a check for the as-batched compositions. The analyzed and as-batched compositions are listed in Table A.1 for CVS-I glasses and Table A.2 for CVS-II Phase 1 and Phase 2 glasses. Only selected CVS-II Phase 3 glasses were submitted for chemical analysis by ICP, the results of which are given in Table A.3. Only selected CVS-II Phase 3 glasses were analyzed because results from previous phases led to the decision to use as-batched glass compositions for modeling and data analyses. The results and reasons for the decision to use as-batched compositions are discussed in Sections A.1, A.2, and A.3.

The as-batched compositions were obtained by starting with the 10 component compositions listed in Table 4.15 and expanding the Others component into its constituents according to the Others mix used. The Others mix in Table 4.1 was used for all glasses except: (1) CVS2-19, CVS2-51, CVS2-97, and CVS2-123 whose Others composition is given in Table 4.8, (2) CVS2-55, CVS2-56, and CVS2-57, whose Others compositions are given in Table 4.10, (3) CVS2-53 and CVS2-54, whose Others compositions are the same as in Table 4.1 (except Nd_2O_3 was replaced by UO_2), and (4) CVS2-64 to CVS2-70, CVS2-95, CVS2-99, CVS2-100, and CVS2-101, whose Others compositions are given in Table 4.13.

In most cases, the analyzed component values are the averages of two ICP results from K/Ni and Na/Zr fusions, although in some cases only one of these two results was available or used. Specifically: (1) only the Na/Zr fusion results were used for SiO_2 for CVS-II Phases 1 and 2, and (2) only the K/Ni fusion results were used for CaO, CeO_2, and LiO_2 on glasses CVS2-20 to CVS2-51 because of a contamination problem with the peroxide fusion reagent. These two statements do not apply to CVS-II Phase 2 glasses CVS2-52 to CVS2-58, which were analyzed at a later time than the other Phase 2 glasses.

In Tables A.1, A.2, and A.3, as-batched composition values were inserted in place of analyzed values when minor components batched into the glass were not detected analytically. This procedure enabled checking how close the sums of the analyzed values plus the assumed as-batched values were to 1.0 (i.e., 100 wt%). Values significantly below or above 1.0 indicate problems with the analyzed compositions.

Observational and statistical comparisons of the as-batched and analyzed glass compositions are contained in Sections A.1 and A.2, respectively. Section A.3 discusses the options considered for representing compositions of CVS glasses. Section A.4 discusses the uncertainties in analyzed glass compositions based on replicate glasses and analyses. The redox state was determined for several CVS glasses, and the results are presented and discussed in Section A.5. Section A.6 contains some conclusions and recommendations regarding glass composition.

A.1 OBSERVATIONS ON AS-BATCHED VERSUS ANALYZED COMPOSITIONS

The following observations were made based on visual comparison of the as-batched and analyzed compositions of CVS-I glasses given in Table A.1, CVS-II Phase 1 and Phase 2 glasses given in Table A.2, and CVS-II Phase 3 glasses given in Table A.3:

1) Although CVS glasses did not nominally contain K_2O, it was detected in CVS-I and CVS-II Phase 1 and 2 glasses. It was not detected in the selected CVS-II Phase 3 glasses analyzed.

2) Although CVS glasses did not nominally contain TiO_2 (except for CVS2-101), it was detected in CVS-I as well as CVS-II Phase 1, 2, and 3 glasses.

3) In all or most CVS phases, Al_2O_3, CaO, MgO, and ZrO_2 were detected in glasses that nominally had zero levels of these components.

4) SiO_2 analyzed values were lower than as-batched values for 22 of the 23 CVS-I glasses, for all 39 CVS-II Phase 2 glasses, and for all 11 of the CVS-II Phase 3 glasses analyzed. The analytical shortfalls were

typically no more than 3-4 wt% for most glasses, but they were as high as 5-8 wt% for a few CVS-II Phase 2 and 3 glasses.

5) For CVS-II Phase 1, SiO_2 analyzed values were higher than as-batched values for 11 of the 19 glasses.

6) Na_2O analyzed values were lower than as-batched values for 15 of 19 CVS-II Phase 1 glasses. Na_2O analyzed values were higher than as-batched values for all 32 of the CVS-II Phase 2 glasses CVS2-20 to CVS2-51, with differences as large as 6 wt%. No consistent Na_2O bias was found for the five glasses CVS2-52 and CVS2-55 through CVS2-58, which were analyzed at a later time than the other CVS-II Phase 2 glasses. Of the 11 CVS-II Phase 3 glasses analyzed, 10 had analyzed Na_2O values less than the as-batched values, but the differences were not large.

7) Co_2O_3, Dy_2O_3, Eu_2O_3, Gd_2O_3, PbO, and V_2O_3 were analyzed as occurring at above analytical detection limit amounts in some CVS2-52 to CVS2-58 glasses which nominally did not contain them. Co_2O_3 was analyzed as occurring in some of the CVS-II Phase 3 glasses, which nominally did not contain it. These oxides had not been previously detected above detection limits for CVS-I or CVS-II Phase 1 and 2 glasses.

8) Glasses CVS1-7, 8, 14, 18, and 22 (a replicate of CVS1-8) had analyzed values of ZrO_2 noticeably lower than the corresponding as-batched values. Most of these differences were around 1 wt%, but the difference was over 3 wt% for CVS1-18.

9) The sums of analyzed component mass fractions, plus as-batched values for components that were not detected analytically, were less than 1.0 for most of the CVS glasses analyzed. The following chart shows the numbers of glasses with sums less than 1.0 for each phase, as well as

the smallest and largest sums.

Phase	Number with Sum < 1.0	Smallest Sum	Largest Sum
CVS-I	18 of 23	0.9544	1.0122
CVS-II Phase 1	12 of 19	0.9465	1.0390
CVS-II Phase 2	24 of 39*	0.8978	1.0530
CVS-II Phase 3	11 of 11**	0.8986	0.9661

* If the analyzed Na_2O values for CVS2-20 to CVS2-51 had not been notably higher than as-batched values, all 32 of those 32 sums would have been less than 1.0. For CVS2-52 to CVS2-58, five of the seven sums were less than 1.0.

** Only 11 of the 43 CVS-II Phase 3 glasses were analyzed.

The above chart shows a wider range of sums for CVS-II Phases 2 and 3 than for CVS-I and CVS-II Phase 1. This could be due to a consolidation of analytical laboratories that occurred after CVS-II Phase 1. Prior to CVS-II Phase 1, a small lab with highly experienced people performed the chemical analyses. After CVS-II Phase 1, the consolidated lab with people less experienced in solids analysis was used.

The problem of detecting components nominally not in the glass (items 1, 2, and 3 in the preceding list) could be due to inappropriate definition of detection limits or to biases in the analytical process. It could also be due to impurities of these elements in chemicals used to batch glasses or to inclusion of these elements by laboratory contamination.

Underanalysis of SiO_2 (item 4) is a recurring problem for analytical laboratories that use fusion processes to dissolve glass. The fusion process can leave undissolved SiO_2, which results in underanalysis of SiO_2. However, this problem did not occur in CVS-II Phase 1 (item 5), which could be due to the fact that CVS-II Phase 1 explored an interior portion of the CVS experimental region involving less extreme compositions.

The significant overanalyses of Na_2O for CVS-II Phase 2 glasses (item 6) is bothersome because of the magnitudes of the differences. Batch chemicals and batching records were checked, and it was determined that batching was not the cause of problems of this magnitude. It is also unlikely that laboratory

contamination was the cause of the problem. Hence, the differences were apparently due to analytical errors or biases of some type.

The reason for finding several minor elements above analytical detections limits in CVS-II Phase 3 even though the glasses did not nominally contain them (item 7) is unknown. As in items 1, 2, and 3, it could be due to inappropriate definition of detection limits or biases in the analytical process, or to trace contaminations of these elements in chemicals used to batch glasses.

The underanalysis of ZrO_2 in some CVS-I glasses (item 8) may be related to the presence of undissolved ZrO_2 or Zr-containing crystals that segregated from the bulk of the melt. Undissolved ZrO_2 or Zr-containing crystals can be difficult to dissolve in the fusion process, thus yielding underanalysis of ZrO_2 concentrations.

The final observation (item 9) concerning sums of component mass fractions typically being less than one is at least partially due to the underanalysis of SiO_2 and selected other elements. The potential remedy to this problem (of normalizing to a sum of one by dividing the analyzed values by the actual sum) is not the proper solution when the sum is significantly below (or above) one. Bias-correction and then normalization was considered, and is discussed in Section A.3. Recommendations for the future are made in Section A.6.

A.2 STATISTICAL COMPARISONS OF AS-BATCHED VERSUS ANALYZED COMPOSITIONS

Tables A.4, A.5, A.6, and A.7 list the results of statistical comparisons of as-batched and analyzed compositions for CVS-I, CVS-II Phase 1, CVS-II Phase 2, and CVS-II Phase 3, respectively. The results in Table A.6 for CVS-II Phase 2 are only for glasses CVS2-20 to CVS2-51, since the results for glasses CVS2-52 to CVS2-58 were different. These latter seven glasses were fabricated and analyzed at later times than the other CVS-II Phase 2 glasses, thus providing a likely reason for the difference in results. The results in Table A.7 are based on analyzed versus as-batched comparisons for 11 CVS-II Phase 3 glasses, since not all of the CVS-II Phase 3 glasses were chemically analyzed.

The statistical comparisons consisted of forming the "analyzed minus as-batched" differences for each glass oxide component, and then for each oxide component, comparing the mean difference across all glasses in the CVS phase to the standard error of the differences. The statistical procedure known as a paired-t test was used to determine if the differences were statistically significant. Differences for a number of components in each phase were statistically significant (based on a two-sided[a] t-test at the 95% confidence level), although several of these may be due to round-off errors or be too small to be of practical consequence. Specific discussions of the statistically significant differences follow.

The results in Tables A.4, A.5, A.6, and A.7 were condensed into Table A.8 to make it easier to compare results across the phases. Focusing on mean differences larger than 0.0010 mass fraction (0.10 wt%) that are statistically significant, the main findings are:

<u>CVS-I</u>

LiO_2, Nd_2O_3, and SiO_2 have analyzed values that tend to be lower than as-batched values. K_2O analyzed values tend to be higher than as-batched values (which are nominally zero for CVS-I glasses).

<u>CVS-II Phase 1</u>

Fe_2O_3, Li_2O, Na_2O, Nd_2O_3, and ZrO_2 analyzed values tend to be lower than as-batched values. K_2O analyzed values tend to be higher than as-batched values (which are nominally zero for CVS-II Phase 1 glasses).

<u>CVS-II Phase 2</u>

Al_2O_3, B_2O_3, Fe_2O_3, LiO_2, MgO, SiO_2, and ZrO_2 analyzed values tend to be lower than as-batched values. CeO_2 and Na_2O analyzed values tend to be higher than as-batched values.

(a) Two-sided refers to the fact that both positive and negative differences are to be detected.

CVS-II Phase 3

Al_2O_3, B_2O_3, Fe_2O_3, LiO_2, MgO, Na_2O, Nd_2O_3, and SiO_2 analyzed values tend to be lower than as-batched values for the selected glasses analyzed. There were no components with analyzed values statistically larger on average compared to as-batched values.

It is clear from the above summary and Tables A.4 through A.8 that analyzed values tend to be less than as-batched values much more than they tend to be greater than as-batched values. Further, differences exist in several or all CVS phases for some components. These differences could be real composition differences (e.g., due to volatilization, batching errors, or trace contaminants in batching materials) or they could be due to analytical biases. While some of the differences could be real, at least some of the differences (especially the larger ones) appear to be due to analytical biases. Unfortunately, during CVS insufficient analyses of representative standard glasses with certified compositions were made to be able to statistically detect or correct for (potential) biases in analyzed values. The ideal protocol would have been to analyze several standard glasses (with compositions representative of several parts of the CVS experimental region) in between every few analyses of CVS glasses. Such an approach was considered for use early in CVS, but for several reasons (e.g., considerable extra cost, lack of adequate representative and certified standard glasses) it was not implemented.

A.3 OPTIONS CONSIDERED FOR REPRESENTING CVS GLASS COMPOSITIONS

Three general options were considered for representing CVS glass compositions: as-analyzed, as-analyzed with "adjustments", and as-batched. The as-analyzed (without adjustments) option was rejected for several reasons:

- It was likely that at least some of the differences between as-batched and as-analyzed compositions discussed in Sections A.1 and A.2 are due to analytical biases (e.g., underanalysis of SiO_2).

- CVS glasses have many minor components at low levels, and some of them were not detected analytically.
- Some components not nominally included in CVS glasses were detected analytically, in some cases at amounts higher than could have occurred due to impurities in batch chemicals.
- The sum of as-analyzed mass fractions of the oxide components differed quite a bit from 1.0 for many glasses.

The option of starting with as-analyzed compositions and making appropriate adjustments was also considered. There are many combinations of adjustments that could be made, and they cannot all be discussed here. Several adjustments that were considered are described below.

1) Assume as-batched levels of minor components are contained in glasses when not detected analytically.
2) Set to zero or reduce the analyzed values of components not nominally in the glass, with the action depending on an assessment of whether the analyzed value could have resulted from impurities in chemicals or from laboratory contamination.
3) Compare analyzed values of representative standard glasses obtained with each CVS phase to certified compositions of the glasses to determine if they differ statistically. If statistically significant differences exist, assume the same differences apply to all glasses in that CVS phase and "bias-correct" the analyzed values accordingly.
4) Divide the as-analyzed composition for each glass by the sum of the analyzed oxide mass fractions (so the adjusted sum would be 1.0).

Option 4) alone was rejected as inappropriate because the oxide mass fraction sums varied quite a bit from 1.0 for many CVS glasses, and the adjustment would then bias the values for correctly-analyzed components. Performing one or both of adjustments 1) or 2) followed by 4) was considered to be a step in the right direction, but the adjusted sums still differed too much from 1.0

for many glasses. Performing all four options was conceptually judged the most reasonable approach, except for issues associated with 3). Ideally, there would have been several standard glasses with different compositions representative of different portions of the large CVS composition experimental region. Further, these standard glasses would ideally have been analyzed in between every few CVS glass samples. It was decided the benefits from following such a rigorous protocol was not worth the time and expense involved, especially since ideal standard glasses did not exist. Instead, calibration standards were analyzed in each CVS phase, the internal standard glass was analyzed in each phase of CVS-II, and one or two standard glasses were analyzed once during later CVS phases. However, this was judged not to be a sufficient basis for performing bias detection and correction.

Ultimately, it was decided to use as-batched compositions in developing glass property models and in other data analyses. No detailed error analysis of the batching process was performed to assess the uncertainties in as-batched compositions. However, all but one of the seven replicate sets of glasses studied in CVS (see Appendix F) included refabricating (i.e., batching and melting) variations as well as variations from retesting/remeasuring of glass properties. The additional variation from refabricating glasses was not noticeable in glass property standard deviations (see Appendix F) compared to the replicate set of the internal standard glass (which was only fabricated once). This indicates that the batching and melting process is fairly stable over time and typical variations do not have major impacts on glass property values.

In summary, although as-batched compositions of CVS glasses are subject to error just as any other representation of glass composition would be, they were judged to be a reasonable basis for developing glass property models and performing other data analyses.

A.4 UNCERTAINTIES IN ANALYZED COMPOSITIONS

Table A.9 gives the as-batched and analyzed compositions for six replicate analyses of glass CVS1-19 conducted over three months. Glass CVS1-19 is a replicate of glass CVS1-1, the center point of the CVS-I composition region. The main observations from Table A.9 are:

- K_2O and TiO_2 were detected for some analyses, although these components are not nominally in CVS1-19.
- SiO_2 was approximately 1.0 wt% low for four of the six analyses.

These results indicate that if indeed the differences seen over the set of 23 CVS glasses are due to biases in the analytical process, then they continued over a three-month period.

Table A.10 gives the means, standard deviations (SD), and percent relative standard deviations (%RSD) of the oxide components based on the six replicate analyses of CVS1-19. The SDs and %RSDs give an indication of the long-term within-lab variation (precision) in analyses that might be expected. The %RSDs tend to be under 5% for components present at more than very minor concentrations, which agrees with results from similar investigations in the past. However, based on the results in Sections A.1 and A.2, analytical bias may be a more important issue than imprecision.

Table A.11 contains the results of three analyses of the CVS internal standard glass tested in CVS-II Phase 1 (CVS2-19), Phase 2 (CVS2-51), and Phase 3 (CVS2-97). Table A.11 also contains the means, SDs, and %RSDs based on the three analyses of the internal standard glass. The %RSDs tend to be under 7% for components present at more than very minor concentrations, which agrees with results in Table A.10 and from similar investigations in the past.

A.5 REDOX STATE OF SELECTED CVS GLASSES

Test glasses contain oxides of several multivalent elements, such as Ce, Cr, Cu, Fe, Mn, Mo, Ni, Pd, Rh, and Ru. Out of these elements only Fe is a major component and thus is an independently-varied composition variable. The rest of the multivalent elements are present at constant proportions in the Others component for most CVS glasses (the ones with Others mix given in Table

4.1). The redox state of multivalent oxides changes with temperature due to mutual reactions and interaction with atmospheric air. The redox state of glass affects crystallinity and, hence, may affect durability.

Several glasses were selected to determine their Fe^{2+}/Fe ratios analytically. Sample analysis was performed using procedure PNL 597 7-40.21 Rev. 1. The results are shown in Table A.12. As this table shows, the Fe^{2+}/Fe ratio in quenched glasses is between 0.016 and 0.040, which is as expected.

A.6 CONCLUSIONS AND RECOMMENDATIONS

The following conclusions and recommendations are made:

- As-batched glass compositions should be (and were) used in developing glass property models and other analyses. They are believed to be closer representations of actual composition than analyzed compositions.
- Because a HLW vitrification plant will have to rely on analyzed feed and glass compositions, it is necessary that appropriate procedures (step-by-step instructions) be developed for laboratory practices and data adjustment techniques. Some aspects of this are recommended below.

  1. Appropriately maintain and analyze laboratory standards, and monitor via statistical control charts so as to detect drifts, calibration problems, or other out-of-control situations in analytical procedures or instruments.

  2. Develop a large quantity of at least two compositionally representative feed and/or glass materials and obtain certified analyses of them. Then, samples of these representative, certified materials (RCM) should be analyzed in between every few actual samples. The RCM results should also be control charted, and statistically compared to the certified values. If statistically significant differences (biases) are found to exist between the analyses of the RCM and its certified values, then the sample results should be bias-corrected.

3. Normalization of compositional analyses to a total mass fraction of 1.0 will be a requirement for the CVS glass property models, otherwise a bias may be introduced into model predictions. An appropriate normalization procedure will need to be developed to take into account the minor glass/feed components that are not detected analytically. The procedure should only be applied to analyzed (or bias-corrected analyzed) compositions that sum within some specified tolerance of 100 wt%. A normalization procedure that accounts for the variances and covariances among analyzed values of glass/feed components is recommended.

TABLE A.1. As-Batched (B) and Analyzed (A) Compositions (in mass fractions) for CVS-I Glasses

Oxide	CVS1-1		CVS1-2		CVS1-3		CVS1-4		CVS1-5	
	B	A	B	A	B	A	B	A	B	A
Al_2O_3	.0636	.0642	.1500	.1500	.1400	.1380	.0000	.0000[a]	.0800	.0803
B_2O_3	.1142	.1160	.0500	.0511	.2000	.2010	.2000	.2000	.0500	.0517
BaO	.0007	.00073	.0002	.00019[b]	.0002	.00018	.0002	.00018	.0002	.00019
CaO	.0275	.0277	.1000	.1020	.0000	.00043	.0200	.0204	.0000	.00104
CdO	.0055	.00554	.0013	.00138	.0013	.00136	.0013	.00140	.0013	.00134
CeO_2	.0011	.0012	.0003	.0003[a]	.0003	.0007	.0003	.0003[a]	.0003	.0003[a]
Cr_2O_3	.0009	.0010	.0002	.0002[a]	.0002	.0003	.0002	.0003	.0002	.0000[a]
Cs_2O	.0011	.0010	.0003	.00025	.0003	.00022	.0003	.00026	.0003	.00024
CuO	.0011	.00111	.0003	.00028	.0003	.00029	.0003	.00031	.0003	.00030
F	.0022	.0022[a]	.0005	.0005[a]	.0005	.0005[a]	.0005	.0005[a]	.0005	.0005[a]
Fe_2O_3	.0568	.0566	.0200	.0203	.0200	.0202	.0200	.0210	.1500	.1490
K_2O	.0000	.0080	.0000	.0040	.0000	.0090	.0000	.0050	.0000	.0090
La_2O_3	.0046	.00441	.0011	.00119	.0011	.00116	.0011	.00116	.0011	.00109
Li_2O	.0376	.0340	.0700	.0615	.0700	.0601	.0100	.00860	.0700	.0620
MgO	.0363	.0359	.0000	.0000[a]	.0800	.0776	.0800	.0791	.0000	.0000[a]
MnO_2	.0011	.00117	.0003	.00032	.0003	.00033	.0003	.00038	.0003	.00037
MoO_3	.0022	.00220	.0005	.00051	.0005	.00054	.0005	.00055	.0005	.00056
Na_2O	.1003	.0891	.0500	.0504	.0500	.0511	.0900	.0893	.0700	.0641
Nd_2O_3	.0090	.00832	.0022	.00207	.0022	.00215	.0022	.00205	.0022	.00205
NiO	.0042	.00443	.0010	.00128	.0010	.00141	.0010	.00136	.0010	.00135
P_2O_5	.0007	.0007[a]	.0002	.0002[a]	.0002	.0002[a]	.0002	.0002[a]	.0002	.0002[a]
PdO	.0004	.0004[a]	.0001	.0001[a]	.0001	.0001[a]	.0001	.0001[a]	.0001	.0001[a]
Pr_6O_{11}	.0007	.0007[a]	.0002	.0002[a]	.0002	.0002[a]	.0002	.0002[a]	.0002	.0002[a]
Rb_2O	.0004	.0004[a]	.0001	.0001[a]	.0001	.0001[a]	.0001	.0001[a]	.0001	.0001[a]
Rh_2O_3	.0004	.0004[a]	.0001	.0001[a]	.0001	.0001[a]	.0001	.0001[a]	.0001	.0001[a]
RuO_2	.0011	.0011[a]	.0003	.0003[a]	.0003	.0003[a]	.0003	.0003[a]	.0003	.0003[a]
SO_3	.0020	.0020[a]	.0005	.0005[a]	.0005	.0005[a]	.0005	.0005[a]	.0005	.0005[a]
SiO_2	.4801	.4770	.5500	.5200	.4200	.4110	.5700	.5460	.5700	.5630
Sm_2O_3	.0004	.0004[a]	.0001	.0001[a]	.0001	.0001[a]	.0001	.0001[a]	.0001	.0001[a]
SrO	.0007	.00076	.0002	.00024	.0002	.00019	.0002	.00020	.0002	.00021
TiO_2	.0000	.00016	.0000	.0000[a]	.0000	.00012	.0000	.0000[a]	.0000	.00012
Y_2O_3	.0004	.00037	.0001	.00010	.0001	.00010	.0001	.00011	.0001	.00010
ZrO_2	.0429	.0418	.0000	.00896	.0100	.00896	.0000	.00049	.0000	.00020
Sum	1.000	0.9910	1.000	0.9787	1.000	0.9885	1.000	0.9806	1.000	0.9907

(a) Below analytical detection limit or not analyzed; as-batched value assumed.

(b) Value from ICP with K/Ni fusion--the value for Na/Zr fusion (.00082) was too high.

TABLE A.1. As-Batched (B) and Analyzed (A) Compositions (in mass fractions) for CVS-I Glasses (continued)

Oxide	CVS1-6		CVS1-7		CVS1-8		CVS1-9		CVS1-10	
	B	A	B	A	B	A	B	A	B	A
Al_2O_3	.0000	.00087	.0000	.00096	.0000	.00090	.0000	.0000[a]	.1200	.1210
B_2O_3	.2000	.1920	.0500	.0507	.0500	.0527	.1962	.2020	.0851	.0848
BaO	.0018	.00164	.0002	.00019	.0002	.00019	.0018	.00176	.0018	.00175
CaO	.0000	.00117	.1000	.1000	.0000	.00027	.0000	.00037	.0000	.00047
CdO	.0134	.0130	.0013	.00139	.0013	.00143	.0134	.0141	.0134	.0118
CeO_2	.0027	.0027	.0003	.0003[a]	.0003	.0003[a]	.0027	.0030	.0027	.0030
Cr_2O_3	.0022	.0022	.0002	.0002[a]	.0002	.0003	.0022	.0022	.0022	.0024
Cs_2O	.0027	.0025	.0003	.00026	.0003	.00028	.0027	.0025	.0027	.0024
CuO	.0027	.00254	.0003	.00029	.0003	.00033	.0027	.00268	.0027	.00268
F	.0054	.0054[a]	.0005	.0005[a]	.0005	.0005[a]	.0054	.0054[a]	0054	.0054[a]
Fe_2O_3	.0200	.0190	.0336	.0334	.1500	.1520	.1400	.1400	.0200	.0206
K_2O	.0000	.0070	.0000	.0070	.0000	.0060	.0000	.0000	.0000	.0050
La_2O_3	.0112	.0100	.0011	.00123	.0011	.00114	.0112	.0111	.0112	.0112
Li_2O	.0700	.0616	.0100	.00871	.0100	.00921	.0100	.00909	.0100	.00873
MgO	.0000	.0000[a]	.0000	.0000[a]	.0800	.0807	.0800	.0816	.0000	.0000[a]
MnO_2	.0027	.00271	.0003	.00031	.0003	.00037	.0027	.00289	.0027	.00281
MoO_3	.0054	.00504	.0005	.00053	.0005	.00061	.0054	.00547	.0054	.00514
Na_2O	.0500	.0537	.0964	.0946	.0837	.0780	.0538	.0562	.0949	.0924
Nd_2O_3	.0221	.0188	.0022	.00212	.0022	.00212	.0221	.0201	.0221	.0201
NiO	.0103	.00942	.0010	.00136	.0010	.00151	.0103	.0106	.0103	.0105
P_2O_5	.0018	.0018[a]	.0002	.0002[a]	.0002	.0002[a]	.0018	.0018[a]	.0018	.0018[a]
PdO	.0009	.0009[a]	.0001	.0001[a]	.0001	.0001[a]	.0009	.0009[a]	.0009	.0009[a]
Pr_6O_{11}	.0018	.0018[a]	.0002	.0002[a]	.0002	.0002[a]	.0018	.0018[a]	.0018	.0018[a]
Rb_2O	.0009	.0009[a]	.0001	.0001[a]	.0001	.0001[a]	.0009	.0009[a]	.0009	.0009[a]
Rh_2O_3	.0009	.0009[a]	.0001	.0001[a]	.0001	.0001[a]	.0009	.0009[a]	.0009	.0009[a]
RuO_2	.0027	.0025	.0003	.0003[a]	.0003	.0003[a]	.0027	.0024	.0027	.0020
SO_3	.0049	.0049[a]	.0005	.0005[a]	.0005	.0005[a]	.0049	.0049[a]	.0049	.0049[a]
SiO_2	.4400	.4150	.5700	.5550	.5363	.5450	.4200	.4140	.5700	.5650
Sm_2O_3	.0009	.0009[a]	.0001	.0001[a]	.0001	.0001[a]	.0009	.0009[a]	.0009	.0009[a]
SrO	.0018	.00168	.0002	.00024	.0002	.00022	.0018	.00180	.0018	.00179
TiO_2	.0000	.00031	.0000	.00032	.0000	.00022	.0000	.0000[a]	.0000	.00013
Y_2O_3	.0009	.00087	.0001	.00012	.0001	.00011	.0009	.00097	.0009	.00100
ZrO_2	.1200	.1160	.1300	.1220	.0800	.0696	.0000	.00020	.0000	.00017
Sum	1.000	0.9598	1.000	0.9833	1.000	1.0056	1.000	1.0025	1.000	0.9944

(a) Below analytical detection limit or not analyzed; as-batched value assumed.

TABLE A.1. As-Batched (B) and Analyzed (A) Compositions (in mass fractions) for CVS-I Glasses (continued)

Oxide	CVS1-11		CVS1-12		CVS1-13		CVS1-14		CVS1-15	
	B	A	B	A	B	A	B	A	B	A
Al_2O_3	.1400	.1450	.0000	.0000[a]	.0038	.00432	.0238	.0240	.0000	.0000[a]
B_2O_3	.1549	.1600	.1764	.1810	.2000	.2030	.2000	.1960	.0500	.0507
BaO	.0014	.00143	.0002	.00021	.0002	.00018	.0002	.00017	.0018	.00169
CaO	.1000	.1030	.1000	.1020	.0000	.00029	.0000	.00015	.0000	.00047
CdO	.0107	.0110	.0013	.00142	.0013	.00137	.0013	.00132	.0134	.0136
CeO_2	.0022	.0023	.0003	.0003[a]	.0003	.0003[a]	.0003	.0003[a]	.0027	.0033
Cr_2O_3	.0018	.0019	.0002	.0003	.0002	.0002[a]	.0002	.0002[a]	.0022	.0023
Cs_2O	.0022	.0020	.0003	.00023	.0003	.00026	.0003	.00024	.0027	.0026
CuO	.0022	.00229	.0003	.00033	.0003	.00030	.0003	.00029	.0027	.00252
F	.0043	.0043[a]	.0005	.0005[a]	.0005	.0005[a]	.0005	.0005[a]	.0054	.0054[a]
Fe_2O_3	.0200	.0206	.1500	.1490	.0200	.0205	.0200	.0194	.0200	.0201
K_2O	.0000	.0000[a]	.0000	.0000[a]	.0000	.0000[a]	.0000	.0060	.0000	.0100
La_2O_3	.0090	.00896	.0011	.00119	.0011	.00113	.0011	.00109	.0112	.0105
Li_2O	.0100	.00982	.0700	.0703	.0100	.00856	.0100	.00925	.0700	.0568
MgO	.0000	.0000[a]	.0000	.0000[a]	.0000	.0000[a]	.0000	.0000[a]	.0800	.0760
MnO_2	.0022	.00233	.0003	.00037	.0003	.00033	.0003	.00031	.0027	.00282
MoO_3	.0043	.00434	.0005	.00051	.0005	.00056	.0005	.00052	.0054	.00527
Na_2O	.0751	.0730	.0736	.0761	.1862	.1740	.1862	.1850	.1211	.1120
Nd_2O_3	.0177	.0163	.0022	.00204	.0022	.00197	.0022	.00202	.0221	.0131
NiO	.0082	.00843	.0010	.00144	.0010	.00133	.0010	.00125	.0103	.0101
P_2O_5	.0014	.0014[a]	.0002	.0002[a]	.0002	.0002[a]	.0002	.0002[a]	.0018	.0018[a]
PdO	.0007	.0007[a]	.0001	.0001[a]	.0001	.0001[a]	.0001	.0001[a]	.0009	.0009[a]
Pr_6O_{11}	.0014	.0014[a]	.0002	.0002[a]	.0002	.0002[a]	.0002	.0002[a]	.0018	.0018[a]
Rb_2O	.0007	.0007[a]	.0001	.0001[a]	.0001	.0001[a]	.0001	.0001[a]	.0009	.0009[a]
Rh_2O_3	.0007	.0007[a]	.0001	.0001[a]	.0001	.0001[a]	.0001	.0001[a]	.0009	.0009[a]
RuO_2	.0022	.0021	.0003	.0003[a]	.0003	.0003[a]	.0003	.0003[a]	.0027	.0021
SO_3	.0039	.0039[a]	.0005	.0005[a]	.0005	.0005[a]	.0005	.0005[a]	.0049	.0049[a]
SiO_2	.4200	.4180	.4200	.4170	.5700	.5510	.4200	.4040	.5589	.5380
Sm_2O_3	.0007	.0007[a]	.0001	.0001[a]	.0001	.0001[a]	.0001	.0001[a]	.0009	.0009[a]
SrO	.0014	.00150	.0002	.00025	.0002	.00021	.0002	.00018	.0018	.00170
TiO_2	.0000	.0000[a]	.0000	.0000[a]	.0000	.0000[a]	.0000	.00025	.0000	.00012
Y_2O_3	.0007	.00077	.0001	.00014	.0001	.00010	.0001	.00010	.0009	.00091
ZrO_2	.0000	.00020	.0000	.00013	.0000	.00058	.1300	.1230	.0000	.00022
Sum	1.000	1.0091	1.000	1.0064	1.000	0.9726	1.000	0.9771	1.000	0.9544

(a) Below analytical detection limit or not analyzed; as-batched value assumed.

TABLE A.1. As-Batched (B) and Analyzed (A) Compositions (in mass fractions) for CVS-I Glasses (continued)

Oxide	CVS1-16		CVS1-17		CVS1-18		CVS1-19		CVS1-20	
	B	A	B	A	B	A	B	A (b)	B	A
Al_2O_3	.1442	.1430	.0000	.0000[a]	.0000	.00089	.0636	.0636	.0636	.0637
B_2O_3	.0500	.0509	.0500	.0513	.0500	.0516	.1142	.1150	.1142	.1160
BaO	.0002	.00017	.0018	.00172	.0016	.00156	.0007	.00071	.0007	.00071
CaO	.0000	.00044	.1000	.0995	.0200	.0220	.0275	.0289	.0275	.0270
CdO	.0013	.00141	.0134	.0136	.0121	.0126	.0055	.00565	.0055	.00550
CeO_2	.0003	.0003[a]	.0027	.0029	.0024	.0026	.0011	.0014	.0011	.0012
Cr_2O_3	.0002	.0002[a]	.0022	.0023	.0020	.0022	.0009	.0010	.0009	.0010
Cs_2O	.0003	.00025	.0027	.0026	.0024	.0022	.0011	.0010	.0011	.0011
CuO	.0003	.00028	.0027	.00260	.0024	.00239	.0011	.00109	.0011	.00112
F	.0005	.0005[a]	.0054	.0054[a]	.0048	.0048[a]	.0022	.0022[a]	.0022	.0022[a]
Fe_2O_3	.0858	.0851	.1400	.1370	.0200	.0202	.0568	.0559	.0568	.0555
K_2O	.0000	.0070	.0000	.0040	.0000	.0130	.0000	.0080	.0000	.0140
La_2O_3	.0011	.00114	.0112	.0108	.0101	.00972	.0046	.00436	.0046	.00433
Li_2O	.0100	.00851	.0100	.00910	.0700	.0616	.0376	.0345	.0376	.0350
MgO	.0800	.0771	.0000	.0000[a]	.0800	.0754	.0363	.0355	.0363	.0344
MnO_2	.0003	.00035	.0027	.00285	.0024	.00248	.0011	.00118	.0011	.00112
MoO_3	.0005	.00053	.0054	.00528	.0048	.00491	.0022	.00220	.0022	.00217
Na_2O	.1873	.1740	.1455	.1540	.1186	.1150	.1003	.0964	.1003	.1100
Nd_2O_3	.0022	.00207	.0221	.0195	.0199	.0179	.0090	.00810	.0090	.00808
NiO	.0010	.00136	.0103	.0104	.0093	.00930	.0042	.00433	.0042	.00443
P_2O_5	.0002	.0002[a]	.0018	.0018[a]	.0016	.0016[a]	.0007	.0007[a]	.0007	.0007[a]
PdO	.0001	.0001[a]	.0009	.0009[a]	.0008	.0008[a]	.0004	.0004[a]	.0004	.0004[a]
Pr_6O_{11}	.0002	.0002[a]	.0018	.0018[a]	.0016	.0016[a]	.0007	.0007[a]	.0007	.0007[a]
Rb_2O	.0001	.0001[a]	.0009	.0009[a]	.0008	.0008[a]	.0004	.0004[a]	.0004	.0004[a]
Rh_2O_3	.0001	.0001[a]	.0009	.0009[a]	.0008	.0008[a]	.0004	.0004[a]	.0004	.0004[a]
RuO_2	.0003	.0003[a]	.0027	.0021	.0024	.0021	.0011	.0016	.0011	.0013
SO_3	.0005	.0005[a]	.0049	.0049[a]	.0044	.0044[a]	.0020	.0020[a]	.0020	.0020[a]
SiO_2	.4327	.4230	.4545	.4380	.4214	.4190	.4801	.4760	.4801	.4750
Sm_2O_3	.0001	.0001[a]	.0009	.0009[a]	.0008	.0008[a]	.0004	.0004[a]	.0004	.0004[a]
SrO	.0002	.00019	.0018	.00179	.0016	.00163	.0007	.00074	.0007	.00074
TiO_2	.0000	.0000[a]	.0000	.0000[a]	.0000	.00028	.0000	.00017	.0000	.00016
Y_2O_3	.0001	.00011	.0009	.00092	.0008	.00083	.0004	.00037	.0004	.00037
ZrO_2	.0000	.00016	.0000	.00037	.1300	.0975	.0429	.0400	.0429	.0411
Sum	1.000	0.9797	1.000	0.9901	1.000	0.9645	1.000	0.9949	1.000	1.0122

(a) Below analytical detection limit or not analyzed; as-batched value assumed.

(b) The first of six replicate analyses is listed here (see Table A.8).

TABLE A.1. As-Batched (B) and Analyzed (A) Compositions (in mass fractions) for CVS-I Glasses (continued)

Oxide	CVS1-21		CVS1-22		CVS1-23	
	B	A	B	A	B	A
Al_2O_3	.0000	.0074	.0000	.00081	.0456	.0434
B_2O_3	.2000	.2010	.0500	.0512	.0956	.0945
BaO	.0002	.00019	.0002	.00019	.0007	.00066
CaO	.0200	.0214	.0000	.00088	.0289	.0294
CdO	.0013	.00137	.0013	.00138	.0053	.00517
CeO_2	.0003	.0003[a]	.0003	.0003[a]	.0011	.0011
Cr_2O_3	.0002	.00035	.0002	.0002[a]	.0009	.0009
Cs_2O	.0003	.00025	.0003	.00025	.0011	.0010
CuO	.0003	.00031	.0003	.00058	.0011	.00102
F	.0005	.0005[a]	.0005	.0005[a]	.0021	.0021[a]
Fe_2O_3	.0200	.0207	.1500	.1480	.1179	.1140
K_2O	.0000	.0000[a]	.0000	.0070	.0000	.0090
La_2O_3	.0011	.00126	.0011	.00108	.0044	.00413
Li_2O	.0100	.00858	.0100	.00955	.0375	.0296
MgO	.0800	.0795	.0800	.0754	.0084	.0078
MnO_2	.0003	.00037	.0003	.00033	.0011	.00115
MoO_3	.0005	.00056	.0005	.00052	.0021	.00210
Na_2O	.0900	.0855	.0837	.0836	.1052	.0943
Nd_2O_3	.0022	.00205	.0022	.00204	.0087	.00761
NiO	.0010	.00140	.0010	.00177	.0040	.00399
P_2O_5	.0002	.0002[a]	.0002	.0002[a]	.0007	.0007[a]
PdO	.0001	.0001[a]	.0001	.0001[a]	.0004	.0004[a]
Pr_6O_{11}	.0002	.0002[a]	.0002	.0002[a]	.0007	.0007[a]
Rb_2O	.0001	.0001[a]	.0001	.0001[a]	.0004	.0004[a]
Rh_2O_3	.0001	.0001[a]	.0001	.0001[a]	.0004	.0004[a]
RuO_2	.0003	.0003[a]	.0003	.0003[a]	.0011	.0011[a]
SO_3	.0005	.0005[a]	.0005	.0005[a]	.0019	.0019[a]
SiO_2	.5700	.5540	.5363	.5340	.5153	.5140[b]
Sm_2O_3	.0001	.0001[a]	.0001	.0001[a]	.0004	.0004[a]
SrO	.0002	.00023	.0002	.00020	.0007	.00070
TiO_2	.0000	.0000[a]	.0000	.00022	.0000	.00011
Y_2O_3	.0001	.00011	.0001	.00011	.0004	.00036
ZrO_2	.0000	.00022	.0800	.0703	.0063	.00640
Sum	1.000	0.9892	1.000	0.9920	1.000	0.9805

(a) Below analytical detection limit or not analyzed; as-batched value assumed.

(b) Value from ICP with K/Ni fusion--value for Na/Zr fusion (.4570) was too low.

TABLE A.2. As-Batched (B) and Analyzed (A) Compositions (in mass fractions) for CVS-II Phase 1 and Phase 2 Glasses

	CVS2-1		CVS2-2		CVS2-3		CVS2-4		CVS2-5	
Oxide	B	A	B	A	B	A	B	A	B	A
Al_2O_3	.08000	.0795	.11000	.1065	.10320	.0995	.06190	.0595	.08000	.0690
B_2O_3	.08740	.0880	.07000	.0705	.13200	.1305	.10950	.1090	.15900	.1545
BaO	.00143	.00135	.00045	.0004	.00045	.0050	.00045	.0004	.00143	.00115
CaO	.00000	.0008	.07000	.0690	.07000	.0690	.07000	.0700	.03480	.0260
CdO	.01074	.0110	.00336	.00335	.00336	.0033	.00336	.0032	.01074	.00595
CeO_2	.00215	.0028	.00067	.00125	.00067	.0015	.00067	.0011	.00215	.00245
Cr_2O_3	.00179	.0021	.00056	.0007	.00056	.00085	.00056	.0008	.00179	.0019
Cs_2O	.00215	.0018	.00067	.0006	.00067	.0005	.00067	.00044	.00215	.0019
CuO	.00215	.00205	.00067	.0007	.00067	.0007	.00067	.0006	.00215	.0019
F	.00430	.00430*	.00134	.00134*	.00134	.00134*	.00134	.00134*	.00430	.00430*
Fe_2O_3	.04000	.0400	.04500	.0425	.04500	.0435	.04000	.03850	.04000	.0345
K_2O	.00000	.03300	.00000	.0150	.00000	.0340	.00000	.0067	.00000	.0170
La_2O_3	.00895	.0083	.00280	.00265	.00280	.00265	.00280	.0025	.00895	.0341
Li_2O	.06000	.0580	.06000	.0530	.04350	.0405	.05360	.0465	.02000	.0170
MgO	.05000	.0465	.00000	.00000*	.01000	.0097	.00000	.00000*	.00000	.00000*
MnO_2	.00215	.0032	.00067	.0014	.00067	.0013	.00067	.00225	.00215	.00245
MoO_3	.00430	.00425	.00134	.0013	.00134	.0013	.00134	.00125	.00430	.0040
Na_2O	.07000	.0700	.08830	.0780	.07000	.0650	.07000	.0630	.10100	.0890
Nd_2O_3	.01767	.0150	.00552	.00475	.00552	.0048	.00552	.0046	.01767	.0130
NiO	.00824	.0088	.00258	.0031	.00258	.0033	.00258	.0030	.00824	.0083
P_2O_5	.00143	.00143*	.00045	.00045*	.00045	.00045*	.00045	.00045*	.00143	.00143*
PdO	.00072	.00072*	.00022	.00022*	.00022	.00022*	.00022	.00022*	.00072	.00072*
Pr_6O_{11}	.00143	.00143*	.00045	.00045*	.00045	.00045*	.00045	.00045*	.00143	.00143*
Rb_2O	.00072	.00072*	.00022	.00022*	.00022	.00022*	.00022	.00022*	.00072	.00072*
Rh_2O_3	.00072	.00072*	.00022	.00022*	.00022	.00022*	.00022	.00022*	.00072	.00072*
RuO_2	.00215	.0023	.00067	.00067*	.00067	.0014	.00067	.00067*	.00215	.0021
SO_3	.00394	.00394*	.00123	.00123*	.00123	.00123*	.00123	.00123*	.00394	.00394*
SiO_2	.52260	.5340	.50170	.5100	.46450	.4670	.56000	.55300	.47510	.4870
Sm_2O_3	.00072	.00072*	.00022	.00022*	.00022	.00022*	.00022	.00022*	.00072	.00072*
SrO	.00143	.0014	.00045	.00045	.00045	.00045*	.00045	.0005	.00143	.0012
TiO_2	.00000	.0002	.00000	.0004	.00000	.0002	.00000	.0003	.00000	.00025
UO_2	.00000	.00000*	.00000	.00000*	.00000	.00000*	.00000	.00000*	.00000	.00000*
Y_2O_3	.00072	.0007	.00022	.0002	.00022	.00025	.00022	.0002	.00072	.0006
ZrO_2	.01000	.0100	.03000	.0280	.03680	.03500	.01000	.01000	.01000	.0073
---	---	---	---	---	---	---	---	---	---	---
Sum	1.0000	1.0390	1.0000	.9988	1.0000	1.0255	1.0000	.9827	1.0000	.9965

* Below analytical detection limit or not analyzed; as-batched value assumed.

TABLE A.2. As-Batched (B) and Analyzed (A) Compositions (in mass fractions) for CVS-II Phase 1 and Phase 2 Glasses (continued)

Oxide	CVS2-6		CVS2-7		CVS2-8		CVS2-9		CVS2-10	
	B	A	B	A	B	A	B	A	B	A
Al_2O_3	.01590	.0155	.09530	.0895	.06100	.0580	.01380	.0140	.10430	.1005
B_2O_3	.07000	.0690	.17000	.1570	.07000	.0695	.09440	.0950	.17000	.1690
BaO	.00115	.0011	.00116	.0011	.00045	.0004	.00045	.0004	.00052	.0005
CaO	.07000	.0680	.00940	.0170	.00000	.0014	.00000	.0006	.00000	.0013
CdO	.00861	.0082	.00870	.0086	.00336	.00325	.00336	.00034	.00387	.0037
CeO_2	.00172	.00205	.00174	.00205	.00067	.0011	.00067	.00012	.00077	.00115
Cr_2O_3	.00144	.00160	.00145	.00170	.00056	.00075	.00056	.00075	.00065	.00085
Cs_2O	.00172	.00155	.00174	.0017	.00067	.0007	.00067	.0006	.00077	.0007
CuO	.00172	.0016	.00174	.00165	.00067	.0007	.00067	.0007	.00077	.0007
F	.00344	.00344*	.00348	.00348*	.00134	.00134*	.00134	.00134*	.00155	.00155*
Fe_2O_3	.12000	.1125	.04000	.0385	.11400	.1065	.07120	.0700	.06690	.0635
K_2O	.00000	.0100	.00000	.0083	.00000	.0190	.00000	.0150	.00000	.0110
La_2O_3	.00717	.00635	.00725	.0066	.00280	.0025	.00280	.00265	.00322	.00295
Li_2O	.03820	.0350	.05910	.0495	.06000	.0540	.06000	.0545	.02000	.00185
MgO	.00460	.00465	.00000	.0000*	.05000	.0445	.00000	.00000*	.00000	.0000*
MnO_2	.00172	.00275	.00174	.0030	.00067	.00185	.00067	.00086	.00077	.0018
MoO_3	.00344	.0032	.00348	.00335	.00134	.00125	.00134	.0013	.00155	.0015
Na_2O	.07000	.0630	.07000	.0770	.09850	.0900	.09240	.0860	.13060	.1180
Nd_2O_3	.01416	.0120	.01431	.0120	.00552	.00465	.00552	.00475	.00636	.00545
NiO	.00660	.0068	.00667	.0066	.00258	.0078	.00258	.0030	.00297	.0033
P_2O_5	.00115	.00115*	.00116	.00116*	.00045	.00045*	.00045	.00045*	.00052	.00052*
PdO	.00058	.00058*	.00058	.00058*	.00022	.00022*	.00022	.00022*	.00026	.00026*
Pr_6O_{11}	.00115	.00115*	.00116	.00116*	.00045	.00045*	.00045	.00045*	.00052	.00052*
Rb_2O	.00058	.00058*	.00058	.00058*	.00022	.00022*	.00022	.00022*	.00026	.00026*
Rh_2O_3	.00058	.00058*	.00058	.00058*	.00022	.00022*	.00022	.00022*	.00026	.00026*
RuO_2	.00172	.00180	.00174	.0017	.00067	.00067*	.00067	.00067*	.00077	.00077*
SO_3	.00316	.00316*	.00319	.00319*	.00123	.00123*	.00123	.00123*	.00142	.00142*
SiO_2	.53730	.5390	.48140	.4690	.51150	.49400	.54310	.54700	.46940	.4680
Sm_2O_3	.00058	.00058*	.00058	.00058*	.00022	.00022*	.00022	.00022*	.00026	.00026*
SrO	.00115	.0011	.00116	.00115	.00045	.00045*	.00045	.00045*	.00052	.00052*
TiO_2	.00000	.0001	.00000	.0001	.00000	.0003	.00000	.0004	.00000	.00025
UO_2	.00000	.00000*	.00000	.00000*	.00000	.00000*	.00000	.00000*	.00000	.00000*
Y_2O_3	.00058	.0006	.00058	.0006	.00022	.0002	.00022	.0002	.00026	.0003
ZrO_2	.01000	.0095	.01000	.0100	.01000	.0049	.10000	.0960	.01000	.0100
Sum	1.0000	.9882	1.0000	.9790	1.0000	.9727	1.0000	.9996	1.0000	.9726

* Below analytical detection limit or not analyzed; as-batched value assumed.

TABLE A.2. As-Batched (B) and Analyzed (A) Compositions (in mass fractions) for CVS-II Phase 1 and Phase 2 Glasses (continued)

Oxide	CVS2-11		CVS2-12		CVS2-13		CVS2-14		CVS2-15	
	B	A	B	A	B	A	B	A	B	A
Al_2O_3	.01000	.0104	.09010	.0900	.08960	.0895	.02430	.0245	.07560	.0745
B_2O_3	.07510	.0745	.17000	.1745	.07000	.0710	.13130	.1320	.07000	.0775
BaO	.00119	.0011	.00045	.00045	.00045	.00045	.00082	.0008	.00143	.0013
CaO	.07000	.068	.07000	.0760	.03000	.0320	.05000	.0310	.06010	.0550
CdO	.00893	.00845	.00336	.00335	.00336	.00340	.00614	.0063	.01074	.0099
CeO_2	.00179	.00235	.00067	.0011	.00067	.0013	.00123	.0019	.00215	.00255
Cr_2O_3	.00149	.00023	.00056	.0007	.00056	.00010	.00102	.0014	.00179	.0018
Cs_2O	.00179	.0018	.00067	.0006	.00067	.0005	.00123	.00114	.00215	.0017
CuO	.00179	.0017	.00067	.0007	.00067	.0007	.00123	.00115	.00215	.00195
F	.00357	.00357*	.00134	.00134*	.00134	.00134*	.00245	.00245*	.00430	.00430*
Fe_2O_3	.04000	.0395	.04000	.0400	.04000	.0405	.04000	.0395	.04000	.0380
K_2O	.00000	.0045	.00000	.0130	.00000	.0370	.00000	.0170	.00000	.0079
La_2O_3	.00744	.00655	.00280	.0027	.00280	.00275	.00511	.00475	.00895	.00785
Li_2O	.06000	.0550	.04660	.0450	.02250	.0215	.04860	.0340	.02140	.0205
MgO	.01000	.0111	.01000	.0100	.05000	.0480	.02000	.0450	.00000	.00000*
MnO_2	.00179	.00305	.00067	.0017	.00067	.00215	.00123	.00225	.00215	.00355
MoO_3	.00357	.0034	.00134	.00135	.00134	.00135	.00245	.0025	.00430	.0040
Na_2O	.08330	.0910	.07000	.0690	.16920	.1620	.08020	.0700	.17000	.1440
Nd_2O_3	.01469	.0120	.00552	.00485	.00552	.00490	.01010	.0085	.01767	.0150
NiO	.00685	.0069	.00258	.0030	.00258	.0031	.00471	.0050	.00824	.0082
P_2O_5	.00119	.00119*	.00045	.00045*	.00045	.00045*	.00082	.00082*	.00143	.00143*
PdO	.00060	.00060*	.00022	.00022*	.00022	.00022*	.00041	.00041*	.00072	.00072*
Pr_6O_{11}	.00119	.00119*	.00045	.00045*	.00045	.00045*	.00082	.00082*	.00143	.00143*
Rb_2O	.00060	.00060*	.00022	.00022*	.00022	.00022*	.00041	.00041*	.00072	.00072*
Rh_2O_3	.00060	.00060*	.00022	.00022*	.00022	.00022*	.00041	.00041*	.00072	.00072*
RuO_2	.00179	.0017	.00067	.00067*	.00067	.0014	.00123	.0014	.00215	.00185
SO_3	.00328	.00328	.00123	.00123*	.00123	.00123*	.00225	.00225*	.00394	.00394*
SiO_2	.49150	.4910	.46830	.4640	.49370	.5050	.46000	.4740	.47290	.4740
Sm_2O_3	.00060	.00060*	.00022	.00022*	.00022	.00022*	.00041	.00041*	.00072	.00072*
SrO	.00119	.00115	.00045	.0005	.00045	.0005	.00082	.0008	.00143	.00135
TiO_2	.00000	.0003	.00000	.00015	.00000	.00025	.00000	.0006	.00000	.00025
UO_2	.00000	.00000*	.00000	.00000*	.00000	.00000*	.00000	.00000*	.00000	.00000*
Y_2O_3	.00060	.0006	.00022	.0002	.00022	.00025	.00041	.0004	.00072	.0007
ZrO_2	.09350	.0870	.01000	.0006	.01000	.0010	.10000	.0900	.01000	.0100
Sum	1.0000	.9949	1.0000	1.0085	1.0000	1.0350	1.0000	1.0039	1.0000	.9773

* Below analytical detection limit or not analyzed; as-batched value assumed.

TABLE A.2. As-Batched (B) and Analyzed (A) Compositions (in mass fractions) for CVS-II Phase 1 and Phase 2 Glasses (continued)

Oxide	CVS2-16		CVS2-17		CVS2-18		CVS2-19		CVS2-20	
	B	A	B	A	B	A	B	A	B	A
Al_2O_3	.02310	.0230	.06360	.0615	.02310	.0235	.0235	.0300	.01000	.00955
B_2O_3	.10530	.1040	.11420	.1135	.10530	.1060	.1048	.1010	.05000	.0486
BaO	.00106	.0010	.00073	.0007	.00106	.0010	.00099	.00230	.00018	.0002
CaO	.00830	.0092	.02750	.0300	.00830	.0093	.0082	.0108	.00000	.0004
CdO	.00795	.0079	.00547	.00565	.00795	.0080	.0065	.00641	.00134	.0012
CeO_2	.00159	.0023	.00109	.0018	.00159	.0022	.00017	.00098	.00027	.0055
Cr_2O_3	.00133	.0016	.00091	.00125	.00133	.0017	.00129	.00104	.00022	.00025
Cs_2O	.00159	.00146	.00109	.0010	.00159	.0015	.0015	.00018	.00027	.00253
CuO	.00159	.0016	.00109	.0010	.00159	.0016	.00158	.00214	.00027	.00025
F	.00318	.00318*	.00219	.00219*	.00318	.00318*	.0019	.0019*	.00054	.00054*
Fe_2O_3	.07190	.0700	.05680	.0550	.07190	.0705	.0733	.0610	.06000	.05635
K_2O	.00000	.0310	.00000	.0180	.00000	.0280	.0000	.0000*	.00000	.00000*
La_2O_3	.00662	.00605	.00455	.0042	.00662	.00615	.0154	.0212	.00112	.00095
Li_2O	.03750	.0360	.03760	.0330	.03750	.0365	.0373	.0344	.06690	.0628
MgO	.00840	.00855	.03630	.0330	.00840	.00855	.0084	.00809	.00000	.00035
MnO_2	.00159	.0024	.00109	.0018	.00159	.0027	.00158	.00241	.00027	.00011
MoO_3	.00318	.00315	.00219	.00219	.00318	.00315	.0031	.00277	.00054	.0005
Na_2O	.11250	.1050	.10030	.0890	.11250	.1090	.1129	.11600	.10310	.1455
Nd_2O_3	.01308	.0110	.00899	.00785	.01308	.0190	.0057	.00700	.00221	.0019
NiO	.00610	.0065	.00419	.0045	.00610	.0066	.0060	.00629	.00103	.0010
P_2O_5	.00106	.00106*	.00073	.00073*	.00106	.00106*	.00099	.00099*	.00018	.00075
PdO	.00053	.00053*	.00037	.00037*	.00053	.00053*	.0000	.0000*	.00009	.00009*
Pr_6O_{11}	.00106	.00106*	.00073	.00073*	.00106	.00106*	.00188	.00188*	.00018	.00018*
Rb_2O	.00053	.00053*	.00037	.00037*	.00053	.00053*	.0000	.0000*	.00009	.00009*
Rh_2O_3	.00053	.00053*	.00037	.00037*	.00053	.00053*	.0000	.0000*	.00009	.00009*
RuO_2	.00159	.0019	.00109	.0013	.00159	.0018	.00151	.00151*	.00027	.0002
SO_3	.00292	.00292*	.00201	.00201*	.00292	.00292*	.0044	.0044*	.00049	.00049*
SiO_2	.53530	.5400	.48010	.4810	.53530	.5320	.5328	.51100	.57000	.5630
Sm_2O_3	.00053	.00053*	.00037	.00037*	.00053	.00053*	.0000	.0000*	.00009	.00009*
SrO	.00106	.0010	.00073	.0007	.00106	.0010	.0000	.0000*	.00018	.0002
TiO_2	.00000	.0002	.00000	.00025	.00000	.00025	.0000	.00103	.00000	.0004
UO_2	.00000	.00000*	.00000	.00000*	.00000	.00000*	.0000	.0000*	.00000	.00000*
Y_2O_3	.00053	.0005	.00037	.0004	.00053	.00055	.0000	.0000*	.00009	.0001
ZnO							.0049	.00482		
ZrO_2	.03850	.0380	.04290	.0410	.03850	.0400	.0392	.0397	.13000	.1180
Sum	1.0000	1.0236	1.0000	.9967	1.0000	1.0309	.9998	.9812	1.0000	1.0222

* Below analytical detection limit or not analyzed; as-batched value assumed.

TABLE A.2. As-Batched (B) and Analyzed (A) Compositions (in mass fractions) for CVS-II Phase 1 and Phase 2 Glasses (continued)

	CVS2-21		CVS2-22		CVS2-23		CVS2-24		CVS2-25	
Oxide	B	A	B	A	B	A	B	A	B	A
Al_2O_3	.06860	.0669	.03650	.0366	.05780	.0561	.09610	.0940	.00330	.00395
B_2O_3	.13140	.1290	.05000	.05015	.05220	.05075	.20000	.20075	.05000	.0496
BaO	.00018	.0002	.00179	.00165	.00018	.0002	.00168	.0015	.00101	.0009
CaO	.00000	.0005	.00000	.0006	.08000	.0760	.00000	.0007	.08000	.0765
CdO	.00134	.0013	.01343	.0123	.00134	.0012	.01261	.01155	.00761	.0072
CeO_2	.00027	.0002	.00269	.0023	.00027	.0001	.00253	.0024	.00153	.0013
Cr_2O_3	.00022	.0003	.00224	.0021	.00022	.0003	.00210	.0020	.00127	.00115
Cs_2O	.00027	.00027	.00269	.00272	.00027	.00036	.00253	.00277	.00153	.00190
CuO	.00027	.0003	.00269	.00245	.00027	.0002	.00253	.0023	.00153	.0014
F	.00054	.00054*	.00537	.00537*	.00054	.00054*	.00504	.00504*	.00304	.00304*
Fe_2O_3	.02000	.0190	.02000	.02025	.02000	.0188	.02000	.0185	.15000	.1415
K_2O	.00000	.00000*	.00000	.0020	.00000	.00000*	.00000	.0200	.00000	.00000*
La_2O_3	.00112	.00095	.01119	.0100	.00112	.00085	.01051	.00925	.00634	.00575
Li_2O	.07000	.0646	.07000	.0703	.01000	.0081	.07000	.0673	.07000	.0663
MgO	.08000	.0705	.08000	.0731	.00000	.0004	.00000	.00015	.00000	.00065
MnO_2	.00027	.00039	.00269	.0024	.00027	.00036	.00253	.00225	.00153	.00128
MoO_3	.00054	.0005	.00537	.0050	.00054	.0005	.00504	.0047	.00304	.00295
Na_2O	.05000	.0847	.07350	.1355	.20000	.2265	.07360	.1290	.08410	.1295
Nd_2O_3	.00221	.00205	.02209	.01915	.00221	.0016	.02074	.01815	.01253	.01165
NiO	.00103	.0010	.01030	.0093	.00103	.0010	.00967	.0087	.00584	.0054
P_2O_5	.00018	.0004	.00179	.0020	.00018	.0002	.00168	.0020	.00101	.0010
PdO	.00009	.00009*	.00090	.00090*	.00009	.00009*	.00085	.00085*	.00051	.00051*
Pr_6O_{11}	.00018	.00018*	.00179	.00179*	.00018	.00018*	.00168	.00168*	.00101	.00101*
Rb_2O	.00009	.00009*	.00090	.00090*	.00009	.00009*	.00085	.00085*	.00051	.00051*
Rh_2O_3	.00009	.00009*	.00090	.00090*	.00009	.00009*	.00085	.00085*	.00051	.00051*
RuO_2	.00027	.0002	.00269	.00145	.00027	.00015	.00253	.00155	.00153	.0009
SO_3	.00049	.00049*	.00493	.00493*	.00049	.00049*	.00463	.00463*	.00280	.00280*
SiO_2	.57000	.5495	.57000	.5560	.57000	.5485	.44640	.4360	.50590	.49025
Sm_2O_3	.00009	.00009*	.00090	.00090*	.00009	.00009*	.00085	.00085*	.00051	.00051*
SrO	.00018	.0002	.00179	.00165	.00018	.0002	.00168	.0015	.00101	.0010
TiO_2	.00000	.0001	.00000	.00015	.00000	.0001	.00000	.0001	.00000	.0001
UO_2	.00000	.00000*	.00000	.00000*	.00000	.00000*	.00000	.00000*	.00000	.00000*
Y_2O_3	.00009	.0001	.00090	.0008	.00009	.0001	.00085	.0008	.00051	.0005
ZrO_2	.00000	.00000*	.00000	.00000*	.00000	.00000*	.00000	.00000*	.00000	.00000*
Sum	1.0000	.9947	1.0000	1.036	1.0000	.9941	1.0000	1.053	1.0000	1.011

* Below analytical detection limit or not analyzed; as-batched value assumed.

TABLE A.2. As-Batched (B) and Analyzed (A) Compositions (in mass fractions) for CVS-II Phase 1 and Phase 2 Glasses (continued)

Oxide	CVS2-26		CVS2-27		CVS2-28		CVS2-29		CVS2-30	
	B	A	B	A	B	A	B	A	B	A
Al_2O_3	.02570	.0250	.07820	.0764	.05550	.04855	.00000	.00045	.04580	.0435
B_2O_3	.2000	.2000	.05000	.0492	.05000	.0443	.20000	.20175	.20000	.1960
BaO	.00018	.00019	.00018	.0002	.00179	.00145	.00179	.0017	.00018	.00015
CaO	.08000	.0770	.00000	.0005	.00000	.0002	.08000	.0758	.00000	.0001
CdO	.00134	.00125	.00134	.0012	.01343	.01085	.01343	.0131	.00134	.0012
CeO_2	.00027	.0048	.00027	.0002	.00269	.0016	.00269	.0065	.00027	.0002
Cr_2O_3	.00022	.0002	.00022	.00025	.00224	.00115	.00224	.0021	.00022	.00025
Cs_2O	.00027	.00055	.00027	.00033	.00269	.00253	.00269	.00282	.00027	.00029
CuO	.00027	.0003	.00027	.0002	.00269	.0022	.00269	.0025	.00027	.00025
F	.00054	.00054*	.00054	.00054*	.00537	.00537*	.00537	.00537*	.00054	.00054*
Fe_2O_3	.02000	.0190	.02000	.0190	.02000	.01745	.02000	.0188	.13200	.12175
K_2O	.00000	.00000*	.00000	.00000*	.00000	.00000*	.00000	.00000*	.00000	.00000*
La_2O_3	.00112	.00079	.00112	.0009	.01119	.0087	.01119	.01005	.00112	.00085
Li_2O	.07000	.0680	.01550	.0168	.01260	.0103	.01000	.0082	.01000	.0084
MgO	.00000	.0010	.08000	.0715	.00000	.0001	.00000	.00065	.00000	.0001
MnO_2	.00027	.00022	.00027	.0002	.00269	.0021	.00269	.00260	.00027	.00012
MoO_3	.00054	.00046	.00054	.0005	.00537	.0044	.00537	.00505	.00054	.00045
Na_2O	.05120	.0520	.20000	.2335	.20000	.2030	.06750	.1080	.08320	.1250
Nd_2O_3	.00221	.0020	.00221	.0017	.02209	.01655	.02209	.0212	.00221	.0015
NiO	.00103	.00089	.00103	.0009	.01030	.0093	.01030	.0093	.00103	.0009
P_2O_5	.00018	.00043	.00018	.00018*	.00179	.0020	.00179	.0020	.00018	.00018*
PdO	.00009	.00009*	.00009	.00009*	.00090	.00090*	.00090	.00090*	.00009	.00009*
Pr_6O_{11}	.00018	.00018*	.00018	.00018*	.00179	.00179*	.00179	.00179*	.00018	.00018*
Rb_2O	.00009	.00009*	.00009	.00009*	.00090	.00090*	.00090	.00090*	.00009	.00009*
Rh_2O_3	.00009	.00009*	.00009	.00009*	.00090	.00090*	.00090	.00090*	.00009	.00009*
RuO_2	.00027	.00015	.00027	.00025	.00269	.00175	.00269	.0015	.00027	.0002
SO_3	.00049	.00049*	.00049	.00049*	.00493	.00493*	.00493	.00493*	.00049	.00049*
SiO_2	.44310	.4300	.54630	.53325	.56190	.4915	.43910	.4170	.51900	.4915
Sm_2O_3	.00009	.00009*	.00009	.00009*	.00090	.00090*	.00090	.00090*	.00009	.00009*
SrO	.00018	.0002	.00018	.0002	.00179	.0014	.00179	.0017	.00018	.0002
TiO_2	.00000	.00026	.00000	.0007	.00000	.00007	.00000	.00025	.00000	.00010
UO_2	.00000	.00000*	.00000	.00000*	.00000	.00000*	.00000	.00000*	.00000	.00000*
Y_2O_3	.00009	.00007	.00009	.0001	.00090	.0007	.00090	.00085	.00009	.0001
ZrO_2	.10000	.0890	.00000	.00000*	.00000	.00000*	.08340	.0736	.00000	.00000*
---	---	---	---	---	---	---	---	---	---	---
Sum	1.0000	.9753	1.0000	1.0097	1.0000	.8978	1.0000	1.003	1.0000	.9949

* Below analytical detection limit or not analyzed; as-batched value assumed.

TABLE A.2. As-Batched (B) and Analyzed (A) Compositions (in mass fractions) for CVS-II Phase 1 and Phase 2 Glasses (continued)

	CVS2-31		CVS2-32		CVS2-33		CVS2-34		CVS2-35	
Oxide	B	A	B	A	B	A	B	A	B	A
Al_2O_3	.05260	.0514	.00270	.00265	.08920	.0875	.13880	.1350	.13400	.1305
B_2O_3	.18430	.1895	.05000	.04905	.05440	.0540	.17430	.1700	.05000	.0493
BaO	.00018	.0002	.00018	.0002	.00179	.0017	.00018	.0002	.00018	.0002
CaO	.08000	.0757	.00000	.0005	.00000	.0005	.00000	.00054	.08000	.0776
CdO	.00134	.00125	.00134	.0012	.01343	.0125	.00134	.0012	.00134	.0012
CeO_2	.00027	.0002	.00027	.0055	.00269	.0029	.00027	.0002	.00027	.0002
Cr_2O_3	.00022	.0001	.00022	.0002	.00224	.0021	.00022	.00015	.00022	.0002
Cs_2O	.00027	.00053	.00027	.00026	.00269	.00280	.00027	.00061	.00027	.00015
CuO	.00027	.0003	.00027	.0002	.00269	.0025	.00027	.00031	.00027	.0002
F	.00054	.00054*	.00054	.00054*	.00537	.00537*	.00054	.00054*	.00054	.00054*
Fe_2O_3	.02000	.0193	.02000	.0194	.02000	.0190	.02000	.0195	.06320	.05965
K_2O	.00000	.00000*	.00000	.00000*	.00000	.00000*	.00000	.00000*	.00000	.00000*
La_2O_3	.00112	.0010	.00112	.00095	.01119	.0101	.00112	.00106	.00112	.0009
Li_2O	.03310	.0295	.04280	.0412	.03640	.0350	.03690	.0350	.04280	.0420
MgO	.00000	.0007	.00000	.0004	.08000	.0710	.00000	.00015	.00000	.0006
MnO_2	.00027	.00035	.00027	.0002	.00269	.00235	.00027	.00026	.00027	.00012
MoO_3	.00054	.0005	.00054	.0005	.00537	.0044	.00054	.00046	.00054	.0005
Na_2O	.05000	.0901	.20000	.2445	.20000	.2200	.20000	.2100	.20000	.2450
Nd_2O_3	.00221	.00205	.00221	.00175	.02209	.0210	.00221	.0020	.00221	.00185
NiO	.00103	.0010	.00103	.0009	.01030	.0092	.00103	.00094	.00103	.0009
P_2O_5	.00018	.0004	.00018	.0009	.00179	.0010	.00018	.00008	.00018	.00018*
PdO	.00009	.00009*	.00009	.00009*	.00090	.00090*	.00009	.00009*	.00009	.00009*
Pr_6O_{11}	.00018	.00018*	.00018	.00018*	.00179	.00179*	.00018	.00018*	.00018	.00018*
Rb_2O	.00009	.00009*	.00009	.00009*	.00090	.00090*	.00009	.00009*	.00009	.00009*
Rh_2O_3	.00009	.00009*	.00009	.00009*	.00090	.00090*	.00009	.00009*	.00009	.00009*
RuO_2	.00027	.0002	.00027	.00025	.00269	.00083	.00027	.0002	.00027	.0002
SO_3	.00049	.00049*	.00049	.00049*	.00493	.00493*	.00049	.00049*	.00049	.00049*
SiO_2	.57000	.5415	.54450	.53825	.42000	.4100	.42000	.4000	.42000	.39775
Sm_2O_3	.00009	.00009*	.00009	.00009*	.00090	.00090*	.00009	.00009*	.00009	.00009*
SrO	.00018	.0002	.00018	.0002	.00179	.00165	.00018	.00019	.00018	.0002
TiO_2	.00000	.00015	.00000	.0003	.00000	.00011	.00000	.00008	.00000	.0001
UO_2	.00000	.00000*	.00000	.00000*	.00000	.00000*	.00000	.00000*	.00000	.00000*
Y_2O_3	.00009	.0001	.00009	.0001	.00090	.00083	.00009	.00004	.00009	.0001
ZrO_2	.00000	.00000*	.13000	.1225	.00000	.00000*	.00000	.00088	.00000	.00000*
Sum	1.0000	1.0078	1.0000	1.033	1.0000	.9887	1.0000	.9806	1.0000	1.0112

* Below analytical detection limit or not analyzed; as-batched value assumed.

TABLE A.2. As-Batched (B) and Analyzed (A) Compositions (in mass fractions) for CVS-II Phase 1 and Phase 2 Glasses (continued)

Oxide	CVS2-36		CVS2-37		CVS2-38		CVS2-39		CVS2-40	
	B	A	B	A	B	A	B	A	B	A
Al_2O_3	.00880	.0088	.14000	.13575	.02720	.0273	.02580	.0247	.10000	.0970
B_2O_3	.05000	.0497	.08390	.0830	.11090	.1100	.05000	.0483	.06390	.0630
BaO	.00018	.0002	.00018	.0002	.00018	.0002	.00018	.00015	.00054	.00046
CaO	.08000	.0780	.00000	.0002	.00000	.0002	.00000	.0005	.02000	.0190
CdO	.00134	.0012	.00134	.0012	.00134	.0013	.00134	.0012	.00403	.00375
CeO_2	.00027	.0002	.00027	.0001	.00027	.0002	.00027	.0032	.00081	.0019
Cr_2O_3	.00022	.0002	.00022	.00025	.00022	.00025	.00022	.0002	.00067	.00065
Cs_2O	.00027	.00020	.00027	.00031	.00027	.00031	.00027	.00039	.00081	.00101
CuO	.00027	.0002	.00027	.00025	.00027	.00025	.00027	.0002	.00081	.00075
F	.00054	.00054*	.00054	.00054*	.00054	.00054*	.00054	.00054*	.00161	.00161*
Fe_2O_3	.15000	.14425	.02000	.01895	.14280	.13375	.07420	.0675	.02000	.0190
K_2O	.00000	.00000*	.00000	.00000*	.00000	.00000*	.00000	.00000*	.00000	.00000*
La_2O_3	.00112	.0009	.00112	.0009	.00112	.00095	.00112	.0008	.00336	.0029
Li_2O	.07000	.0692	.07000	.0642	.01000	.0085	.07000	.0643	.04210	.0400
MgO	.00000	.0005	.00000	.00000	.08000	.0706	.08000	.06895	.05000	.0440
MnO_2	.00027	.0002	.00027	.00032	.00027	.0003	.00027	.00016	.00081	.00074
MoO_3	.00054	.0005	.00054	.0005	.00054	.0005	.00054	.00045	.00161	.0014
Na_2O	.08910	.1395	.10610	.1405	.10440	.1435	.13620	.1725	.15000	.1660
Nd_2O_3	.00221	.00195	.00221	.00165	.00221	.0019	.00221	.0017	.00663	.00625
NiO	.00103	.0009	.00103	.0009	.00103	.0010	.00103	.0009	.00309	.0028
P_2O_5	.00018	.00018*	.00018	.0004	.00018	.00045	.00018	.0005	.00054	.00053
PdO	.00009	.00009*	.00009	.00009*	.00009	.00009*	.00009	.00009*	.00027	.00027*
Pr_6O_{11}	.00018	.00018*	.00018	.00018*	.00018	.00018*	.00018	.00018*	.00054	.00054*
Rb_2O	.00009	.00009*	.00009	.00009*	.00009	.00009*	.00009	.00009*	.00027	.00027*
Rh_2O_3	.00009	.00009*	.00009	.00009*	.00009	.00009*	.00009	.00009*	.00027	.00027*
RuO_2	.00027	.0001	.00027	.0002	.00027	.0001	.00027	.0002	.00081	.00045
SO_3	.00049	.00049*	.00049	.00049*	.00049	.00049*	.00049	.00049*	.00148	.00148*
SiO_2	.54210	.53375	.57000	.55075	.51470	.5005	.48380	.4551	.50400	.4900
Sm_2O_3	.00009	.00009*	.00009	.00009*	.00009	.00009*	.00009	.00009*	.00027	.00027*
SrO	.00018	.0002	.00018	.0002	.00018	.0002	.00018	.0002	.00054	.00049
TiO_2	.00000	.00015	.00000	.0001	.00000	.00015	.00000	.0002	.00000	.00011
UO_2	.00000	.00000*	.00000	.00000*	.00000	.00000*	.00000	.00000*	.00000	.00000*
Y_2O_3	.00009	.0001	.00009	.0001	.00009	.0001	.00009	.0001	.00027	.00013
ZrO_2	.00000	.00000*	.00000	.00000*	.00000	.00000*	.07000	.0601	.02000	.0160
---	---	---	---	---	---	---	---	---	---	---
Sum	1.0000	1.0327	1.0000	1.0025	1.0000	1.0041	1.0000	.9740	1.0000	.9830

* Below analytical detection limit or not analyzed; as-batched value assumed.

TABLE A.2. As-Batched (B) and Analyzed (A) Compositions (in mass fractions) for CVS-II Phase 1 and Phase 2 Glasses (continued)

	CVS2-41		CVS2-42		CVS2-43		CVS2-44		CVS2-45	
Oxide	B	A	B	A	B	A	B	A	B	A
Al_2O_3	.10000	.0970	.03000	.0290	.05000	.04765	.06230	.0610	.05920	.0575
B_2O_3	.06940	.0680	.05000	.0490	.14770	.14175	.10780	.1050	.11060	.1100
BaO	.00054	.0052	.00054	.00500	.00054	.0005	.00054	.00049	.00125	.0012
CaO	.05000	.0480	.03200	.03100	.02000	.0209	.05000	.0470	.02000	.0190
CdO	.00403	.0039	.00403	.0037	.00403	.0037	.00403	.00038	.00940	.00875
CeO_2	.00081	.0019	.00081	.0014	.00081	.0039	.00081	.0018	.00188	.0030
Cr_2O_3	.00067	.00064	.00067	.00063	.00067	.00065	.00067	.00064	.00157	.0014
Cs_2O	.00081	.00108	.00081	.00092	.00081	.00115	.00081	.00104	.00188	.00220
CuO	.00081	.00078	.00081	.00074	.00081	.0008	.00081	.00075	.00188	.00175
F	.00161	.00161*	.00161	.00161*	.00161	.00161*	.00161	.00161*	.00376	.00376*
Fe_2O_3	.03000	.0285	.10000	.0930	.03000	.0283	.02000	.0190	.03080	.0290
K_2O	.00000	.00000*	.00000	.00000*	.00000	.00000*	.00000	.00000*	.00000	.00000*
La_2O_3	.00336	.0033	.00336	.00295	.00336	.0028	.00336	.0029	.00783	.00705
Li_2O	.07000	.0660	.07000	.0660	.06530	.0593	.06990	.0650	.05950	.0560
MgO	.02000	.0180	.03800	.0335	.03000	.02655	.02000	.0175	.05000	.0445
MnO_2	.00081	.00067	.00081	.00071	.00081	.00081	.00081	.00068	.00188	.00165
MoO_3	.00161	.00145	.00161	.0014	.00161	.0014	.00161	.0014	.00376	.0035
Na_2O	.07810	.1200	.06250	.0660	.05000	.0809	.05000	.0530	.05000	.0520
Nd_2O_3	.00663	.0069	.00663	.0060	.00663	.0060	.00663	.0061	.01546	.0145
NiO	.00309	.0030	.00309	.0029	.00309	.0030	.00309	.0029	.00721	.0065
P_2O_5	.00054	.00055	.00054	.00055	.00054	.0008	.00054	.00053	.00125	.0010
PdO	.00027	.00027*	.00027	.00027*	.00027	.00027*	.00027	.00027*	.00063	.00063*
Pr_6O_{11}	.00054	.00054*	.00054	.00054*	.00054	.00054*	.00054	.00054*	.00125	.00125*
Rb_2O	.00027	.00027*	.00027	.00027*	.00027	.00027*	.00027	.00027*	.00063	.00063*
Rh_2O_3	.00027	.00027*	.00027	.00027*	.00027	.00027*	.00027	.00027*	.00063	.00063*
RuO_2	.00081	.00045	.00081	.00038	.00081	.0006	.00081	.00045	.00188	.00135
SO_3	.00148	.00148*	.00148	.00148*	.00148	.00148*	.00148	.00148*	.00345	.00345*
SiO_2	.53250	.5100	.56750	.5500	.50700	.4870	.57000	.4900	.52990	.4700
Sm_2O_3	.00027	.00027*	.00027	.00027*	.00027	.00027*	.00027	.00027*	.00063	.00063*
SrO	.00054	.00057	.00054	.00051	.00054	.0005	.00054	.0005	.00125	.0012
TiO_2	.00000	.00013	.00000	.00013	.00000	.00025	.00000	.00016	.00000	.00013
UO_2	.00000	.00000*	.00000	.00000*	.00000	.00000*	.00000	.00000*	.00000	.00000*
Y_2O_3	.00027	.00022	.00027	.00018	.00027	.0003	.00027	.0002	.00063	.00058
ZrO_2	.02000	.0170	.02000	.0170	.07000	.0610	.02000	.0160	.02000	.0170
Sum	1.0000	1.0079	1.0000	.9673	1.0000	.9852	1.0000	.8991	1.0000	.9217

* Below analytical detection limit or not analyzed; as-batched value assumed.

TABLE A.2. As-Batched (B) and Analyzed (A) Compositions (in mass fractions) for CVS-II Phase 1 and Phase 2 Glasses (continued)

Oxide	CVS2-46		CVS2-47		CVS2-48		CVS2-49		CVS2-50	
	B	A	B	A	B	A	B	A	B	A
Al_2O_3	.07460	.0721	.04000	.0390	.08540	.0835	.07850	.0763	.06360	.0625
B_2O_3	.12590	.1225	.05000	.0495	.14420	.1300	.13570	.1325	.11420	.1150
BaO	.00117	.0011	.00125	.00150	.00098	.00092	.00054	.0005	.00073	.00062
CaO	.02000	.0196	.05000	.04900	.05000	.0490	.02000	.0191	.02750	.0270
CdO	.00878	.0081	.00940	.0088	.00733	.0069	.00403	.00375	.00547	.0051
CeO_2	.00176	.0023	.00188	.00405	.00147	.0016	.00081	.0018	.00109	.0030
Cr_2O_3	.00146	.00135	.00157	.00165	.00122	.0011	.00067	.00007	.00091	.00084
Cs_2O	.00176	.00237	.00188	.00203	.00147	.00166	.00081	.00113	.00109	.00118
CuO	.00176	.00165	.00188	.00175	.00147	.0014	.00081	.0008	.00109	.00010
F	.00351	.00351*	.00376	.00376*	.00293	.00293*	.00161	.00161*	.00219	.00219*
Fe_2O_3	.02000	.01935	.02000	.0190	.02000	.0190	.05150	.04935	.05680	.0535
K_2O	.00000	.00000*	.00000	.00000*	.00000	.00000*	.00000	.00000*	.00000	.00000*
La_2O_3	.00732	.0066	.00783	.0069	.00611	.00565	.00336	.0031	.00455	.0038
Li_2O	.07000	.0632	.04290	.0400	.03900	.0380	.04130	.0368	.03760	.0370
MgO	.02000	.0181	.02000	.0175	.02000	.0175	.02000	.0176	.03630	.03165
MnO_2	.00176	.00182	.00188	.0018	.00147	.00145	.00081	.00088	.00109	.00095
MoO_3	.00351	.0034	.00376	.0035	.00293	.00285	.00161	.00145	.00219	.00205
Na_2O	.05770	.0927	.12770	.1300	.09680	.1100	.09570	.1280	.10030	.1100
Nd_2O_3	.01445	.0135	.01546	.0145	.01206	.0110	.00663	.0062	.00899	.0081
NiO	.00674	.0065	.00721	.0065	.00562	.0051	.00309	.0031	.00419	.0037
P_2O_5	.00117	.0010	.00125	.0015	.00098	.0010	.00054	.0006	.00073	.00065
PdO	.00059	.00059*	.00063	.00063*	.00049	.00049*	.00027	.00027*	.00037	.00037*
Pr_6O_{11}	.00117	.00117*	.00125	.00125*	.00098	.00098*	.00054	.00054*	.00073	.00073*
Rb_2O	.00059	.00059*	.00063	.00063*	.00049	.00049*	.00027	.00027*	.00037	.00037*
Rh_2O_3	.00059	.00059*	.00063	.00063*	.00049	.00049*	.00027	.00027*	.00037	.00037*
RuO_2	.00176	.00075	.00188	.0010	.00147	.00068	.00081	.0006	.00109	.00060
SO_3	.00322	.00322*	.00345	.00345*	.00269	.00269*	.00148	.00148*	.00201	.00201*
SiO_2	.52640	.5060	.52940	.5200	.47000	.4600	.50730	.4800	.48010	.4400
Sm_2O_3	.00059	.00059*	.00063	.00063*	.00049	.00049*	.00027	.00027*	.00037	.00037*
SrO	.00117	.0011	.00125	.00115	.00098	.00092	.00054	.0005	.00073	.00065
TiO_2	.00000	.0002	.00000	.00021	.00000	.00012	.00000	.0001	.00000	.00015
UO_2	.00000	.00000*	.00000	.00000*	.00000	.00000*	.00000	.00000*	.00000	.00000*
Y_2O_3	.00059	.0006	.00063	.00059	.00049	.00031	.00027	.0003	.00037	.00036
ZrO_2	.02000	.0150	.05000	.0440	.02000	.0170	.02000	.0167	.04290	.0370
---	---	---	---	---	---	---	---	---	---	---
Sum	1.0000	.9912	1.0000	.9764	1.0000	.9752	1.0000	.9859	1.0000	.9519

* Below analytical detection limit or not analyzed; as-batched value assumed.

TABLE A.2. As-Batched (B) and Analyzed (A) Compositions (in mass fractions) for CVS-II Phase 1 and Phase 2 Glasses (continued)

	CVS2-51		CVS2-52[a]		CVS2-53		CVS2-54		CVS2-55[a]	
Oxide	B	A	B	A	B	A	B	A	B	A
Al_2O_3	.02350	.02850	.02330	.02600	.08000	.08400	.02350	.03300	.02350	.02700
B_2O_3	.10480	.09750	.08180	.08750	.08740	.09100	.10480	.11000	.10480	.11500
BaO	.00099	.00215	.00106	.00105	.00143	.00130	.00099	.00090	.00000	.00002
CaO	.00820	.00990	.00080	.00120	.00000	.00180	.00820	.00940	.00820	.00690
CdO	.00650	.00590	.00792	.00745	.01074	.01000	.00650	.00620	.00000	.00000
CeO_2	.00017	.00210	.00159	.00155	.00215	.00200	.00017	.00017*	.00000	.00000
Co_2O_3	.00000	.00000*	.00000	.00010	.00000	.00000*	.00000	.00000*	.00000	.00001
Cr_2O_3	.00129	.00096	.00132	.00125	.00179	.00170	.00129	.00130	.00894	.00820
Cs_2O	.00150	.00158	.00159	.00159*	.00215	.00215*	.00150	.00150*	.00000	.00000*
CuO	.00158	.00185	.00159	.00150	.00215	.00200	.00150	.00150	.00000	.00002
Dy_2O_3	.00000	.00000	.00000	.00000*	.00000	.00000*	.00000	.00000*	.00000	.00005
Eu_2O_3	.00000	.00000	.00000	.00002	.00000	.00000*	.00000	.00000*	.00000	.00000*
F	.00190	.00190*	.00317	.00317*	.00430	.00430*	.00190	.00190*	.00298	.00298*
Fe_2O_3	.07330	.05700	.07200	.07550	.04000	.03600	.07330	.06600	.07330	.07650
Gd_2O_3	.00000	.00000	.00000	.00000*	.00000	.00000*	.00000	.00000*	.00000	.00000*
K_2O	.00000	.00000*	.00000	.00000*	.00000	.00000*	.00000	.00000*	.00000	.00000*
La_2O_3	.01540	.02050	.00660	.00610	.00895	.00810	.01541	.01400	.00000	.00000*
Li_2O	.03730	.03200	.07880	.08300	.06000	.06300	.03730	.03900	.03730	.04050
MgO	.00840	.00720	.00090	.00005	.05000	.04400	.00840	.00750	.00840	.00710
MnO_2	.00158	.00210	.00159	.00155	.00215	.00210	.00158	.00160	.02801	.02500
MoO_3	.00310	.00280	.00317	.00315	.00430	.00420	.00310	.00300	.00000	.00000
Na_2O	.11290	.12000	.04500	.06800	.07000	.06500	.11290	.10000	.11290	.11000
Nd_2O_3	.00570	.00645	.01302	.01300	.00000	.00000*	.00000	.00000*	.01669	.01700
NiO	.00600	.00590	.00608	.00000	.00824	.00770	.00600	.00560	.00000	.00000*
P_2O_5	.00099	.00150	.00106	.00200	.00143	.00200	.00099	.00100	.00000	.00040
PbO	.00000	.00000	.00000	.00010	.00000	.00020	.00000	.00000*	.00000	.00010
PdO	.00000	.00000*	.00053	.00053*	.00072	.00100	.00000	.00000*	.00000	.00000*
Pr_6O_{11}	.00188	.00188*	.00106	.00106*	.00143	.00143*	.00188	.00188*	.00000	.00000*
Rb_2O	.00000	.00000*	.00053	.00053*	.00072	.00072*	.00000	.00000*	.00000	.00000*
Rh_2O_3	.00000	.00000*	.00053	.00053*	.00072	.00072*	.00000	.00000*	.00000	.00000*
RuO_2	.00151	.00130	.00159	.00159*	.00215	.00150	.00150	.00100	.00000	.00000*
SO_3	.00440	.00440*	.00290	.00290*	.00394	.00394*	.00401	.00401*	.00298	.00298*
SiO_2	.53280	.46000	.60000	.58000	.52260	.50000	.53280	.51000	.53280	.52000
Sm_2O_3	.00000	.00000*	.00053	.00053*	.00072	.00072*	.00000	.00000*	.00000	.00000*
SrO	.00000	.00000*	.00106	.00105	.00143	.00140	.00000	.00003	.00000	.00000*
TiO_2	.00000	.00106	.00000	.00020	.00000	.00010	.00000	.00020	.00000	.00020
UO_2	.00000	.00000*	.00000	.00400	.01767	.02000	.00570	.00600	.00000	.00400
V_2O_3	.00000	.00000	.00000	.00002	.00000	.00000*	.00000	.00000*	.00000	.00000*
Y_2O_3	.00000	.00000*	.00053	.00050	.00072	.00070	.00000	.00000*	.00000	.00000*
ZnO	.00490	.00430	.00000	.00000*	.00000	.00000*	.00000	.00450	.00000	.00000*
ZrO_2	.03920	.03400	.03850	.03900	.01000	.00910	.03920	.03500	.03920	.03900
---	---	---	---	---	---	---	---	---	---	---
Sum	.9998	.9147	1.0000	1.0173	1.0000	.9739	1.0000	.9662	1.0000	1.0030

* Below analytical detection limit or not analyzed; as-batched value assumed.

(a) Co_2O_3, Dy_2O_3, Eu_2O_3, Gd_2O_3, PbO, and V_2O_3 were analyzed as occurring at above analytical detection limit amounts in some CVS2-52 and CVS2-55 to CVS2-58 glasses. These oxides had not been previously detected above detection limits for CVS-I or CVS-II Phase 1 or 2 glasses.

TABLE A.2. As-Batched (B) and Analyzed (A) Compositions (in mass fractions) for CVS-II Phase 1 and Phase 2 Glasses (continued)

Oxide	CVS2-56[a] B	CVS2-56[a] A	CVS2-57[a] B	CVS2-57[a] A	CVS2-58[a] B	CVS2-58[a] A
Al_2O_3	.02350	.0260	.02350	.0250	.1500	.1500
B_2O_3	.10480	.1100	.10480	.1100	.2000	.2050
BaO	.00000	.00000*	.00000	.00002	.00018	.0002
CaO	.00820	.0066	.00820	.00665	.02000	.0190
CdO	.00000	.00000*	.00000	.00000*	.00134	.0012
CeO_2	.00000	.00015	.00000	.00000*	.00027	.0002
Co_2O_3	.00000	.00010	.00000	.0001	.00000	.00010
Cr_2O_3	.00715	.0066	.00536	.0049	.00022	.0002
Cs_2O	.00000	.00000*	.00000	.00000*	.00027	.00027
CuO	.00000	.0066	.00000	.00000*	.00027	.00025
Dy_2O_3	.00000	.00010	.00000	.00000*	.00000	.00000*
Eu_2O_3	.00000	.00002	.00000	.00000*	.00000	.00000*
F	.00298	.00298*	.00298	.00298*	.00053	.00053*
Fe_2O_3	.07330	.0760	.07330	.07550	.02000	.02100
Gd_2O_3	.00000	.00000*	.00000	.00030	.00000	.00000*
K_2O	.00000	.00000*	.00000	.00000*	.00000	.00000*
La_2O_3	.00000	.00000*	.00000	.00000*	.00119	.00100
Li_2O	.03730	.0405	.03730	.0385	.07000	.07150
MgO	.00840	.0069	.00840	.00675	.08000	.07550
MnO_2	.04649	.0385	.00000	.00004	.00027	.00025
MoO_3	.00000	.00000*	.00000	.00000*	.00054	.0005
Na_2O	.11290	.0940	.11290	.10000	.05000	.0670
Nd_2O_3	.00000	.00000*	.05126	.05050	.00221	.00195
NiO	.00000	.00000*	.00000	.00000*	.00103	.0007
P_2O_5	.00000	.0004	.00000	.0006	.00018	.0004
PbO	.00000	.00010	.00000	.00020	.00000	.00010
PdO	.00000	.00000*	.00000	.00000*	.00009	.00009*
Pr_6O_{11}	.00000	.00000*	.00000	.00000*	.00018	.00018*
Rb_2O	.00000	.00000*	.00000	.00000*	.00009	.00009*
Rh_2O_3	.00000	.00000*	.00000	.00000*	.00009	.00009*
RuO_2	.00000	.00000*	.00000	.00000*	.00027	.0002
SO_3	.00298	.00298*	.00000	.00000*	.00049	.00049*
SiO_2	.53280	.5000	.53280	.49000	.39000	.3600
Sm_2O_3	.00000	.00000*	.00000	.00000*	.00000	.00000*
SrO	.00000	.00000*	.00000	.00000*	.00018	.0002
TiO_2	.00000	.0002	.00000	.0002	.00000	.00010
UO_2	.00000	.0020	.00000	.0085	.00000	.00020
V_2O_3	.00000	.00000*	.00000	.00002	.00000	.00002
Y_2O_3	.00000	.00000*	.00000	.00000*	.00009	.0001
ZnO	.00000	.00000*	.0000	.00000*	.0000	.00000*
ZrO_2	.03920	.03700	.03920	.03800	.01000	.0086
Sum	1.0000	.9577	1.0000	.9588	1.0000	.9872

* Below analytical detection limit or not analyzed; as-batched value assumed.

(a) Co_2O_3, Dy_2O_3, Eu_2O_3, Gd_2O_3, PbO, and V_2O_3 were analyzed as occurring at above analytical detection limit amounts in some CVS2-52 and CVS2-55 to CVS2-58 glasses. These oxides had not been previously detected above detection limits for CVS-I or CVS-II Phase 1 or 2 glasses.

TABLE A.3. As-Batched (B) and Analyzed (A) Compositions (in mass fractions) for Selected CVS-II Phase 3 Glasses

	CVS2-59		CVS2-69		CVS2-70		CVS2-74		CVS2-79	
Oxide	B	A	B	A	B	A	B	A	B	A
Al2O3	.11500	.10550	.08160	.07740	.18190	.16700	.08160	.07410	.02000	.02000
As2O3	.00000	.00000*	.00000	.00000	.00106	.00075	.00000	.00000*	.00000	.00000*
B2O3	.17180	.16200	.07810	.07680	.14180	.13350	.07810	.07505	.16000	.15650
BaO	.00018	.00020	.00000	.00000*	.00000	.00000*	.00164	.00145	.00161	.00150
BeO	.00000	.00000*	.00000	.00000*	.00000	.00000*	.00000	.00000*	.00000	.00000*
CaO	.03750	.03305	.00790	.00590	.00080	.00080*	.00790	.00695	.00500	.00455
CdO	.00137	.00118	.00110	.00080	.00109	.00098	.01230	.01040	.01209	.01065
CeO2	.00027	.00027*	.00000	.00000*	.00131	.00095	.00246	.00205	.00242	.00210
Co2O3	.00000	.00015	.00000	.00000*	.00000	.00000*	.00000	.00000*	.00000	.00000*
Cr2O3	.00023	.00030	.02375	.02230	.01168	.01060	.00205	.00185	.00202	.00190
Cs2O	.00027	.00027*	.00000	.00000*	.00000	.00000*	.00246	.00246*	.00242	.00242*
CuO	.00027	.00028	.00183	.00165	.00164	.00151	.00246	.00216	.00242	.00226
Dy2O3	.00000	.00000*	.00000	.00000*	.00000	.00000*	.00000	.00000*	.00000	.00000*
Eu2O3	.00000	.00000*	.00000	.00000*	.00000	.00000*	.00000	.00000*	.00000	.00000*
F	.00055	.00055*	.00110	.00110*	.00000	.00000*	.00492	.00492*	.00483	.00483*
Fe2O3	.02000	.01725	.03340	.03060	.00800	.00641	.03340	.02930	.10500	.09990
FeO	.00000	.00000*	.00000	.00000*	.00000	.00000*	.00000	.00000*	.00000	.00000*
Gd2O3	.00000	.00000*	.00000	.00000*	.00000	.00000*	.00000	.00000*	.00000	.00000*
K2O	.00000	.00000*	.00000	.00000*	.00000	.00000*	.00000	.00000*	.00000	.00000*
La2O3	.00114	.00100	.00000	.00000*	.00055	.00040	.01025	.00842	.01007	.00861
Li2O	.07270	.06580	.07130	.06645	.06910	.06230	.07130	.06375	.01210	.01145
MgO	.00050	.00080	.00320	.00295	.00080	.00080*	.00320	.00270	.00500	.00435
MnO	.00000	.00000*	.00000	.00000*	.00000	.00000*	.00000	.00000*	.00000	.00000*
MnO2	.00027	.00041	.01495	.01420	.00353	.00334	.00246	.00215	.00242	.00237
MoO3	.00055	.00055	.00000	.00000*	.00000	.00000*	.00492	.00435	.00483	.00450
Na2O	.12680	.11400	.06640	.06550	.08120	.07460	.06640	.06230	.05000	.04750
Nd2O3	.00225	.00195	.00174	.00125	.00055	.00035	.02023	.01695	.01988	.01740
NiO	.00105	.00290	.00000	.00030	.00082	.00080	.00943	.00809	.00927	.00850
P2O5	.00018	.00018*	.03255	.01670	.00067	.00067*	.00164	.00200	.00161	.00150
PbO	.00000	.00000*	.00147	.00200	.00000	.00000*	.00000	.00000*	.00000	.00000*
PdO	.00009	.00009*	.00137	.00137*	.00137	.00137*	.00082	.00082*	.00081	.00081*
Pr6O11	.00018	.00018*	.00000	.00000*	.00000	.00000*	.00164	.00164*	.00161	.00161*
Rb2O	.00009	.00009*	.00000	.00000*	.00000	.00000*	.00082	.00082*	.00081	.00081*
Rh2O3	.00009	.00009*	.00064	.00064*	.00067	.00067*	.00082	.00082*	.00081	.00081*
RuO2	.00027	.00027*	.00064	.00064*	.00071	.00055	.00246	.00170	.00242	.00170
SeO2	.00000	.00000*	.00357	.00357*	.00353	.00353*	.00000	.00000*	.00000	.00000*
SO3	.00050	.00050*	.00688	.00688*	.00027	.00027*	.00452	.00452*	.00444	.00444*
Sb2O3	.00000	.00000*	.00000	.00000*	.00049	.00049*	.00000	.00000*	.00000	.00000*
SiO2	.43800	.39800	.56600	.52400	.48540	.44600	.56600	.51650	.54790	.52400
Sm2O3	.00009	.00009*	.00000	.00000*	.00000	.00000*	.00082	.00082*	.00081	.00081*
SrO	.00018	.00019	.00000	.00000*	.00000	.00000*	.00164	.00145	.00161	.00150
TeO2	.00000	.00000*	.00000	.00000*	.00055	.00055*	.00000	.00000*	.00000	.00000*
ThO2	.00000	.00000*	.00000	.00000*	.00000	.00000*	.00000	.00000*	.00000	.00000*
TiO2	.00000	.00021	.00000	.00028	.00000	.00010	.00000	.00016	.00000	.00015
UO2	.00000	.00000*	.00000	.00000*	.00000	.00000*	.00000	.00000*	.00000	.00000*
V2O3	.00000	.00000*	.00000	.00000*	.00000	.00000*	.00000	.00000*	.00000	.00000*
Y2O3	.00009	.00009*	.00000	.00000*	.00000	.00000*	.00082	.00070	.00081	.00072
ZnO	.00000	.00000*	.00000	.00000*	.00000	.00000*	.00000	.00000*	.00000	.00000*
ZrO2	.00750	.00640	.00050	.00050*	.00050	.00063	.00050	.00075	.00500	.00480
Sum	1.0000	.91479	1.0000	.92378	1.0000	.91992	1.0000	.91210	1.0000	.95495

* Below analytical detection limit or not analyzed; as-batched value assumed.

TABLE A.3. As-Batched (B) and Analyzed (A) Compositions (in mass fractions) for Selected CVS-II Phase 3 Glasses (continued)

	CVS2-91		CVS2-95		CVS2-96		CVS2-97		CVS2-98	
Oxide	B	A	B	A	B	A	B	A	B	A
Al2O3	.02000	.01850	.03670	.03390	.06360	.05965	.02350	.02870	.13880	.12750
As2O3	.00000	.00000*	.00000	.00000*	.00000	.00000*	.00000	.00000*	.00000	.00000*
B2O3	.16000	.15450	.11120	.10550	.11420	.11200	.10480	.09940	.17430	.16450
BaO	.00161	.00145	.00055	.00055*	.00073	.00068	.00099	.00233	.00018	.00020
BeO	.00000	.00000*	.00000	.00000*	.00000	.00000*	.00000	.00000*	.00000	.00000*
CaO	.00500	.00440	.01130	.01070	.02750	.02470	.00820	.00975	.00000	.00081
CdO	.01209	.01024	.00416	.00416*	.00547	.00473	.00653	.00601	.00134	.00112
CeO2	.00242	.00205	.00083	.00083*	.00109	.00100	.00017	.00017*	.00027	.00027*
Co2O3	.00000	.00000*	.00000	.00009	.00000	.00000*	.00000	.00043	.00000	.00000*
Cr2O3	.00202	.00185	.00069	.00069*	.00091	.00090	.00130	.00105	.00022	.00025
Cs2O	.00242	.00242*	.00083	.00083*	.00109	.00109*	.00151	.00151*	.00027	.00027*
CuO	.00242	.00219	.00083	.00083*	.00109	.00100	.00151	.00199	.00027	.00031
Dy2O3	.00000	.00000*	.00000	.00000*	.00000	.00000*	.00000	.00000*	.00000	.00000*
Eu2O3	.00000	.00000*	.00000	.00000*	.00000	.00000*	.00000	.00000*	.00000	.00000*
F	.00483	.00483*	.00166	.00166*	.00219	.00219*	.00191	.00191*	.00054	.00054*
Fe2O3	.00500	.00356	.08970	.08325	.05680	.05270	.07330	.05900	.02000	.01720
FeO	.00000	.00000*	.00000	.00000*	.00000	.00000*	.00000	.00000*	.00000	.00000*
Gd2O3	.00000	.00000*	.00000	.00000*	.00000	.00000*	.00000	.00000*	.00000	.00000*
K2O	.00000	.00000*	.00000	.00000*	.00000	.00000*	.00000	.00000*	.00000	.00000*
La2O3	.01007	.00831	.00347	.00345	.00455	.00385	.01548	.01960	.00112	.00073
Li2O	.01000	.00910	.04280	.04065	.03760	.03465	.03730	.03280	.03690	.03330
MgO	.04000	.03420	.01660	.01400	.03630	.03170	.00840	.00775	.00000	.00000*
MnO	.00000	.00000*	.00000	.00000*	.00000	.00000*	.00000	.00000*	.00000	.00000*
MnO2	.00242	.00222	.00083	.01250	.00109	.00110	.00159	.00230	.00027	.00027
MoO3	.00483	.00430	.00166	.00166*	.00219	.00200	.00312	.00290	.00054	.00050
Na2O	.10500	.09990	.16710	.16000	.10030	.09940	.11290	.11400	.20000	.18400
Nd2O3	.01988	.01665	.00685	.00685*	.00899	.00770	.00573	.00655	.00221	.00150
NiO	.00927	.00808	.00319	.00550	.00419	.00360	.00603	.00600	.00103	.00084
P2O5	.00161	.00200	.00055	.00055*	.00073	.00073*	.00099	.00150	.00018	.00018*
PbO	.00000	.00000*	.00000	.00000*	.00000	.00000*	.00000	.00000*	.00000	.00000*
PdO	.00081	.00081*	.00028	.00028*	.00037	.00037*	.00000	.00000*	.00009	.00009*
Pr6O11	.00161	.00161*	.00055	.00055*	.00073	.00073*	.00189	.00189*	.00018	.00018*
Rb2O	.00081	.00081*	.00028	.00028*	.00037	.00037*	.00000	.00000*	.00009	.00009*
Rh2O3	.00081	.00081*	.00028	.00028*	.00037	.00037*	.00000	.00000*	.00009	.00009*
RuO2	.00242	.00175	.00083	.00083*	.00109	.00109*	.00152	.00100	.00027	.00027*
SeO2	.00000	.00000*	.00000	.00000*	.00000	.00000*	.00000	.00000*	.00000	.00000*
SO3	.00444	.00444*	.00153	.00153*	.00201	.00201*	.00442	.00442*	.00049	.00049*
Sb2O3	.00000	.00000*	.00000	.00000*	.00000	.00000*	.00000	.00000*	.00000	.00000*
SiO2	.56000	.48950	.48950	.46300	.48010	.44600	.53280	.48500	.42000	.38400
Sm2O3	.00081	.00081*	.00028	.00028*	.00037	.00037*	.00000	.00000*	.00009	.00009*
SrO	.00161	.00144	.00055	.00055*	.00073	.00068	.00000	.00000*	.00018	.00014
TeO2	.00000	.00000*	.00000	.00000*	.00000	.00000*	.00000	.00000*	.00000	.00000*
ThO2	.00000	.00000*	.00000	.00000*	.00000	.00000*	.00000	.00000*	.00000	.00000*
TiO2	.00000	.00023	.00000	.00649	.00000	.00028	.00000	.00115	.00000	.00009
UO2	.00000	.00000*	.00000	.00000*	.00000	.00000*	.00000	.00000*	.00000	.00000*
V2O3	.00000	.00000*	.00000	.00000*	.00000	.00000*	.00000	.00000*	.00000	.00000*
Y2O3	.00081	.00070	.00028	.00028*	.00037	.00032	.00000	.00000*	.00009	.00009*
ZnO	.00000	.00000*	.00000	.00000*	.00000	.00000*	.00492	.00480	.00000	.00000*
ZrO2	.00500	.00498	.00410	.00360	.04290	.03980	.03920	.03670	.00000	.00010
---	---	---	---	---	---	---	---	---	---	---
Sum	1.0000	.89864	1.0000	.96610	1.0000	.93776	1.0000	.94061	1.0000	.92001

* Below analytical detection limit or not analyzed; as-batched value assumed.

TABLE A.3. As-Batched (B) and Analyzed (A) Compositions (in mass fractions) for Selected CVS-II Phase 3 Glasses (continued)

	CVS2-101		ARM-1		ARG-1	
Oxide	B	A	N (a)	A	N (a)	A
Al2O3	.0367	.03410	.0559	.05300	.0453	.04410
As2O3						
B2O3	.1112	.10550	.1130	.11200	.0839	.08100
BaO			.0066	.00614	.0004	.00083
BeO						.00006
CaO	.0113	.01000	.0223	.02060	.0153	.01335
CdO	.0000	.00009		.00005		
CeO2			.0151	.01250		
Co2O3	.0000	.00009				.00009
Cr2O3					.00096	.00094
Cs2O			.0116	.0116*		
CuO					.00008	.00008*
Dy2O3						
Eu2O3						
F						
Fe2O3	.0808	.08495		.00045	.1385	.13200
FeO	.0089	(b)				
Gd2O3						
K2O	.0004	.00000			.0259	.02500
La2O3	.0041	.00380		.00014		
Li2O	.0428	.04150	.0508	.04730	.0326	.02990
MgO	.0166	.01550			.0085	.00770
MnO	.0134	.00000				
MnO2	.0000	.01530		.00010	.0239	.02160
MoO3			.0167	.01770		
Na2O	.1671	.16500	.0967	.10100	.1136	.11000
Nd2O3			.0596	.05060		
NiO	.0061	.00540			.0103	.01010
P2O5			.0065	.00530	.0025	.00200
PbO				.00050		.00060
PdO						
Pr6O11						
Rb2O						
Rh2O3						
RuO2						
SeO2						
SO3						
Sb2O3						
SiO2	.4895	.46100	.4650	.43700	.4860	.42800
Sm2O3						
SrO			.0045	.00452	.00006	.00006
TeO2						
ThO2						
TiO2	.0071	.00641	.0321	.03155	.0112	.01020
UO2						
V2O3						.00015
Y2O3						
ZnO	.0000	.00020	.0146	.01460	.00014	.00020
ZrO2	.0041	.00430	.0180	.01820	.00128	.00120
---	---	---	---	---	---	---
Sum	1.0000	.95314	.9890	.94485	1.0004	.91916

* Below analytical detection limit or not analyzed; as-batched value assumed.

(a) ARM-1 and ARG-1 are reference/standard glasses whose nominal compositions are given. These two glasses were not part of CVS, but were merely analyzed along with the CVS glasses.

(b) All Fe was considered to be Fe_2O_3.

TABLE A.4. Results of Statistical Tests on Differences Between Analyzed and As-Batched Values of Oxide Components for CVS-I Glasses

Oxide	Analyzed - As-Batched Differences[b] Mean	SD	SE	t	Significantly Different at 95% Confidence Level
Al2O3 (a)	.00062	.001989	.00041475	1.48	
B2O3 (a)	.00102	.002823	.00058858	1.73	
BaO	-.00003	.000043	.00000899	-2.95	x (c)
CaO (a)	.00078	.000862	.00017966	4.33	x (d)
CdO	.00004	.000411	.00008578	0.47	
CeO2	.00011	.000166	.00003461	3.27	x (d)
Cr2O3	.00006	.000086	.00001796	3.27	x (c)
Cs2O	-.00010	.000074	.00001549	-6.20	x (c)
CuO	-.00001	.000086	.00001802	-0.41	
F	.00000	.000000	.00000000	----	
Fe2O3 (a)	-.00042	.001302	.00027141	-1.54	
K2O	.00600	.004034	.00084114	7.13	x (e)
La2O3	-.00014	.000311	.00006488	-2.10	x (d)
Li2O (a)	-.00372	.003917	.00081676	-4.56	x
MgO (a)	-.00093	.001674	.00034904	-2.65	x (d)
MnO2	.00007	.000048	.00000994	6.78	x (c)
MoO3	-.00001	.000112	.00002337	-0.33	
Na2O (a)	-.00263	.006102	.00127235	-2.06	
Nd2O3	-.00120	.001945	.00040548	-2.95	x
NiO	.00022	.000310	.00006462	3.47	x (d)
P2O5	.00000	.000000	.00000000	----	
PdO	.00000	.000000	.00000000	----	
Pr6O11	.00000	.000000	.00000000	----	
Rb2O	.00000	.000000	.00000000	----	
Rh2O3	.00000	.000000	.00000000	----	
RuO2	-.00009	.000264	.00005514	-1.66	
SO3	.00000	.000000	.00000000	----	
SiO2 (a)	-.01016	.009469	.00197435	-5.15	x
Sm2O3	.00000	.000000	.00000000	----	
SrO	.00001	.000047	.00000979	0.84	
TiO2	.00012	.000112	.00002327	5.03	x (d),(e)
Y2O3	.00001	.000034	.00000719	1.51	
ZrO2 (a)	-.00289	.007660	.00159719	-1.81	

(a) Major CVS component.

(b) SD = standard deviation; SE = standard error ($SD/\sqrt{23}$); t = t-statistic (Mean/SE), which is compared to $\pm t_{0.975}(22) = \pm 2.074$.

(c) Average absolute difference is less than or equal to 0.0001 (0.01 wt%), which is not of practical significance.

(d) Average absolute difference is less than or equal to 0.001 (0.1 wt%), which may not be of practical significance.

(e) Not nominally contained in CVS-I glasses.

TABLE A.5. Results of Statistical Tests on Differences Between Analyzed and As-Batched Values of Oxide Components for CVS-II Phase 1 Glasses

Oxide	Analyzed - As-Batched Differences[b] Mean	SD	SE	t	Significantly Different at 95% Confidence Level
Al2O3 (a)	-0.00157	0.003427	0.000786	-2.00	
B2O3 (a)	-0.00065	0.003961	0.000909	-0.71	
BaO	0.00025	0.001089	0.000250	1.00	
CaO (a)	-0.00064	0.005695	0.001307	-0.49	
CdO	-0.00051	0.001259	0.000289	-1.75	x (d)
CeO2	0.00048	0.000301	0.000069	7.04	x (d)
Cr2O3	0.00009	0.000386	0.000089	0.96	
Cs2O	-0.00020	0.000296	0.000068	-2.94	x (d)
CuO	-0.00002	0.000163	0.000037	-0.56	
F	0.00000	0.000000	0.000000	----	
Fe2O3 (a)	-0.00274	0.003260	0.000748	-3.66	x
K2O	0.01713	0.010764	0.002469	6.94	x (e)
La2O3	0.00124	0.005970	0.001370	0.91	
Li2O (a)	-0.00514	0.004672	0.001072	-4.79	x
MgO (a)	0.00061	0.006132	0.001407	0.43	
MnO2	0.00098	0.000366	0.000084	11.68	x (d)
MoO3	-0.00010	0.000116	0.000027	-3.69	x (c)
Na2O (a)	-0.00619	0.007684	0.001763	-3.51	x
Nd2O3	-0.00111	0.002107	0.000483	-2.29	x
NiO	0.00059	0.001142	0.000262	2.23	x (d)
P2O5	0.00000	0.000000	0.000000	----	
PdO	0.00000	0.000000	0.000000	----	
Pr6O11	0.00000	0.000000	0.000000	----	
Rb2O	0.00000	0.000000	0.000000	----	
Rh2O3	0.00000	0.000000	0.000000	----	
RuO2	0.00011	0.000256	0.000059	1.89	
SO3	0.00000	0.000000	0.000000	----	
SiO2 (a)	0.00018	0.009797	0.002248	0.08	
Sm2O3	0.00000	0.000000	0.000000	----	
SrO	-0.00002	0.000062	0.000014	-1.70	
TiO2	0.00030	0.000210	0.000048	6.33	x (d),(e)
Y2O3	0.00006	0.000036	0.000008	-0.71	
ZrO2 (a)	-0.00271	0.003619	0.000830	-3.26	x

(a) Major CVS component.

(b) SD = standard deviation; SE = standard error ($SD/\sqrt{19}$); t = t-statistic (Mean/SE), which is compared to $\pm t_{0.975}(18) = \pm 2.101$.

(c) Average absolute difference is less than or equal to 0.0001 (0.01 wt%), which is not of practical significance.

(d) Average absolute difference is less than or equal to 0.001 (0.1 wt%), which may not be of practical significance.

(e) Not nominally contained in CVS-II Phase 1 glasses.

TABLE A.6. Results of Statistical Tests on Differences Between Analyzed and As-Batched Values of Oxide Components for CVS-II Phase 2 Glasses CVS2-20 to CVS2-51

Oxide	Analyzed - As-Batched Differences[b] Mean	SD	SE	t	Significantly Different at 95% Confidence Level
Al2O3 (a)	-0.00150	0.001947	0.000344	-4.36	x
B2O3 (a)	-0.00184	0.003268	0.000578	-3.19	x
BaO	0.00029	0.001144	0.000202	1.43	
CaO (a)	-0.00085	0.001663	0.000294	-2.89	x (d)
CdO	-0.00051	0.000754	0.000133	-3.85	x (d)
CeO2	0.00109	0.001702	0.000301	3.61	x
Cr2O3	-0.00010	0.000223	0.000039	-2.52	x (c)
Cs2O	0.00022	0.000406	0.000072	3.02	x (d)
CuO	-0.00010	0.000201	0.000036	-2.84	x (c)
F	0.00000	0.000000	0.000000	----	
Fe2O3 (a)	-0.00309	0.003674	0.000649	-4.76	x
K2O	0.00069	0.003542	0.000626	1.10	(e)
La2O3	-0.00036	0.001113	0.000197	-1.82	
Li2O (a)	-0.00289	0.001994	0.000352	-8.21	x
MgO (a)	-0.00274	0.003673	0.000649	-4.22	x
MnO2	-0.00008	0.000182	0.000032	-2.49	x (c)
MoO3	0.00019	0.000228	0.000040	-4.73	x (d)
Na2O (a)	0.02821	0.017961	0.003175	8.88	x
Nd2O3	-0.00080	0.001098	0.000194	-4.13	x (d)
NiO	-0.00033	0.000353	0.000062	-5.21	x (d)
P2O5	0.00011	0.000267	0.000047	2.28	x (d)
PdO	0.00000	0.000000	0.000000	----	
Pr6O11	0.00000	0.000000	0.000000	----	
Rb2O	0.00000	0.000000	0.000000	----	
Rh2O3	0.00000	0.000000	0.000000	----	
RuO2	-0.00043	0.000455	0.000080	-5.38	x (d)
SO3	0.00000	0.000000	0.000000	----	
SiO2 (a)	-0.02458	0.019389	0.003428	-7.17	x
Sm2O3	0.00000	0.000000	0.000000	----	
SrO	-0.00004	0.000086	0.000015	-2.49	x (c)
TiO2	0.00020	0.000198	0.000035	5.74	x (d),(e)
Y2O3	-0.00003	0.000059	0.000010	-2.98	x (c)
ZrO2 (a)	-0.00324	0.003863	0.000683	-4.75	x

(a) Major CVS component.

(b) SD = standard deviation; SE = standard error ($SD/\sqrt{32}$); t = t-statistic (Mean/SE), which is compared to $\pm t_{0.975}(31) = \pm 2.040$.

(c) Average absolute difference is less than or equal to 0.0001 (0.01 wt%), which is not of practical significance.

(d) Average absolute difference is less than or equal to 0.001 (0.1 wt%), which may not be of practical significance.

(e) Not nominally contained in CVS-II Phase 2 glasses.

TABLE A.7. Results of Statistical Tests on Differences Between Analyzed and As-Batched Values of Oxide Components for Selected CVS-II Phase 3 Glasses

Oxide	Analyzed - As-Batched Differences[b] Mean	SD	SE	t	Significantly Different at 95% Confidence Level
Al2O3 (a)	-0.00482	0.005635	0.001699	-2.83	x
As2O3	-0.00003	0.000093	0.000028	-1.00	
B2O3 (a)	-0.00547	0.002889	0.000871	-6.29	x
BaO	0.00008	0.000424	0.000128	0.62	
CaO (a)	-0.00098	0.001662	0.000501	-1.96	
CdO	-0.00065	0.000737	0.000222	-2.94	x (d)
CeO2	-0.00014	0.000180	0.000054	-2.59	x (d)
Co2O3	0.00007	0.000131	0.000039	1.75	
Cr2O3	-0.00029	0.000500	0.000151	-1.92	
Cs2O	0.00000	0.000000	0.000000	----	
CuO	-0.00005	0.000207	0.000062	-0.81	
F	0.00000	0.000000	0.000000	----	
Fe2O3 (a)	-0.00375	0.004426	0.001334	-2.81	x
K2O	-0.00004	0.000121	0.000036	-1.00	
La2O3	-0.00024	0.001603	0.000483	-0.49	
Li2O (a)	-0.00383	0.002496	0.000753	-5.09	x
MgO (a)	-0.00144	0.002029	0.000612	-2.36	x
MnO2	0.00239	0.005554	0.001675	1.43	
MoO3	-0.00017	0.000219	0.000066	-2.59	x (d)
Na2O (a)	-0.00518	0.005242	0.001580	-3.28	x
Nd2O3	-0.00101	0.001387	0.000418	-2.43	x
NiO	-0.00003	0.001162	0.000351	-0.10	
P2O5	-0.00133	0.004818	0.001453	-0.92	
PbO	0.00005	0.000160	0.000048	1.00	
PdO	0.00000	0.000000	0.000000	----	
Pr6O11	0.00000	0.000000	0.000000	----	
Rb2O	0.00000	0.000000	0.000000	----	
Rh2O3	0.00000	0.000000	0.000000	----	
RuO2	-0.00026	0.000334	0.000101	-2.56	x (d)
SO3	0.00000	0.000000	0.000000	----	
Sb2O3	0.00000	0.000000	0.000000	----	
SiO2 (a)	-0.03984	0.013076	0.003943	-10.10	x
Sm2O3	0.00000	0.000000	0.000000	----	
SrO	-0.00005	0.000073	0.000022	-2.26	x (c)
TiO2	0.00077	0.001943	0.000586	1.31	
UO2	0.00000	0.000000	0.000000	----	
Y2O3	-0.00003	0.000050	0.000015	-2.25	x (c)
ZnO	0.00000	0.000073	0.000022	0.33	
ZrO2 (a)	-0.00061	0.001156	0.000349	-1.76	

(a) Major CVS component.

(b) SD = standard deviation; SE = standard error ($SD/\sqrt{11}$); t = t-statistic (Mean/SE), which is compared to $\pm t_{0.975}(10) = \pm 2.228$.

(c) Average absolute difference is less than or equal to 0.0001 (0.01 wt%), which is not of practical significance.

(d) Average absolute difference is less than or equal to 0.001 (0.1 wt%), which may not be of practical significance.

TABLE A.8. Summary of Analyzed - Batched (A-B) Differences By Oxide Component for CVS-I, CVS-II Phase 1, CVS-II Phase 2, and CVS-II Phase 3 Glasses

Oxide	CVS-I A-B Mean	CVS-I # of 23 (b)	CVS-II Phase 1 A-B Mean	CVS-II Phase 1 # of 19 (b)	CVS-II Phase 2 (CVS2-20 to -51) A-B Mean	CVS-II Phase 2 # of 32 (b)	CVS-II Phase 3 (selected glasses) A-B Mean	CVS-II Phase 3 # of 11 (b)
Al2O3 (a)	0.00062	20	-0.00157	14	-0.00150 (e)	26	-0.00482 (e)	9
As2O3.	-----	--	-----	--	-----	--	-0.00003	1
B2O3 (a)	0.00102	19	-0.00065	11	-0.00184 (e)	26	-0.00547 (e)	11
BaO	-0.00003 (c)	18	0.00025	15	0.00029	16	0.00008	3
CaO (a)	0.00078 (d)	21	-0.00064	12	-0.00085 (d)	17	-0.00098	8
CdO	0.00004	20	-0.00051 (d)	14	-0.00051 (d)	32	-0.00065 (d)	9
CeO2	0.00011 (d)	23	0.00048 (d)	18	0.00109 (e)	18	-0.00014 (d)	5
Co2O3	-----	--	-----	--	-----	--	0.00007	4
Cr2O3	0.00006 (c)	22	0.00009	16	-0.00010 (c)	24	-0.00029	7
Cs2O	-0.00010 (c)	22	-0.00020 (d)	17	0.00022 (d)	28	-----	--
CuO	-0.00001	10	-0.00002	10	-0.00010 (c)	27	-0.00005	6
F	-----	--	-----	--	-----	--	-----	--
Fe2O3 (a)	-0.00042	12	-0.00274 (e)	17	-0.00309 (e)	31	-0.00375 (e)	10
K2O (f)	0.00600 (e)	23	0.01713 (e)	19	0.00069	32	-0.00004	1
La2O3	-0.00014 (d)	13	0.00124	17	-0.00036	31	-0.00024	9
Li2O (a)	-0.00372 (e)	22	-0.00514 (e)	19	-0.00289 (e)	30	-0.00383 (e)	11
MgO (a)	-0.00093 (d)	11	0.00061	13	-0.00274 (e)	18	-0.00144 (e)	8
MnO2	0.00007 (c)	23	0.00098 (d)	18	-0.00008 (c)	23	0.00239	4
MoO3	0.00001	19	-0.00010 (c)	15	-0.00019 (d)	31	-0.00017 (d)	6
Na2O (a)	-0.00263	16	-0.00619 (e)	15	0.02821 (e)	32	-0.00518 (e)	10
Nd2O3	-0.00120 (e)	23	-0.00111 (e)	17	-0.00080 (d)	31	-0.00101 (e)	9
NiO	0.00022 (d)	20	0.00059 (d)	17	-0.00033 (d)	31	-0.00003	8
P2O5	-----	--	-----	--	0.00011 (d)	24	-0.00133	2
PdO	-----	--	-----	--	-----	--	-----	--
Pr6O11	-----	--	-----	--	-----	--	-----	--
Rb2O	-----	--	-----	--	-----	--	-----	--
Rh2O3	-----	--	-----	--	-----	--	-----	--
RuO2	-0.00009	16	0.00011	15	-0.00043 (d)	32	-0.00026 (d)	5
SO3	-----	--	-----	--	-----	--	-----	--
SiO2 (a)	-0.01016 (e)	22	0.00018	11	-0.02458 (e)	32	-0.03984 (e)	11
Sm2O3	-----	--	-----	--	-----	--	-----	--
SrO	0.00001	16	-0.00002	9	-0.00004 (c)	17	-0.00005 (c)	5
TiO2 (f)	0.00012 (d)	23	0.00030 (d)	19	0.00020 (d)	32	0.00077	10
Y2O3	0.00001	18	-0.00006	10	-0.00003 (c)	16	-0.00003 (c)	4
ZrO2 (a)	-0.00289	10	-0.00271 (e)	12	-0.00324 (e)	17	-0.00061	6

(a) Major CVS component.

(b) Number of glasses of total that had Analyzed - Batched difference of the same sign as the mean difference shown. The total number of glasses for CVS-I is 19, for CVS-II Phase 1 is 23, for CVS-II Phase 2 (CVS2-20 to CVS2-51) is 32, and for CVS-II Phase 3 (selected glasses) is 11.

(c) Statistically different from zero at 95% confidence level, but average absolute difference is less than or equal to 0.0001 (0.01 wt%), which is not of practical significance.

(d) Statistically different from zero at 95% confidence level, but average absolute difference is less than or equal to 0.001 (0.1 wt%), which may not be of practical significance.

(e) Statistically different from zero at 95% confidence level, with average absolute difference greater than 0.001.

(f) Not nominally contained in CVS glasses, except CVS2-101 in CVS-II Phase 3.

TABLE A.9. As-Batched and Analyzed Compositions (in mass fractions) for Six Replicate Analyses of CVS-I Glass CVS1-19 Conducted Over Three Months

		Replicate Analyses and Dates[a]					
K/Ni Fusion		4/20/89	4/15/89	5/17/89	6/30/89	6/30/89	7/25/89
Na/Zr Fusion		4/21/89	4/20/89	5/17/89	6/30/89	6/30/89	7/25/89
Oxide	As-Batched	19-1	19-2	19-3	19-4	19-5	19-6
Al2O3	.0636	.0636	.0630	.0668	.0626	.0630	.0637
B2O3	.1142	.1150	.1140	.1200	.1140	.1140	.1170
BaO	.0007	.00071	.00070	.00073	.00071	.00071	.00070
CaO	.0275	.0289	.0275	.0288	.0277	.0290	.0273
CdO	.0055	.00565	.00558	.00564	.00532	.00536	.00532
CeO2	.0011	.0014	.0013	.0011(b)	.0012	.0011	.00116
Cr2O3	.0009	.00095	.0010	.00102	.00100	.00099	.00091
Cs2O	.0011	.0010	.0010	.0012	.0012	.0012	.0010
CuO	.0011	.00109	.00103	.00112	.00110	.00108	.00108
F	.0022	.0022(b)	.0022(b)	.0022(b)	.0022(b)	.0022(b)	.0022(b)
Fe2O3	.0568	.0559	.0548	.0558	.0544	.0548	.0542
K2O (c)	.0000	.0080	.0170	.0000(b)	.0040	.0040	.0000(b)
La2O3	.0046	.00436	.00429	.0045	.00428	.00432	.00430
Li2O	.0376	.0345	.0354	.0368	.0392	.0384	.0382
MgO	.0363	.0355	.0358	.0368	.0344	.0347	.0346
MnO2	.0011	.00118	.00115	.00120	.00113	.00113	.00114
MoO3	.0022	.00220	.00215	.00202	.0021	.00210	.0020
Na2O	.1003	.0964	.1110	.0976	.1020	.1000	.1050
Nd2O3	.0090	.00810	.00784	.00804	.00817	.00823	.0082
NiO	.0042	.00433	.00435	.00427	.00442	.00426	.0042
P2O5	.0007	.0007(b)	.0007(b)	.0007(b)	.0007(b)	.0007(b)	.0007(b)
PdO	.0004	.0004(b)	.0004(b)	.0004(b)	.0004(b)	.0004(b)	.0004(b)
Pr6O11	.0007	.0007(b)	.0007(b)	.0007(b)	.0007(b)	.0007(b)	.0007(b)
Rb2O	.0004	.0004(b)	.0004(b)	.0004(b)	.0004(b)	.0004(b)	.0004(b)
Rh2O3	.0004	.0004(b)	.0004(b)	.0004(b)	.0004(b)	.0004(b)	.0004(b)
RuO2	.0011	.0016	.0012	.0011(b)	.0011	.0011	.0011(b)
SO3	.0020	.0020(b)	.0020(b)	.0020(b)	.0020(b)	.0020(b)	.0020(b)
SiO2	.4801	.4760	.4670	.4900	.4700	.4700	.4710
Sm2O3	.0004	.0004(b)	.0004(b)	.0004(b)	.0004(b)	.0004(b)	.0004(b)
SrO	.0007	.00074	.00073	.00076	.00074	.00073	.00072
TiO2 (c)	.0000	.00017	.00015	.00016	.00026	.00026	.0000(b)
Y2O3	.0004	.00037	.00037	.00039	.00036	.00037	.00036
ZrO2	.0429	.0400	.0400	.0426	.0399	.0396	.0379
Sum	1.000	0.99485	1.00554	1.01565	0.98849	0.98764	0.98829

(a) Results are averages of K/Ni and Na/Zr fusions except for K and Ni (Na/Zr results used) and Na and Zr (K/Ni results used).

(b) Below analytical detection limit or not analyzed; as-batched value assumed.

(c) Not nominally contained in the glass.

TABLE A.10. Summary Statistics for Six Replicate Analyses of CVS-I Glass CVS1-19 Conducted Over Three Months

Oxide	As-Batched	Analyzed Values[b] Mean	SD	%RSD
Al2O3 (a)	.0636	.06378	.001534	2.40
B2O3 (a)	.1142	.11566	.002422	2.09
BaO	.0007	.00071	.000011	1.54
CaO (a)	.0275	.02820	.000780	2.77
CdO	.0055	.00547	.000161	2.94
CeO2	.0011	.00121	.000119	9.85 (c)
Cr2O3	.0009	.00097	.000041	4.16
Cs2O	.0011	.00110	.000110	9.96
CuO	.0011	.00108	.000030	2.78
F	.0022	.00220	.000000	0.00 (d)
Fe2O3 (a)	.0568	.05498	.000711	1.29
K2O	.0000	.00550	.006380	115.99 (e)
La2O3	.0046	.00434	.000082	1.90
Li2O (a)	.0376	.03708	.001846	4.98
MgO (a)	.0363	.03530	.000916	2.60
MnO2	.0011	.00115	.000029	2.49
MoO3	.0022	.00209	.000076	3.62
Na2O (a)	.1003	.10200	.005380	5.27
Nd2O3	.0090	.00809	.000143	1.77
NiO	.0042	.00430	.000078	1.80
P2O5	.0007	.00070	.000000	0.00 (d)
PdO	.0004	.00040	.000000	0.00 (d)
Pr6O11	.0007	.00070	.000000	0.00 (d)
Rb2O	.0004	.00040	.000000	0.00 (d)
Rh2O3	.0004	.00040	.000000	0.00 (d)
RuO2	.0011	.00120	.000200	16.67 (c)
SO3	.0020	.00200	.000000	0.00 (d)
SiO2 (a)	.4801	.47400	.008367	1.76
Sm2O3	.0004	.00040	.000000	0.00 (d)
SrO	.0007	.00073	.000014	1.86
TiO2	.0000	.00016	.000095	57.26 (e)
Y2O3	.0004	.00037	.000011	2.96
ZrO2 (a)	.0429	.04000	.001506	3.76

(a) Major CVS component.

(b) SD = standard deviation; %RSD = percent relative standard deviation.

(c) One or more values set equal to the as-batched value (since the oxide was not detected) were used for the computations.

(d) The oxide was not detected in any of the replicate analyses, and hence all data values were set equal to the as-batched value. This yields a mean equal to the as-batched value and zero SD and %RSD.

(e) Oxide was not present in the glass, but was detected in one or more replicates. The summary statistics are based on the positive values as well as the non-detects set equal to zero (the as-batched value). This yields a smaller mean and larger SD and %RSD than would be obtained by omitting non-detects.

TABLE A.11. As-Batched and Analyzed Compositions (in mass fractions) for Replicate Analyses of the CVS Internal Standard Glass

Oxide	Internal Standard As-Batched	Replicate Analyses and Dates 8/07/90 CVS2-19	7/12/91 CVS2-51	3/17/93 CVS2-97	Mean	SD	%RSD
Al2O3(a)	.0235	.0300	.0285	.0287	.02907	.00081	2.8
B2O3(a)	.1048	.1010	.0975	.0994	.09930	.00175	1.8
BaO	.00099	.00230	.00215	.00233	.00226	.00010	4.3
CaO(a)	.0082	.0108	.0099	.00975	.01015	.00057	5.6
CdO	.0065	.00641	.0059	.00601	.00611	.00027	4.4
CeO2	.00017	.00098	.0021	.00017(b)	.00108	.00097	89.5
Co2O3	.00000	.0000 (b)	.0000 (b)	.00043	.00014	.00025	173.2 (d)
Cr2O3	.00129	.00104	.00096	.00105	.00102	.00005	4.9
Cs2O	.0015	.00018	.00158	.0015 (b)	.00109	.00079	72.4
CuO	.00158	.00214	.00185	.00199	.00199	.00015	7.3
F	.0019	.0019 (b)	.0019 (b)	.0019 (b)	.00190	.00000	0.0 (c)
Fe2O3(a)	.0733	.0610	.0570	.0590	.05900	.00200	3.4
K2O	.0000	.0000 (b)	.0000 (b)	.0000 (b)	.00000	.00000	0.0 (c)
La2O3	.0154	.0212	.0205	.0196	.02043	.00080	3.9
Li2O(a)	.0373	.0344	.0320	.0328	.03307	.00122	3.7
MgO(a)	.0084	.00809	.0072	.00775	.00768	.00045	5.8
MnO2	.00158	.00241	.0021	.00230	.00227	.00016	6.9
MoO3	.0031	.00277	.0028	.0029	.00282	.00007	2.4
Na2O(a)	.1129	.1160	.1200	.1140	.11667	.00306	2.6
Nd2O3	.0057	.00700	.00645	.00655	.00667	.00029	4.4
NiO	.0060	.00629	.0059	.0060	.00606	.00020	3.3
P2O5	.00099	.00099(b)	.0015	.0015	.00133	.00029	22.1
PdO	.0000	.0000 (b)	.0000 (b)	.0000 (b)	.00000	.00000	0.0 (c)
Pr6O11	.00188	.00188(b)	.00188(b)	.00188(b)	.00188	.00000	0.0 (c)
Rb2O	.0000	.0000 (b)	.0000 (b)	.0000 (b)	.00000	.00000	0.0 (c)
Rh2O3	.0000	.0000 (b)	.0000 (b)	.0000 (b)	.00000	.00000	0.0 (c)
RuO2	.00151	.00151(b)	.0013	.0010	.00127	.00026	20.2
SO3	.0044	.0044 (b)	.0044 (b)	.0044 (b)	.00440	.00000	0.0 (c)
SiO2(a)	.5328	.5110	.4600	.4850	.48533	.02550	5.3
Sm2O3	.0000	.0000 (b)	.0000 (b)	.0000 (b)	.00000	.00000	0.0 (c)
SrO	.0000	.0000 (b)	.00008	.0000 (b)	.00003	.00005	173.2 (d)
TiO2	.0000	.00103	.00106	.00115	.00108	.00006	5.8
Y2O3	.0000	.0000 (b)	.0000 (b)	.0000 (b)	.00000	.00000	0.0 (c)
ZnO	.0049	.00482	.0043	.0048	.00464	.00029	6.3
ZrO2(a)	.0392	.0397	.0340	.0367	.03680	.00285	7.7
Sum	.9998	.9812	.9148	.9406			

(a) Major CVS component.

(b) Below analytical detection limit or not analyzed; as-batched value assumed.

(c) The oxide was not detected in any of the replicate analyses, and hence all data values were set equal to the as-batched value. This yields a mean equal to the as-batched value and zero SD and %RSD.

(d) Oxide was not present in the glass, but was detected in one or more replicates. The summary statistics are based on the positive values as well as the non-detects set equal to zero (the as-batched value). This yields a smaller mean and larger SD and %RSD than would be obtained by omitting non-detects.

TABLE A.12. Redox Ratios of Selected Test Glasses

Glass	Analytical Total Fe Mass Fraction	Analytical Fe^{2+}/Fe Ratio	Target Oxide Mass Fractions Fe_2O_3	Others
CVS1-12	0.1066	0.040	0.1500	0.0100
CVS1-17	0.1003	0.016	0.1400	0.1000
CVS1-20	0.0416	0.022	0.0568	0.0407
CVS2-10	0.0499	0.027	0.0669	0.0288
CVS2-25	0.1073	0.030	0.1500	0.0567
CVS2-30	0.0953	0.035	0.1320	0.0100

APPENDIX B

VISCOSITY AT TEMPERATURE DATA AND RESULTS FROM FITTING THE FULCHER EQUATION

APPENDIX B

VISCOSITY AT TEMPERATURE DATA AND RESULTS FROM FITTING THE FULCHER EQUATION

Viscosity was measured at three to five temperatures for each of the CVS-I glasses and a few CVS-II Phase 1 glasses. A revised viscosity procedure was used for the balance of CVS-II and involved obtaining 10 measurements at 7 temperatures between 950°C and 1250°C. See Section 5.2 for further discussion of the viscosity measurement procedures. Table B.1 contains the viscosity at temperature data.

Table B.2 contains the results of fitting the viscosity at temperature data for each glass to the Fulcher equation:

$$\ln \eta = A + B/(T - T_0), \tag{B.1}$$

where A, B, and T_0 are the Fulcher equation coefficients and T is temperature in °C. Included in Table B.2 are the estimated viscosity values at 1150°C (η_{1150}).

Note that it was necessary to omit from the fits a few viscosity at temperature values for some of the CVS-I glasses because of concern that results were affected by crystals in the glasses. The number of data points for each glass that were used to fit the Fulcher equation varied between two and five for the CVS-I glasses. Because the Fulcher equation contains three coefficients, the equation fit the data exactly or nearly exactly in these cases. Physically meaningless values of the Fulcher equation coefficients were obtained for glass CVS1-18, which only had three data points. The new 10-point viscosity measurement procedure was adopted in CVS-II to avoid some of these problems and to provide a better basis for modeling the dependence of viscosity on temperature.

TABLE B.1. Viscosity at Temperature Data for CVS-I and CVS-II Phase 1, 2, and 3 Glasses

Glass	ID #	Temp. (°C)	Viscosity (Pa·s)	Glass	ID #	Temp. (°C)	Viscosity (Pa·s)
CVS1-1	1	1250	2.54	CVS1-10	10	1449	7.98 (a)
CVS1-1	1	1150	5.81	CVS1-10	10	1350	13.83
CVS1-1	1	1050	16.69	CVS1-10	10	1250	30.80
CVS1-1	1	949	72.38	CVS1-10	10	1150	83.47
CVS1-2	2	1248	5.81	CVS1-11	11	1251	5.68
CVS1-2	2	1149	13.58	CVS1-11	11	1152	14.48
CVS1-2	2	1050	38.32	CVS1-11	11	1052	153.94 (c)
CVS1-2	2	951	156.46	CVS1-11	11	952	277.82 (c)
CVS1-3	3	1149	2.39	CVS1-12	12	1148	0.42
CVS1-3	3	1050	6.48	CVS1-12	12	1049	0.88
CVS1-3	3	951	21.78	CVS1-12	12	952	2.31
CVS1-3	3	852	121.81 (a)	CVS1-12	12	852	10.47 (a)
CVS1-4	4	1149	8.79	CVS1-12	12	752	131.67 (a)
CVS1-4	4	1051	28.95	CVS1-13	13	1247	1.55
CVS1-4	4	951	140.45	CVS1-13	13	1148	3.36
CVS1-5	5	1348	3.19	CVS1-13	13	1049	9.83
CVS1-5	5	1250	6.02	CVS1-13	13	949	46.75
CVS1-5	5	1150	13.18	CVS1-14	14	1249	1.41
CVS1-5	5	1050	35.11	CVS1-14	14	1150	3.37
CVS1-5	5	950	118.89	CVS1-14	14	1051	11.38
CVS1-6	6	1052	5.59	CVS1-14	14	950	61.29
CVS1-6	6	952	22.73	CVS1-15	15	1251	1.30
CVS1-6	6	851	171.56 (a)	CVS1-15	15	1151	2.53
CVS1-7	7	1348	6.75	CVS1-15	15	1051	5.88
CVS1-7	7	1248	19.47	CVS1-15	15	951	17.80
CVS1-7	7	1148	75.15	CVS1-15	15	851	79.16 (a)
CVS1-8	8	1350	4.57	CVS1-16	16	1348	2.89
CVS1-8	8	1252	10.21	CVS1-16	16	1249	6.48
CVS1-8	8	1152	36.16 (b)	CVS1-16	16	1149	18.02
CVS1-9	9	1251	1.58	CVS1-16	16	1049	113.81 (b)
CVS1-9	9	1152	3.98	CVS1-17	17	1252	1.04
CVS1-9	9	1052	36.16 (b)	CVS1-17	17	1152	2.22

(a) This data point was not used in modeling viscosity as a function of temperature and glass composition due to the outlying temperature value.

(b) This data point was not used in fitting the Fulcher equation for this glass (see Table B.2) nor in modeling viscosity as a function of temperature and glass composition due to the change in viscosity from initial to final determinations.

(c) This data point was not used in modeling viscosity as a function of temperature and glass composition due to the large viscosity value.

TABLE B.1. Viscosity at Temperature Data for CVS-I and CVS-II Phase 1, 2, and 3 Glasses (continued)

Glass	ID #	Temp. (°C)	Viscosity (Pa·s)	
CVS1-17	17	1052	5.83	
CVS1-17	17	953	23.10	
CVS1-18	18	1251	0.77	(f)
CVS1-18	18	1152	.	(d,f)
CVS1-18	18	1052	4.62	(f)
CVS1-18	18	952	12.23	(e,f)
CVS1-19	19	1251	2.46	
CVS1-19	19	1151	5.73	
CVS1-19	19	1051	16.35	
CVS1-19	19	951	64.53	
CVS1-20	20	1252	2.52	
CVS1-20	20	1152	5.51	
CVS1-20	20	1053	15.31	
CVS1-20	20	953	53.90	
CVS1-21	21	1249	4.14	
CVS1-21	21	1150	9.58	
CVS1-21	21	1049	28.12	(g)
CVS1-21	21	950	138.75	
CVS1-22	22	1351	4.43	
CVS1-22	22	1252	11.20	
CVS1-22	22	1153	35.97	(b)
CVS1-23	23	1252	2.66	
CVS1-23	23	1153	5.55	
CVS1-23	23	1053	13.91	
CVS1-23	23	953	44.72	
CVS2-1	24	1199	5.11	
CVS2-1	24	1123	9.81	
CVS2-1	24	1048	21.29	
CVS2-1	24	948	70.77	
CVS2-2	25	1149	6.21	
CVS2-2	25	1097	10.44	
CVS2-2	25	1047	17.22	
CVS2-2	25	1100	9.72	
CVS2-2	25	1150	6.14	
CVS2-2	25	1199	4.24	
CVS2-2	25	1249	2.90	
CVS2-2	25	1147	6.47	
CVS2-2	25	999	30.68	
CVS2-2	25	948	60.06	
CVS2-3	26	1148	5.60	
CVS2-3	26	1096	9.65	
CVS2-3	26	1048	15.67	
CVS2-3	26	1100	8.82	
CVS2-3	26	1150	5.54	
CVS2-3	26	1198	3.58	
CVS2-3	26	1249	2.56	
CVS2-3	26	1147	5.86	
CVS2-3	26	998	30.09	
CVS2-3	26	949	61.85	
CVS2-4	27	1198	4.37	
CVS2-4	27	1124	7.81	
CVS2-4	27	1048	17.36	
CVS2-4	27	948	59.47	
CVS2-5	28	1149	7.89	
CVS2-5	28	1097	13.60	
CVS2-5	28	1047	23.82	
CVS2-5	28	1100	13.65	
CVS2-5	28	1150	8.07	
CVS2-5	28	1200	5.41	

(b) This data point was not used in fitting the Fulcher equation for this glass (see Table B.2) nor in modeling viscosity as a function of temperature and glass composition due to the change in viscosity from initial to final determinations.

(d) Temperature data errors.

(e) Unknown noise in results.

(f) Results not used in fitting Fulcher-mixture or Arrhenius-mixture models in Section 7.1 of Chapter 7.

(g) Reduced time due to bumped spindle.

TABLE B.1. Viscosity at Temperature Data for CVS-I and CVS-II Phase 1, 2, and 3 Glasses (continued)

Glass	ID #	Temp. (°C)	Viscosity (Pa·s)
CVS2-5	28	1250	3.72
CVS2-5	28	1147	8.53
CVS2-5	28	999	46.32
CVS2-5	28	948	98.42
CVS2-6	29	1149	6.18
CVS2-6	29	1098	10.01
CVS2-6	29	1048	17.25
CVS2-6	29	1100	9.96
CVS2-6	29	1150	6.16
CVS2-6	29	1199	4.10
CVS2-6	29	1250	2.87
CVS2-6	29	1148	6.44
CVS2-6	29	999	33.30
CVS2-6	29	949	68.39
CVS2-7	30	1148	4.35
CVS2-7	30	1098	6.57
CVS2-7	30	1048	10.67
CVS2-7	30	1099	6.54
CVS2-7	30	1150	4.23
CVS2-7	30	1199	2.85
CVS2-7	30	1250	2.17
CVS2-7	30	1149	4.37
CVS2-7	30	998	19.03
CVS2-7	30	949	35.50
CVS2-8	31	1148	4.35
CVS2-8	31	1097	7.08
CVS2-8	31	1046	11.22
CVS2-8	31	1100	6.59
CVS2-8	31	1150	4.27
CVS2-8	31	1200	2.93
CVS2-8	31	1250	2.13
CVS2-8	31	1299	1.57
CVS2-8	31	1145	4.64
CVS2-8	31	995	19.86
CVS2-8	31	947	35.44
CVS2-9	32	1198	4.68
CVS2-9	32	1123	9.57
CVS2-9	32	1048	23.07
CVS2-9	32	943	111.05
CVS2-9A	32	1149	7.33
CVS2-9A	32	1099	12.43
CVS2-9A	32	1048	22.09
CVS2-9A	32	1100	12.01
CVS2-9A	32	1150	7.23
CVS2-9A	32	1200	4.52
CVS2-9A	32	1250	3.04
CVS2-9A	32	1148	7.38
CVS2-9A	32	999	42.76
CVS2-9A	32	948	93.07
CVS2-10	33	1149	8.67
CVS2-10	33	1098	14.54
CVS2-10	33	1048	24.11
CVS2-10	33	1100	14.24
CVS2-10	33	1150	8.70
CVS2-10	33	1200	6.07
CVS2-10	33	1250	4.39
CVS2-10	33	1147	9.43
CVS2-10	33	999	44.78
CVS2-10	33	949	88.75
CVS2-11	34	1198	2.01
CVS2-11	34	1123	3.98
CVS2-11	34	1048	9.22
CVS2-11	34	948	38.83
CVS2-12	35	1198	2.37
CVS2-12	35	1123	4.18
CVS2-12	35	1048	8.93
CVS2-12	35	945	35.62
CVS2-13	36	1148	7.17
CVS2-13	36	1096	12.50
CVS2-13	36	1046	20.52
CVS2-13	36	1099	11.77
CVS2-13	36	1149	7.02
CVS2-13	36	1199	4.85
CVS2-13	36	1248	3.32
CVS2-13	36	1146	7.67
CVS2-13	36	997	39.31
CVS2-13	36	948	72.40

TABLE B.1. Viscosity at Temperature Data for CVS-I and CVS-II Phase 1, 2, and 3 Glasses (continued)

Glass	ID #	Temp. (°C)	Viscosity (Pa·s)
CVS2-14	37	1149	2.88
CVS2-14	37	1099	5.03
CVS2-14	37	1048	8.86
CVS2-14	37	1100	4.99
CVS2-14	37	1150	2.88
CVS2-14	37	1199	2.00
CVS2-14	37	1249	1.33
CVS2-14	37	1148	2.99
CVS2-14	37	998	17.54
CVS2-14	37	949	38.36
CVS2-15	38	1149	4.40
CVS2-15	38	1099	7.18
CVS2-15	38	1048	11.71
CVS2-15	38	1100	6.95
CVS2-15	38	1150	4.44
CVS2-15	38	1199	2.94
CVS2-15	38	1249	2.16
CVS2-15	38	1148	4.74
CVS2-15	38	998	22.69
CVS2-15	38	949	42.40
CVS2-16	39	1199	4.27
CVS2-16	39	1123	8.38
CVS2-16	39	1048	18.88
CVS2-16	39	948	65.71
CVS2-16A	39	1148	6.68
CVS2-16A	39	1097	11.24
CVS2-16A	39	1047	18.61
CVS2-16A	39	1099	10.59
CVS2-16A	39	1149	6.71
CVS2-16A	39	1198	4.42
CVS2-16A	39	1248	2.93
CVS2-16A	39	1147	6.91
CVS2-16A	39	998	34.49
CVS2-16A	39	948	70.62
CVS2-17	40	1149	5.57
CVS2-17	40	1098	8.85
CVS2-17	40	1048	14.90
CVS2-17	40	1100	8.53
CVS2-17	40	1149	5.37
CVS2-17	40	1199	3.45
CVS2-17	40	1250	2.46
CVS2-17	40	1147	5.69
CVS2-17	40	999	27.35
CVS2-17	40	949	57.68
CVS2-18	41	1148	6.46
CVS2-18	41	1097	10.53
CVS2-18	41	1047	17.78
CVS2-18	41	1099	10.51
CVS2-18	41	1150	6.47
CVS2-18	41	1199	4.20
CVS2-18	41	1248	2.89
CVS2-18	41	1145	6.84
CVS2-18	41	997	33.96
CVS2-18	41	948	66.75
CVS2-19	42	1149	6.76
CVS2-19	42	1097	11.51
CVS2-19	42	1048	18.73
CVS2-19	42	1100	11.02
CVS2-19	42	1150	6.76
CVS2-19	42	1200	4.44
CVS2-19	42	1249	2.95
CVS2-19	42	1148	7.14
CVS2-19	42	999	36.93
CVS2-19	42	949	77.01

TABLE B.1. Viscosity at Temperature Data for CVS-I and CVS-II Phase 1, 2, and 3 Glasses (continued)

Glass	ID #	Temp. (°C)	Viscosity (Pa·s)
CVS2-20	43	1144	12.77
CVS2-20	43	1094	23.52
CVS2-20	43	1044	44.72
CVS2-20	43	1094	23.47
CVS2-20	43	1144	13.12
CVS2-20	43	1194	7.80
CVS2-20	43	1245	5.07
CVS2-20	43	1144	13.02
CVS2-20	43	994	94.97
CVS2-20	43	944	218.42
CVS2-21	44	1145	6.17
CVS2-21	44	1096	9.85
CVS2-21	44	1046	16.20
CVS2-21	44	1096	9.66
CVS2-21	44	1146	6.23
CVS2-21	44	1195	4.16
CVS2-21	44	1244	2.93
CVS2-21	44	1145	6.40
CVS2-21	44	995	28.76
CVS2-21	44	946	55.62
CVS2-22	45	1148	5.97
CVS2-22	45	1098	9.36
CVS2-22	45	1047	15.63
CVS2-22	45	1098	9.31
CVS2-22	45	1148	6.17
CVS2-22	45	1198	4.10
CVS2-22	45	1248	2.79
CVS2-22	45	1148	6.05
CVS2-22	45	997	28.16
CVS2-22	45	947	54.27
CVS2-23	46	1145	10.16
CVS2-23	46	1095	16.96
CVS2-23	46	1045	29.41
CVS2-23	46	1096	16.96
CVS2-23	46	1145	10.45
CVS2-23	46	1194	6.76
CVS2-23	46	1243	4.63
CVS2-23	46	1144	10.64
CVS2-23	46	995	53.72
CVS2-23	46	945	117.22
CVS2-24	47	1147	2.11
CVS2-24	47	1097	3.06
CVS2-24	47	1047	4.66
CVS2-24	47	1098	2.99
CVS2-24	47	1148	2.02
CVS2-24	47	1199	1.41
CVS2-24	47	1247	1.03
CVS2-24	47	1144	1.99
CVS2-24	47	997	7.33
CVS2-24	47	947	13.11
CVS2-25	48	1147	1.38
CVS2-25	48	1097	2.00
CVS2-25	48	1048	3.14
CVS2-25	48	1098	1.98
CVS2-25	48	1148	1.37
CVS2-25	48	1197	0.97
CVS2-25	48	1246	0.72
CVS2-25	48	1148	1.44
CVS2-25	48	998	5.45
CVS2-25	48	947	10.11
CVS2-26	49	1146	1.27
CVS2-26	49	1095	2.13
CVS2-26	49	1046	3.48
CVS2-26	49	1097	2.09
CVS2-26	49	1147	1.30
CVS2-26	49	1194	0.88
CVS2-26	49	1244	0.63
CVS2-26	49	1145	1.30
CVS2-26	49	996	6.34
CVS2-26	49	946	13.65

TABLE B.1. Viscosity at Temperature Data for CVS-I and CVS-II Phase 1, 2, and 3 Glasses (continued)

Glass	ID #	Temp. (°C)	Viscosity (Pa·s)
CVS2-27	50	1144	15.11
CVS2-27	50	1094	25.10
CVS2-27	50	1045	42.92
CVS2-27	50	1094	24.94
CVS2-27	50	1144	15.06
CVS2-27	50	1194	9.77
CVS2-27	50	1241	6.61
CVS2-27	50	1143	15.85
CVS2-27	50	993	88.73
CVS2-27	50	943	173.11
CVS2-28	51	1147	13.32
CVS2-28	51	1097	22.01
CVS2-28	51	1046	37.50
CVS2-28	51	1097	21.65
CVS2-28	51	1148	13.73
CVS2-28	51	1197	9.21
CVS2-28	51	1246	6.28
CVS2-28	51	1146	14.54
CVS2-28	51	996	75.70
CVS2-28	51	946	145.16
CVS2-29	52	1149	5.22
CVS2-29	52	1098	9.89
CVS2-29	52	1048	20.38
CVS2-29	52	1099	9.75
CVS2-29	52	1149	5.43
CVS2-29	52	1199	3.23
CVS2-29	52	1248	2.06
CVS2-29	52	1149	5.45
CVS2-29	52	998	46.62
CVS2-29	52	949	124.81
CVS2-30	53	1147	26.59
CVS2-30	53	1096	46.78
CVS2-30	53	1047	78.55
CVS2-30	53	1098	46.67
CVS2-30	53	1148	28.22
CVS2-30	53	1197	18.61
CVS2-30	53	1247	12.56
CVS2-30	53	1147	28.92
CVS2-30	53	998	155.75
CVS2-31	54	1146	10.50
CVS2-31	54	1096	17.58
CVS2-31	54	1047	29.96
CVS2-31	54	1096	17.80
CVS2-31	54	1146	10.80
CVS2-31	54	1195	6.82
CVS2-31	54	1245	4.84
CVS2-31	54	1146	11.08
CVS2-31	54	996	64.17
CVS2-31	54	947	141.91
CVS2-32	55	1142	8.59
CVS2-32	55	1092	15.71
CVS2-32	55	1043	28.16
CVS2-32	55	1093	15.09
CVS2-32	55	1143	8.66
CVS2-32	55	1193	5.27
CVS2-32	55	1243	3.35
CVS2-32	55	1143	8.78
CVS2-32	55	994	57.52
CVS2-32	55	943	128.61
CVS2-33	56	1148	2.14
CVS2-33	56	1098	3.26
CVS2-33	56	1048	5.20
CVS2-33	56	1099	3.22
CVS2-33	56	1149	2.17
CVS2-33	56	1198	1.52
CVS2-33	56	1247	1.08
CVS2-33	56	1148	2.24
CVS2-33	56	999	8.74
CVS2-33	56	948	15.52
CVS2-34	57	1145	1.97
CVS2-34	57	1095	2.80
CVS2-34	57	1046	4.14
CVS2-34	57	1097	2.77
CVS2-34	57	1046	1.96
CVS2-34	57	1195	1.44
CVS2-34	57	1244	1.07
CVS2-34	57	1145	1.98
CVS2-34	57	996	6.57
CVS2-34	57	945	11.29

TABLE B.1. Viscosity at Temperature Data for CVS-I and CVS-II Phase 1, 2, and 3 Glasses (continued)

Glass	ID #	Temp. (°C)	Viscosity (Pa·s)
CVS2-35	58	1144	2.87
CVS2-35	58	1093	4.45
CVS2-35	58	1043	7.12
CVS2-35	58	1094	4.42
CVS2-35	58	1144	2.95
CVS2-35	58	1193	2.04
CVS2-35	58	1244	1.51
CVS2-35	58	1143	3.01
CVS2-35	58	993	12.06
CVS2-35	58	943	21.65
CVS2-36	59	1146	1.96
CVS2-36	59	1095	2.94
CVS2-36	59	1045	4.67
CVS2-36	59	1096	2.93
CVS2-36	59	1145	1.98
CVS2-36	59	1196	1.38
CVS2-36	59	1246	1.01
CVS2-36	59	1145	1.95
CVS2-36	59	995	7.50
CVS2-36	59	945	13.65
CVS2-37	60	1146	12.43
CVS2-37	60	1095	20.05
CVS2-37	60	1046	31.75
CVS2-37	60	1097	19.48
CVS2-37	60	1146	12.74
CVS2-37	60	1195	8.70
CVS2-37	60	1244	6.20
CVS2-37	60	1146	13.05
CVS2-37	60	997	54.67
CVS2-37	60	947	102.97
CVS2-38	61	1147	12.21
CVS2-38	61	1096	21.19
CVS2-38	61	1047	38.80
CVS2-38	61	1097	21.27
CVS2-38	61	1147	12.41
CVS2-38	61	1197	7.75
CVS2-38	61	1247	5.14
CVS2-38	61	1147	12.44
CVS2-38	61	998	77.06
CVS2-39	62	1145	2.14
CVS2-39	62	1095	3.34
CVS2-39	62	1047	5.45
CVS2-39	62	1097	3.15
CVS2-39	62	1147	2.02
CVS2-39	62	1196	1.33
CVS2-39	62	1143	2.08
CVS2-39	62	994	9.61
CVS2-39	62	944	20.00
CVS2-40	63	1147	6.81
CVS2-40	63	1097	11.42
CVS2-40	63	1048	18.83
CVS2-40	63	1098	11.19
CVS2-40	63	1148	6.78
CVS2-40	63	1197	4.72
CVS2-40	63	1247	3.24
CVS2-40	63	1147	7.16
CVS2-40	63	998	35.11
CVS2-40	63	947	68.10
CVS2-41	64	1147	6.40
CVS2-41	64	1097	10.23
CVS2-41	64	1047	16.80
CVS2-41	64	1098	10.01
CVS2-41	64	1147	6.30
CVS2-41	64	1197	4.16
CVS2-41	64	1246	2.97
CVS2-41	64	1147	6.46
CVS2-41	64	998	29.58
CVS2-41	64	947	61.73
CVS2-42	65	1147	5.66
CVS2-42	65	1096	9.05
CVS2-42	65	1047	14.95
CVS2-42	65	1098	8.94
CVS2-42	65	1148	5.71
CVS2-42	65	1197	3.68
CVS2-42	65	1247	2.58
CVS2-42	65	1147	5.75
CVS2-42	65	998	26.70
CVS2-42	65	948	54.54

TABLE B.1. Viscosity at Temperature Data for CVS-I and CVS-II Phase 1, 2, and 3 Glasses (continued)

Glass	ID #	Temp. (°C)	Viscosity (Pa·s)
CVS2-43	66	1147	4.55
CVS2-43	66	1097	7.23
CVS2-43	66	1047	12.43
CVS2-43	66	1097	7.27
CVS2-43	66	1148	4.59
CVS2-43	66	1197	2.94
CVS2-43	66	1247	2.08
CVS2-43	66	1147	4.70
CVS2-43	66	997	25.21
CVS2-43	66	947	53.29
CVS2-44	67	1147	6.19
CVS2-44	67	1097	10.01
CVS2-44	67	1047	16.63
CVS2-44	67	1098	9.80
CVS2-44	67	1148	6.19
CVS2-44	67	1197	4.12
CVS2-44	67	1246	2.88
CVS2-44	67	1147	6.30
CVS2-44	67	998	30.39
CVS2-44	67	948	59.96
CVS2-45	68	1148	6.05
CVS2-45	68	1098	9.73
CVS2-45	68	1049	16.44
CVS2-45	68	1100	9.55
CVS2-45	68	1149	6.08
CVS2-45	68	1198	4.09
CVS2-45	68	1248	2.75
CVS2-45	68	1149	6.29
CVS2-45	68	998	32.61
CVS2-45	68	948	64.17
CVS2-46	69	1148	4.79
CVS2-46	69	1097	7.31
CVS2-46	69	1048	12.26
CVS2-46	69	1100	7.16
CVS2-46	69	1150	4.82
CVS2-46	69	1199	3.27
CVS2-46	69	1248	2.25
CVS2-46	69	1148	4.90
CVS2-46	69	998	22.41
CVS2-46	69	948	44.39
CVS2-47	70	1148	6.60
CVS2-47	70	1098	10.99
CVS2-47	70	1048	19.29
CVS2-47	70	1100	11.03
CVS2-47	70	1149	7.07
CVS2-47	70	1198	4.32
CVS2-47	70	1248	2.90
CVS2-47	70	1148	6.81
CVS2-47	70	999	37.34
CVS2-47	70	948	80.59
CVS2-48	71	1148	3.94
CVS2-48	71	1098	6.32
CVS2-48	71	1048	10.51
CVS2-48	71	1099	6.23
CVS2-48	71	1149	4.00
CVS2-48	71	1198	2.69
CVS2-48	71	1248	1.90
CVS2-48	71	1148	4.06
CVS2-48	71	999	19.64
CVS2-48	71	948	39.72
CVS2-49	72	1147	6.65
CVS2-49	72	1098	10.47
CVS2-49	72	1048	17.56
CVS2-49	72	1098	10.31
CVS2-49	72	1147	6.63
CVS2-49	72	1198	4.35
CVS2-49	72	1247	3.09
CVS2-49	72	1147	6.72
CVS2-49	72	998	31.31
CVS2-49	72	948	64.85
CVS2-50	73	1147	5.96
CVS2-50	73	1096	9.57
CVS2-50	73	1047	16.49
CVS2-50	73	1098	9.46
CVS2-50	73	1147	5.87
CVS2-50	73	1197	3.78
CVS2-50	73	1247	2.57
CVS2-50	73	1147	5.85
CVS2-50	73	998	31.28
CVS2-50	73	948	63.53

TABLE B.1. Viscosity at Temperature Data for CVS-I and CVS-II Phase 1, 2, and 3 Glasses (continued)

Glass	ID #	Temp. (°C)	Viscosity (Pa·s)
CVS2-51	74	1149	6.97
CVS2-51	74	1099	11.73
CVS2-51	74	1048	19.96
CVS2-51	74	1099	11.55
CVS2-51	74	1149	7.03
CVS2-51	74	1198	4.75
CVS2-51	74	1248	3.26
CVS2-51	74	1148	7.28
CVS2-51	74	999	39.58
CVS2-51	74	948	82.16
CVS2-52	75	1148	9.20
CVS2-52	75	1098	14.82
CVS2-52	75	1048	25.92
CVS2-52	75	1099	14.71
CVS2-52	75	1149	9.43
CVS2-52	75	1198	6.23
CVS2-52	75	1249	4.26
CVS2-52	75	1149	9.56
CVS2-52	75	999	48.56
CVS2-52	75	949	100.65
CVS2-53	76	(h)	(h)
CVS2-54	77	(h)	(h)
CVS2-55	78	1147	6.35
CVS2-55	78	1096	10.55
CVS2-55	78	1046	17.76
CVS2-55	78	1097	10.36
CVS2-55	78	1147	6.49
CVS2-55	78	1197	4.18
CVS2-55	78	1247	2.89
CVS2-55	78	1147	6.53
CVS2-55	78	997	33.88
CVS2-55	78	946	70.30
CVS2-56	79	1146	6.22
CVS2-56	79	1096	10.07
CVS2-56	79	1047	17.05
CVS2-56	79	1097	10.05
CVS2-56	79	1147	6.32
CVS2-56	79	1197	4.12
CVS2-56	79	1247	2.89
CVS2-56	79	1147	6.44
CVS2-56	79	996	32.52
CVS2-56	79	946	65.92
CVS2-57	80	1147	7.00
CVS2-57	80	1096	11.35
CVS2-57	80	1046	19.90
CVS2-57	80	1097	11.29
CVS2-57	80	1147	6.97
CVS2-57	80	1197	4.49
CVS2-57	80	1247	3.04
CVS2-57	80	1147	6.90
CVS2-57	80	996	38.62
CVS2-57	80	945	82.58
CVS2-58	81	1146	1.93
CVS2-58	81	1096	2.96
CVS2-58	81	1046	4.75
CVS2-58	81	1097	2.89
CVS2-58	81	1146	1.92
CVS2-58	81	1195	1.31
CVS2-58	81	1245	0.94
CVS2-58	81	1146	1.88
CVS2-58	81	997	8.05
CVS2-58	81	946	15.25 (i)

(h) Viscosity measurements were not made on the radioactive glasses CVS2-53 and CVS2-54.

(i) This value was originally reported as 15.2, which was used in all data analyses. The second decimal place was later determined as shown.

TABLE B.1. Viscosity at Temperature Data for CVS-I and CVS-II Phase 1, 2, and 3 Glasses (continued)

Glass	ID #	Temp. (°C)	Viscosity (Pa·s)
CVS2-59	82	1147	1.19
CVS2-59	82	1097	1.67
CVS2-59	82	1048	2.41
CVS2-59	82	1098	1.59
CVS2-59	82	1147	1.19
CVS2-59	82	1196	0.89
CVS2-59	82	1246	0.62
CVS2-59	82	1147	1.23
CVS2-59	82	998	3.77
CVS2-59	82	947	6.82
CVS2-60	83	1147	2.62
CVS2-60	83	1098	3.78
CVS2-60	83	1048	5.74
CVS2-60	83	1098	3.88
CVS2-60	83	1147	2.69
CVS2-60	83	1196	1.92
CVS2-60	83	1246	1.45
CVS2-60	83	1147	2.63
CVS2-60	83	998	9.12
CVS2-60	83	947	15.18
CVS2-61	84	1147	13.14
CVS2-61	84	1097	20.57
CVS2-61	84	1047	33.64
CVS2-61	84	1098	20.36
CVS2-61	84	1148	13.10
CVS2-61	84	1197	8.78
CVS2-61	84	1246	6.21
CVS2-61	84	1147	13.60
CVS2-61	84	998	60.13
CVS2-61	84	948	111.03
CVS2-62	85	1147	9.82
CVS2-62	85	1097	17.03
CVS2-62	85	1047	30.72
CVS2-62	85	1097	17.09
CVS2-62	85	1147	10.36
CVS2-62	85	1195	6.70
CVS2-62	85	1245	4.54
CVS2-62	85	1146	10.58
CVS2-62	85	997	65.34
CVS2-62	85	946	149.73
CVS2-63	86	1147	2.40
CVS2-63	86	1097	3.77
CVS2-63	86	1047	6.06
CVS2-63	86	1098	3.68
CVS2-63	86	1147	2.43
CVS2-63	86	1197	1.65
CVS2-63	86	1246	1.25
CVS2-63	86	1147	2.45
CVS2-63	86	998	10.92
CVS2-63	86	947	20.93
CVS2-64	87	1149	8.88
CVS2-64	87	1099	14.82
CVS2-64	87	1049	24.81
CVS2-64	87	1100	14.55
CVS2-64	87	1149	9.03
CVS2-64	87	1199	5.79
CVS2-64	87	1249	3.87
CVS2-64	87	1149	8.85
CVS2-64	87	999	45.69
CVS2-64	87	948	91.58
CVS2-65	88	1146	8.53
CVS2-65	88	1096	15.14
CVS2-65	88	1046	29.64
CVS2-65	88	1096	15.26
CVS2-65	88	1146	8.60
CVS2-65	88	1196	5.06
CVS2-65	88	1246	3.21
CVS2-65	88	1146	8.73
CVS2-65	88	996	62.62
CVS2-65	88	945	149.06
CVS2-66	89	1150	8.13
CVS2-66	89	1100	12.86
CVS2-66	89	1050	20.69
CVS2-66	89	1100	12.74
CVS2-66	89	1150	8.28
CVS2-66	89	1200	5.55
CVS2-66	89	1250	3.90
CVS2-66	89	1150	8.38
CVS2-66	89	1000	37.33
CVS2-66	89	949	70.70

TABLE B.1. Viscosity at Temperature Data for CVS-I and CVS-II Phase 1, 2, and 3 Glasses (continued)

Glass	ID #	Temp. (°C)	Viscosity (Pa·s)	
CVS2-67	90	1146	9.17	
CVS2-67	90	1096	14.20	
CVS2-67	90	1046	22.44	
CVS2-67	90	1096	14.29	
CVS2-67	90	1146	9.30	
CVS2-67	90	1195	6.37	
CVS2-67	90	1244	4.51	
CVS2-67	90	1146	9.42	
CVS2-67	90	996	39.41	
CVS2-67	90	946	72.63	
CVS2-68	91	1151	16.13	(f)
CVS2-68	91	1101	23.90	(f)
CVS2-68	91	1051	39.77	(f)
CVS2-68	91	1101	24.29	(f)
CVS2-68	91	1151	17.83	(f)
CVS2-68	91	1201	11.39	(f)
CVS2-68	91	1250	8.54	(f)
CVS2-68	91	1150	17.68	(f)
CVS2-68	91	1000	74.27	(f)
CVS2-68	91	950	106.71	(f)
CVS2-69	92	1150	21.97	(f)
CVS2-69	92	1101	36.91	(f)
CVS2-69	92	1051	66.83	(f)
CVS2-69	92	1101	36.91	(f)
CVS2-69	92	1151	22.56	(f)
CVS2-69	92	1201	13.60	(f,i)
CVS2-69	92	1251	8.63	(f,i)
CVS2-69	92	1151	19.77	(f,i)
CVS2-69	92	1000	105.67	(f,i)
CVS2-70	93	1154	9.98	
CVS2-70	93	1104	16.19	
CVS2-70	93	1053	27.16	
CVS2-70	93	1105	15.97	
CVS2-70	93	1154	10.52	
CVS2-70	93	1204	7.39	
CVS2-70	93	1253	4.87	
CVS2-70	93	1153	10.30	
CVS2-70	93	1003	43.48	
CVS2-70	93	953	79.55	
CVS2-71	94	1150	8.84	
CVS2-71	94	1100	13.86	
CVS2-71	94	1050	23.40	
CVS2-71	94	1100	13.89	
CVS2-71	94	1150	8.62	
CVS2-71	94	1200	5.49	
CVS2-71	94	1250	3.56	
CVS2-71	94	1150	8.33	
CVS2-71	94	1000	43.34	
CVS2-71	94	950	87.96	
CVS2-72	95	1150	8.02	
CVS2-72	95	1100	12.16	
CVS2-72	95	1050	19.29	
CVS2-72	95	1101	11.89	
CVS2-72	95	1150	7.74	
CVS2-72	95	1200	5.28	
CVS2-72	95	1249	3.69	
CVS2-72	95	1150	7.84	
CVS2-72	95	1000	34.41	
CVS2-72	95	950	63.40	
CVS2-73	96	1149	8.83	
CVS2-73	96	1098	13.63	
CVS2-73	96	1049	21.49	
CVS2-73	96	1100	13.37	
CVS2-73	96	1149	8.72	
CVS2-73	96	1199	5.98	
CVS2-73	96	1248	4.12	
CVS2-73	96	1149	8.75	
CVS2-73	96	999	38.40	
CVS2-73	96	949	69.65	
CVS2-74	97	1151	9.28	
CVS2-74	97	1101	14.73	
CVS2-74	97	1050	24.26	
CVS2-74	97	1102	14.70	
CVS2-74	97	1151	9.54	
CVS2-74	97	1201	6.39	
CVS2-74	97	1251	4.42	
CVS2-74	97	1151	9.69	
CVS2-74	97	1001	44.16	
CVS2-74	97	950	84.97	

(f) Results not used in fitting Fulcher-mixture or Arrhenius-mixture models in Section 7.1 of Chapter 7.

(i) Data questionable due to problems or changes during measurement.

TABLE B.1. Viscosity at Temperature Data for CVS-I and CVS-II Phase 1, 2, and 3 Glasses (continued)

Glass	ID #	Temp. (°C)	Viscosity (Pa·s)	
CVS2-75	98	1150	8.87	
CVS2-75	98	1100	13.41	
CVS2-75	98	1050	21.28	
CVS2-75	98	1100	13.19	
CVS2-75	98	1150	8.53	
CVS2-75	98	1200	5.93	
CVS2-75	98	1249	4.13	
CVS2-75	98	1150	8.72	
CVS2-75	98	1000	37.21	
CVS2-75	98	950	69.65	
CVS2-76	99	1148	1.18	
CVS2-76	99	1098	1.66	
CVS2-76	99	1048	2.47	
CVS2-76	99	1098	1.69	
CVS2-76	99	1148	1.20	
CVS2-76	99	1198	0.88	
CVS2-76	99	1248	0.69	
CVS2-76	99	1148	1.23	
CVS2-76	99	999	3.42	
CVS2-76	99	947	6.07	
CVS2-77	100	1150	1.52	
CVS2-77	100	1099	2.44	
CVS2-77	100	1049	4.06	
CVS2-77	100	1100	2.46	
CVS2-77	100	1149	1.60	
CVS2-77	100	1199	1.04	
CVS2-77	100	1247	0.75	
CVS2-77	100	1148	1.59	
CVS2-77	100	999	7.69	
CVS2-77	100	948	15.29	
CVS2-78	101	1149	26.93	
CVS2-78	101	1099	47.63	
CVS2-78	101	1050	97.61	
CVS2-78	101	1100	54.86	
CVS2-78	101	1150	28.28	
CVS2-78	101	1200	16.79	
CVS2-78	101	1250	10.91	
CVS2-78	101	1149	27.31	
CVS2-78	101	999	187.57	
CVS2-79	102	1151	69.68	
CVS2-79	102	1101	121.28	
CVS2-79	102	1051	235.79	
CVS2-79	102	1102	124.22	
CVS2-79	102	1151	71.59	
CVS2-79	102	1203	34.75	(f,i)
CVS2-79	102	1252	14.46	(f,i)
CVS2-79	102	1152	32.87	(f,i)
CVS2-79	102	1002	199.92	(f,i)
CVS2-80	103	1150	54.77	
CVS2-80	103	1100	136.93	
CVS2-80	103	1101	128.15	
CVS2-80	103	1150	57.93	
CVS2-80	103	1200	27.62	
CVS2-80	103	1252	17.32	(f,i)
CVS2-80	103	1149	110.88	(f,i)
CVS2-81	104	1150	0.72	
CVS2-81	104	1099	0.99	
CVS2-81	104	1050	1.40	
CVS2-81	104	1099	1.00	
CVS2-81	104	1149	0.76	
CVS2-81	104	1198	0.54	
CVS2-81	104	1248	0.35	
CVS2-81	104	1149	0.74	
CVS2-81	104	1000	3.88	
CVS2-81	104	949	7.89	
CVS2-82	105	1147	1.56	
CVS2-82	105	1097	2.26	
CVS2-82	105	1047	3.31	
CVS2-82	105	1098	2.24	
CVS2-82	105	1146	1.54	
CVS2-82	105	1196	1.26	
CVS2-82	105	1246	1.02	
CVS2-82	105	1146	1.52	
CVS2-82	105	997	5.26	
CVS2-82	105	946	9.17	

(f) Results not used in fitting Fulcher-mixture or Arrhenius-mixture models in Section 7.1 of Chapter 7.

(i) Data questionable due to problems or changes during measurement.

TABLE B.1. Viscosity at Temperature Data for CVS-I and CVS-II Phase 1, 2, and 3 Glasses (continued)

Glass	ID #	Temp. (°C)	Viscosity (Pa·s)
CVS2-83	106	1147	0.77
CVS2-83	106	1097	1.08
CVS2-83	106	1048	1.55
CVS2-83	106	1098	1.08
CVS2-83	106	1148	0.77
CVS2-83	106	1196	0.56
CVS2-83	106	1246	0.39
CVS2-83	106	1148	0.78
CVS2-83	106	999	2.75
CVS2-83	106	948	5.00
CVS2-84	107	1152	1.16
CVS2-84	107	1101	1.75
CVS2-84	107	1051	2.74
CVS2-84	107	1102	1.80
CVS2-84	107	1152	1.18
CVS2-84	107	1201	0.82
CVS2-84	107	1250	0.61
CVS2-84	107	1152	1.18
CVS2-84	107	1002	4.60
CVS2-84	107	951	8.55
CVS2-85	108	1148	4.06
CVS2-85	108	1099	6.18
CVS2-85	108	1049	9.66
CVS2-85	108	1098	6.21
CVS2-85	108	1148	4.06
CVS2-85	108	1198	2.79
CVS2-85	108	1247	1.99
CVS2-85	108	1148	4.16
CVS2-85	108	999	16.19
CVS2-85	108	948	29.05
CVS2-86	109	1150	30.22
CVS2-86	109	1100	50.16
CVS2-86	109	1049	90.26
CVS2-86	109	1100	49.92
CVS2-86	109	1150	29.75
CVS2-86	109	1199	18.49
CVS2-86	109	1249	12.14
CVS2-86	109	1149	30.75
CVS2-86	109	999	185.81
CVS2-87	110	1150	18.13
CVS2-87	110	1100	31.37
CVS2-87	110	1050	56.56
CVS2-87	110	1100	30.90
CVS2-87	110	1150	17.98
CVS2-87	110	1198	11.13
CVS2-87	110	1248	7.26
CVS2-87	110	1149	17.89
CVS2-87	110	999	114.01
CVS2-87	110	949	247.66
CVS2-88	111	1152	3.50
CVS2-88	111	1102	5.62
CVS2-88	111	1052	9.48
CVS2-88	111	1102	5.58
CVS2-88	111	1151	3.51
CVS2-88	111	1200	2.32
CVS2-88	111	1250	1.63
CVS2-88	111	1150	3.63
CVS2-88	111	1001	17.69
CVS2-88	111	951	35.32
CVS2-89	112	1149	2.77
CVS2-89	112	1099	4.53
CVS2-89	112	1049	7.86
CVS2-89	112	1100	4.53
CVS2-89	112	1149	2.83
CVS2-89	112	1199	1.85
CVS2-89	112	1248	1.29
CVS2-89	112	1149	2.78
CVS2-89	112	999	14.70
CVS2-89	112	949	31.52
CVS2-90	113	1149	3.64
CVS2-90	113	1099	5.52
CVS2-90	113	1049	8.80
CVS2-90	113	1100	5.52
CVS2-90	113	1149	3.68
CVS2-90	113	1199	2.58
CVS2-90	113	1248	1.86
CVS2-90	113	1149	3.68
CVS2-90	113	999	15.06
CVS2-90	113	948	28.52

TABLE B.1. Viscosity at Temperature Data for CVS-I and CVS-II Phase 1, 2, and 3 Glasses (continued)

Glass	ID #	Temp. (°C)	Viscosity (Pa·s)
CVS2-91	114	1150	13.91
CVS2-91	114	1100	23.93
CVS2-91	114	1049	44.34
CVS2-91	114	1100	23.87
CVS2-91	114	1150	14.29
CVS2-91	114	1200	9.14
CVS2-91	114	1250	6.09
CVS2-91	114	1150	14.82
CVS2-91	114	1000	97.17
CVS2-91	114	949	219.91
CVS2-92	115	1149	1.00
CVS2-92	115	1099	1.52
CVS2-92	115	1049	2.36
CVS2-92	115	1099	1.54
CVS2-92	115	1148	1.03
CVS2-92	115	1197	0.70
CVS2-92	115	1247	0.51
CVS2-92	115	1148	1.01
CVS2-92	115	999	4.06
CVS2-92	115	949	7.72
CVS2-93	116	1148	0.64
CVS2-93	116	1099	0.90
CVS2-93	116	1049	1.30
CVS2-93	116	1099	0.90
CVS2-93	116	1148	0.64
CVS2-93	116	1198	0.48
CVS2-93	116	1247	0.36
CVS2-93	116	1148	0.67
CVS2-93	116	999	2.04
CVS2-93	116	949	3.36
CVS2-94	117	1148	0.81
CVS2-94	117	1098	1.17
CVS2-94	117	1048	1.62
CVS2-94	117	1099	1.14
CVS2-94	117	1148	0.82
CVS2-94	117	1197	0.61
CVS2-94	117	1247	0.48
CVS2-94	117	1148	0.82
CVS2-94	117	999	2.54
CVS2-94	117	948	4.39
CVS2-95	118	1152	1.59
CVS2-95	118	1102	2.26
CVS2-95	118	1051	3.43
CVS2-95	118	1102	2.25
CVS2-95	118	1152	1.55
CVS2-95	118	1202	1.18
CVS2-95	118	1251	0.89
CVS2-95	118	1152	1.55
CVS2-95	118	1002	5.55
CVS2-95	118	951	9.95
CVS2-96	119	1150	5.53
CVS2-96	119	1099	9.11
CVS2-96	119	1049	15.88
CVS2-96	119	1100	9.17
CVS2-96	119	1149	5.56
CVS2-96	119	1199	3.60
CVS2-96	119	1250	2.51
CVS2-96	119	1149	5.56
CVS2-96	119	999	31.16
CVS2-96	119	948	66.15
CVS2-97	120	1151	7.14
CVS2-97	120	1100	11.67
CVS2-97	120	1051	19.97
CVS2-97	120	1101	11.53
CVS2-97	120	1151	7.23
CVS2-97	120	1200	4.72
CVS2-97	120	1250	3.16
CVS2-97	120	1150	7.49
CVS2-97	120	1001	39.29
CVS2-97	120	950	80.52
CVS2-98	121	1147	1.95
CVS2-98	121	1096	2.75
CVS2-98	121	1047	4.19
CVS2-98	121	1098	2.73
CVS2-98	121	1147	1.95
CVS2-98	121	1196	1.43
CVS2-98	121	1246	1.08
CVS2-98	121	1146	1.93
CVS2-98	121	997	6.53
CVS2-98	121	947	11.22

TABLE B.1. Viscosity at Temperature Data for CVS-I and CVS-II Phase 1, 2, and 3 Glasses (continued)

Glass	ID #	Temp. (°C)	Viscosity (Pa·s)
CVS2-99	122	1146	8.80
CVS2-99	122	1096	14.33
CVS2-99	122	1045	24.52
CVS2-99	122	1098	14.07
CVS2-99	122	1148	8.74
CVS2-99	122	1198	5.67
CVS2-99	122	1247	3.93
CVS2-99	122	1146	8.81
CVS2-99	122	997	45.71
CVS2-99	122	946	93.86
CVS2-100	123	1147	6.92
CVS2-100	123	1097	11.32
CVS2-100	123	1047	19.14
CVS2-100	123	1098	11.22
CVS2-100	123	1148	6.96
CVS2-100	123	1197	4.61
CVS2-100	123	1247	3.19
CVS2-100	123	1145	7.27
CVS2-100	123	998	36.92
CVS2-100	123	947	74.36
CVS2-101	124	1153	1.46
CVS2-101	124	1103	2.09
CVS2-101	124	1053	3.21
CVS2-101	124	1103	2.11
CVS2-101	124	1152	1.50
CVS2-101	124	1202	1.09
CVS2-101	124	1251	0.81
CVS2-101	124	1152	1.49
CVS2-101	124	1002	5.05
CVS2-101	124	952	8.82

TABLE B.2. Results of Fitting the Fulcher Equation to the Viscosity at Temperature Data for Each CVS-I and CVS-II Phase 1, 2, and 3 Glass

Glass	# Data Points	Fulcher Equation Coefficients A	B	T_0	Fulcher Predicted η_{1150} (Pa·s)
CVS1-1	4	-5.31	5390.83	387.05	5.78
CVS1-2	4	-5.14	6367.00	326.47	13.29
CVS1-3	4	-6.47	6286.50	294.28	2.39
CVS1-4	3	-7.11	7998.68	287.57	8.70
CVS1-5	5	-5.72	7937.47	194.09	13.24
CVS1-6	3	-6.30	5392.86	379.94	2.01
CVS1-7	3	-6.86	8127.95	420.63	72.88
CVS1-8	2 (a)	-5.67	7000.00	375.91	29.26
CVS1-9	2 (a)	-7.18	7000.00	333.99	4.06
CVS1-10	4	-2.56	4100.51	563.65	83.83
CVS1-11	4	(b)	(b)	(b)	14.50 (b)
CVS1-12	5	-5.18	2995.90	454.08	0.42
CVS1-13	5	-4.48	3586.72	518.39	3.31
CVS1-14	4	-5.99	5055.15	449.86	3.42
CVS1-15	5	-5.47	5493.19	293.09	2.55
CVS1-16	3 (a)	-6.15	7080.86	365.44	17.81
CVS1-17	4	-5.14	4146.93	451.94	2.23
CVS1-18	3	-34.31	135565.10	-2730.03	1.87 (c)
CVS1-19	4	-6.45	7170.87	275.46	5.76
CVS1-20	4	-6.53	7629.94	228.06	5.71
CVS1-21	4	-3.90	4025.10	494.15	9.36
CVS1-22	2 (a)	-6.16	7000.00	435.70	38.11
CVS1-23	4	-6.00	7237.84	214.12	5.69
CVS2-1	4	-7.66	10547.27	63.07	7.74
CVS2-2	10	-5.83	6776.14	265.76	6.26
CVS2-3	10	-5.47	5748.80	349.90	5.56
CVS2-4	4	-5.63	6567.10	272.32	6.37
CVS2-5	10	-4.67	5076.07	400.58	8.18
CVS2-6	10	-4.77	4954.98	398.91	6.19
CVS2-7	10	-4.67	4761.86	371.35	4.26

(a) Viscosity data at certain temperature values were not used in the fitting process due to high rates of change (see Table B.1), which are indicative of crystallinity. These data are marked with footnote (b) in Table B.1.

(b) The nonlinear least squares routine did not converge for this glass. The predicted η_{1150} value was determined graphically from a plot of the data.

(c) The η_{1150} value is reasonable in spite of the odd Fulcher coefficients.

TABLE B.2. Results of Fitting the Fulcher Equation to the Viscosity at Temperature Data for Each CVS-I and CVS-II Phase 1, 2, and 3 Glass (continued)

Glass	# Data Points	Fulcher Equation Coefficients A	B	T_0	Fulcher Predicted η_{1150} (Pa·s)
CVS2-8	11	-5.83	6627.35	242.42	4.36
CVS2-9	4 (d)	-6.15	6722.43	324.08	7.30
CVS2-9A	10 (d)	-6.50	7389.73	278.00	7.23
CVS2-10	10	-4.02	4618.29	406.77	8.99
CVS2-11	4	-6.37	5985.39	351.41	3.07
CVS2-12	4	-4.24	3704.99	470.67	3.38
CVS2-13	10	-6.36	7751.57	221.29	7.27
CVS2-14	10	-5.65	4912.78	420.85	2.97
CVS2-15	10	-5.34	5529.18	341.84	4.47
CVS2-16	4 (d)	-5.28	5621.98	364.03	6.57
CVS2-16A	10 (d)	-6.70	8140.32	202.92	6.61
CVS2-17	10	-5.44	5744.01	343.47	5.37
CVS2-18	10	-6.12	7093.77	260.62	6.41
CVS2-19	10	-5.69	6319.75	319.03	6.76
CVS2-20	10	-6.53	7702.25	298.49	12.31
CVS2-21	10	-5.82	6876.21	246.69	6.01
CVS2-22	10	-5.57	6443.11	273.26	5.92
CVS2-23	10	-5.27	6320.83	313.98	9.91
CVS2-24	10	-6.84	7662.12	131.74	1.99
CVS2-25	10	-5.15	4096.93	398.47	1.35
CVS2-26	10	-5.99	4592.64	411.51	1.26
CVS2-27	10	-6.07	8126.56	220.07	14.41
CVS2-28	10	-4.57	5824.32	337.01	13.44
CVS2-29	10	-5.91	5180.47	466.54	5.32
CVS2-30	9	-3.39	4967.63	408.69	27.42
CVS2-31	10	-3.94	4316.83	462.00	10.30
CVS2-32	10	-7.67	9122.28	214.78	8.07
CVS2-33	10	-6.66	7113.98	191.83	2.15
CVS2-34	10	-1.87	1173.64	671.69	1.79
CVS2-35	10	-5.49	5647.30	283.96	2.82
CVS2-36	10	-5.93	5863.67	258.71	1.91
CVS2-37	10	-4.80	6610.03	246.37	12.34
CVS2-38	9	-5.26	6086.86	364.62	12.02
CVS2-39	9	-7.06	6961.55	250.19	1.98

(d) Viscosity data for glasses CVS2-9 and CVS2-16 were obtained using the old procedure (4 data points) and the new procedure (10 data points) in order to compare results.

TABLE B.2. Results of Fitting the Fulcher Equation to the Viscosity at Temperature Data for Each CVS-I and CVS-II Phase 1, 2, and 3 Glass (continued)

Glass	# Data Points	Fulcher Equation Coefficients A	B	T_0	Fulcher Predicted η_{1150} (Pa·s)
CVS2-40	10	-5.75	6742.38	271.62	6.88
CVS2-41	10	-5.40	6099.51	305.66	6.20
CVS2-42	10	-5.74	6416.85	288.43	5.51
CVS2-43	10	-4.86	4564.37	430.53	4.43
CVS2-44	10	-5.65	6415.57	290.01	6.08
CVS2-45	10	-5.46	5948.95	330.69	6.03
CVS2-46	10	-4.81	4922.26	375.69	4.70
CVS2-47	10	-5.90	6497.30	316.28	6.64
CVS2-48	10	-5.06	4906.65	387.16	3.94
CVS2-49	10	-4.99	5515.20	345.32	6.46
CVS2-50	10	-6.13	6769.05	289.66	5.71
CVS2-51	10	-4.93	5280.77	383.49	7.07
CVS2-52	10	-4.43	5054.41	390.32	9.22
CVS2-53	(e)	(e)	(e)	(e)	(e)
CVS2-54	(e)	(e)	(e)	(e)	(e)
CVS2-55	10	-5.48	6007.61	329.16	6.26
CVS2-56	10	-5.22	5672.65	343.32	6.12
CVS2-57	10	-5.51	6014.17	338.91	6.74
CVS2-58	10	-6.53	6403.64	253.59	1.85
CVS2-59	10	-5.35	4588.72	313.48	1.15
CVS2-60	10	-5.68	6413.79	184.20	2.61
CVS2-61	10	-5.39	7522.86	203.81	12.90
CVS2-62	10	-4.29	4595.09	452.47	9.95
CVS2-63	10	-5.02	4410.76	400.45	2.38
CVS2-64	10	-7.14	9409.83	140.36	8.89
CVS2-65	10	-7.47	8445.48	268.33	8.20
CVS2-66	10	-5.34	6683.87	253.16	8.24
CVS2-67	10	-5.23	6894.45	221.22	8.97
CVS2-68	10	-5.99	9991.45	18.11	17.05
CVS2-69	5	-6.07	8377.90	235.63	21.97 (f)
CVS2-70	10	-6.89	10305.91	37.89	10.80

(e) Viscosity measurements were not made on the radioactive glasses CVS2-53 and CVS2-54.

(f) The Fulcher model was first fit to all 9 data points given in Table B.1, but odd coefficients resulted. The η_{1150} value obtained (22.15) was reasonable, however, and was used in fitting models to η_{1150} data.

TABLE B.2. Results of Fitting the Fulcher Equation to the Viscosity at Temperature Data for Each CVS-I and CVS-II Phase 1, 2, and 3 Glass (continued)

Glass	# Data Points	Fulcher Equation Coefficients A	B	T_0	Fulcher Predicted η_{1150} (Pa·s)
CVS2-71	10	-7.34	9636.07	133.89	8.50
CVS2-72	10	-5.86	7570.66	193.65	7.81
CVS2-73	10	-5.88	7844.44	174.32	8.67
CVS2-74	10	-5.11	6427.61	277.16	9.55
CVS2-75	10	-5.34	6896.99	229.66	8.66
CVS2-76	10	-5.33	4925.24	254.58	1.18
CVS2-77	10	-6.28	5333.94	356.37	1.55
CVS2-78	9	-7.05	10022.81	184.77	28.12
CVS2-79	5	-3.37	5588.22	418.24	71.38 (g)
CVS2-80	5	-3.97	4098.99	637.80	56.30 (h)
CVS2-81	10	-3.82	1666.90	667.51	0.69
CVS2-82	10	-2.99	2066.37	550.60	1.58
CVS2-83	10	-5.51	3926.44	395.30	0.74
CVS2-84	10	-6.13	5274.80	313.34	1.19
CVS2-85	10	-6.99	8887.61	90.21	4.02
CVS2-86	9	-5.33	7632.33	275.12	29.69
CVS2-87	10	-6.86	9243.27	201.98	17.98
CVS2-88	10	6.28	6455.00	295.58	3.57
CVS2-89	10	-5.75	5167.78	387.33	2.78
CVS2-90	10	-4.95	5090.70	334.61	3.65
CVS2-91	10	-4.20	4818.26	447.80	14.31
CVS2-92	10	-6.34	5237.82	323.83	1.00
CVS2-93	10	-6.17	5113.18	255.81	0.64
CVS2-94	10	-4.78	3416.96	401.23	0.81
CVS2-95	10	-4.21	3304.95	443.20	1.60
CVS2-96	10	-5.39	5539.08	370.69	5.55
CVS2-97	10	-5.72	6451.33	312.06	7.25
CVS2-98	10	-4.75	4415.06	330.91	1.90
CVS2-99	10	-5.40	6369.71	305.31	8.53
CVS2-100	10	-5.33	5934.93	332.06	6.85
CVS2-101	10	-5.26	4730.46	315.57	1.51

(g) The Fulcher model was first fit to all 9 data points given in Table B.1, but odd coefficients resulted. The η_{1150} value obtained (57.26) was was used in fitting models to η_{1150} data in Chapter 7.

(h) The Fulcher model was first fit to all 7 data points given in Table B.1, but odd coefficients resulted. The η_{1150} value obtained (66.25) was was used in fitting models to η_{1150} data in Chapter 7.

APPENDIX C

ELECTRICAL CONDUCTIVITY AT TEMPERATURE DATA AND RESULTS FROM FITTING THE ARRHENIUS EQUATION

APPENDIX C

ELECTRICAL CONDUCTIVITY AT TEMPERATURE DATA AND RESULTS FROM FITTING THE ARRHENIUS EQUATION

Electrical conductivity was measured at three to five temperatures for each of the CVS glasses. A new automated measurement procedure was adopted beginning with CVS-II Phase 3 (glasses numbered CVS2-59 and higher). See Section 5.3 for discussion of the measurement procedure. Table C.1 contains the electrical conductivity at temperature data for CVS-I and CVS-II Phases 1 and 2 glasses. Table C.2 contains the electrical conductivity at temperature data for CVS-II Phase 3 glasses. The electrical conductivity values for the 1k frequency in Table C.2 were used in CVS.

Table C.3 contains the results of fitting the electrical conductivity at temperature data for each glass to the Arrhenius equation:

$$\ln \epsilon = A + B/T, \tag{C.1}$$

where A and B are the coefficients and T is temperature in K. Included in Table C.3 are the estimated electrical conductivity values at 1150°C (ϵ_{1150}). The ϵ_{1150} values for the CVS-II Phase 3 glasses were computed from the 1k frequency data from Table C.2.

TABLE C.1. Electrical Conductivity at Temperature Data for CVS-I and CVS-II Phase 1 and 2 Glasses

Glass	ID #	Temp. (°C)	Electrical Conductivity (S/m)
CVS1-1	1	1239	25.1
CVS1-1	1	1140	18.4
CVS1-1	1	1040	12.2
CVS1-1	1	940	6.6
CVS1-2	2	1239	35.3
CVS1-2	2	1141	25.5
CVS1-2	2	1041	16.8
CVS1-2	2	941	9.6
CVS1-3	3	1137	33.3
CVS1-3	3	1040	21.1
CVS1-3	3	941	12.5
CVS1-3	3	841	6.2
CVS1-4	4	1239	14.3
CVS1-4	4	1141	8.7
CVS1-4	4	1042	4.9
CVS1-4	4	942	2.3
CVS1-5	5	1339	51.8
CVS1-5	5	1241	42.7
CVS1-5	5	1141	31.6
CVS1-5	5	1040	20.7
CVS1-5	5	939	12.3
CVS1-6	6	1238	75.4
CVS1-6	6	1139	43.1
CVS1-6	6	1040	24.6
CVS1-6	6	940	13.9
CVS1-7	7	1337	16.4
CVS1-7	7	1240	10.8
CVS1-7	7	1140	6.7
CVS1-7	7	1041	3.6
CVS1-8	8	1338	19.7
CVS1-8	8	1241	13.6
CVS1-8	8	1141	8.4
CVS1-9	9	1239	13.3
CVS1-9	9	1141	8.1
CVS1-9	9	1041	4.2
CVS1-9	9	943	2.3
CVS1-10	10	1438	46.6
CVS1-10	10	1340	35.2
CVS1-10	10	1241	28.2
CVS1-10	10	1142	19.9
CVS1-11	11	1239	11.7
CVS1-11	11	1141	7.3
CVS1-11	11	1041	3.9
CVS1-11	11	940	1.8
CVS1-12	12	1138	55.6
CVS1-12	12	1040	35.2
CVS1-12	12	940	19.5
CVS1-12	12	842	8.7
CVS1-12	12	742	2.8
CVS1-13	13	1238	46.6
CVS1-13	13	1141	33.2
CVS1-13	13	1041	21.8
CVS1-13	13	941	13.6
CVS1-14	14	1238	46.6
CVS1-14	14	1142	34.7
CVS1-14	14	1041	22.7
CVS1-14	14	942	13.9
CVS1-15	15	1239	78.0
CVS1-15	15	1141	55.4
CVS1-15	15	1041	39.8
CVS1-15	15	942	24.5
CVS1-16	16	1239	35.2
CVS1-16	16	1140	26.1
CVS1-16	16	1040	17.1
CVS1-16	16	938	10.1
CVS1-17	17	1239	40.2
CVS1-17	17	1142	28.3
CVS1-17	17	1042	17.3
CVS1-17	17	942	9.7
CVS1-18	18	1239	90.1
CVS1-18	18	1141	61.3
CVS1-18	18	1042	42.8
CVS1-18	18	942	25.6
CVS1-18	18	843	12.6
CVS1-19	19	1238	33.3
CVS1-19	19	1142	24.5
CVS1-19	19	1042	15.0
CVS1-19	19	944	8.4

TABLE C.1. Electrical Conductivity at Temperature Data for CVS-I and CVS-II Phase 1 and 2 Glasses (continued)

Glass	ID #	Temp. (°C)	Electrical Conductivity (S/m)
CVS1-20	20	1238	39.5
CVS1-20	20	1142	25.3
CVS1-20	20	1042	15.9
CVS1-20	20	939	9.4
CVS1-21	21	1240	12.9
CVS1-21	21	1140	7.6
CVS1-21	21	1040	4.2
CVS1-21	21	939	1.9
CVS1-22	22	1338	19.7
CVS1-22	22	1242	14.0
CVS1-22	22	1142	8.9
CVS1-22	22	1040	5.3
CVS1-23	23	1239	40.2
CVS1-23	23	1142	27.0
CVS1-23	23	1042	16.8
CVS1-23	23	940	10.3
CVS2-1	24	1189	37.3
CVS2-1	24	1117	28.7
CVS2-1	24	1042	20.9
CVS2-1	24	943	12.4
CVS2-2	25	1138	31.6
CVS2-2	25	1043	21.2
CVS2-2	25	943	12.3
CVS2-2	25	1238	45.7
CVS2-3	26	1139	20.9
CVS2-3	26	1043	13.3
CVS2-3	26	944	7.3
CVS2-3	26	1238	33.0
CVS2-4	27	1190	27.4
CVS2-4	27	1117	20.3
CVS2-4	27	1043	14.5
CVS2-4	27	943	8.1
CVS2-5	28	1139	16.6
CVS2-5	28	1042	10.6
CVS2-5	28	943	5.8
CVS2-5	28	1239	23.7
CVS2-6	29	1139	18.7
CVS2-6	29	1043	11.6
CVS2-6	29	943	6.2
CVS2-6	29	1238	28.7
CVS2-7	30	1139	29.7
CVS2-7	30	1044	20.4
CVS2-7	30	945	12.3
CVS2-7	30	1238	40.3
CVS2-8	31	1140	38.1
CVS2-8	31	1043	25.9
CVS2-8	31	945	15.6
CVS2-8	31	1238	51.5
CVS2-9	32	1188	40.7
CVS2-9	32	1117	31.8
CVS2-9	32	1043	23.5
CVS2-9	32	944	14.3
CVS2-10	33	1138	23.2
CVS2-10	33	1043	15.9
CVS2-10	33	942	9.6
CVS2-10	33	1238	30.9
CVS2-11	34	1189	41.0
CVS2-11	34	1117	30.7
CVS2-11	34	1042	21.7
CVS2-11	34	943	12.1
CVS2-12	35	1190	27.2
CVS2-12	35	1117	20.2
CVS2-12	35	1042	14.1
CVS2-12	35	942	7.7
CVS2-13	36	1139	33.2
CVS2-13	36	1042	23.2
CVS2-13	36	943	14.4
CVS2-13	36	1238	44.3
CVS2-14	37	1139	26.9
CVS2-14	37	1044	17.2
CVS2-14	37	943	9.5
CVS2-14	37	1238	37.9
CVS2-15	38	1139	35.3
CVS2-15	38	1043	24.7
CVS2-15	38	944	15.3
CVS2-15	38	1239	46.6
CVS2-16	39	1189	31.8
CVS2-16	39	1118	24.2
CVS2-16	39	1043	17.5
CVS2-16	39	943	10.2

TABLE C.1. Electrical Conductivity at Temperature Data for CVS-I and CVS-II Phase 1 and 2 Glasses (continued)

Glass	ID #	Temp. (°C)	Electrical Conductivity (S/m)
CVS2-17	40	1139	24.9
CVS2-17	40	1043	16.2
CVS2-17	40	944	9.1
CVS2-17	40	1237	36.7
CVS2-18	41	1138	27.4
CVS2-18	41	1044	18.4
CVS2-18	41	945	10.9
CVS2-18	41	1238	38.6
CVS2-19	42	1139	26.9
CVS2-19	42	1043	18.3
CVS2-19	42	943	10.8
CVS2-19	42	1238	36.8
CVS2-20	43	1241	54.0
CVS2-20	43	1143	35.9
CVS2-20	43	1044	24.7
CVS2-20	43	944	15.1
CVS2-21	44	1241	43.1
CVS2-21	44	1144	31.3
CVS2-21	44	1045	20.9
CVS2-21	44	948	12.4
CVS2-22	45	1243	50.4
CVS2-22	45	1144	36.8
CVS2-22	45	1045	24.7
CVS2-22	45	945	14.7
CVS2-23	46	1242	44.7
CVS2-23	46	1143	35.1
CVS2-23	46	1045	25.2
CVS2-23	46	946	15.7
CVS2-24	47	1241	54.9
CVS2-24	47	1143	40.6
CVS2-24	47	1044	27.4
CVS2-24	47	944	16.5
CVS2-25	48	1241	70.2
CVS2-25	48	1146	50.6
CVS2-25	48	1046	33.0
CVS2-25	48	947	19.2
CVS2-26	49	1241	48.2
CVS2-26	49	1145	34.2
CVS2-26	49	1045	21.8
CVS2-26	49	946	12.1
CVS2-27	50	1241	48.8
CVS2-27	50	1143	37.6
CVS2-27	50	1044	24.3
CVS2-27	50	944	15.9
CVS2-28	51	1242	55.6
CVS2-28	51	1144	43.0
CVS2-28	51	1045	31.0
CVS2-28	51	945	20.3
CVS2-29	52	1242	11.6
CVS2-29	52	1144	6.8
CVS2-29	52	1045	3.5
CVS2-29	52	946	1.4
CVS2-30	53	1242	15.0
CVS2-30	53	1144	10.8
CVS2-30	53	1045	7.1
CVS2-30	53	946	4.0
CVS2-31	54	1241	16.5
CVS2-31	54	1144	10.7
CVS2-31	54	1045	6.4
CVS2-31	54	945	3.3
CVS2-32	55	1242	72.9
CVS2-32	55	1143	56.8
CVS2-32	55	1044	41.2
CVS2-32	55	944	26.7
CVS2-33	56	1242	81.2
CVS2-33	56	1145	60.3
CVS2-33	56	1046	42.0
CVS2-33	56	947	26.7
CVS2-34	57	1242	66.4
CVS2-34	57	1143	51.6
CVS2-34	57	1045	39.2
CVS2-34	57	945	26.7

TABLE C.1. Electrical Conductivity at Temperature Data for CVS-I and CVS-II Phase 1 and 2 Glasses (continued)

Glass	ID #	Temp. (°C)	Electrical Conductivity (S/m)
CVS2-35	58	1242	74.2
CVS2-35	58	1142	57.2
CVS2-35	58	1044	41.5
CVS2-35	58	944	26.7
CVS2-36	59	1243	59.2
CVS2-36	59	1144	38.6
CVS2-36	59	1045	24.1
CVS2-36	59	946	13.6
CVS2-37	60	1241	54.1
CVS2-37	60	1144	41.4
CVS2-37	60	1044	29.2
CVS2-37	60	945	18.4
CVS2-38	61	1242	19.9
CVS2-38	61	1145	13.3
CVS2-38	61	1045	8.4
CVS2-38	61	946	4.6
CVS2-39	62	1242	82.8
CVS2-39	62	1144	60.6
CVS2-39	62	1045	41.0
CVS2-39	62	946	24.8
CVS2-40	63	1242	52.1
CVS2-40	63	1144	37.7
CVS2-40	63	1046	25.3
CVS2-40	63	946	15.1
CVS2-41	64	1242	42.7
CVS2-41	64	1144	30.5
CVS2-41	64	1045	20.2
CVS2-41	64	946	11.8
CVS2-42	65	1241	44.7
CVS2-42	65	1144	31.4
CVS2-42	65	1045	20.4
CVS2-42	65	947	11.9
CVS2-43	66	1241	43.6
CVS2-43	66	1144	31.0
CVS2-43	66	1044	20.3
CVS2-43	66	945	11.7
CVS2-44	67	1241	39.1
CVS2-44	67	1144	28.4
CVS2-44	67	1045	18.8
CVS2-44	67	946	11.1
CVS2-45	68	1242	33.2
CVS2-45	68	1144	26.0
CVS2-45	68	1046	16.6
CVS2-45	68	947	9.4
CVS2-46	69	1242	47.8
CVS2-46	69	1144	34.4
CVS2-46	69	1045	22.9
CVS2-46	69	946	13.5
CVS2-47	70	1242	35.0
CVS2-47	70	1144	26.4
CVS2-47	70	1045	18.8
CVS2-47	70	946	11.5
CVS2-48	71	1242	32.1
CVS2-48	71	1145	22.3
CVS2-48	71	1046	14.2
CVS2-48	71	947	7.8
CVS2-49	72	1242	32.3
CVS2-49	72	1145	23.2
CVS2-49	72	1046	15.4
CVS2-49	72	946	8.9
CVS2-50	73	1241	35.0
CVS2-50	73	1144	24.7
CVS2-50	73	1045	15.6
CVS2-50	73	946	8.7
CVS2-51	74	1242	39.1
CVS2-51	74	1145	28.2
CVS2-51	74	1046	18.5
CVS2-51	74	946	10.8
CVS2-52	75	1242	46.0
CVS2-52	75	1144	34.7
CVS2-52	75	1046	25.0
CVS2-52	75	946	15.8

TABLE C.1. Electrical Conductivity at Temperature Data for CVS-I and CVS-II Phase 1 and 2 Glasses (continued)

Glass	ID #	Temp. (°C)	Electrical Conductivity (S/m)
CVS2-53	76	(a)	(a)
CVS2-54	77	(a)	(a)
CVS2-55	78	1242	36.3
CVS2-55	78	1145	27.3
CVS2-55	78	1046	18.2
CVS2-55	78	946	10.6
CVS2-56	79	1242	38.8
CVS2-56	79	1145	27.7
CVS2-56	79	1046	18.0
CVS2-56	79	946	10.4
CVS2-57	80	1241	39.1
CVS2-57	80	1144	27.9
CVS2-57	80	1045	18.1
CVS2-57	80	946	10.4
CVS2-58	81	1242	44.5
CVS2-58	81	1144	32.8
CVS2-58	81	1045	22.0
CVS2-58	81	946	12.9

(a) Electrical conductivity measurements were not made for the radioactive glasses CVS2-53 and CVS2-54.

TABLE C.2. Electrical Conductivity at Temperature Data for CVS-II Phase 3 Glasses

Glass	ID #	Temp. (°C)	Electrical Conductivity (S/m)[a] .1k	1k	10k	100k
CVS2-59	82	1241	46.94	62.78	69.42	69.81
CVS2-59	82	1143	33.94	48.21	51.94	52.01
CVS2-59	82	1044	25.37	34.10	35.74	35.78
CVS2-59	82	945	16.81	21.19	21.87	21.91
CVS2-60	83	1241	55.39	86.11	97.31	97.28
CVS2-60	83	1143	43.82	68.75	75.14	75.25
CVS2-60	83	1044	37.04	50.98	54.42	54.45
CVS2-60	83	945	25.95	34.20	35.68	35.69
CVS2-61	84	1244	39.11	59.92	65.77	66.09
CVS2-61	84	1146	30.70	45.78	48.94	49.01
CVS2-61	84	1048	25.06	32.55	33.93	33.95
CVS2-61	84	948	17.26	20.60	21.15	21.19
CVS2-62	85	1245	17.79	22.08	22.96	22.99
CVS2-62	85	1147	12.96	15.32	15.69	15.71
CVS2-62	85	1048	8.57	9.53	9.66	9.66
CVS2-62	85	948	4.74	5.06	5.10	5.11
CVS2-63	86	1244	35.74	46.67	49.63	49.54
CVS2-63	86	1147	27.13	34.16	35.75	35.79
CVS2-63	86	1048	18.94	22.97	23.77	23.74
CVS2-63	86	949	11.97	13.70	13.95	13.93
CVS2-64	87	1247	48.44	54.28	56.56	56.51
CVS2-64	87	1149	35.14	39.86	41.36	41.34
CVS2-64	87	1050	23.64	27.18	28.02	28.03
CVS2-64	87	951	14.54	16.61	17.02	17.04
CVS2-65	88	1246	38.42	50.38	54.36	54.57
CVS2-65	88	1148	28.49	36.69	38.92	39.04
CVS2-65	88	1049	19.80	24.64	25.68	25.73
CVS2-65	88	950	12.39	14.61	15.07	15.12
CVS2-66	89	1247	46.37	51.68	53.75	53.83
CVS2-66	89	1149	34.01	38.10	39.49	39.59
CVS2-66	89	1049	22.95	25.95	26.88	26.99
CVS2-66	89	950	14.06	15.77	16.32	16.39
CVS2-67	90	1244	36.52	48.17	51.82	52.01
CVS2-67	90	1147	27.58	36.36	38.39	38.47
CVS2-67	90	1048	20.18	25.44	26.26	26.29
CVS2-67	90	949	13.22	15.62	16.05	16.08
CVS2-68	91	1243	36.32	46.64	50.61	50.98
CVS2-68	91	1145	27.54	35.31	37.57	37.91
CVS2-68	91	1046	19.75	24.38	26.04	26.03
CVS2-68	91	946	13.11	15.54	16.02	16.08

(a) Electrical conductivity was measured at four frequencies as discussed in Section 5.3.

TABLE C.2. Electrical Conductivity at Temperature Data for CVS-II Phase 3 Glasses (continued)

Glass	ID #	Temp. (°C)	Electrical Conductivity (S/m)[a] .1k	1k	10k	100k
CVS2-69	92	1248	43.78	49.23	51.20	51.46
CVS2-69	92	1150	32.21	36.43	37.90	38.12
CVS2-69	92	1051	22.55	25.46	26.36	26.50
CVS2-69	92	952	13.40	14.91	15.35	15.43
CVS2-70	93	1248	42.63	50.09	52.66	52.94
CVS2-70	93	1150	32.20	37.34	38.97	39.11
CVS2-70	93	1051	22.79	26.07	26.98	27.10
CVS2-70	93	951	14.50	16.28	16.75	16.80
CVS2-71	94	1242	46.62	51.71	53.86	54.07
CVS2-71	94	1145	33.79	38.23	39.59	39.52
CVS2-71	94	1045	22.94	26.12	26.72	26.84
CVS2-71	94	946	14.14	15.84	16.23	16.23
CVS2-72	95	1243	40.64	49.53	52.07	52.15
CVS2-72	95	1145	30.43	36.79	38.24	38.29
CVS2-72	95	1046	21.17	25.16	25.92	25.98
CVS2-72	95	946	13.52	15.37	15.74	15.77
CVS2-73	96	1246	35.93	49.72	53.1	53.18
CVS2-73	96	1148	28.71	37.12	38.96	39.01
CVS2-73	96	1049	20.63	25.68	26.50	26.53
CVS2-73	96	949	13.49	15.76	16.13	16.16
CVS2-74	97	1248	41.77	48.60	50.72	50.90
CVS2-74	97	1150	31.39	35.92	37.37	37.30
CVS2-74	97	1051	21.76	24.33	25.44	25.43
CVS2-74	97	952	13.57	15.29	15.54	15.60
CVS2-75	98	1242	36.58	48.28	51.14	51.21
CVS2-75	98	1144	29.04	36.23	37.79	37.84
CVS2-75	98	1045	20.66	25.02	25.81	25.85
CVS2-75	98	945	13.33	15.44	15.81	15.84
CVS2-76	99	1246	91.19	106.69	111.64	110.85
CVS2-76	99	1148	67.72	80.32	84.47	84.34
CVS2-76	99	1049	47.65	57.17	60.33	60.42
CVS2-76	99	950	29.73	36.33	38.71	39.05
CVS2-77	100	1247	89.66	112.64	121.34	121.38
CVS2-77	100	1149	67.41	85.80	92.24	92.09
CVS2-77	100	1050	48.01	62.04	66.13	66.40
CVS2-77	100	951	33.23	41.25	43.20	43.58
CVS2-78	101	1248	14.19	14.95	15.31	15.33
CVS2-78	101	1149	9.51	10.11	10.30	10.28
CVS2-78	101	1050	5.86	6.19	6.27	6.27
CVS2-78	101	951	3.13	3.27	3.31	3.31

(a) Electrical conductivity was measured at four frequencies as discussed in Section 5.3.

TABLE C.2. Electrical Conductivity at Temperature Data for CVS-II Phase 3 Glasses (continued)

Glass	ID #	Temp. (°C)	Electrical Conductivity (S/m)[a] .1k	1k	10k	100k
CVS2-79	102	1248	20.34	22.42	23.39	23.49
CVS2-79	102	1150	7.94	8.51	8.77	8.86
CVS2-79	102	1051	4.64	4.92	5.02	5.10
CVS2-79	102	951	2.44	2.56	2.62	2.70
CVS2-80	103	1246	11.80	12.38	12.44	12.46
CVS2-80	103	1149	7.84	8.09	8.16	8.17
CVS2-80	103	1050	4.74	4.88	4.92	4.93
CVS2-80	103	952	2.47	2.6	2.74	2.91
CVS2-81	104	1244	25.14	27.94	29.78	30.14
CVS2-81	104	1147	15.80	19.25	20.64	20.96
CVS2-81	104	1048	9.53	12.06	13.10	13.28
CVS2-81	104	949	5.14	6.69	7.24	7.35
CVS2-82	105	1246	62.45	97.73	109.73	109.51
CVS2-82	105	1148	49.44	77.10	84.58	84.36
CVS2-82	105	1049	38.09	56.66	60.92	60.89
CVS2-82	105	950	28.25	37.67	39.62	39.65
CVS2-83	106	1247	97.21	121.43	130.70	130.75
CVS2-83	106	1149	74.42	94.34	101.74	102.54
CVS2-83	106	1050	54.87	69.69	75.05	76.05
CVS2-83	106	951	37.91	47.60	50.61	51.46
CVS2-84	107	1246	91.21	107.96	113.27	113.03
CVS2-84	107	1149	67.90	81.93	86.92	86.85
CVS2-84	107	1050	47.33	58.80	62.54	62.55
CVS2-84	107	950	29.41	37.52	40.26	40.44
CVS2-85	108	1246	65.35	93.99	102.57	102.83
CVS2-85	108	1148	50.78	72.72	77.84	77.71
CVS2-85	108	1050	37.98	52.52	55.62	55.56
CVS2-85	108	951	28.21	34.62	36.03	36.10
CVS2-86	109	1247	33.87	41.91	44.06	44.16
CVS2-86	109	1149	25.43	31.19	32.42	32.50
CVS2-86	109	1051	18.17	21.72	22.26	22.33
CVS2-86	109	951	11.81	13.44	13.72	13.76
CVS2-87	110	1241	33.74	45.09	47.92	47.96
CVS2-87	110	1144	27.05	34.01	35.32	35.35
CVS2-87	110	1044	19.17	23.40	23.96	24.03
CVS2-87	110	945	12.50	14.36	14.64	14.67
CVS2-88	111	1246	54.49	74.40	80.94	80.72
CVS2-88	111	1148	42.28	58.18	62.19	62.03
CVS2-88	111	1049	30.72	40.42	42.47	42.46
CVS2-88	111	950	19.04	24.78	25.89	25.98

(a) Electrical conductivity was measured at four frequencies as discussed in Section 5.3.

TABLE C.2. Electrical Conductivity at Temperature Data for CVS-II Phase 3 Glasses (continued)

Glass	ID #	Temp. (°C)	Electrical Conductivity (S/m)[a] .1k	1k	10k	100k
CVS2-89	112	1247	47.04	51.76	53.28	53.27
CVS2-89	112	1150	33.47	37.32	38.52	38.58
CVS2-89	112	1051	22.07	24.93	25.75	25.80
CVS2-89	112	951	12.89	14.7	15.18	15.25
CVS2-90	113	1246	41.40	45.05	46.40	46.44
CVS2-90	113	1148	29.75	32.67	33.78	33.81
CVS2-90	113	1049	19.71	22.09	22.70	22.73
CVS2-90	113	950	11.84	13.26	13.55	13.57
CVS2-91	114	1248	16.54	19.04	19.62	19.65
CVS2-91	114	1150	12.00	13.22	13.40	13.42
CVS2-91	114	1051	7.63	8.19	8.29	8.32
CVS2-91	114	952	4.17	4.39	4.44	4.45
CVS2-92	115	1247	61.91	74.74	79.02	78.83
CVS2-92	115	1149	45.82	54.6	57.28	57.19
CVS2-92	115	1050	31.82	36.98	38.34	38.38
CVS2-92	115	951	19.52	22.07	22.66	22.72
CVS2-93	116	1246	89.03	98.26	101.05	100.58
CVS2-93	116	1148	66.94	73.86	76.24	75.99
CVS2-93	116	1049	46.59	51.86	53.68	53.62
CVS2-93	116	950	29.71	32.85	33.91	33.9
CVS2-94	117	1246	67.06	89.37	96.89	96.89
CVS2-94	117	1148	51.17	68.76	74.03	73.88
CVS2-94	117	1050	36.80	49.48	52.55	52.60
CVS2-94	117	950	25.51	31.86	33.20	33.22
CVS2-95	118	1247	62.42	72.86	76.31	76.37
CVS2-95	118	1149	46.08	54.27	57.17	57.28
CVS2-95	118	1050	31.99	38.18	40.09	40.12
CVS2-95	118	950	19.87	23.90	24.78	24.82
CVS2-96	119	1247	32.82	36.44	37.61	37.65
CVS2-96	119	1149	22.82	25.32	26.07	26.13
CVS2-96	119	1050	14.48	16.17	16.50	16.53
CVS2-96	119	951	8.26	8.97	9.11	9.13
CVS2-97	120	1243	30.82	34.28	35.37	35.38
CVS2-97	120	1145	21.98	24.47	25.14	25.16
CVS2-97	120	1046	14.33	15.93	16.30	16.33
CVS2-97	120	946	8.39	9.19	9.33	9.36
CVS2-98	121	1244	49.82	76.05	84.60	84.67
CVS2-98	121	1147	39.44	60.37	65.26	65.27
CVS2-98	121	1048	32.66	44.51	47.09	47.04
CVS2-98	121	949	22.62	29.36	30.48	30.50

(a) Electrical conductivity was measured at four frequencies as discussed in Section 5.3.

TABLE C.2. Electrical Conductivity at Temperature Data for CVS-II Phase 3 Glasses (continued)

Glass	ID #	Temp. (°C)	Electrical Conductivity (S/m)[a] .1k	1k	10k	100k
CVS2-99	122	1244	(b)	28.00	(b)	(b)
CVS2-99	122	1147	(b)	19.70	(b)	(b)
CVS2-99	122	1048	(b)	12.80	(b)	(b)
CVS2-99	122	948	(b)	7.10	(b)	(b)
CVS2-100	123	1246	(b)	38.00	(b)	(b)
CVS2-100	123	1148	(b)	27.40	(b)	(b)
CVS2-100	123	1049	(b)	18.10	(b)	(b)
CVS2-100	123	948	(b)	10.70	(b)	(b)
CVS2-101	124	1247	69.03	78.38	83.78	85.56
CVS2-101	124	1149	49.97	58.72	63.07	63.02
CVS2-101	124	1050	33.85	40.94	43.12	43.15
CVS2-101	124	950	20.93	25.32	26.27	26.24

(a) Electrical conductivity was measured at four frequencies as discussed in Section 5.3.

(b) Data not taken at these frequencies.

TABLE C.3. Results of Fitting the Arrhenius Equation to the Electrical Conductivity at Temperature Data for Each CVS-I and CVS-II Phase 1, 2, and 3 Glass

Glass	# Points Fitted	Arrhenius Equation Coefficients A	Arrhenius Equation Coefficients B	Arrhenius Predicted ϵ_{1150} (S/m)
CVS1-1	4	8.68	-8184.8	18.65
CVS1-2	4	8.89	-8022.7	25.97
CVS1-3	4	9.82	-8886.9	35.64
CVS1-4	4	10.13	-11272.0	9.11
CVS1-5	5	8.42	-7107.9	30.74
CVS1-6	4	11.14	-10366.0	47.29
CVS1-7	4	9.51	-10792.0	6.87
CVS1-8	3	9.11	-9869.6	8.84
CVS1-9	4	9.87	-11014.0	8.37
CVS1-10	4	7.81	-6810.4	20.61
CVS1-11	4	10.11	-11527.0	7.47
CVS1-12	5	11.77	-10802.0	65.44
CVS1-13	4	8.89	-7627.4	34.17
CVS1-14	4	8.86	-7554.1	34.92
CVS1-15	4	9.03	-7069.4	58.20
CVS1-16	4	8.65	-7646.3	26.36
CVS1-17	4	9.57	-8852.5	28.53
CVS1-18	5	9.98	-8254.0	65.50
CVS1-19	4	9.31	-8704.5	24.27
CVS1-20	4	9.44	-8747.3	26.88
CVS1-21	4	10.25	-11624.0	8.05
CVS1-22	4	8.81	-9368.9	9.24
CVS1-23	4	9.22	-8379.0	28.03
CVS2 -1	4	9.08	-7971.4	32.55
CVS2 -2	4	9.23	-8153.7	33.08
CVS2 -3	4	9.69	-9370.7	22.36
CVS2 -4	4	9.32	-8772.7	23.43
CVS2 -5	4	8.99	-8758.6	17.00
CVS2 -6	4	9.67	-9528.5	19.63
CVS2 -7	4	8.66	-7468.4	30.39
CVS2 -8	4	8.94	-7516.5	38.78
CVS2 -9	4	8.95	-7639.8	35.84
CVS2-10	4	8.28	-7291.0	23.58
CVS2-11	4	9.77	-8828.7	35.30
CVS2-12	4	9.52	-9064.1	23.26
CVS2-13	4	8.45	-7007.6	33.95
CVS2-14	4	9.40	-8661.7	27.40
CVS2-15	4	8.48	-6969.4	35.85
CVS2-16	4	9.09	-8219.3	27.54

TABLE C.3. Results of Fitting the Arrhenius Equation to the Electrical Conductivity at Temperature Data for Each CVS-I and CVS-II Phase 1, 2, and 3 Glass (continued)

Glass	# Points Fitted	Arrhenius Equation Coefficients A	Arrhenius Equation Coefficients B	Arrhenius Predicted ϵ_{1150} (S/m)
CVS2-17	4	9.39	-8720.0	26.06
CVS2-18	4	8.93	-7952.8	28.34
CVS2-19	4	8.69	-7644.6	27.55
CVS2-20	4	9.13	-7807.7	38.08
CVS2-21	4	8.97	-7858.5	31.58
CVS2-22	4	8.98	-7646.3	37.02
CVS2-23	4	8.15	-6542.4	34.97
CVS2-24	4	8.97	-7476.4	40.91
CVS2-25	4	9.66	-8152.8	50.70
CVS2-26	4	9.62	-8653.2	34.30
CVS2-27	4	8.60	-7094.0	36.98
CVS2-28	4	8.17	-6269.5	43.25
CVS2-29	4	11.19	-13175.6	6.89
CVS2-30	4	8.18	-8245.5	10.85
CVS2-31	4	9.43	-10011.5	10.96
CVS2-32	4	8.42	-6221.7	57.11
CVS2-33	4	9.01	-6967.2	60.94
CVS2-34	4	7.92	-5630.8	52.63
CVS2-35	4	8.50	-6324.7	57.81
CVS2-36	4	10.10	-9126.6	39.89
CVS2-37	4	8.45	-6722.4	41.60
CVS2-38	4	9.00	-9097.4	13.62
CVS2-39	4	9.40	-7526.7	61.14
CVS2-40	4	9.08	-7734.2	38.09
CVS2-41	4	9.07	-8019.9	30.87
CVS2-42	4	9.30	-8312.1	31.90
CVS2-43	4	9.20	-8187.3	31.42
CVS2-44	4	8.90	-7890.7	28.60
CVS2-45	4	8.86	-8024.8	25.00
CVS2-46	4	9.09	-7888.1	34.77
CVS2-47	4	8.14	-6918.7	26.65
CVS2-48	4	9.34	-8856.5	22.48
CVS2-49	4	8.80	-8036.9	23.38
CVS2-50	4	9.35	-8731.4	24.81
CVS2-51	4	9.00	-8043.2	28.30

TABLE C.3. Results of Fitting the Arrhenius Equation to the Electrical Conductivity at Temperature Data for Each CVS-I and CVS-II Phase 1, 2, and 3 Glass (continued)

Glass	# Points Fitted	Arrhenius Equation Coefficients A	B	Arrhenius Predicted ϵ_{1150} (S/m)
CVS2-52	4	8.23	-6646.8	35.17
CVS2-53	(a)	(a)	(a)	(a)
CVS2-54	(a)	(a)	(a)	(a)
CVS2-55	4	8.72	-7715.3	27.02
CVS2-56	4	9.11	-8228.9	27.83
CVS2-57	4	9.17	-8296.3	28.13
CVS2-58	4	8.93	-7736.3	32.87
CVS2-59	4	8.64	-6770.5	48.41
CVS2-60	4	8.28	-5793.9	68.96
CVS2-61	4	8.52	-6690.3	45.69
CVS2-62	4	9.19	-9208.2	15.18
CVS2-63	4	8.94	-7705.7	34.05
CVS2-64	4	8.91	-7445.9	39.53
CVS2-65	4	9.06	-7773.0	36.43
CVS2-66	4	8.85	-7482.2	37.74
CVS2-67	4	8.56	-7074.5	36.20
CVS2-68	4	8.39	-6871.7	35.28
CVS2-69	4	8.84	-7481.5	36.01
CVS2-70	4	8.56	-7041.8	36.97
CVS2-71	4	8.83	-7376.6	38.46
CVS2-72	4	8.73	-7292.5	36.88
CVS2-73	4	8.66	-7186.8	36.85
CVS2-74	4	8.70	-7304.8	35.40
CVS2-75	4	8.58	-7097.5	36.40
CVS2-76	4	9.13	-6747.8	80.23
CVS2-77	4	8.88	-6309.3	85.62
CVS2-78	4	8.99	-9528.3	9.96
CVS2-79	4	11.57	-13130.0	10.44
CVS2-80	4	9.02	-9864.0	8.08
CVS2-81	4	9.28	-8991.3	19.24
CVS2-82	4	8.55	-5990.6	76.39
CVS2-83	4	8.68	-5883.6	94.09
CVS2-84	4	9.05	-6619.6	81.62
CVS2-85	4	8.71	-6306.0	72.19
CVS2-86	4	8.46	-7150.5	30.93
CVS2-87	4	8.55	-7139.3	34.12

(a) Electrical conductivity was not measured for radioactive glasses CVS2-53 and CVS2-54.

TABLE C.3. Results of Fitting the Arrhenius Equation to the Electrical Conductivity at Temperature Data for Each CVS-I and CVS-II Phase 1, 2, and 3 Glass (continued)

Glass	# Points Fitted	Arrhenius Equation Coefficients A	Arrhenius Equation Coefficients B	Arrhenius Predicted ϵ_{1150} (S/m)
CVS2-88	4	8.91	-6939.8	56.70
CVS2-89	4	9.17	-7909.3	36.92
CVS2-90	4	8.87	-7671.6	32.58
CVS2-91	4	9.06	-9257.8	12.90
CVS2-92	4	9.38	-7664.4	54.07
CVS2-93	4	9.13	-6878.1	73.54
CVS2-94	4	8.78	-6479.2	68.27
CVS2-95	4	8.89	-6966.2	54.06
CVS2-96	4	9.41	-8805.4	25.08
CVS2-97	4	8.97	-8207.1	24.56
CVS2-98	4	8.30	-5984.7	59.92
CVS2-99	4	9.01	-8572.8	19.71
CVS2-100	4	8.86	-7904.7	27.21
CVS2-101	4	9.03	-7073.1	58.16

APPENDIX D

NORMALIZED ELEMENTAL RELEASES AND STANDARD DEVIATIONS FROM DUPLICATE MCC-1 AND PCT DISSOLUTION TESTS

APPENDIX D

NORMALIZED ELEMENTAL RELEASES AND STANDARD DEVIATIONS FROM DUPLICATE MCC-1 AND PCT DISSOLUTION TESTS

Normalized elemental releases and solution pH values from duplicate 28-day MCC-1 and 7-day PCT dissolution tests of CVS glasses are given in Tables D.1 and D.2, respectively. Variations in duplicate dissolution test results are a function of how the duplicate dissolution tests were performed and how the chemical analyses of the two solutions for each glass were performed. In CVS-I the dissolution tests were performed in two groups, with the duplicates of each glass in the same group. In CVS-II, tests were again done in two groups, but with one replicate of each glass in one group and the other replicate of each glass in another group. This change was made to avoid confounding group differences with glass effects, and to instead include group-to-group variations in the estimate of experimental (testing and chemical analysis) variation. Solutions from different glasses and duplicate tests of the same glass were analyzed in random order, so that more than very short-term variations in the analytical process and instrumentation are included.

Standard deviations (SD) and percent relative standard deviations (%RSD) for normalized B release (before and after natural log transformations) from the duplicate MCC-1 and PCT dissolution tests are given in Tables D.3 and D.4, respectively. Short-term variations in MCC-1 and PCT B normalized release results are relatively constant with size of release on a relative (or log transformed) basis. The pooled (i.e., "averaged" over all CVS glasses, except that outliers were removed) %RSD is 2.92% for B release in MCC-1 (Table D.3) and is 3.85% for B release in PCT (Table D.4). These values should be considered as estimates of short-term dissolution test and analytical standard deviations.

TABLE D.1. Normalized Elemental Release and pH Data from Duplicate 28-day MCC-1 Tests (90°C, DIW, $10m^{-1}$) Performed on CVS-I and CVS-II Glasses

Glass	ID[b] #	PS[c]	Normalized[a] Elemental Release Rates (g/m^2) Si	B	Li	Mo	Na	Cs	pH
CVS1-1	1	M	8.81	12.33	11.78	12.14	12.15	10.65	9.92
CVS1-1	1	M	9.17	12.61	12.12	12.34	12.58	8.72	9.98
CVS1-2	2	1	6.92	7.59	7.19	8.93	7.38	8.28	10.17
CVS1-2	2	1	6.72	7.33	7.19	7.54	7.44	8.67	9.91
CVS1-3	3	1	10.18	14.90	14.99	14.80	14.99	9.86	9.41
CVS1-3	3	1	11.50	16.24	16.13	16.19	16.25	10.64	9.74
CVS1-4	4	1	65.60	191.32	162.58	178.68	181.19	102.50	9.65
CVS1-4	4	1	64.10	188.10	161.29	175.89	179.70	102.50	9.65
CVS1-5	5	1	10.12	11.19	10.35	11.17	10.63	13.80	10.01
CVS1-5	5	1	10.72	11.77	10.57	12.00	11.03	14.19	10.12
CVS1-6	6	1	45.94	119.61	105.99	116.70	90.57	9.86	10.06
CVS1-6	6	1	44.82	122.99	111.21	120.05	95.42	9.86	9.76
CVS1-7	7	1	7.42	10.80	10.28	11.73	10.57	9.46	9.81
CVS1-7	7	1	7.57	11.19	10.73	10.89	10.93	11.04	9.89
CVS1-8	8	1	11.59	17.94	16.71	18.71	17.23	15.37	9.71
CVS1-8	8	1	11.87	17.81	16.75	17.87	17.39	15.77	9.72
CVS1-9	9	1	45.79	158.64	148.82	123.40	150.30	67.80	9.24
CVS1-9	9	1	45.79	158.80	148.82	124.80	150.30	70.96	9.24
CVS1-10	10	1	2.51	2.57	3.18	2.23	2.60	2.17	8.65
CVS1-10	10	1	2.88	2.92	3.48	2.51	3.01	2.60	8.37
CVS1-11	11	1	6.72	8.22	8.17	7.78	8.31	5.92	9.15
CVS1-11	11	1	6.82	8.28	8.17	7.88	8.33	5.92	9.18
CVS1-12	12	1	49.35	118.48	122.58	120.05	122.68	114.32	10.86
CVS1-12	12	1	49.35	118.48	122.58	117.26	122.68	98.55	10.87
CVS1-13	13	1	179.56	672.03	632.26	647.72	617.40	98.55	10.55
CVS1-13	13	1	195.68	709.00	673.12	684.02	657.21	106.44	10.63
CVS1-14	14	1	24.01	75.24	69.68	47.18	58.92	9.86	10.04
CVS1-14	14	1	23.86	72.03	66.45	44.67	56.46	10.25	10.14
CVS1-15	15	1	73.02	213.50	174.50	199.90	174.72	57.95	12.37
CVS1-15	15	1	73.79	207.07	169.58	198.50	170.27	56.77	12.37
CVS1-16	16	1	10.07	15.50	14.04	18.15	14.46	14.98	10.42
CVS1-16	16	1	12.69	18.20	16.71	17.87	17.56	17.74	10.54

(a) Elemental releases normalized using as-batched compositions from Table A.1.

(b) ID# is a consecutive integer numbering of all CVS glasses.

(c) PS is the plotting symbol used in plots associated with this data: 1 = CVS-I boundary, 2 = CVS-II Phase 1 interior, 3 = CVS-II Phase 2a boundary, 4 = CVS-II Phase 2b interior, 5 = CVS-II Phase 3 boundary, 6 = CVS-II Phase 4 one-component-at-a-time, M = middle compositions, O = other than NCAW waste glasses, A = EA glass.

TABLE D.1. Normalized Elemental Release and pH Data from Duplicate 28-day MCC-1 Tests (90°C, DIW, $10m^{-1}$) Performed on CVS-I and CVS-II Glasses (continued)

Glass	ID[b] #	PS[c]	Normalized[a] Elemental Release Rates (g/m^2) Si	B	Li	Mo	Na	Cs	pH
CVS1-17	17	1	20.08	38.84	40.64	37.69	40.57	34.69	10.94
CVS1-17	17	1	20.40	39.36	41.08	38.53	41.13	39.42	10.98
CVS1-18	18	1	5.93	24.44	24.33	20.61	23.98	14.90	10.59
CVS1-18	18	1	5.88	23.67	22.98	20.52	22.50	11.39	11.47
CVS1-19	19	M	8.72	12.73	12.93	11.98	12.76	9.68	9.84
CVS1-19	19	M	9.17	13.32	13.44	12.60	13.34	10.65	9.92
CVS1-20	20	M	8.68	12.28	12.18	11.78	12.19	9.30	9.88
CVS1-20	20	M	8.99	12.73	12.81	12.05	12.79	9.10	9.88
CVS1-21	21	1	60.73	204.18	178.28	192.64	190.18	102.50	9.66
CVS1-21	21	1	61.48	207.40	177.20	195.43	194.67	102.50	9.64
CVS1-22	22	1	11.16	17.04	16.75	17.59	16.75	15.77	9.80
CVS1-22	22	1	12.07	17.68	17.44	17.31	17.23	15.77	9.73
CVS1-23	23	M	------ Results Discarded as Obviously Erroneous ------						
CVS1-23	23	M	12.02	15.37	15.71	14.64	15.63	14.00	9.96
CVS2-1	24	2	9.39	12.42	12.98	11.99	11.94	(d)	9.48
CVS2-1	24	2	9.35	12.06	12.24	11.99	11.74	12.96	9.44
CVS2-2	25	2	7.12	8.21	9.33	(d)	8.98	7.07	9.62
CVS2-2	25	2	7.47	8.67	9.74	9.23	9.33	8.48	9.60
CVS2-3	26	2	7.34	8.87	9.56	(d)	9.12	9.33	9.27
CVS2-3	26	2	7.39	8.87	9.56	9.23	9.12	11.03	9.32
CVS2-4	27	2	9.53	9.73	11.10	(d)	10.48	12.05	9.51
CVS2-4	27	2	9.57	9.73	10.64	10.79	10.27	14.46	9.54
CVS2-5	28	2	9.00	10.20	11.76	10.49	10.90	7.81	9.03
CVS2-5	28	2	9.44	10.61	11.89	10.49	11.05	10.05	9.06
CVS2-6	29	2	13.35	17.24	19.05	18.27	18.61	13.68	9.65
CVS2-6	29	2	13.78	17.71	18.43	18.74	19.04	16.42	9.68
CVS2-7	30	2	9.46	5.12	4.78	13.87	24.85	11.23	9.78
CVS2-7	30	2	9.51	4.92	4.78	13.87	23.63	11.48	9.74
CVS2-8	31	2	15.36	18.97	20.71	20.39	19.62	14.54	9.81
CVS2-8	31	2	14.70	18.04	19.12	17.99	18.72	13.63	9.82

(a) Elemental releases normalized using as-batched compositions from Table A.1.

(b) ID# is a consecutive integer numbering of all CVS glasses.

(c) PS is the plotting symbol used in plots associated with this data: 1 = CVS-I boundary, 2 = CVS-II Phase 1 interior, 3 = CVS-II Phase 2a boundary, 4 = CVS-II Phase 2b interior, 5 = CVS-II Phase 3 boundary, 6 = CVS-II Phase 4 one-component-at-a-time, M = middle compositions, O = other than NCAW waste glasses, A = EA glass.

(d) Missing or erroneous values.

TABLE D.1. Normalized Elemental Release and pH Data from Duplicate 28-day MCC-1 Tests (90°C, DIW, $10m^{-1}$) Performed on CVS-I and CVS-II Glasses (continued)

Glass	ID[b] #	PS[c]	Normalized[a] Elemental Release Rates (g/m^2) Si	B	Li	Mo	Na	Cs	pH
CVS2-9	32	2	11.36	13.20	14.60	13.84	13.48	(d)	9.53
CVS2-9	32	2	11.48	13.20	14.21	13.84	12.85	11.13	9.50
CVS2-10	33	2	10.97	12.18	12.79	11.99	12.68	5.45	8.93
CVS2-10	33	2	11.01	12.37	12.79	11.99	9.37	9.54	8.92
CVS2-11	34	2	11.73	19.85	22.29	20.28	18.07	14.14	9.93
CVS2-11	34	2	11.59	19.85	21.11	20.28	17.77	17.08	9.96
CVS2-12	35	2	8.32	9.77	10.51	11.11	9.57	8.48	9.26
CVS2-12	35	2	8.55	9.95	10.04	10.00	9.77	10.60	9.24
CVS2-13	36	2	10.45	13.13	14.00	12.85	17.72	14.42	9.73
CVS2-13	36	2	10.81	13.59	14.00	12.85	15.47	14.00	9.74
CVS2-14	37	2	8.50	15.71	16.20	16.96	15.39	7.95	9.51
CVS2-14	37	2	7.98	14.48	14.85	15.60	14.54	8.15	9.44
CVS2-15	38	2	10.83	24.48	32.52	9.75	5.24	6.55	9.02
CVS2-15	38	2	11.38	25.72	33.57	9.75	5.52	10.48	9.04
CVS2-16	39	M	14.47	18.24	18.52	17.61	18.35	13.80	9.41
CVS2-16	39	M	14.35	17.93	17.92	17.13	18.10	15.69	9.51
CVS2-17	40	M	9.09	12.18	13.69	12.85	13.17	(d)	9.31
CVS2-17	40	M	9.37	12.47	14.34	12.85	13.78	10.60	9.32
CVS2-18	41	M	15.66	19.72	20.62	19.51	24.48	14.14	9.42
CVS2-18	41	M	15.82	19.72	20.03	19.04	22.26	15.55	9.34
CVS2-19	42	M	11.37	14.01	14.38	15.15	13.59	9.43	9.31
CVS2-19	42	M	11.00	13.37	13.13	14.07	12.55	9.90	9.37
CVS2-20	43	3	7.31	8.49	7.39	(e)	7.74	6.31	9.62
CVS2-20	43	3	7.12	8.36	7.17	(e)	7.63	6.31	9.47
CVS2-21	44	3	9.67	12.16	10.63	(e)	11.56	12.22	9.41
CVS2-21	44	3	9.11	11.45	9.98	(e)	10.94	6.31	9.32

(a) Elemental releases normalized using as-batched compositions from Table A.1.

(b) ID# is a consecutive integer numbering of all CVS glasses.

(c) PS is the plotting symbol used in plots associated with this data: 1 = CVS-I boundary, 2 = CVS-II Phase 1 interior, 3 = CVS-II Phase 2a boundary, 4 = CVS-II Phase 2b interior, 5 = CVS-II Phase 3 boundary, 6 = CVS-II Phase 4 one-component-at-a-time, M = middle compositions, O = other than NCAW waste glasses, A = EA glass.

(d) Missing or erroneous values.

(e) Mo release was determined as not of interest, and so data were no longer collected beginning with Phase 2 of CVS-II.

TABLE D.1. Normalized Elemental Release and pH Data from Duplicate 28-day MCC-1 Tests (90°C, DIW, $10m^{-1}$) Performed on CVS-I and CVS-II Glasses (continued)

Glass	ID[b] #	PS[c]	Normalized[a] Elemental Release Rates (g/m^2) Si	B	Li	Mo	Na	Cs	pH
CVS2-22	45	3	11.51	15.76	13.67	(e)	14.67	10.25	9.75
CVS2-22	45	3	11.36	15.43	13.33	(e)	14.45	11.04	9.73
CVS2-23	46	3	10.31	11.21	10.56	(e)	11.66	9.86	9.87
CVS2-23	46	3	10.23	11.21	10.41	(e)	11.59	10.25	9.84
CVS2-24	47	3	10.05	19.94	17.54	(e)	15.89	0.84	9.40
CVS2-24	47	3	10.15	19.77	17.20	(e)	15.95	1.05	9.35
CVS2-25	48	3	21.20	34.53	31.64	(e)	33.49	31.88*	10.32
CVS2-25	48	3	21.33	34.47	31.34	(e)	33.81	33.27*	10.22
CVS2-26	49	3	17.36	37.94	34.10	(e)	36.06	9.46	9.75
CVS2-26	49	3	18.23	40.35	35.94	(e)	38.43	8.67	9.75
CVS2-27	50	3	8.84	11.25	9.91	(e)	10.98	13.01	9.73
CVS2-27	50	3	8.72	11.19	9.88	(e)	10.98	9.86	9.54
CVS2-28	51	3	8.75	9.77	8.81	(e)	9.84	8.28	9.51
CVS2-28	51	3	8.97	9.90	8.93	(e)	10.11	7.88	9.51
CVS2-29	52	3	20.54	41.80	37.42	(e)	40.13	24.44	9.14
CVS2-29	52	3	20.97	42.77	38.06	(e)	41.13	26.81	9.14
CVS2-30	53	3	8.32	25.08	21.72	(e)	18.79	1.97	8.79
CVS2-30	53	3	7.90	23.79	20.43	(e)	17.82	1.97	8.72
CVS2-31	54	3	22.49	46.93	42.69	(e)	44.20	17.74	9.40
CVS2-31	54	3	22.30	47.11	42.69	(e)	44.20	14.19	9.41
CVS2-32	55	3	13.73	16.78	14.32	(e)	16.11	9.46	10.07
CVS2-32	55	3	13.50	16.46	13.92	(e)	15.97	7.10	10.07
CVS2-33	56	3	9.00	14.24	12.41	(e)	13.61	9.46	10.27
CVS2-33	56	3	9.46	14.78	13.00	(e)	14.29	10.25	10.24
CVS2-34	57	3	12.82	29.52	26.11	(e)	22.78	3.94	9.96
CVS2-34	57	3	12.77	28.96	26.23	(e)	22.84	3.15	10.00
CVS2-35	58	3	9.67	11.64	10.95	(e)	12.13	14.19	10.23
CVS2-35	58	3	9.62	11.58	10.70	(e)	11.93	11.83	10.20

(a) Elemental releases normalized using as-batched compositions from Table A.1.

(b) ID# is a consecutive integer numbering of all CVS glasses.

(c) PS is the plotting symbol used in plots associated with this data: 1 = CVS-I boundary, 2 = CVS-II Phase 1 interior, 3 = CVS-II Phase 2a boundary, 4 = CVS-II Phase 2b interior, 5 = CVS-II Phase 3 boundary, 6 = CVS-II Phase 4 one-component-at-a-time, M = middle compositions, O = other than NCAW waste glasses, A = EA glass.

(e) Mo release was determined as not of interest, and so data were no longer collected beginning with Phase 2 of CVS-II.

* Solution was re-analyzed to rectify different results from first analysis.

TABLE D.1. Normalized Elemental Release and pH Data from Duplicate 28-day MCC-1 Tests (90°C, DIW, $10m^{-1}$) Performed on CVS-I and CVS-II Glasses (continued)

Glass	ID[b] #	PS[c]	Normalized[a] Elemental Release Rates (g/m^2) Si	B	Li	Mo	Na	Cs	pH
CVS2-36	59	3	15.41	21.09	18.96	(e)	20.27	17.35	10.13
CVS2-36	59	3	15.57	21.09	19.05	(e)	20.42	19.71	10.12
CVS2-37	60	3	9.07	9.50	8.23	(e)	8.78	7.88	9.32
CVS2-37	60	3	9.52	9.77	8.57	(e)	9.32	7.10	9.33
CVS2-38	61	3	17.10	23.95	20.65	(e)	22.59	15.37	9.27
CVS2-38	61	3	16.77	23.34	20.06	(e)	22.07	14.98	9.27
CVS2-39	62	3	10.73	16.72	14.59	(e)	15.63	10.25	10.22
CVS2-39	62	3	10.25	15.88	13.82	(e)	15.04	10.25	10.12
CVS2-40	63	4	9.45	12.13	10.52	(e)	11.59	7.36	9.70
CVS2-40	63	4	9.45	12.28	10.78	(e)	11.77	11.17	9.88
CVS2-41	64	4	7.78	9.17	7.86	(e)	8.63	8.67	9.50
CVS2-41	64	4	8.07	9.68	8.33	(e)	9.23	5.78	9.69
CVS2-42	65	4	10.99	14.15	12.20	(e)	13.33	12.61	9.86
CVS2-42	65	4	10.99	14.47	12.20	(e)	13.48	17.08	9.86
CVS2-43	66	4	8.64	11.34	9.95	(e)	10.84	6.70	9.21
CVS2-43	66	4	8.60	11.32	9.88	(e)	10.89	8.41	9.24
CVS2-44	67	4	8.77	10.17	8.77	(e)	9.70	8.94	9.55
CVS2-44	67	4	8.81	10.38	8.92	(e)	10.05	5.52	9.57
CVS2-45	68	4	8.75	11.48	9.79	(e)	10.81	11.26	9.39
CVS2-45	68	4	8.83	11.72	9.90	(e)	11.00	6.19	9.46
CVS2-46	69	4	9.05	11.01	9.62	(e)	10.25	7.23	9.36
CVS2-46	69	4	9.09	10.96	9.55	(e)	10.46	9.64	9.27
CVS2-47	70	4	8.64	11.34	9.73	(e)	10.66	11.83	9.78
CVS2-47	70	4	8.88	11.77	10.28	(e)	11.19	9.57	9.88
CVS2-48	71	4	8.32	10.46	9.15	(e)	9.98	6.50	9.41
CVS2-48	71	4	8.50	10.79	9.26	(e)	10.23	4.76	9.42
CVS2-49	72	4	9.39	11.26	9.69	(e)	10.63	5.26	8.96
CVS2-49	72	4	9.56	11.44	9.89	(e)	10.79	8.80	9.06

(a) Elemental releases normalized using as-batched compositions from Table A.1.

(b) ID# is a consecutive integer numbering of all CVS glasses.

(c) PS is the plotting symbol used in plots associated with this data: 1 = CVS-I boundary, 2 = CVS-II Phase 1 interior, 3 = CVS-II Phase 2a boundary, 4 = CVS-II Phase 2b interior, 5 = CVS-II Phase 3 boundary, 6 = CVS-II Phase 4 one-component-at-a-time, M = middle compositions, O = other than NCAW waste glasses, A = EA glass.

(e) Mo release was determined as not of interest, and so data were no longer collected beginning with Phase 2 of CVS-II.

TABLE D.1. Normalized Elemental Release and pH Data from Duplicate 28-day MCC-1 Tests (90°C, DIW, $10m^{-1}$) Performed on CVS-I and CVS-II Glasses (continued)

Glass	ID[b] #	PS[c]	Normalized[a] Elemental Release Rates (g/m^2) Si	B	Li	Mo	Na	Cs	pH
CVS2-50	73	M	8.41	11.40	9.78	(e)	10.75	11.62	9.44
CVS2-50	73	M	8.32	11.46	9.89	(e)	10.87	8.23	9.45
CVS2-51	74	M	10.31	12.40	10.26	(e)	12.18	5.29	9.47
CVS2-51	74	M	10.15	12.30	10.38	(e)	12.18	9.92	9.49
CVS2-52	75	4	8.76	9.84	8.62	(e)	9.34	9.35	9.47
CVS2-52	75	4	9.22	10.31	8.79	(e)	9.76	6.35	9.46
CVS2-53	76	4	(f)	(f)	(f)	(f)	(f)	(f)	(f)
CVS2-53	76	4	(f)	(f)	(f)	(f)	(f)	(f)	(f)
CVS2-54	77	M	(f)	(f)	(f)	(f)	(f)	(f)	(f)
CVS2-54	77	M	(f)	(f)	(f)	(f)	(f)	(f)	(f)
CVS2-55	78	0	13.19	15.95	13.61	(e)	14.80	0.33	9.53
CVS2-55	78	0	13.03	15.86	13.84	(e)	15.04	0.33	9.50
CVS2-56	79	0	14.12	16.91	14.70	(e)	16.00	0.33	9.56
CVS2-56	79	0	14.60	17.55	15.28	(e)	16.59	0.33	9.57
CVS2-57	80	0	11.71	14.67	12.80	(e)	13.73	0.33	9.57
CVS2-57	80	0	12.55	15.89	13.84	(e)	15.04	0.33	9.52
CVS2-58	81	4	8.22	12.52	10.97	(e)	12.02	4.34	9.39
CVS2-58	81	4	9.09	13.78	11.92	(e)	13.42	4.34	9.32
CVS2-59	82	5	9.76	12.35	10.35	(e)	11.69	12.00	9.84
CVS2-59	82	5	9.76	11.60	10.06	(e)	11.69	5.03	9.86
CVS2-60	83	5	10.92	16.52	14.76	(e)	16.41	1.47	10.38
CVS2-60	83	5	10.52	16.52	14.47	(e)	16.41	1.84	10.49
CVS2-61	84	5	10.12	10.65	9.43	(e)	10.44	7.26	9.64
CVS2-61	84	5	10.52	11.14	9.72	(e)	11.01	8.21	9.86
CVS2-62	85	5	9.96	12.21	11.03	(e)	11.98	11.18	9.34
CVS2-62	85	5	9.96	12.57	12.13	(e)	13.18	4.97	9.31
CVS2-63	86	5	7.93	9.55	8.43	(e)	9.22	11.04	9.60
CVS2-63	86	5	7.93	9.74	12.65	(e)	9.93	5.91	9.62

(a) Elemental releases normalized using as-batched compositions from Table A.1.

(b) ID# is a consecutive integer numbering of all CVS glasses.

(c) PS is the plotting symbol used in plots associated with this data: 1 = CVS-I boundary, 2 = CVS-II Phase 1 interior, 3 = CVS-II Phase 2a boundary, 4 = CVS-II Phase 2b interior, 5 = CVS-II Phase 3 boundary, 6 = CVS-II Phase 4 one-component-at-a-time, M = middle compositions, 0 = other than NCAW waste glasses, A = EA glass.

(e) Mo release was determined as not of interest, and so data were no longer collected beginning with Phase 2 of CVS-II.

(f) Radioactive glasses were not tested by MCC-1.

TABLE D.1. Normalized Elemental Release and pH Data from Duplicate 28-day MCC-1 Tests (90°C, DIW, $10m^{-1}$) Performed on CVS-I and CVS-II Glasses (continued)

Glass	ID[b] #	PS[c]	Normalized[a] Elemental Release Rates (g/m^2) Si	B	Li	Mo	Na	Cs	pH
CVS2-64	87	0	10.88	12.00	10.72	(e)	12.09	9.84	9.83
CVS2-64	87	0	10.50	12.63	10.72	(e)	12.53	10.66	9.87
CVS2-65	88	0	8.00	9.69	8.64	(e)	9.25	(g)	9.67
CVS2-65	88	0	7.60	9.12	8.02	(e)	8.78	(g)	9.51
CVS2-66	89	0	10.32	11.57	10.28	(e)	11.13	(g)	9.60
CVS2-66	89	0	10.32	11.92	10.69	(e)	12.24	(g)	9.62
CVS2-67	90	0	10.69	10.94	9.59	(e)	10.92	(g)	9.07
CVS2-67	90	0	11.16	11.35	10.33	(e)	11.54	(g)	9.15
CVS2-68	91	0	10.18	10.44	9.27	(e)	10.31	(g)	9.24
CVS2-68	91	0	10.18	10.68	9.58	(e)	10.82	(g)	9.18
CVS2-69	92	0	9.44	9.88	8.75	(e)	9.74	(g)	9.46
CVS2-69	92	0	9.44	9.88	8.75	(e)	9.95	(g)	9.44
CVS2-70	93	0	11.01	11.56	10.58	(e)	11.78	(g)	9.28
CVS2-70	93	0	11.01	11.56	10.27	(e)	11.78	(g)	9.16
CVS2-71	94	5	10.13	12.00	10.38	(e)	11.51	9.52	9.83
CVS2-71	94	5	10.13	12.00	10.72	(e)	12.09	9.52	9.74
CVS2-72	95	5	10.32	11.57	10.28	(e)	12.24	8.78	9.67
CVS2-72	95	5	10.32	11.92	10.69	(e)	12.24	8.97	9.75
CVS2-73	96	5	5.94	6.41	5.56	(e)	6.09	6.07	9.07
CVS2-73	96	5	6.36	6.88	6.18	(e)	6.59	5.12	9.13
CVS2-74	97	5	8.68	9.88	8.75	(e)	9.74	8.18	9.54
CVS2-74	97	5	8.68	9.88	8.75	(e)	9.95	8.18	9.44
CVS2-75	98	5	7.92	8.62	7.78	(e)	8.63	5.82	9.11
CVS2-75	98	5	7.92	8.62	7.78	(e)	8.63	5.82	9.13
CVS2-76	99	5	20.01	26.26	23.82	(e)	26.95	19.71	10.70
CVS2-76	99	5	20.44	26.80	23.48	(e)	27.70	19.71	10.71
CVS2-77	100	5	26.30	48.77	43.01	(e)	44.17	13.14	11.13
CVS2-77	100	5	26.77	50.38	43.01	(e)	46.42	13.14	11.21

(a) Elemental releases normalized using as-batched compositions from Table A.1.

(b) ID# is a consecutive integer numbering of all CVS glasses.

(c) PS is the plotting symbol used in plots associated with this data: 1 = CVS-I boundary, 2 = CVS-II Phase 1 interior, 3 = CVS-II Phase 2a boundary, 4 = CVS-II Phase 2b interior, 5 = CVS-II Phase 3 boundary, 6 = CVS-II Phase 4 one-component-at-a-time, M = middle compositions, O = other than NCAW waste glasses, A = EA glass.

(e) Mo release was determined as not of interest, and so data were no longer collected beginning with Phase 2 of CVS-II.

(g) This glass did not contain Cs.

TABLE D.1. Normalized Elemental Release and pH Data from Duplicate 28-day MCC-1 Tests (90°C, DIW, $10m^{-1}$) Performed on CVS-I and CVS-II Glasses (continued)

Glass	ID[b] #	PS[c]	Normalized[a] Elemental Release Rates (g/m^2) Si	B	Li	Mo	Na	Cs	pH
CVS2-78	101	5	20.60	32.15	27.94	(e)	29.65	12.42	9.13
CVS2-78	101	5	20.22	32.15	27.94	(e)	32.35	7.88	9.17
CVS2-79	102	5	23.40	32.15	28.44	(e)	29.65	10.95	8.82
CVS2-79	102	5	23.40	32.15	30.21	(e)	32.35	13.58	8.87
CVS2-80	103	5	27.79	48.23	41.54	(e)	45.82	19.12	9.09
CVS2-80	103	5	24.42	42.20	36.66	(e)	40.43	11.04	9.11
CVS2-81	104	5	48.56	107.18	89.09	(e)	93.27	38.65	11.57
CVS2-81	104	5	48.56	107.18	89.09	(e)	101.04	40.58	11.63
CVS2-82	105	5	366.30	643.09	522.27	(e)	591.49	118.27	11.76
CVS2-82	105	5	358.67	643.09	491.55	(e)	591.49	57.16	11.82
CVS2-83	106	5	28.78	37.19	33.84	(e)	36.69	25.84	10.70
CVS2-83	106	5	29.22	37.19	33.84	(e)	38.93	31.10	10.74
CVS2-84	107	5	22.54	29.47	26.11	(e)	29.20	17.35	10.78
CVS2-84	107	5	23.01	30.55	26.11	(e)	30.70	19.71	10.73
CVS2-85	108	5	15.54	18.76	15.98	(e)	18.72	17.51	10.50
CVS2-85	108	5	15.05	18.22	15.98	(e)	19.47	16.64	10.40
CVS2-86	109	5	7.18	8.04	7.27	(e)	8.24	6.74	9.57
CVS2-86	109	5	7.18	8.57	8.54	(e)	8.98	7.71	9.49
CVS2-87	110	5	7.72	9.24	8.24	(e)	9.73	8.28	9.58
CVS2-87	110	5	7.72	9.65	9.08	(e)	9.73	7.49	9.58
CVS2-88	111	5	6.97	9.11	8.29	(e)	9.41	7.29	10.09
CVS2-88	111	5	6.97	9.11	8.29	(e)	9.61	7.69	10.03
CVS2-89	112	5	20.88	38.44	34.41	(e)	37.44	21.68	10.00
CVS2-89	112	5	21.37	38.44	34.41	(e)	38.19	17.94	10.07
CVS2-90	113	5	25.56	28.14	25.81	(e)	29.84	12.61	9.55
CVS2-90	113	5	26.71	30.14	26.11	(e)	29.84	15.57	9.57
CVS2-91	114	5	26.33	44.21	38.71	(e)	43.64	11.39	9.07
CVS2-91	114	5	26.33	44.21	38.71	(e)	43.64	14.02	9.18
CVS2-92	115	5	20.40	84.41	70.66	(e)	71.43	4.82	10.58
CVS2-92	115	5	20.88	88.42	70.66	(e)	74.12	6.13	10.54

(a) Elemental releases normalized using as-batched compositions from Table A.1.

(b) ID# is a consecutive integer numbering of all CVS glasses.

(c) PS is the plotting symbol used in plots associated with this data: 1 = CVS-I boundary, 2 = CVS-II Phase 1 interior, 3 = CVS-II Phase 2a boundary, 4 = CVS-II Phase 2b interior, 5 = CVS-II Phase 3 boundary, 6 = CVS-II Phase 4 one-component-at-a-time, M = middle compositions, O = other than NCAW waste glasses, A = EA glass.

(e) Mo release was determined as not of interest, and so data were no longer collected beginning with Phase 2 of CVS-II.

TABLE D.1. Normalized Elemental Release and pH Data from Duplicate 28-day MCC-1 Tests (90°C, DIW, $10m^{-1}$) Performed on CVS-I and CVS-II Glasses (continued)

Glass	ID[b] #	PS[c]	Normalized[a] Elemental Release Rates (g/m^2) Si	B	Li	Mo	Na	Cs	pH
CVS2-93	116	5	97.13	211.64	178.19	(e)	189.67	43.80	10.87
CVS2-93	116	5	97.13	221.26	175.12	(e)	200.21	52.56	10.91
CVS2-94	117	5	58.28	118.57	106.30	(e)	112.31	13.40	10.84 (i)
CVS2-94	117	5	31.08	56.27	49.06	(e)	56.15	17.15	10.64 (i)
CVS2-95	118	A	34.05	49.16	41.20	(e)	45.97	(h)	10.21
CVS2-95	118	A	34.92	49.16	40.70	(e)	47.59	(h)	10.31
CVS2-96	119	M	8.90	12.39	10.87	(e)	12.36	8.13	9.56
CVS2-96	119	M	8.90	12.67	11.44	(e)	12.90	9.68	9.58
CVS2-97	120	M	10.43	12.89	10.95	(e)	13.13	10.58	9.56
CVS2-97	120	M	10.43	12.89	10.95	(e)	13.13	10.58	9.42
CVS2-98	121	5	13.23	29.52	27.97	(e)	25.61	1.58	10.07
CVS2-98	121	5	13.23	31.36	27.39	(e)	26.28	1.97	10.08
CVS2-99	122	5	10.27	14.27	12.08	(e)	12.65	(h)	9.50
CVS2-99	122	5	9.86	13.61	11.48	(e)	12.24	(h)	9.47
CVS2-100	123	5	10.03	13.91	11.91	(e)	12.49	(h)	9.63
CVS2-100	123	5	10.03	14.34	11.91	(e)	12.49	(h)	9.61
CVS2-101	124	A	48.20	92.20	76.62	(e)	79.84	(h)	10.63
CVS2-101	124	A	48.20	89.32	76.62	(e)	79.04	(h)	10.64

(a) Elemental releases normalized using as-batched compositions from Table A.1.

(b) ID# is a consecutive integer numbering of all CVS glasses.

(c) PS is the plotting symbol used in plots associated with this data: 1 = CVS-I boundary, 2 = CVS-II Phase 1 interior, 3 = CVS-II Phase 2a boundary, 4 = CVS-II Phase 2b interior, 5 = CVS-II Phase 3 boundary, 6 = CVS-II Phase 4 one-component-at-a-time, M = middle compositions, O = other than NCAW waste glasses, A = EA glass.

(e) Mo release was determined as not of interest, and so data were no longer collected beginning with Phase 2 of CVS-II.

(h) This glass did not contain Cs.

(i) The duplicate results for CVS2-94 are clearly different, but re-analysis of the dissolution solutions by ICP confirmed the results, indicating the difference is due to something other than analytical error. Model predictions suggest the first duplicate with the larger release values may be the erroneous one.

TABLE D.1. Normalized Elemental Release and pH Data from Duplicate 28-day MCC-1 Tests (90°C, DIW, $10m^{-1}$) Performed on CVS-I and CVS-II Glasses (continued)

Glass	ID[b] #	PS[c]	Normalized[a] Elemental Release Rates (g/m^2) Si	B	Li	Mo	Na	Cs	pH
CVS2-102	125	M	15.57	19.54	17.78	(e)	17.97	(g)	9.52
CVS2-102	125	M	15.17	18.93	17.20	(e)	16.77	(g)	9.55
CVS2-103	126	6	25.54	52.91	49.70	(e)	45.30	(g)	10.23
CVS2-103	126	6	26.06	52.91	49.70	(e)	46.24	(g)	10.20
CVS2-104	127	6	20.42	30.97	29.06	(e)	28.33	(g)	9.88
CVS2-104	127	6	19.94	30.97	27.61	(e)	27.32	(g)	9.85
CVS2-105	128	6	17.01	22.53	20.88	(e)	20.73	(g)	9.66
CVS2-105	128	6	17.01	22.81	20.88	(e)	20.73	(g)	9.69
CVS2-106	129	6	11.25	13.54	13.01	(e)	12.82	(g)	9.37
CVS2-106	129	6	10.87	13.21	12.40	(e)	12.04	(g)	9.37
CVS2-107	130	6	10.15	12.22	11.89	(e)	11.28	(g)	9.58
CVS2-107	130	6	10.15	12.86	11.89	(e)	11.28	(g)	9.53
CVS2-108	131	6	24.79	21.44	28.37	(e)	28.62	(g)	9.48
CVS2-108	131	6	22.69	24.01	27.68	(e)	27.48	(g)	9.46
CVS2-109	132	6	49.11	93.25	83.45	(e)	77.70	(g)	9.41
CVS2-109	132	6	44.65	88.65	83.45	(e)	75.02	(g)	9.39
CVS2-110	133	6	8.58	10.27	9.65	(e)	9.43	(g)	9.09
CVS2-110	133	6	8.58	9.99	9.12	(e)	9.16	(g)	9.07
CVS2-111	134	6	20.42	26.13	24.56	(e)	24.26	(g)	9.88
CVS2-111	134	6	20.00	25.81	23.96	(e)	23.36	(g)	9.86
CVS2-112	135	6	53.14	98.26	89.08	(e)	80.86	(g)	10.79
CVS2-112	135	6	53.14	98.26	89.08	(e)	80.86	(g)	10.73
CVS2-113	136	6	10.87	13.06	11.18	(e)	11.65	(g)	9.20
CVS2-113	136	6	10.09	12.47	10.97	(e)	11.42	(g)	9.15
CVS2-114	137	6	21.25	20.33	20.43	(e)	20.11	(g)	9.95
CVS2-114	137	6	20.84	20.33	19.71	(e)	19.38	(g)	9.77

(a) Elemental releases normalized using as-batched compositions from Table A.1.

(b) ID# is a consecutive integer numbering of all CVS glasses.

(c) PS is the plotting symbol used in plots associated with this data: 1 = CVS-I boundary, 2 = CVS-II Phase 1 interior, 3 = CVS-II Phase 2a boundary, 4 = CVS-II Phase 2b interior, 5 = CVS-II Phase 3 boundary, 6 = CVS-II Phase 4 one-component-at-a-time, M = middle compositions, O = other than NCAW waste glasses, A = EA glass.

(e) Mo release was determined as not of interest, and so data were no longer collected beginning with Phase 2 of CVS-II.

(g) Cs releases were not measured for CVS-II Phase 4 glasses.

TABLE D.1. Normalized Elemental Release and pH Data from Duplicate 28-day MCC-1 Tests (90°C, DIW, $10m^{-1}$) Performed on CVS-I and CVS-II Glasses (continued)

Glass	ID[b] #	PS[c]	Normalized[a] Elemental Release Rates (g/m^2) Si	B	Li	Mo	Na	Cs	pH
CVS2-115	138	6	22.31	29.40	26.11	(e)	26.04	(g)	10.06
CVS2-115	138	6	22.31	29.40	26.42	(e)	26.04	(g)	10.04
CVS2-116	139	6	14.95	20.08	17.97	(e)	18.18	(g)	9.60
CVS2-116	139	6	14.54	19.46	17.39	(e)	16.97	(g)	9.53
CVS2-117	140	6	15.83	19.38	17.64	(e)	17.81	(g)	9.52
CVS2-117	140	6	16.63	20.59	18.77	(e)	19.00	(g)	9.59
CVS2-118	141	6	15.75	20.69	19.13	(e)	19.39	(g)	9.59
CVS2-118	141	6	15.35	20.08	17.97	(e)	18.18	(g)	9.58
CVS2-119	142	6	38.60	56.67	49.84	(e)	49.14	(g)	9.76
CVS2-119	142	6	38.60	56.67	50.40	(e)	49.14	(g)	9.76
CVS2-120	143	6	11.49	13.82	12.37	(e)	12.32	(g)	9.42
CVS2-120	143	6	10.67	13.19	12.37	(e)	12.20	(g)	9.48
CVS2-121	144	6	8.23	9.94	8.70	(e)	8.98	(g)	9.21
CVS2-121	144	6	8.66	10.28	9.32	(e)	9.37	(g)	9.26
CVS2-122	145	6	7.80	9.48	8.58	(e)	8.40	(g)	8.97
CVS2-122	145	6	7.80	9.13	8.58	(e)	7.98	(g)	8.88
CVS2-123	146	M	12.83	16.26	13.84	(e)	15.52	(g)	9.47
CVS2-123	146	M	12.03	15.03	13.26	(e)	14.32	(g)	9.52

(a) Elemental releases normalized using as-batched compositions from Table A.1.

(b) ID# is a consecutive integer numbering of all CVS glasses.

(c) PS is the plotting symbol used in plots associated with this data: 1 = CVS-I boundary, 2 = CVS-II Phase 1 interior, 3 = CVS-II Phase 2a boundary, 4 = CVS-II Phase 2b interior, 5 = CVS-II Phase 3 boundary, 6 = CVS-II Phase 4 one-component-at-a-time, M = middle compositions, O = other than NCAW waste glasses, A = EA glass.

(e) Mo release was determined as not of interest, and so data were no longer collected beginning with Phase 2 of CVS-II.

(g) Cs releases were not measured for CVS-II Phase 4 glasses.

TABLE D.2. Normalized Elemental Release and pH Data from Duplicate 7-day PCTs (90°C, DIW, 2000m^{-1}) Performed on CVS-I and CVS-II Glasses

Glass	ID[b] #	PS[c]	Normalized[a] Elemental Release Rates (g/m²) Si	B	Li	Mo	Na	Cs	pH
CVS1-1	1	M	0.167	0.521	0.515	0.439	0.403	0.058	10.92
CVS1-1	1	M	0.167	0.521	0.543	0.439	0.403	0.053	10.92
CVS1-2	2	1	0.054	0.066	0.154	0.061	0.064	0.057	11.43
CVS1-2	2	1	---------- No Sample Analyzed ----------						11.41
CVS1-3	3	1	0.176	0.900	0.814	0.487	0.593	0.051	9.85
CVS1-3	3	1	0.168	0.828	0.768	0.449	0.566	0.034	9.85
CVS1-4	4	1	0.482	20.289	16.667	22.335	16.697	1.498	9.67
CVS1-4	4	1	0.598	20.989	17.204	23.731	17.370	1.971	9.67
CVS1-5	5	1	0.321	0.357	0.464	0.325	0.192	0.130	11.22
CVS1-5	5	1	0.315	0.354	0.461	0.328	0.190	0.166	11.22
CVS1-6	6	1	0.313	6.053	4.854	4.188	3.032	0.126	10.07
CVS1-6	6	1	0.311	6.174	4.931	4.188	3.059	0.122	10.07
CVS1-7	7	1	0.114	0.287	0.330	0.306	0.340	0.136	10.91
CVS1-7	7	1	0.114	0.287	0.331	0.302	0.338	0.150	10.91
CVS1-8	8	1	0.265	1.254	0.745	1.161	0.805	0.075	10.42
CVS1-8	8	1	0.265	1.222	0.743	1.159	0.805	0.073	10.43
CVS1-9	9	1	0.346	10.816	8.495	7.259	7.803	0.915	8.69
CVS1-9	9	1	0.343	11.169	8.710	7.538	7.991	0.930	8.69
CVS1-10	10	1	0.103	0.125	0.382	0.094	0.095	0.030	9.78
CVS1-10	10	1	0.105	0.128	0.390	0.095	0.095	0.028	9.74
CVS1-11	11	1	0.043	0.104	0.188	0.065	0.109	0.054	10.00
CVS1-11	11	1	0.038	0.093	0.186	0.067	0.090	0.059	9.98
CVS1-12	12	1	0.842	4.794	4.301	4.928	4.541	1.577	11.12
CVS1-12	12	1	0.809	4.530	4.040	4.551	4.248	1.636	11.13
CVS1-13	13	1	0.759	14.132	12.903	13.262	12.449	1.183	10.37
CVS1-13	13	1	0.813	14.011	12.903	12.982	12.377	1.025	10.37
CVS1-14	14	1	0.153	9.968	8.172	1.256	5.863	0.473	9.63
CVS1-14	14	1	0.145	9.727	7.849	1.368	5.718	0.150	9.64
CVS1-15	15	1	0.990	18.971	11.275	19.404	14.134	2.957	13.04
CVS1-15	15	1	0.944	18.585	11.121	18.845	13.855	2.641	13.02
CVS1-16	16	1	0.247	0.524	0.265	0.470	0.540	0.150	12.02
CVS1-16	16	1	0.235	0.521	0.267	0.466	0.540	0.154	11.99

(a) Elemental releases normalized using as-batched compositions from Table A.1.

(b) ID# is a consecutive integer numbering of all CVS glasses.

(c) PS is the plotting symbol used in plots associated with this data: 1 = CVS-I boundary, 2 = CVS-II Phase 1 interior, 3 = CVS-II Phase 2a boundary, 4 = CVS-II Phase 2b interior, 5 = CVS-II Phase 3 boundary, 6 = CVS-II Phase 4 one-component-at-a-time, M = middle compositions, O = other than NCAW waste glasses, A = EA glass.

TABLE D.2. Normalized Elemental Release and pH Data from Duplicate 7-day PCTs (90°C, DIW, $2000m^{-1}$) Performed on CVS-I and CVS-II Glasses (continued)

Glass	ID[b] #	PS[c]	Normalized[a] Elemental Release Rates (g/m^2) Si	B	Li	Mo	Na	Cs	pH
CVS1-17	17	1	0.630	2.241	2.075	2.234	2.177	0.986	11.57
CVS1-17	17	1	0.696	2.228	2.075	2.234	2.431	0.895	11.58
CVS1-18	18	1	1.516	11.125	7.957	10.631	7.954	1.429	12.25
CVS1-18	18	1	1.547	11.350	8.172	10.833	8.125	1.709	12.25
CVS1-19	19	M	0.165	0.517	0.529	0.439	0.430	0.063	10.29
CVS1-19	19	M	0.167	0.529	0.538	0.456	0.437	0.068	10.29
CVS1-20	20	M	0.156	0.453	0.466	0.391	0.394	0.053	10.17
CVS1-20	20	M	0.156	0.458	0.469	0.401	0.397	0.048	10.15
CVS1-21	21	1	0.467	19.051	15.806	19.543	15.723	1.735	9.68
CVS1-21	21	1	0.452	18.650	15.376	19.543	15.349	1.754	9.68
CVS1-22	22	1	0.259	1.122	0.704	1.125	0.762	0.065	9.81
CVS1-22	22	1	0.259	1.116	0.703	1.120	0.758	0.069	9.81
CVS1-23	23	M	0.230	0.521	0.530	0.483	0.484	0.060	10.28
CVS1-23	23	M	0.228	0.528	0.539	0.490	0.489	0.065	10.30
CVS2-1	24	2	0.173	0.320	0.386	0.300	0.218	0.047	10.20
CVS2-1	24	2	0.166	0.305	0.352	0.300	0.198	0.049	10.22
CVS2-2	25	2	0.075	0.132	0.292	0.121	0.171	0.064	10.92
CVS2-2	25	2	0.075	0.123	0.260	0.115	0.204	0.071	10.93
CVS2-3	26	2	0.065	0.140	0.231	(d)	0.130	0.067	10.09
CVS2-3	26	2	0.064	0.134	0.212	0.121	0.120	0.059	10.08
CVS2-4	27	2	0.100	0.155	0.298	0.150	0.168	0.105	10.42
CVS2-4	27	2	0.102	0.162	0.301	0.150	0.196	0.096	10.39
CVS2-5	28	2	0.104	0.278	0.373	0.163	0.283	0.026	9.57
CVS2-5	28	2	0.107	0.290	0.392	0.167	0.285	0.033	9.58
CVS2-6	29	2	0.410	1.186	1.346	1.242	1.284	0.251	10.47
CVS2-6	29	2	0.432	1.184	1.260	1.265	1.284	0.226	10.49
CVS2-7	30	2	0.169	0.763	0.852	0.210	0.344	0.004	9.90
CVS2-7	30	2	0.159	0.716	0.773	0.197	0.342	0.005	9.88
CVS2-8	31	2	0.263	0.477	0.510	0.474	0.439	0.055	10.73
CVS2-8	31	2	0.263	0.490	0.536	0.492	0.451	0.034	10.77

(a) Elemental releases normalized using as-batched compositions from Table A.1.

(b) ID# is a consecutive integer numbering of all CVS glasses.

(c) PS is the plotting symbol used in plots associated with this data: 1 = CVS-I boundary, 2 = CVS-II Phase 1 interior, 3 = CVS-II Phase 2a boundary, 4 = CVS-II Phase 2b interior, 5 = CVS-II Phase 3 boundary, 6 = CVS-II Phase 4 one-component-at-a-time, M = middle compositions, O = other than NCAW waste glasses, A = EA glass.

(d) Missing or erroneous values.

TABLE D.2. Normalized Elemental Release and pH Data from Duplicate 7-day PCTs (90°C, DIW, 2000m^{-1}) Performed on CVS-I and CVS-II Glasses (continued)

Glass	ID[b] #	PS[c]	Normalized[a] Elemental Release Rates (g/m²) Si	B	Li	Mo	Na	Cs	pH
CVS2-9	32	2	0.241	0.564	0.647	0.565	0.366	0.011	10.35
CVS2-9	32	2	0.241	0.555	0.594	0.571	0.382	0.016	10.34
CVS2-10	33	2	0.114	1.332	1.325	0.130	0.857	0.006	9.46
CVS2-10	33	2	0.116	1.332	1.319	0.125	0.799	0.005	9.46
CVS2-11	34	2	0.510	1.590	1.582	1.676	1.333	0.127	11.46
CVS2-11	34	2	0.510	1.584	1.546	1.676	1.407	0.026	11.45
CVS2-12	35	2	0.074	0.190	0.256	0.133	0.179	0.069	9.91
CVS2-12	35	2	0.076	0.197	0.268	0.133	0.188	0.053	9.89
CVS2-13	36	2	0.186	0.371	0.380	0.316	0.499	0.102	11.16
CVS2-13	36	2	0.179	0.349	0.345	0.300	0.458	0.059	11.13
CVS2-14	37	2	0.261	1.595	1.444	1.730	1.268	0.212	10.47
CVS2-14	37	2	0.261	1.718	1.491	1.832	1.268	0.497	10.46
CVS2-15	38	2	0.178	0.322	0.446	0.281	0.608	0.125	11.31
CVS2-15	38	2	0.183	0.340	0.456	0.281	0.608	0.192	11.30
CVS2-16	39	M	0.547	2.937	2.485	2.832	2.182	0.019	10.37
CVS2-16	39	M	0.568	2.937	2.213	2.689	2.182	0.015	10.36
CVS2-17	40	M	0.167	0.496	0.570	0.464	0.473	0.025	10.27
CVS2-17	40	M	0.167	0.494	0.573	0.464	0.476	0.021	10.27
CVS2-18	41	M	0.546	2.578	2.192	2.475	1.855	0.020	10.34
CVS2-18	41	M	0.546	2.578	1.997	2.475	1.916	0.011	10.34
CVS2-19	42	M	0.439	1.910	1.700	2.030	1.394	0.159	10.34
CVS2-19	42	M	0.460	2.069	1.607	2.111	1.568	0.097	10.36
CVS2-20	43	3	0.187	0.347	0.386	(e)	0.279	0.048*	10.99
CVS2-20	43	3	0.187	0.347	0.387	(e)	0.279	0.048*	10.78
CVS2-21	44	3	0.487	3.671	2.458	(e)	2.022	0.034	10.26
CVS2-21	44	3	0.525	4.038	2.611	(e)	2.156	0.073	10.25

(a) Elemental releases normalized using as-batched compositions from Table A.1.

(b) ID# is a consecutive integer numbering of all CVS glasses.

(c) PS is the plotting symbol used in plots associated with this data: 1 = CVS-I boundary, 2 = CVS-II Phase 1 interior, 3 = CVS-II Phase 2a boundary, 4 = CVS-II Phase 2b interior, 5 = CVS-II Phase 3 boundary, 6 = CVS-II Phase 4 one-component-at-a-time, M = middle compositions, O = other than NCAW waste glasses, A = EA glass.

(e) Mo release was determined as not of interest, and so data were no longer collected beginning with Phase 2 of CVS-II.

* Solution was re-analyzed to rectify different results from first analysis.

TABLE D.2. Normalized Elemental Release and pH Data from Duplicate 7-day PCTs (90°C, DIW, 2000m^{-1}) Performed on CVS-I and CVS-II Glasses (continued)

Glass	ID[b] #	PS[c]	Normalized[a] Elemental Release Rates (g/m²) Si	B	Li	Mo	Na	Cs	pH
CVS2-22	45	3	2.249	9.646	5.376	(e)	6.051	0.453	11.72
CVS2-22	45	3	2.249	9.646	5.530	(e)	6.143	0.414	11.71
CVS2-23	46	3	0.146	0.173	0.605	(e)	0.809	0.076*	11.83
CVS2-23	46	3	0.142	0.173	0.602	(e)	0.809	0.079*	11.79
CVS2-24	47	3	0.179	4.662	3.226	(e)	2.106	0.038	9.78
CVS2-24	47	3	0.179	4.381	3.226	(e)	2.014	0.046	9.81
CVS2-25	48	3	1.140	4.180	2.611	(e)	3.365	0.522	11.90
CVS2-25	48	3	1.288	5.145	2.919	(e)	3.686	0.278	11.91
CVS2-26	49	3	0.275	1.624	1.429	(e)	1.342	0.069	10.11
CVS2-26	49	3	0.275	1.632	1.444	(e)	1.356	0.177	10.10
CVS2-27	50	3	0.860	3.003	1.769	(e)	2.291	0.158	11.86
CVS2-27	50	3	0.919	3.537	1.901	(e)	2.392	0.375	11.88
CVS2-28	51	3	1.597	5.466	3.593	(e)	3.369	0.237	11.55
CVS2-28	51	3	1.711	4.823	3.772	(e)	3.706	0.414	11.52
CVS2-29	52	3	0.194	1.286	1.355	(e)	1.298	0.158	9.09
CVS2-29	52	3	0.191	1.286	1.355	(e)	1.248	0.473	9.12
CVS2-30	53	3	0.173	6.592	4.161	(e)	2.511	0.010	8.72
CVS2-30	53	3	0.175	6.431	4.226	(e)	2.592	0.020	8.76
CVS2-31	54	3	0.121	0.409	0.458	(e)	0.318	0.315	9.54
CVS2-31	54	3	0.121	0.413	0.461	(e)	0.319	0.026	9.53
CVS2-32	55	3	2.747	9.646	5.527	(e)	6.065	0.375	12.30
CVS2-32	55	3	2.747	9.646	5.527	(e)	5.728	0.552	12.31
CVS2-33	56	3	0.524	1.714	1.412	(e)	1.600	0.256	11.94
CVS2-33	56	3	0.509	1.732	1.465	(e)	1.617	0.493	11.94
CVS2-34	57	3	0.265	4.409	3.497	(e)	2.729	0.054	11.54
CVS2-34	57	3	0.265	4.271	3.439	(e)	2.672	0.053	11.55
CVS2-35	58	3	0.207	0.321	0.633	(e)	0.910	0.189	11.88
CVS2-35	58	3	0.200	0.318	0.528	(e)	0.910	0.335	11.91

(a) Elemental releases normalized using as-batched compositions from Table A.1.

(b) ID# is a consecutive integer numbering of all CVS glasses.

(c) PS is the plotting symbol used in plots associated with this data: 1 = CVS-I boundary, 2 = CVS-II Phase 1 interior, 3 = CVS-II Phase 2a boundary, 4 = CVS-II Phase 2b interior, 5 = CVS-II Phase 3 boundary, 6 = CVS-II Phase 4 one-component-at-a-time, M = middle compositions, O = other than NCAW waste glasses, A = EA glass.

(e) Mo release was determined as not of interest, and so data were no longer collected beginning with Phase 2 of CVS-II.

* Solution was re-analyzed to rectify different results from first analysis.

TABLE D.2. Normalized Elemental Release and pH Data from Duplicate 7-day PCTs (90°C, DIW, 2000m^{-1}) Performed on CVS-I and CVS-II Glasses (continued)

Glass	ID[b] #	PS[c]	Normalized[a] Elemental Release Rates (g/m²) Si	B	Li	Mo	Na	Cs	pH
CVS2-36	59	3	0.276	0.482	0.636	(e)	0.662	0.197	11.33
CVS2-36	59	3	0.276	0.479	0.624	(e)	0.646	0.296	11.35
CVS2-37	60	3	0.206	0.251	0.301	(e)	0.176	0.022	10.44
CVS2-37	60	3	0.206	0.241	0.298	(e)	0.178	0.051	10.45
CVS2-38	61	3	0.270	1.135	0.733	(e)	0.839	0.041	9.56
CVS2-38	61	3	0.291	1.103	0.720	(e)	0.775	0.089	9.56
CVS2-39	62	3	1.568	12.219	6.452	(e)	7.421	0.591	12.48
CVS2-39	62	3	1.656	13.183	6.605	(e)	7.916	0.926	12.52
CVS2-40	63	4	0.174	0.337	0.332	(e)	0.401	0.361	11.12
CVS2-40	63	4	0.171	0.337	0.324	(e)	0.397	0.059	11.13
CVS2-41	64	4	0.106	0.181	0.264	(e)	0.192	0.092	10.89
CVS2-41	64	4	0.101	0.173	0.255	(e)	0.183	0.085	10.89
CVS2-42	65	4	0.584	1.768	1.229	(e)	1.380	0.118	11.20
CVS2-42	65	4	0.565	1.621	1.212	(e)	1.294	0.118	11.17
CVS2-43	66	4	0.200	0.788	0.721	(e)	0.468	0.018	9.96
CVS2-43	66	4	0.193	0.746	0.673	(e)	0.434	0.007	9.97
CVS2-44	67	4	0.131	0.261	0.298	(e)	0.198	0.059	10.30
CVS2-44	67	4	0.125	0.249	0.291	(e)	0.190	0.062	10.31
CVS2-45	68	4	0.186	0.507	0.483	(e)	0.376	0.023	10.04
CVS2-45	68	4	0.185	0.494	0.473	(e)	0.371	0.042	10.05
CVS2-46	69	4	0.148	0.313	0.341	(e)	0.187	0.033	10.18
CVS2-46	69	4	0.149	0.321	0.350	(e)	0.189	0.021	10.20
CVS2-47	70	4	0.444	1.164	1.135	(e)	1.055	0.217	11.38
CVS2-47	70	4	0.424	1.154	1.113	(e)	1.055	0.158	11.39
CVS2-48	71	4	0.102	0.305	0.312	(e)	0.280	0.032	10.06
CVS2-48	71	4	0.103	0.309	0.323	(e)	0.287	0.065	10.11
CVS2-49	72	4	0.138	0.309	0.341	(e)	0.222	0.020	9.96
CVS2-49	72	4	0.135	0.297	0.328	(e)	0.212	0.011	9.97

(a) Elemental releases normalized using as-batched compositions from Table A.1.

(b) ID# is a consecutive integer numbering of all CVS glasses.

(c) PS is the plotting symbol used in plots associated with this data: 1 = CVS-I boundary, 2 = CVS-II Phase 1 interior, 3 = CVS-II Phase 2a boundary, 4 = CVS-II Phase 2b interior, 5 = CVS-II Phase 3 boundary, 6 = CVS-II Phase 4 one-component-at-a-time, M = middle compositions, O = other than NCAW waste glasses, A = EA glass.

(e) Mo release was determined as not of interest, and so data were no longer collected beginning with Phase 2 of CVS-II.

TABLE D.2. Normalized Elemental Release and pH Data from Duplicate 7-day PCTs (90°C, DIW, 2000m^{-1}) Performed on CVS-I and CVS-II Glasses (continued)

Glass	ID[b] #	PS[c]	Normalized[a] Elemental Release Rates (g/m²) Si	B	Li	Mo	Na	Cs	pH
CVS2-50	73	M	0.152	0.450	0.438	(e)	0.377	0.036	10.24
CVS2-50	73	M	0.149	0.434	0.415	(e)	0.359	0.024	10.22
CVS2-51	74	M	0.421	1.841	1.505	(e)	1.313	0.083	10.31
CVS2-51	74	M	0.401	1.687	1.488	(e)	1.253	0.030	10.29
CVS2-52	75	4	0.303	0.571	0.566	(e)	0.268	0.025	10.17
CVS2-52	75	4	0.285	0.543	0.542	(e)	0.253	0.019	10.15
CVS2-53	76	4	0.174	0.294	0.305	(e)	0.202	0.059	10.02
CVS2-53	76	4	0.178	0.313	0.305	(e)	0.202	0.062	10.03
CVS2-54	77	M	0.541	2.608	1.730	(e)	1.612	0.119	10.26
CVS2-54	77	M	0.602	2.915	1.701	(e)	1.612	0.106	10.20
CVS2-55	78	0	0.359	1.365	1.153	(e)	0.907	0.002	10.20
CVS2-55	78	0	0.345	1.319	1.101	(e)	0.854	0.002	10.18
CVS2-56	79	0	0.369	1.442	1.277	(e)	0.961	0.002	10.21
CVS2-56	79	0	0.367	1.396	1.159	(e)	0.931	0.002	10.19
CVS2-57	80	0	0.361	1.213	1.116	(e)	0.895	0.002	10.27
CVS2-57	80	0	0.331	1.115	1.046	(e)	0.788	0.002	10.24
CVS2-58	81	4	0.139	0.793	0.639	(e)	0.628	0.035	9.84
CVS2-58	81	4	0.137	0.764	0.634	(e)	0.611	0.032	9.89
CVS2-59	82	5	0.268	1.591	1.287	(e)	1.222	0.017	11.41
CVS2-59	82	5	0.268	1.591	1.287	(e)	1.222	0.021	11.53
CVS2-60	83	5	0.405	1.652	1.158	(e)	1.523	0.046	11.97
CVS2-60	83	5	0.425	1.597	1.158	(e)	1.523	0.024	11.95
CVS2-61	84	5	0.192	0.220	0.280	(e)	0.230	0.062	10.97
CVS2-61	84	5	0.198	0.223	0.280	(e)	0.230	0.066	10.81
CVS2-62	85	5	0.268	1.002	0.827	(e)	0.898	0.029	9.57
CVS2-62	85	5	0.268	1.002	0.896	(e)	0.958	0.023	9.54
CVS2-63	86	5	0.079	0.328	0.232	(e)	0.390	0.191	10.74
CVS2-63	86	5	0.079	0.337	0.211	(e)	0.390	0.181	10.43

(a) Elemental releases normalized using as-batched compositions from Table A.1.

(b) ID# is a consecutive integer numbering of all CVS glasses.

(c) PS is the plotting symbol used in plots associated with this data: 1 = CVS-I boundary, 2 = CVS-II Phase 1 interior, 3 = CVS-II Phase 2a boundary, 4 = CVS-II Phase 2b interior, 5 = CVS-II Phase 3 boundary, 6 = CVS-II Phase 4 one-component-at-a-time, M = middle compositions, 0 = other than NCAW waste glasses, A = EA glass.

(e) Mo release was determined as not of interest, and so data were no longer collected beginning with Phase 2 of CVS-II.

TABLE D.2. Normalized Elemental Release and pH Data from Duplicate 7-day PCTs (90°C, DIW, $2000m^{-1}$) Performed on CVS-I and CVS-II Glasses (continued)

Glass	ID[b] #	PS[c]	Normalized[a] Elemental Release Rates (g/m^2) Si	B	Li	Mo	Na	Cs	pH
CVS2-64	87	0	0.225	0.379	0.368	(e)	0.342	0.057	10.70
CVS2-64	87	0	0.244	0.379	0.385	(e)	0.342	0.051	10.53
CVS2-65	88	0	0.150	0.342	0.355	(e)	0.204	(f)	10.62
CVS2-65	88	0	0.146	0.328	0.355	(e)	0.196	(f)	10.63
CVS2-66	89	0	0.163	0.210	0.247	(e)	0.223	(f)	10.56
CVS2-66	89	0	0.165	0.210	0.247	(e)	0.223	(f)	10.51
CVS2-67	90	0	0.228	0.507	0.480	(e)	0.211	(f)	9.72
CVS2-67	90	0	0.232	0.517	0.480	(e)	0.217	(f)	9.74
CVS2-68	91	0	0.254	0.308	0.340	(e)	0.127	(f)	9.88
CVS2-68	91	0	0.254	0.308	0.340	(e)	0.127	(f)	9.81
CVS2-69	92	0	0.185	0.226	0.302	(e)	0.112	(f)	10.14
CVS2-69	92	0	0.187	0.226	0.302	(e)	0.112	(f)	10.21
CVS2-70	93	0	0.286	0.306	0.373	(e)	0.124	(f)	9.89
CVS2-70	93	0	0.286	0.317	0.389	(e)	0.133	(f)	9.89
CVS2-71	94	5	0.244	0.411	0.419	(e)	0.342	0.026	10.79
CVS2-71	94	5	0.244	0.411	0.435	(e)	0.357	0.036	10.78
CVS2-72	95	5	0.153	0.210	0.226	(e)	0.228	0.021	10.60
CVS2-72	95	5	0.153	0.210	0.226	(e)	0.228	0.056	10.36
CVS2-73	96	5	0.148	0.214	0.278	(e)	0.063	0.011	9.85
CVS2-73	96	5	0.210	0.273	0.324	(e)	0.085	0.009	10.06
CVS2-74	97	5	0.164	0.226	0.271	(e)	0.152	0.054	10.41
CVS2-74	97	5	0.162	0.226	0.287	(e)	0.142	0.041	10.41
CVS2-75	98	5	0.220	0.272	0.327	(e)	0.100	0.034	9.88
CVS2-75	98	5	0.220	0.283	0.342	(e)	0.100	0.030	9.89
CVS2-76	99	5	4.045	15.005	7.656	(e)	12.728	3.548	12.46
CVS2-76	99	5	4.045	14.737	7.486	(e)	12.354	2.858	12.46
CVS2-77	100	5	2.301	9.378	6.144	(e)	6.364	1.643	12.26
CVS2-77	100	5	2.278	9.646	6.298	(e)	6.739	1.226	12.26

(a) Elemental releases normalized using as-batched compositions from Table A.1.

(b) ID# is a consecutive integer numbering of all CVS glasses.

(c) PS is the plotting symbol used in plots associated with this data: 1 = CVS-I boundary, 2 = CVS-II Phase 1 interior, 3 = CVS-II Phase 2a boundary, 4 = CVS-II Phase 2b interior, 5 = CVS-II Phase 3 boundary, 6 = CVS-II Phase 4 one-component-at-a-time, M = middle compositions, 0 = other than NCAW waste glasses, A = EA glass.

(e) Mo release was determined as not of interest, and so data were no longer collected beginning with Phase 2 of CVS-II.

(f) This glass did not contain Cs.

TABLE D.2. Normalized Elemental Release and pH Data from Duplicate 7-day PCTs (90°C, DIW, 2000m^{-1}) Performed on CVS-I and CVS-II Glasses (continued)

Glass	ID[b] #	PS[c]	Normalized[a] Elemental Release Rates (g/m²) Si	B	Li	Mo	Na	Cs	pH
CVS2-78	101	5	0.191	0.864	0.720	(e)	0.593	0.013	9.25
CVS2-78	101	5	0.191	1.005	0.677	(e)	0.593	0.011	9.17
CVS2-79	102	5	0.187	0.754	0.675	(e)	0.674	0.050	9.03
CVS2-79	102	5	0.193	0.734	0.693	(e)	0.647	0.020	8.90
CVS2-80	103	5	0.194	0.754	0.672	(e)	0.593	0.005	9.14
CVS2-80	103	5	0.196	0.774	0.672	(e)	0.606	0.005	9.16
CVS2-81	104	5	3.157	17.417	8.449	(e)	13.601	0.386	12.50
CVS2-81	104	5	2.914	15.809	7.680	(e)	12.047	0.290	12.52
CVS2-82	105	5	18.124	47.385	21.505	(e)	37.436	8.771	12.15
CVS2-82	105	5	15.644	40.616	18.433	(e)	33.318	8.377	12.20
CVS2-83	106	5	9.376	30.430	16.921	(e)	24.334	0.854	12.31
CVS2-83	106	5	13.518	38.883	21.536	(e)	31.447	0.810	12.35
CVS2-84	107	5	0.775	12.594	6.759	(e)	8.236	0.759	12.41
CVS2-84	107	5	0.211	12.326	6.605	(e)	8.236	1.084	12.44
CVS2-85	108	5	0.291	0.456	0.415	(e)	0.749	0.162	11.65
CVS2-85	108	5	0.291	0.456	0.430	(e)	0.749	0.131	11.70
CVS2-86	109	5	0.081	0.115	0.087	(e)	0.251	0.079	11.02
CVS2-86	109	5	0.083	0.115	0.095	(e)	0.258	0.070	10.94
CVS2-87	110	5	0.114	0.179	0.131	(e)	0.285	0.053	10.91
CVS2-87	110	5	0.114	0.177	0.131	(e)	0.288	0.054	10.88
CVS2-88	111	5	0.163	0.322	0.384	(e)	0.475	0.108	11.52
CVS2-88	111	5	0.160	0.295	0.369	(e)	0.471	0.079	11.51
CVS2-89	112	5	0.364	1.648	1.183	(e)	1.310	0.043	11.04
CVS2-89	112	5	0.364	1.785	1.290	(e)	1.385	0.045	11.05
CVS2-90	113	5	0.706	5.527	3.687	(e)	3.357	0.035	9.98
CVS2-90	113	5	0.725	5.627	3.840	(e)	3.605	0.038	9.99
CVS2-91	114	5	0.458	8.441	6.774	(e)	6.418	0.329	9.38
CVS2-91	114	5	0.477	8.842	6.774	(e)	7.059	0.162	9.39
CVS2-92	115	5	1.166	18.087	12.135	(e)	11.456	0.372	11.12
CVS2-92	115	5	1.263	19.092	12.750	(e)	12.129	1.358	11.12

(a) Elemental releases normalized using as-batched compositions from Table A.1.

(b) ID# is a consecutive integer numbering of all CVS glasses.

(c) PS is the plotting symbol used in plots associated with this data: 1 = CVS-I boundary, 2 = CVS-II Phase 1 interior, 3 = CVS-II Phase 2a boundary, 4 = CVS-II Phase 2b interior, 5 = CVS-II Phase 3 boundary, 6 = CVS-II Phase 4 one-component-at-a-time, M = middle compositions, O = other than NCAW waste glasses, A = EA glass.

(e) Mo release was determined as not of interest, and so data were no longer collected beginning with Phase 2 of CVS-II.

TABLE D.2. Normalized Elemental Release and pH Data from Duplicate 7-day PCTs (90°C, DIW, $2000m^{-1}$) Performed on CVS-I and CVS-II Glasses (continued)

Glass	ID[b] #	PS[c]	Normalized[a] Elemental Release Rates (g/m^2) Si	B	Li	Mo	Na	Cs	pH
CVS2-93	116	5	2.234	13.227	7.680	(e)	10.010	0.942	11.74
CVS2-93	116	5	1.700	13.227	7.834	(e)	10.010	2.190	11.79
CVS2-94	117	5	0.923	4.019	3.066	(e)	3.332	0.128	11.85
CVS2-94	117	5	0.947	4.120	3.066	(e)	3.369	0.118	11.83
CVS2-95	118	A	1.986	9.687	4.271	(e)	7.259	(g)	11.81
CVS2-95	118	A	2.030	10.265	4.271	(e)	7.259	(g)	11.81
CVS2-96	119	M	0.158	0.493	0.429	(e)	0.410	0.018	10.29
CVS2-96	119	M	0.160	0.493	0.429	(e)	0.410	0.047	10.19
CVS2-97	120	M	0.381	1.457	1.009	(e)	1.074	0.083	10.28
CVS2-97	120	M	0.401	1.411	1.095	(e)	1.194	0.050	10.22
CVS2-98	121	5	0.254	4.520	3.497	(e)	2.796	0.022	11.62
CVS2-98	121	5	0.280	4.520	3.497	(e)	2.796	0.108	11.55
CVS2-99	122	5	0.131	0.232	0.245	(e)	0.199	(g)	10.07
CVS2-99	122	5	0.131	0.232	0.248	(e)	0.199	(g)	10.12
CVS2-100	123	5	0.170	0.326	0.343	(e)	0.226	(g)	10.34
CVS2-100	123	5	0.170	0.326	0.343	(e)	0.226	(g)	10.34
CVS2-101	124	A	1.797	8.644	3.831	(e)	6.387	(g)	11.91
CVS2-101	124	A	1.841	8.644	3.831	(e)	6.786	(g)	11.94
CVS2-102	125	M	0.559	2.748	1.978	(e)	1.737	(h)	10.30
CVS2-102	125	M	0.559	2.596	1.864	(e)	1.617	(h)	10.25
CVS2-103	126	6	0.678	5.772	3.840	(e)	3.869	(h)	11.59
CVS2-103	126	6	0.704	6.373	4.292	(e)	4.294	(h)	11.63

(a) Elemental releases normalized using as-batched compositions from Table A.1.

(b) ID# is a consecutive integer numbering of all CVS glasses.

(c) PS is the plotting symbol used in plots associated with this data: 1 = CVS-I boundary, 2 = CVS-II Phase 1 interior, 3 = CVS-II Phase 2a boundary, 4 = CVS-II Phase 2b interior, 5 = CVS-II Phase 3 boundary, 6 = CVS-II Phase 4 one-component-at-a-time, M = middle compositions, O = other than NCAW waste glasses, A = EA glass.

(e) Mo release was determined as not of interest, and so data were no longer collected beginning with Phase 2 of CVS-II.

(g) This glass did not contain Cs.

(h) Cs releases were not measured for CVS-II Phase 4 glasses.

TABLE D.2. Normalized Elemental Release and pH Data from Duplicate 7-day PCTs (90°C, DIW, 2000m^{-1}) Performed on CVS-I and CVS-II Glasses (continued)

Glass	ID[b] #	PS[c]	Normalized[a] Elemental Release Rates (g/m²) Si	B	Li	Mo	Na	Cs	pH
CVS2-104	127	6	0.712	5.548	3.633	(e)	3.693	(h)	11.29
CVS2-104	127	6	0.712	5.548	3.633	(e)	3.642	(h)	11.29
CVS2-105	128	6	0.676	4.450	3.132	(e)	2.946	(h)	10.81
CVS2-105	128	6	0.698	4.729	3.132	(e)	3.001	(h)	10.82
CVS2-106	129	6	0.444	1.651	1.332	(e)	1.165	(h)	10.17
CVS2-106	129	6	0.450	1.651	1.363	(e)	1.165	(h)	10.18
CVS2-107	130	6	0.357	0.804	0.675	(e)	0.620	(h)	10.69
CVS2-107	130	6	0.338	0.772	0.648	(e)	0.620	(h)	10.67
CVS2-108	131	6	0.357	2.144	1.631	(e)	1.387	(h)	9.79
CVS2-108	131	6	0.357	2.144	1.661	(e)	1.387	(h)	9.79
CVS2-109	132	6	0.313	5.707	4.494	(e)	3.550	(h)	9.53
CVS2-109	132	6	0.313	5.707	4.494	(e)	3.617	(h)	9.54
CVS2-110	133	6	0.158	0.314	0.402	(e)	0.116	(h)	9.61
CVS2-110	133	6	0.162	0.314	0.402	(e)	0.120	(h)	9.61
CVS2-111	134	6	1.209	6.214	3.894	(e)	4.088	(h)	11.35
CVS2-111	134	6	1.188	6.055	3.894	(e)	3.998	(h)	11.34
CVS2-112	135	6	0.686	14.231	7.953	(e)	9.771	(h)	12.03
CVS2-112	135	6	0.221	14.569	7.635	(e)	9.434	(h)	12.04
CVS2-113	136	6	0.214	0.612	0.635	(e)	0.501	(h)	9.62
CVS2-113	136	6	0.218	0.612	0.624	(e)	0.518	(h)	9.64
CVS2-114	137	6	1.816	6.881	4.892	(e)	4.599	(h)	11.41
CVS2-114	137	6	1.860	7.350	4.964	(e)	4.599	(h)	11.41
CVS2-115	138	6	1.921	9.169	5.837	(e)	5.765	(h)	11.54
CVS2-115	138	6	1.962	9.643	5.837	(e)	5.765	(h)	11.56
CVS2-116	139	6	0.606	2.934	2.145	(e)	1.939	(h)	10.42
CVS2-116	139	6	0.606	3.089	2.261	(e)	2.121	(h)	10.43
CVS2-117	140	6	0.435	1.514	1.309	(e)	1.069	(h)	10.18
CVS2-117	140	6	0.455	1.665	1.365	(e)	1.128	(h)	10.20

(a) Elemental releases normalized using as-batched compositions from Table A.1.

(b) ID# is a consecutive integer numbering of all CVS glasses.

(c) PS is the plotting symbol used in plots associated with this data: 1 = CVS-I boundary, 2 = CVS-II Phase 1 interior, 3 = CVS-II Phase 2a boundary, 4 = CVS-II Phase 2b interior, 5 = CVS-II Phase 3 boundary, 6 = CVS-II Phase 4 one-component-at-a-time, M = middle compositions, O = other than NCAW waste glasses, A = EA glass.

(e) Mo release was determined as not of interest, and so data were no longer collected beginning with Phase 2 of CVS-II.

(h) Cs releases were not measured for CVS-II Phase 4 glasses.

TABLE D.2. Normalized Elemental Release and pH Data from Duplicate 7-day PCTs (90°C, DIW, 2000m^{-1}) Performed on CVS-I and CVS-II Glasses (continued)

Glass	ID[b] #	PS[c]	Normalized[a] Elemental Release Rates (g/m²) Si	B	Li	Mo	Na	Cs	pH
CVS2-118	141	6	0.586	3.398	2.493	(e)	2.303	(h)	10.38
CVS2-118	141	6	0.626	3.861	2.724	(e)	2.485	(h)	10.41
CVS2-119	142	6	0.838	3.878	2.744	(e)	2.632	(h)	10.32
CVS2-119	142	6	0.819	3.728	2.632	(e)	2.515	(h)	10.32
CVS2-120	143	6	0.152	0.283	0.324	(e)	0.234	(h)	10.09
CVS2-120	143	6	0.156	0.298	0.324	(e)	0.228	(h)	10.09
CVS2-121	144	6	0.128	0.199	0.311	(e)	0.137	(h)	10.05
CVS2-121	144	6	0.130	0.199	0.311	(e)	0.137	(h)	10.06
CVS2-122	145	6	0.128	0.193	0.363	(e)	0.089	(h)	9.91
CVS2-122	145	6	0.128	0.193	0.363	(e)	0.089	(h)	9.91
CVS2-123	146	M	0.381	1.411	1.067	(e)	1.015	(h)	10.21
CVS2-123	146	M	0.401	1.534	1.182	(e)	1.134	(h)	10.23

(a) Elemental releases normalized using as-batched compositions from Table A.1.

(b) ID# is a consecutive integer numbering of all CVS glasses.

(c) PS is the plotting symbol used in plots associated with this data: 1 = CVS-I boundary, 2 = CVS-II Phase 1 interior, 3 = CVS-II Phase 2a boundary, 4 = CVS-II Phase 2b interior, 5 = CVS-II Phase 3 boundary, 6 = CVS-II Phase 4 one-component-at-a-time, M = middle compositions, 0 = other than NCAW waste glasses, A = EA glass.

(e) Mo release was determined as not of interest, and so data were no longer collected beginning with Phase 2 of CVS-II.

(h) Cs releases were not measured for CVS-II Phase 4 glasses.

TABLE D.3. Standard Deviations (SD) and Percent Relative Standard Deviations (%RSD)[a] Before and After Natural Logarithmic Transformations of Normalized[b] Si, B, Li, and Na Release Data From Duplicate 28-Day MCC-1 Dissolution Tests

		# Glasses With Dups	Untransformed SD (g/m²)	Untransformed RSD (%)	Ln Transformed SD (g/m²)	Ln Transformed RSD (%)
Si Release						
All Data	CVS-I	22	2.5007	5.06	0.0507	2.81
	CVS-II Phase 1	19	0.2289	2.20	0.0220	0.97
	CVS-II Phase 2	37	0.2503	2.35	0.0235	1.04
	CVS-II Phase 3	43	3.0772	6.90	0.0710	1.98
	CVS-II Phase 4	22	0.8052	3.09	0.0310	1.12
	All Phases	143	1.9830	4.67	0.0476	1.73
Outliers Removed (c)	CVS-I	21	0.6035	5.01	0.0502	2.86
	CVS-II Phase 1	19	0.2289	2.20	0.0220	0.97
	CVS-II Phase 2	37	0.2503	2.35	0.0235	1.04
	CVS-II Phase 3	41	0.4459	2.15	0.0216	0.83
	CVS-II Phase 4	22	0.8052	3.09	0.0310	1.12
	All Phases	140	0.4883	2.96	0.0296	1.43
B Release						
All Data	CVS-I	22	5.7649	3.93	0.0393	2.26
	CVS-II Phase 1	19	0.3824	2.52	0.0252	1.02
	CVS-II Phase 2	37	0.4582	2.45	0.0245	0.92
	CVS-II Phase 3	43	6.8623	8.17	0.0851	2.08
	CVS-II Phase 4	22	0.8743	2.99	0.0299	1.05
	All Phases	143	4.4119	5.12	0.0528	1.62
Outliers Removed (c)	CVS-I	21	1.5081	3.93	0.0394	2.30
	CVS-II Phase 1	19	0.3824	2.52	0.0252	1.02
	CVS-II Phase 2	37	0.4582	2.45	0.0245	0.92
	CVS-II Phase 3	41	1.4336	2.85	0.0285	1.03
	CVS-II Phase 4	22	0.8743	2.99	0.0299	1.05
	All Phases	140	1.0670	2.92	0.0293	1.28

(a) The standard deviations (SD) and percent relative standard deviations (%RSD) reported are pooled over various sets of glasses by forming the root-mean-square of the SD and %RSD values for individual glasses (i.e., the square root of the sum of the squares of the values in a set, divided by the number in the set).

(b) Normalized with respect to as-batched compositions.

(c) Duplicate results for glasses CVS1-13, CVS2-84, and CVS2-94 had larger SDs or %RSDs than the other glasses and were excluded from computations.

TABLE D.3. Standard Deviations (SD) and Percent Relative Standard Deviations (%RSD)[a] Before and After Natural Logarithmic Transformations of Normalized[b] Si, B, Li, and Na Release Data From Duplicate 28-Day MCC-1 Dissolution Tests (continued)

		# Glasses With Dups	Untransformed SD (g/m²)	Untransformed RSD (%)	Ln Transformed SD (g/m²)	Ln Transformed RSD (%)
Li Release						
All Data	CVS-I	22	6.2999	3.85	0.0385	1.68
	CVS-II Phase 1	19	0.5439	3.30	0.0330	1.22
	CVS-II Phase 2	37	0.3865	2.48	0.0248	1.00
	CVS-II Phase 3	43	7.0559	9.69	0.1004	3.10
	CVS-II Phase 4	22	0.4416	2.51	0.0251	0.95
	All Phases	143	4.6026	5.88	0.0605	1.98
Outliers Removed (c)	CVS-I	21	1.3518	3.82	0.0382	1.72
	CVS-II Phase 1	19	0.5439	3.30	0.0330	1.22
	CVS-II Phase 2	37	0.3865	2.48	0.0248	1.00
	CVS-II Phase 3	41	0.8653	5.64	0.0569	2.46
	CVS-II Phase 4	22	0.4416	2.51	0.0251	0.95
	All Phases	140	0.7770	3.95	0.0397	1.68
Na Release						
All Data	CVS-I	22	6.1642	4.48	0.0449	2.53
	CVS-II Phase 1	19	0.8351	6.13	0.0616	2.48
	CVS-II Phase 2	37	0.4488	2.71	0.0271	1.07
	CVS-II Phase 3	43	6.2879	8.04	0.0829	2.15
	CVS-II Phase 4	22	0.6747	3.07	0.0307	1.12
	All Phases	143	4.2367	5.55	0.0567	1.92
Outliers Removed (c)	CVS-I	21	1.4397	4.48	0.0449	2.59
	CVS-II Phase 1	19	0.8351	6.13	0.0616	2.48
	CVS-II Phase 2	37	0.4488	2.71	0.0271	1.07
	CVS-II Phase 3	41	1.7333	3.67	0.0368	1.34
	CVS-II Phase 4	22	0.6747	3.07	0.0307	1.12
	All Phases	140	1.1875	3.93	0.0394	1.69

(a) The standard deviations (SD) and percent relative standard deviations (%RSD) reported are pooled over various sets of glasses by forming the root-mean-square of the SD and %RSD values for individual glasses (i.e., the square root of the sum of the squares of the values in a set, divided by the number in the set).

(b) Normalized with respect to as-batched compositions.

(c) Duplicate results for glasses CVS1-13, CVS2-84, and CVS2-94 had larger SDs or %RSDs than the other glasses and were excluded from computations.

TABLE D.4. Standard Deviations (SD) and Percent Relative Standard Deviations (%RSD)[a] Before and After Natural Logarithmic Transformations of Normalized[b] Si, B, Li, and Na Release Data From Duplicate 7-Day PCT Dissolution Tests

		# Glasses With Dups	Untransformed SD (g/m²)	Untransformed RSD (%)	Ln Transformed SD (g/m²)	Ln Transformed RSD (%)
Si Release						
All Data	CVS-I	22	0.0241	4.52	0.0453	22.81
	CVS-II Phase 1	19	0.0065	2.08	0.0208	1.93
	CVS-II Phase 2	39	0.0265	3.19	0.0319	10.32
	CVS-II Phase 3	43	0.5282	14.05	0.1558	17.55
	CVS-II Phase 4	22	0.0715	15.59	0.1720	18.55
	All Phases	145	0.2894	10.09	0.1110	15.86
Outliers Removed (c)	CVS-I	22	0.0241	4.52	0.0453	22.81
	CVS-II Phase 1	19	0.0065	2.08	0.0208	1.93
	CVS-II Phase 2	39	0.0265	3.19	0.0319	10.32
	CVS-II Phase 3	40	0.0676	5.43	0.0547	8.35
	CVS-II Phase 4	21	0.0142	2.09	0.0209	4.12
	All Phases	141	0.0402	3.95	0.0397	15.94
B Release						
All Data	CVS-I	22	0.1609	2.58	0.0259	8.86
	CVS-II Phase 1	19	0.0341	3.16	0.0316	4.9[illegible]
	CVS-II Phase 2	39	0.1954	4.59	0.0460	8.77
	CVS-II Phase 3	43	1.1893	4.92	0.0494	23.35
	CVS-II Phase 4	22	0.1749	3.86	0.0386	5.69
	All Phases	145	0.6622	4.18	0.0419	14.22
Outliers Removed (c)	CVS-I	22	0.1609	2.58	0.0259	8.86
	CVS-II Phase 1	19	0.0341	3.16	0.0316	4.96
	CVS-II Phase 2	39	0.1954	4.59	0.0460	8.77
	CVS-II Phase 3	41	0.2310	3.91	0.0392	23.89
	CVS-II Phase 4	22	0.1749	3.86	0.0386	5.69
	All Phases	143	0.1859	3.85	0.0385	14.32

(a) The standard deviations (SD) and percent relative standard deviations (%RSD) reported are pooled over various sets of glasses by forming the root-mean-square of the SD and %RSD values for individual glasses (i.e., the square root of the sum of the squares of the values in a set, divided by the number in the set).

(b) Normalized with respect to as-batched compositions.

(c) Duplicate Si release results for glasses CVS2-82, CVS2-83, CVS2-84, and CVS2-112 had larger SDs or %RSDs than the other glasses, and were excluded from computations. For B, Li, and Na releases, results for CVS2-82 and CVS2-83 were excluded.

TABLE D.4. Standard Deviations (SD) and Percent Relative Standard Deviations (%RSD)[a] Before and After Natural Logarithmic Transformations of Normalized[b] Si, B, Li, and Na Release Data From Duplicate 7-Day PCT Dissolution Tests (continued)

		# Glasses With Dups	Untransformed SD (g/m²)	Untransformed RSD (%)	Ln Transformed SD (g/m²)	Ln Transformed RSD (%)
Li Release						
All Data	CVS-I	22	0.1324	1.94	0.0194	4.09
	CVS-II Phase 1	19	0.0619	4.98	0.0498	10.36
	CVS-II Phase 2	39	0.0582	3.45	0.0346	13.10
	CVS-II Phase 3	43	0.6086	4.51	0.0452	19.37
	CVS-II Phase 4	22	0.0979	3.20	0.0321	13.38
	All Phases	145	0.3397	3.82	0.0383	14.26
Outliers Removed (c)	CVS-I	22	0.1324	1.94	0.0194	4.09
	CVS-II Phase 1	19	0.0619	4.98	0.0498	10.36
	CVS-II Phase 2	39	0.0582	3.45	0.0346	13.10
	CVS-II Phase 3	41	0.1170	3.38	0.0339	19.81
	CVS-II Phase 4	22	0.0979	3.20	0.0321	13.88
	All Phases	143	0.0976	3.46	0.0346	14.35
Na Release						
All Data	CVS-I	22	0.1441	3.70	0.0370	2.85
	CVS-II Phase 1	19	0.0353	5.27	0.0527	8.91
	CVS-II Phase 2	39	0.0924	3.39	0.0339	13.30
	CVS-II Phase 3	43	0.9109	5.31	0.0533	13.41
	CVS-II Phase 4	22	0.0982	3.46	0.0346	25.54
	All Phases	145	0.5031	4.36	0.0437	14.54
Outliers Removed (c)	CVS-I	22	0.1441	3.70	0.0370	2.85
	CVS-II Phase 1	19	0.0353	5.27	0.0527	8.91
	CVS-II Phase 2	39	0.0924	3.39	0.0339	13.30
	CVS-II Phase 3	41	0.2155	4.47	0.0449	13.71
	CVS-II Phase 4	22	0.0982	3.46	0.0346	25.54
	All Phases	143	0.1431	4.06	0.0407	14.64

(a) The standard deviations (SD) and percent relative standard deviations (%RSD) reported are pooled over various sets of glasses by forming the root-mean-square of the SD and %RSD values for individual glasses (i.e., the square root of the sum of the squares of the values in a set, divided by the number in the set).

(b) Normalized with respect to as-batched compositions.

(c) Duplicate Si release results for glasses CVS2-82, CVS2-83, CVS2-84, and CVS2-112 had larger SDs or %RSDs than the other glasses, and were excluded from computations. For B, Li, and Na releases, results for CVS2-82 and CVS2-83 were excluded.

TABLE D.5. Normalized Elemental Release and pH Data from Duplicate 7-day PCTs (90°C, DIW, 2000m^{-1}) Performed on CVS-II Phase 4 Glasses

Glass	ID[b] #	PS[c]	Normalized[a] Elemental Release Rates (g/m²) Si	B	Li	Mo	Na	Cs	pH
CVS2-102	125	M	0.524	2.722	1.894	(d)	1.755	(e)	10.3
CVS2-102	125	M	0.548	2.553	1.865	(d)	1.689	(e)	10.3
CVS2-103	126	6	0.780	5.732	4.363	(d)	4.247	(e)	11.5
CVS2-103	126	6	0.806	6.070	4.431	(d)	4.252	(e)	11.5
CVS2-104	127	6	0.818	6.396	4.656	(d)	4.206	(e)	11.2
CVS2-104	127	6	0.792	6.474	4.389	(d)	4.075	(e)	11.1
CVS2-105	128	6	0.640	3.595	2.981	(d)	2.735	(e)	10.7
CVS2-105	128	6	0.672	3.483	3.059	(d)	2.751	(e)	10.7
CVS2-106	129	6	0.398	1.305	1.117	(d)	0.978	(e)	10.0
CVS2-106	129	6	0.388	1.355	1.086	(d)	0.893	(e)	10.0
CVS2-107	130	6	0.263	0.708	0.508	(d)	0.468	(e)	10.5
CVS2-107	130	6	0.256	0.612	0.459	(d)	0.429	(e)	10.5
CVS2-108	131	6	0.379	2.233	1.843	(d)	1.551	(e)	9.8
CVS2-108	131	6	0.360	2.147	1.722	(d)	1.419	(e)	9.8
CVS2-109	132	6	0.326	4.250	3.820	(d)	3.002	(e)	9.4
CVS2-109	132	6	0.335	4.411	3.916	(d)	3.062	(e)	9.4
CVS2-110	133	6	0.231	2.642	2.172	(d)	1.577	(e)	9.8
CVS2-110	133	6	0.241	2.628	2.306	(d)	1.537	(e)	9.8
CVS2-111	134	6	1.456	3.017	5.004	(d)	5.032	(e)	11.2
CVS2-111	134	6	1.202	6.258	4.135	(d)	4.264	(e)	11.2
CVS2-112	135	6	0.459	15.893	8.374	(d)	10.177	(e)	12.0
CVS2-112	135	6	0.448	14.757	7.515	(d)	9.638	(e)	12.1
CVS2-113	136	6	0.194	0.520	0.484	(d)	0.419	(e)	9.6
CVS2-113	136	6	0.210	0.595	0.545	(d)	0.454	(e)	9.6
CVS2-114	137	6	1.717	6.881	4.462	(d)	4.108	(e)	11.3
CVS2-114	137	6	1.798	7.194	4.534	(d)	4.231	(e)	11.4

(a) Elemental releases normalized using as-batched compositions from Table 4.14.

(b) ID# is a consecutive integer numbering of all CVS glasses.

(c) PS is the plotting symbol used in plots associated with this data: 1 = CVS-I boundary, 2 = CVS-II Phase 1 interior, 3 = CVS-II Phase 2a boundary, 4 = CVS-II Phase 2b interior, 5 = CVS-II Phase 3 boundary, 6 = CVS-II Phase 4 one-component-at-a-time, M = middle compositions, O = other than NCAW waste glasses, A = EA glass.

(d) Mo release was determined as not of interest, and so data were no longer collected beginning with Phase 2 of CVS-II.

(e) Cs releases were not measured for CVS-II Phase 4 glasses.

TABLE D.5. Normalized Elemental Release and pH Data from Duplicate 7-day PCTs (90°C, DIW, $2000m^{-1}$) Performed on CVS-II Phase 4 Glasses (continued)

Glass	ID[b] #	PS[c]	Normalized[a] Elemental Release Rates (g/m^2) Si	B	Li	Mo	Na	Cs	pH
CVS2-115	138	6	1.826	9.606	5.827	(d)	5.735	(e)	11.5
CVS2-115	138	6	1.828	9.337	5.581	(d)	5.487	(e)	11.6
CVS2-116	139	6	0.578	2.769	2.004	(d)	1.892	(e)	10.4
CVS2-116	139	6	0.562	2.739	2.033	(d)	1.952	(e)	10.4
CVS2-117	140	6	0.440	1.622	1.423	(d)	1.153	(e)	10.2
CVS2-117	140	6	0.432	1.577	1.309	(d)	1.129	(e)	10.2
CVS2-118	141	6	0.576	2.831	2.207	(d)	2.007	(e)	10.3
CVS2-118	141	6	0.534	2.785	2.004	(d)	1.928	(e)	10.3
CVS2-119	142	6	0.826	3.600	3.028	(d)	2.821	(e)	10.4
CVS2-119	142	6	0.828	3.585	3.000	(d)	2.809	(e)	10.3
CVS2-120	143	6	0.140	0.299	0.310	(d)	0.221	(e)	10.1
CVS2-120	143	6	0.136	0.283	0.301	(d)	0.211	(e)	10.1
CVS2-121	144	6	0.121	0.166	0.269	(d)	0.132	(e)	10.0
CVS2-121	144	6	0.117	0.183	0.271	(d)	0.137	(e)	10.0
CVS2-122	145	6	0.115	0.250	0.310	(d)	0.089	(e)	9.9
CVS2-122	145	6	0.117	0.176	0.307	(d)	0.088	(e)	9.9
CVS2-123	146	M	0.353	1.260	1.039	(d)	1.015	(e)	10.2
CVS2-123	146	M	0.359	1.444	1.068	(d)	0.997	(e)	10.2

(a) Elemental releases normalized using as-batched compositions from Table 4.14.

(b) ID# is a consecutive integer numbering of all CVS glasses.

(c) PS is the plotting symbol used in plots associated with this data: 1 = CVS-I boundary, 2 = CVS-II Phase 1 interior, 3 = CVS-II Phase 2a boundary, 4 = CVS-II Phase 2b interior, 5 = CVS-II Phase 3 boundary, 6 = CVS-II Phase 4 one-component-at-a-time, M = middle compositions, O = other than NCAW waste glasses, A = EA glass.

(d) Mo release was determined as not of interest, and so data were no longer collected beginning with Phase 2 of CVS-II.

(e) Cs releases were not measured for CVS-II Phase 4 glasses.

APPENDIX E

THERMAL PROPERTY AND LIQUIDUS TEMPERATURE DATA

APPENDIX E

THERMAL PROPERTY AND LIQUIDUS TEMPERATURE DATA

Glass transition temperature, coefficients of thermal expansion for solid and molten glass, and early liquidus temperature data are given in Table E.1. The data for glass transition temperature and coefficients of thermal expansion for solid and molten glass table are also given in Tables 9.1 and 10.1 in the main body of the report, respectively.

The liquidus temperature data given in Table E.1 are those generated during CVS-I (determination whether liquidus temperature was above or below 1050°C) and by Corning glass for CVS-II Phase 1 glasses. However, these data are superseded by the data given in Tables 11.3 and 11.4 in Chapter 11, since liquidus temperature was subsequently measured for all CVS glasses. The older "above or below 1050°C" determinations and Corning measurements are reported here for completeness.

TABLE E.1. Glass Transition Temperature (T_g), Thermal Expansion Coefficients for Solid Glass (α_s) and Molten Glass (α_m), and Older Liquidus Temperature Results for CVS-I and CVS-II Phase 1, 2, and 3 Glasses

Glass (a)	(b) ID #	(c) PS	T_g (°C)	α_s (10^{-6}/K)	α_m (10^{-6}/K)	Older Liquidus (d) Temp. (°C) Results
CVS1-1 (1)	1	M	486.2	8.9	103.0	< 1050
CVS1-2	2	1	487.6	9.4	72.0	< 1050
CVS1-3	3	1	486.3	9.2	111.3	< 1050
CVS1-4 (2)	4	1	524.6	6.9	69.7	< 1050
CVS1-5	5	1	450.9	9.1	103.5	< 1050
CVS1-6	6	1	490.5	8.6	96.5	> 1050
CVS1-7	7	1	579.1	8.0	60.7	> 1050
CVS1-8 (3)	8	1	547.0	8.1	79.8	> 1050
CVS1-9	9	1	516.9	6.6	82.8	> 1050
CVS1-10	10	1	519.4	6.6	53.7	> 1050
CVS1-11	11	1	537.1	8.5	57.1	< 1050
CVS1-12	12	1	469.3	10.3	132.3	< 1050
CVS1-13	13	1	526.7	10.0	120.4	< 1050
CVS1-14	14	1	520.4	9.4	95.1	< 1050
CVS1-15	15	1	429.6	10.6	96.1	< 1050
CVS1-16	16	1	488.5	10.9	58.6	> 1050
CVS1-17	17	1	490.4	11.1	117.8	< 1050
CVS1-18	18	1	429.3	12.4	75.7	> 1050
CVS1-19 (1)	19	M	491.3	8.3	87.8	< 1050
CVS1-20 (1)	20	M	496.3	9.5	91.6	< 1050
CVS1-21 (2)	21	1	543.5	5.6	101.0	< 1050
CVS1-22 (3)	22	1	559.9	7.1	49.2	> 1050
CVS1-23	23	M	486.5	9.1	123.0	< 1050
CVS2-1	24	2	474.5	8.8	114.2	885
CVS2-2	25	2	479.8	8.9	81.6	765

(a) The numbers in parentheses represent replicate sets of glasses.

(b) ID# is a consecutive integer numbering of all CVS glasses.

(c) PS is the plotting symbol used in plots associated with this data: 1 = CVS-I boundary, 2 = CVS-II Phase 1 interior, 3 = CVS-II Phase 2a boundary, 4 = CVS-II Phase 2b interior, 5 = CVS-II Phase 3 boundary, M = middle compositions, O = other than NCAW waste glasses, A = EA glass.

(d) During CVS-I, liquidus temperature was not measured, but only determined to be above or below 1050°C. The liquidus temperatures of CVS-II Phase 1 glasses measured by Corning are reported here, but these values were subsequently determined to be of questionable accuracy compared to results obtained as part of CVS-II work (see Tables 11.3 and 11.4).

TABLE E.1. Glass Transition Temperature (T_g), Thermal Expansion Coefficients for Solid Glass (α_s) and Molten Glass (α_m), and Older Liquidus Temperature Results for CVS-I and CVS-II Phase 1, 2, and 3 Glasses (continued)

Glass (a)	(b) ID #	(c) PS	T_g (°C)	α_s (10^{-6}/K)	α_m (10^{-6}/K)	Older Liquidus (d) Temp. (°C) Results
CVS2-3	26	2	522.1	9.1	81.5	825
CVS2-4	27	2	497.6	8.4	89.3	755
CVS2-5	28	2	519.3	7.9	59.3	895
CVS2-6	29	2	497.7	8.8	108.2	855
CVS2-7	30	2	475.5	11.2	88.4	740
CVS2-8	31	2	465.4	10.3	120.9	1080
CVS2-9	32	2	483.6	9.0	83.3	785
CVS2-10	33	2	490.8	7.9	74.2	685
CVS2-11	34	2	482.3	9.5	83.7	890
CVS2-12	35	2	500.6	8.3	99.0	760
CVS2-13	36	2	480.2	10.7	77.8	860
CVS2-14	37	2	516.6	9.6	78.3	1120
CVS2-15	38	2	480.8	8.3	88.1	840
CVS2-16 (4)	39	M	487.4	9.0	98.0	750
CVS2-17 (1)	40	M	492.9	8.6	97.7	830
CVS2-18 (4)	41	M	483.2	9.4	88.1	810
CVS2-19 (5)	42	M	493.0	9.8	99.3	825
CVS2-20	43	3	489.0	9.23	52.8	---
CVS2-21	44	3	487.7	8.38	93.2	---
CVS2-22	45	3	469.0	9.65	106.2	---
CVS2-23	46	3	498.4	11.32	68.8	---
CVS2-24	47	3	462.8	8.83	86.8	---
CVS2-25	48	3	455.1	10.95	107.0	---
CVS2-26	49	3	511.2	7.98	108.0	---

(a) The numbers in parentheses represent replicate sets of glasses.

(b) ID# is a consecutive integer numbering of all CVS glasses.

(c) PS is the plotting symbol used in plots associated with this data: 1 = CVS-I boundary, 2 = CVS-II Phase 1 interior, 3 = CVS-II Phase 2a boundary, 4 = CVS-II Phase 2b interior, 5 = CVS-II Phase 3 boundary, M = middle compositions, O = other than NCAW waste glasses, A = EA glass.

(d) During CVS-I, liquidus temperature was not measured, but only determined to be above or below 1050°C. The liquidus temperatures of CVS-II Phase 1 glasses measured by Corning are reported here, but these values were subsequently determined to be of questionable accuracy compared to results obtained as part of CVS-II work (see Tables 11.3 and 11.4).

TABLE E.1. Glass Transition Temperature (T_g), Thermal Expansion Coefficients for Solid Glass (α_s) and Molten Glass (α_m), and Older Liquidus Temperature Results for CVS-I and CVS-II Phase 1, 2, and 3 Glasses (continued)

Glass (a)	(b) ID #	(c) PS	T_g (°C)	α_s (10^{-6}/K)	α_m (10^{-6}/K)
CVS2-27	50	3	480.1	10.99	69.1
CVS2-28	51	3	476.3	11.38	64.0
CVS2-29	52	3	561.6	6.28	94.3
CVS2-30	53	3	490.1	6.38	96.4
CVS2-31	54	3	528.9	6.52	72.4
CVS2-32	55	3	475.3	10.76	61.5
CVS2-33	56	3	412.0	12.19	72.4
CVS2-34 (6)	57	3	455.6	11.04	84.9
CVS2-35	58	3	422.2	13.13	60.1
CVS2-36	59	3	472.7	10.27	149.3
CVS2-37	60	3	470.3	10.59	63.0
CVS2-38	61	3	527.8	7.69	98.4
CVS2-39	62	3	447.3	11.83	81.8
CVS2-40	63	4	464.3	10.82	71.3
CVS2-41	64	4	472.5	9.15	97.8
CVS2-42	65	4	477.9	8.85	96.7
CVS2-43	66	4	499.2	8.23	92.8
CVS2-44	67	4	483.8	8.41	78.4
CVS2-45	68	4	492.8	8.20	101.4
CVS2-46	69	4	480.1	7.09	82.3
CVS2-47	70	4	481.3	10.32	151.4
CVS2-48	71	4	489.5	8.70	99.7
CVS2-49	72	4	486.6	8.81	98.0
CVS2-50 (1)	73	M	491.2	8.72	80.6
CVS2-51 (5)	74	M	478.0	9.39	94.2
CVS2-52	75	4	479.0	8.39	91.8
CVS2-53	76	4	(e)	(e)	(e)
CVS2-54	77	M	(e)	(e)	(e)
CVS2-55	78	0	502.2	8.73	85.8
CVS2-56	79	0	496.6	9.05	98.9

(a) The numbers in parentheses represent replicate sets of glasses.

(b) ID# is a consecutive integer numbering of all CVS glasses.

(c) PS is the plotting symbol used in plots associated with this data: 1 = CVS-I boundary, 2 = CVS-II Phase 1 interior, 3 = CVS-II Phase 2a boundary, 4 = CVS-II Phase 2b interior, 5 = CVS-II Phase 3 boundary, M = middle compositions, 0 = other than NCAW waste glasses, A = EA glass.

(e) Properties not measured for radioactive glasses CVS2-53 and CVS2-54.

TABLE E.1. Glass Transition Temperature (T_g), Thermal Expansion Coefficients for Solid Glass (α_s) and Molten Glass (α_m), and Older Liquidus Temperature Results for CVS-I and CVS-II Phase 1, 2, and 3 Glasses (continued)

Glass (a)	(b) ID #	(c) PS	T_g (°C)	α_s (10^{-6}/K)	α_m (10^{-6}/K)
CVS2-57	80	0	512.1	8.95	87.6
CVS2-58	81	4	499.1	7.98	96.7
CVS2-59	82	5	453.8	10.5	86.1
CVS2-60	83	5	432.0	9.70	71.8
CVS2-61	84	5	460.4	10.6	62.7
CVS2-62	85	5	537.2	8.0	112.3
CVS2-63	86	5	488.6	12.5	62.9
CVS2-64	87	0	471.8	10.0	80.9
CVS2-65	88	0	514.3	9.4	68.5
CVS2-66	89	0	470.1	8.8	79.3
CVS2-67	90	0	479.3	8.0	60.6
CVS2-68	91	0	465.7	7.7	74.0
CVS2-69	92	0	488.2	8.9	62.5
CVS2-70	93	0	484.2	8.4	94.0
CVS2-71	94	5	470.9	8.7	97.1
CVS2-72	95	5	462.7	8.4	76.3
CVS2-73	96	5	476.4	8.3	71.7
CVS2-74	97	5	470.3	8.8	83.3
CVS2-75	98	5	469.1	77.1 (f)	713.0 (f)
CVS2-76	99	5	428.9	13.8	97.0
CVS2-77	100	5	426.0	11.7	76.1
CVS2-78	101	5	519.4	6.0	72.5
CVS2-79	102	5	497.8	4.7	56.1
CVS2-80	103	5	530.4	5.6	93.4
CVS2-81	104	5	392.8	13.7	79.5
CVS2-82	105	5	438.5	13.7	77.5
CVS2-83	106	5	415.5	13.4	73.1
CVS2-84	107	5	418.8	11.2	83.5
CVS2-85	108	5	416.1	8.4	64.0

(a) The numbers in parentheses represent replicate sets of glasses.

(b) ID# is a consecutive integer numbering of all CVS glasses.

(c) PS is the plotting symbol used in plots associated with this data: 1 = CVS-I boundary, 2 = CVS-II Phase 1 interior, 3 = CVS-II Phase 2a boundary, 4 = CVS-II Phase 2b interior, 5 = CVS-II Phase 3 boundary, M = middle compositions, O = other than NCAW waste glasses, A = EA glass.

(f) These values appear to be erroneous and were not used in fitting models or other data analyses.

TABLE E.1. Glass Transition Temperature (T_g), Thermal Expansion Coefficients for Solid Glass (α_s) and Molten Glass (α_m), and Older Liquidus Temperature Results for CVS-I and CVS-II Phase 1, 2, and 3 Glasses (continued)

Glass (a)	(b) ID #	(c) PS	T_g (°C)	α_s (10^{-6}/K)	α_m (10^{-6}/K)
CVS2-86	109	5	510.2	10.6	78.2
CVS2-87	110	5	497.2	8.7	59.5
CVS2-88	111	5	441.7	11.2	61.5
CVS2-89	112	5	512.3	10.4	101.7
CVS2-90	113	5	486.1	6.8	94.8
CVS2-91	114	5	525.3	7.0	90.8
CVS2-92	115	5	467.8	8.0	79.6
CVS2-93	116	5	450.1	12.3	105.4
CVS2-94	117	5	454.4	11.3	103.5
CVS2-95 (7)	118	A	453.1	11.3	90.3
CVS2-96 (1)	119	M	494.0	9.6	96.4
CVS2-97 (5)	120	M	489.3	10.1	104.1
CVS2-98 (6)	121	5	461.1	11.5	78.6
CVS2-99	122	5	482.6	8.6	74.0
CVS2-100	123	5	476.4	9.3	96.2
CVS2-101(7)	124	A	(g)	(g)	(g)

(a) The numbers in parentheses represent replicate sets of glasses.

(b) ID# is a consecutive integer numbering of all CVS glasses.

(c) PS is the plotting symbol used in plots associated with this data: 1 = CVS-I boundary, 2 = CVS-II Phase 1 interior, 3 = CVS-II Phase 2a boundary, 4 = CVS-II Phase 2b interior, 5 = CVS-II Phase 3 boundary, M = middle compositions, O = other than NCAW waste glasses, A = EA glass.

(g) Properties not measured for this glass.

APPENDIX F

PROPERTY VALUE UNCERTAINTIES

APPENDIX F

PROPERTY VALUE UNCERTAINTIES

Several glass compositions were fabricated and/or tested more than once over the course of the CVS in order to estimate uncertainties in measured property values. Property values for the replicated compositions are given in Table F.1 (for viscosity, electrical conductivity, and thermal properties), Table F.2 (for PCT releases), and Table F.3 (for MCC-1 Releases). Table F.4 contains means (Mean), standard deviations (SD), and percent relative standard deviations (%RSD) estimated from the property data in Table F.1, as well as for natural logarithm transformed values of the property data where applicable. The SDs and %RSDs in Table F.4 correspond to longer-term replicate fabrication[(a)] and property measurement of glasses. Tables F.5 and F.6 contain means (Mean) and standard deviations (SD) estimated from natural logarithms of the PCT and MCC-1 data in Tables F.2 and F.3. The SDs in Tables F.5 and F.6 correspond to duplicate dissolution tests of each glass as well as longer-term replicate dissolution tests of glasses. In most cases, these longer-term standard deviations are larger than the shorter-term duplicate dissolution test standard deviations. This is as expected, because replicate dissolution tests conducted over time include variations due to refabricating glasses[(a)] as well as longer-term sources of variation in dissolution testing and chemical analyses of solutions.

Tables F.4, F.5, and F.6 also contain pooled values of SDs and %RSDs (for Table F.4 only) over all replicates for each property. The pooled SD for

---

(a) Glasses in Replicate Set #5 were subsamples of the CVS internal standard glass, which was only fabricated once. Hence, SDs computed from replicate property values for Replicate Set #5 do not contain variation due to refabricating the glass.

a given property was calculated from the SDs for each replicate set as

$$Pooled\ SD = \sqrt{\frac{\sum_{i=1}^{n} df_i\ SD_i^2}{\sum_{i=1}^{n} df_i}} \qquad (F.1)$$

where df_i and SD_i represent the degrees of freedom and SD from the i-th replicate set, and n represents the number of replicate sets. A similar formula was used to compute the pooled %RSDs in Table F.4.

Because the replicate data are a mix of shorter-term and longer-term replicates, resulting pooled SDs and %RSDs will estimate somewhere between short-term and long-term variation due to glass fabrication and property testing. As an example of how to interpret the pooled SDs or %RSDs, consider the pooled SDs and %RSDs for viscosity at 1150°C in Table F.4 (w/o Set 3). Because viscosity has a natural logarithm transformation applied, attention should be focused on the transformed pooled SD = 0.0345 and the untransformed pooled %RSD = 3.44[a]. These values indicate the combined short- and long-term standard deviation in viscosity at 1150°C data for repeated fabrication[b] and measurement of a given glass is about 0.0345 ln(Pa·s), which is roughly equivalent to an untransformed %RSD of 3.44%.

(a) Note that for log transformed properties, the untransformed %RSD will typically be equal or close to 100 times the transformed SD.

(b) Glasses in Replicate Set #5 were subsamples of the CVS internal standard glass, which was only fabricated once. Hence, SDs computed from replicate property values for Replicate Set #5 do not contain variation due to refabricating the glass.

TABLE F.1. Viscosity, Electrical Conductivity, and Thermal Property Values for Glasses Replicated During CVS

(a) Rep. Set	Glass	CVS Phase	(b) η_{1150} (Pa·s)	(c) ϵ_{1150} (S/m)	T_g (°C)	α_s (10^{-6}/K)	α_m (10^{-6}/K)
1	CVS1-1	1.0	5.78	18.65	486.2	8.9	103.0
	CVS1-19	1.0	5.76	24.27	491.3	8.3	87.8
	CVS1-20	1.0	5.71	26.88	496.3	9.5	91.6
	CVS2-17	2.1	5.37	26.06	492.9	8.6	97.7
	CVS2-50	2.2	5.71	24.81	491.2	8.72	80.6
	CVS2-96	2.3	5.55	25.08	494.0	9.6	96.4
2	CVS1-4	1.0	8.70	9.11	524.6	6.9	69.7
	CVS1-21	1.0	9.36	8.05	543.5	5.6	101.0
3	CVS1-8	1.0	29.26	8.84	547.0	8.1	79.8
	CVS1-22	1.0	38.11	9.24	559.9	7.1	49.2
4	CVS2-16	2.1	6.61	27.54	487.4	9.0	98.0
	CVS2-18	2.1	6.41	28.34	483.2	9.4	88.1
5	CVS2-19	2.1	6.76	27.55	493.0	9.8	99.3
	CVS2-51	2.2	7.07	28.30	478.0	9.39	94.2
	CVS2-97	2.3	7.25	24.56	489.3	10.1	104.1
6	CVS2-34	2.2	1.79	52.63	455.6	11.04	84.9
	CVS2-98	2.3	1.90	59.92	461.1	11.5	78.6
7	CVS2-95	2.3	1.60	54.06	453.1	11.3	90.3
	CVS2-101	2.3	1.51	58.16	(d)	(d)	(d)

(a) Glasses in each replicate set were independently fabricated and tested except for #5. This set involved the CVS internal standard glass, which was fabricated only once and then tested multiple times.

(b) Viscosity at 1150°C predicted using Fulcher equations fitted for each glass.

(c) Electrical conductivity at 1150°C predicted using Arrhenius equations fitted for each glass.

(d) Property not measured for this glass.

TABLE F.2. PCT Elemental Releases for Glasses Replicated During CVS

Replicate Set (a)	Glass	CVS Phase	Test #	PCT Releases (g/m^2) Si	B	Li	Na	Cs	PCT pH
1	CVS1-1	1.0	1	0.167	0.521	0.515	0.403	0.058	10.92
			2	0.167	0.521	0.543	0.403	0.053	10.92
	CVS1-19	1.0	1	0.165	0.517	0.529	0.430	0.063	10.29
			2	0.167	0.529	0.538	0.437	0.068	10.29
	CVS1-20	1.0	1	0.156	0.453	0.466	0.394	0.053	10.17
			2	0.156	0.458	0.469	0.397	0.048	10.15
	CVS2-17	2.1	1	0.167	0.496	0.570	0.473	0.025	10.27
			2	0.167	0.494	0.573	0.476	0.021	10.27
	CVS2-50	2.2	1	0.152	0.450	0.438	0.377	0.036	10.24
			2	0.149	0.434	0.415	0.359	0.024	10.22
	CVS2-96	2.3	1	0.158	0.493	0.429	0.410	0.018	10.29
			2	0.160	0.493	0.429	0.410	0.047	10.19
2	CVS1-4	1.0	1	0.482	20.289	16.667	16.697	1.498	9.67
			2	0.598	20.989	17.204	17.370	1.971	9.67
	CVS1-21	1.0	1	0.467	19.051	15.806	15.723	1.735	9.68
			2	0.452	18.650	15.376	15.349	1.754	9.68
3	CVS1-8	1.0	1	0.265	1.254	0.745	0.805	0.075	10.42
			2	0.265	1.222	0.743	0.805	0.073	10.43
	CVS1-22	1.0	1	0.259	1.122	0.704	0.762	0.065	9.81
			2	0.259	1.116	0.703	0.758	0.069	9.81
4	CVS2-16	2.1	1	0.547	2.937	2.485	2.182	0.019	10.37
			2	0.568	2.937	2.213	2.182	0.015	10.36
	CVS2-18	2.1	1	0.546	2.578	2.192	1.855	0.020	10.34
			2	0.546	2.578	1.997	1.916	0.011	10.34
	CVS2-102	2.4	1	0.559	2.748	1.978	1.737	(b)	10.30
			2	0.559	2.596	1.864	1.617	(b)	10.25
5	CVS2-19	2.1	1	0.439	1.910	1.700	1.394	0.159	10.34
			2	0.460	2.069	1.607	1.568	0.097	10.36
	CVS2-51	2.2	1	0.421	1.841	1.505	1.313	0.083	10.31
			2	0.401	1.687	1.488	1.253	0.030	10.29
	CVS2-97	2.3	1	0.381	1.457	1.009	1.074	0.083	10.28
			2	0.401	1.411	1.095	1.194	0.050	10.22
	CVS2-123	2.4	1	0.381	1.411	1.067	1.015	(b)	10.21
			2	0.401	1.534	1.182	1.134	(b)	10.23
6	CVS2-34	2.2	1	0.265	4.409	3.497	2.729	0.054	11.54
			2	0.265	4.271	3.439	2.672	0.053	11.55
	CVS2-98	2.3	1	0.254	4.520	3.497	2.796	0.022	11.62
			2	0.280	4.520	3.497	2.796	0.108	11.55
7	CVS2-95	2.3	1	1.986	9.687	4.271	7.259	(b)	11.81
			2	2.030	10.265	4.271	7.259	(b)	11.81
	CVS2-101	2.3	1	1.797	8.644	3.831	6.387	(b)	11.91
			2	1.841	8.644	3.831	6.786	(b)	11.94

(a) Glasses in each replicate set were independently fabricated and tested except for Set #5. This set involved the CVS internal standard glass, which was fabricated only once and then tested multiple times.

(b) Cs release was not measured for CVS2-102 and CVS2-123. CVS2-95 and CVS2-101 did not contain Cs.

TABLE F.3. MCC-1 Elemental Releases for Glasses Replicated During CVS

Replicate Set (a)	Glass	CVS Phase	Test #	MCC-1 Releases (g/m^2) Si	B	Li	Na	Cs	MCC-1 pH
1	CVS1-1	1.0	1	8.81	12.33	11.78	12.15	10.65	9.92
			2	9.17	12.61	12.12	12.58	8.72	9.98
	CVS1-19	1.0	1	8.72	12.73	12.93	12.76	9.68	9.84
			2	9.17	13.32	13.44	13.34	10.65	9.92
	CVS1-20	1.0	1	8.68	12.28	12.18	12.19	9.30	9.88
			2	8.99	12.73	12.81	12.79	9.10	9.88
	CVS2-17	2.1	1	9.09	12.18	13.69	13.17	(b)	9.31
			2	9.37	12.47	14.34	13.78	10.60	9.32
	CVS2-50	2.2	1	8.41	11.40	9.78	10.75	11.62	9.44
			2	8.32	11.46	9.89	10.87	8.23	9.45
	CVS2-96	2.3	1	8.90	12.39	10.87	12.36	8.13	9.56
			2	8.90	12.67	11.44	12.90	9.68	9.58
2	CVS1-4	1.0	1	65.60	191.32	162.58	181.19	102.50	9.65
			2	64.10	188.10	161.29	179.70	102.50	9.65
	CVS1-21	1.0	1	60.73	204.18	178.28	190.18	102.50	9.66
			2	61.48	207.40	177.20	194.67	102.50	9.64
3	CVS1-8	1.0	1	11.59	17.94	16.71	17.23	15.37	9.71
			2	11.87	17.81	16.75	17.39	15.77	9.72
	CVS1-22	1.0	1	11.16	17.04	16.75	16.75	15.77	9.80
			2	12.07	17.68	17.44	17.23	15.77	9.73
4	CVS2-16	2.1	1	14.47	18.24	18.52	18.35	13.80	9.41
			2	14.35	17.93	17.92	18.10	15.69	9.51
	CVS2-18	2.1	1	15.66	19.72	20.62	24.48	14.14	9.42
			2	15.82	19.72	20.03	22.26	15.55	9.34
	CVS2-102	2.4	1	15.57	19.54	17.78	17.97	(b)	9.52
			2	15.17	18.93	17.20	16.77	(b)	9.55
5	CVS2-19	2.1	1	11.37	14.01	14.38	13.59	9.43	9.31
			2	11.00	13.37	13.13	12.55	9.90	9.37
	CVS2-51	2.2	1	10.31	12.40	10.26	12.18	5.29	9.47
			2	10.15	12.30	10.38	12.18	9.92	9.49
	CVS2-97	2.3	1	10.43	12.89	10.95	13.13	10.58	9.56
			2	10.43	12.89	10.95	13.13	10.58	9.42
	CVS2-123	2.4	1	12.83	16.26	13.84	15.52	(b)	9.47
			2	12.03	15.03	13.26	14.32	(b)	9.52
6	CVS2-34	2.2	1	12.82	29.52	26.11	22.78	3.94	9.96
			2	12.77	28.96	26.23	22.84	3.15	10.00
	CVS2-98	2.3	1	13.23	29.52	27.97	25.61	1.58	10.07
			2	13.23	31.36	27.39	26.28	1.97	10.08
7	CVS2-95	2.3	1	34.05	49.16	41.20	45.97	(b)	10.21
			2	34.92	49.16	40.70	47.59	(b)	10.31
	CVS2-101	2.3	1	48.20	92.20	76.62	79.84	(b)	11.91
			2	48.20	89.32	76.62	79.04	(b)	11.94

(a) Glasses in each replicate set were independently fabricated and tested except for Set #5. This set involved the CVS internal standard glass, which was fabricated only once and then tested multiple times.

(b) Cs release was not measured for CVS2-17, -102, and -123. CVS2-95 and CVS2-101 did not contain Cs.

TABLE F.4. Standard Deviations of Untransformed and Transformed Glass and Melt Property Data from Replicate Glasses

Property	Replicate Set (a)	df	Untransformed Property Mean	SD	%RSD	Transformed Property Mean	SD	%RSD
η_{1150}	1	5	5.6467	0.1578	2.79	1.7307	0.0283	1.64
	2	1	9.0300	0.4667	5.17	2.1999	0.0517	2.35
	3	1	33.6850	6.2579	18.58	3.5083	0.1869	5.33
	4	1	6.5100	0.1414	2.17	1.8732	0.0217	1.16
	5	2	7.0267	0.2479	3.53	1.9493	0.0354	1.82
	6	1	1.8450	0.0778	4.22	0.6120	0.0422	6.89
	7	1	1.5550	0.0636	4.09	0.4411	0.0409	9.28
	Pooled	12		1.8179	6.29		0.0633	3.97
	w/o Set 3	11		0.2122	3.44		0.0345	3.82
ϵ_{1150}	1	5	24.2917	2.9170	12.01	3.1834	0.1313	4.13
	2	1	8.5800	0.7495	8.74	2.1475	0.0875	4.07
	3	1	9.0400	0.2828	3.13	2.2014	0.0313	1.42
	4	1	27.9400	0.5657	2.02	3.3300	0.0202	0.61
	5	2	26.8033	1.9786	7.38	3.2867	0.0753	2.29
	6	1	56.2750	5.1548	9.16	4.0281	0.0917	2.28
	7	1	56.1100	2.8991	5.17	4.0266	0.0517	1.28
	Pooled	12		2.6820	9.27		0.0990	3.18
T_g	1	5	491.9833	3.4079	0.69			
	2	1	534.0500	13.3643	2.50			
	3	1	553.4500	9.1217	1.65	T_g was not transformed		
	4	1	485.3000	2.9698	0.61			
	5	2	486.7667	7.8143	1.61			
	6	1	458.3500	3.8891	0.85			
	Pooled	11		6.5084	1.27			
α_s	1	5	8.9367	0.5147	5.76			
	2	1	6.2500	0.9192	14.71			
	3	1	7.6000	0.7071	9.30	α_s was not transformed		
	4	1	9.2000	0.2828	3.07			
	5	2	9.7633	0.3564	3.65			
	6	1	11.2700	0.3253	2.89			
	Pooled	11		0.5317	6.83			
α_m	1	5	92.8500	7.9533	8.57			
	2	1	85.3500	22.1324	25.93			
	3	1	64.5000	21.6375	33.55	α_m was not transformed		
	4	1	93.0500	7.0004	7.52			
	5	2	99.2000	4.9508	4.99			
	6	1	81.7500	4.4548	5.45			
	Pooled	11		11.2499	14.46			
	w/o Sets 2 & 3	9		6.9454	7.48			

(a) Glasses in each replicate set were independently fabricated and tested except for Set #5. This set involved the CVS internal standard glass, which was fabricated only once and then tested multiple times.

TABLE F.5. Standard Deviations of Natural Log Transformed PCT Si, B, Li, and Na Release (g/m^2) Data from Replicate Glasses

Element	Rep. Set	df	Mean	Glass[a] SD	Duplicate[b] SD	Total[c] SD #1	Total[d] SD #2
Si	1	5	-1.8277	0.0428	0.0076	0.0435	0.0431
	2	1	-0.6999	0.0786	0.1091	0.1344	0.1101
	3	1	-1.3395	0.0162	0.0000	0.0162	0.0162
	4	2	-0.5904	0.0068	0.0154	0.0168	0.0128
	5	3	-0.8920	0.0609	0.0350	0.0703	0.0657
	6	1	-1.3249	0.0000	0.0487	0.0487	0.0344
	7	1	0.6476	0.0689	0.0163	0.0709	0.0699
	Pooled (e)			0.0449	0.0408	0.0607	0.0534
B	1	5	-0.7213	0.0686	0.0128	0.0698	0.0692
	2	1	2.9818	0.0624	0.0200	0.0655	0.0640
	3	1	0.1629	0.0708	0.0132	0.0720	0.0714
	4	2	1.0023	0.0654	0.0232	0.0694	0.0674
	5	3	0.5000	0.1503	0.0524	0.1592	0.1548
	6	1	1.4881	0.0265	0.0159	0.0309	0.0288
	7	1	2.2283	0.0989	0.0290	0.1031	0.1010
	Pooled (e)			0.0924	0.0284	0.0967	0.0946

(a) Longer-term variability due to refabricating (except for Set #5) and retesting glasses of the same nominal composition.

(b) Shorter-term variability from duplicate dissolution tests of a glass conducted during the same phase of CVS.

(c) The Total SD #1 for each replicate set was calculated as $[(\text{Glass SD})^2 + (\text{Duplicate SD})^2]^{0.5}$, which is the standard deviation for a single PCT test on a single sample of glass.

(d) The Total SD #2 for each replicate set was calculated as $[(\text{Glass SD})^2 + (\text{Duplicate SD})^2/2]^{0.5}$, which is the standard deviation for the average of duplicate PCT tests on a single sample of glass.

(e) The Pooled Glass SD and Pooled Duplicate SD were calculated using variance component estimation software. The Pooled Total SDs were calculated as $[(\text{Pooled Glass SD})^2 + (\text{Pooled Duplicate SD})^2]^{0.5}$.

TABLE F.5. Standard Deviations of Natural Log Transformed PCT Si, B, Li, and Na Release (g/m^2) Data from Replicate Glasses (continued)

Element	Rep. Set	df	Mean	Glass SD [a]	Duplicate SD [b]	Total SD #1 [c]	Total SD #2 [d]
Li	1	5	-0.7140	0.1222	0.0225	0.1243	0.1232
	2	1	2.7879	0.0565	0.0210	0.0603	0.0584
	3	1	-0.3237	0.0396	0.0015	0.0396	0.0396
	4	2	0.7476	0.0890	0.0653	0.1104	0.1003
	5	3	0.2679	0.2161	0.0506	0.2219	0.2190
	6	1	1.2477	0.0000	0.0084	0.0084	0.0059
	7	1	1.3975	0.0769	0.0000	0.0769	0.0769
		Pooled (e)		0.1314	0.0360	0.1363	0.1338
Na	1	5	-0.8849	0.0860	0.0151	0.0873	0.0867
	2	1	2.7890	0.0629	0.0231	0.0670	0.0650
	3	1	-0.2457	0.0406	0.0026	0.0407	0.0406
	4	2	0.6436	0.1302	0.0321	0.1341	0.1322
	5	3	0.2086	0.1338	0.0703	0.1511	0.1427
	6	1	1.0108	0.0235	0.0106	0.0257	0.0247
	7	1	1.9334	0.0657	0.0303	0.0723	0.0691
		Pooled (e)		0.0985	0.0361	0.1049	0.1018

(a) Longer-term variability due to refabricating (except for Set #5) and retesting glasses of the same nominal composition.

(b) Shorter-term variability from duplicate dissolution tests of a glass conducted during the same phase of CVS.

(c) The Total SD #1 for each replicate set was calculated as $[(\text{Glass SD})^2 + (\text{Duplicate SD})^2]^{0.5}$, which is the standard deviation for a single PCT test on a single sample of glass.

(d) The Total SD #2 for each replicate set was calculated as $[(\text{Glass SD})^2 + (\text{Duplicate SD})^2/2]^{0.5}$, which is the standard deviation for the average of duplicate PCT tests on a single sample of glass.

(e) The Pooled Glass SD and Pooled Duplicate SD were calculated using variance component estimation software. The Pooled Total SDs were calculated as $[(\text{Pooled Glass SD})^2 + (\text{Pooled Duplicate SD})^2]^{0.5}$.

TABLE F.6. Standard Deviations of Natural Log Transformed MCC-1 Si, B, Li, and Na Release (g/m^2) Data from Replicate Glasses

Element	Rep. Set	df	Mean	Glass[a] SD	Duplicate[b] SD	Total[c] SD #1	Total[d] SD #2
Si	1	5	2.1829	0.0280	0.0231	0.0364	0.0324
	2	1	4.1423	0.0410	0.0131	0.0430	0.0420
	3	1	2.4568	0.0000	0.0410	0.0410	0.0290
	4	2	2.7189	0.0449	0.0119	0.0464	0.0457
	5	3	2.4010	0.0859	0.0236	0.0898	0.0875
	6	1	2.5658	0.0236	0.0020	0.0237	0.0236
	7	1	3.7079	0.2367	0.0126	0.2370	0.2369
	Pooled (e)			0.0791	0.0222	0.0822	0.0806
	w/o Rep #7:			0.0493	0.0230	0.0544	0.0519
B	1	5	2.5153	0.0405	0.0203	0.0453	0.0430
	2	1	5.2861	0.0570	0.0115	0.0581	0.0578
	3	1	2.8687	0.0160	0.0188	0.0247	0.0208
	4	2	2.9444	0.0433	0.0147	0.0458	0.0446
	5	3	2.6090	0.1001	0.0325	0.1052	0.1027
	6	1	3.3954	0.0170	0.0317	0.0360	0.0281
	7	1	4.2016	0.4333	0.0159	0.4336	0.4334
	Pooled (e)			0.1292	0.0227	0.1312	0.1302
	w/o Rep #7:			0.0594	0.0233	0.0638	0.0616

(a) Longer-term variability due to refabricating (except for Set #5) and retesting glasses of the same nominal composition.

(b) Shorter-term variability from duplicate dissolution tests of a glass conducted during the same phase of CVS.

(c) The Total SD #1 for each replicate set was calculated as $[(\text{Glass SD})^2 + (\text{Duplicate SD})^2]^{0.5}$, which is the standard deviation for a single PCT test on a single sample of glass.

(d) The Total SD #2 for each replicate set was calculated as $[(\text{Glass SD})^2 + (\text{Duplicate SD})^2/2]^{0.5}$, which is the standard deviation for the average of duplicate PCT tests on a single sample of glass.

(e) The Pooled Glass SD and Pooled Duplicate SD were calculated using variance component estimation software. The Pooled Total SDs were calculated as $[(\text{Pooled Glass SD})^2 + (\text{Pooled Duplicate SD})^2]^{0.5}$.

TABLE F.6. Standard Deviations of Natural Log Transformed MCC-1 Si, B, Li, and Na Release (g/m^2) Data from Replicate Glasses (continued)

Element	Rep. Set	df	Mean	Glass[a] SD	Duplicate[b] SD	Total[c] SD #1	Total[d] SD #2
Li	1	5	2.4870	0.1244	0.0285	0.1276	0.1240
	2	1	5.1338	0.0658	0.0050	0.0659	0.0659
	3	1	2.8279	0.0049	0.0202	0.0208	0.0151
	4	2	2.9252	0.0760	0.0225	0.0793	0.0776
	5	3	2.4885	0.1440	0.0358	0.1489	0.1462
	6	1	3.2926	0.0389	0.0107	0.0403	0.0396
	7	1	4.0256	0.4430	0.0061	0.4430	0.4430
	Pooled (e)			0.1590	0.0246	0.1608	0.1600
	w/o Rep #7:			0.1101	0.0258	0.1133	0.1116
Na	1	5	2.5207	0.0730	0.0281	0.0782	0.0757
	2	1	5.2275	0.0446	0.0124	0.0462	0.0455
	3	1	2.8419	0.0080	0.0149	0.0169	0.0132
	4	2	2.9691	0.1551	0.0483	0.1625	0.1588
	5	3	2.5865	0.0793	0.0400	0.0888	0.0842
	6	1	3.1915	0.0905	0.0130	0.0915	0.0910
	7	1	4.1101	0.3743	0.0180	0.3748	0.3745
	Pooled (e)			0.1322	0.0308	0.1357	0.1340
	w/o Rep #7:			0.0896	0.0318	0.0950	0.0934

(a) Longer-term variability due to refabricating (except for Set #5) and retesting glasses of the same nominal composition.

(b) Shorter-term variability from duplicate dissolution tests of a glass conducted during the same phase of CVS.

(c) The Total SD #1 for each replicate set was calculated as $[(\text{Glass SD})^2 + (\text{Duplicate SD})^2]^{0.5}$, which is the standard deviation for a single PCT test on a single sample of glass.

(d) The Total SD #2 for each replicate set was calculated as $[(\text{Glass SD})^2 + (\text{Duplicate SD})^2/2]^{0.5}$, which is the standard deviation for the average of duplicate PCT tests on a single sample of glass.

(e) The Pooled Glass SD and Pooled Duplicate SD were calculated using variance component estimation software. The Pooled Total SDs were calculated as $[(\text{Pooled Glass SD})^2 + (\text{Pooled Duplicate SD})^2]^{0.5}$.

TABLE F.7. Standard Deviations of PCT pH and MCC-1 pH Data from Replicate Glasses

PCT pH	Rep. Set	df	Mean	Glass[a] SD	Duplicate[b] SD	Total[c] SD #1	Total[d] SD #2
	1	5	10.3517	0.2812	0.0300	0.2827	0.2820
	2	1	9.6750	0.0071	0.0000	0.0071	0.0071
	3	1	10.1175	0.4349	0.0050	0.4349	0.4349
	4	2	10.3267	0.0441	0.0208	0.0487	0.0465
	5	3	10.2800	0.0545	0.0245	0.0598	0.0572
	6	1	11.5650	0.0132	0.0354	0.0377	0.0283
	7	1	11.8675	0.0806	0.0150	0.0820	0.0813
		Pooled (e)		0.2077	0.0240	0.2091	0.2084
MCC-1 pH							
	1	5	9.6733	0.2649	0.0297	0.2666	0.2657
	2	1	9.6500	0.0000	0.0100	0.0100	0.0071
	3	1	9.7400	0.0250	0.0354	0.0433	0.0354
	4	2	9.4583	0.0676	0.0537	0.0863	0.0775
	5	3	9.4513	0.0625	0.0571	0.0847	0.0744
	6	1	10.0275	0.0656	0.0206	0.0687	0.0672
	7	1	11.0925	1.1768	0.0522	1.1779	1.1774
		Pooled (e)		0.3547	0.0414	0.5956	0.1340
		w/o Rep #7:		0.1703	0.0401	0.1750	0.1726

(a) Longer-term variability due to refabricating (except for Set #5) and retesting glasses of the same nominal composition.

(b) Shorter-term variability from duplicate dissolution tests of a glass conducted during the same phase of CVS.

(c) The Total SD #1 for each replicate set was calculated as $[(\text{Glass SD})^2 + (\text{Duplicate SD})^2]^{0.5}$, which is the standard deviation for a single PCT test on a single sample of glass.

(d) The Total SD #2 for each replicate set was calculated as $[(\text{Glass SD})^2 + (\text{Duplicate SD})^2/2]^{0.5}$, which is the standard deviation for the average of duplicate PCT tests on a single sample of glass.

(e) The Pooled Glass SD and Pooled Duplicate SD were calculated using variance component estimation software. The Pooled Total SDs were calculated as $[(\text{Pooled Glass SD})^2 + (\text{Pooled Duplicate SD})^2]^{0.5}$.

TABLE F.8. Liquidus Temperature Data and Their Means, Standard Deviations, and % Relative Standard Deviations for Glasses Replicated During CVS

Rep. Set	Glass	Crystals Other Than Spinel T_L (°C)	Phase	Spinel T_L (°C)
1	CVS1-1 (a)	959/903	zircon/clinopyroxene	977
	CVS1-19	916	zircon/clinopyroxene	961
	CVS1-20	913	zircon/clinopyroxene	966
	CVS2-17	925	zircon/clinopyroxene	971
	CVS2-50	922	zircon/clinopyroxene	1025
	CVS2-96	946	zircon/clinopyroxene	1010
	Mean	924.4		986.6
	SD	12.97		28.92
	%RSD	1.40		2.93
2	CVS1-4	957	SiO2	none
	CVS1-21	957	SiO2	none
	Mean	957		(b)
	SD	0.00		(b)
	%RSD	0.00		(b)
3	CVS1-8	>1118	zircon	>1118
	CVS1-22	>1118	zircon	>1118
	Mean	(b)		(b)
	SD	(b)		(b)
	%RSD	(b)		(b)
4	CVS2-16	877	clinopyroxene	906
	CVS2-18	865	clinopyroxene	895
	Mean	871.0		900.5
	SD	8.49		7.78
	%RSD	0.97		0.86
5	CVS2-19	862	clinopyroxene/Na•Zr silicate	>883
	CVS2-51	856	clinopyroxene/Na•Zr silicate	899
	CVS2-97	858	clinopyroxene/Na•Zr silicate	887
	Mean	858.7		893.0
	SD	3.06		8.49
	%RSD	0.36		0.95
6	CVS2-34	736	nepheline	none
	CVS2-98	740	nepheline	none
	Mean	738.0		(b)
	SD	2.83		(b)
	%RSD	0.38		(b)

(a) Data from CVS1-1 were excluded from computing a mean and a standard deviation for Set #1 because of unexplainable different results obtained for this glass.

(b) "Greater than" T_L values or "no crystals (none)" cases do not permit computing a mean and a standard deviation.

APPENDIX G

DATA FOR VALIDATING FITTED PROPERTY MODELS

APPENDIX G

DATA FOR VALIDATING FITTED PROPERTY MODELS

A database of glass composition and property data for use in validating the CVS property models was compiled from several sources. The model validation database consists of three main parts, all of which are logically tied together by unique identifiers. The three parts are:

- Glass Composition - The composition of each glass, expressed as oxide mass fractions of the 10 components: SiO_2, B_2O_3, Na_2O, Li_2O, CaO, MgO, Fe_2O_3, Al_2O_3, ZrO_2, and Others. Complete composition information (i.e., with reported components not grouped into the Others category) is available in an intermediate version of the database if it is required in the future.

- Durability - Normalized elemental releases (g/m^2) for the MCC-1 28-day and the PCT 7-day static dissolution tests. Only data for tests conducted at 90°C in de-ionized water were included in the database. Where available, B, Li, Si, and Na normalized elemental releases were included in the database.

- Other Properties - Data for several other properties were included in the model validation database, including: viscosity (Pa·s) at various temperatures (°C), electrical conductivity (S/m) at various temperatures (°C), glass transition temperature (°C), and coefficients of thermal expansion of solid and molten glass (10^{-6}/K).

The unique identifiers constructed to tie the parts of the model validation database together were the source of the data and the location within that source, determined either by a record number in a source electronic database or a line position in a referenced table for hard copy sources. This approach was required because of the lack of naming conventions for glasses gathered from a variety of sources.

An acronym and brief description of the data sources used to build the model validation database follows:

MCC_LEACH	The MCC Static Leach Test Database, restricted to MCC-1, 90°C, 28-day, DIW leachant, 10^{-1}m SA/V
MCC_PROP	The MCC Thermal and Processing Properties Database
WVMCC1	Data available from MCC-1 testing of West Valley glasses
WVPCT	Data available from PCT testing of the same West Valley glasses as WVMCC1
HWVP	Data available in several older HWVP reports or associated with results in these reports
CVS1	Data available from the CVS-I model validation effort

A complete bibliographic reference is given for each data source at the end of this appendix. A general summary of the contents of the model validation database by data source is given in Table G.1. The MCC_LEACH and MCC_PROP sources are from a database generated a few years ago by the MCC, using data from various sites around the country including Hanford.

All glass compositions present in the data sources that had property data of interest were included in the database. Data for compositions within the composition region studied during CVS are of primary interest for validation purposes, since in general extrapolation with empirical models is not recommended. However, compositions outside the CVS study region were retained in the database to assess the extrapolative ability of the fitted property models.

Table G.2 displays relaxed CVS component lower and upper bounds (which are referred to in Chapters 7, 8, and 9) along with the original CVS composition region lower and upper bounds. The relaxed bounds define a composition region somewhat larger than the CVS composition region within which the glass property models may be assumed to be applicable without extrapolating too much.

TABLE G.1. Summary of Model Validation Database Contents

Data Source	# Glasses	Number of Glasses Having Data for Each Property[a]					
		Durability	Viscosity	Conductivity	T_g	Solid	Molten
MCC_LEACH	505	462 MCC-1	-	-	-	-	-
MCC_PROP	680	-	523/1150	250/818	143	??	??
WVMCC1	24	24 MCC-1	-	-	-	-	-
WVPCT	44	44 PCT	-	-	-	-	-
HWVP	78	65 MCC-1	43/43	35/35	-	-	-
CVS1	24	17 MCC-1	24/32	19/19	-	-	-

(a) For viscosity and electrical conductivity, the number before the slash is the number of glasses for which there is data, while the number after the slash is the total number of property values at various temperatures.

TABLE G.2. Oxide Composition Regions in Mass Fractions Delimited by Nominal CVS Oxide Component Bounds and Relaxed CVS Bounds

Oxide	Nominal CVS Bounds		Relaxed CVS Bounds	
	Lower	Upper	Lower	Upper
SiO_2	.42	.57	.406[a]	.591[a]
B_2O_3	.05	.20	.05	.21[a]
Na_2O	.05	.20	.05	.21[a]
Li_2O	.01	.07	.01	.07
CaO	.0	.10	.0	.10
MgO	.0	.08	.0	.08
Fe_2O_3	.02	.15	.02	.18[a]
Al_2O_3	.0	.17	.0	.17
ZrO_2	.0	.13	.0	.13
Others	.0	.10	.0	.11[a]

(a) Indicates bounds slightly relaxed to allow more data points.

Historical data sets used to calculate property model predictions for validation purposes are displayed in Tables G.3 (viscosity), G.4 (electrical conductivity), and G.5 (transition temperature) in order to document the source data. Data sets for validating each model are listed separately for clarity, although the same glasses may appear in several tables. Oxide compositions in mass fractions, measured property values (or in some cases values calculated from measured values), and predicted property values for the four models considered for each property are shown. For each property, a first-order mixture model and three candidate second-order mixture models (see Section 6.1.1 for the general forms of these models) were considered for validation.

The "Bnds" columns in Tables G.3, G.4, and G.5 indicate the number of relaxed CVS oxide composition bounds (Table G.2) satisfied by each glass. Glasses that satisfy 10 bounds lie completely within the CVS relaxed single-component constraints. Due to space limitations, the 95% prediction intervals shown on the validation plots in Chapters 7, 8, and 9 are not listed.

Oxide mixtures in the MCC_PROP data set were originally provided in mole percents; these data were converted to mass fractions to conform with the property models. Oxide mixtures for the other data sets were provided in mass percents, which were converted to mass fractions.

A few data points in the MCC_PROP data set were found to have incorrect data, which had to be corrected or discarded. These data points included glass sequence numbers 586 through 588 which had Young's modulus values entered for viscosity, and thermal diffusivity values in place of electrical conductivity. Glasses 586 through 588 were deleted from the analysis for viscosity and electrical conductivity. In addition, for sequence numbers 661 through 664, the electrical conductivity at 1200 poise data were unusable. For sequence numbers 577 and 579, the electrical conductivity data were unusable. A number of electrical conductivity values for 1200, 1400, and 1700°C were found to be incorrectly calculated; these values were recalculated and salvaged. These cases included the MCC_PROP glasses with sequence numbers 15 through 38, 62 through 72, 74 through 81, 83 through 96, 99, 100, 102, and 104 through 111. Other MCC_PROP glasses requiring corrections to electrical

conductivity data were 586 through 588, 604 through 607, 651 through 660, 673, and 675. Finally, electrical conductivity data from the Bansal data set (Bansal and Doremus 1986) were found to be incorrectly converted to common logs in the MCC_PROP data set. Other questions about the applicability of these data also existed, however, so they were deleted from the electrical conductivity model validation data set.

No oxide mixtures were found to be incorrect in any of the data sets, including MCC_PROP. No incorrect or inconsistent oxide mixtures or property data were found in the data set designated HWVP.

TABLE G.3. Data for 160 Glasses from Historical Database Used to Validate Models for Viscosity at 1150°C

Glass	(a) Seq	Mass Fractions SiO2	B2O3	Na2O	Li2O	CaO	MgO	Fe2O3	Al2O3	ZrO2	Others	(b) Bnds	(c) V.1150	(d) VIS.1	(d) VIS.2.1	(d) VIS.2.2	(d) VIS.2.3
WVBM 4 (WV205)	1	.4405	.0907	.1094	.0344	.0079	.0142	.1316	.0335	.0304	.1073	10	6.10	4.01	2.87	2.73	3.62
WVCM 5	2	.5043	.0692	.1412	.0321	.0070	.0047	.1288	.0209	.0294	.0623	10	6.40	5.68	4.75	4.49	4.90
WVCM 17	3	.4450	.0999	.1013	.0290	.0082	.0133	.1197	.0367	.0291	.1178	10	5.59	5.26	3.83	3.64	4.85
WVCM 20	4	.4640	.1037	.1091	.0306	.0071	.0117	.1142	.0370	.0294	.0931	10	5.30	5.47	4.33	4.15	5.05
WVBM 20 (WVCM 10+3.5	5	.4373	.0959	.1068	.0290	.0059	.0120	.1143	.0657	.0301	.1029	10	9.10	6.79	5.27	5.00	6.34
WVBM 21 (WVCM 20+7 Z	6	.4230	.0928	.1033	.0280	.0057	.0116	.1106	.0309	.0947	.0993	10	11.00	7.44	5.48	5.66	6.12
WVCM 30	7	.4639	.0801	.1072	.0313	.0112	.0098	.1420	.0324	.0104	.1117	10	8.70	5.00	3.74	3.41	4.61
WVCM 32	8	.4172	.1325	.1124	.0311	.0108	.0038	.1410	.0303	.0178	.1031	10	3.20	2.40	2.01	1.87	2.46
WVCM 39	9	.4335	.0974	.1327	.0271	.0099	.0096	.1247	.0306	.0056	.1288	10	3.69	2.83	2.12	1.94	2.60
WVCM 43	10	.4498	.0903	.0994	.0276	.0087	.0119	.1134	.0651	.0041	.1298	10	8.69	6.96	5.68	5.17	7.37
WVCM 44	11	.4547	.0840	.0933	.0278	.0099	.0139	.1132	.0625	.0030	.1376	9	8.70	7.59	6.10	5.55	8.03
WVCM 45	12	.4706	.0665	.0957	.0289	.0090	.0140	.1186	.0748	.0022	.1197	10	15.59	10.61	8.85	8.15	11.86
WVCM 46	13	.4597	.0936	.0868	.0208	.0079	.0138	.1167	.0772	.0026	.1208	10	16.50	12.27	10.20	9.42	13.88
WVCM 47	14	.4233	.1238	.0921	.0202	.0060	.0132	.1213	.0798	.0029	.1173	10	10.79	7.45	6.61	5.95	9.00
06-71	228	.3555	.0000	.3002	.0000	.1516	.0000	.0697	.1230	.0000	.0000	5	3.00	1.38	2.54	2.37	1.96
40-47	262	.4712	.0954	.2078	.0000	.0775	.0000	.0974	.0507	.0000	.0000	9	3.00	4.04	4.00	4.57	3.82
49-13	271	.5175	.2005	.1280	.0000	.1511	.0000	.0000	.0029	.0000	.0000	8	3.00	2.73	2.60	3.12	2.64
S1	461	.7742	.0000	.1209	.0000	.1017	.0000	.0000	.0019	.0000	.0013	6	254.14	133.08	363.99	274.68	238.16
S2	462	.6657	.0000	.1077	.0000	.1049	.0168	.0000	.0825	.0000	.0225	6	402.79	134.57	271.90	295.32	235.79
S3	463	.6671	.0000	.1058	.0000	.1196	.0074	.0000	.0600	.0000	.0401	6	237.36	99.12	225.98	231.26	175.71
S4	464	.6708	.0000	.1088	.0000	.0961	.0216	.0000	.0401	.0000	.0627	7	183.99	88.13	208.01	199.67	154.83
S5	465	.6655	.0000	.1050	.0000	.1118	.0125	.0000	.0225	.0000	.0827	6	113.61	65.41	173.19	158.97	116.27
S6	466	.6882	.0000	.1188	.0000	.1334	.0185	.0000	.0409	.0000	.0002	6	195.58	77.97	170.83	170.63	138.13
S7	467	.7175	.0000	.1250	.0000	.1015	.0077	.0000	.0222	.0000	.0261	6	187.14	93.71	223.28	200.27	164.86
S8	468	.6905	.0000	.1210	.0000	.1188	.0217	.0000	.0036	.0000	.0444	6	98.49	54.11	137.12	121.84	95.75
S9	469	.6579	.0000	.1131	.0000	.0852	.0119	.0000	.0713	.0000	.0607	7	270.02	115.80	248.29	258.82	200.81
S10	470	.6493	.0000	.1128	.0000	.1004	.0000	.0000	.0536	.0000	.0840	6	149.46	80.79	192.24	194.23	141.27
S11	471	.6750	.0000	.1274	.0000	.1177	.0064	.0000	.0732	.0000	.0003	6	275.08	102.20	199.68	218.85	177.81
S12	472	.6849	.0000	.1268	.0000	.0882	.0231	.0000	.0539	.0000	.0231	7	251.94	103.76	211.23	213.68	179.16
S13	473	.6765	.0000	.1277	.0000	.1069	.0120	.0000	.0337	.0000	.0432	6	133.20	68.17	153.22	150.91	118.78

(a) Sequence number from MCC-PROP data set.

(b) BNDS is the number of relaxed CVS component bounds (Table G.2) satisfied.

(c) V.1150 is the measured or estimated viscosity at 1150°C value (Pa·s).

(d) VIS.1 is the value predicted by the first-order mass fraction model in Table 7.5. VIS.2.1, VIS.2.2, and VIS.2.3 are the values predicted by the three candidate second-order mass fraction models in Table 7.5. All have units of Pa·s.

TABLE G.3. Data for 160 Glasses from Historical Database Used to Validate Models for Viscosity at 1150°C (continued)

Glass	(a) Seq	Mass Fractions SiO2	B2O3	Na2O	Li2O	CaO	MgO	Fe2O3	Al2O3	ZrO2	Others	(b) Bnds	(c) V.1150	(d) VIS.1	(d) VIS.2.1	(d) VIS.2.2	(d) VIS.2.3
S14	474	.6665	.0000	.1249	.0000	.1210	.0000	.0000	.0226	.0000	.0650	6	83.44	52.35	128.13	124.64	92.03
S15	475	.6722	.0000	.1271	.0000	.0964	.0169	.0000	.0000	.0000	.0874	7	68.91	46.44	118.43	106.88	80.96
S16	476	.7019	.0000	.1416	.0000	.1113	.0225	.0000	.0225	.0000	.0004	6	138.87	64.07	134.92	130.18	111.07
S17	477	.6951	.0000	.1389	.0000	.1297	.0110	.0000	.0016	.0000	.0237	6	75.42	44.09	103.91	97.13	77.39
S18	478	.6554	.0000	.1346	.0000	.0944	.0000	.0000	.0717	.0000	.0440	7	191.21	88.53	177.65	193.77	151.51
S19	479	.6362	.0000	.1277	.0000	.1056	.0172	.0000	.0510	.0000	.0623	6	109.53	56.97	122.51	129.80	98.21
S20	480	.6547	.0000	.1344	.0000	.0857	.0072	.0000	.0359	.0000	.0820	7	98.80	59.92	133.97	135.12	102.71
S21	481	.6817	.0000	.1533	.0000	.0978	.0126	.0000	.0545	.0000	.0002	7	171.06	74.80	137.93	148.56	126.94
S22	482	.6749	.0000	.1464	.0000	.1131	.0000	.0000	.0416	.0000	.0241	6	112.38	59.96	121.99	129.34	103.14
S23	483	.6805	.0000	.1495	.0000	.0888	.0175	.0000	.0196	.0000	.0442	7	93.38	52.98	111.62	109.99	90.30
S24	484	.6737	.0000	.1469	.0000	.1059	.0054	.0000	.0037	.0000	.0643	6	55.63	38.90	89.08	87.03	67.05
S25	485	.5954	.0000	.1316	.0000	.1098	.0198	.0000	.0673	.0000	.0760	6	77.68	43.77	91.36	102.64	74.60
S26	486	.7205	.0000	.1121	.0000	.1008	.0199	.0000	.0218	.0000	.0249	6	233.56	108.01	266.41	230.80	191.75
S27	487	.6938	.0000	.1198	.0000	.0821	.0127	.0000	.0235	.0000	.0681	7	159.26	88.19	216.21	194.45	153.98
S28	488	.7302	.0000	.1298	.0000	.1122	.0066	.0000	.0204	.0000	.0008	6	196.59	93.28	216.58	194.59	164.50
S29	489	.7052	.0000	.1385	.0000	.0886	.0000	.0000	.0216	.0000	.0462	7	136.96	78.19	178.68	166.98	135.30
S30	490	.6362	.0000	.1366	.0000	.1032	.0218	.0000	.0230	.0000	.0791	6	57.31	37.69	83.72	86.10	64.68
D1	491	.7241	.0000	.1419	.0000	.1217	.0000	.0000	.0123	.0000	.0000	6	129.01	67.85	154.27	142.75	119.01
D2	492	.7255	.0000	.1385	.0018	.1219	.0000	.0000	.0123	.0000	.0000	6	124.84	66.85	153.43	139.74	117.71
D3	493	.7283	.0000	.1315	.0054	.1224	.0000	.0000	.0124	.0000	.0000	6	117.87	65.10	152.32	134.35	115.52
D4	494	.7327	.0000	.1209	.0109	.1231	.0000	.0000	.0124	.0000	.0000	7	107.63	62.34	150.15	126.09	111.93
D5	495	.6840	.0000	.1341	.0000	.0830	.0000	.0000	.0116	.0000	.0873	7	101.95	61.03	150.15	138.02	105.55
D6	496	.6506	.0000	.1274	.0000	.0450	.0000	.0000	.0110	.0000	.1660	6	81.69	57.73	152.23	138.43	98.48
D7	497	.7039	.0000	.1380	.0000	.0985	.0000	.0000	.0119	.0000	.0477	7	127.44	65.57	155.49	142.88	114.05
D8	498	.6937	.0000	.1359	.0000	.0647	.0000	.0000	.0118	.0000	.0939	7	144.54	72.82	178.67	160.24	125.15
D9	499	.7093	.0205	.1390	.0000	.1192	.0000	.0000	.0120	.0000	.0000	6	81.35	54.68	101.04	95.35	80.95
D10	500	.6949	.0403	.1362	.0000	.1168	.0000	.0000	.0118	.0000	.0000	6	52.42	44.45	69.13	66.31	57.20
D13	501	.6895	.0000	.1351	.0000	.0997	.0000	.0000	.0117	.0000	.0640	7	102.05	58.22	140.83	130.94	101.30
D14	502	.6606	.0000	.1294	.0000	.0761	.0000	.0000	.0112	.0000	.1227	7	85.69	52.76	134.73	125.21	91.01
D15	503	.6813	.0592	.1335	.0000	.1145	.0000	.0000	.0116	.0000	.0000	7	35.38	36.47	49.35	47.96	41.95

(a) Sequence number from MCC-PROP data set.

(b) BNDS is the number of relaxed CVS component bounds (Table G.2) satisfied.

(c) V.1150 is the measured or estimated viscosity at 1150°C value (Pa·s).

(d) VIS.1 is the value predicted by the first-order mass fraction model in Table 7.5. VIS.2.1, VIS.2.2, and VIS.2.3 are the values predicted by the three candidate second-order mass fraction models in Table 7.5. All have units of Pa·s.

TABLE G.3. Data for 160 Glasses from Historical Database Used to Validate Models for Viscosity at 1150°C (continued)

Glass	(a) Seq	Mass Fractions SiO2	B2O3	Na2O	Li2O	CaO	MgO	Fe2O3	Al2O3	ZrO2	Others	(b) Bnds	(c) V.1150	(d) VIS.1	(d) VIS.2.1	(d) VIS.2.2	(d) VIS.2.3
D17	504	.6201	.1437	.1215	.0000	.1042	.0000	.0000	.0105	.0000	.0000	7	16.80	15.02	14.80	14.79	13.53
F2	505	.7364	.0028	.1383	.0000	.1012	.0000	.0000	.0163	.0000	.0050	6	173.32	91.41	203.53	182.05	156.01
F3	506	.7329	.0050	.1392	.0000	.1011	.0000	.0000	.0168	.0000	.0050	6	161.54	87.08	187.74	169.69	145.62
F4	507	.7364	.0000	.1289	.0100	.1029	.0000	.0000	.0168	.0000	.0050	6	126.00	72.38	166.96	143.15	128.15
F5	508	.7305	.0027	.1313	.0100	.1042	.0000	.0000	.0165	.0000	.0048	7	109.11	65.08	143.60	125.28	112.26
F6	509	.7277	.0056	.1309	.0105	.1040	.0000	.0000	.0165	.0000	.0048	7	99.62	61.64	131.59	115.19	103.71
F7	510	.7339	.0000	.1210	.0205	.1030	.0000	.0000	.0169	.0000	.0048	7	83.85	53.62	122.99	101.72	95.90
F8	511	.7339	.0029	.1200	.0205	.1020	.0000	.0000	.0160	.0000	.0048	7	80.52	53.02	118.91	97.82	92.52
F9	512	.7324	.0046	.1201	.0200	.1020	.0000	.0000	.0160	.0000	.0049	7	78.75	52.58	115.86	95.70	90.38
F10	513	.7335	.0000	.1121	.0300	.1031	.0000	.0000	.0165	.0000	.0048	7	60.76	42.09	97.19	77.04	76.12
F11	514	.7297	.0031	.1129	.0300	.1030	.0000	.0000	.0163	.0000	.0050	7	54.91	39.52	87.75	70.18	69.47
F12	515	.7275	.0048	.1131	.0300	.1031	.0000	.0000	.0168	.0000	.0047	7	52.38	38.46	83.45	67.16	66.58
F13	516	.7257	.0000	.1389	.0100	.1040	.0000	.0000	.0165	.0000	.0049	6	98.74	58.58	127.87	114.84	102.73
F14	517	.7197	.0000	.1369	.0200	.1029	.0000	.0000	.0160	.0000	.0045	7	59.99	40.20	84.93	75.18	70.80
F15	518	.7136	.0000	.1389	.0270	.0999	.0000	.0000	.0160	.0000	.0046	8	41.06	29.84	60.64	53.83	52.51
FAL 1	519	.7200	.0000	.1500	.0000	.1100	.0000	.0000	.0200	.0000	.0000	6	134.89	70.29	148.75	143.61	121.75
FAL 2	520	.6800	.0000	.1300	.0000	.1300	.0000	.0000	.0600	.0000	.0000	6	200.51	84.15	171.51	184.40	147.29
FAL 3	521	.6800	.0000	.1300	.0000	.1100	.0200	.0000	.0600	.0000	.0000	6	244.22	91.83	180.07	190.37	159.17
FAL 4	522	.6800	.0000	.1100	.0000	.1300	.0000	.0000	.0600	.0000	.0200	6	251.03	102.58	230.27	236.90	182.48
FAL 5	523	.6800	.0000	.1100	.0000	.1100	.0200	.0000	.0600	.0000	.0200	6	300.03	111.94	238.96	244.57	197.20
FAL 6	524	.6600	.0000	.1700	.0000	.1100	.0000	.0000	.0600	.0000	.0000	6	101.10	52.10	90.37	105.40	87.35
FAL 7	525	.6600	.0000	.1500	.0000	.1300	.0000	.0000	.0600	.0000	.0000	6	117.64	56.97	107.58	122.35	97.77
FAL 8	526	.6600	.0000	.1500	.0000	.1100	.0200	.0000	.0600	.0000	.0000	6	148.07	62.17	114.28	126.31	105.66
FAL 9	527	.6600	.0000	.1300	.0000	.1300	.0000	.0000	.0600	.0000	.0200	6	149.87	69.45	144.44	157.18	121.13
FAL 10	528	.6600	.0000	.1300	.0000	.1100	.0200	.0000	.0600	.0000	.0200	6	184.88	75.78	151.65	162.27	130.90
FAL 11	529	.7100	.0000	.1500	.0000	.0900	.0300	.0000	.0200	.0000	.0000	7	149.92	68.94	139.76	132.20	117.90
FAL 12	530	.7000	.0000	.1500	.0000	.0700	.0600	.0000	.0200	.0000	.0000	7	160.12	67.61	131.31	121.71	114.17
FAL 13	531	.7133	.0000	.1500	.0000	.0967	.0200	.0000	.0200	.0000	.0000	7	145.32	69.35	142.62	135.84	119.11
FAL 14	532	.7033	.0000	.1500	.0000	.0767	.0500	.0000	.0200	.0000	.0000	7	157.36	68.02	134.00	125.05	115.34
HAHP	533	.4540	.1030	.1113	.0314	.0043	.0135	.1061	.0650	.0189	.0923	10	6.11	6.09	5.13	4.86	5.96

(a) Sequence number from MCC-PROP data set.

(b) BNDS is the number of relaxed CVS component bounds (Table G.2) satisfied.

(c) V.1150 is the measured or estimated viscosity at 1150°C value (Pa·s).

(d) VIS.1 is the value predicted by the first-order mass fraction model in Table 7.5. VIS.2.1, VIS.2.2, and VIS.2.3 are the values predicted by the three candidate second-order mass fraction models in Table 7.5. All have units of Pa·s.

TABLE G.3. Data for 160 Glasses from Historical Database Used to Validate Models for Viscosity at 1150°C (continued)

Glass	(a) Seq	Mass Fractions SiO2	B2O3	Na2O	Li2O	CaO	MgO	Fe2O3	Al2O3	ZrO2	Others	(b) Bnds	(c) V.1150	(d) VIS.1	(d) VIS.2.1	(d) VIS.2.2	(d) VIS.2.3
HAHF	534	.4526	.1027	.1060	.0314	.0022	.0130	.1775	.0518	.0068	.0559	10	4.38	5.26	4.94	4.73	5.69
HALF	535	.4555	.1034	.1162	.0314	.0063	.0139	.1040	.0518	.0298	.0877	10	4.79	5.45	4.42	4.26	5.00
Centroid	536	.4548	.1031	.1141	.0314	.0054	.0137	.1407	.0297	.0253	.0817	10	3.48	4.25	3.38	3.22	3.92
AL-001	537	.4548	.1032	.1148	.0314	.0057	.0138	.1488	.0168	.0268	.0839	10	3.02	3.69	2.85	2.71	3.30
AL-002	538	.4549	.1032	.1144	.0314	.0056	.0137	.1447	.0232	.0260	.0828	10	3.17	3.95	3.10	2.95	3.59
AL-003	539	.4548	.1031	.1141	.0314	.0054	.0137	.1407	.0297	.0253	.0817	10	3.48	4.25	3.38	3.22	3.92
AL-004	540	.4545	.1031	.1136	.0314	.0053	.0137	.1348	.0389	.0242	.0804	10	3.84	4.68	3.79	3.62	4.41
AL-005	541	.4543	.1031	.1130	.0314	.0050	.0136	.1267	.0518	.0227	.0784	10	4.70	5.38	4.48	4.27	5.19
CR-001	542	.4544	.1030	.1141	.0314	.0055	.0137	.1416	.0298	.0255	.0810	10	3.42	4.25	3.38	3.22	3.92
CR-002	543	.4559	.1034	.1145	.0315	.0055	.0137	.1316	.0299	.0255	.0885	10	3.17	4.24	3.33	3.17	3.90
CR-003	544	.4548	.1031	.1141	.0314	.0054	.0137	.1407	.0297	.0253	.0817	10	3.48	4.25	3.38	3.22	3.92
CR-004	545	.4546	.1031	.1140	.0314	.0054	.0137	.1388	.0295	.0249	.0845	10	3.40	4.21	3.33	3.17	3.89
CR-005	546	.4545	.1031	.1138	.0314	.0054	.0137	.1370	.0294	.0246	.0871	10	3.44	4.20	3.30	3.13	3.87
FE-001	547	.4560	.1034	.1185	.0314	.0072	.0141	.1039	.0348	.0352	.0953	10	3.91	4.55	3.53	3.42	4.09
FE-002	548	.4554	.1033	.1163	.0314	.0063	.0139	.1223	.0322	.0302	.0885	10	3.80	4.39	3.43	3.29	4.01
FE-003	549	.4548	.1031	.1141	.0314	.0054	.0137	.1407	.0297	.0253	.0817	10	3.48	4.25	3.38	3.22	3.92
FE-004	550	.4539	.1030	.1119	.0314	.0046	.0135	.1590	.0272	.0203	.0752	10	3.46	4.09	3.33	3.17	3.79
FE-005	551	.4535	.1028	.1097	.0314	.0037	.0133	.1774	.0246	.0153	.0682	10	3.41	3.95	3.33	3.17	3.66
MN-001	552	.4551	.1033	.1148	.0314	.0057	.0138	.1479	.0304	.0266	.0710	10	3.76	4.33	3.53	3.40	4.00
MN-002	553	.4548	.1032	.1144	.0314	.0056	.0137	.1442	.0300	.0259	.0767	10	3.71	4.28	3.44	3.29	3.95
MN-003	554	.4548	.1031	.1141	.0314	.0054	.0137	.1407	.0297	.0253	.0817	10	3.48	4.25	3.38	3.22	3.92
MN-004	555	.4545	.1031	.1136	.0314	.0053	.0137	.1348	.0292	.0242	.0902	10	3.50	4.17	3.26	3.09	3.85
MN-005	556	.4544	.1031	.1132	.0314	.0051	.0136	.1290	.0286	.0231	.0985	10	3.24	4.10	3.16	2.99	3.77
NI-001	557	.4548	.1032	.1143	.0314	.0055	.0137	.1429	.0299	.0257	.0785	10	3.37	4.27	3.42	3.26	3.94
NI-002	558	.4548	.1031	.1142	.0314	.0055	.0137	.1418	.0298	.0255	.0801	10	3.85	4.26	3.39	3.24	3.93
NI-003	559	.4548	.1031	.1141	.0314	.0054	.0137	.1407	.0297	.0253	.0817	10	3.48	4.25	3.38	3.22	3.92
NI-004	560	.4546	.1031	.1140	.0314	.0054	.0137	.1387	.0295	.0249	.0846	10	3.17	4.21	3.33	3.17	3.89
NI-005	561	.4546	.1031	.1138	.0314	.0054	.0137	.1368	.0293	.0246	.0873	10	3.06	4.19	3.29	3.13	3.86
P-001	562	.4547	.1032	.1145	.0314	.0056	.0138	.1452	.0301	.0261	.0754	10	3.97	4.29	3.46	3.31	3.96
P-002	563	.4548	.1032	.1143	.0314	.0055	.0137	.1429	.0299	.0257	.0785	10	3.34	4.27	3.42	3.26	3.94

(a) Sequence number from MCC-PROP data set.

(b) BNDS is the number of relaxed CVS component bounds (Table G.2) satisfied.

(c) V.1150 is the measured or estimated viscosity at 1150°C value (Pa·s).

(d) VIS.1 is the value predicted by the first-order mass fraction model in Table 7.5. VIS.2.1, VIS.2.2, and VIS.2.3 are the values predicted by the three candidate second-order mass fraction models in Table 7.5. All have units of Pa·s.

TABLE G.3. Data for 160 Glasses from Historical Database Used to Validate Models for Viscosity at 1150°C (continued)

Glass	(a) Seq	Mass Fractions SiO2	B2O3	Na2O	Li2O	CaO	MgO	Fe2O3	Al2O3	ZrO2	Others	(b) Bnds	(c) V.1150	(d) VIS.1	(d) VIS.2.1	(d) VIS.2.2	(d) VIS.2.3
P-003	564	.4548	.1031	.1141	.0314	.0054	.0137	.1407	.0297	.0253	.0817	10	3.48	4.25	3.38	3.22	3.92
P-004	565	.4545	.1031	.1136	.0314	.0052	.0137	.1340	.0291	.0240	.0914	10	3.33	4.16	3.25	3.07	3.83
P-005	566	.4544	.1031	.1130	.0314	.0050	.0136	.1274	.0284	.0228	.1008	10	3.78	4.08	3.14	2.96	3.76
Frit 18	567	.5250	.1000	.2250	.0000	.0500	.0000	.0000	.0000	.0000	.1000	8	2.80	3.25	2.08	3.32	2.80
Frit 18- 25 HI	568	.3938	.0750	.1687	.0000	.0480	.0000	.1535	.0140	.0000	.1470	7	2.20	2.52	1.54	1.45	2.00
Frit 21	569	.5250	.1000	.1850	.0400	.0500	.0000	.0000	.0000	.0000	.1000	10	1.67	1.25	0.93	1.24	1.13
Frit 21- 25 HI	570	.3938	.0750	.1387	.0300	.0480	.0000	.1535	.0140	.0000	.1470	8	1.10	1.23	0.74	0.70	1.01
Frit 21- 30 HI	571	.3675	.0700	.1295	.0280	.0476	.0000	.1842	.0168	.0000	.1564	8	0.98	1.23	0.63	0.56	0.98
Frit 21- 10 HA	572	.4725	.0900	.1665	.0360	.0454	.0000	.0060	.0863	.0000	.0973	10	3.30	3.15	2.92	3.33	2.94
Frit 21- 15 HA	573	.4463	.0850	.1572	.0340	.0431	.0000	.0090	.1294	.0000	.0960	10	5.10	5.00	5.34	5.46	4.81
Frit 21- 20 HA	574	.4200	.0800	.1480	.0320	.0408	.0000	.0120	.1726	.0000	.0946	9	8.20	7.93	9.97	8.96	7.94
Frit 21- 25 HA	575	.3938	.0750	.1387	.0300	.0385	.0000	.0150	.2157	.0000	.0933	8	13.90	12.59	18.96	14.70	13.23
Frit 21- 35 HA	576	.3413	.0650	.1202	.0260	.0339	.0000	.0210	.3020	.0000	.0906	8	50.90	31.69	72.85	39.61	37.81
Frit 18- 25 HA	577	.3938	.0750	.1687	.0000	.0385	.0000	.0150	.2157	.0000	.0933	7	25.00	25.77	40.16	30.21	26.12
Frit 18- 25 SA	578	.3938	.0750	.1687	.0000	.0450	.0000	.1087	.0645	.0000	.1443	7	5.50	4.48	3.60	3.32	4.51
Frit 18- 35 SA	579	.3413	.0650	.1462	.0000	.0430	.0000	.1522	.0903	.0000	.1620	7	6.10	5.10	3.73	2.83	5.99
Frit 21- 25 SA	580	.3938	.0750	.1387	.0300	.0450	.0000	.1087	.0645	.0000	.1443	8	2.10	2.19	1.74	1.60	2.29
Frit 21- 30 SA	581	.3675	.0700	.1295	.0280	.0440	.0000	.1305	.0774	.0000	.1531	8	2.20	2.45	1.85	1.57	2.74
Frit 18- 25 SC	582	.3938	.0750	.1687	.0000	.0457	.0000	.0790	.1160	.0000	.1218	8	10.00	8.02	8.36	7.30	9.10
Frit 21- 20 SC	583	.4200	.0800	.1480	.0320	.0466	.0000	.0632	.0928	.0000	.1174	10	4.00	3.12	3.01	2.91	3.33
Frit 21- 25 SC	584	.3938	.0750	.1387	.0300	.0457	.0000	.0790	.1160	.0000	.1218	9	4.00	3.92	3.99	3.51	4.61
Frit 21- 30 SC	585	.3675	.0700	.1295	.0280	.0449	.0000	.0948	.1392	.0000	.1261	9	5.40	4.92	5.26	4.19	6.50
SRL 165 HiFe	586	.4889	.0698	.1178	.0486	.0115	.0076	.1484	.0181	.0093	.0801	10	3.01	2.84	2.35	2.18	2.45
SRL 165 TDS	587	.5509	.0692	.1049	.0479	.0153	.0081	.1202	.0418	.0122	.0295	10	5.55	7.80	7.92	7.71	7.63
SRL 165 HiAl	588	.5429	.0739	.1176	.0514	.0114	.0080	.0635	.0928	.0101	.0285	10	4.60	9.64	9.71	9.83	10.07
#1	589	.8009	.0000	.0000	.1991	.0000	.0000	.0000	.0000	.0000	.0000	6	11.58	1.16	6.73	2.69	2.40
#2	590	.8578	.0000	.0000	.1422	.0000	.0000	.0000	.0000	.0000	.0000	6	27.53	13.69	81.22	30.04	28.00
#3	591	.8894	.0000	.0000	.1106	.0000	.0000	.0000	.0000	.0000	.0000	6	340.19	53.99	323.68	114.73	109.60
#4	592	.6597	.0000	.3403	.0000	.0000	.0000	.0000	.0000	.0000	.0000	6	27.74	8.58	6.46	11.58	12.16
#5	593	.7441	.0000	.2559	.0000	.0000	.0000	.0000	.0000	.0000	.0000	6	76.99	44.53	56.58	65.41	68.56

(a) Sequence number from MCC-PROP data set.

(b) BNDS is the number of relaxed CVS component bounds (Table G.2) satisfied.

(c) V.1150 is the measured or estimated viscosity at 1150°C value (Pa·s).

(d) VIS.1 is the value predicted by the first-order mass fraction model in Table 7.5. VIS.2.1, VIS.2.2, and VIS.2.3 are the values predicted by the three candidate second-order mass fraction models in Table 7.5. All have units of Pa·s.

TABLE G.3. Data for 160 Glasses from Historical Database Used to Validate Models for Viscosity at 1150°C (continued)

Glass	(a) Seq	Mass Fractions SiO2	B2O3	Na2O	Li2O	CaO	MgO	Fe2O3	Al2O3	ZrO2	Others	(b) Bnds	(c) V.1150	(d) VIS.1	(d) VIS.2.1	(d) VIS.2.2	(d) VIS.2.3
#6	594	.7950	.0000	.2050	.0000	.0000	.0000	.0000	.0000	.0000	.0000	7	162.42	120.08	209.21	185.62	194.33
#7	595	.5606	.0000	.0000	.0000	.0000	.0000	.0000	.0000	.0000	.4394	6	72.79	96.25	594.39	372.57	176.77
#8	596	.6568	.0000	.0000	.0000	.0000	.0000	.0000	.0000	.0000	.3432	5	164.58	242.48	1499.74	803.11	452.67
#9	597	.7184	.0000	.0000	.0000	.0000	.0000	.0000	.0000	.0000	.2816	5	330.76	438.34	2713.82	1313.79	826.90
#10	598	.5057	.0000	.0000	.0000	.0000	.0000	.0000	.0000	.0000	.4943	6	131.04	56.82	350.58	240.40	103.39
#11	599	.6054	.0000	.0000	.0000	.0000	.0000	.0000	.0000	.0000	.3946	5	346.14	148.13	915.38	533.14	274.12
SM513FR	604	.5860	.1470	.0650	.0470	.0510	.0230	.0000	.0300	.0000	.0510	10	9.34	6.24	6.60	5.75	5.81
SM513LW08	605	.5399	.1354	.0836	.0433	.0470	.0212	.0121	.0343	.0037	.0796	10	6.45	4.52	4.48	4.29	4.18
SM513LW11	606	.5225	.1311	.0906	.0419	.0455	.0205	.0166	.0359	.0050	.0904	10	5.93	4.01	3.87	3.81	3.69
SM513LW14	607	.5052	.1267	.0976	.0405	.0440	.0198	.0212	.0375	.0064	.1011	10	4.90	3.55	3.35	3.37	3.26

(a) Sequence number from MCC-PROP data set.

(b) BNDS is the number of relaxed CVS component bounds (Table G.2) satisfied.

(c) V.1150 is the measured or estimated viscosity at 1150°C value (Pa·s).

(d) VIS.1 is the value predicted by the first-order mass fraction model in Table 7.5. VIS.2.1, VIS.2.2, and VIS.2.3 are the values predicted by the three candidate second-order mass fraction models in Table 7.5. All have units of Pa·s.

TABLE G.4. Data for 209 Glasses from Historical Database Used to Validate Models for Electrical Conductivity at 1150°C

Data Set / Glass	(a) Seq	Mass Fractions SiO2	B2O3	Na2O	Li2O	CaO	MgO	Fe2O3	Al2O3	ZrO2	Others	(b) Bnds	(c) E.1150	(d) EC.1	(d) EC.2.1	(d) EC.2.2	(d) EC.2.3
MCC 01-09	223	.6180	.0000	.1636	.0000	.0039	.0000	.2043	.0102	.0000	.0000	6	23.50	17.41	17.26	20.15	21.72
MCC 02-38	224	.4213	.2044	.1736	.0000	.0462	.0000	.0596	.0329	.0012	.0608	9	29.00	24.88	22.60	24.48	24.19
MCC 03-15	225	.4398	.0000	.1239	.0000	.0031	.0000	.2086	.0134	.0042	.2070	6	19.30	19.31	20.96	16.14	17.11
MCC 04-44	226	.4416	.0763	.1872	.0000	.0590	.0000	.0743	.0875	.0015	.0726	9	30.00	25.25	31.50	30.70	31.56
MCC 05-40	227	.4221	.0631	.2873	.0000	.0508	.0000	.0620	.0346	.0016	.0785	8	89.00	74.25	100.98	114.93	124.02
MCC 06-71	228	.3555	.0000	.3002	.0000	.1516	.0000	.0697	.1230	.0000	.0000	5	64.00	64.95	72.81	69.30	76.39
MCC 07-34	229	.4533	.0841	.1917	.0000	.0625	.0000	.0810	.0451	.0016	.0807	9	30.00	27.47	33.61	34.51	36.47
MCC 08-62	230	.5410	.1101	.1639	.0000	.0123	.0000	.1163	.0564	.0000	.0000	9	21.50	18.17	25.01	26.11	25.38
MCC 09-03	231	.6267	.0000	.1200	.0000	.0000	.0000	.1719	.0814	.0000	.0000	7	15.00	10.32	12.82	13.74	10.94
MCC 10-30	232	.3700	.0000	.3003	.0000	.1527	.0000	.1701	.0069	.0000	.0000	5	105.00	74.76	116.70	99.20	96.53
MCC 11-57	233	.3598	.0911	.2977	.0000	.0021	.0000	.0000	.0440	.0041	.2012	5	80.00	108.75	146.74	157.20	181.58
MCC 12-65	234	.6084	.1186	.1561	.0000	.0000	.0000	.1090	.0079	.0000	.0000	7	19.50	16.50	20.66	22.16	25.21
MCC 13-60	235	.4757	.0898	.1613	.0000	.0225	.0000	.1348	.0092	.0021	.1046	9	28.50	22.85	26.17	27.05	29.85
MCC 14-67	236	.6251	.0859	.0689	.0000	.0040	.0000	.2063	.0098	.0000	.0000	7	6.10	6.96	7.05	7.50	8.38
MCC 15-74	237	.3784	.2096	.0926	.0000	.0000	.0000	.1974	.1221	.0000	.0000	7	12.00	11.21	7.96	7.78	7.72
MCC 16-58	238	.3728	.0717	.1818	.0000	.1515	.0000	.2121	.0101	.0000	.0000	6	37.00	24.00	43.67	27.30	27.28
MCC 17-21	239	.3742	.1126	.2979	.0000	.0022	.0000	.2050	.0081	.0000	.0000	6	92.00	93.45	125.67	160.82	164.65
MCC 18-69	240	.3659	.0000	.2921	.0000	.0030	.0000	.0000	.1283	.0042	.2065	4	83.00	91.46	120.86	95.15	112.82
MCC 19-73	241	.3533	.1455	.0752	.0000	.0943	.0000	.0000	.1244	.0041	.2031	6	5.90	10.08	5.71	6.29	7.54
MCC 20-22	242	.3741	.0000	.2956	.0000	.0039	.0000	.2085	.0104	.0022	.1054	5	91.00	100.73	125.99	135.30	137.81
MCC 21-36	243	.6021	.0514	.1633	.0000	.0423	.0000	.0524	.0292	.0012	.0580	8	22.00	17.02	21.78	22.55	24.08
MCC 22-27	244	.3555	.1982	.2891	.0000	.0746	.0000	.0000	.0827	.0000	.0000	6	80.00	69.76	71.30	82.87	86.82
MCC 23-61	245	.5355	.0637	.1344	.0000	.0131	.0000	.1344	.0091	.0022	.1077	9	18.30	16.36	18.53	18.30	20.66
MCC 24-41	246	.4628	.0916	.2010	.0000	.0060	.0000	.0906	.0498	.0020	.0963	9	43.00	32.80	41.28	44.00	46.61
MCC 25-64	247	.5988	.1159	.1563	.0000	.0042	.0000	.0000	.1249	.0000	.0000	7	17.70	14.10	28.32	26.64	19.74
MCC 26-10	248	.6120	.1931	.1186	.0000	.0020	.0000	.0680	.0064	.0000	.0000	8	11.80	11.40	12.69	11.97	13.00
MCC 27-02	249	.6145	.0000	.2996	.0000	.0021	.0000	.0000	.0838	.0000	.0000	5	57.00	57.44	109.16	121.97	101.41
MCC 28-45	250	.4721	.0977	.2082	.0000	.0793	.0000	.0000	.0504	.0018	.0905	8	38.00	30.21	33.12	40.43	42.80
MCC 29-37	251	.4735	.0000	.2095	.0000	.0768	.0000	.0956	.0524	.0018	.0904	8	44.00	30.80	39.25	34.53	34.53
MCC 30-14	252	.4168	.0000	.1272	.0000	.1548	.0000	.0000	.0880	.0043	.2090	5	11.40	14.30	12.32	10.43	10.97

(a) Sequence number from data set.

(b) BNDS is the number of relaxed CVS component bounds (Table G.2) satisfied.

(c) E.1150 is the measured or estimated electrical conductivity at 1150°C value (S/m).

(d) EC.1 is the value predicted by the first-order mass fraction model in Table 8.4. EC.2.1, EC.2.2, and EC.2.3 are the values predicted by the three candidate second-order mass fraction models in Table 8.4. All have units of S/m.

TABLE G.4. Data for 209 Glasses from Historical Database Used to Validate Models for Electrical Conductivity at 1150°C (continued)

Data Set / Glass	(a) Seq	Mass Fractions SiO2	B2O3	Na2O	Li2O	CaO	MgO	Fe2O3	Al2O3	ZrO2	Others	(b) Bnds	(c) E.1150	(d) EC.1	(d) EC.2.1	(d) EC.2.2	(d) EC.2.3
MCC 31-01	253	.6025	.0000	.1665	.0000	.1496	.0000	.0000	.0815	.0000	.0000	5	18.00	12.85	13.40	17.02	14.06
MCC 32-70	254	.3578	.1983	.1123	.0000	.0021	.0000	.0000	.1255	.0041	.1999	6	16.00	16.58	8.96	10.69	12.26
MCC 33-06	255	.6043	.1922	.1189	.0000	.0014	.0000	.0000	.0832	.0000	.0000	7	6.80	10.39	15.96	13.81	11.22
MCC 34-18	256	.3892	.1992	.1215	.0000	.0020	.0000	.0000	.0847	.0041	.1993	6	15.40	18.18	11.49	13.75	14.67
MCC 35-35	257	.3894	.1044	.2193	.0000	.0805	.0000	.0580	.0551	.0019	.0914	7	49.00	38.25	42.42	46.61	50.58
MCC 36-19	258	.4062	.0000	.2984	.0000	.0026	.0000	.2031	.0898	.0000	.0000	6	94.00	79.81	83.95	109.11	109.30
MCC 37-31	259	.3478	.0000	.2813	.0000	.1531	.0000	.0000	.0040	.0043	.2096	3	80.00	78.33	70.15	88.04	92.10
MCC 38-53	260	.6038	.0000	.2944	.0000	.0017	.0000	.0427	.0064	.0010	.0500	6	79.00	65.05	94.02	102.45	117.19
MCC 39-59	261	.5699	.0000	.0700	.0000	.1370	.0000	.0430	.1240	.0011	.0550	7	3.00	5.49	7.48	5.69	4.25
MCC 40-47	262	.4712	.0954	.2078	.0000	.0775	.0000	.0974	.0507	.0000	.0000	9	36.00	27.90	38.28	39.03	39.67
MCC 41-63	263	.5426	.0973	.1625	.0000	.0120	.0000	.0602	.1254	.0000	.0000	9	21.00	16.23	26.75	26.51	21.64
MCC 42-34	264	.4569	.0810	.1973	.0000	.0633	.0000	.0800	.0446	.0015	.0754	9	35.00	28.64	35.52	36.70	38.72
MCC 43-11	265	.6023	.0000	.1204	.0000	.0031	.0000	.0000	.0642	.0042	.2058	5	15.00	13.21	21.52	14.29	13.58
MCC 44-23	266	.3634	.0000	.3013	.0000	.0016	.0000	.1151	.0090	.0042	.2054	5	120.00	118.99	179.99	153.69	162.77
MCC 45-17	267	.4064	.0000	.2984	.0000	.0007	.0000	.0000	.0825	.0042	.2078	5	77.00	97.34	153.93	120.54	132.39
MCC 46-56	268	.3693	.0000	.1231	.0000	.0810	.0000	.2020	.0913	.0027	.1306	5	16.80	15.74	19.40	11.05	11.74
MCC 47-04	269	.6055	.0601	.1328	.0000	.0015	.0000	.0000	.0041	.0039	.1921	6	11.30	15.88	20.28	17.42	21.62
MCC 48-32	270	.4337	.0000	.1097	.0000	.0040	.0000	.1749	.0818	.0039	.1920	7	28.00	15.24	16.00	12.07	12.30
MCC 49-13	271	.5175	.2005	.1280	.0000	.1511	.0000	.0000	.0029	.0000	.0000	7	10.70	11.31	7.10	10.34	10.65
MCC 50-05	272	.6053	.0000	.1816	.0000	.0013	.0000	.0000	.0104	.0040	.1974	5	29.00	25.25	37.74	27.56	32.34
MCC 51-66	273	.6058	.1031	.1454	.0000	.0053	.0000	.0473	.0563	.0007	.0361	8	21.30	14.31	21.30	21.31	20.50
MCC 52-42	274	.4399	.0657	.1814	.0000	.1511	.0000	.0646	.0365	.0012	.0597	8	30.00	21.70	22.82	24.67	25.89
MCC 53-52	275	.6036	.0000	.1205	.0000	.1489	.0000	.0557	.0064	.0013	.0636	6	10.20	9.78	8.01	8.82	9.80
MCC 54-72	276	.3474	.1974	.1833	.0000	.1511	.0000	.0000	.1208	.0000	.0000	6	22.00	21.48	15.68	16.82	18.27
MCC 55-27	277	.3476	.1962	.3038	.0000	.0707	.0000	.0000	.0817	.0000	.0000	6	110.00	81.97	85.72	100.77	106.75
MCC 56-68	278	.5894	.0000	.0733	.0000	.1094	.0000	.0000	.0083	.0044	.2152	5	3.60	7.83	6.51	5.86	6.78
MCC 57-07	279	.6237	.0000	.1227	.0000	.0423	.0000	.2002	.0111	.0000	.0000	6	15.00	10.93	11.53	11.16	11.92
MCC 58-39	280	.4785	.0929	.1237	.0000	.0709	.0000	.0919	.0524	.0018	.0879	9	25.50	13.55	15.61	14.65	15.11
MCC 59-06	281	.6014	.1945	.1193	.0000	.0016	.0000	.0000	.0832	.0000	.0000	7	8.50	10.48	15.92	13.75	11.17
MCC 60-20	282	.3657	.2356	.1172	.0000	.0024	.0000	.1943	.0848	.0000	.0000	6	44.00	15.15	10.83	10.30	9.78

(a) Sequence number from data set.

(b) BNDS is the number of relaxed CVS component bounds (Table G.2) satisfied.

(c) E.1150 is the measured or estimated electrical conductivity at 1150°C value (S/m).

(d) EC.1 is the value predicted by the first-order mass fraction model in Table 8.4. EC.2.1, EC.2.2, and EC.2.3 are the values predicted by the three candidate second-order mass fraction models in Table 8.4. All have units of S/m.

TABLE G.4. Data for 209 Glasses from Historical Database Used to Validate Models for Electrical Conductivity at 1150°C (continued)

Data Set / Glass	(a) Seq	Mass Fractions SiO2	B2O3	Na2O	Li2O	CaO	MgO	Fe2O3	Al2O3	ZrO2	Others	(b) Bnds	(c) E.1150	(d) EC.1	(d) EC.2.1	(d) EC.2.2	(d) EC.2.3
MCC 61-60	283	.4715	.0891	.1629	.0000	.0246	.0000	.1281	.0101	.0023	.1114	8	33.00	23.40	26.86	27.62	30.48
MCC 62-54	284	.3549	.2004	.1232	.0000	.1545	.0000	.0000	.0438	.0025	.1207	5	13.60	14.81	6.98	10.76	10.96
MCC 63-34	285	.4524	.0802	.1984	.0000	.0627	.0000	.0792	.0442	.0017	.0812	9	38.00	29.36	36.21	37.39	39.59
MCC 64-28	286	.3732	.1997	.1251	.0000	.0918	.0000	.2017	.0085	.0000	.0000	7	16.70	15.42	18.77	13.41	12.52
MCC 65-49	287	.3784	.0000	.1251	.0000	.1545	.0000	.1713	.0095	.0032	.1580	5	9.30	15.99	22.78	12.20	12.31
MCC 66-33	288	.3453	.1918	.3069	.0000	.1535	.0000	.0000	.0025	.0000	.0000	4	79.00	82.11	66.90	115.18	110.78
MCC 67-75	289	.3684	.0000	.3048	.0000	.0019	.0000	.1968	.1282	.0000	.0000	5	80.00	85.64	78.60	103.33	111.47
MCC 68-50	290	.3535	.0000	.3010	.0000	.1500	.0000	.0503	.0842	.0012	.0598	5	78.00	73.43	77.71	81.41	88.33
MCC 69-16	291	.4226	.0000	.1273	.0000	.1568	.0000	.2037	.0896	.0000	.0000	6	9.10	11.70	20.37	9.60	9.14
MCC 70-55	292	.3512	.1977	.3101	.0000	.0025	.0000	.0933	.0452	.0000	.0000	7	89.00	102.67	128.34	143.16	144.11
MCC 71-33	293	.3427	.0911	.2745	.0000	.0666	.0000	.0000	.0428	.0036	.1787	5	81.00	78.80	82.85	102.43	116.81
MCC 72-02	294	.6047	.0000	.3084	.0000	.0033	.0000	.0000	.0836	.0000	.0000	5	71.00	63.36	119.34	134.83	113.42
MCC 73-01	295	.5900	.0000	.1740	.0000	.1530	.0000	.0000	.0830	.0000	.0000	5	18.00	13.98	14.42	18.46	15.36
MCC 74-12	296	.5436	.0000	.3034	.0000	.1492	.0000	.0000	.0038	.0000	.0000	5	63.00	58.12	45.52	85.43	93.34
MCC 75-26	297	.3533	.0830	.1229	.0000	.1502	.0000	.0000	.0854	.0041	.2011	5	15.60	15.24	10.23	11.59	13.57
MCC 76-29	298	.3560	.1925	.1221	.0000	.1112	.0000	.0000	.0046	.0043	.2093	5	17.00	18.08	8.32	14.14	14.41
MCC 77-25	299	.3534	.1976	.1253	.0000	.1548	.0000	.0845	.0845	.0000	.0000	7	14.50	12.84	12.13	9.32	9.47
MCC 78-48	300	.4233	.0577	.1792	.0000	.0433	.0000	.0566	.0350	.0041	.2008	8	32.00	30.01	35.09	32.49	36.02
MCC 79-43	301	.4544	.0870	.2077	.0000	.0686	.0000	.0849	.0077	.0018	.0880	9	42.00	33.50	39.85	43.56	47.78
MCC 80-46	302	.4304	.0553	.1742	.0000	.0430	.0000	.1998	.0359	.0012	.0602	8	32.00	24.95	31.03	28.76	29.86
MCC 81-34	303	.4523	.0802	.1963	.0000	.0637	.0000	.0791	.0442	.0017	.0825	9	39.00	28.77	35.33	36.38	38.53
MCC 82-24	304	.3381	.1909	.2933	.0000	.0000	.0000	.0000	.0034	.0035	.1709	5	97.00	111.11	114.09	149.33	153.24
MCC 83-08	305	.5881	.1947	.2103	.0000	.0025	.0000	.0000	.0044	.0000	.0000	7	30.00	28.38	38.04	37.25	40.92
MCC 84-51	306	.3659	.1974	.1234	.0000	.0020	.0000	.1490	.0093	.0031	.1500	7	21.50	20.53	14.16	17.31	17.22
MCC 85-16	307	.4274	.0000	.1259	.0000	.1584	.0000	.2000	.0883	.0000	.0000	6	11.80	11.44	19.82	9.45	8.96
MCC 86-88	308	.6100	.0000	.2668	.0000	.0010	.0000	.0000	.1222	.0000	.0000	5	39.00	40.22	82.50	87.56	62.57
MCC 87-86	309	.3959	.0000	.2811	.0000	.1384	.0000	.0462	.0791	.0012	.0581	5	59.00	58.10	63.63	67.51	69.97
MCC 88-91	310	.5154	.0592	.1819	.0000	.1517	.0000	.0256	.0050	.0012	.0600	8	29.00	20.09	16.59	23.68	26.47
MCC 89-77	311	.4501	.1666	.1219	.0000	.0016	.0000	.1798	.0800	.0000	.0000	9	19.00	13.94	14.23	14.57	13.90
MCC 90-85	312	.4497	.0000	.1218	.0000	.1228	.0000	.1264	.0070	.0034	.1688	6	15.50	14.73	17.35	11.77	12.43

(a) Sequence number from data set.

(b) BNDS is the number of relaxed CVS component bounds (Table G.2) satisfied.

(c) E.1150 is the measured or estimated electrical conductivity at 1150°C value (S/m).

(d) EC.1 is the value predicted by the first-order mass fraction model in Table 8.4. EC.2.1, EC.2.2, and EC.2.3 are the values predicted by the three candidate second-order mass fraction models in Table 8.4. All have units of S/m.

TABLE G.4. Data for 209 Glasses from Historical Database Used to Validate Models for Electrical Conductivity at 1150°C (continued)

Data Set / Glass	(a) Seq	Mass Fractions SiO2	B2O3	Na2O	Li2O	CaO	MgO	Fe2O3	Al2O3	ZrO2	Others	(b) Bnds	(c) E.1150	(d) EC.1	(d) EC.2.1	(d) EC.2.2	(d) EC.2.3
MCC 91-89	313	.4170	.0961	.1513	.0000	.0019	.0000	.1014	.1246	.0022	.1056	9	26.00	20.17	20.61	21.18	22.41
MCC 92-84	314	.4417	.0673	.1871	.0000	.0512	.0000	.0664	.0364	.0030	.1469	8	39.00	29.40	34.77	34.43	37.50
MCC 93-81	315	.4754	.1749	.1288	.0000	.0838	.0000	.0000	.0031	.0027	.1314	7	12.80	15.48	10.47	14.57	15.82
MCC 94-92	316	.5118	.0587	.1875	.0000	.0025	.0000	.0000	.0344	.0041	.2010	7	30.00	30.09	42.77	37.63	42.05
MCC 95-90	317	.4077	.0000	.1525	.0000	.0997	.0000	.1027	.1281	.0022	.1071	8	20.00	17.53	21.19	14.12	14.45
MCC 96-76	318	.6017	.0000	.2654	.0000	.1297	.0000	.0000	.0032	.0000	.0000	4	54.00	38.08	30.62	52.46	59.19
MCC 97-82	319	.4835	.0000	.2270	.0000	.1176	.0000	.0000	.0027	.0034	.1658	4	49.00	38.23	35.42	41.42	45.98
MCC 98-79	320	.4424	.0000	.2658	.0000	.0044	.0000	.0964	.0061	.0037	.1812	6	82.00	72.77	105.64	90.59	98.68
MCC 99-78	321	.4889	.0000	.1279	.0000	.1217	.0000	.1454	.0092	.0021	.1048	7	37.00	13.79	16.58	11.86	12.44
MCC 100-93	322	.5541	.0000	.1026	.0000	.0781	.0000	.1086	.0461	.0022	.1084	8	8.30	9.98	12.14	9.21	9.02
MCC 101-80	323	.4314	.1707	.1196	.0000	.1309	.0000	.0747	.0727	.0000	.0000	8	13.30	11.34	12.15	10.49	10.20
MCC 102-87	324	.4277	.1689	.0997	.0000	.0019	.0000	.0000	.1165	.0037	.1816	7	10.50	13.07	10.29	10.99	11.40
MCC 103-83	325	.5217	.1456	.2210	.0000	.1084	.0000	.0000	.0033	.0000	.0000	6	46.00	29.34	27.86	40.61	44.74
MCC Centroid	536	.4548	.1031	.1141	.0314	.0054	.0137	.1407	.0297	.0253	.0817	10	28.62	29.27	29.44	31.24	31.86
MCC AL-001	537	.4548	.1032	.1148	.0314	.0057	.0138	.1488	.0168	.0268	.0839	10	34.63	29.95	30.21	32.26	32.85
MCC AL-002	538	.4549	.1032	.1144	.0314	.0056	.0137	.1447	.0232	.0260	.0828	10	29.61	29.60	29.82	31.74	32.35
MCC AL-004	540	.4545	.1031	.1136	.0314	.0053	.0137	.1348	.0389	.0242	.0804	10	26.72	28.78	28.90	30.52	31.16
MCC AL-005	541	.4543	.1031	.1130	.0314	.0050	.0136	.1267	.0518	.0227	.0784	10	26.03	28.14	28.18	29.57	30.23
MCC CR-001	542	.4544	.1030	.1141	.0314	.0055	.0137	.1416	.0298	.0255	.0810	10	25.70	29.23	29.42	31.22	31.82
MCC CR-002	543	.4559	.1034	.1145	.0315	.0055	.0137	.1316	.0299	.0255	.0885	10	25.20	29.54	29.73	31.38	32.11
MCC CR-004	545	.4546	.1031	.1140	.0314	.0054	.0137	.1388	.0295	.0249	.0845	10	25.30	29.35	29.51	31.29	31.95
MCC CR-005	546	.4545	.1031	.1138	.0314	.0054	.0137	.1370	.0294	.0246	.0871	10	28.70	29.38	29.54	31.29	31.98
MCC FE-001	547	.4560	.1034	.1185	.0314	.0072	.0141	.1039	.0348	.0352	.0953	10	26.77	29.97	30.55	31.46	32.33
MCC FE-002	548	.4554	.1033	.1163	.0314	.0063	.0139	.1223	.0322	.0302	.0885	10	29.89	29.62	30.01	31.36	32.10
MCC FE-004	550	.4539	.1030	.1119	.0314	.0046	.0135	.1590	.0272	.0203	.0752	10	29.84	28.92	28.87	31.13	31.62
MCC FE-005	551	.4535	.1028	.1097	.0314	.0037	.0133	.1774	.0246	.0153	.0682	10	23.71	28.59	28.27	31.04	31.40
MCC MN-001	552	.4551	.1033	.1148	.0314	.0057	.0138	.1479	.0304	.0266	.0710	10	29.93	29.04	29.24	31.11	31.58
MCC MN-002	553	.4548	.1032	.1144	.0314	.0056	.0137	.1442	.0300	.0259	.0767	10	28.02	29.16	29.35	31.19	31.73
MCC MN-004	555	.4545	.1031	.1136	.0314	.0053	.0137	.1348	.0292	.0242	.0902	10	27.10	29.45	29.60	31.33	32.06
MCC MN-005	556	.4544	.1031	.1132	.0314	.0051	.0136	.1290	.0286	.0231	.0985	10	26.38	29.66	29.80	31.46	32.31

(a) Sequence number from data set.

(b) BNDS is the number of relaxed CVS component bounds (Table G.2) satisfied.

(c) E.1150 is the measured or estimated electrical conductivity at 1150°C value (S/m).

(d) EC.1 is the value predicted by the first-order mass fraction model in Table 8.4. EC.2.1, EC.2.2, and EC.2.3 are the values predicted by the three candidate second-order mass fraction models in Table 8.4. All have units of S/m.

TABLE G.4. Data for 209 Glasses from Historical Database Used to Validate Models for Electrical Conductivity at 1150°C (continued)

Data Set / Glass	(a) Seq	Mass Fractions SiO2	B2O3	Na2O	Li2O	CaO	MgO	Fe2O3	Al2O3	ZrO2	Others	(b) Bnds	(c) E.1150	(d) EC.1	(d) EC.2.1	(d) EC.2.2	(d) EC.2.3
MCC NI-001	557	.4548	.1032	.1143	.0314	.0055	.0137	.1429	.0299	.0257	.0785	10	24.85	29.20	29.38	31.21	31.78
MCC NI-002	558	.4548	.1031	.1142	.0314	.0055	.0137	.1418	.0298	.0255	.0801	10	28.58	29.23	29.41	31.22	31.81
MCC NI-004	560	.4546	.1031	.1140	.0314	.0054	.0137	.1387	.0295	.0249	.0846	10	28.35	29.35	29.52	31.29	31.95
MCC NI-005	561	.4546	.1031	.1138	.0314	.0054	.0137	.1368	.0293	.0246	.0873	10	27.76	29.39	29.56	31.30	31.99
MCC P-001	562	.4547	.1032	.1145	.0314	.0056	.0138	.1452	.0301	.0261	.0754	10	26.63	29.12	29.31	31.16	31.69
MCC P-002	563	.4548	.1032	.1143	.0314	.0055	.0137	.1429	.0299	.0257	.0785	10	28.73	29.20	29.38	31.21	31.78
MCC P-004	565	.4545	.1031	.1136	.0314	.0052	.0137	.1340	.0291	.0240	.0914	10	26.84	29.50	29.65	31.37	32.12
MCC P-005	566	.4544	.1031	.1130	.0314	.0050	.0136	.1274	.0284	.0228	.1008	10	28.34	29.71	29.84	31.49	32.37
MCC SM513FR	604	.5860	.1470	.0650	.0470	.0510	.0230	.0000	.0300	.0000	.0510	9	17.34	19.60	16.45	18.34	18.90
MCC SM513LW08	605	.5399	.1354	.0836	.0433	.0470	.0212	.0121	.0343	.0037	.0796	9	18.39	23.73	20.82	23.15	23.78
MCC SM513LW11	606	.5225	.1311	.0906	.0419	.0455	.0205	.0166	.0359	.0050	.0904	9	21.67	25.50	22.70	25.16	25.86
MCC SM513LW14	607	.5052	.1267	.0976	.0405	.0440	.0198	.0212	.0375	.0064	.1011	10	22.82	27.40	24.71	27.28	28.09
MCC Table V	651	.3720	.0000	.0000	.0000	.0000	.0000	.0000	.0000	.0000	.6280	4	17.86	10.19	17.02	4.80	5.71
MCC Table VI	652	.0000	.0000	.0000	.0000	.0000	.0000	.0000	.0000	.0000	1.0000	4	15.15	26.83	63.63	8.94	9.49
MCC Table VI	653	.0000	.2791	.0000	.0000	.0000	.0000	.0000	.0000	.0000	.7209	4	13.33	20.28	0.99	5.38	4.46
MCC Table VI	654	.0000	.0000	.0000	.0000	.0000	.0000	.0000	.0000	.0000	1.0000	4	5.56	26.83	63.63	8.94	9.49
MCC FRIT 18	655	.5250	.1000	.2250	.0000	.0500	.0000	.0000	.0000	.0000	.1000	7	8.33	37.11	42.35	52.51	61.71
MCC FRIT 18- HA 25	656	.3938	.0750	.1687	.0000	.0385	.0000	.0150	.2157	.0000	.0933	6	7.69	20.26	20.18	18.46	21.00
MCC FRIT 18- HA 35	657	.3413	.0650	.1462	.0000	.0339	.0000	.0210	.3020	.0000	.0906	7	10.99	15.90	10.18	8.85	13.53
MCC FRIT 18- HA 45	658	.2888	.0550	.1237	.0000	.0293	.0000	.0270	.3883	.0000	.0879	7	15.38	12.48	4.12	3.54	8.68
MCC FRIT 18- HI 25	659	.3938	.0750	.1687	.0000	.0480	.0000	.1535	.0140	.0000	.1470	7	8.33	27.94	32.68	30.52	32.81
MCC FRIT 18- HI 35	660	.3413	.0650	.1462	.0000	.0472	.0000	.2149	.0196	.0000	.1658	6	4.55	24.94	28.79	23.92	25.28
MCC FRIT 18- HI 45	661	.2888	.0550	.1237	.0000	.0464	.0000	.2763	.0252	.0000	.1846	6	15.87	22.26	25.04	18.47	19.39
MCC FRIT 18- SA 25	662	.3938	.0750	.1687	.0000	.0450	.0000	.1087	.0645	.0000	.1443	7	12.50	26.06	28.98	27.07	29.66
MCC FRIT 18- SA 35	663	.3413	.0650	.1462	.0000	.0430	.0000	.1522	.0903	.0000	.1620	7	12.50	22.63	22.23	18.80	21.94
MCC FRIT 18- SA 45	664	.2888	.0550	.1237	.0000	.0410	.0000	.1957	.1161	.0000	.1797	6	10.53	19.64	15.99	12.34	16.16
MCC FRIT 21	665	.5250	.1000	.1850	.0400	.0500	.0000	.0000	.0000	.0000	.1000	9	15.38	65.94	47.44	58.45	63.09
MCC FRIT 21- HA 25	666	.3938	.0750	.1387	.0300	.0385	.0000	.0150	.2157	.0000	.0933	7	15.87	31.18	24.57	22.86	29.68
MCC FRIT 21- HA 35	667	.3413	.0650	.1202	.0260	.0339	.0000	.0210	.3020	.0000	.0906	8	16.13	23.10	12.56	11.15	20.47
MCC FRIT 21- HA 45	668	.2888	.0550	.1017	.0220	.0293	.0000	.0270	.3883	.0000	.0879	8	15.38	17.12	5.08	4.47	13.57

(a) Sequence number from data set.

(b) BNDS is the number of relaxed CVS component bounds (Table G.2) satisfied.

(c) E.1150 is the measured or estimated electrical conductivity at 1150°C value (S/m).

(d) EC.1 is the value predicted by the first-order mass fraction model in Table 8.4. EC.2.1, EC.2.2, and EC.2.3 are the values predicted by the three candidate second-order mass fraction models in Table 8.4. All have units of S/m.

TABLE G.4. Data for 209 Glasses from Historical Database Used to Validate Models for Electrical Conductivity at 1150°C (continued)

Data Set / Glass	(a) Seq	Mass Fractions SiO2	B2O3	Na2O	Li2O	CaO	MgO	Fe2O3	Al2O3	ZrO2	Others	(b) Bnds	(c) E.1150	(d) EC.1	(d) EC.2.1	(d) EC.2.2	(d) EC.2.3
MCC FRIT 21- HI 25	669	.3938	.0750	.1387	.0300	.0480	.0000	.1535	.0140	.0000	.1470	8	15.38	42.99	47.75	45.71	46.38
MCC FRIT 21- HI 45	671	.2888	.0550	.1017	.0220	.0464	.0000	.2763	.0252	.0000	.1846	7	15.38	30.54	39.30	30.04	30.31
MCC FRIT 21- I 35	672	.3413	.0650	.1202	.0260	.0325	.0000	.3500	.0000	.0000	.0650	8	13.89	34.83	43.56	41.02	37.75
MCC FRIT 21- I 45	673	.2888	.0550	.1017	.0220	.0275	.0000	.4500	.0000	.0000	.0550	8	15.38	29.03	36.02	33.92	29.81
MCC FRIT 21- SA 30	675	.3675	.0700	.1295	.0280	.0440	.0000	.1305	.0774	.0000	.1531	8	12.99	36.31	36.60	33.37	37.49
CR 2	681	.5250	.0978	.1030	.0386	.0286	.0091	.1130	.0450	.0060	.0339	10	35.00	26.09	26.46	26.86	26.95
CR 1	682	.5220	.0974	.1010	.0378	.0286	.0089	.1130	.0453	.0060	.0400	10	29.00	25.38	25.89	26.21	26.36
CR 3	683	.5190	.0969	.1020	.0384	.0286	.0089	.1120	.0452	.0059	.0431	10	26.00	26.21	26.63	27.01	27.20
CR 4	684	.5170	.0955	.1020	.0381	.0284	.0090	.1110	.0447	.0067	.0476	10	27.00	26.21	26.63	26.99	27.24
CR 5	685	.5200	.0963	.1020	.0387	.0282	.0090	.1120	.0447	.0057	.0434	10	27.00	26.40	26.75	27.17	27.38
CVS1 22	686	.5278	.1053	.1125	.0450	.0083	.0084	.0719	.0231	.0385	.0592	10	29.60	34.24	32.85	33.59	34.72
CVS1 23	687	.5353	.1053	.1050	.0375	.0120	.0122	.0719	.0231	.0385	.0592	10	25.00	25.96	25.75	25.97	27.04
CVS1 24	688	.5353	.1053	.1125	.0375	.0083	.0084	.0719	.0231	.0385	.0592	10	25.90	28.27	27.80	28.14	29.33
CVS1 3	689	.5122	.0956	.1050	.0375	.0289	.0084	.1172	.0453	.0063	.0436	10	29.00	26.70	27.23	27.60	27.80
CVS1 11	690	.5188	.0983	.1124	.0371	.0279	.0089	.0863	.0311	.0076	.0716	10	31.00	29.33	28.56	29.54	30.51
CVS1 13	691	.5583	.0967	.0738	.0379	.0277	.0082	.1486	.0000	.0030	.0458	10	20.00	20.00	19.19	19.73	21.45
CVS1 14	692	.5215	.0973	.1113	.0361	.0281	.0084	.0873	.0311	.0076	.0713	10	48.00	28.23	27.61	28.46	29.43
CVS1 16	693	.5576	.0946	.0735	.0362	.0292	.0086	.0483	.0855	.0072	.0593	10	24.00	17.00	18.95	18.15	17.22
CVS1 5	694	.5214	.0949	.1139	.0380	.0280	.0095	.0849	.0320	.0073	.0701	10	36.00	30.17	29.22	30.20	31.15
CVS1 15	700	.5046	.0983	.0742	.0361	.0281	.0071	.1455	.0021	.0853	.0187	10	22.00	17.73	19.60	18.75	19.27
CVS1 17	701	.5060	.0957	.1700	.0356	.0285	.0079	.0519	.0845	.0000	.0199	10	48.00	44.75	43.16	45.25	43.90
CVS1 18	702	.5504	.0962	.1784	.0371	.0275	.0085	.0501	.0018	.0028	.0472	10	64.00	53.57	43.82	49.11	52.91
CVS1 6	703	.5495	.0949	.1758	.0370	.0271	.0078	.0509	.0539	.0005	.0026	10	50.00	46.81	42.86	46.06	44.98
CVS1 7	704	.5032	.0963	.0717	.0334	.0285	.0118	.1504	.0845	.0000	.0202	10	23.00	16.67	18.83	18.01	17.42
CVS1 9	705	.5096	.0962	.0753	.0367	.0297	.0092	.1309	.0000	.0122	.1002	10	26.00	22.02	22.27	22.61	24.13
CVS1 4	706	.5144	.0967	.0738	.0369	.0299	.0110	.0484	.0000	.0199	.1690	9	24.00	22.66	21.83	22.30	24.64
CVS1 12	707	.5070	.0974	.0733	.0371	.0296	.0110	.0502	.0000	.0191	.1753	9	27.00	23.12	22.46	22.97	25.27
CVS1 8	708	.5071	.0958	.1744	.0363	.0272	.0071	.1522	.0000	.0000	-.0001	9	66.00	52.66	47.90	53.20	54.20
CVS1 10	709	.5082	.0971	.0753	.0357	.0293	.0089	.1110	.0000	.0123	.1222	9	27.00	22.02	21.97	22.36	24.10
MAS 1	710	.4880	.0930	.1680	.0000	.0288	.0076	.1070	.0440	.0070	.0566	9	30.00	20.97	26.22	26.75	27.65

(a) Sequence number from data set.

(b) BNDS is the number of relaxed CVS component bounds (Table G.2) satisfied.

(c) E.1150 is the measured or estimated electrical conductivity at 1150°C value (S/m).

(d) EC.1 is the value predicted by the first-order mass fraction model in Table 8.4. EC.2.1, EC.2.2, and EC.2.3 are the values predicted by the three candidate second-order mass fraction models in Table 8.4. All have units of S/m.

TABLE G.4. Data for 209 Glasses from Historical Database Used to Validate Models for Electrical Conductivity at 1150°C (continued)

Data Set / Glass	(a) Seq	Mass Fractions SiO2	B2O3	Na2O	Li2O	CaO	MgO	Fe2O3	Al2O3	ZrO2	Others	(b) Bnds	(c) E.1150	(d) EC.1	(d) EC.2.1	(d) EC.2.2	(d) EC.2.3
MAS 2	711	.5440	.1040	.0015	.0950	.0313	.0087	.1190	.0500	.0065	.0400	8	47.00	36.80	54.65	57.34	60.64
MAS 3	712	.4490	.0840	.0015	.0000	.0251	.0068	.0997	.0390	.0050	.2899	7	11.00	5.84	4.95	4.00	4.45
MAS 4	713	.4890	.0900	.0580	.0270	.0262	.0074	.1050	.0410	.0065	.1499	9	15.00	15.47	16.23	15.42	16.29
MAS 5	714	.4700	.0910	.0840	.0000	.0285	.0075	.1080	.0410	.0058	.1642	8	15.00	10.84	11.05	10.18	10.88
MAS 6	715	.4900	.0940	.0015	.0440	.0282	.0079	.1070	.0420	.0058	.1796	8	11.00	13.86	16.60	15.73	16.93
SS1 3	716	.5106	.0956	.0994	.0375	.0288	.0083	.0946	.0365	.0049	.0838	10	29.00	26.76	26.75	27.26	28.13
SS1 4	717	.5107	.0956	.0996	.0375	.0288	.0083	.0954	.0369	.0050	.0822	10	30.00	26.75	26.76	27.26	28.10
SS1 1	718	.5116	.0956	.1031	.0750	.0289	.0084	.1097	.0424	.0057	.0196	9	30.00	63.14	57.35	61.74	61.47
SS1 2	719	.5117	.0956	.1034	.0375	.0289	.0084	.1110	.0429	.0058	.0548	10	29.00	26.71	27.09	27.50	27.88
SS1 5	720	.5121	.0956	.1050	.0375	.0289	.0085	.1177	.0455	.0062	.0430	10	29.00	26.68	27.22	27.59	27.78
U28 1	721	.5190	.0965	.1070	.0373	.0287	.0081	.1090	.0433	.0056	.0455	10	25.00	26.96	27.19	27.68	27.96
U28 2	722	.5120	.0954	.1050	.0366	.0283	.0084	.1060	.0422	.0061	.0600	10	28.00	26.70	26.99	27.42	27.89
U28 3	723	.5170	.0950	.1030	.0362	.0285	.0094	.0991	.0402	.0060	.0656	10	27.00	25.88	26.07	26.47	27.04
U28 4	724	.5130	.0950	.1030	.0360	.0279	.0103	.0890	.0377	.0049	.0832	10	28.00	26.49	26.44	26.94	27.77
U28 5	725	.5050	.0933	.0965	.0362	.0279	.0076	.0807	.0317	.0045	.1166	9	27.00	26.55	26.40	26.80	28.14
U28 6	726	.5000	.0930	.0974	.0361	.0283	.0079	.0723	.0287	.0042	.1321	9	25.00	27.42	27.10	27.57	29.15
U28 7	727	.5130	.0939	.1000	.0353	.0288	.0077	.1070	.0424	.0056	.0663	10	27.00	24.82	25.32	25.53	26.04
ZR 1	728	.5250	.0990	.1020	.0400	.0294	.0086	.1030	.0390	.0000	.0540	10	27.10	27.73	27.43	28.18	28.69
ZR 5	729	.5720	.1090	.1030	.0430	.0310	.0084	.0680	.0270	.0000	.0386	10	27.20	27.78	25.23	26.47	27.53
ZR 6	730	.5710	.1080	.0860	.0430	.0310	.0086	.0000	.0000	.1570	-.0046	7	16.80	17.94	17.65	16.70	17.95
ZR 7	731	.5230	.0980	.0870	.0400	.0280	.0072	.0360	.0130	.1570	.0108	9	21.80	18.35	20.07	18.53	19.05
ZR 8	732	.4760	.0910	.0870	.0360	.0262	.0074	.0680	.0270	.1570	.0244	9	20.50	17.98	20.92	18.90	18.99
ZR 9	733	.4830	.0900	.1030	.0350	.0260	.0080	.1360	.0530	.0000	.0660	10	26.20	26.64	27.53	27.76	28.16
ZR 10	734	.5700	.1080	.0860	.0430	.0310	.0083	.0000	.0000	.1580	-.0043	7	16.00	17.95	17.70	16.73	17.98
ZR 11	735	.4830	.0880	.1040	.0360	.0270	.0075	.1390	.0520	.0000	.0635	10	26.10	27.50	28.41	28.62	29.01
ZR 12	736	.5730	.1070	.1040	.0430	.0310	.0084	.0690	.0250	.0000	.0396	10	27.30	28.11	25.35	26.65	27.84
ZR 2	737	.5630	.1070	.0950	.0430	.0320	.0077	.0350	.0120	.0790	.0263	10	22.20	22.98	21.74	21.76	23.05
ZR 3	738	.4970	.0820	.0950	.0340	.0250	.0068	.1000	.0490	.0750	.0362	10	20.70	20.29	22.14	20.98	21.04
ZR 4	739	.5260	.0980	.0950	.0400	.0290	.0073	.0700	.0250	.0790	.0307	10	21.90	22.58	23.39	22.81	23.37

(a) Sequence number from data set.

(b) BNDS is the number of relaxed CVS component bounds (Table G.2) satisfied.

(c) E.1150 is the measured or estimated electrical conductivity at 1150°C value (S/m).

(d) EC.1 is the value predicted by the first-order mass fraction model in Table 8.4. EC.2.1, EC.2.2, and EC.2.3 are the values predicted by the three candidate second-order mass fraction models in Table 8.4. All have units of S/m.

TABLE G.5. Data for 143 Glasses from Historical Database Used to Validate Models for Glass Transition Temperature

Glass	(a) Seq	Mass Fractions SiO2	B2O3	Na2O	Li2O	CaO	MgO	Fe2O3	Al2O3	ZrO2	Others	(b) Bnds	(c) Tg	(d) TG.1	(d) TG.2.1	(d) TG.2.2	(d) TG.2.3
02-38	224	.4213	.2044	.1736	.0000	.0462	.0000	.0596	.0329	.0012	.0608	9	524.0	499.2	514.5	504.4	508.0
03-15	225	.4398	.0000	.1239	.0000	.0031	.0000	.2086	.0134	.0042	.2070	6	519.0	472.0	453.9	455.0	508.7
04-44	226	.4416	.0763	.1872	.0000	.0590	.0000	.0743	.0875	.0015	.0726	9	522.0	487.0	479.8	479.8	488.5
05-40	227	.4221	.0631	.2873	.0000	.0508	.0000	.0620	.0346	.0016	.0785	8	445.0	439.7	425.6	436.1	440.2
07-34	229	.4533	.0841	.1917	.0000	.0625	.0000	.0810	.0451	.0016	.0807	9	508.0	484.7	484.6	481.9	489.6
08-62	230	.5410	.1101	.1639	.0000	.0123	.0000	.1163	.0564	.0000	.0000	9	522.0	512.1	509.3	499.3	508.6
09-03	231	.6267	.0000	.1200	.0000	.0000	.0000	.1719	.0814	.0000	.0000	7	540.0	528.1	536.5	533.9	544.4
10-30	232	.3700	.0000	.3003	.0000	.1527	.0000	.1701	.0069	.0000	.0000	5	477.0	439.9	454.0	455.6	468.0
11-57	233	.3598	.0911	.2977	.0000	.0021	.0000	.0000	.0440	.0041	.2012	5	438.0	410.9	381.0	417.0	398.2
12-65	234	.6084	.1186	.1561	.0000	.0000	.0000	.1090	.0079	.0000	.0000	7	539.0	521.3	526.8	512.6	508.3
13-60	235	.4757	.0898	.1613	.0000	.0225	.0000	.1348	.0092	.0021	.1046	9	522.0	488.2	484.9	478.1	497.5
14-67	236	.6251	.0859	.0689	.0000	.0040	.0000	.2063	.0098	.0000	.0000	7	510.0	552.0	524.3	531.9	524.9
15-74	237	.3784	.2096	.0926	.0000	.0000	.0000	.1974	.1221	.0000	.0000	7	497.0	526.3	475.6	475.7	529.7
16-58	238	.3728	.0717	.1818	.0000	.1515	.0000	.2121	.0101	.0000	.0000	6	466.0	492.2	527.1	511.1	538.7
17-21	239	.3742	.1126	.2979	.0000	.0022	.0000	.2050	.0081	.0000	.0000	6	416.0	430.2	424.7	395.9	475.4
18-69	240	.3659	.0000	.2921	.0000	.0030	.0000	.0000	.1283	.0042	.2065	4	519.0	408.9	333.2	389.2	339.3
19-73	241	.3533	.1455	.0752	.0000	.0943	.0000	.0000	.1244	.0041	.2031	6	572.0	519.1	534.0	519.3	517.6
20-22	242	.3741	.0000	.2956	.0000	.0039	.0000	.2085	.0104	.0022	.1054	5	434.0	407.9	378.5	382.2	458.0
21-36	243	.6021	.0514	.1633	.0000	.0423	.0000	.0524	.0292	.0012	.0580	8	539.0	513.1	526.4	525.3	523.8
22-27	244	.3555	.1982	.2891	.0000	.0746	.0000	.0000	.0827	.0000	.0000	6	451.0	460.1	478.8	477.5	485.1
23-61	245	.5355	.0637	.1344	.0000	.0131	.0000	.1344	.0091	.0022	.1077	9	537.0	502.7	502.1	497.8	508.8
24-41	246	.4628	.0916	.2010	.0000	.0060	.0000	.0906	.0498	.0020	.0963	9	527.0	473.3	467.7	464.6	480.4
25-64	247	.5988	.1159	.1563	.0000	.0042	.0000	.0000	.1249	.0000	.0000	7	585.0	529.9	538.6	537.0	543.1
26-10	248	.6120	.1931	.1186	.0000	.0020	.0000	.0680	.0064	.0000	.0000	8	546.0	545.2	541.0	535.2	513.7
27-02	249	.6145	.0000	.2996	.0000	.0021	.0000	.0000	.0838	.0000	.0000	5	487.0	462.4	467.7	482.3	476.6
28-45	250	.4721	.0977	.2082	.0000	.0793	.0000	.0000	.0504	.0018	.0905	8	532.0	486.3	485.7	489.1	486.8
29-37	251	.4735	.0000	.2095	.0000	.0768	.0000	.0956	.0524	.0018	.0904	8	532.0	473.1	467.9	474.6	469.7
30-14	252	.4168	.0000	.1272	.0000	.1548	.0000	.0000	.0880	.0043	.2090	5	616.0	499.3	487.2	474.6	439.1
31-01	253	.6025	.0000	.1665	.0000	.1496	.0000	.0000	.0815	.0000	.0000	5	588.0	533.3	524.7	536.2	536.5
32-70	254	.3578	.1983	.1123	.0000	.0021	.0000	.0000	.1255	.0041	.1999	6	517.0	497.9	512.0	518.5	514.9

(a) Sequence number from MCC-PROP data set.

(b) BNDS is the number of relaxed CVS component bounds (Table G.2) satisfied.

(c) Tg is the measured or estimated glass transition temperature (°C).

(d) TG.1 is the value predicted by the first-order mass fraction model in Table 9.4. TG.2.1, TG.2.2, and TG.2.3 are the values predicted by the three candidate second-order mass fraction models in Table 9.4. All have units of °C.

TABLE G.5. Data for 143 Glasses from Historical Database Used to Validate Models for Glass Transition Temperature (continued)

Glass	(a) Seq	Mass Fractions SiO2	B2O3	Na2O	Li2O	CaO	MgO	Fe2O3	Al2O3	ZrO2	Others	(b) Bnds	(c) Tg	(d) TG.1	(d) TG.2.1	(d) TG.2.2	(d) TG.2.3
33-06	255	.6043	.1922	.1189	.0000	.0014	.0000	.0000	.0832	.0000	.0000	7	550.0	550.1	557.1	556.8	551.2
34-18	256	.3892	.1992	.1215	.0000	.0020	.0000	.0000	.0847	.0041	.1993	6	537.0	496.7	513.6	518.9	512.8
35-35	257	.3894	.1044	.2193	.0000	.0805	.0000	.0580	.0551	.0019	.0914	7	499.0	469.6	468.1	466.6	474.9
36-19	258	.4062	.0000	.2984	.0000	.0026	.0000	.2031	.0898	.0000	.0000	6	451.0	427.8	398.6	399.4	470.5
38-53	260	.6038	.0000	.2944	.0000	.0017	.0000	.0427	.0064	.0010	.0500	6	470.0	451.5	468.7	473.2	467.2
39-59	261	.5699	.0000	.0700	.0000	.1370	.0000	.0430	.1240	.0011	.0550	7	684.0	559.0	559.8	563.1	552.8
40-47	262	.4712	.0954	.2078	.0000	.0775	.0000	.0974	.0507	.0000	.0000	9	508.0	493.4	498.2	490.9	500.3
41-63	263	.5426	.0973	.1625	.0000	.0120	.0000	.0602	.1254	.0000	.0000	9	547.0	517.0	513.4	510.6	518.9
42-34	264	.4569	.0810	.1973	.0000	.0633	.0000	.0800	.0446	.0015	.0754	9	523.0	483.5	483.4	481.0	488.2
43-11	265	.6023	.0000	.1204	.0000	.0031	.0000	.0000	.0642	.0042	.2058	5	621.0	505.4	525.6	525.1	508.5
44-23	266	.3634	.0000	.3013	.0000	.0016	.0000	.1151	.0090	.0042	.2054	5	468.0	395.0	346.8	375.6	393.3
45-17	267	.4064	.0000	.2984	.0000	.0007	.0000	.0000	.0825	.0042	.2078	5	507.0	409.2	349.2	399.7	354.4
46-56	268	.3693	.0000	.1231	.0000	.0810	.0000	.2020	.0913	.0027	.1306	5	577.0	486.8	479.3	478.5	523.8
47-04	269	.6055	.0601	.1328	.0000	.0015	.0000	.0000	.0041	.0039	.1921	6	607.0	505.2	528.8	527.3	520.6
48-32	270	.4337	.0000	.1097	.0000	.0040	.0000	.1749	.0818	.0039	.1920	7	569.0	483.3	459.6	462.3	503.9
49-13	271	.5175	.2005	.1280	.0000	.1511	.0000	.0000	.0029	.0000	.0000	7	580.0	552.2	561.4	556.9	559.0
50-05	272	.6053	.0000	.1816	.0000	.0013	.0000	.0000	.0104	.0040	.1974	5	515.0	479.9	501.1	505.2	487.9
51-66	273	.6058	.1031	.1454	.0000	.0053	.0000	.0473	.0563	.0007	.0361	8	557.0	524.6	533.8	528.6	529.8
52-42	274	.4399	.0657	.1814	.0000	.1511	.0000	.0646	.0365	.0012	.0597	8	527.0	500.1	506.3	500.8	497.7
53-52	275	.6036	.0000	.1205	.0000	.1489	.0000	.0557	.0064	.0013	.0636	6	567.0	538.0	550.7	560.5	546.0
54-72	276	.3474	.1974	.1833	.0000	.1511	.0000	.0000	.1208	.0000	.0000	6	457.0	513.0	537.7	519.2	532.3
55-27	277	.3476	.1962	.3038	.0000	.0707	.0000	.0000	.0817	.0000	.0000	6	527.0	452.5	469.3	470.5	478.3
56-68	278	.5894	.0000	.0733	.0000	.1094	.0000	.0000	.0083	.0044	.2152	5	650.0	532.9	546.8	544.9	530.1
57-07	279	.6237	.0000	.1227	.0000	.0423	.0000	.2002	.0111	.0000	.0000	6	522.0	528.0	547.8	550.8	546.9
58-39	280	.4785	.0929	.1237	.0000	.0709	.0000	.0919	.0524	.0018	.0879	9	550.0	516.0	515.5	513.3	518.6
59-06	281	.6014	.1945	.1193	.0000	.0016	.0000	.0000	.0832	.0000	.0000	7	547.0	549.8	556.8	556.6	550.5
60-20	282	.3657	.2356	.1172	.0000	.0024	.0000	.1943	.0848	.0000	.0000	6	499.0	515.9	478.4	470.4	517.3
61-60	283	.4715	.0891	.1629	.0000	.0246	.0000	.1281	.0101	.0023	.1114	8	542.0	486.6	484.0	477.8	496.0
62-54	284	.3549	.2004	.1232	.0000	.1545	.0000	.0000	.0438	.0025	.1207	5	572.0	520.0	554.9	533.0	538.7
63-34	285	.4524	.0802	.1984	.0000	.0627	.0000	.0792	.0442	.0017	.0812	9	518.0	481.6	481.0	478.9	486.1

(a) Sequence number from MCC-PROP data set.

(b) BNDS is the number of relaxed CVS component bounds (Table G.2) satisfied.

(c) Tg is the measured or estimated glass transition temperature (°C).

(d) TG.1 is the value predicted by the first-order mass fraction model in Table 9.4. TG.2.1, TG.2.2, and TG.2.3 are the values predicted by the three candidate second-order mass fraction models in Table 9.4. All have units of °C.

TABLE G.5. Data for 143 Glasses from Historical Database Used to Validate Models for Glass Transition Temperature (continued)

Glass	(a) Seq	Mass Fractions SiO2	B2O3	Na2O	Li2O	CaO	MgO	Fe2O3	Al2O3	ZrO2	Others	(b) Bnds	(c) Tg	(d) TG.1	(d) TG.2.1	(d) TG.2.2	(d) TG.2.3
64-28	286	.3732	.1997	.1251	.0000	.0918	.0000	.2017	.0085	.0000	.0000	7	526.0	518.7	523.5	508.0	531.7
65-49	287	.3784	.0000	.1251	.0000	.1545	.0000	.1713	.0095	.0032	.1580	5	562.0	491.2	516.2	508.4	512.2
66-33	288	.3453	.1918	.3069	.0000	.1535	.0000	.0000	.0025	.0000	.0000	4	446.0	458.1	488.2	473.9	484.1
69-16	291	.4226	.0000	.1273	.0000	.1568	.0000	.2037	.0896	.0000	.0000	6	560.0	518.5	542.7	543.0	551.5
70-55	292	.3512	.1977	.3101	.0000	.0025	.0000	.0933	.0452	.0000	.0000	7	477.0	436.2	449.3	432.4	465.9
71-33	293	.3427	.0911	.2745	.0000	.0666	.0000	.0000	.0428	.0036	.1787	5	441.0	429.3	405.8	428.0	412.5
72-02	294	.6047	.0000	.3084	.0000	.0033	.0000	.0000	.0836	.0000	.0000	5	489.0	457.7	459.0	476.1	469.1
73-01	295	.5900	.0000	.1740	.0000	.1530	.0000	.0000	.0830	.0000	.0000	5	568.0	529.2	518.3	529.9	528.6
74-12	296	.5436	.0000	.3034	.0000	.1492	.0000	.0000	.0038	.0000	.0000	5	493.0	467.6	444.0	469.5	459.0
75-26	297	.3533	.0830	.1229	.0000	.1502	.0000	.0000	.0854	.0041	.2011	5	571.0	500.5	505.5	485.2	472.7
76-29	298	.3560	.1925	.1221	.0000	.1112	.0000	.0000	.0046	.0043	.2093	5	567.0	501.2	535.2	520.5	519.2
77-25	299	.3534	.1976	.1253	.0000	.1548	.0000	.0845	.0845	.0000	.0000	7	545.0	532.4	560.2	539.2	551.2
78-48	300	.4233	.0577	.1792	.0000	.0433	.0000	.0566	.0350	.0041	.2008	8	544.0	466.2	458.7	462.5	459.4
79-43	301	.4544	.0870	.2077	.0000	.0686	.0000	.0849	.0077	.0018	.0880	9	512.0	476.8	482.2	477.7	484.0
80-46	302	.4304	.0553	.1742	.0000	.0430	.0000	.1998	.0359	.0012	.0602	8	516.0	480.9	474.1	466.8	512.8
81-34	303	.4523	.0802	.1963	.0000	.0637	.0000	.0791	.0442	.0017	.0825	9	519.0	482.4	481.9	479.8	486.8
82-24	304	.3381	.1909	.2933	.0000	.0000	.0000	.0000	.0034	.0035	.1709	5	470.0	420.6	436.9	452.6	447.6
84-51	306	.3659	.1974	.1234	.0000	.0020	.0000	.1490	.0093	.0031	.1500	7	516.0	489.6	474.0	468.6	508.1
85-16	307	.4274	.0000	.1259	.0000	.1584	.0000	.2000	.0883	.0000	.0000	6	567.0	520.0	544.3	544.9	550.9
86-88	308	.6100	.0000	.2668	.0000	.0010	.0000	.0000	.1222	.0000	.0000	5	501.0	476.4	479.2	492.2	486.8
87-86	309	.3959	.0000	.2811	.0000	.1384	.0000	.0462	.0791	.0012	.0581	5	486.0	449.9	413.2	434.1	412.9
88-91	310	.5154	.0592	.1819	.0000	.1517	.0000	.0256	.0050	.0012	.0600	8	537.0	509.4	512.1	512.8	508.7
89-77	311	.4501	.1666	.1219	.0000	.0016	.0000	.1798	.0800	.0000	.0000	9	502.0	519.1	485.4	478.6	511.9
90-85	312	.4497	.0000	.1218	.0000	.1228	.0000	.1264	.0070	.0034	.1688	6	580.0	497.9	511.7	509.8	500.3
91-89	313	.4170	.0961	.1513	.0000	.0019	.0000	.1014	.1246	.0022	.1056	9	531.0	488.6	467.5	468.6	496.3
92-84	314	.4417	.0673	.1871	.0000	.0512	.0000	.0664	.0364	.0030	.1469	8	510.0	473.9	470.0	471.3	473.5
93-81	315	.4754	.1749	.1288	.0000	.0838	.0000	.0000	.0031	.0027	.1314	7	569.0	518.6	535.6	531.5	529.0
94-92	316	.5118	.0587	.1875	.0000	.0025	.0000	.0000	.0344	.0041	.2010	7	546.0	471.4	476.0	483.4	468.5
95-90	317	.4077	.0000	.1525	.0000	.0997	.0000	.1027	.1281	.0022	.1071	8	477.0	491.2	478.8	479.4	477.8
96-76	318	.6017	.0000	.2654	.0000	.1297	.0000	.0000	.0032	.0000	.0000	4	492.0	487.7	481.2	499.9	497.0

(a) Sequence number from MCC-PROP data set.

(b) BNDS is the number of relaxed CVS component bounds (Table G.2) satisfied.

(c) Tg is the measured or estimated glass transition temperature (°C).

(d) TG.1 is the value predicted by the first-order mass fraction model in Table 9.4. TG.2.1, TG.2.2, and TG.2.3 are the values predicted by the three candidate second-order mass fraction models in Table 9.4. All have units of °C.

TABLE G.5. Data for 143 Glasses from Historical Database Used to Validate Models for Glass Transition Temperature (continued)

Glass	(a) Seq	Mass Fractions SiO2	B2O3	Na2O	Li2O	CaO	MgO	Fe2O3	Al2O3	ZrO2	Others	(b) Bnds	(c) Tg	(d) TG.1	(d) TG.2.1	(d) TG.2.2	(d) TG.2.3
97-82	319	.4835	.0000	.2270	.0000	.1176	.0000	.0000	.0027	.0034	.1658	4	516.0	465.0	446.6	461.6	433.5
98-79	320	.4424	.0000	.2658	.0000	.0044	.0000	.0964	.0061	.0037	.1812	6	474.0	423.5	401.6	417.6	420.4
99-78	321	.4889	.0000	.1279	.0000	.1217	.0000	.1454	.0092	.0021	.1048	7	425.0	507.8	525.6	528.1	519.3
100-93	322	.5541	.0000	.1026	.0000	.0781	.0000	.1086	.0461	.0022	.1084	8	537.0	523.3	533.5	537.8	528.9
101-80	323	.4314	.1707	.1196	.0000	.1309	.0000	.0747	.0727	.0000	.0000	8	549.0	539.1	548.9	539.4	542.8
102-87	324	.4277	.1689	.0997	.0000	.0019	.0000	.0000	.1165	.0037	.1816	7	524.0	511.3	519.1	523.7	518.8
103-83	325	.5217	.1456	.2210	.0000	.1084	.0000	.0000	.0033	.0000	.0000	6	528.0	505.2	517.9	512.4	518.0
#1	331	.4300	.0800	.0000	.0000	.0000	.0000	.0000	.0500	.0000	.4400	6	572.0	505.2	524.7	512.9	485.8
#2	332	.0500	.3000	.0000	.0000	.0000	.0000	.0000	.0500	.0000	.6000	4	560.0	454.3	564.1	561.2	567.4
#3	333	.0400	.3100	.0000	.0000	.0000	.0000	.0000	.0500	.0000	.6000	4	560.0	453.9	570.2	568.2	576.0
#4	334	.1000	.2400	.0000	.0000	.0000	.0000	.0000	.0000	.0000	.6600	4	565.0	445.4	528.2	518.3	510.4
#5	335	.1600	.5500	.0000	.0000	.0000	.0000	.0000	.0300	.0000	.2600	4	535.0	534.9	683.9	728.9	632.4
Centroid	536	.4548	.1031	.1141	.0314	.0054	.0137	.1407	.0297	.0253	.0817	10	462.5	477.1	464.5	461.7	485.3
AL-001	537	.4548	.1032	.1148	.0314	.0057	.0138	.1488	.0168	.0268	.0839	10	465.5	476.1	463.4	460.2	485.3
AL-002	538	.4549	.1032	.1144	.0314	.0056	.0137	.1447	.0232	.0260	.0828	10	461.5	476.6	464.0	461.0	485.3
AL-004	540	.4545	.1031	.1136	.0314	.0053	.0137	.1348	.0389	.0242	.0804	10	461.0	477.8	465.3	462.8	485.3
AL-005	541	.4543	.1031	.1130	.0314	.0050	.0136	.1267	.0518	.0227	.0784	10	467.0	478.7	466.4	464.2	485.3
CR-001	542	.4544	.1030	.1141	.0314	.0055	.0137	.1416	.0298	.0255	.0810	10	454.5	477.2	464.5	461.6	485.5
CR-002	543	.4559	.1034	.1145	.0315	.0055	.0137	.1316	.0299	.0255	.0885	10	460.0	476.6	465.3	462.6	483.8
CR-004	545	.4546	.1031	.1140	.0314	.0054	.0137	.1388	.0295	.0249	.0845	10	465.5	476.7	464.4	461.7	484.8
CR-005	546	.4545	.1031	.1138	.0314	.0054	.0137	.1370	.0294	.0246	.0871	10	466.0	476.4	464.4	461.7	484.4
FE-001	547	.4560	.1034	.1185	.0314	.0072	.0141	.1039	.0348	.0352	.0953	10	470.0	478.2	469.9	468.0	483.1
FE-002	548	.4554	.1033	.1163	.0314	.0063	.0139	.1223	.0322	.0302	.0885	10	462.0	477.7	467.3	464.9	484.1
FE-004	550	.4539	.1030	.1119	.0314	.0046	.0135	.1590	.0272	.0203	.0752	10	460.0	476.5	461.5	458.4	486.5
FE-005	551	.4535	.1028	.1097	.0314	.0037	.0133	.1774	.0246	.0153	.0682	10	458.5	475.9	458.4	455.0	487.8
MN-001	552	.4551	.1033	.1148	.0314	.0057	.0138	.1479	.0304	.0266	.0710	10	463.5	478.4	464.9	461.8	487.1
MN-002	553	.4548	.1032	.1144	.0314	.0056	.0137	.1442	.0300	.0259	.0767	10	467.0	477.7	464.6	461.7	486.2
MN-004	555	.4545	.1031	.1136	.0314	.0053	.0137	.1348	.0292	.0242	.0902	10	461.5	476.1	464.3	461.7	483.8
MN-005	556	.4544	.1031	.1132	.0314	.0051	.0136	.1290	.0280	.0231	.0985	10	461.5	475.0	464.1	461.7	482.3
NI-001	557	.4548	.1032	.1143	.0314	.0055	.0137	.1429	.0299	.0257	.0785	10	461.5	477.5	464.6	461.7	485.9

(a) Sequence number from MCC-PROP data set.

(b) BNDS is the number of relaxed CVS component bounds (Table G.2) satisfied.

(c) Tg is the measured or estimated glass transition temperature (°C).

(d) TG.1 is the value predicted by the first-order mass fraction model in Table 9.4. TG.2.1, TG.2.2, and TG.2.3 are the values predicted by the three candidate second-order mass fraction models in Table 9.4. All have units of °C.

TABLE G.5. Data for 143 Glasses from Historical Database Used to Validate Models for Glass Transition Temperature (continued)

Glass	(a) Seq	Mass Fractions SiO2	B2O3	Na2O	Li2O	CaO	MgO	Fe2O3	Al2O3	ZrO2	Others	(b) Bnds	(c) Tg	(d) TG.1	(d) TG.2.1	(d) TG.2.2	(d) TG.2.3
NI-002	558	.4548	.1031	.1142	.0314	.0055	.0137	.1418	.0298	.0255	.0801	10	462.0	477.3	464.6	461.7	485.6
NI-004	560	.4546	.1031	.1140	.0314	.0054	.0137	.1387	.0295	.0249	.0846	10	464.5	476.7	464.4	461.7	484.8
NI-005	561	.4546	.1031	.1138	.0314	.0054	.0137	.1368	.0293	.0246	.0873	10	461.5	476.4	464.4	461.7	484.4
P-001	562	.4547	.1032	.1145	.0314	.0056	.0138	.1452	.0301	.0261	.0754	10	464.5	477.9	464.7	461.7	486.4
P-002	563	.4548	.1032	.1143	.0314	.0055	.0137	.1429	.0299	.0257	.0785	10	463.5	477.5	464.6	461.7	485.9
P-004	565	.4545	.1031	.1136	.0314	.0052	.0137	.1340	.0291	.0240	.0914	10	460.5	475.9	464.2	461.6	483.6
P-005	566	.4544	.1031	.1130	.0314	.0050	.0136	.1274	.0284	.0228	.1008	10	462.0	474.7	464.0	461.6	481.9
SRL 165 HiFe	586	.4889	.0698	.1178	.0486	.0115	.0076	.1484	.0181	.0093	.0801	10	458.0	453.3	446.6	443.2	462.0
SRL 165 TDS	587	.5509	.0692	.1049	.0479	.0153	.0081	.1202	.0418	.0122	.0295	10	458.0	477.4	475.5	473.7	478.3
SRL 165 HiAl	588	.5429	.0739	.1176	.0514	.0114	.0080	.0635	.0928	.0101	.0285	10	460.0	471.2	471.3	469.6	471.8
Table V	643	.0000	.0942	.0000	.0000	.0000	.0000	.0000	.0000	.0000	.9058	5	280.0	386.9	425.5	384.8	315.0
Table V	644	.0000	.1332	.0000	.0000	.0000	.0000	.0000	.0000	.0000	.8668	5	350.0	395.6	451.1	416.7	369.9
Table V	645	.0000	.1721	.0000	.0000	.0000	.0000	.0000	.0000	.0000	.8279	5	360.0	404.2	476.7	448.7	420.9
Table V	646	.0000	.2378	.0000	.0000	.0000	.0000	.0000	.0000	.0000	.7622	4	430.0	418.7	519.7	502.4	498.1
Table V	647	.0000	.3877	.0000	.0000	.0000	.0000	.0000	.0000	.0000	.6123	4	500.0	451.9	618.1	625.3	633.0
Table V	648	.1522	.0000	.0000	.0000	.0000	.0000	.0000	.0000	.0000	.8478	4	350.0	405.9	414.2	369.0	256.5
Table V	649	.2121	.0000	.0000	.0000	.0000	.0000	.0000	.0000	.0000	.7879	4	420.0	421.6	434.0	393.1	292.0
Table V	650	.2876	.0000	.0000	.0000	.0000	.0000	.0000	.0000	.0000	.7124	4	460.0	441.4	459.1	423.5	336.9
Table V	651	.3720	.0000	.0000	.0000	.0000	.0000	.0000	.0000	.0000	.6280	4	507.0	463.5	487.1	457.5	386.9
Table VI	652	.0000	.0000	.0000	.0000	.0000	.0000	.0000	.0000	.0000	1.000	4	400.0	366.1	363.7	307.7	166.2
Table VI	653	.0000	.2791	.0000	.0000	.0000	.0000	.0000	.0000	.0000	.7209	4	405.0	427.9	546.9	536.3	541.0
Table VI	654	.0000	.0000	.0000	.0000	.0000	.0000	.0000	.0000	.0000	1.000	4	280.0	366.1	363.7	307.7	166.2

(a) Sequence number from MCC-PROP data set.

(b) BNDS is the number of relaxed CVS component bounds (Table G.2) satisfied.

(c) Tg is the measured or estimated glass transition temperature (°C).

(d) TG.1 is the value predicted by the first-order mass fraction model in Table 9.4. TG.2.1, TG.2.2, and TG.2.3 are the values predicted by the three candidate second-order mass fraction models in Table 9.4. All have units of °C.

Data Sources

MCC_LEACH Kindle, C.H., K.M. Olson, G.B. Mellinger, and M.R. Kreiter. 1988. Comprehensive Data Base Data Files Report, Volume 1: 1985-1988 Data from Static Glass Durability Tests, Materials Characterization Center, Pacific Northwest Laboratory, Richland, Washington.

Kindle, C.H., K.M. Olson, G.B. Mellinger, and M.R. Kreiter. 1988. Comprehensive Data Base Data Files Report, Volume 2: 1979-1984 Data from Static Glass Durability Tests, Materials Characterization Center, Pacific Northwest Laboratory, Richland, Washington.

MCC_PROP Kindle, C.H., K.M. Olson, G.B. Mellinger, and M.R. Kreiter. 1988. Comprehensive Data Base Data Files Report, Volume 3: Glass Durability Flowing Test Data; Data on Thermal and Processing Properties, Materials Characterization Center, Pacific Northwest Laboratory, Richland, Washington.

WVMCC1 Reimus, M.A.H., G.F. Piepel, G.B. Mellinger, and L.R. Brunell. 1988. West Valley Glass Product Qualification Durability Studies, FY 1987-1988: Effects of Composition, Redox State, Thermal History, and Groundwater, PNL-6723, Pacific Northwest Laboratory, Richland, Washington.

WVPCT Olson, K.M., S.C. Marschman, and G.F. Piepel. 1991. Product Consistency Testing of West Valley Compositional Variability Glasses, Limited Distribution Letter Report, Pacific Northwest Laboratory, Richland, Washington.

HWVP Bates, S.O. and W.M. Bowen. 1986. Report on Composition Variability Testing Conducted for the Hanford Waste Vitrification Program, Interim Milestone HWVP-86-V1122C, Pacific Northwest Laboratory, Richland, Washington.

Bates, S.O. 1987a. Report on FY87 Glass Variability Testing Conducted for the Hanford Waste Vitrification Program, Interim Milestone HWVP-87-V110202C, Pacific Northwest Laboratory, Richland, Washington.

Bates, S.O. 1987b. Composition Variability Studies to Increase Processing Flexibility for the Hanford Waste Vitrification Plant, Interim Milestone HWVP-87-V110202E, Pacific Northwest Laboratory, Richland, Washington.

Bates, S.O., G.F. Piepel, and J.W. Johnston. 1989. Leach Testing of Simulated Hanford Waste Vitrification Plant Reference Glass HW-39, PNL-6884, Pacific Northwest Laboratory, Richland, Washington.

CVS1 Piepel, G.F., P.R. Hrma, S.O. Bates, M.J. Schweiger, and D. E. Smith. 1993. First-Order Study of Property/Composition Relationships for Hanford Waste Vitrification Plant Glass, PNL-8502, Pacific Northwest Laboratory, Richland, Washington.

APPENDIX H

MODELING NORMALIZED BORON RELEASE AS A FUNCTION OF COMPUTED FREE ENERGY OF HYDRATION

APPENDIX H

MODELING NORMALIZED BORON RELEASE AS A FUNCTION OF COMPUTED FREE ENERGY OF HYDRATION

In this appendix, the relationship between normalized B release and computed free energy of hydration is investigated for both the 28-day MCC-1 and 7-day PCT dissolution tests. Jantzen and Plodinec (1984) and Jantzen (1988) discuss the free energy of hydration approach for predicting glass durability, including corrections for pH of the solution. Basically, their modeling approach involves calculating free energy of hydration values for the glasses to be used in developing the model, and then fitting a line to (x,y) data, where x = calculated free energy of hydration and y = logarithm of dissolution test elemental release.

Table H.1 contains the computed free energy of hydration values for the CVS-I and CVS-II Phase 1, 2, and 3 glasses in units of kcal/mol[(a)]. These computed free energy of hydration values were recomputed for all CVS glasses using updated oxide free energy values obtained in 1993 from Carol Jantzen at the Savannah River Technology Center (SRTC). Table H.1 also contains pH values from the PCT and MCC-1 tests for each CVS glass, as well as PCT and MCC-1 pH-corrected (Si and B) free energy of hydration values for each CVS glass.

Figure H.1 contains a plot of the natural log of 28-day MCC-1 normalized boron release versus uncorrected free energy of hydration (kcal/mol units). Figure H.2 contains a similar plot, except the MCC-1 pH-corrected free energy of hydration values from Table H.1 are used. Figures H.3 and H.4 are similar to Figures H.1 and H.2, except the natural log of 7-day PCT normalized boron release is plotted. The plotting symbols in Figures H.1 through H.4 are explained in a Table H.1 footnote.

(a) Free energy of hydration was also calculated in units of kcal/kg glass, but those values are not reported here.

TABLE H.1. Computed Free Energy of Hydration Values With and Without PCT and MCC-1 pH Corrections Versus PCT and MCC-1 Normalized Boron Releases

Glass	(a) PS	ΔG kcal/mol	PCT pH	(b) PCT ΔG′ kcal/mol	MCC-1 pH	(b) MCC-1 ΔG′ kcal/mol	PCT B rel. g/m²	MCC-1 B rel. g/m²
CVS1-1	M	-4.91	10.92	-8.67	9.95	-6.43	0.521	12.47
CVS1-2	1	-2.28	11.42	-7.46	10.04	-3.97	0.066	7.46
CVS1-3	1	-3.50	9.85	-4.85	9.58	-4.44	0.864	15.57
CVS1-4	1	-5.60	9.67	-6.67	9.65	-6.64	20.639	189.71
CVS1-5	1	-2.76	11.22	-7.35	10.07	-4.51	0.355	11.48
CVS1-6	1	-4.77	10.07	-6.52	9.91	-6.22	6.113	121.30
CVS1-7	1	-3.12	10.91	-6.86	9.85	-4.47	0.287	11.00
CVS1-8	1	-2.00	10.43	-4.53	9.72	-3.14	1.238	17.88
CVS1-9	1	-4.23	8.69	-4.43	9.24	-4.78	10.993	158.72
CVS1-10	1	-1.60	9.76	-2.80	8.51	-1.73	0.127	2.74
CVS1-11	1	-2.95	9.99	-4.55	9.17	-3.44	0.099	8.25
CVS1-12	1	-8.15	11.13	-12.48	10.87	-11.77	4.662	118.48
CVS1-13	1	-9.83	10.37	-12.21	10.59	-12.74	14.072	690.51
CVS1-14	1	-8.51	9.64	-9.53	10.09	-10.30	9.847	73.63
CVS1-15	1	-8.63	13.03	-20.21	12.37	-17.17	18.778	210.29
CVS1-16	1	-6.50	12.01	-13.64	10.48	-9.15	0.523	16.85
CVS1-17	1	-8.95	11.58	-14.63	10.96	-12.81	2.235	39.10
CVS1-18	1	-7.73	12.25	-15.78	11.03	-11.79	11.238	24.05
CVS1-19	M	-4.91	10.29	-7.12	9.88	-6.31	0.523	13.02
CVS1-20	M	-4.91	10.16	-6.84	9.88	-6.31	0.455	12.50
CVS1-21	1	-5.60	9.68	-6.68	9.65	-6.64	18.850	205.79
CVS1-22	1	-2.00	9.81	-3.28	9.77	-3.22	1.119	17.36
CVS1-23	M	-5.39	10.29	-7.60	9.96	-6.93	0.525	15.37
CVS2-1	2	-3.96	10.21	-5.99	9.46	-4.74	0.313	12.24
CVS2-2	2	-4.22	10.93	-8.00	9.61	-5.19	0.128	8.44
CVS2-3	2	-3.35	10.09	-5.14	9.30	-3.96	0.137	8.87
CVS2-4	2	-4.41	10.41	-6.89	9.53	-5.28	0.159	9.73
CVS2-5	2	-4.88	9.58	-5.81	9.05	-5.27	0.284	10.40
CVS2-6	2	-4.45	10.48	-7.10	9.67	-5.52	1.185	17.48
CVS2-7	2	-4.23	9.89	-5.65	9.76	-5.43	0.740	5.02
CVS2-8	2	-5.20	10.75	-8.51	9.82	-6.50	0.484	18.50
CVS2-9	2	-4.43	10.35	-6.77	9.52	-5.29	0.560	13.20
CVS2-10	2	-5.17	9.46	-5.95	8.93	-5.49	1.332	12.28
CVS2-11	2	-5.66	11.46	-10.97	9.95	-7.19	1.587	19.85
CVS2-12	2	-4.57	9.90	-6.00	9.25	-5.12	0.194	9.86
CVS2-13	2	-7.44	11.15	-11.83	9.74	-8.61	0.360	13.36

(a) PS is the plotting symbol used in plots associated with this data: 1 = CVS-I boundary, 2 = CVS-II Phase 1 interior, 3 = CVS-II Phase 2a boundary, 4 = CVS-II Phase 2b interior, 5 = CVS-II Phase 3 boundary, M = middle compositions, O = other than NCAW waste glasses, A = EA glass.

(b) ΔG′ denotes free energy of hydration corrected for pH.

TABLE H.1. Computed Free Energy of Hydration Values With and Without PCT and MCC-1 pH Corrections Versus PCT and MCC-1 Normalized Boron Releases (continued)

Glass	(a) PS	ΔG kcal/mol	PCT pH	(b) PCT ΔG′ kcal/mol	MCC-1 pH	(b) MCC-1 ΔG′ kcal/mol	PCT B rel. g/m²	MCC-1 B rel. g/m²
CVS2-50	M	-4.91	10.23	-6.99	9.45	-5.68	0.442	11.43
CVS2-51	M	-5.77	10.30	-8.00	9.48	-6.57	1.764	12.35
CVS2-52	4	-3.28	10.16	-5.21	9.47	-4.07	0.557	10.08
CVS2-53	4	-3.95	10.02	-5.61	(c)	(c)	0.304	(c)
CVS2-54	M	-5.77	10.23	-7.85	(c)	(c)	2.761	(c)
CVS2-55	0	-6.00	10.19	-7.99	9.52	-6.85	1.342	15.90
CVS2-56	0	-6.08	10.20	-8.10	9.57	-7.01	1.419	17.23
CVS2-57	0	-5.97	10.26	-8.11	9.55	-6.87	1.164	15.28
CVS2-58	4	-3.71	9.87	-5.09	9.36	-4.37	0.779	13.15
CVS2-59	5	-7.79	11.47	-13.13	9.85	-9.14	1.591	11.98
CVS2-60	5	-9.00	11.96	-15.95	10.44	-11.55	1.624	16.52
CVS2-61	5	-4.37	10.89	-8.04	9.75	-5.55	0.222	10.90
CVS2-62	5	-5.60	9.56	-6.51	9.33	-6.23	1.002	12.39
CVS2-63	5	-8.62	10.59	-11.53	9.61	-9.59	0.332	9.64
CVS2-64	0	-4.79	10.62	-7.77	9.85	-6.14	0.379	12.32
CVS2-65	0	-4.42	10.63	-7.43	9.59	-5.37	0.335	9.40
CVS2-66	0	-5.24	10.54	-8.02	9.61	-6.21	0.210	11.74
CVS2-67	0	-3.73	9.73	-4.88	9.11	-4.16	0.512	11.14
CVS2-68	0	-3.10	9.85	-4.45	9.21	-3.62	0.308	10.56
CVS2-69	0	-4.06	10.18	-6.03	9.45	-4.83	0.226	9.88
CVS2-70	0	-2.89	9.89	-4.31	9.22	-3.42	0.312	11.56
CVS2-71	5	-4.87	10.79	-8.28	9.79	-6.12	0.411	12.00
CVS2-72	5	-5.29	10.48	-7.93	9.71	-6.41	0.210	11.74
CVS2-73	5	-3.29	9.96	-4.83	9.10	-3.72	0.244	6.64
CVS2-74	5	-3.94	10.41	-6.42	9.49	-4.76	0.226	9.88
CVS2-75	5	-3.02	9.89	-4.44	9.12	-3.46	0.278	8.62
CVS2-76	5	-10.80	12.46	-19.72	10.71	-14.01	14.871	26.53
CVS2-77	5	-10.24	12.26	-18.33	11.17	-14.69	9.512	49.58
CVS2-78	5	-2.03	9.21	-2.55	9.15	-2.50	0.934	32.15
CVS2-79	5	-2.00	8.97	-2.33	8.85	-2.26	0.744	32.15
CVS2-80	5	-1.28	9.15	-1.75	9.10	-1.71	0.764	45.22
CVS2-81	5	-11.31	12.51	-20.43	11.60	-17.05	16.613	107.18
CVS2-82	5	-10.73	12.18	-18.51	11.79	-17.10	44.000	643.09

(a) PS is the plotting symbol used in plots associated with this data: 1 = CVS-I boundary, 2 = CVS-II Phase 1 interior, 3 = CVS-II Phase 2a boundary, 4 = CVS-II Phase 2b interior, 5 = CVS-II Phase 3 boundary, M = middle compositions, 0 = other than NCAW waste glasses, A = EA glass.

(b) ΔG′ denotes free energy of hydration corrected for pH.

(c) MCC-1 dissolution tests were not performed on the radioactive glasses CVS2-53 and CVS2-54.

TABLE H.1. Computed Free Energy of Hydration Values With and Without PCT and MCC-1 pH Corrections Versus PCT and MCC-1 Normalized Boron Releases (continued)

Glass	(a) PS	ΔG kcal/mol	PCT pH	(b) PCT ΔG′ kcal/mol	MCC-1 pH	(b) MCC-1 ΔG′ kcal/mol	PCT B rel. g/m²	MCC-1 B rel. g/m²
CVS2-14	2	-4.90	10.47	-7.52	9.48	-5.71	1.657	15.10
CVS2-15	2	-8.47	11.31	-13.33	9.03	-8.85	0.331	25.10
CVS2-16	M	-5.78	10.37	-8.17	9.46	-6.56	2.937	18.08
CVS2-17	M	-4.91	10.27	-7.08	9.32	-5.54	0.495	12.32
CVS2-18	M	-5.78	10.34	-8.10	9.38	-6.47	2.578	19.72
CVS2-19	M	-5.77	10.35	-8.11	9.34	-6.41	1.990	13.69
CVS2-20	3	-4.35	10.89	-8.03	9.55	-5.25	0.347	8.42
CVS2-21	3	-3.85	10.26	-5.99	9.37	-4.53	3.855	11.80
CVS2-22	3	-5.47	11.72	-11.60	9.74	-6.64	9.646	15.60
CVS2-23	3	-9.13	11.81	-15.56	9.86	-10.50	0.173	11.21
CVS2-24	3	-5.65	9.80	-6.91	9.38	-6.34	4.522	19.86
CVS2-25	3	-7.05	11.91	-13.83	10.27	-9.22	4.663	34.50
CVS2-26	3	-5.15	10.11	-6.98	9.75	-6.33	1.628	39.14
CVS2-27	3	-8.33	11.87	-14.97	9.64	-9.35	3.270	11.22
CVS2-28	3	-8.98	11.54	-14.53	9.51	-9.83	5.145	9.84
CVS2-29	3	-4.70	9.11	-5.14	9.14	-5.16	1.286	42.28
CVS2-30	3	-3.16	8.74	-3.38	8.76	-3.38	6.512	24.44
CVS2-31	3	-3.56	9.54	-4.45	9.41	-4.29	0.411	47.02
CVS2-32	3	-8.91	12.31	-17.20	10.07	-10.66	9.646	16.62
CVS2-33	3	-10.42	11.94	-17.30	10.26	-12.56	1.723	14.51
CVS2-34	3	-9.44	11.55	-15.02	9.98	-11.02	4.340	29.24
CVS2-35	3	-9.63	11.90	-16.38	10.22	-11.69	0.320	11.61
CVS2-36	3	-6.67	11.34	-11.61	10.13	-8.54	0.481	21.09
CVS2-37	3	-4.19	10.45	-6.77	9.33	-4.83	0.246	9.64
CVS2-38	3	-4.55	9.56	-5.46	9.27	-5.12	1.119	23.64
CVS2-39	3	-7.62	12.50	-16.70	10.17	-9.57	12.701	16.30
CVS2-40	4	-6.72	11.13	-11.06	9.79	-7.97	0.337	12.20
CVS2-41	4	-4.28	10.89	-7.96	9.60	-5.25	0.177	9.42
CVS2-42	4	-4.26	11.19	-8.77	9.86	-5.63	1.695	14.31
CVS2-43	4	-3.43	9.97	-4.99	9.23	-3.97	0.767	11.33
CVS2-44	4	-3.84	10.31	-6.10	9.56	-4.75	0.255	10.28
CVS2-45	4	-3.63	10.05	-5.34	9.43	-4.38	0.501	11.60
CVS2-46	4	-4.12	10.19	-6.12	9.32	-4.75	0.317	10.98
CVS2-47	4	-6.70	11.39	-11.79	9.83	-8.01	1.159	11.56
CVS2-48	4	-5.40	10.09	-7.19	9.42	-6.14	0.307	10.62
CVS2-49	4	-4.63	9.97	-6.19	9.01	-4.99	0.303	11.35

(a) PS is the plotting symbol used in plots associated with this data: 1 = CVS-I boundary, 2 = CVS-II Phase 1 interior, 3 = CVS-II Phase 2a boundary, 4 = CVS-II Phase 2b interior, 5 = CVS-II Phase 3 boundary, M = middle compositions, O = other than NCAW waste glasses, A = EA glass.

(b) ΔG′ denotes free energy of hydration corrected for pH.

TABLE H.1. Computed Free Energy of Hydration Values With and Without PCT and MCC-1 pH Corrections Versus PCT and MCC-1 Normalized Boron Releases (continued)

Glass	(a) PS	ΔG kcal/mol	PCT pH	(b) PCT ΔG′ kcal/mol	MCC-1 pH	(b) MCC-1 ΔG′ kcal/mol	PCT B rel. g/m²	MCC-1 B rel. g/m²
CVS2-83	5	-12.10	12.33	-20.47	10.72	-15.33	34.656	37.19
CVS2-84	5	-9.92	12.43	-18.71	10.76	-13.26	12.460	30.01
CVS2-85	5	-8.26	11.68	-14.26	10.45	-10.83	0.456	18.49
CVS2-86	5	-6.05	10.98	-9.97	9.53	-6.92	0.115	8.30
CVS2-87	5	-6.47	10.90	-10.18	9.58	-7.41	0.178	9.44
CVS2-88	5	-6.64	11.52	-12.13	10.06	-8.38	0.308	9.11
CVS2-89	5	-8.81	11.05	-12.93	10.04	-10.51	1.716	38.44
CVS2-90	5	-4.63	9.99	-6.23	9.56	-5.54	5.577	29.14
CVS2-91	5	-5.67	9.39	-6.37	9.13	-6.12	8.642	44.21
CVS2-92	5	-7.69	11.12	-12.00	10.56	-10.53	18.590	86.42
CVS2-93	5	-9.59	11.77	-15.88	10.89	-13.27	13.227	216.45
CVS2-94	5	-10.71	11.84	-17.25	10.74	-14.00	4.070	87.42(d)
CVS2-95	A	-9.33	11.81	-15.76	10.26	-11.47	9.976	49.16
CVS2-96	M	-4.91	10.24	-7.01	9.57	-5.83	0.493	12.53
CVS2-97	M	-5.77	10.25	-7.89	9.49	-6.59	1.434	12.89
CVS2-98	5	-9.44	11.59	-15.15	10.08	-11.21	4.520	30.44
CVS2-99	5	-5.44	10.10	-7.25	9.49	-6.26	0.232	13.94
CVS2-100	5	-4.14	10.34	-6.46	9.62	-5.13	0.326	14.12
CVS2-101	A	-9.33	11.93	-16.14	10.63	-12.31	8.644	90.76

(a) PS is the plotting symbol used in plots associated with this data: 1 = CVS-I boundary, 2 = CVS-II Phase 1 interior, 3 = CVS-II Phase 2a boundary, 4 = CVS-II Phase 2b interior, 5 = CVS-II Phase 3 boundary, M = middle compositions, O = other than NCAW waste glasses, A = EA glass.

(b) ΔG′ denotes free energy of hydration corrected for pH.

(d) The two duplicate MCC-1 tests yielded significantly different elemental releases (see Table D.1 in Appendix D). Because it is not clear which (if either) of the two results is correct, the average is used here.

Figures H.1 to H.4 show essentially no relationship between PCT or MCC-1 normalized boron release rates (g/m^2) and free energy of hydration for CVS data, and that pH corrections to free energy of hydration do not really improve matters. Lines fitted to the data in Figures H.1 to H.4 had R^2 values (proportion of variability in release values accounted for by linear relationships to free energy) of 0.182, 0.314, 0.241, and 0.284, respectively. Not only did these lines fit the data poorly, but they had negative slopes, indicating a tendency for release to decrease with increasing free energy of hydration (which is visible in Figures H.1 to H.4). However, work at SRTC indicates that release should increase with increasing free energy of hydration.

The reasons for the poor performance of free energy of hydration as a predictor of PCT and MCC-1 durability for CVS glasses is not clear. Carol Jantzen of SRTC, one of the developers of the technique, has suggested that glasses with phase separation or crystallinity may disrupt the relationship. Using the method discussed in Sections 12.11.4.2 and 12.11.4.4, only nine of the 123 CVS glasses are predicted as prone to amorphous phase separation. For samples having a thermal history corresponding to a predicted centerline canister cooling (CCC) schedule, phase separation has been experimentally confirmed (by SEM/TEM) for three (CVS1-4, CVS2-29, and CVS2-31) of the nine prone glasses. Three other CCC glasses (CVS1-9, CVS2-78, and CVS2-80) lying within the miscibility boundary were found to be highly crystallized. The extensive crystallization is believed to be the result of prior amorphous phase separation acting as a precursor to crystallization. In fact, amorphous phase separation and less extensive crystallization was observed in a quenched sample of CVS1-9 by SEM, showing the effect of thermal history. The CCC cooling schedule is kinetically more favorable for the development of phase separation (both crystalline and amorphous) than quenching the glass.

Given the limited number of CCC glasses found or predicted prone to be phase separated and the limiting kinetics involved, it is unlikely that the number of quenched glasses possessing amorphous phase separation should exceed that for the CCC schedule. The more rapid cooling schedule would limit the development of amorphous phase separation and crystallization. In fact, very

few quenched CVS glasses contain crystals. Thus, it appears that the data scatter in Figures H.1 through H.4 (based on quenched glasses) should not be related to the development of amorphous phase separation or crystallization.

The free energy of hydration values calculated and plotted in this appendix are based on the approach and enhancements developed at SRTC through late 1993/early 1994. SRTC has developed additional enhancements of the methodology, but the documentation was not yet available at the time this report went to press. Hence, it was not possible to investigate the effects of the enhancements for the CVS data nor include discussion of the enhancements here.

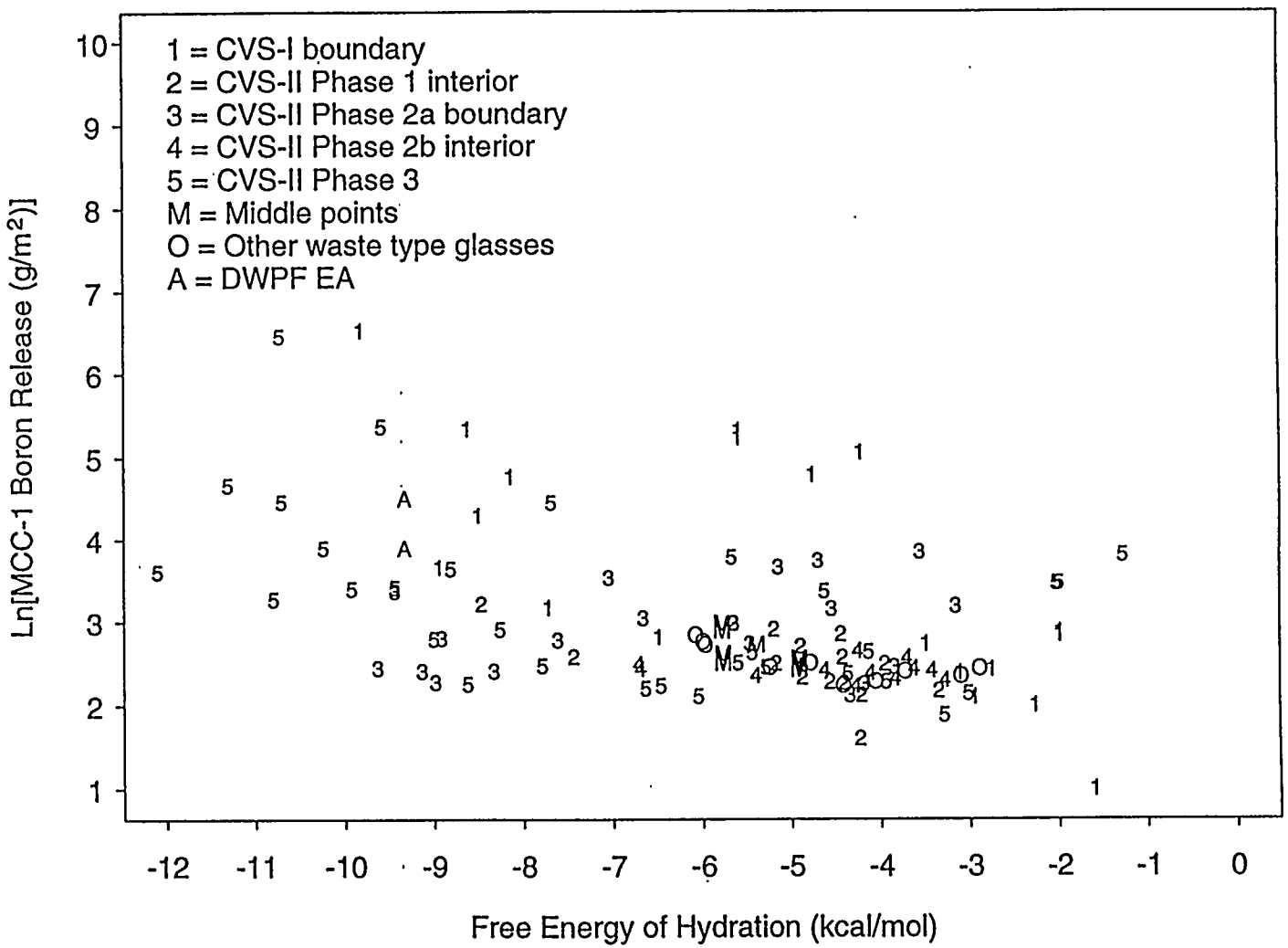

FIGURE H.1. Natural Log of 28-Day MCC-1 Boron Release Versus Free Energy of Hydration for CVS Glasses

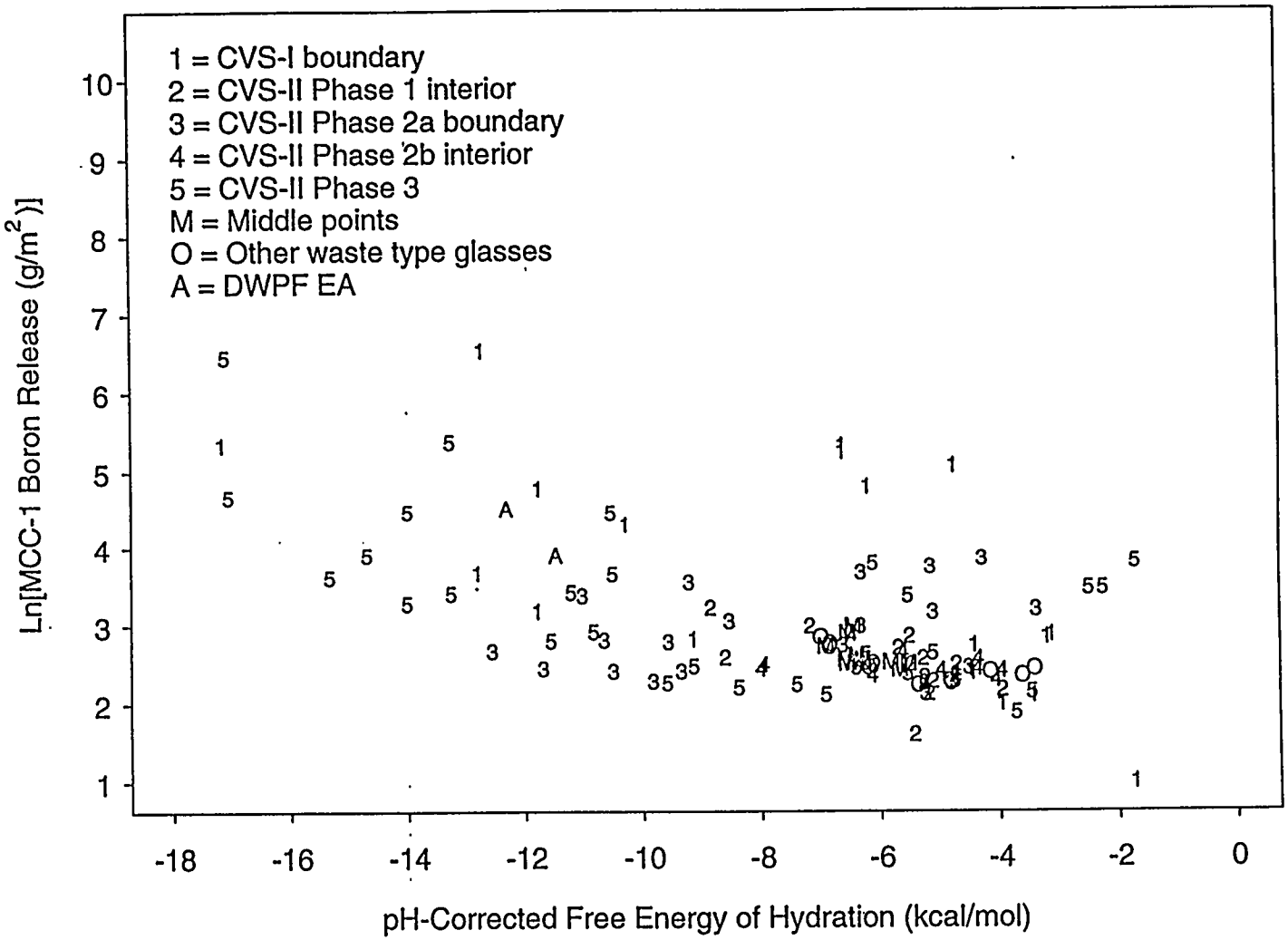

FIGURE H.2. Natural Log of 28-Day MCC-1 Boron Release Versus pH-Corrected Free Energy of Hydration for CVS Glasses

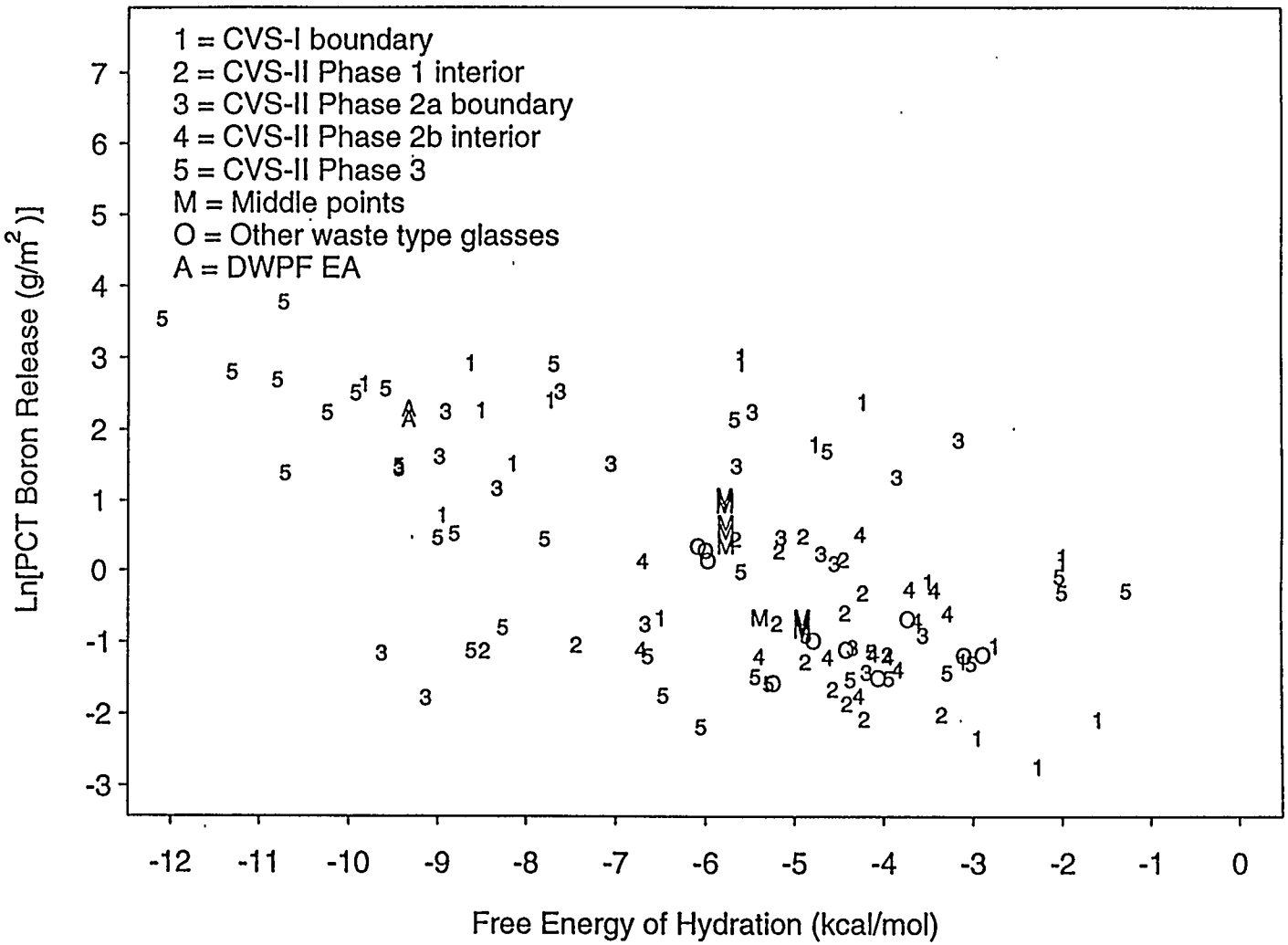

FIGURE H.3. Natural Log of 7-Day PCT Boron Release Versus Free Energy of Hydration for CVS Glasses

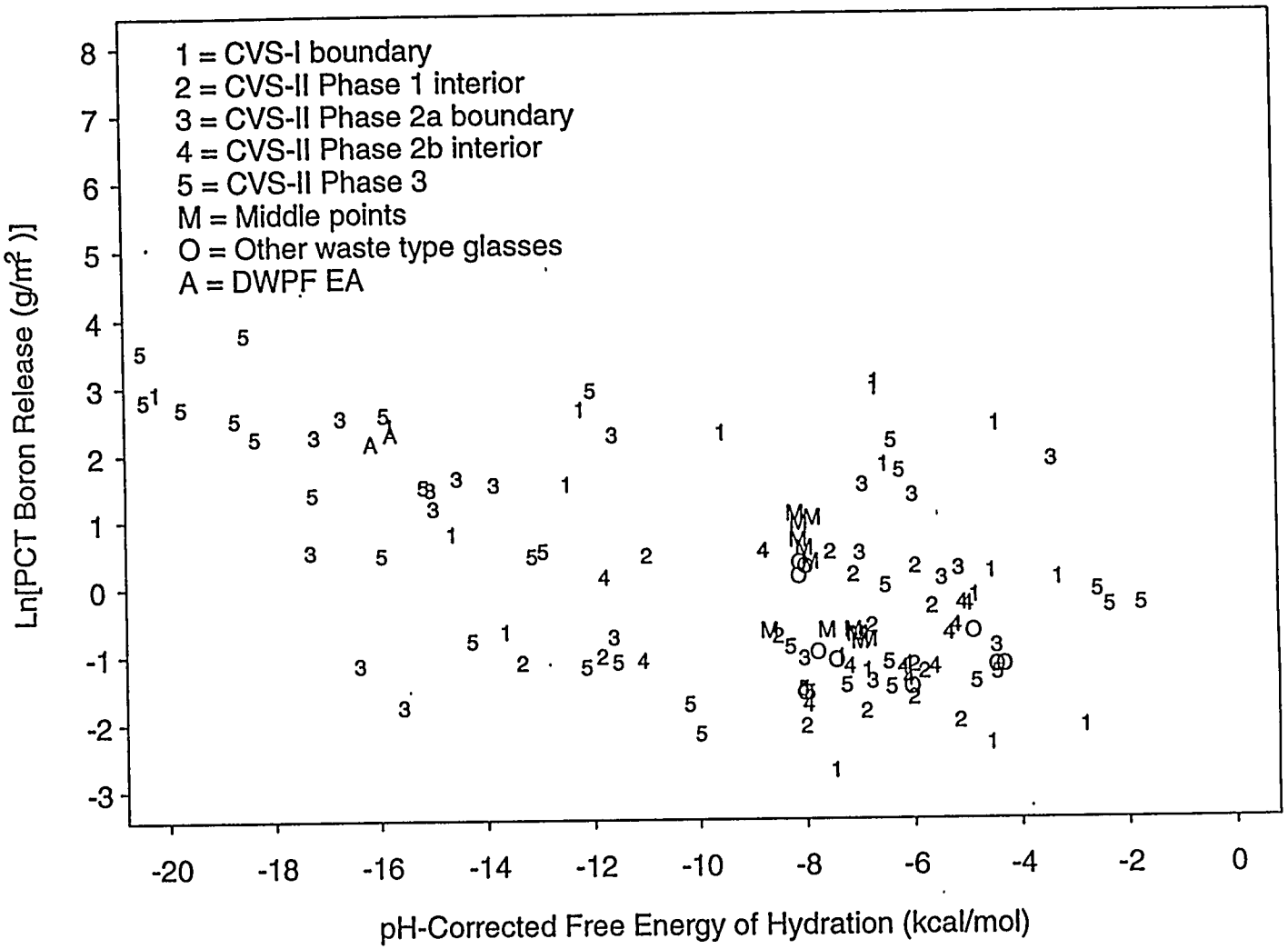

FIGURE H.4. Natural Log of 7-Day PCT Boron Release Versus pH-Corrected Free Energy of Hydration for CVS Glasses

APPENDIX I

UNCERTAINTIES AND STATISTICAL INTERVALS FOR GLASS PROPERTY MODEL PREDICTIONS

APPENDIX I

UNCERTAINTIES AND STATISTICAL INTERVALS FOR GLASS PROPERTY MODEL PREDICTIONS

Equations for the standard deviations of CVS model predictions are developed, presented, and illustrated. Section I.1 gives the necessary notational and least-squares theory background. Section I.2 contains the covariance matrices corresponding to the fitted property models. Section I.3 presents the standard deviation equations that quantify the uncertainty in glass property predictions due to model (i.e., estimated coefficient) uncertainty. Section I.4 presents the equations for various statistical intervals and bands (simultaneous intervals) for predictions made with fitted property models. Section I.5 presents the standard deviation equation that quantifies the uncertainty in glass property predictions due to estimated composition uncertainties.

I.1 LEAST SQUARES BACKGROUND

Models linear in their coefficients[a], and the data points the model will be fitted to, can be written in the general matrix form:

$$\mathbf{y} = \mathbf{X}\boldsymbol{\beta} + \boldsymbol{\epsilon} \tag{I.1}$$

where $\mathbf{y}$ is an n x 1 vector of (possibly transformed) property values corresponding to the n glasses used to fit the model, $\mathbf{X}$ is a known matrix with n rows corresponding to the glasses used to fit the model and p columns corresponding to the terms in the model, $\boldsymbol{\beta}$ is a p x 1 vector consisting of the model coefficients to be estimated from the data, and $\boldsymbol{\epsilon}$ is an n x 1 vector of independent and identically distributed random errors with mean 0 and variance σ^2. Although least squares theory does not depend on it, subsequent statistical methods often require the additional assumption that the random

(a) Linearity in the coefficients is different than linearity in the predictor variables. All of the first- and second-order empirical models discussed in Section 6.1.1 are linear in their coefficients, with the exception of viscosity models based on the Fulcher equation.

errors are normally distributed (Gaussian). The (unweighted) least squares estimates of the model coefficients are given by:

$$\hat{\beta} = (X'X)^{-1}X'y \tag{I.2}$$

and the covariance matrix of $\hat{\beta}$ is given by:

$$\mathrm{Cov}(\hat{\beta}) = (X'X)^{-1}\,\hat{\sigma}^2 \tag{I.3}$$

If the random errors are not identically or independently distributed, the coefficients must be estimated by weighted or generalized least squares. In the CVS, the random errors are generally expected to be independent and have identical distributions (in some cases after mathematically transforming the properties). Hence, it is not necessary to discuss weighted or generalized least squares further here.

The above notation and theory provides the background for discussing the model prediction uncertainty equations in Section I.3. The uncertainty equations presented later are valid for models linear in the coefficients, assuming the fitted models do not have a significant lack-of-fit (i.e., they do not yield significantly biased predictions over the CVS experimental region).

I.2 COVARIANCE MATRICES FOR FITTED MODELS

The $(X'X)^{-1}$ portions of the covariance matrices [see Equation (I.3)] for first-order property models are given in Tables I.1 to I.11. These matrices are symmetric, so only the diagonals and lower triangular portions are shown in the tables. Note that the $(X'X)^{-1}$ matrices depend only on the glass compositions used to fit each model. Hence, the $(X'X)^{-1}$ matrix in some tables holds for several first-order property models where the same glass compositions were used to fit those models. There is not much difference among the $(X'X)^{-1}$ matrices in Tables I.1 to I.8 because the same compositions (CVS-I and CVS-II Phase 1, 2, and 3) were used to fit all the corresponding models, with a few exceptions for particular models. Only small subsets of the data were used to fit the liquidus temperature models for clinopyroxene, spinel, and Zr-containing primary phases, so the $(X'X)^{-1}$ matrices in Tables I.9, I.10, and I.11 are quite different from those in Tables I.1 to I.8.

The $\hat{\sigma}^2$ values for first-order property models are given in Table I.12. These values were calculated for each model according to the equation

$$\hat{\sigma}^2 = \frac{\sum_{i=1}^{n} (y_i - \hat{y}_i)^2}{n-p} \tag{I.4}$$

where

- n = the number of data points used to fit the model,
- p = the number of terms in the model,
- y_i = the measured property value for the ith data point,
- $\hat{y}_i$ = the predicted property value for the ith data point.

For all CVS property models except the three liquidus temperature models, n ranged from 114 to 124 (the total number of CVS-I and CVS-II Phase 1, 2, and 3 data points). For the three liquidus temperature models, n ranged from 22 to 29. For first-order models, p = 10.

Because the $\hat{\sigma}^2$ values depend on the measured as well as predicted property values, they are different for every property model, regardless of whether first-order property models shared the same $(X'X)^{-1}$ matrix or not.

TABLE I.1. $(X'X)^{-1}$ for the First-Order Mixture Model Using Mass Fractions for ln(Viscosity at 1150°C) (from Table 7.3)

	SiO_2	B_2O_3	Na_2O	Li_2O	CaO	MgO	Fe_2O_3	Al_2O_3	ZrO_2	Others
SiO_2	0.874									
B_2O_3	-0.757	3.045								
Na_2O	-0.860	0.524	3.575							
Li_2O	-1.816	1.130	1.941	17.785						
CaO	-0.510	-0.327	0.021	1.223	9.727					
MgO	-0.787	-0.122	0.068	1.178	2.775	11.885				
Fe_2O_3	-1.100	0.323	0.024	0.167	-0.586	-0.165	5.985			
Al_2O_3	-0.453	-0.768	-1.191	-2.774	-0.424	0.549	2.226	5.032		
ZrO_2	-0.634	-0.291	-0.668	-2.168	-0.037	0.649	1.405	2.956	7.336	
Others	-0.900	-0.151	-0.246	-1.442	0.337	0.246	0.881	1.554	1.117	9.030

TABLE I.2. $(X'X)^{-1}$ for the First-Order Mixture Model Using Mass Fractions for ln(Electrical Conductivity at 1150°C) (from Table 8.2)

	SiO_2	B_2O_3	Na_2O	Li_2O	CaO	MgO	Fe_2O_3	Al_2O_3	ZrO_2	Others
SiO_2	0.914									
B_2O_3	-0.767	3.056								
Na_2O	-0.948	0.562	3.815							
Li_2O	-1.973	1.165	2.305	18.480						
CaO	-0.518	-0.331	-0.014	1.171	9.862					
MgO	-0.856	-0.114	0.166	1.375	2.904	12.012				
Fe_2O_3	-1.152	0.336	0.168	0.431	-0.637	-0.120	6.098			
Al_2O_3	-0.420	-0.789	-1.309	-2.934	-0.367	0.550	2.153	5.105		
ZrO_2	-0.565	-0.329	-0.847	-2.366	-0.097	0.504	1.337	3.030	7.569	
Others	-0.968	-0.138	-0.096	-1.204	0.359	0.374	0.981	1.496	0.971	9.201

TABLE I.3. $(X'X)^{-1}$ for the First-Order Mixture Models Using Mass Fractions for ln(PCT Elemental Releases) (from Table 12.10a) and for PCT pH (from Table 12.18)

	SiO_2	B_2O_3	Na_2O	Li_2O	CaO	MgO	Fe_2O_3	Al_2O_3	ZrO_2	Others
SiO_2	0.878									
B_2O_3	-0.760	3.046								
Na_2O	-0.871	0.538	3.631							
Li_2O	-1.823	1.152	1.999	17.830						
CaO	-0.515	-0.340	-0.010	1.180	9.809					
MgO	-0.806	-0.092	0.111	1.118	2.904	11.891				
Fe_2O_3	-1.095	0.325	0.034	0.193	-0.616	-0.177	5.993			
Al_2O_3	-0.450	-0.774	-1.223	-2.820	-0.377	0.541	2.215	5.057		
ZrO_2	-0.607	-0.328	-0.762	-2.180	-0.110	0.579	1.408	2.997	7.514	
Others	-0.915	-0.117	-0.191	-1.478	0.430	0.213	0.876	1.527	1.065	8.970

TABLE I.4. $(X'X)^{-1}$ for the First-Order Mixture Models Using Mass Fractions for ln(MCC-1 Elemental Releases) Fitted to the "Reduced Data" (from Table 12.3a)

	SiO_2	B_2O_3	Na_2O	Li_2O	CaO	MgO	Fe_2O_3	Al_2O_3	ZrO_2	Others
SiO_2	1.057									
B_2O_3	-0.697	3.678								
Na_2O	-0.729	0.633	3.965							
Li_2O	-1.945	0.766	2.181	19.265						
CaO	-0.542	-0.570	-0.149	1.192	10.091					
MgO	-0.622	0.290	0.077	0.930	3.122	14.334				
Fe_2O_3	-1.650	-0.014	-0.540	0.031	-0.460	-0.963	8.112			
Al_2O_3	-0.984	-1.437	-1.902	-2.790	-0.066	-0.518	4.290	7.431		
ZrO_2	-1.176	-0.734	-1.407	-1.934	0.042	-0.741	3.324	5.173	9.924	
Others	-1.509	-0.314	-0.773	-1.023	0.444	0.140	2.652	3.203	2.849	11.461

TABLE I.5. $(X'X)^{-1}$ for the First-Order Mixture Models Using Mass Fractions for ln(MCC-1 Elemental Releases) Fitted to the "Full Data" (from Table 12.2a) and for T_g (from Table 9.2)

	SiO_2	B_2O_3	Na_2O	Li_2O	CaO	MgO	Fe_2O_3	Al_2O_3	ZrO_2	Others
SiO_2	0.880									
B_2O_3	-0.763	3.055								
Na_2O	-0.874	0.552	3.654							
Li_2O	-1.828	1.146	1.989	17.861						
CaO	-0.526	-0.330	0.004	1.207	9.860					
MgO	-0.808	-0.12	0.062	1.173	2.916	12.036				
Fe_2O_3	-1.094	0.329	0.041	0.182	-0.622	-0.202	6.000			
Al_2O_3	-0.451	-0.785	-1.241	-2.801	-0.375	0.593	2.206	5.076		
ZrO_2	-0.608	-0.324	-0.755	-2.185	-0.107	0.563	1.410	2.991	7.516	
Others	-0.903	-0.146	-0.237	-1.479	0.375	0.284	0.870	1.555	1.052	9.079

TABLE I.6. $(X'X)^{-1}$ for the First-Order Mixture Model Using Mass Fractions for MCC-1 pH (from Table 12.18)

	SiO_2	B_2O_3	Na_2O	Li_2O	CaO	MgO	Fe_2O_3	Al_2O_3	ZrO_2	Others
SiO_2	0.882									
B_2O_3	-0.770	3.079								
Na_2O	-0.869	0.535	3.666							
Li_2O	-1.805	1.067	2.045	18.123						
CaO	-0.525	-0.335	0.008	1.225	9.861					
MgO	-0.778	-0.223	0.136	1.514	2.939	12.479				
Fe_2O_3	-1.113	0.393	-0.005	-0.031	-0.637	-0.478	6.170			
Al_2O_3	-0.470	-0.720	-1.288	-3.016	-0.390	0.314	2.381	5.252		
ZrO_2	-0.628	-0.253	-0.805	-2.417	-0.123	0.261	1.598	3.181	7.722	
Others	-0.888	-0.197	-0.201	-1.312	0.386	0.501	0.735	1.418	0.904	9.185

TABLE I.7. $(X'X)^{-1}$ for the First-Order Mixture Model Using Mass Fractions for Thermal Expansion of Molten Glass (from Table 10.2)

	SiO_2	B_2O_3	Na_2O	Li_2O	CaO	MgO	Fe_2O_3	Al_2O_3	ZrO_2	Others
SiO_2	0.884									
B_2O_3	-0.776	3.100								
Na_2O	-0.874	0.542	3.677							
Li_2O	-1.837	1.179	1.968	17.894						
CaO	-0.507	-0.407	0.052	1.131	10.036					
MgO	-0.803	-0.146	0.094	1.137	2.999	12.084				
Fe_2O_3	-1.110	0.381	0.035	0.216	-0.703	-0.224	6.061			
Al_2O_3	-0.454	-0.755	-1.300	-2.746	-0.501	0.511	2.225	5.224		
ZrO_2	-0.603	-0.338	-0.760	-2.190	-0.094	0.561	1.391	3.001	7.523	
Others	-0.890	-0.192	-0.231	-1.510	0.447	0.305	0.815	1.536	1.068	9.127

TABLE I.8. $(X'X)^{-1}$ for the First-Order Mixture Model Using Mass Fractions for Thermal Expansion of Solid Glass (from Table 10.2)

	SiO_2	B_2O_3	Na_2O	Li_2O	CaO	MgO	Fe_2O_3	Al_2O_3	ZrO_2	Others
SiO_2	0.890									
B_2O_3	-0.756	3.119								
Na_2O	-0.895	0.479	3.769							
Li_2O	-1.865	1.176	1.976	18.152						
CaO	-0.514	-0.402	0.098	0.982	10.105					
MgO	-0.808	-0.173	0.118	1.184	2.972	12.161				
Fe_2O_3	-1.100	0.344	0.029	0.204	-0.647	-0.214	6.002			
Al_2O_3	-0.486	-0.795	-1.222	-2.637	-0.523	0.512	2.215	5.351		
ZrO_2	-0.609	-0.329	-0.757	-2.155	-0.131	0.575	1.409	3.010	7.524	
Others	-0.931	-0.170	-0.149	-1.535	0.454	0.196	0.871	1.655	1.025	9.327

TABLE I.9. $(X'X)^{-1}$ for the First-Order Mixture Model Using Mass Fractions for Liquidus Temperature of Clinopyroxene (from Table 11.7)

	SiO_2	B_2O_3	Na_2O	Li_2O	CaO	MgO	Fe_2O_3	Al_2O_3	ZrO_2	Others
SiO_2	12.275									
B_2O_3	-7.244	39.169								
Na_2O	-5.775	2.323	51.210							
Li_2O	-25.040	59.514	20.676	297.293						
CaO	-1.204	36.715	-10.790	145.960	156.221					
MgO	-11.811	5.523	-3.520	-38.854	-17.067	122.956				
Fe_2O_3	-20.927	-4.344	-12.446	-19.180	-32.634	38.697	76.297			
Al_2O_3	-12.618	-45.500	0.935	-92.132	-89.119	25.892	58.369	135.834		
ZrO_2	-21.186	-16.462	-4.134	11.113	-14.820	-9.816	39.321	61.969	153.298	
Others	-14.211	-18.248	-32.305	-84.043	-71.182	26.738	60.805	62.869	54.480	137.199

TABLE I.10. $(X'X)^{-1}$ for the First-Order Mixture Model Using Mass Fractions for Liquidus Temperature of Spinel (from Table 11.7)

	SiO_2	B_2O_3	Na_2O	Li_2O	CaO	MgO	Fe_2O_3	Al_2O_3	ZrO_2	Others
SiO_2	15.337									
B_2O_3	2.727	50.733								
Na_2O	-7.731	2.867	34.057							
Li_2O	-45.885	-6.967	31.071	329.138						
CaO	-11.572	7.301	12.778	2.600	134.699					
MgO	-7.632	41.119	1.185	-2.932	28.470	254.933				
Fe_2O_3	-22.452	-32.992	-21.495	30.209	-16.323	-10.803	115.278			
Al_2O_3	-23.542	-62.556	-13.528	17.174	-31.903	-95.392	109.328	190.362		
ZrO_2	-34.683	-47.156	-6.867	155.712	-13.790	-86.424	75.481	115.687	270.422	
Others	-23.313	-22.247	-10.241	-24.133	51.179	36.057	33.155	43.202	9.810	157.153

TABLE I.11. $(X'X)^{-1}$ for the First-Order Mixture Model Using Mass Fractions for Liquidus Temperature of Zr-Containing Phases (from Table 11.7)

	SiO_2	B_2O_3	Na_2O	Li_2O	CaO	MgO	Fe_2O_3	Al_2O_3	ZrO_2	Others
SiO_2	24.938									
B_2O_3	-22.652	60.439								
Na_2O	0.301	24.763	70.612							
Li_2O	25.961	-11.386	14.951	308.044						
CaO	29.981	-49.383	36.517	67.424	186.396					
MgO	-11.211	-15.397	-6.595	-64.971	27.453	159.677				
Fe_2O_3	-64.602	32.207	-39.636	-94.414	-73.775	20.963	246.104			
Al_2O_3	-46.428	21.410	-52.940	-135.753	-129.957	5.105	136.969	210.061		
ZrO_2	-78.984	33.317	-78.496	-242.419	-153.374	77.633	244.126	247.826	438.622	
Others	-28.797	-14.396	-55.653	-54.161	-63.379	17.840	107.931	103.936	151.187	143.174

TABLE I.12. $\hat{\sigma}^2$ Values Corresponding to First-Order Mass Fraction Property Models

First-Order Property Model	From Table	$\hat{\sigma}^2$
ln(Viscosity at 1150°C)	7.3	0.064
ln(Electrical Conductivity at 1150°C)	8.2	0.025
ln(PCT B Release)	12.10a	0.471
ln(PCT Li Release)	12.10a	0.365
ln(PCT Na Release)	12.10a	0.352
ln(PCT Si Release)	12.10a	0.293
ln(MCC-1 B Release) "Full Data"	12.2a	0.311
ln(MCC-1 Li Release) "Full Data"	12.2a	0.307
ln(MCC-1 Na Release) "Full Data"	12.2a	0.292
ln(MCC-1 Si Release) "Full Data"	12.2a	0.198
ln(MCC-1 B Release) "Reduced Data"	12.3a	0.173
ln(MCC-1 Li Release) "Reduced Data"	12.3a	0.166
ln(MCC-1 Na Release) "Reduced Data"	12.3a	0.163
ln(MCC-1 Si Release) "Reduced Data"	12.3a	0.109
MCC-1 pH	12.18	0.087
PCT pH	12.18	0.083
Transition Temperature	9.2	127.310
Thermal Expansion of Solid Glass	10.2	0.450
Thermal Expansion of Molten Glass	10.2	198.766
Liquidus Temperature of Clinopyroxene	11.7	312.213
Liquidus Temperature of Spinel	11.7	2565.216
Liquidus Temperature of Zr-containing Phases	11.7	2667.672

I.3 MODEL UNCERTAINTY

The estimated standard deviation (due to model uncertainty) of a model prediction $\hat{y}(x) = x'\hat{\beta}$ for glass composition x, considered as a prediction of the long-term mean value, is given by:

$$SD_{m1}[\hat{y}(x)] = [x'(X'X)^{-1}x]^{0.5}\,\hat{\sigma}\ . \tag{I.5}$$

The estimated standard deviation (due to model uncertainty) of a model prediction $\hat{y}(x) = x'\hat{\beta}$ for glass composition x, considered as a prediction of the mean of k observations, is given by:

$$SD_{m2}[\hat{y}(x)] = [1/k + x'(X'X)^{-1}x]^{0.5}\,\hat{\sigma}\ . \tag{I.6}$$

The estimated standard deviation (due to model uncertainty) of a model prediction $\hat{y}(x) = x'\hat{\beta}$ for glass composition x, considered as a prediction of an individual observation, is given by:

$$SD_{m3}[\hat{y}(x)] = [1 + x'(X'X)^{-1}x]^{0.5}\,\hat{\sigma}\ . \tag{I.7}$$

Note that equation (I.7) is a special case of (I.6) when k = 1. Under the assumption that the model does not have a statistically significant lack-of-fit, the square root of the error mean square given in Equation (I.4) can be used as the estimate $\hat{\sigma}$ in (I.5), (I.6), and (I.7).

An equation for propagating glass composition uncertainty through a model linear in its coefficients is given in Section I.5. Combining model and composition uncertainties is discussed at the end of Section I.5.

I.4 STATISTICAL INTERVALS AND BANDS

Three basic types of statistical statements can be made about glass property model predictions: confidence intervals, prediction intervals, and tolerance intervals. A confidence interval is a statement about the mean property value for a given point (composition), a prediction interval is a statement about a single property value for a given point (composition), while

a tolerance interval is a statement about a specified proportion of the distribution of property values for a given point (composition). Confidence, prediction, and tolerance intervals can be one-sided lower, one-sided upper, or two-sided.

Each of the three basic types of statements can be made about one point (composition) at a time, or about all possible points (compositions) simultaneously. In the simultaneous cases, the statements are referred to as simultaneous confidence intervals (sometimes referred to as confidence bands), simultaneous prediction intervals (sometimes referred to as prediction bands), and simultaneous tolerance intervals (sometimes referred to as tolerance bands).

Equations for one-sided lower, one-sided upper, and two-sided statistical confidence, prediction, and tolerance intervals and bands (simultaneous intervals) for predictions made with fitted glass property models are presented in this section. Intervals for model predictions at a single point (composition) are presented in Section I.4.1, while simultaneous intervals (bands) for model predictions at many points (compositions) are presented in Section I.4.2.

I.4.1 Intervals for Predictions at Single Points

Confidence, prediction, and tolerance intervals for model predictions made at single points (compositions) are discussed in this section.

Confidence Intervals

A one-sided upper $(1-\alpha)100\%$ confidence interval for the mean property value at a single composition x is given by

$$\hat{y}(x) + t_{1-\alpha}(n-p) * SD_{ml}[\hat{y}(x)] \qquad (I.8a)$$

where $t_{1-\alpha}(n-p)$ is the $(1-\alpha)100$-th percentile of a t-distribution with n-p degrees of freedom [the point below which $(1-\alpha)100\%$ of the distribution falls] and $SD_{ml}[\hat{y}(x)]$ is given in (I.5). As indicated in Section I.1, n is the number of points used to fit the model and p is the number of terms in the model.

A one-sided lower $(1-\alpha)100\%$ confidence interval for the mean property value at a single composition x is given by

$$\hat{y}(x) - t_{1-\alpha}(n-p) * SD_{m1}[\hat{y}(x)] \tag{I.8b}$$

where $t_{1-\alpha}(n-p)$ is as defined in the previous paragraph and $SD_{m1}[\hat{y}(x)]$ is given in (I.5).

A two-sided $(1-\alpha)100\%$ confidence interval for the mean property value at a single composition x is given by

$$\hat{y}(x) \pm t_{1-\alpha/2}(n-p) * SD_{m1}[\hat{y}(x)] \tag{I.8c}$$

where $t_{1-\alpha/2}(n-p)$ is the $(1-\alpha/2)100$-th percentile of a t-distribution with n-p degrees of freedom [the point below which $(1-\alpha/2)100\%$ of the distribution falls] and $SD_{m1}[\hat{y}(x)]$ is given in (I.5).

Confidence intervals for a mean of k results instead of a long-term mean can be obtained by substituting SD_{m2} [from (I.6)] for SD_{m1} in (I.8a), (I.8b), or (I.8c) above.

Prediction Intervals

A one-sided upper $(1-\alpha)100\%$ prediction interval for an individual property value at a single composition x is given by

$$\hat{y}(x) + t_{1-\alpha}(n-p) * SD_{m3}[\hat{y}(x)] \tag{I.9a}$$

where $t_{1-\alpha}(n-p)$ is the $(1-\alpha)100$-th percentile of a t-distribution with n-p degrees of freedom [the point below which $(1-\alpha)100\%$ of the distribution falls] and $SD_{m3}[\hat{y}(x)]$ is given in (I.7).

A one-sided lower $(1-\alpha)100\%$ prediction interval for an individual property value at a single composition x is given by

$$\hat{y}(x) - t_{1-\alpha}(n-p) * SD_{m3}[\hat{y}(x)] \tag{I.9b}$$

where $t_{1-\alpha}(n-p)$ is as defined previously and $SD_{m3}[\hat{y}(x)]$ is given in (I.7).

A two-sided $(1-\alpha)100\%$ prediction interval for an individual property value at a single composition x is given by

$$\hat{y}(x) \pm t_{1-\alpha/2}(n-p) * SD_{m3}[\hat{y}(x)] \tag{I.9c}$$

where $t_{1-\alpha/2}(n-p)$ is the $(1-\alpha/2)100$-th percentile of a t-distribution with n-p degrees of freedom [the point below which $(1-\alpha/2)100\%$ of the distribution falls] and $SD_{m3}[\hat{y}(x)]$ is given in (I.7).

Note that the only difference between the confidence intervals in (I.8) and the prediction intervals in (I.9) is the use of SD_{m1} in the former and SD_{m3} in the latter.

Tolerance Intervals

A one-sided upper Q%/P% tolerance interval is a Q% confidence statement about the P-th percentile (P > 50) of the distribution of property values y(x) at a single composition x. It is obtained using the model prediction $\hat{y}(x)$ at x and the uncertainty of the prediction, and is given by

$$\hat{y}(x) + t_{1-\alpha}(n-p,\delta) * SD_{m1}[\hat{y}(x)] \tag{I.10a}$$

where $Q = (1 - \alpha)100$, $t_{1-\alpha}(n-p,\delta)$ is the $(1-\alpha)100$-th percentile of the noncentral t-distribution with n-p degrees of freedom and noncentrality parameter $\delta = N_p\hat{\sigma}/SD_{m1}[\hat{y}(x)]$, $SD_{m1}[\hat{y}(x)]$ is given in (I.5), and N_p is the P-th percentile of a standard normal distribution (see Graybill 1976, pp. 270-275, although the notation used here is different than that of Graybill's).

A one-sided lower Q%/P% tolerance interval is a Q% confidence statement about the P-th percentile (P < 50) of the distribution of property values y(x) at a single composition x, and is given by

$$\hat{y}(x) - t_{1-\alpha}(n-p,\delta) * SD_{m1}[\hat{y}(x)] \tag{I.10b}$$

where $t_{1-\alpha}(n-p,\delta)$ is as previously defined and $SD_{m1}[\hat{y}(x)]$ is given in (I.5).

A two-sided Q%/P% tolerance interval is a Q% confidence statement about the middle P-th percent of the distribution of property values y(x) at a single composition x, and is given by

$$\hat{y}(x) \pm t_{1-\alpha/2}(n-p,\delta) * SD_{m1}[\hat{y}(x)] \qquad (I.10c)$$

where $t_{1-\alpha/2}(n-p,\delta)$ is the $(1-\alpha/2)100$-th percentile of the noncentral t-distribution with n-p degrees of freedom and noncentrality parameter $\delta = N_p\hat{\sigma}/SD_{m1}[\hat{y}(x)]$, $SD_{m1}[\hat{y}(x)]$ is given in (I.5), and N_p is the P-th percentile of a standard normal distribution.

I.4.2 Simultaneous Intervals (Bands) for Predictions at Many Points

Confidence, prediction, and tolerance simultaneous intervals (bands) for model predictions made at many points (compositions) are discussed in this section.

Simultaneous Confidence Intervals (Bands)

A one-sided upper $(1-\alpha)100\%$ confidence band for the mean property values at all compositions x is given by

$$\hat{y}(x) + [p\ F_{2\alpha}(p,n-p)]^{0.5} * SD_{m1}[\hat{y}(x)] \qquad (I.11a)$$

where $F_{2\alpha}(p,n-p)$ is the $(2\alpha)100$-th percentile of a F-distribution with p and n-p degrees of freedom [the point below which $(2\alpha)100\%$ of the distribution falls] and $SD_{m1}[\hat{y}(x)]$ is given in (I.5). As indicated in Section I.1, n is the number of points used to fit the model and p is the number of terms in the model.

A one-sided lower $(1-\alpha)100\%$ confidence band for the mean property values at all compositions x is given by

$$\hat{y}(x) - [p\ F_{2\alpha}(p,n-p)]^{0.5} * SD_{m1}[\hat{y}(x)] \qquad (I.11b)$$

where $F_{2\alpha}(p,n-p)$ is as defined in the previous paragraph and $SD_{m1}[\hat{y}(x)]$ is given in (I.5).

A two-sided $(1-\alpha)100\%$ confidence band for the mean property values at all compositions x is given by

$$\hat{y}(x) \pm [p\ F_{1-\alpha}(p,n-p)]^{0.5} * SD_{m1}[\hat{y}(x)] \qquad (I.11c)$$

where $F_{1-\alpha}(p,n-p)$ is the $(1-\alpha)100$-th percentile of a F-distribution with p and n-p degrees of freedom [the point below which $(1-\alpha)100\%$ of the distribution falls] and $SD_{m1}[\hat{y}(x)]$ is given in (I.5).

Confidence bands for the mean property values over k results (instead of a long-term mean) for all compositions x can be obtained by substituting SD_{m2} [from (I.6)] for SD_{m1} in (I.11a), (I.11b), or (I.11c) above.

Simultaneous Prediction Intervals (Bands)

A one-sided upper $(1-\alpha)100\%$ prediction band for individual property values at all compositions x is given by

$$\hat{y}(x) + [p\ F_{1-\alpha/2}(p,n-p)]^{0.5} * SD_{m3}[\hat{y}(x)] \qquad (I.12a)$$

where $F_{1-\alpha/2}(p,n-p)$ is the $(1-\alpha/2)100$-th percentile of a F-distribution with p and n-p degrees of freedom [the point below which $(1-\alpha/2)100\%$ of the distribution falls] and $SD_{m3}[\hat{y}(x)]$ is given in (I.7).

A one-sided lower $(1-\alpha)100\%$ prediction band for individual property values at all compositions x is given by

$$\hat{y}(x) - [p\ F_{1-\alpha/2}(p,n-p)]^{0.5} * SD_{m3}[\hat{y}(x)] \qquad (I.12b)$$

where $F_{1-\alpha/2}(p,n-p)$ is as defined in the previous paragraph and $SD_{m3}[\hat{y}(x)]$ is given in (I.7).

A two-sided $(1-\alpha)100\%$ prediction band for individual property values at all compositions x is given by

$$\hat{y}(x) \pm [p\ F_{1-\alpha}(p,n-p)]^{0.5} * SD_{m3}[\hat{y}(x)] \qquad (I.12c)$$

where $F_{1-\alpha}(p,n-p)$ is the $(1-\alpha)100$-th percentile of a F-distribution with p and n-p degrees of freedom [the point below which $(1-\alpha)100\%$ of the distribution

falls] and $SD_{m3}[\hat{y}(x)]$ is given in (I.7).

Note that the only difference between the confidence bands in (I.11) and the prediction bands in (I.12) is the use of SD_{m1} in the former and SD_{m3} in the latter.

Simultaneous Tolerance Intervals (Bands)

The formulas for simultaneous tolerance intervals (bands) are quite complicated and no need is envisioned for them at this time in CVS or in a high-level waste vitrification plant. The interested reader is referred to Miller (1981, pp. 123-125).

I.5 COMPOSITION UNCERTAINTY

Assume that a glass composition is estimated with covariance matrix Λ^{-1}. The standard deviation of the predicted property value due to uncertainty in composition x is given by:

$$SD_c[x'\hat{\beta}] = [\hat{\beta}' \Lambda^{-1} \hat{\beta}]^{0.5} \qquad (I.13)$$

This equation is very general, and assumes that any effective reduction in variability/uncertainty obtained by averaging results from replicate samples or replicate analyses is included in the covariance matrix. Further, (I.13) is general in that the covariance matrix Λ^{-1} might be for one source of variation (e.g., batch-to-batch variation, sampling/inhomogeneity uncertainty, or analytical uncertainty) or for several sources of variation combined.

The total standard deviation due to model uncertainty and composition uncertainty can be obtained by squaring, adding, and then taking the square root of the two separate standard deviations [that is, (I.13) and the appropriate one of (I.5), (I.6), or (I.7)].

Estimating composition covariance matrices and propagating them through the CVS glass property models is not within the CVS work scope, and so this topic is not discussed further or illustrated here. Such activities fall under the Process and Product Model Development activity of the PVTD project.

The statistical intervals discussed in Section I.4 can be adapted to handle composition uncertainty or composition and model uncertainty combined. However, a discussion of the formulas for such adapted statistical intervals is beyond the scope of this report.

APPENDIX J

QUALITY ASSURANCE

APPENDIX J

QUALITY ASSURANCE

J.1 DATA QUALITY ASSURANCE

All testing that generated licensing-related data described in this report was conducted under Quality Assurance (QA) requirements commensurate with other licensing-related programs conducted at PNL. These general requirements are described in PNL-MA-70 (PNL 1989) under QA Impact Level I and supplemental controls for DOE/RW-0214 (DOE 1990). Specific QA requirements applicable to this work are defined in the PNL Vitrification Technology Development (PVTD) project QA plan WTC-006. Testing was conducted so that all instrument calibrations and materials were traceable, test procedures and associated training activities were documented in detail, and test methods complied with the above noted QA program requirements. Glasses were archived in compliance with conditions specified by DOE/RW-0214 as implemented in procedure PHTD-PSP-801-S.

The laboratory record books used for CVS are BNW-51795 (labeled "HWVP-89-1"), BNW-53669 (labeled "HWVP-90-1"), BNW-53990 (labeled "HWVP-91"), BNW-53973 (labeled "CVS2-Special"), BNW-54448 (labeled "HWVP-92-93"), BNW-54449 (labeled "CVS XRD and SEM Analyses"), BNW-55078 (labeled "HWVP-93-1"), and BNW-55079 (labeled "HWVP-93-94").

J.2 SOFTWARE QUALITY ASSURANCE

PNL-MA-70 Impact Level I QA Software Control Procedures (SCPs) are the applicable software control procedures for: (1) software used to generate experimental designs (test matrices) for the various phases of CVS-I and CVS-II, and (2) statistical data analysis and other software used to analyze data and fit empirical property models. Supplemental procedures PHTD-PSP-SCP-1 through PHTD-PSP-SCP-5 address additional DOE/RW-0214 requirements beyond PNL-MA-70, but these do not apply to the statistical and other software being used in CVS. Specifically, statistical experimental design and data analysis

work for CVS uses software in the "system maintained" and "support" software categories of PNL-MA-70. DOE/RW-0214 addresses only the development of "engineering/scientific" software, the third category of software covered by PNL-MA-70. DOE/RW-0214 has additional requirements beyond PNL-MA-70 for the "engineering/scientific" category of software, but does not address at all the other two classes of software. Hence, PNL-MA-70 Level I software control procedures are applicable for all statistical experimental design and data analysis software runs leading to reportable results.

Because of the large number of experimental design and data analysis results (contained in tables and figures) in this report, it was decided (by a team of technical staff and quality engineers) that the PNL-MA-70 requirements need not be satisfied for all results. Rather, it was decided to classify results as "verification required" and "no verification required". The following descriptions clarify the "verification required" and "no verification required" classes of results.

Verification Required--This class of results includes those that have been determined to be of primary importance and are most likely to be directly used to make decisions or guide work for high-level waste vitrification. Specific examples are the test matrices (how they were selected) for the various CVS phases, and the regression modeling efforts that produce property prediction equations that will be used to formulate glass and frit compositions, direct future work, and help operate/control the eventual HLW vitrification plant.

No Verification Required--This class of results includes those that are reported, but are not of primary importance, will not be directly used to make decisions or guide high-level waste vitrification work, or are easily reproduced. Specific examples are: (1) plots of data, (2) plots developed from property models such as property model predicted versus measured plots or component effects plots which display results of predictions made with glass property models, (3) comparisons of CVS property models to those developed at other sites which do not perform as well and will not be used for CVS or high-level waste vitrification

purposes, (4) preliminary model validation exercises to assess how well our glass property models predict for data not used to develop them.

Nearly all statistical experimental design, modeling, and other data analysis results are from commercial software with predetermined calculations and output formats. Hence, the software control requirements for the "verification required" class essentially consist of documenting the software used, compiling an application package of inputs and outputs, and performing an independent technical review to serve as verification/validation. The associated paperwork is a part of formal project records.

The "No Verification Required" classification of results is justified because: (1) such results are either not primary results or are only for general information and understanding, (2) little chance exists of making errors that are not detected due to the substantial use of commercial statistical software with predetermined calculations and output formats, (3) such results can reasonably be reproduced given data in the report and primary results (such as glass property models) for which the SCP documentation will be completed, and (4) the report is independently reviewed prior to issue.

Table J.1 lists the results in this report classified as "verification required". Table J.2 lists the "no verification required" results organized under general rationales for the classification. Because results are presented in tables and figures in this report, table and figure numbers are used in Tables J.1 and J.2 to classify the results.

Because Tables J.1 and J.2 are from the perspective of QA requirements (primarily Software Control Procedure requirements) for the experimental design and data analysis aspects of CVS, the data themselves are listed as not requiring verification under SCPs. All data were collected following the appropriate QA requirements (see Section J.1). Hence, the QA requirements for experimental design, data collection, and data analysis are all satisfied.

TABLE J.1. Design and Analysis Results That Require QA SCP Verification

Chapter	Table Numbers	Figure Numbers
1	None	None
2	None	None
3	None	None
4	4.4, 4.7, 4.9, 4.12, 4.14, 4.15	None
5	None	None
6	None	None
7	7.1a to 7.4, 7.10	None
8	8.1a to 8.3	None
9	9.2, 9.3	None
10	10.2 to 10.4	None
11	11.7, 11.13	None
12	12.2a to 12.7, 12.10a to 12.14, 12.18	None
13	None	None
14	None	None
15	15.1	None
16	None	None
APP A	None	None
APP B	B.2	None
APP C	C.3	None
APP D	D.3, D.4	None
APP E	None	None
APP F	F.4 to F.8	None
APP G	None	None
APP H	None	None
APP I	I.1 to I.12	None
APP J	None	None
APP K	None	None

TABLE J.2. Design and Analysis Results That Do Not Require QA SCP Verification, Organized by Reason Why

1. Inputs or Starting Information--QA Not Applicable

Table Numbers: 3.1, 4.1 to 4.3, 4.6, 4.10, 4.11, 5.1, 6.1, 11.2, 14.1, 14.2

2. Data Listings--No Experimental Design or Data Analysis Involved

Table Numbers: 4.8, 4.13, 9.1, 10.1, 11.1 to 11.6, 12.1, 12.9, 12.23, 13.3 to 13.6, 13.8, A.1 to A.3, A.11, A.12, B.1, C.1, C.2, D.1, D.2, D.5, E.1, F.1 to F.3, G.3 to G.5, H.1

3. Results That Are Easily Reproduced

Table Numbers: 13.7, 4.17 to 4.18

Figure Numbers: 7.1a to 7.3b, 7.5, 7.14a, 7.14b, 7.16, 7.17, 8.1a to 8.2b, 8.4, 8.10, 9.1a, 9.1b, 9.3, 9.11, 9.12, 10.1a to 10.2b, 10.5 to 10.7, 11.7 to 11.14, 12.1a to 12.2b, 12.4, 12.7a, 12.7b, 12.9, 12.12a to 12.14b, 12.17, 12.18, 12.20 to 12.27, 12.32 to 12.34

4. Results Used for Understanding and Informational Purposes

Table Numbers: 4.5, 4.16, 7.5 to 7.9, 8.4, 9.4, 12.8, 12.15 to 12.17, 12.19 to 12.22, 13.1, 13.2, A.4 to A.10, G.1, G.2

Figure Numbers: 7.4, 7.6 to 7.13, 7.15, 8.3, 8.5 to 8.9, 9.2, 9.4 to 9.10c, 10.3, 10.4, 11.1 to 11.6, 11.15 to 11.17, 12.3, 12.5 to 12.6c, 12.8, 12.10 to 12.11c, 12.15, 12.16, 12.19, 12.28 to 12.31, 13.1 to 13.4, H.1 to H.4

5. Preliminary Results for Which Verification is Premature

Table Numbers: 11.8 to 11.11, 14.3 to 14.7

Figure Numbers: 11.18 to 11.22, 14.1, 14.2

J.3 REPORT QUALITY ASSURANCE

A draft version of this report was formally reviewed and commented on by Westinghouse Hanford Company, two staff of the Technology Development Program Office, and a PNL staff member. Both materials science and statistics disciplines were represented among the reviewers. The DOE Richland Field Office also reviewed the report, but had no comments. All formal comments (and many informal ones) were responded to and corresponding revisions made to the report to yield the final version. The formal comments and responses are documented in project records.

APPENDIX K

ACRONYMS, TERMS, SYMBOLS, AND ABBREVIATIONS

APPENDIX K

ACRONYMS, TERMS, SYMBOLS, AND ABBREVIATIONS

The following is a list of acronyms, terms, symbols, and abbreviations and their definitions or explanations.

ACRONYMS, ABBREVIATIONS, TERMS, AND SYMBOLS

Acronyms, Abbreviations, Terms and Symbols	Meaning
α_m	Coefficient of thermal expansion for molten glass in units of 10^{-6}/K.
α_s	Coefficient of thermal expansion for solid glass in units of 10^{-6}/K.
ϵ_{1150}	Electrical conductivity at 1150°C in units of S/m.
η_{1150}	Viscosity at 1150°C in units of Pa·s.
ϱ	Glass density.
$(a_B)_i$	Coefficient of the i-th component in the first-order mixture model for normalized B release. Can be either PCT or MCC-1 dissolution test.
$(a_{Si})_i$	Coefficient of the i-th component in the first-order mixture model for normalized Si release. Can be either PCT or MCC-1 dissolution test.
Accurate, Accuracy	Closeness of agreement between an estimated or measured value of a quantity and the true value (or an accepted reference value) for the quantity.
Amorphous phase separation	The separation of a homogeneous liquid into one or more liquid phases upon cooling.
ANL	Argonne National Laboratory.
A/V	Surface area to volume ratio used in dissolution testing of glass samples.
BET	Brunauer-Emmett-Teller.
Bias	A systematic (i.e., not random) difference between an estimated or measured value of a quantity and the true value (or an accepted reference value) for the quantity.

Acronyms, Abbreviations, Terms and Symbols	Meaning
CC	Complexant Concentrate. One of the four major waste types from double shell tanks at Hanford.
CCC	Canister Centerline Cooling.
CELS	Corning Engineering Laboratory Services.
Coefficient of Variation	A percentage measure of the standard deviation of a set of data relative to its mean [CV=100(standard deviation/mean)].
Confidence Interval	An interval that captures a single fixed true value (e.g., the mean of a population) with specified confidence (e.g., 95%). A specific confidence interval either does or does not capture the single fixed true value (i.e., the probability is zero or one). Thus, confidence refers not to whether a specific confidence interval captures the value, but the percentage of times the procedure would yield a specific confidence interval that captures the single fixed true value if applied many times.
Confidence Band	A collection of simultaneous confidence intervals that captures many fixed true values with specified confidence (e.g., 95%). The confidence is that all intervals simultaneously capture their corresponding fixed true values. A specific confidence band either does or does not capture all fixed true values intended to be captured (i.e., the probability is zero or one). Thus, confidence refers not to whether a specific confidence band captures all fixed true values, but the percentage of times the procedure would yield a specific confidence band that captures all fixed true values if applied many times.

Acronyms, Abbreviations, Terms and Symbols	Meaning
Confounded	Two variables (glass components in this report) are said to be confounded when they are highly correlated, such that it is difficult or impossible to separate the effect of varying one from the effect of varying the other. The experimental strategy of replacing one component with another (this strategy was not used in CVS) leaves the effects of the two components completely confounded.
Covariance matrix	A representation of the uncertainties and interrelationships between individual quantities that make up a multivariate datum. A covariance matrix is symmetric with variance of the individual quantities on the diagonal and the pairwise covariances in the off diagonal positions. In this report, we primarily encounter covariance matrices of estimated coefficient vectors corresponding to glass property models fitted to experimental data.
Cross-Product Terms	Terms of the form $x_i x_j$ in second-order mixture models.
CVS	Composition Variation Study. The two major parts of the study are CVS-I and CVS-II. CVS-II was performed in four phases, referred to as CVS-II Phases 1, 2, 3, and 4.
DBT	Dissolving boundary temperature.
Degrees of Freedom	The number of independent pieces of information used to compute a sum of squares or variance. Denoted by df or DF.
Disilicates	Double island silicates.
DOE	Department of Energy.
DST	Double Shell Tanks.

Acronyms, Abbreviations, Terms and Symbols	Meaning
Durability Risers	Components that increase durability.
Durability Reducers	Components that decrease durability.
DWPF	Defense Waste Processing Facility.
EA glass	The DWPF Environmental Assessment glass.
EDS	Energy Dispersion Spectroscopy.
Experimental region	The portion of glass composition space explored in CVS experimental work.
F Value	In general, the value of a statistical hypothesis test based on the F-distribution. In this report F = Model Mean Square/Error Mean Square, which tests whether a significant portion of the data variation for a glass property is accounted for by the fitted model.
HLW	High Level Waste.
HWVP	Hanford Waste Vitrification Plant. This was the name of the originally planned Hanford HLW vitrification plant, but a subsequent change in plans scrapped this name. A new name for the eventual Hanford HLW vitrification plant has not yet been selected.
ICP	Inductively Coupled Plasma Spectroscopy.
Ill-Conditioning	Instability in the numerical estimation of model coefficients via least square regression.
Immiscibility dome	A compositional region in which amorphous phase separation is thermodynamically favorable.
Lithium-depleted depth	Denoted by $\delta=(r_{Li} - r_B)/\varrho$.

Acronyms, Abbreviations, Terms and Symbols	Meaning
LOF	Lack of Fit. A statistical test for lack-of-fit checks whether the differences between measured and predicted property values from a fitted model are larger than expected based on the experimental and measurement uncertainty in the data. If the predicted versus measured differences are larger than data uncertainty at a high enough statistical confidence (e.g., greater than 90%), the model is said to have a statistically significant lack-of-fit.
Long-term uncertainties	Experimental or analytical uncertainties that occur in replicate results obtained over a longer period of time (e.g., over several days, weeks, or months).
$M_1M_2[Si_2O_6]$	Generalized chemical composition of clinopyroxenes, where M_1 represents Na, Ca, or Li and M_2 represents Al, Fe, Cr or Mg.
MCC	Materials Characterization Center.
MCC-1	A durability test developed by the Materials Characterization Center in which a small monolith of glass is leached for 28 days in deionized water at 90°C.
Mean Square	Sum of squares/degrees of freedom (SS/df). Denoted by MS.
MFT	Melter Feed Tank.
M&TE	Measurement and Test Equipment.
Multicollinearity	Approximate linear relationships exist between the terms in the model being considered.
NCAW	Neutralized Current Acid Waste. One of the four major waste types from double shell tanks at Hanford.

Acronyms, Abbreviations, Terms and Symbols	Meaning
NCRW	Neutralized Cladding Removal Waste. One of the four major waste types from double shell tanks at Hanford.
NO_x	Nitrous Oxide.
OED	Optimal Experimental Design.
Orthosilicates	Island silicates.
PACR	Predicted Acceptable Composition Region. The subregion of composition space explored during CVS within which compositions are predicted to have property values within specified limits. The uncertainty in the models used to predict property values is not accounted for.
PCT	Product Consistency Test. A durability test in which crushed glass is leached for 7 days in deionized water at 90°C.
Pearson Correlation Coefficient	Indicator of the strength of the linear relationship between a pair of variables. Takes values between -1.0 and +1.0, where values of -1 and +1 denote perfect linear relationships with negative and positive slopes respectively, and a value of 0 denotes complete lack of a linear relationship.
PFP	Plutonium Finishing Plant. One of the four major waste types from double shell tanks at Hanford.
PNL	Pacific Northwest Laboratory.
Precise, Precision	Closeness of agreement between test results, measurements, or estimates of a quantity obtained under similar conditions. There is no such thing as the precision of a test, measurement, or estimation method--a separate precision statement will apply to each combination of sources of variability included in the set of similar conditions.

Acronyms, Abbreviations, Terms and Symbols	Meaning
Prediction Interval	An interval that captures a single random true value (e.g., an individual from a population) with specified confidence (e.g., 95%). A specific prediction interval either does or does not capture the single random true value (i.e., the probability is zero or one). Thus, confidence refers not to whether a specific prediction interval captures the value, but the percentage of times the procedure would yield a specific prediction interval that captures the single random true value if applied many times.
Prediction Band	A collection of simultaneous prediction intervals that captures many random true values with specified confidence (e.g., 95%). The confidence is that all intervals simultaneously capture their corresponding random true values. A specific prediction band either does or does not capture all fixed true values intended to be captured (i.e., the probability is zero or one). Thus, confidence refers not to whether a specific prediction band captures all random true values, but the percentage of times the procedure would yield a specific prediction band that captures all random true values if applied many times.
PRESS	Predicted Residual Sum of Squares.
Prob > F	Probability of seeing an F-distribution value larger than the test statistic calculated. In this report, the notation occurs in software output related to fitting property models, and involves testing whether the model does not account for a significant portion of the variability in the data.

Acronyms, Abbreviations, Terms and Symbols	Meaning
Prob > |T|	Probability of seeing an t-distribution value larger than the absolute value of the test statistic calculated. In this report, the notation occurs in software output related to testing the significance of fitted property model coefficients. In that context, it is the probability that the coefficient is not significantly different than zero.
PVTD	PNL Vitrification Technology Development.
QA	Quality Assurance.
QCR	Qualified Composition Region. The subregion of composition space explored during CVS within which compositions are predicted to have property values within specified limits, after accounting for uncertainty in the models used to predict property values.
R^2	Fraction of variability in the property data accounted for by a fitted model.
R^2(ADJ)	Fraction of variability in the property data accounted for by a fitted model, adjusted for the number of parameters and number of data points used in fitting the model.
R^2(PRESS)	Fraction of variability in the property data accounted for by a fitted model, where each data point is "left out of the fit" in evaluating how well the model predicts the property for that data point.
R^2(VAL)	Fraction of variability in a set of property data not used to fit the model (i.e., a validation set of data) accounted for by a fitted model.
r_B	Normalized boron release in units of g/m^2.
r_{Li}	Normalized lithium release in units of g/m^2.
r_{Si}	Normalized silicon release in units of g/m^2.

ACRONYMS, ABBREVIATIONS, TERMS, AND SYMBOLS (continued)

Acronyms, Abbreviations, Terms and Symbols	Meaning
Redox	Reduction-oxidation state of a glass, indicated by Fe^{2+}/Fe.
Root Mean Square Error	Square root of the Mean Square Error. Denoted by √MSE.
RSD (%RSD)	Relative Standard Deviation (RSD=SD/Mean) and Percent Relative Standard Deviation (%RSD=100*SD/Mean).
SCP	Software Control Procedures.
SD	Standard Deviation.
Short-term uncertainties	Experimental or analytical uncertainties that occur in replicate results obtained at the same time or within a short period of time.
SEM	Scanning Electron Microscopy.
SME	Slurry Mix Evaporator.
Spinel	One of the major crystalline phases identified during the study.
Squared Terms	Terms of the form x_i^2 that can occur in "less than complete" versions of second-order mixture models.
SRTC	Savannah River Technology Center.
SST	Single Shell Tanks.
Sum of Squares	A general statistical term usually referring to a sum of squared differences (e.g., differences between measured and model predicted glass property values).
T	Temperature in °C or K, where the units will be made clear where the abbreviation is used.
TEM	Transmission Electron Microscopy.

Acronyms, Abbreviations, Terms and Symbols	Meaning
T_0	Temperature at which viscosity approaches infinity and thus glass becomes purely elastic.
T_g	Glass transition temperature.
T_L	Glass liquidus temperature.
TOC	Total Organic Carbon.
Tolerance Interval	An interval that captures a predefined proportion of a single population with specified confidence (e.g., 95%). A specific tolerance interval either does or does not capture the predefined proportion of the single population (i.e., the probability is zero or one). Thus, confidence refers not to whether a specific tolerance interval captures the proportion of the population, but the percentage of times the procedure would yield a specific tolerance interval that captures the proportion of the population if applied many times.
Tolerance Band	A collection of simultaneous tolerance intervals that captures predefined proportions of many populations with specified confidence (e.g., 95%). The confidence is that all tolerance intervals simultaneously capture the corresponding proportions of the populations. A specific tolerance band either does or does not capture the proportions of all populations intended to be captured (i.e., the probability is zero or one). Thus, confidence refers not to whether a specific tolerance band captures all predefined proportions of populations, but the percentage of times the procedure would yield a specific tolerance band that captures all predefined proportions of populations if applied many times.

ACRONYMS, ABBREVIATIONS, TERMS, AND SYMBOLS (continued)

Acronyms, Abbreviations, Terms and Symbols	Meaning
TPA	Tri-Party Agreement. An agreement among the U.S. Department of Energy, the U.S. Environmental Protection Agency, and the state of Washington that governs the cleanup of the Hanford site.
TRUEX	Transuranic Extraction.
TTT	Time-Temperature Transformation.
t-value	Calculated value of a t-statistic. In this report calculated t-values are used to test whether a coefficient in a glass property model is statistically different from 0.
TWEAT	Ternary Waste Envelope Assessment Tool.
Vertices	The "corner points" of a glass composition region defined by lower and upper bounds on glass components or linear combinations of glass components. Such points are the most extreme compositions that satisfy all of the constraints defining the glass composition region.
WAPS	Waste Acceptance Product Specifications.
WFQ	Waste Form Qualification.
WVDP	West Valley Demonstration Project.
XRD	X-ray Diffraction.
$\bar{y}$	Average of n measured property values y_i.
$\hat{y}_{(i)}$	Predicted property value for the ith data point made using a model fitted to all data points except the ith.
y_i	Measured property value for the ith data point.

Acronyms, Abbreviations, Terms and Symbols	Meaning
y_i	Predicted property value for the ith data point made using a model fitted to all data points.

DISTRIBUTION

No. of
Copies

OFFSITE

12 DOE/Office of Scientific and Technical Information

S. M. Barnes
West Valley Nuclear Services
P. O. Box 191
West Valley, NY 14171

J. K. Bates
Argonne National Laboratory
9700 S. Cass Avenue
Argonne, IL 60439-4837

S. O. Bates
EG&G Idaho, Inc.
812 Dickson
Idaho Falls, ID 83402

N. E. Bibler
Westinghouse Savannah River Co.
P.O. Box 616
Aiken, SC 29802

D. F. Bickford
Westinghouse Savannah River Co.
P.O. Box 616
Aiken, SC 29802

R. R. Borisch
West Valley Nuclear Services
P. O. Box 191
West Valley, NY 14171

H. Brandt
DOE Savannah River Operations
P.O. Box A
Aiken, SC 29801

No. of
Copies

K. G. Brown
Westinghouse Savannah River Co.
P.O. Box 616
Aiken, SC 29802

L. H. Cadoff
West Valley Nuclear Services
P. O. Box 191
West Valley, NY 14171

K. A. Chacey, EM-361
DOE Office of Environmental Management
19901 Germantown Road
Germantown, MD 20585

D. Clark
University of Florida
Advanced Materials Research
One Progress Blvd. #14
Alachua, FL 32615

J. A. Colemen, EM-35
DOE Office of Environmental Management
19901 Germantown Road
Germantown, MD 20585

C. R. Cooley, EM-55
DOE Office of Environmental Management
19901 Germantown Road
Germantown, MD 20585

A. R. Cooper
Case Western Reserve Univ.
Dept. Materials Science & Eng.
10900 Euclid Avenue
Cleveland, OH 44106

No. of
Copies

S. Cowan, EM-30
DOE Office of Environmental
Management
19901 Germantown Road
Germantown, MD 20585

D. E. Day
Univertiy of Missouri-Rolla
Materials Research Center
Rolla, MO 65401

I. J. Dempster
West Valley Nuclear Services
P. O. Box 191
West Valley, NY 14171

R. H. Doremus
Rensselaer Polytechnic Inst.
Materials Engineering Dept.
Troy, NY 12180-3950

D. Dreyfus, RW-1
DPE Office of Civilian
Radioactive Waste Management
1000 Independence Ave. S.W.
Washington, D.C. 20585

A. Drobot
West Valley Nuclear Services
P. O. Box 191
West Valley, NY 14171

W. Ebert
Argonne National Laboratory
9700 S. Cass Avenue
Argonne, IL 60439-4837

T. B. Edwards
Westinghouse Savannah River Co.
P.O. Box 616
Aiken, SC 29802

No. of
Copies

J. J. Einerson
EG&G Idaho, Inc.
2525 Fremont Avenue
Idaho Falls, ID 83415

A. Ellison
Argonne National Laboratory
9700 S. Cass Avenue
Argonne, IL 60439-4837

R. E. Ewing
University of New Mexico
Albuquerque, NM 87131

J. J. Fiore, EM-423
DOE Office of Environmental
Management
19901 Germantown Road
Germantown, MD 20585

C. Frank, EM-50
DOE Office of Environmental
Management
19901 Germantown Road
Germantown, MD 20585

M. Frei, EM-34
DOE Office of Environmental
Management
19901 Germantown Road
Germantown, MD 20585

T. Grumbly, EM-1
Assistant Secretary
DOE Office of Environmental
Management
1000 Independence Ave. S.W.
Washington, D.C. 20585

No. of
Copies

L. L. Hench
University of Florida
Advanced Materials Research
One Progress Blvd. #14
Alachua, FL 32615

J. Hennessey, EM-361
DOE Office of Environmental
Management
19901 Germantown Road
Germantown, MD 20585

E. W. Holtzscheiter
Westinghouse Savannah River Co.
P.O. Box 616
Aiken, SC 29802

N. D. Hudson
Westinghouse Savannah River Co.
P.O. Box 616
Aiken, SC 29802

V. J. Jain
West Valley Nuclear Services
P. O. Box 191
West Valley, NY 14171

C. M. Jantzen
Westinghouse Savannah River Co.
P.O. Box 616
Aiken, SC 29802

D. E. Karl
West Valley Nuclear Services
P. O. Box 191
West Valley, NY 14171

W. S. Ketola
DOE West Valley Project
P.O. Box 191
West Valley, NY 14171

No. of
Copies

R. B. King
Regents Professor of Chemistry
University of Georgia
1001 Cedar Street
Athens, GA 30602

J. R. Knight
Westinghouse Savannah River Co.
P.O. Box 616
Aiken, SC 29802

W. LaCourse
Alfred University
NYS College of Ceramics
Alfred, NY 14802

W. Lutze
Hahn-Meitner-Institut Berlin
D-1000
Berlin 39
Germany

J. E. Lytle, EM-30
DOE Office of Environmental
Management
19901 Germantown Road
Germantown, MD 20585

P. Macedo
Vitreous State Laboratory
Catholic University of Amierica
Washington, D.C. 20064

J. L. Mahoney
West Valley Nuclear Services
P. O. Box 191
West Valley, NY 14171

S. L. Marra
Westinghouse Savannah River Co.
P.O. Box 616
Aiken, SC 29802

No. of
Copies

L. B. McEwen
DOE Oakland Operations Office
1301 Clay Street
Oakland, CA 94612

T. W. McIntosh, EM-323
DOE Office of Environmental
Management
19901 Germantown Road
Germantown, MD 20585

C. E. Miller, EM-323
DOE Office of Environmental
Management
19901 Germantown Road
Germantown, MD 20585

R. A. Palmer
West Valley Nuclear Services
P. O. Box 191
West Valley, NY 14171

K. G. Picha, Jr., EM-323
DOE Office of Environmental
Management
19901 Germantown Road
Germantown, MD 20585

M. J. Plodinec
Westinghouse Savannah River Co.
P.O. Box 616
Aiken, SC 29802

A. A. Ramsey
Westinghouse Savannah River Co.
P.O. Box 616
Aiken, SC 29802

No. of
Copies

W. G. Ramsey
Westinghouse Savannah River Co.
P.O. Box 616
Aiken, SC 29802

C. T. Randall
Westinghouse Savannah River Co.
P.O. Box 616
Aiken, SC 29802

C. P. Reeve
Westinghouse Savannah River Co.
P.O. Box 616
Aiken, SC 29802

J. L. Resce
Environmental Systems Eng.
Rich Environmental Res. Lab
Clemson Research Park
Clemson, SC 29634-0919

M. Smith
Westinghouse Savannah River Co.
P.O. Box 616
Aiken, SC 29802

J. F. Sproull
Westinghouse Savannah River Co.
P.O. Box 616
Aiken, SC 29802

M. Tomozawa
Rensselaer Polytechnic Inst.
Materials Engineering Dept.
Troy, NY 12180-3950

J. C. Tseng, EM-36
DOE Office of Environmental
Management
19901 Germantown Road
Germantown, MD 20585

No. of
Copies

D. R. Uhlmann
Arizona Materials Laboratory
University of Arizona
4715 E. Fort Lowell Road
Tucson, AZ 85712

A. K. Varshneya
Alfred University
NYS College of Ceramics
Alfred, NY 14802

H. F. Walter, EM-323
DOE Office of Environmental
Management
19901 Germantown Road
Germantown, MD 20585

F. E. Woolley
Corning Incorporated
HP-ME-2-38-E6
Corning, NY 14831

R. G. Wymar
ORNL Consultant
188-A Outer Drive
Oak Ridge, TN 37830

ONSITE

9 DOE/Richland Operations Office

K. W. Bracken	S7-50
N. R. Brown	S7-53
S. T. Burnum	S7-53
M. Dev	S7-53
L. Erickson	S7-53
P. E. LaMont	S7-53
J. C. Peshcong	S7-53
G. H. Sanders	S7-53
T. R. Sheridan	S7-50

No. of
Copies

25 Westinghouse Hanford Company

J. N. Appel	G3-21
A. L. Boldt	H5-49
K. D. Boomer	H5-49
R. B. Calmus	H5-27
R. P. Colburn	H5-27
T. W. Crawford	H5-49
J. S. Garfield	H5-49
R. L. Gibby	H5-27
J. W. Hales	H5-60
B. A. Higley	H5-27
J. O. Honeyman	S7-81
A. A. Kruger	H5-27
W. C. Miller	S4-55
R. M. Orme	H5-27
R. W. Powell	H4-14
E. H. Randklev	H5-27
P. S. Schaus	H4-14
R. G. Seymour	H5-27
G. E. Stegen	H5-27
D. J. Washenfelder	H5-27
R. A. Watrous	H5-27
E. T. Weber, III	H5-27
C. N. Wilson	H5-27
D. D. Wodrich	S7-84
G. Woodcock	H5-27

3 TDPO

J. A. Carr	K9-81
J. H. Holbrook	K9-81
G. B. Mellinger	K9-81

95 Pacific Northwest Laboratory

C. S. Amrine	P8-44
R. M. Bean	K9-76
G. H. Beeman	S7-71
W. F. Bonner	K9-14
M. F. Bryan	K5-12
C. C. Chapman	P7-41
J. M. Creer	K9-80
M. L. Elliott	P7-41

No. of Copies		
	X. D. Feng	P8-44
	N. D. Foote	K7-10
	W. K. Hahn	P8-44
	S. A. Hartley	K5-12
	L. K. Holton	P7-43
	M. Hoza	K7-22
	P. R. Hrma (20)	P8-37
	G. A. Jensen	P7-19
	B. M. Johnson	K1-78
	J. W. Johnston	K5-12
	D. S. Kim	P8-44
	M. H. Langowski	P8-44
	D. E. Larson (10)	K9-80
	H. Li	P8-44
	C. A. LoPresti	K5-12
	B. P. McGrail	K2-38
	P. J. Mellinger	K9-76
	E. V. Morrey	P7-19

No. of Copies		
	D. K. Peeler	P8-44
	J. M. Perez, Jr.	P7-41
	R. D. Peters	P7-41
	G. F. Piepel (20)	K5-12
	P. E. Redgate	K5-12
	R. J. Robertus	P8-38
	M. J. Schweiger	P8-37
	P. A. Scott	P7-43
	G. J. Sevigny	P7-33
	P. Sliva	P7-18
	D. E. Smith	P8-37
	P. A. Smith	P7-14
	D. M. Strachen	K2-44
	J. D. Vienna	P8-44
	J. H. Westsik, Jr.	P7-19
	K. D. Wiemers	P7-14
	Publishing Coordination Technical Report Files (5)	